(2)

AFWL-TR-87-101

AFWL-TR-
87-101

AD-A195 351

ISST STRUCTURE WITH SIFCON -- HFC-2 TEST

Bruce Schneider, et al

New Mexico Engineering Research Institute
University of New Mexico
Albuquerque, New Mexico 87131

April 1988

Final Report

Approved for public release; distribution unlimited.

AIR FORCE WEAPONS LABORATORY
Air Force Systems Command
Kirtland Air Force Base, NM 87117-6008

AFWL-TR-87-101

This final report was prepared by the New Mexico Engineering Research Institute, University of New Mexico, Albuquerque, New Mexico under Contract F29601-84-C-0080, Job Order 8809131G with the Air Force Weapons Laboratory, Kirtland Air Force Base, New Mexico. Captain Susan M. Cheney (NTES) was the Laboratory Project Officer-in-Charge.

This technical report has been reviewed and is approved for publication.

Susan M. Cheney

SUSAN M. CHENEY
Captain, USAF
Project Officer

FOR THE COMMANDER

Thomas E. Bretz, Jr

THOMAS E. BRETZ, JR
Lt Col, USAF
Chief, Applications Branch

Carl L. Davidson

CARL L. DAVIDSON
Colonel, USAF
Chief, Civil Engrg Research Division

UNCLASSIFIED
SECURITY CLASSIFICATION OF THIS PAGE

REPORT DOCUMENTATION PAGE

1a. REPORT SECURITY CLASSIFICATION UNCLASSIFIED	1b. RESTRICTIVE MARKINGS
2a. SECURITY CLASSIFICATION AUTHORITY 2b. DECLASSIFICATION / DOWNGRADING SCHEDULE	3. DISTRIBUTION / AVAILABILITY OF REPORT Approved for public release; distribution unlimited.
4. PERFORMING ORGANIZATION REPORT NUMBER(S) NMERI WA8-25 (8.16)	5. MONITORING ORGANIZATION REPORT NUMBER(S) AFWL-TR-87-101
6a. NAME OF PERFORMING ORGANIZATION New Mexico Engineering Research Institute 6b. OFFICE SYMBOL (If applicable) NMERI	7a. NAME OF MONITORING ORGANIZATION Air Force Weapons Laboratory
6c. ADDRESS (City, State, and ZIP Code) Box 25, University of New Mexico Albuquerque, NMex 87131	7b. ADDRESS (City, State, and ZIP Code) Kirtland Air Force Base, NM 87117-6008
8a. NAME OF FUNDING / SPONSORING ORGANIZATION 8b. OFFICE SYMBOL (If applicable)	9. PROCUREMENT INSTRUMENT IDENTIFICATION NUMBER F29601-84-C-0080
8c. ADDRESS (City, State, and ZIP Code)	10. SOURCE OF FUNDING NUMBERS PROGRAM ELEMENT NO 62601F; PROJECT NO 8809; TASK NO 13; WORK UNIT ACCESSION NO 1G

11. TITLE (Include Security Classification)
ISST STRUCTURE WITH SIFCON--HFC-2 TEST

12. PERSONAL AUTHOR(S)
Schneider, Bruce; Mondragon, Ray; Kirst, Jon; and Berglund, Jerry

13a. TYPE OF REPORT	13b. TIME COVERED	14. DATE OF REPORT (Year, Month, Day)	15. PAGE COUNT
Final	FROM Nov 83 TO Sep 84	1988 April	382

16. SUPPLEMENTARY NOTATION

17. COSATI CODES FIELD	GROUP	SUB-GROUP	18. SUBJECT TERMS (Continue on reverse if necessary and identify by block number)
13	13		Missile silo; Hardened structures; SIFCON; Blast effects; Fiber concrete

19. ABSTRACT (Continue on reverse if necessary and identify by block number)

In 1983 a new material, slurry-infiltrated fiber concrete (SIFCON), was brought to the attention of the Air Force Weapons Laboratory (AFWL) by Dr David Lankard of the Lankard Materials Laboratory (LML) in Columbus, Ohio. A review and analysis of the material by AFWL showed that SIFCON possessed the characteristics of both high strength as well as ductility. These properties indicated that the material had a potential use in a superhard silo structure.

Because the material showed such promise, AFWL proposed a program to construct and test a scale model of a generic superhard silo structure using the SIFCON material. AFWL decided to place the structure in a scheduled calibration test that was part of the Intercontinental Ballistic Missile Silo Superhardening Technology (ISST) testing program in Yuma, Arizona. NMERI then began a program to develop a slurry mix design for use in the structure, as well as construction techniques for placing the SIFCON in the wall of the model. (over)

20. DISTRIBUTION / AVAILABILITY OF ABSTRACT ☐ UNCLASSIFIED/UNLIMITED ☒ SAME AS RPT ☐ DTIC USERS	21. ABSTRACT SECURITY CLASSIFICATION UNCLASSIFIED
22a. NAME OF RESPONSIBLE INDIVIDUAL Susan M. Cheney, Captain, USAF	22b. TELEPHONE (Include Area Code) (505) 866-4656 22c. OFFICE SYMBOL NTES

DD FORM 1473, 84 MAR
83 APR edition may be used until exhausted.
All other editions are obsolete.

SECURITY CLASSIFICATION OF THIS PAGE
UNCLASSIFIED

19. ABSTRACT (Continued)

The report discusses the design, construction, instrumentation and placement of the structure in the test-bed and tabulates the results of the static testing of the SIFCON material. In addition, the report includes the results and analysis of sonic static and dynamic testing of SIFCON. Analysis of the data obtained from the gages mounted on the model and comparison to the pretest predictions were conducted by AFWL and the results published in a separate document.

CONTENTS

CONTENTS (Continued)

CONTENTS (Continued)

CONTENTS (Concluded)

ILLUSTRATIONS

ILLUSTRATIONS (Continued)

ILLUSTRATIONS (Concluded)

TABLES

I. OVERVIEW

INTRODUCTION

In 1983 a new material, slurry-infiltrated fiber concrete (SIFCON), was brought to the attention of the Air Force Weapons Laboratory (AFWL) by Dr. David Lankard of the Lankard Materials Laboratory (LML) in Columbus, Ohio. Dr. Lankard had done some pioneer work in the development of the material, as well as some applications using the material in the paving and metal fabrication industries. A review and analysis of the material by AFWL showed that SIFCON possessed the characteristics of both high strength as well as ductility. These properties indicated that the material had a potential use in a superhard silo structure.

Because the material showed such promise, AFWL proposed a program to construct and test a scale model of a generic superhard silo structure using the SIFCON material. Limited funds and time prevented the building of a specific explosive test environment for the structure. As a result, AFWL decided to place the structure in a scheduled calibration test that was part of the Intercontinental Ballistic Missile Silo Superhardening Technology (ISST) testing program in Yuma, Arizona. Unfortunately, the environment of the calibration test would have required a much larger scale model than could be constructed with the funding and time available. To proceed with the program, AFWL selected a much smaller scale size for the structure. Although the structure would be subjected to a more severe environment than an equivalent scale baseline-type structure, AFWL felt that the structure fabricated from SIFCON would still generally survive the test and provide valuable data for future work.

On November 15, 1983, several New Mexico Engineering Institute (NMERI) engineers and technicians were instructed by Dr. Lankard on the manufacture of SIFCON. It was clear at that time that there was not a large amount of test data covering one specific mix design or fiber percentage but only a few results on many different mixes. In addition, no data covering dynamic loading were available.

Following the instruction, NMERI began a program to develop a slurry mix design for use in the structure, as well as construction techniques for placing the SIFCON in the wall of the model. Again, time constraints permitted

only a brief study of mix designs before a decision had to be made. With advice from Mr. Lankard, a mix was selected and the design and construction of the model began in early January 1984.

SCOPE

This report is divided into four sections. Section I is an overview of the program. Section II discusses the design, construction, instrumentation, and placement of the structure in the test-bed as well as tabulating the results of the static testing of the SIFCON material. Section III analyzes the results of the static and dynamic testing of SIFCON. Section IV presents some qualitative posttest observations of the model. Analysis of the data obtained from the gages mounted on the model and comparison to the pretest predictions will be conducted by AFWL, with the results to be published in a separate document.

GOALS

The goal of fabricating and testing a generic ISST scaled model of SIFCON was to demonstrate the survivability of a superhard silo structure using innovative design concepts and unconventional materials.

APPROACH

The approach was to use the Ballistic Missile Office (BMO) ISST test series, specifically HFC-2 (High-Fidelity Calibration) event (Ref. 1), as a test-bed for evaluating the materials and design concepts of a superhard silo constructed with SIFCON. The HFC-2 test was designed to be a 379-MPa (55 k/in^2), 225-kt nuclear airblast simulation test. This environment, on the

---

1. Bedsun, David A., Site Characterization of the HFC-2 Testbed, Luke AFB, AZ, NMERI TA8-61, Task Report, Air Force Weapons Laboratory, Kirtland Air Force Base, New Mexico, March 1984.

one-eighth scale ISST structure, would scale to an environment of 115 Mt and 379 MPa (55 k/in^2) for a full-size Peacekeeper-type missile silo. Reference 2 gives specific details of the simulator design and structure placement in the test-bed as well as the predicted airblast and ground shock environments.

TEST OBJECTIVES

The first objective was to design a structure that would reduce some of the relative soil structure motions and thus reduce structural loading. The method that was used to accomplish the reduced silo structure motions and structural loading is discussed in Section II. A second objective in the test was to use materials that have high strength and ductility while at the same time improving constructability. SIFCON, with the percentage of steel used in the structure, was such a material. The high strength and ductility characteristics and the constructability issues of SIFCON are discussed in Sections II and III.

---

2. Bedsun, David A., HFC-2 Pretest Report, NMERI TA7-29, Task Report, Air Force Weapons Laboratory, Kirtland Air Force Base, New Mexico, May 1984.

II. CONSTRUCTION AND FIELDING OPERATIONS

INTRODUCTION

This section is limited to a documentation of the construction and fielding procedures and material test results performed by NMERI during the fabrication of a scale model of a generic hard silo structure. The model was constructed for AFWL as part of the ISST testing program.

This section begins with a discussion of the development of the SIFCON mix design and construction techniques. Next, a review of the silo design procedure is presented followed by a step-by-step documentation of the construction of the model and installation of the instrumentation. Also included is documentation of the results of the Materials Testing Program.

DEMONSTRATION PROGRAM

Introduction--Basically, the manufacture of SIFCON involves first filling a form with short, small-diameter steel fibers. Although the form will appear to be filled solid with fiber, the actual volume occupied by fiber is only about 5 to 15 percent of the form volume. In practice the exact volume occupied by the fiber is mainly a function of the type of fiber used. For a specific-type fiber used, a specific percentage of volume occupied will result. This value is relatively constant and cannot be significantly increased by vibration or compressing the mass of fiber. Certain form geometries such as narrow walls or sharp curves may also cause slight variation in the percentage value due to a phenomenon designated as "edge effects" which is discussed later.

After the form is filled with fiber, a portland-cement-based slurry is poured on the surface of the fiber mass and allowed to infiltrate the voids between the fibers. The slurry is poured until the form is full, and then allowed to set up and cure.

Procedure--To gain some knowledge concerning the properties of SIFCON for design purposes, as well as to determine construction methods necessary to

to fabricate the model, a small demonstration-type program was undertaken by NMERI. The program consisted of the fabrication of a mold approximately simulating the wall of the model. This mold, as shown in Figure 1, consisted of a 6-mm (0.25-in)-thick steel plate for the back of the mold and a 6-mm (0.25-in)-thick clear acrylic plastic plate for the front face. Both plates were secured to a wood frame comprising the sides and bottom. The wood frame was cut from standard 2 by 8 lumber cut down to 152 mm (6 in) wide. Headed anchor studs, 6 mm (0.25 in) in diameter and 64 mm (2.5 in) long, were welded to the steel backplate. In addition, headed anchor studs, of the same geometry as the steel studs, were fabricated from clear acrylic plastic rods and glued to the clear acrylic front plate. The studs were arranged in a staggered pattern on the front and back plates so that no studs were directly opposite each other. The clear acrylic front plate permitted observation of the fibers and slurry mix during placement. From this observation, the following questions could be answered:

1. What was the best method of placing the fiber into the form and hopefully into the wall of the model?

2. What was the effect of the anchor studs on the placement of the fiber?

3. What was the effect of form vibration on the placing of both the fiber and the slurry?

4. Was the slurry mix the proper consistency to completely infiltrate the fiber mass?

5. What was the best technique to make a horizontal construction joint between consecutive pours?

In addition to the form simulating the wall of the model, three 204-mm (8-in) cubes of SIFCON were fabricated. These specimens were used to determine fiber densities as well as to produce core samples. The cored specimens, taken both horizontally and vertically from the cube, were used to study the effect of fiber orientation versus compressive strength. Standard 102-mm (4-in)-diam by 204-mm (8-in)-long cylindrical specimens of both SIFCON and the slurry were also prepared.

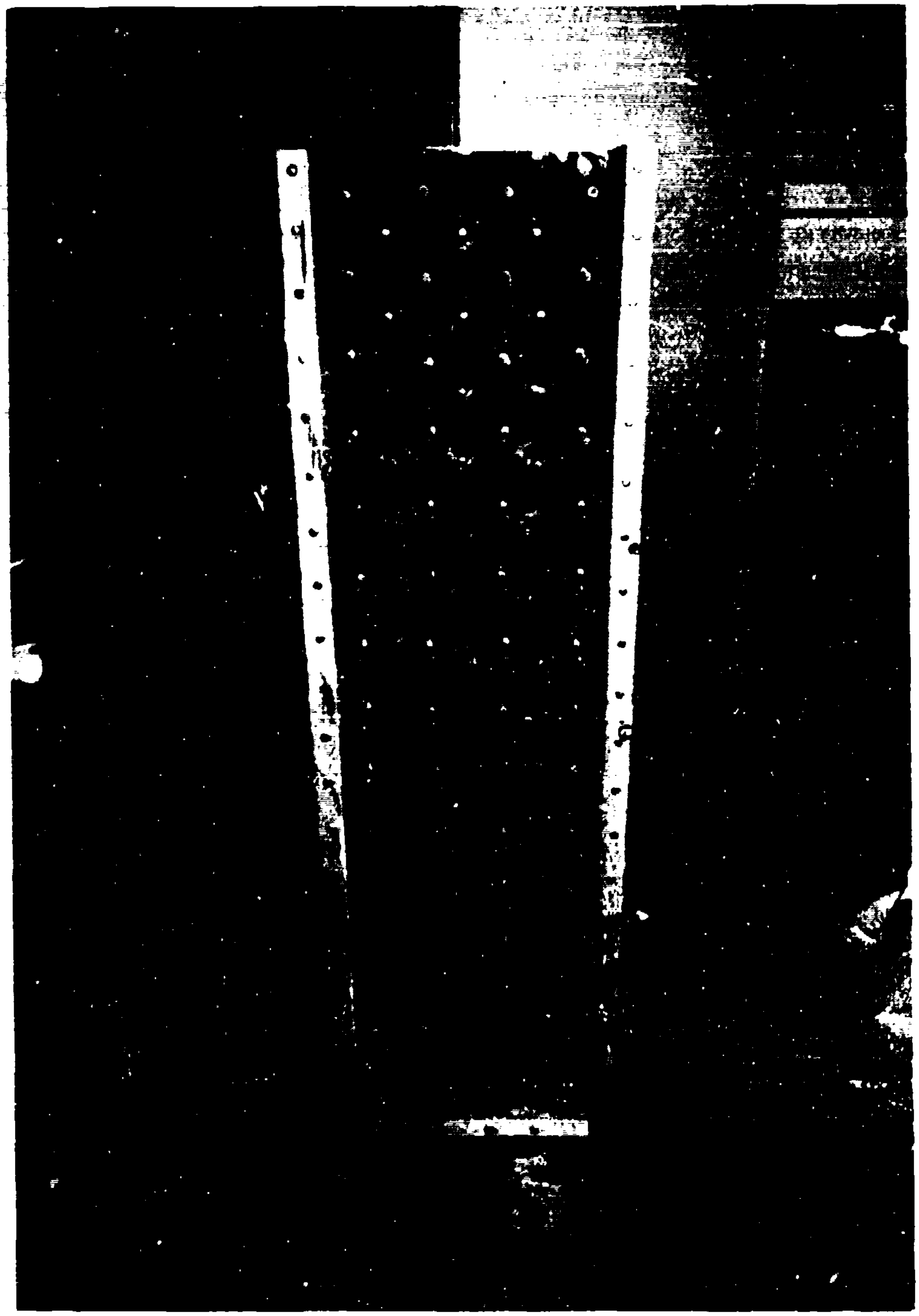

Figure 1. Wall mold for demonstration program.

Results--From this program it was determined that the fiber could be placed by hand by sprinkling the fibers into the form or by just dropping a handful of fibers into the form and allowing the anchor studs to break up the clump of fibers as they fell. In general, both techniques produced undiscernible differences in fiber densities throughout the height of the wall except near the top of the form. In the upper 152 to 305 mm (6 to 12 in) of the form, the fibers had to be sprinkled because there were not enough anchor studs to break up clumps of fibers.

In addition, visual inspection showed that the headed anchor studs were not detrimental to placing the fiber, provided the form was continuously vibrated during the placement procedure. In fact, the fibers interlocked around the studs so well that the form could be turned upside down and the fibers would not fall out.

Four different slurry mixes were tried until one was found with the proper consistency to flow down through a depth of 1.5 to 1.8 m (5 to 6 ft) of fiber. It was also determined that even a relatively thick mix could be worked into the fibers if the form was vibrated properly.

After several trials, a method for making a horizontal construction joint was developed. This technique involved stopping the slurry placement when the level of the slurry was about 50 mm (2 in) below the surface of the fiber mass.

These results and the experience gained in working with the fibers and slurry permitted the design of the structural details to begin. In addition, construction plans were also developed (Ref. 3). It should be noted that the demonstration program proved to be invaluable in providing the necessay experience for working with such a new and unconventional material.

DESIGN

Introduction--Due to an almost total lack of data concerning material properties for the SIFCON at the beginning of the project, the design of the

---

3. Mondragon, R., Generic Hard Silo Structures Test Program, NMERI TA9-11, Management Plan prepared for Air Force Weapons Laboratory, Kirtland Air Force Base, New Mexico, December 1983.

structure was actually an effort to determine only a few of the critical dimensions for the model. These included the wall thickness of the cylinder portion, the length of the reduced section in the headworks area, the thickness of the closure, and the liner plate thicknesses. An illustration of terminology used in this section is given in Figure 2. The internal geometry was selected by AFWL from a study of the current ISST baseline structure.

SIFCON mix design--The design of the SIFCON was based on recommendations by Dr. Lankard and the results of the Demonstration Program performed at NMERI.

The fiber selected was manufactured by the Bekaert Steel Wire Corporation under the registered trade name of DRAMIX and designated as ZL 30/.50 by the manufacturer. The fiber was 30 mm (1.2 in) long with a 0.50-mm (0.02-in) diameter. Each fiber had a slight kink at each end as shown in Figure 3. The fiber was manufactured from low carbon, cold drawn steel wire having a specified minimum tensile yield strength of 1170 MPa (170,000 lb/in^2). Other properties of the fiber are shown in Table 1.

The mix design for the slurry is shown in Table 2. The ratio of water to cement plus fly ash was 0.35. The ratio of the cement to fly ash was 70/30 by weight. The superplasticizer dosage rate was 887 mL/45 kg (30 oz/100 lb) of cement plus fly ash.

The type of cement desired was Type III because of its high-early-strength property. However, Type III cement is difficult and costly to obtain in the New Mexico area in bagged form; as a result, Type I (Special) was selected. This is a cement, manufactured locally, which has some properties of Type III cement, specifically the high-early-strength characteristic. In actual practice, most any type of cement would be satisfactory depending upon the desired results; however, the test schedule at the time dictated the use of a high-early-strength cement. The fly ash selected was Type C having some cementitious qualities which were felt would be of some benefit to the mix.

One of the trial mixes performed in the Demonstration Program was found to perform extremely well during the pouring operation and the early test results indicated a satisfactory strength. At the time, it was felt certain

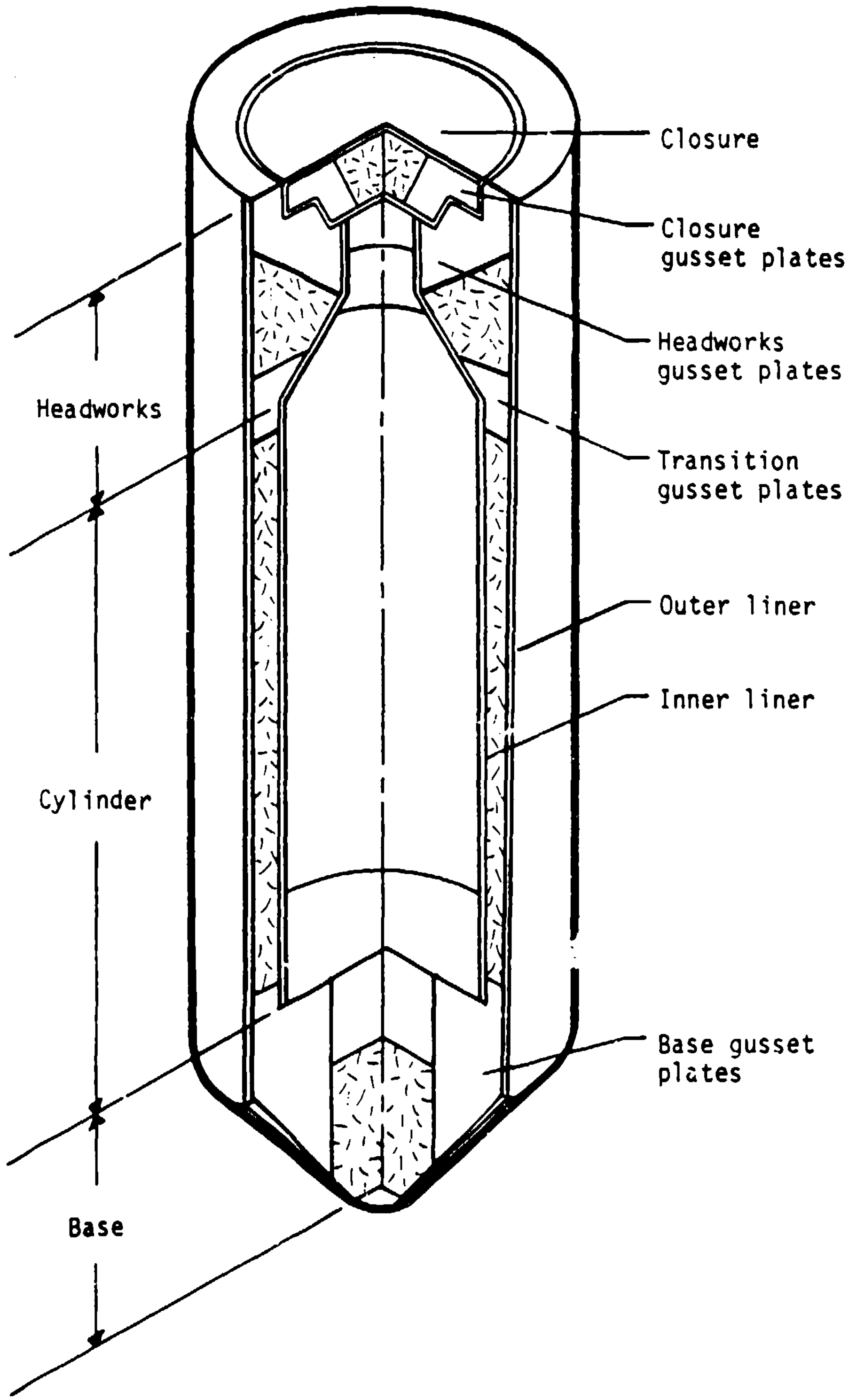

Figure 2. ISST terminology.

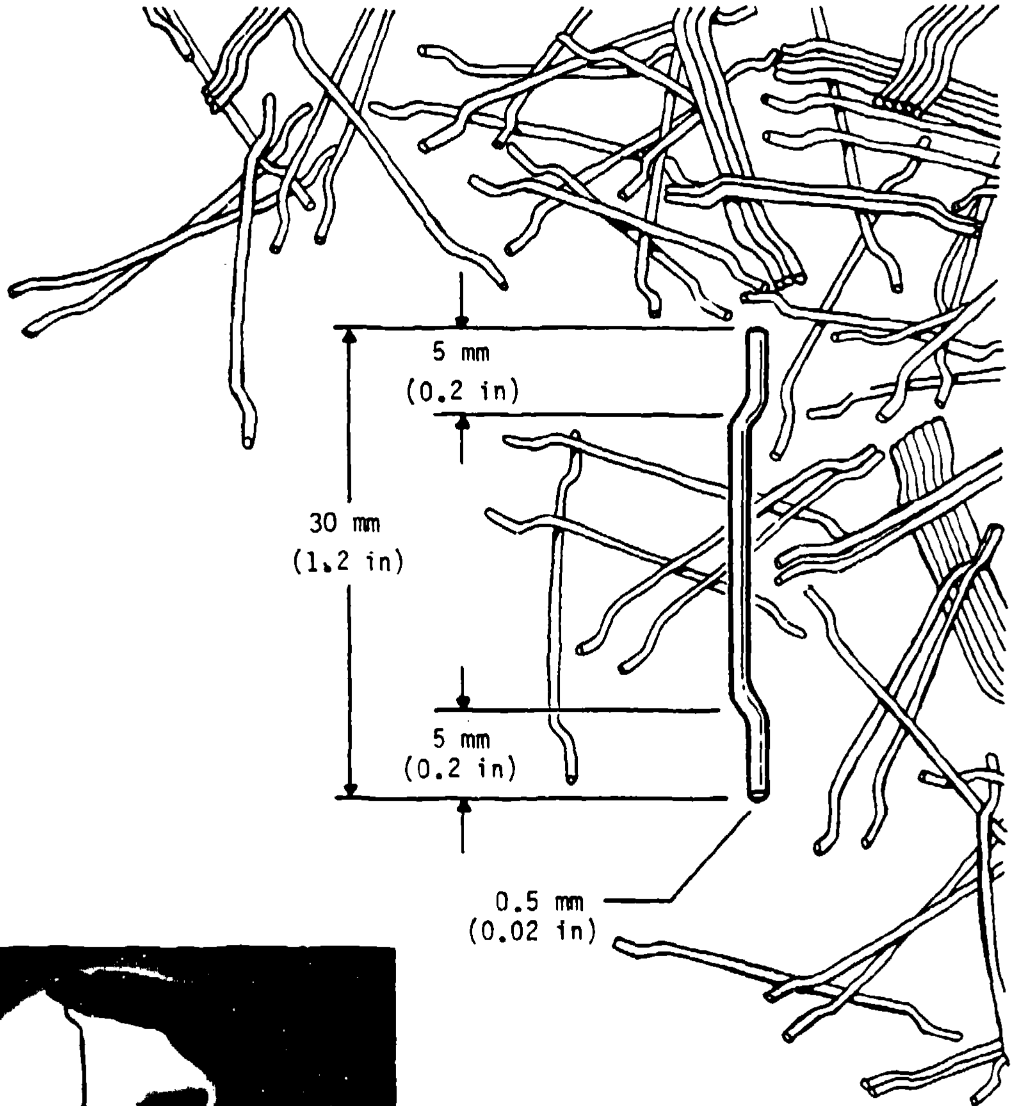

Figure 3. Steel fiber for ISST SIFCON.

TABLE 1. FIBER PROPERTIES

Fiber type	ZL 30/.50
Dimensions	Length: l = 30 mm (1.18 in)
	Diameter: d = 0.50 mm (0.02 in)
	Z = hooked
	L = loose
Aspect ratio	l/d = 60
Tensile yield strength	1172 MPa (170,000 lb/in^2)
Tolerances	Length ±5 percent maximum
	Diameter ±4 percent maximum
	Aspect ratio ±10 percent maximum

TABLE 2. SLURRY MIX DESIGN

Ingredient	Specification	Manufacturer	Weight
Portland cement	Type I (Special)	Ideal Basic Industries Tijeras Canyon, NM	42.6 kg (94.00 lb)
Fly ash	Type C	Panhandle Fly Ash Amarillo, TX	18.3 kg (40.29 lb)
Water	Potable		21.3 kg (47.01 lb)
Superplastizer	LA-8 (400N)	Master Builders Cleveland, OH	1191 ml (40.29 oz)
Yield			0.043 m^3 (1.51 ft^3)
Calculated unit weight			2528.0 kg/m^3 (157.8 lb/ft^3)

minor adjustments could be made in the cement/fly ash ratio, the water/cement ratio, and the superplastizer dosage rate which might improve the workability or strength of the slurry mix. However, time and cost constraints prevented further development and refinement of the mix.

Liners--The material selected for the outer liner plate was 6-mm (0.25-in)-thick A572 Grade 50 steel plate. The main reason for selecting this material was that it was readily available within the time frame required. Secondly, it was reasoned, intuitively, that the higher the confining pressure the SIFCON would experience, the higher the axial compression strength would be. Therefore, while a thinner plate would be adequate for construction conditions, a thicker plate would provide a higher confining pressure. Under yield conditions, the 6-mm (0.25-in)-thick plate would exert a confining pressure of 4.0 MPa (580 lb/in^2).

The material selected for the inner liner plate was also 6 mm (0.25 in) thick, A572 Grade 50 steel plate. It was also selected for reasons of availability.

A 10-mm (0.375-in)-thick steel plate of A572 Grade 50 was selected for the inner liner of the headworks region. Again, the thickness was chosen based on availability from suppliers. Also this thickness provided approximately the same cross-sectional area of steel in the reduced section of the headworks as the 6-mm (0.25-in)-thick plate did in the cylindrical section. This was done in the hopes of avoiding large and sudden variations of stress in the liner from one area to another during loading.

Steel-headed anchor studs, 64 mm (2.5 in) long by 6 mm (0.25 in) in diameter with a tensile strength of 380 MPa (55,000 lb/in^2), were provided on both the inner and outer liner plates. Use of studs on the outer liner was studied for some time, and it was finally decided to provide them with the idea that even if they did not contribute to the strength of the system, they would probably not be significantly detrimental either. The stud length and spacing selected was somewhat arbitrary because the mechanisms of shear and pullout failures of the SIFCON were not known at the time. The stud pattern was selected to avoid studs on the inner and outer liners from being directly opposite each other. This was done as a precaution to prevent preferential

cracking or failure planes from developing through the thickness of the wall. However, it was felt this would probably not be a problem with SIFCON. Also, by staggering the studs on the inner and outer liners it was felt that the steel fibers would not bridge between studs on opposite liners as the fibers were being placed. The stud length, although not to scale, was selected as being a standard stocked item from several suppliers. A shorter stud was actually desired due to the scale of the model; however, time and cost constraints did not permit a special order.

Wall thickness--The thickness of the wall in the cylinder section of the model was selected following a preliminary calculation using a spring-mass model performed by the Theoretics Division at NMERI (Ref. 4). Based on the calculation, a wall thickness of 152 mm (6 in) of SIFCON was chosen. From this dimension, the thickness of the walls in the headworks section was determined.

Base section--The concept of the conical end at the base of the model was developed by AFWL. Originally, a steel floor plate was designed in the inside of the cylinder section. However, it was eliminated early in the design process to simplify placing of the SIFCON in the base. Also, from a structural response point of view, it did not add to the strength because the base was a conical section rather than a flat plate.

A series of six 13-mm (0.5-in)-thick steel gusset plates was selected by AFWL as stiffeners at the intersection of the wall of the cylinder and the base section. These gussets were designed to be welded to both the inner and outer liner and connected to each other with 13-mm (0.5-in)-thick plates (Ref. 5). These gussets were designed to prevent a potential shear failure mechanism from developing at the wall and base as detailed in Figure 4.

Although it was felt that the SIFCON alone would have been able to resist the failure, the possibility of losing data from the calibration test warranted the inclusion of the gussets as a precautionary measure.

---

4. Rudeen, D., and Morrison, D., Preliminary Pretest Predictions of the ISST 1/8 Scale Structure Response, NMERI Task Report, Air Force Weapons Laboratory, Kirtland Air Force Base, New Mexico, February 1984.

5. Schneider, Bruce, Engineering Drawings For ISST Structure With SIFCON--HFC-2 Test, NMERI WA8-56, Task Report, Air Force Weapons Laboratory, Kirtland Air Force Base, New Mexico, September 1984.

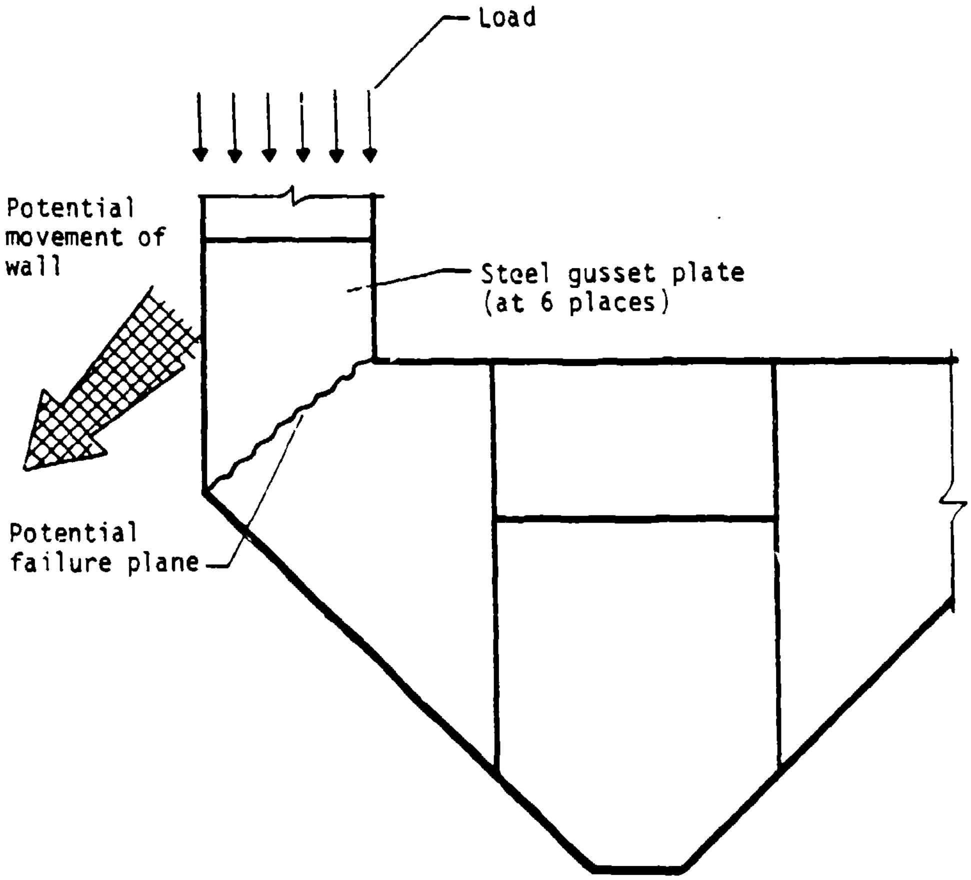

Figure 4. Base gusset plates.

Headworks section--The headworks was detailed with a horizontal bearing plane for the closure. The width of the bearing plane was selected by AFWL. Some concern was expressed concerning the ability to place fiber under a wide horizontal surface such as the bearing plate. An inward sloping bearing surface, such as on one of the reinforced concrete baseline structures, was considered but rejected in favor of the horizontal surface since it was simpler to fabricate in the allotted time.

Again, as in the base section, twelve 13-mm (0.5-in)-thick steel gusset plates were provided as a precautionary measure against failure in the bearing area (Fig. 5). The gussets were welded to the inner liner but not to the outer liner because of limited access for welding. Instead, a steel angle was welded to each side of the gusset plate to engage a large section of the SIFCON wall to help resist potential movement.

Later calculations (Refs. 6 and 7) indicated that the wall section at the transition of the headworks and the cylinder section might suffer a significant amount of distress. To stiffen that area, twelve 13-mm (0.5-in)-thick steel gusset plates were added as shown in Figure 2.

Intuitively, it was felt that the gusset plates were probably not necessary or that at least the size could be significantly reduced. However, as stated earlier, the risk of losing the data on the calibration test dictated that the precaution be taken.

Closure--The general geometry of the closure was selected by AFWL. The steel plates used were A572 Grade 50 with 13-mm (0.5-in) thickness selected for the bottom plate and 10-mm (0.375-in) thickness for the sides. As before, these thicknesses were selected mainly for availability and timely delivery from suppliers.

---

6. Berglund, J. W., Pretest Prediction Report for the Generic Hard Silo Model, NMERI TA8-59, Task Report, Air Force Weapons Laboratory, Kirtland Air Force Base, New Mexico, March 1984.

7. Berglund, J. W., Analysis of ST and LT Calculation Results, NMERI Task Report, Air Force Weapons Laboratory, Kirtland Air Force Base, New Mexico, March 1984.

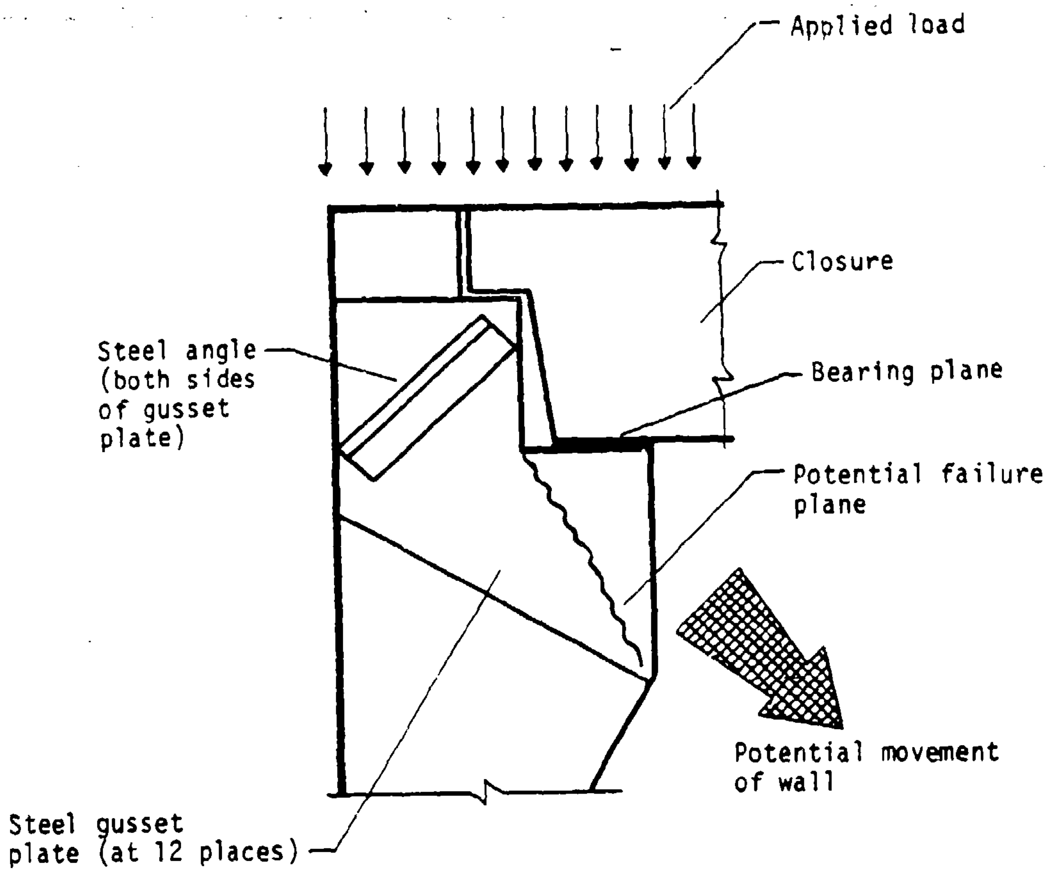

Figure 5. Headworks gusset plates.

Gusset plates, of 13-mm (0.5-in)-thick steel, were provided in the closure (Ref. 5). These gusset plates were designed to greatly stiffen the closure as a precautionary measure against failure. The plates were located in the closure in a pattern corresponding with the gusset plates in the bearing area of the headworks. In addition, sleeves for six 22-mm (0.88-in)-diam, ASTM A-490 bolts were provided to match the location of high-tensile strength threaded concrete inserts located under the bearing plate.

The bolts were designed to keep the closure attached to the structure as the closure rebounded from the load. To prevent the bolts from breaking in the root of the threaded portion, as past experience had shown they would, the body of the bolt was detailed to be machined down to a diameter of 18 mm ± 0.25 mm (0.71 in ± 0.01 in) as shown in Figure 6. This detail would hopefully force the body of the bolt to yield first where large ductile deformations could occur, thereby absorbing the rebound energy without sudden failure.

To provide for a uniform distribution of load from the closure into the structure, a 6-mm (0.25-in)-thick lead plate was provided at the bearing interface. This soft material was designed to conform to the slight irregularities always present in steel plate, thus preventing concentrated or asymmetrical loading into the structure. In addition, the lead plate was designed to be an air seal to prevent the blast pressure from leaking inside the structure. As an added benefit, the deformation of the lead plate as it was loaded would act like a type of crushable link to "soften" the load going into the structure. Whether the reduction would be of much significance was doubtful, but even a small amount was considered helpful.

CONSTRUCTION PROCEDURES

Component fabrication--

Liner subcontract--A contract was entered into with D & R Tank of Albuquerque, New Mexico, to fabricate the necessary steel liner components for the model. The liner plate joint welds were tested 100 percent ultrasonically and spot checked radiographically. After testing, any needed repairs were performed and then the welds were retested. After the weld repairs were completed, the liners exceeded all of the contract specifications.

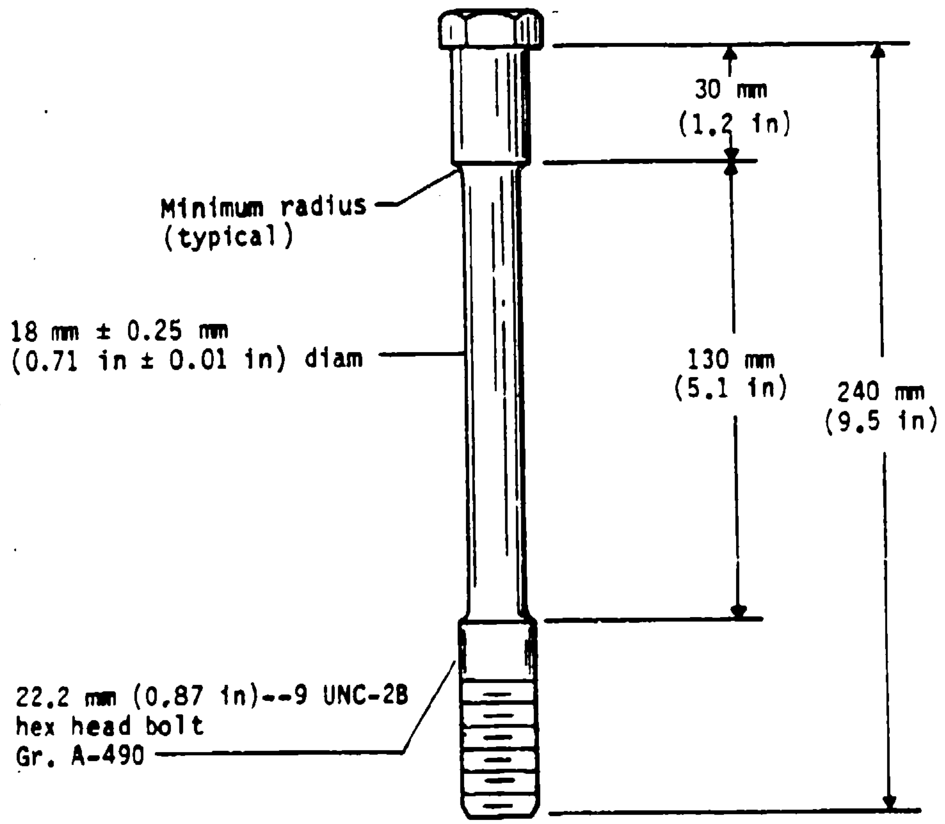

Figure 6. Closure bolt.

Base section--The base section was composed of a 178-mm (7-in)-diam base plate, a conical outer liner section, the lower portion of the outer liner, and six gusset plates. All edges to receive full penetration welds were beveled. The conical section was first welded to the lower outer liner with full penetration welds (Fig. 7). The 178-mm (7-in)-diam base plate was next welded to the bottom of the conical section. These welds were tested ultrasonically and radiographically. The necessary repairs were made before further work was performed. Gusset plates were cut to the shape noted in Reference 5 and fitted in the base section. These gusset plates were then welded in place, as shown in Figure 8, and the welds tested. The anchor studs were then welded in place according to the spacings noted in Reference 5. A 25-mm (1-in)-diam high-tensile concrete insert was welded at the center of the 178-mm (7-in)-diam plate for handling purposes. After completion of welding, the required instrumentation was installed, completing this phase of construction.

Bottom section of inner liner--The 305-mm (12-in)-long inner liner section required no additional welding except for installing the anchor studs. All edges that eventually would be full penetration welded were beveled. One strain gage was placed on the inside of the liner (Fig. 9).

Cylinder inner liner section--The major portion of the cylinder inner liner was manufactured in three identical 1.5-m (5-ft) sections. All edges to receive full penetration welds were beveled. The liner sections were fitted together so that the vertical joint welds of each section were staggared at least 90 deg. These three sections were welded to each other with full penetration welds. Each weld was tested ultrasonically with additional spot testing radiographically. After all repairs were made, the anchor studs were welded to the three liner sections (Fig. 10).

Headworks inner liner--The headworks inner liner was composed of manufactured rolled plate sections and 13-mm (0.5-in)-thick flat plates. All flat plates were cut from sheets and all the required holes were drilled. The individual plates and rolled sections were then tack-welded together beginning from the top to the bottom. All dimensions were checked before further welding. Backup plates were welded at the joint of the 10-mm (0.375-in)-thick

Figure 7. Welding base section.

Figure 8. Base section with welding completed.

Figure 9. Bottom section of inner liner.

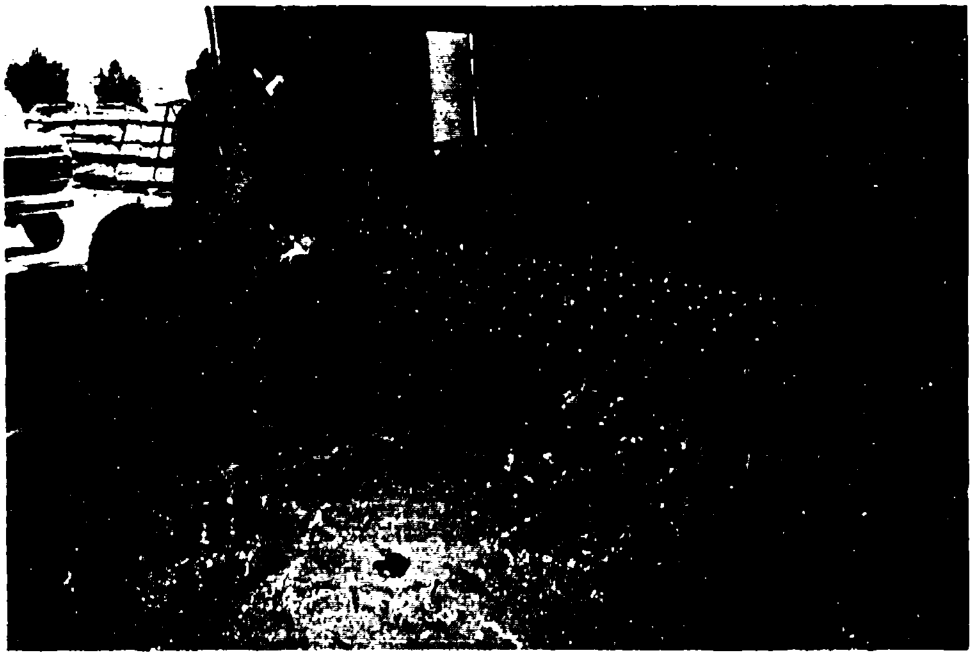

Figure 10. Cylinder inner liner section.

conical section plate and the 6-mm (0.25-in)-thick cylinder liner plate. This was needed because of the change in steel thicknesses. A root pass was first welded on all the joints inside the liner. Then a bead of weld was placed on all outside joints. Next, all the final full penetration weld passes were performed (Fig. 11). All welds were tested ultrasonically and radiographically. The test results indicated that minor repairs were required at the backup plates. The backup plates were removed and the needed repairs were made. The headworks fabrication was concluded with the welding of the anchor studs and closure bolt inserts.

Gusset plates for the headworks area were also fabricated from flat plate but not installed to the liner. These plates would later be fitted and welded just prior to the installation of the last outer liner section.

Closure--The closure was composed of manufactured rolled sections, 13-mm (0.5-in) flat plates, and gusset plates. All plates were cut from sheets and the required holes were drilled in the bottom plate. The individual plates and sections were then tack-welded together. All dimensions were checked and match-fitted to the headworks section before any further welding. A root pass was first welded on all inside joints. Then a bead of weld was placed on all outside joints. Next, all final weld passes were performed (Fig. 12). All welds were tested as described earlier. The gusset plates were fitted and welded in place inside the closure as shown in Reference 5. Six bolt sleeves, manufactured from 32-mm (1.25-in) and 64-mm (2.5-in) standard pipe, were welded onto the closure bottom. A temporary lifting eye was also welded to the top of the gusset plates at the center of the closure. The purpose of the lifting eye was to enable not only the lifting of the closure but the lifting of the entire model with the closure bolted in place. The appropriate instrumentation was then installed to the closure.

A 6-mm (0.25-in)-thick lead plate was cut to match the size and hole pattern of the horizontal bearing plate where the closure was to seat. The lead plate would be installed in the field.

Outer liners--The 1.5-m (5-ft)-long outer liners were each fitted with anchor studs using the configuration noted in Reference 5. A series of small-diameter holes was drilled and tapped in each of the 1.5-m (5-ft) outer

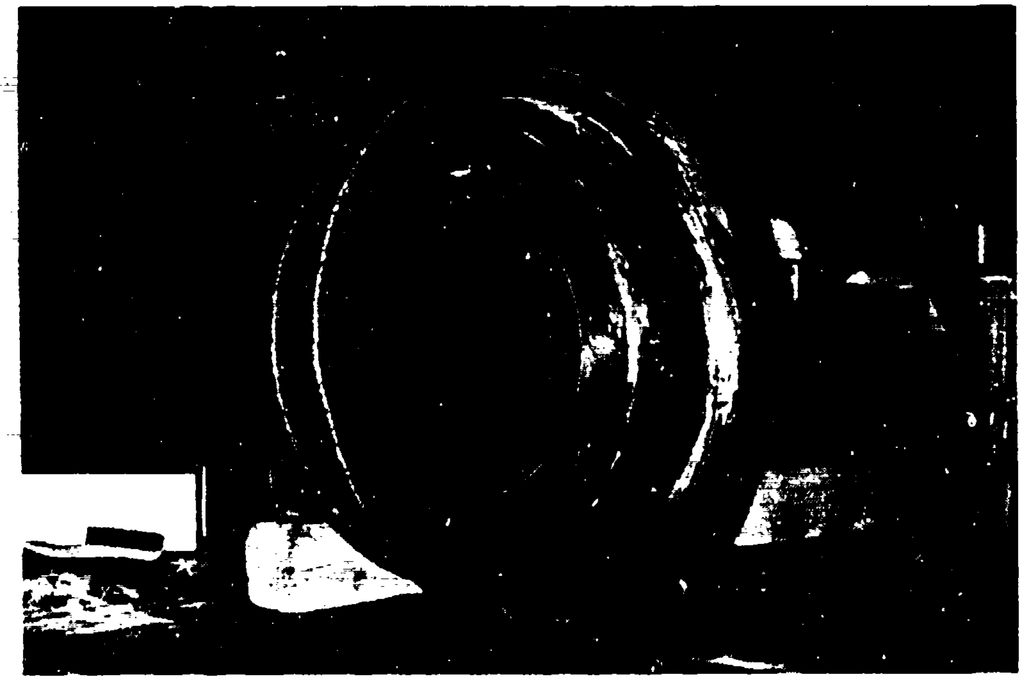

Figure 11. Headworks.

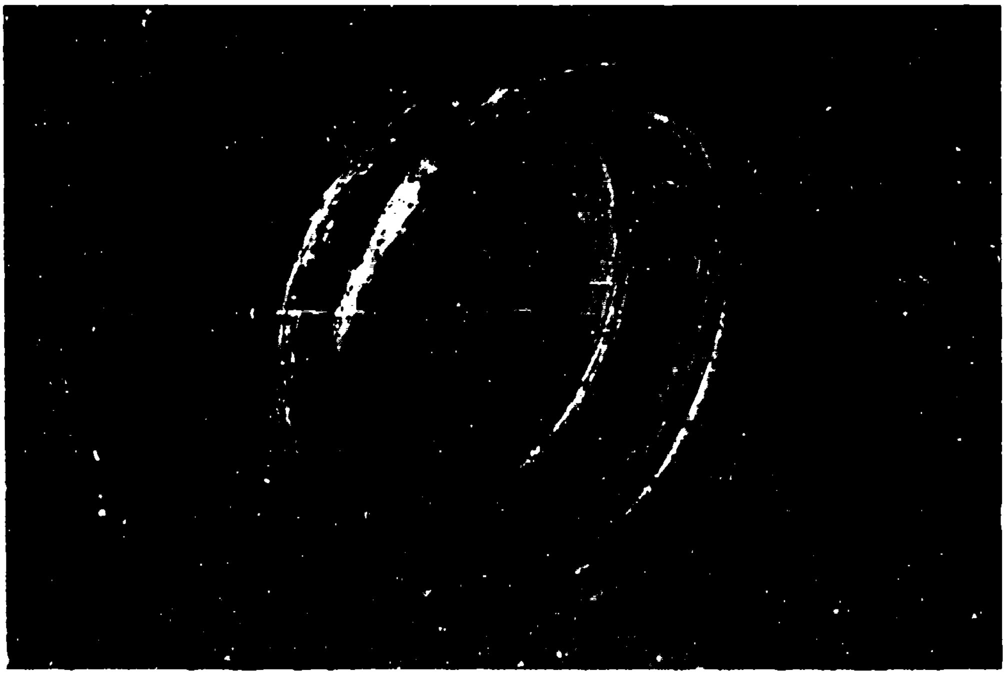

Figure 12. Closure.

liners at approximately 0.30-m (1-ft) spacing on four vertical lines located 90 deg apart. The purpose of these holes was to give a visual indication of slurry levels during the slurry placement. As the level of slurry reached the location of a hole and began to flow out, a screw would be inserted to seal off the slurry.

Concrete support structure--Because of the long slender shape and the conical base of the model, a means of supporting the structure in an upright position during construction was needed. To meet this need a concrete structure (Ref. 5), molded to the shape of the model base, was constructed using the following procedures. The support structure was formed so that it could be poured upside down. The actual conical steel base section for the model was placed upside down in the center of the form so that the concrete would conform exactly to the shape of the model base. A 200-mm (8-in) layer of styrofoam was placed on the bottom of the form around the model base section. Plastic sheets were taped on all surface areas of the base section to be exposed to the concrete so that the base section would not bond to the concrete. After all reinforcing steel, high-tensile inserts, anchor plates, and lifting brackets were installed, the concrete was placed in the form and finished. After the forms were stripped the concrete structure was turned over and transported to the location where the model was to be constructed.

Assembly of components and SIFCON placement--

First SIFCON placement, model base section--The outer liner base section was set in the concrete support structure and leveled in preparation of SIFCON placement (Fig. 13). The steel fibers described earlier were sprinkled into the base section in such a way as to prevent clumps of fibers from forming (Fig. 14). The base section liner was vibrated using pneumatic form vibrators while fibers were being sprinkled. Vibration and filling of fibers continued until there was no more consolidation of fibers and the level of the fibers had reached the level of the floor inside the model. As noted in Table 3, a careful accounting was kept of the weight of the fiber placed in the base section in order to calculate the percentage of fiber.

On January 19, 1984, after fiber placement, the concrete slurry was batched using the mix proportions decribed earlier. It was determined during

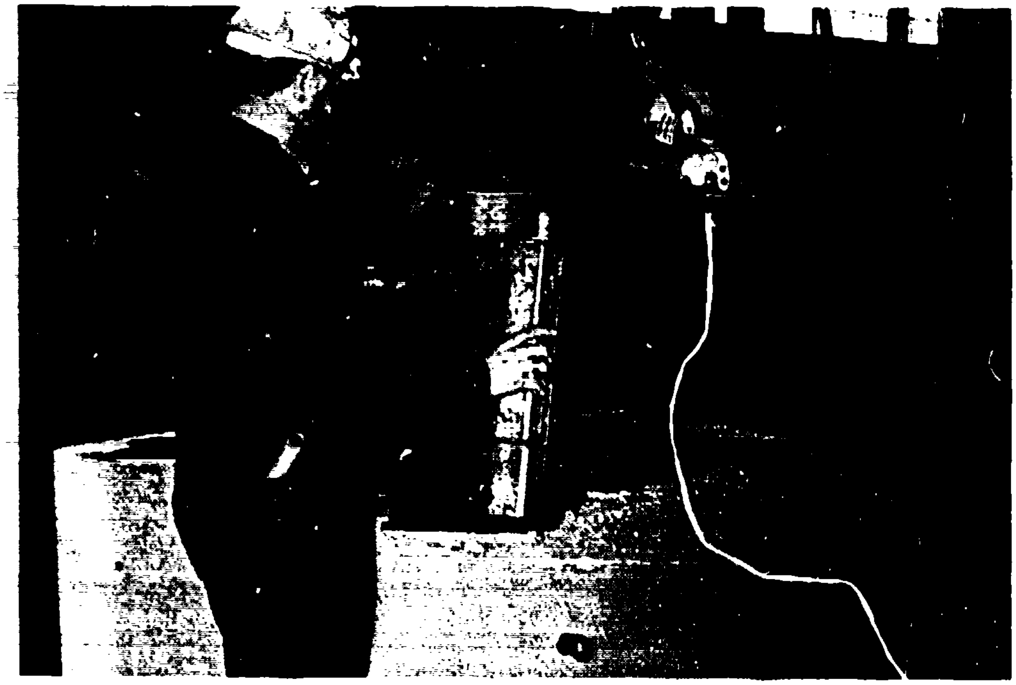

Figure 13. Placement of base section in concrete support structure.

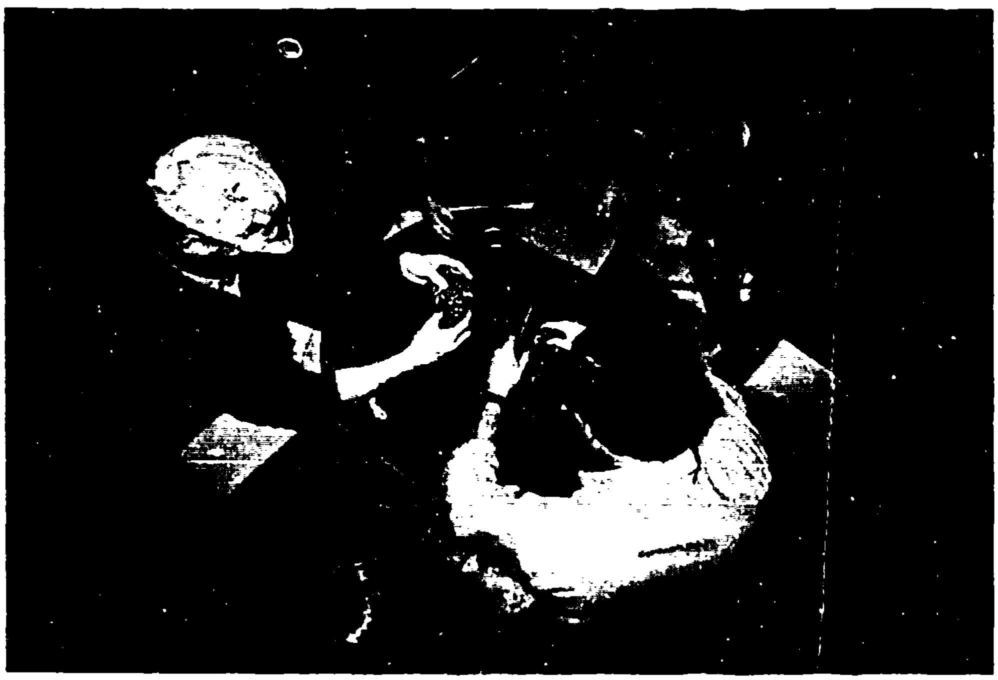

Figure 14. Placing steel fiber into base section.

TABLE 3. SIFCON QUANTITIES

	Model					Closure	Totals
Test series	6	7	8	9	10	10	
Pour number and date	1st-1/19	2nd-2/03	3rd-2/22	4th-3/12	5th-4/02	5th-4/02	
Calculated SIFCON volume, m³ (ft³)	0.331 (11.68)	0.765 (27.02)	0.673 (23.78)	0.673 (23.76)	0.840 (29.65)	0.076 (2.70)	3.358 (118.58)
Steel Fiber							
Weight, kg (lb)	290 (640)	615 (1365)	538 (1186)	554 (1222)	681 (1501)	65 (144)	2743 (6048)
Volume of steel, m³ (ft³)	0.038 (1.31)	0.078 (2.77)	0.069 (2.42)	0.071 (2.49)	0.087 (3.06)	0.008 (0.29)	0.349 (12.34)
Volume occupied, m³ (ft³)	0.331 (11.68)	0.787 (27.81)	0.673 (23.78)	0.673 (23.76)	0.817 (28.86)	0.076 (2.70)	3.358 (118.59)
Steel percent	11.19	9.95	10.18	10.49	10.61	10.92	---
Cumulative percent	11.19	10.31	10.26	10.32	10.40	10.41	10.41
Slurry volumes, m³ (ft³)							
Volume batched	0.391 (13.81)	0.869 (30.68)	0.760 (26.85)	0.880 (31.09)	1.100 (38.25)		4.001 (141.28)
Volume occupied[a]	0.294 (10.37)	0.689 (24.33)	0.605 (21.36)	0.602 (21.26)	0.751 (26.51)	0.068 (2.40)	3.001 (106.23)
Volume samples	0.072 (2.55)	0.095 (3.35)	0.095 (3.35)	0.178 (5.29)	0.230 (8.11)		0.669 (23.64)
Volume left over	0.003 (0.11)	0.023 (0.82)	0.012 (0.44)	0.067 (2.36)	0.036 (1.27)		0.142 (5.00)
Total volume accounted	0.316 (11.15)	0.751 (26.51)	0.653 (23.06)	0.635 (22.44)	0.835 (29.48)		3.190 (112.64)
Volume unaccounted[b]	0.022 (0.78)	0.062 (2.18)	0.048 (1.70)	0.033 (1.17)	0.016 (0.57)		0.181 (6.40)

[a]The volume occupied is based on the actual calculated steel percent.

[b]Volume unaccounted is mainly a result of spillage. However, some of the unaccounted slurry may be considered to be in the model and the samples as a result of the actual dimensions being slightly larger than those used for calculations. As long as Volume Unaccounted was a positive value it was one indication that the model had been completely filled.

the Demonstration Program that a normal concrete mixer would not adequately mix the cement and fly ash because they had a tendency to lump. Therefore an impeller-type grout mixer was used (Fig. 15). This mixer was equipped with rubber-tipped blades that scraped against the walls of the mixer drum with each rotation.

It was eventually discovered that the best mixing sequence involved the following procedure:

1. Pre-weigh all the fly ash and water for a batch using two standard sacks [85.3 kg (188-lb)] of cement. Also, pre-measure the needed superplasticizer.

2. Mix the superplasticizer with water just prior to batching.

3. Place approximately 80 percent of the water into the mixer.

4. Set the mixer paddles in rotation at a moderate speed.

5. Slowly add all fly ash into the mixer, allowing the water to mix well.

6. Slowly add two sacks of cement.

7. Wash off the mixer paddles with the last portion of water.

8. Allow the batch to mix 3 to 5 min or until thoroughly mixed.

After the batch was mixed, the slurry was poured into the base section using buckets. It was learned that it was best to pour the slurry at designated areas, allowing the other areas to remain free of slurry to permit air to escape as the voids around the fibers were filled (Fig. 16). The slurry was poured until the base was filled to the level of the interior floor of the model. All slurry placement was performed under continuous vibration using the same setup as for the fiber installation. (See Table 4 for vibrator locations.) An approximately 25-mm (1-in) thickness of additional fiber was placed along the walls of the base section, in the area where the cylinder walls would be built, and fully worked into the slurry. The purpose of this was to establish a good bond between this pour and the next. At the beginning and end of the slurry placement, several fiber concrete test samples were molded as described under Material Testing Program later in this section.

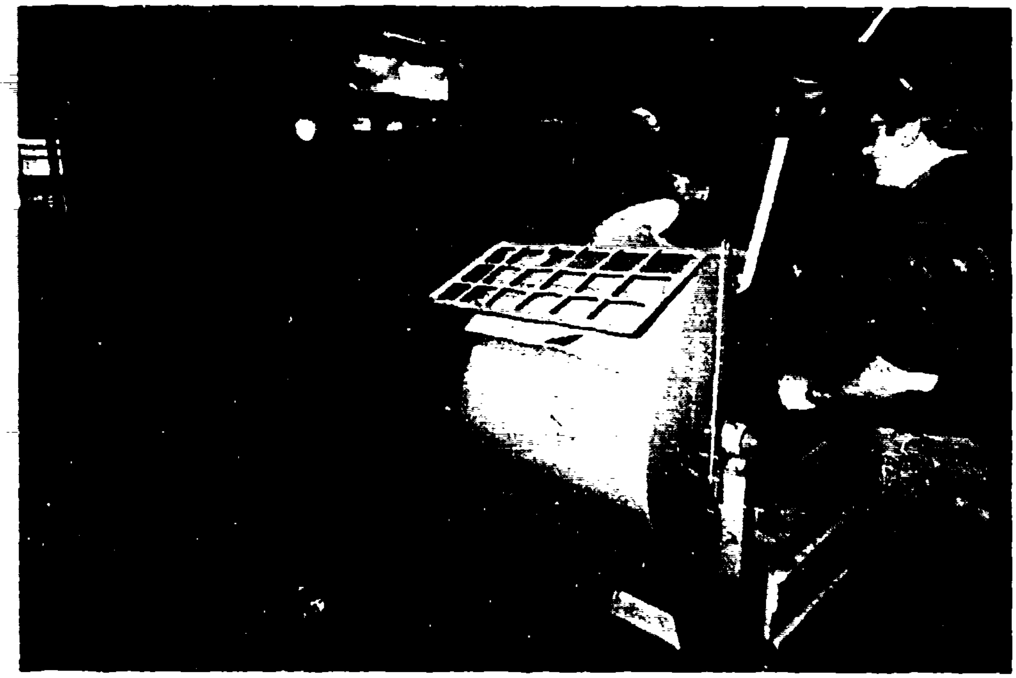

Figure 15. Mixing slurry.

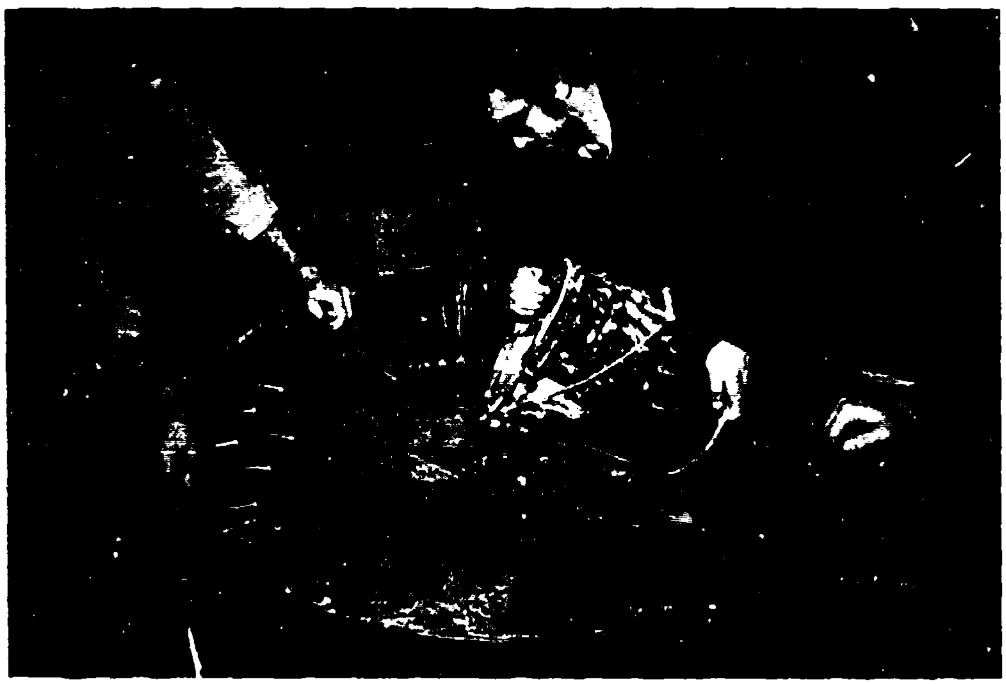

Figure 16. Slurry placement.

TABLE 4. FORM VIBRATOR LOCATIONS

	Outer liner		Inner liner	
Pour No.	Elevation, m (ft)	Azimuth, deg	Elevation, m (ft)	Azimuth, deg
1	6.2 (20.4)	135 and ---	---	---
2	5.3 (17.5)	45 and 225	---	---
3	3.7 (12.3)	135 and 315	---	---
4	2.3 (7.5)	120 and 315	---	---
5	0.8 (2.5)	45 and 225	0.7 (2.2)	135

Second SIFCON placement, first 1.5-m (5-ft) core section--The 305-mm (12-in)-long bottom section of the inner liner was welded to the gusset plates of the base section. The three-sectioned, 4.6-m (15-ft) inner liner section was then welded, using full penetration welds, to this lower liner section. All welds were tested ultrasonically and radiographically before any other work was performed. Any needed repairs were made. Next, the first 1.5-m (5-ft) outer liner section was welded to the base section (Fig. 17). These welds were tested and repaired as the others. The appropriate instrumentation was placed at the locations noted in Reference 5. Steel fibers were placed under vibration after the manner described earlier (Fig. 18). The fiber volume for this section was calculated to be 9.95 percent. Fiber was placed to within 50 mm (2 in) of the top of the outer liner. As determined in the Demonstration Program, small depressions about 100 mm (4 in) deep in the top surface of the fiber were formed at four locations 90 deg apart. These were formed for the purpose of permitting the slurry level to be visually observed as it reached the bottom of the depressions (Fig. 19).

On February 3, 1984, the slurry was mixed and placed as described earlier. The slurry was placed at the four points between the depressions in the surface of the fiber as noted in Figure 19. The weep holes in the outer liner provided a visual indication of slurry levels at various stages of the pour. They gave assurance that the slurry was fully penetrating to the bottom of the lift. Slurry placement continued until it reached the level of the bottom of the 100-mm (4-in) depressions. At the end of the slurry placement several test samples were molded as before.

Figure 17. Placement of first 1.5-m (5-ft) outer section.

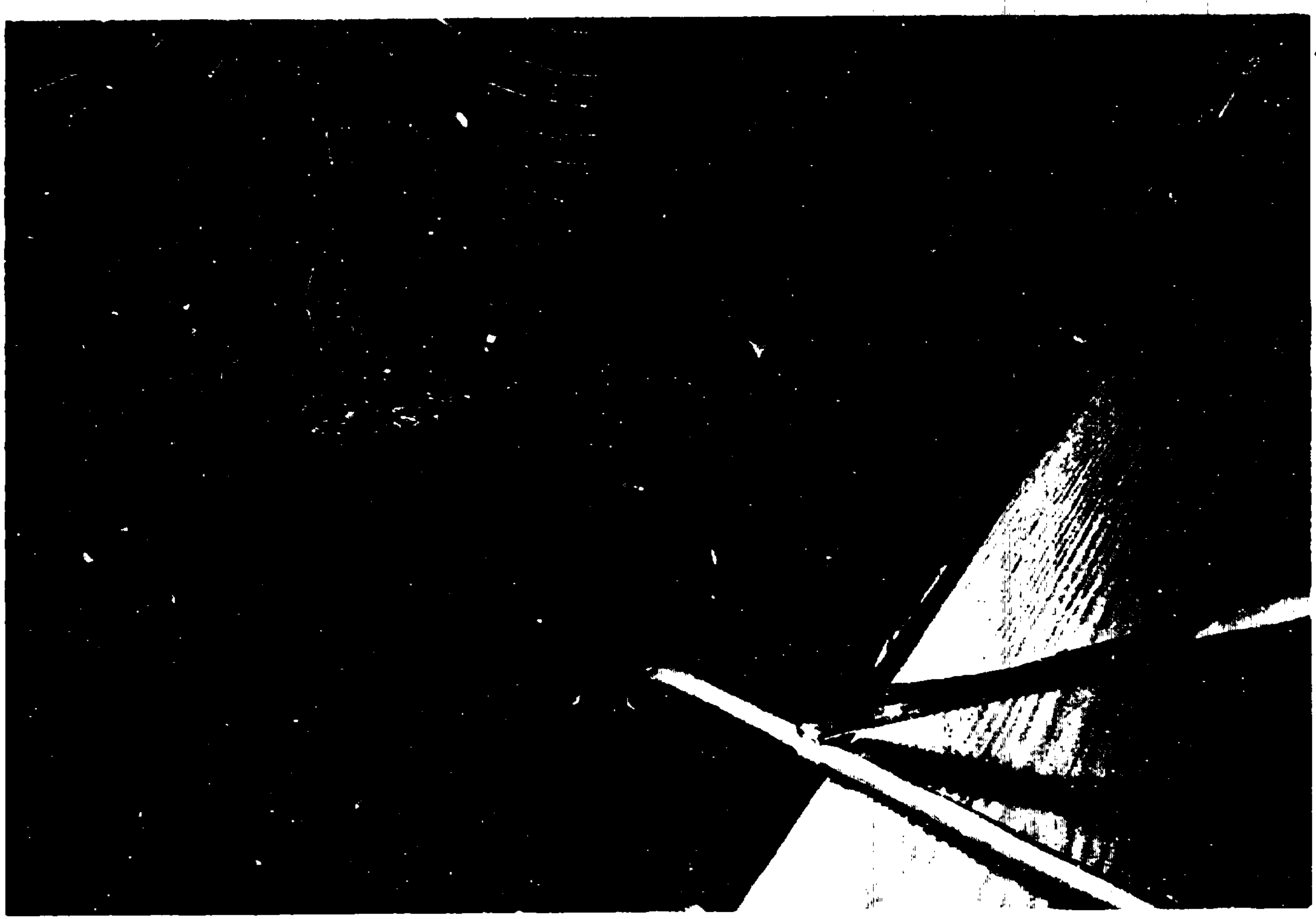

Figure 18. Completion of fiber placement of second SIFCON pour.

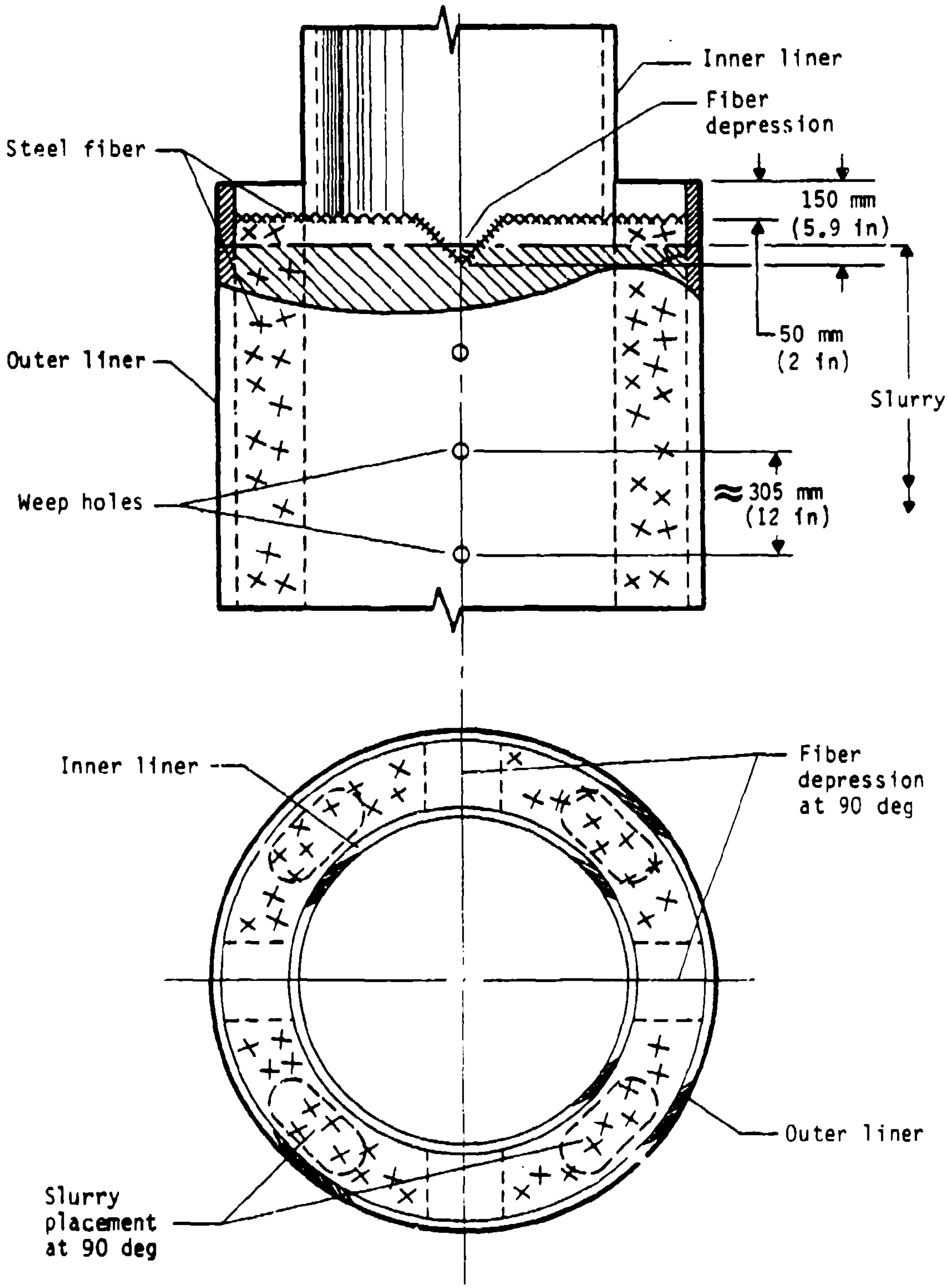

Figure 19. Fiber and slurry placement.

Third SIFCON placement, second 1.5-m (5-ft) cylinder section--While trying to fit the second 1.5-m (5-ft) outer liner section to the first 1.5-m (5-ft) outer liner section, it was discovered that the inner liner was slightly out of alignment. If left unchanged it would have created a minor misalignment at the top. The inner liner was then cut and refitted to correct the situation. After fitting and rewelding the liner together, the welds were tested as before. The second 1.5-m (5-ft) outer liner section was then welded to the first 1.5-m (5-ft) liner section using the same procedures as before. These welds were also tested and repaired the same as before. A hole was cut through both liners to fit a section of 102-mm (4-in)-diameter, Schedule 160 pipe that would serve to access power to the internal high-speed diagnostic camera. The 102-mm (4-in) pipe was then welded to both liners, establishing a watertight seal. The appropriate instrumentation was installed on and between the liners. Fibers and slurry were placed on February 22, 1984, using the same procedures described for the second SIFCON placement. The only difference was the use of wire window screens to filter out the lumps in the slurry as it was being poured (Fig. 20). At the end of the slurry placement, several test samples were molded as before.

Fourth SIFCON placement, third 1.5-m (5-ft) cylinder section--The inner liner headworks was first fitted and welded to the top of the inner liner. These welds also were tested and repaired in the same manner as the other welds. Next, the third 1.5-m (5-ft) outer liner section was welded to the second section, and then tested and repaired as before. A hole was cut through both liners to fit a 127-mm (5-in)-diameter, Schedule 160 pipe that would serve as an instrumentation cable egress port. The 127-mm (5-in) pipe was welded to both liners in the same manner as the 102-mm (4-in) pipe of the second 1.5-m (5-ft) section. Finally, the required instrumentation was installed. On March 12, 1984, fibers and slurry were placed using the same procedures as before. Throughout the duration of the slurry placement, several test samples were molded as before.

Final SIFCON placment, headworks and closure--All the gusset plates were fitted and tack-welded to the inner liner headworks. Before welding of the plates, the outer liner was set and fitted to ensure a proper fit and then removed. All welds were performed, tested, and repaired as before. Following

Figure 20. Slurry placement of silo walls.

the welding, the final instrumentation was installed. Then the final 1.5-m (5-ft) outer liner section was fitted and welded to the third section using the same procedure as before.

On April 2, 1984, fibers were placed in the headworks and closure (Fig. 21) using the same procedures as before. After completion of fiber placement it was discovered that there was a substantial settlement of fibers under the horizontal bearing plate supporting the closure in the headworks. There was concern that even further settlement would take place when the slurry was placed and vibrated, leaving localized areas with no fiber. A decision was made to remove approximately 230 mm (9 in) of the fiber down to the level of the bearing plate. Next, slurry was placed to 50 mm (2 in) below the level of the fiber; this was immediately followed by replacing the removed fiber and completing the placement of the slurry. The closure was also filled with fiber and slurry using the same procedures as for the model. Throughout the duration of the slurry placement, several test samples were molded.

INSTRUMENTATION

Introduction--The following paragraphs describe the instrumentation procedures used to implement gage requirements for the ISST model. A complete list of these requirements along with a measurement list is provided in Appendix A.

Several new techniques, designed by NMERI personnel, were incorporated in the instrumentation of the model. One involved the modification of a 16-mm (0.6-in)-diam by 38-mm (1.5-in) bolt to provide for direct mounting of an accelerometer making a radial measurement, or attaching an accelerometer mounting block for making vertical acceleration measurements. The purpose of this mount* was to provide isolation of the gage from the inner liner. Details of this mount are listed later in this section under Accelerometers.

* Designed by Bruce Schneider and Jon Kirst of NMERI.

Figure 21. Completion of fiber placement in closure.

Another new technique was the modification of the Waterways Experimental Station (WES) cable exit.* In the past there have been problems with the ability of cables exiting a structure in high-pressure HEST environments to survive long enough to provide sufficient data. The original WES design allowed for protection of cables exiting the structure just at the structure-soil interface. The new design extends the use of the WES protection concept into the test-bed. The modification is designed to allow the cable to undergo a large amount of vertical and lateral displacement, while still being protected by a casing of heavy steel pipe. Details of this cable protection scheme are given later in this section.

A final new technique being employed by NMERI involved the mounting of the camera used to provide high-speed motion picture documentation inside the model during the test. The method developed** was designed to allow the camera to free-fall inside the model after the explosives have been detonated. Since very little lateral movement of the model was expected, this technique was designed to protect the camera from being bounced around inside the model, as has been the experience on some previous tests. The details are given later in this section under Photo Documentation.

Strain gage instrumentation--The appropriate gages were procured upon receipt of initial strain gage requirements in November 1983.

SIFCON strain--Micromeasurements strain gages, type EA-06-500350, were used to measure strain in the SIFCON material of the test structure during loading. Manufacturer's specifications indicate that overall length could change by 5 percent without gage failure. This gage is a one-fourth bridge, 350- device with a gage factor of 2.05, mounted on a length of No. 2 deformed steel reinforcing bar. The bar was fabricated with hooks on each end to provide proper anchorage in the SIFCON.

---

* By Bruce Schneider, Jon Kirst, and Steve Pickett of NMERI.

** By Steve Pickett and Manuel Davila of NMERI.

Preparation--Each piece of rebar was formed as shown in Figure 22. The center of the rebar on both sides was cleaned and sanded to provide a flat surface for the strain gage. Epoxy (EPY 150) was applied to these surfaces and strain gages placed in the epoxy so that the longitudinal axis of each gage was parallel to the longitudinal axis of the rebar. The gages were mounted directly opposite (180 deg) each other and held in place by tape while the epoxy cured. Wires were then soldered to the strain gages. The wires attached to the strain gage were fastened to the rebar in such a fashion as to provide a strain relief, reducing the possibility of their breaking during the loading of the structure. The entire gage, including wire connections, was covered with a waterproofing compound.

Installation--The rebar was placed between the steel liners of the model at the appropriate location as specified by the measurement list (Appendix A) before the fibers were placed and the slurry was poured. Gage electrical wires were run into the model through the inner liner via a small hole.

Quality control--The resistance of each rebar gage was measured prior to the placing of the fiber slurry. The acceptable gage resistance was 350 Ω ± 1 percent. This value was also rechecked after the SIFCON was cured. All SIFCON strain gages were found to be in working order upon completion of the construction of the model.

Steel liner strain--Initially, Micromeasurements strain gages, type CEA-06-125UM-350, were planned for liner strain measurements. These gages were epoxied to the liner, using standard procedures. They were, however, used for only two measurements, numbers 3025 and 3024. After placement of these first gages, additional welding work on the liner was required. Upon completion of this work, the gages were rechecked, and the strain gage used for measurement number 3024 was found to be defective. To prevent this problem from reoccurring, the use of the Ailtech SG159-11-10-6 weldable strain gage, which had a greater tolerance of high temperatures, was investigated as a replacement for the epoxy gages.

Engineers from both Micromeasurements and Ailtech were contacted. Neither would confirm performance of their respective gage past their published specifications. Micromeasurements stated that their gages were capable

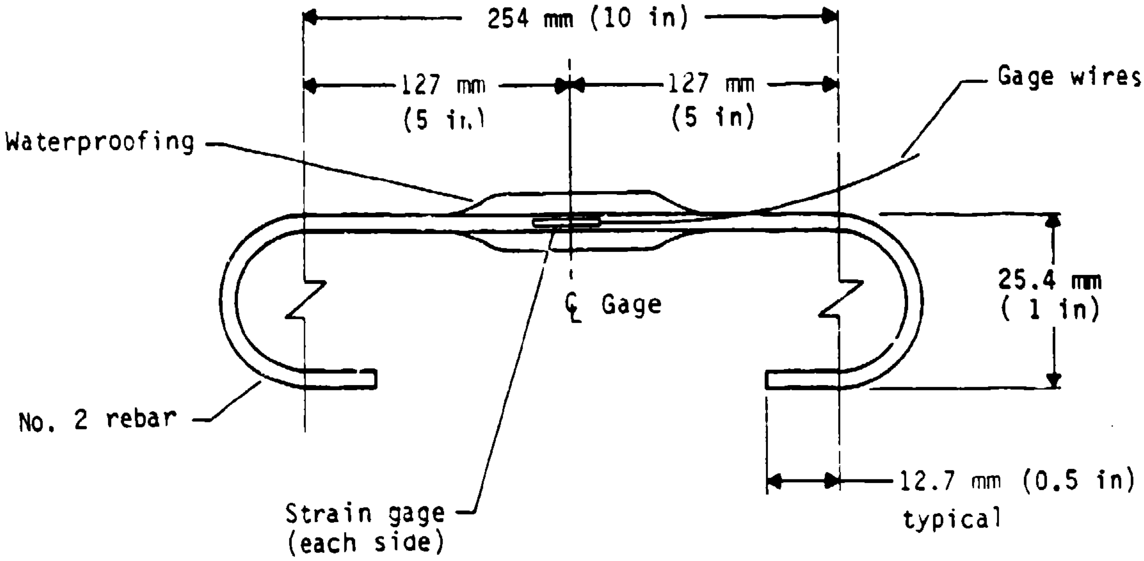

Figure 22. SIFCON strain transducer.

of measuring 50,000 με with a gage factor of 2.05 ± 5 percent. Ailtech strain gages were capable of measuring 20,000 με with a gage factor of 2.0 ± 3 percent. Both were one-fourth bridge, 350-Ω gages. Even though the manufacturer's specifications indicated that the Ailtech gage did not have as large a range as the Micromeasurements gage, a study sponsored by the Defense Nuclear Agency (DNA) at NMERI indicated that the Ailtech gage had an equal or better range than the Micromeasurements gage (Ref. 8). On the basis of this information, the Ailtech weldable strain gages were used at locations specified by measurement numbers 3001 through 3023.

Installation--When the exact locations of the strain gages on the liner were determined, the liner was sanded to ensure a good bond. The Ailtech gages were then spot welded to the liner. The gage wires were then secured to the steel liner in such a manner as to provide strain relief. The entire gage, including the wire connections, was finally covered with a waterproofing compound.

8. Gay, H., Static and Dynamic Performance Comparison Tests on Foil and Weldable Strain Gages, AFWL-TR-81-37, Air Force Weapons Laboratory, Kirtland Air Force Base, New Mexico, July 1981.

Quality control--The resistance of the gages was measured and recorded after the gages had been placed. The acceptable gage resistance was 3.50 Ω ± 1. The resistance between gage and liner was also measured. Acceptable resistance was greater than 10 MΩ. Liner gages that contacted concrete were rechecked when the SIFCON had cured. All the gages were found acceptable and in working order upon completion of the model.

Accelerometer gages--On the basis of preliminary predictions, NMERI procured the required 2K Endevco 2264A accelerometers. In February 1984 a set of updated predictions indicated that the range of these gages was insufficient for the test requirements. NMERI was able to procure the necessary gages from stock, averting any delays that might have been caused by ordering new gages at that time. Nine Endevco model 2264A and one Endevco model 7270 (AFWL experimental gage) accelerometers were used. Locations of these gages, ranges, and predicted levels of acceleration are indicated in the measurement list in Appendix A. The accelerometers were calibrated using NMERI's calibration facilities; All AFWL experimental gages were calibrated by AFWL.

To provide for installation of accelerometers located at the inner liner, a special 16-mm (0.625-in)-diameter by 32-mm (1.25-in) bolt was threaded through a 38-mm (1.5-in) hole in the inner liner into a recessed concrete insert so that the top of the head of the bolt was flush with the inner surface of the liner. The head of the bolt was machined and tapped to accommodate either an Endevco model 2254A- or model 2260A-type accelerometer. Details of this mount are shown in Reference 5. For measurement numbers 1601 and 1702 on the measurement list, a special epoxy mounting block was located at the inner liner at the location specified. Two Endevco 2264A accelerometers were attached to the mount and the wires run into the model through a hole in the inner liner.

To mount the accelerometer specified for the floor of the structure, the hub formed by the union of the gusset plates was drilled and tapped to receive the accelerometer.

The bottom plate of the closure lid was also drilled and tapped at the appropriate location specified by the measurement list to provide mounting capabilities.

Experimental gages--AFWL specified the following gages be used for experimental measurements:

- 2 NMERI normal stress (NS) gages
- 1 NMERI structure-media interaction (SMI) gage
- 1 Endevco 2264A accelerometer with a special "soft" mounting system
- 1 Endevco 7270 accelerometer (a new type of high-range accelerometer) with a special "hard" mounting system
- 2 Internally strain-gaged (ISG) transducers

Except for the two ISG transducers, these gages were supplied by AFWL and installed by NMERI personnel. The NS and SMI gages were calibrated by NMERI. The two internally strain gaged (ISG) transducers (one a one-fourth bridge and the other a full bridge device) were supplied and installed by AFWL. These gages were calibrated by NMERI.

Gage mount installation--Mounting hardware for the two NS gages and the SMI gage was supplied and installed by NMERI at the locations specified on the measurement list (Appendix A). The special "soft" and "hard" mounts were supplied by AFWL and installed in the model by NMERI.

Relative displacement (passive)--Two scratch gages were mounted to the sides of the liner at locations specified by the measurement list. These gages had position indicators which were physically measured before and after loading. Since these gages are strictly mechanical, no electrical accommodations were necessary for them.

Final gage installation--When the completed model was delivered to NMERI, the remaining accelerometers, inner liner strain gages, and the AFWL experimental gages were installed.

For the measurement of radial acceleration, the accelerometer was mounted directly to the special bolt head noted earlier at the appropriate location. To measure vertical acceleration, a mounting block was first bolted to the special bolt head at the location specified by the measurement list. The accelerometer was then attached to the block with the proper orientation.

The NS and SMI gages were installed so that they were flush with the top edge of their fixtures. The SMI gage was also installed into its mount, using a torque of 339 N • m. The AFWL experimental accelerometers were installed on their appropriate mounts.

Belden No. 8723 4-conductor cable [approximately 37 m (120 ft) in length] was spliced to each gage pigtail inside the model, using a color-to-color wiring scheme as noted in Appendix A. In the case of the ISG gage, the clear lead from the gages was spliced to the white lead from the Belden cable. All cables were marked with the measurement numbers, bundled, foam-wrapped, and fed through the cable exit in the wall of the structure.

Prior to shipment to the test site, all connections were checked. At this time it was determined that the SMI gage had become defective and it was replaced. All other gages (with the exception of measurement 3024, as noted previously) were noted to be in working order.

Cable--The following paragraphs outline the cable requirements, splicing techniques, and routing requirements necessary to achieve the acquisition of data as specified by the measurement plan. Also included is information concerning cable trenching, wiring, and the cable exit. Cable from the van to the junction box was supplied by AFWL. NMERI supplied and installed all cable from the junction box to the model.

Cable requirements--The following cable types were used:

Concrete strain: Belden No. 8723 (4-conductor)

Steel liner, floor, and lid strain: Belden No. 8723 (4-conductor)

Accelerometers (including experimental): Belden No. 8723 (4 conductor)

Trunkline cable: 20-pair cable

Experimental gages: specifications by AFWL

NS, SMI gages: Belden No. 8723 (4-conductor)

Cable splicing--Twenty-pair cable was spliced where necessary using crimp tools, sealing compound, and plastic tape. The drain wire was also spliced. A tape shield was used when necessary. Splices were avoided in the test-bed surrounding the structure by providing continuous cable runs from the perimeter of the test-bed to the inside of the structure.

Cable routing--The cables for structure measurements were tied together in bundles to minimize cable motion. The cable bundles were secured to eyebolts or welded brackets attached to the inner liner of the structure, routed through the structure, and out the cable exit of the structure. The power cable for the internal camera was kept separate from the other cables both in the structure and also in the cable trenches.

Cable exit--A modified version of the WES cable exit was used as requested by AFWL. As shown in Figure 23, a short section of 127-mm (5-in)-diam, Schedule 160 steel pipe was inserted in the wall of the structure. Next, a section of 76-mm (3-in)-diam, Schedule 160 pipe with a steel flange, as shown in Figure 23, was slipped through the 127-mm (5-in) pipe sleeve in the structure. The instrumentation cable was then pulled through the 76-mm (3-in) pipe and into the cable trench.

In the trench, and in the cable exit, the bundled cable was wrapped with 13-mm (0.5-in)-thick foam and placed inside 1.5-m (5-ft) sections of 76-mm (3-in)-diam, Schedule 160 pipe. The 76.2-mm-diam pipe sections were then connected together with pipe sleeves made from 127-mm (5-in)-diam, Schedule 160 pipe, as shown in Figure 24. This system was designed to allow for considerable horizontal and vertical movement without the pipe segments separating to expose the cable.

Cable protection--Trenches were constructed by the test site contractor between the structure and the perimeter of the test-bed, and then backfilled after all the cables had been laid, hooked up, and protected. The trenching scheme is given in Figure 25.

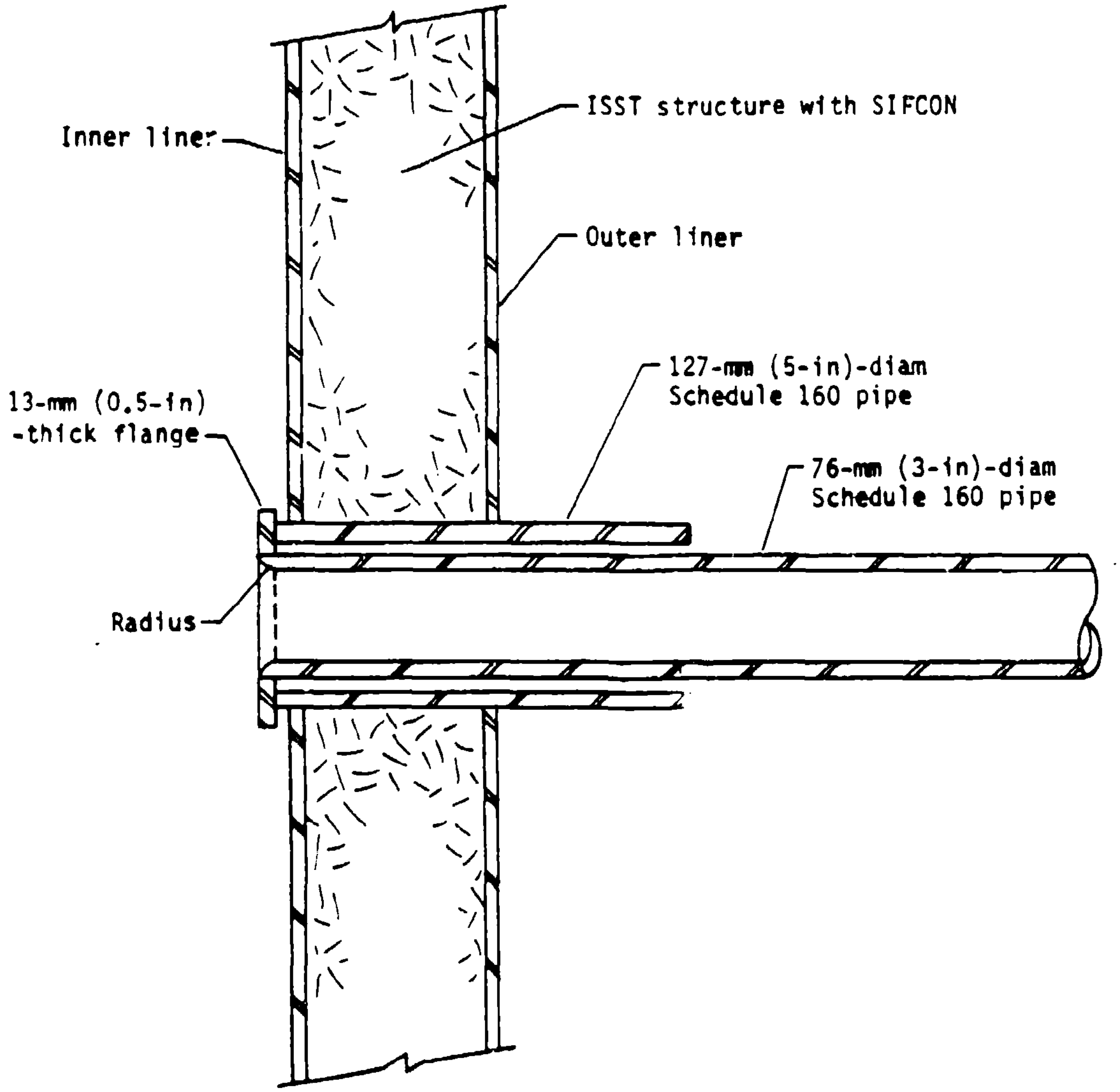

Figure 23. Cable exit detail.

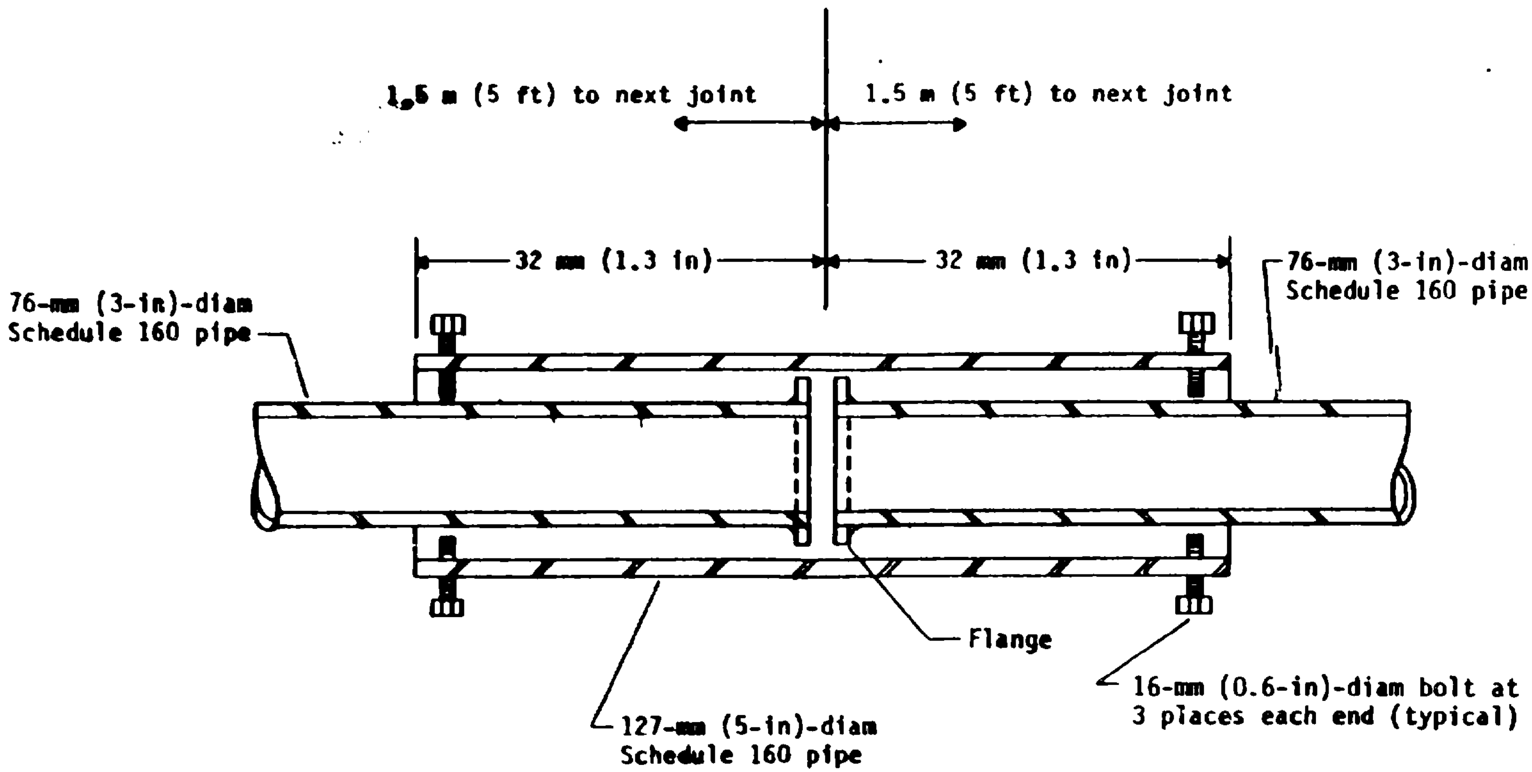

Figure 24. Slip joint detail.

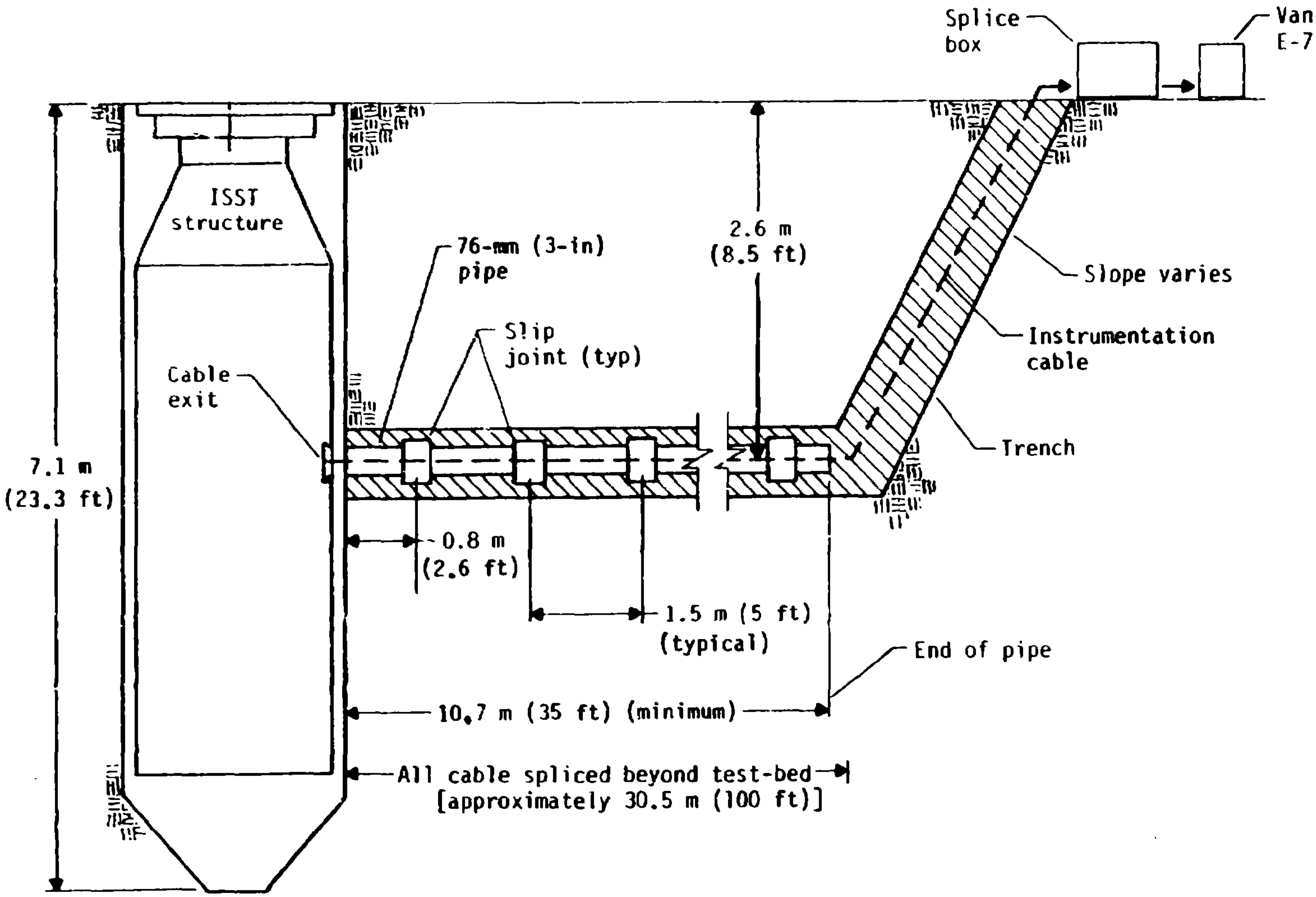

Figure 25. Cable routing.

Cable wiring--The following describes cable interconnection for the different types of transducers used on this test.

Concrete strain--A 1.8-m (6-ft) pigtail of Belden No. 1121 cable was connected to each individual strain gage (Appendix A). Both pigtails from each strain gage on the piece of rebar were spliced to the 4-conductor (Belden No. 8723) cable and the gages configured into a bridge at the junction box (Appendix A).

Steel liner, floor, and lid strain--Steel liner strain gages also had a 1.8-m (6-ft) pigtail of Belden No. 1121 cable (Appendix A). These cables were also spliced to Belden No. 8723 (4-conductor) cable in the structure and configured into a bridge at the splice bunker (Appendix A).

Accelerometers--Accelerometers were bridge-configured internally and had a 0.30- to 1.2-m (1- to 4-ft) pigtail supplied by the manufacturer. Belden No. 8723 4-conductor cable was spliced to the pigtail in the structure (Appendix A.)

Experimental gages--Belden No. 8723 (4-conductor) cable was spliced to the pigtails of the experimental gages. All experimental gages were full-bridge devices (except the one-fourth bridge ISG gage, measurement No. E004, and the vertical SMI, measurement No. E006A, which was a one-half bridge device) (Appendix A). The cabling was the same as that of accelerometers.

Quality control--After the model had been delivered to Yuma and installed in the test-bed, all gages were checked and, except as previously noted, all appeared to be functioning.

Photo documentation--

Construction documentation--Throughout the construction of the ISST model, NMERI took photographs documenting the work. Both 125- by 180-mm (5- by 7-in) black and white prints and 35-mm colored slides were taken. In addition, videotape was also provided covering the major activities of the construction such as liner installation, fiber and slurry placement, gage installation, and so on.

Structural response documentation--To document the response of the structure during the test, NMERI installed a Hycam II high-speed camera (model number 41-0064) inside the model.

The camera was enclosed in a steel box with a clear Lexan viewing port. The box was located in the model as shown in Figure 26 to provide a view of the closure and headworks area down to a point about 1.0 m (3.25 ft) from the top of the structure. A cardboard mockup of the inside of the model was used to determine the exact location of the camera for obtaining the proper view and lighting requirements.

Lighting inside the structure was provided using Sylvania FF-33 Flood Flash bulbs. The bulbs were mounted on a plywood ring above the camera. The ring was positioned in relation to the camera and the headworks to minimize obstructions of the critical viewing area. The exact location of the ring was determined using the cardboard mockup.

To reference the photography to the detonation of the charge, a time-zero bulb was incorporated into the field of view. For dimensional reference, an orthogonal grid of black stripes on a white background was painted on the underside of the closure. In addition, black circumferential stripes on a white background were painted throughout the viewing area.

The power cable for the camera entered through a port in the wall of the structure similar to the one used for the cable exit. The location of this port was selected to minimize the effects of the a.c. power on the gage signals. In addition, the power cable was shielded in a flexible conduit and installed in a steel pipe protection system.

The camera and light ring were installed as shown in Figure 26. The system was designed so that during the test, as the structure is accelerated downward, the camera would free-fall at 1 g. As the camera falls it would strike the Styrofoam disk, breaking it. The camera would then continue to fall into the net.

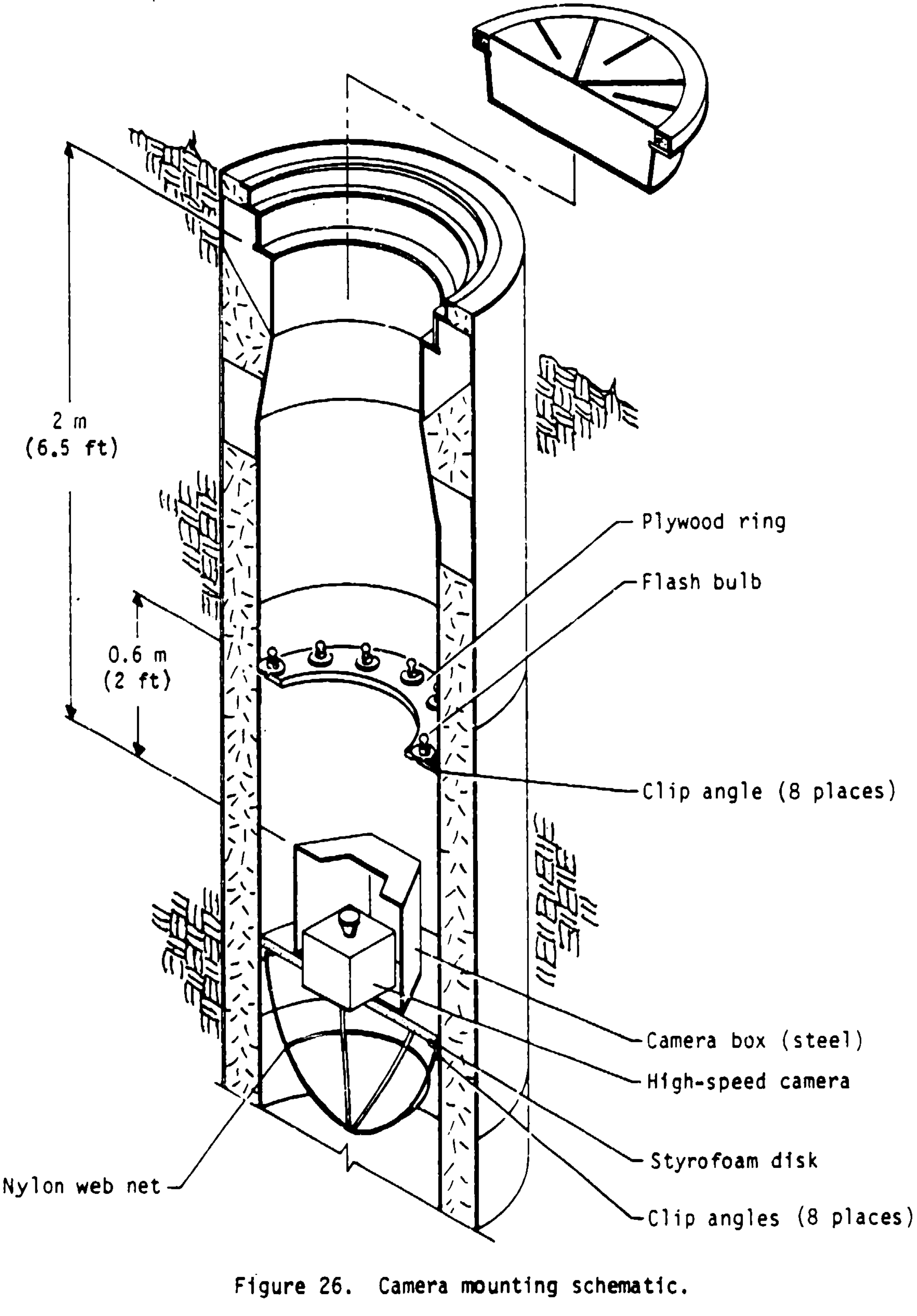

Figure 26. Camera mounting schematic.

FIELD OPERATIONS

Field construction--

Preparations for shipment of model to Yuma, Arizona--The following preparations were made at NMERI prior to shipment of the model to the test-bed near Yuma, Arizona. The closure was set, aligned in the headworks, and bolted in place. A short wire-rope sling was attached to the lifting device on the closure and hooked to an overhead crane. The model was slowly lifted in the vertical position over its support structure. Next, the model was moved and laid on its side on wood cribbing by first setting the bottom on a styrofoam cushion and then lowering the structure to a horizontal position (Fig. 27). Using a platform scale, the weight of the model was measured at 11,090 kg (24,450 lb). Next, the model was lifted in a horizontal position and set on the flatbed trailer that would be used to transport it to the test-bed (Fig. 28).

While on the trailer, the remaining gages and transducers on the inner liner were installed and all gages were hooked up to instrumentation cable. The cables were then marked, bundled, and prepared for shipment as described previously under Instrumentation. Next, all camera and light ring support mounts were welded in place. Finally, the exterior was painted with a prime coat of dark blue while the bottom of the closure and the headworks inner liner walls were painted white with black stripes for photographic reference (Ref. 5). Finally, the closure was reattached and the model was transported to the testbed on April 23, 1984.

Field placement--At the test site the model was first lifted horizontally, removed from the trailer, and set on wood cribbing using a hydraulic crane (Fig. 29). The short wire rope sling noted earlier was then connected to the lifting eye on the closure and to the crane. The model was next lifted to a vertical position while the conical base rested on the ground. It was then moved and lowered into a 1.4-m (4.5-ft)-diam by 7-m (23-ft)-deep hole that had been previously drilled at the center of the test-bed (Fig. 30). The model was lowered to the bottom of the drilled shaft, compacting some loose sand present at the bottom of the hole. It was then raised approximately 1.02 mm (4 in) and held at that elevation by the crane. A low-strength grout

Figure 27. Setting silo in horizontal position.

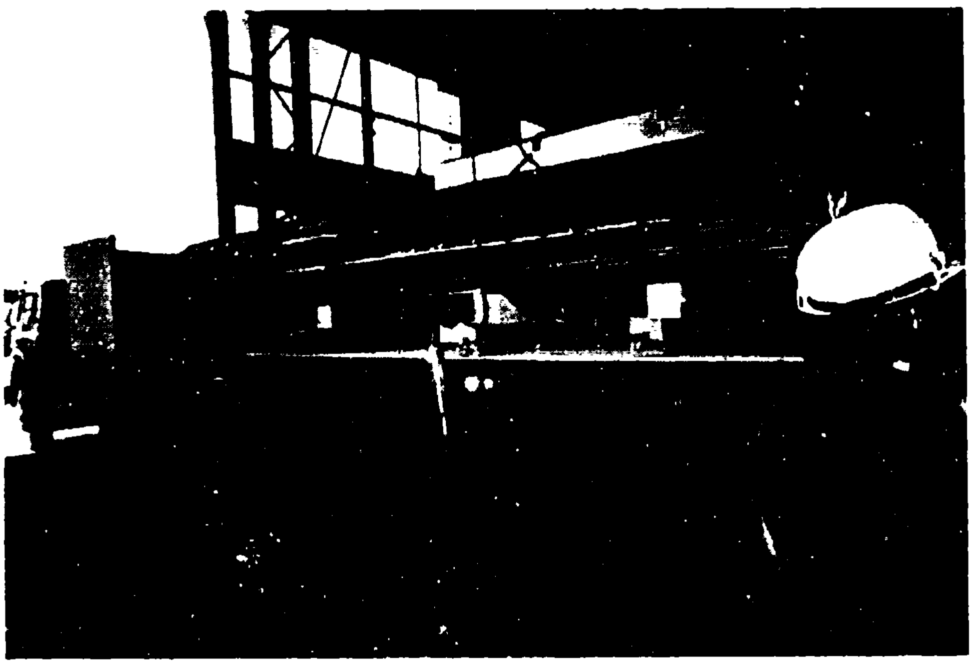

Figure 28. Shipment of silo.

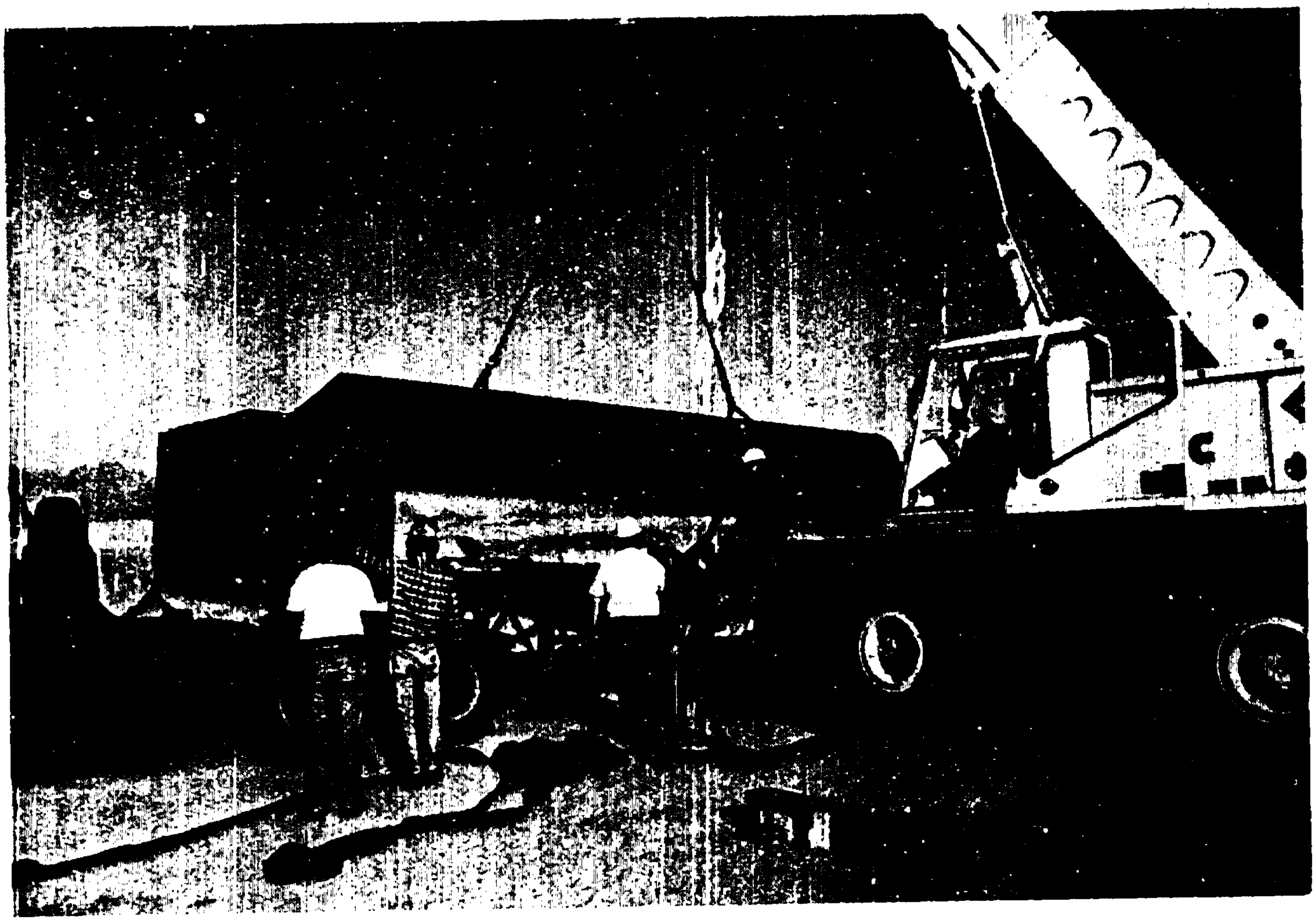

Figure 29. Field placement of silo.

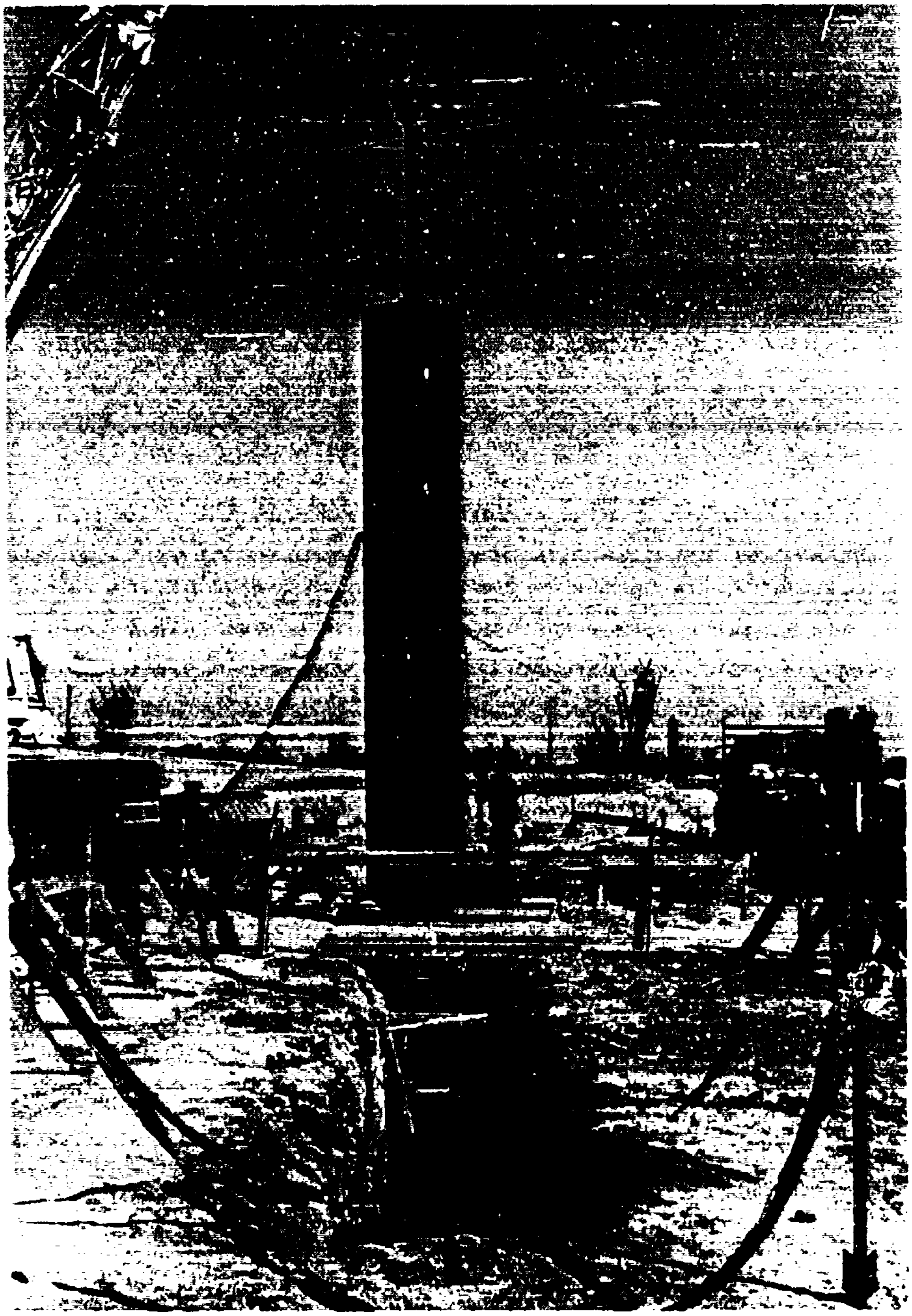

Figure 30. Placement of silo in excavation.

composed of masonry sand, cement, barite, Aqua Gel, and water was mixed on site (Table 5). The grout was poured into the drilled shaft using two 76-mm (3-in)-diameter pipes (Fig. 31). Grout was placed up to a level 585 mm (23 in) above the lowest point on the base of the model. The crane held the model in place for 24 hours, allowing the grout to set up thoroughly. After the grout had set up, a dry sand was rained into the drilled shaft around the sides of the model up to a level approximately 3 m (9.8 ft) from the bottom of the model. This elevation was the level of the existing instrumentation cable trenches (Fig. 32).

Steel cable protection sleeves were installed according to the engineering drawings (Ref. 5). Next, the instrumentation cable trenches were backfilled and compacted. All model instrumentation was spliced and hooked up to the junction box and to the instrumentation van. The camera was installed in the model and the camera wiring hooked up. The lead seal was fitted onto the bearing plate of the model and the closure bolted in place. The lifting eye was cut off and ground flush, completing field placement.

TABLE 5. MIX DESIGN FOR YUMA BACKFILL GROUT

Ingredient	Weight
Masonry sand	28.26 kg (62.3 lb)
Portland cement	5.58 kg (12.3 lb)
Barite	8.30 kg (18.3 lb)
Aqua Gel	1.95 kg (4.3 lb)
Water	12.84 kg (28.3 lb)
Density	2010.32 kg/m^3 (124.14 lb/ft^3)
Yield	0.028 m^3 (1 ft^3)

Figure 31. Grouting bottom of silo.

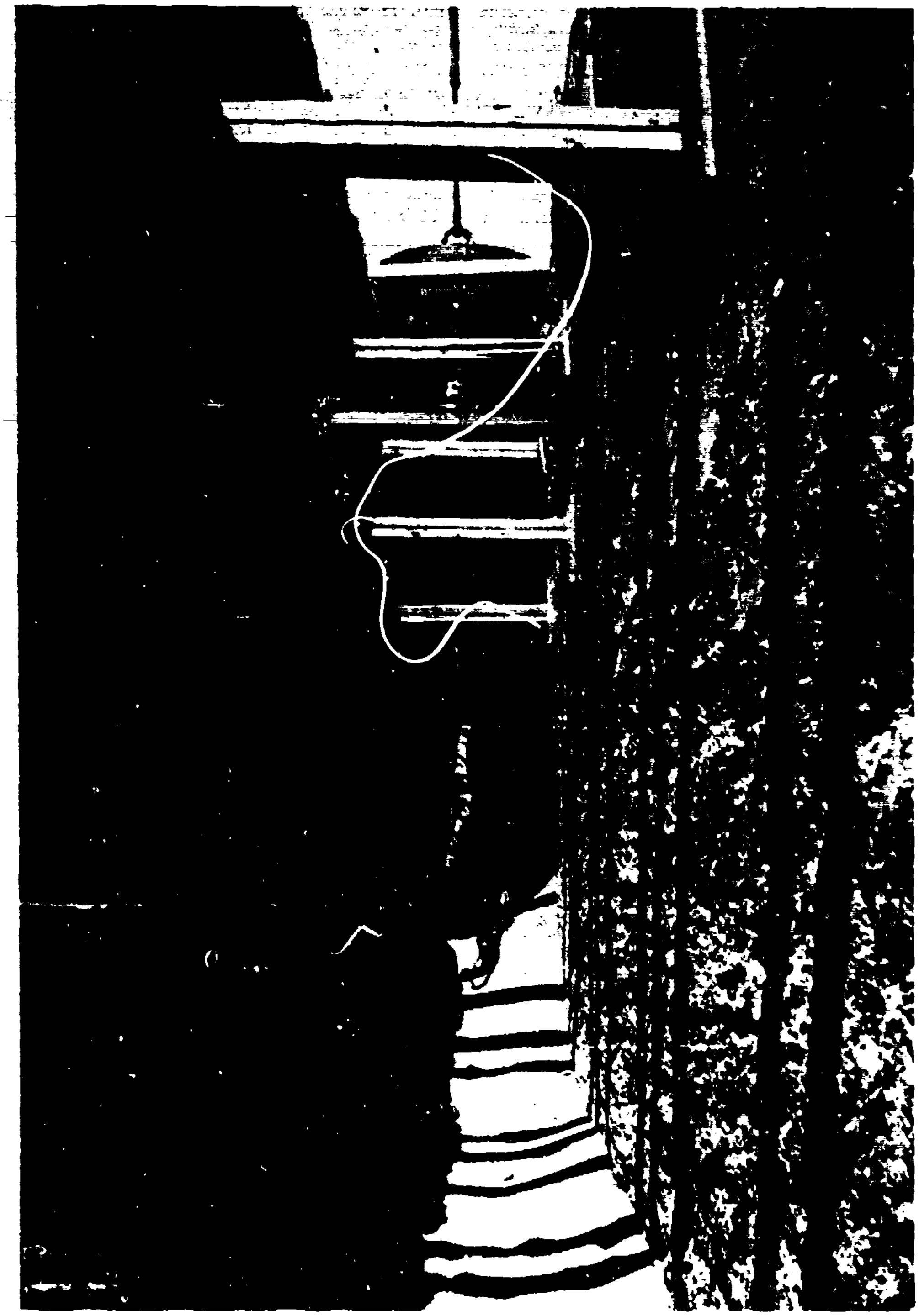

Figure 32. Instrumentation trenches for silo.

MATERIAL TESTING PROGRAM

SIFCON--With SIFCON being such a new and relatively untested material, very little data were available on which to establish a testing program. As a result, the program "grew up" as the construction of the model progressed and test data became available.

The program began, patterned after a conventional concrete quality control program, with the preparation of six 102-mm (4-in)-diam by 203-mm (8-in)-long compressive test specimens of SIFCON, molded in standard plastic cylindrical molds. In addition, six 102- by 102- by 457-mm (4- by 4- by 18-in) flexural test specimens of SIFCON were made in single-use wood molds. The 102-mm (4-in)-diam specimens were chosen over the standard 152-mm- (6-in)-diam specimens because the maximum capacity of the testing machine at NMERI is only 136,078 kg (300,000 lb). With the expected strength of the SIFCON in excess of 82.7 MPa (12,000 lb/in^2), a 152-mm (6-in) specimen would require a machine with a capacity of at least 154,221 kg (340,000 lb). The 102- by 102-mm (4- by 4-in) beam size was selected as an economy effort to minimize the use of steel fiber, since it was quite expensive. Wood forms were selected because steel forms of this size were not available.

The SIFCON samples were fabricated by raining the fibers into the mold or form using the same techniques as for the model. This was followed by pouring the slurry into the forms. Care was taken not to cover the top surface of the fiber mass with slurry to prevent air from being trapped inside the specimen. Both the placing of the steel fibers and the pouring of the slurry into the molds was done with vibration on a shake-table. The samples were then moved to an area near the model, covered with plastic sheeting, and allowed to cure for 24 hours. The next day the molds of those specimens to be cured under standard conditions were removed and the samples transferred to the wet room. The remaining samples were left undisturbed in their molds until testing.

The initial plan was to cure the test samples in a wet room environment; however, NMERI was directed by AFWL to cure the samples at ambient conditions near the model. Later in the program it was decided to increase the number of specimens and cure half in a wet room environment and half in ambient conditions.

Early in the program, data became available which tended to indicate that specimens cored from a slab yielded generally higher and more consistent results than from 102-mm (4-in)-diam molded specimens of the same mix. As a result, a 305- by 305-mm by 102-mm (12- by 12- by 4-in)-thick slab of SIFCON was prepared for each lift. From this slab nine 51-mm (2-in)-diam cores were cut as shown in Figure 33. These cores were tested in axial compressions.

Also, early in the program, it was determined that the SIFCON apparently possessed different strengths, depending on the direction of the applied load versus the direction the fibers were placed in the form. Based on these data it was decided to prepare a set of flexural test specimens by forming and placing the SIFCON as a vertical column but testing it in a standard horizontal flexural mode.

When the model was about 60 percent complete, with two more lifts to construct, AFWL requested a test specimen be constructed to model the wall section of the structure. It was as tall as the depth of a lift in the model. A form for such a specimen was fabricated as shown in Figure 34.

The plan was to prepare a slab of SIFCON from which cored samples would be taken throughout its height and tested. The purpose was to determine if a variation in strength existed through the height of the wall as a result o ambient curing conditions.

To simulate the correct fiber orientation in the cored sample, as compared to the actual wall of the model, the fiber was placed with the form in a horizontal position. The steel plate was then bolted in place, the form was turned to a vertical position, and the slurry poured from the top.

In an effort to match as closely as possible the conditions in the structure, the following plan was used in preparation of the test specimens from this slab:

1. After the slurry was poured the specimen w [illegible] an ambient condition next to the model.

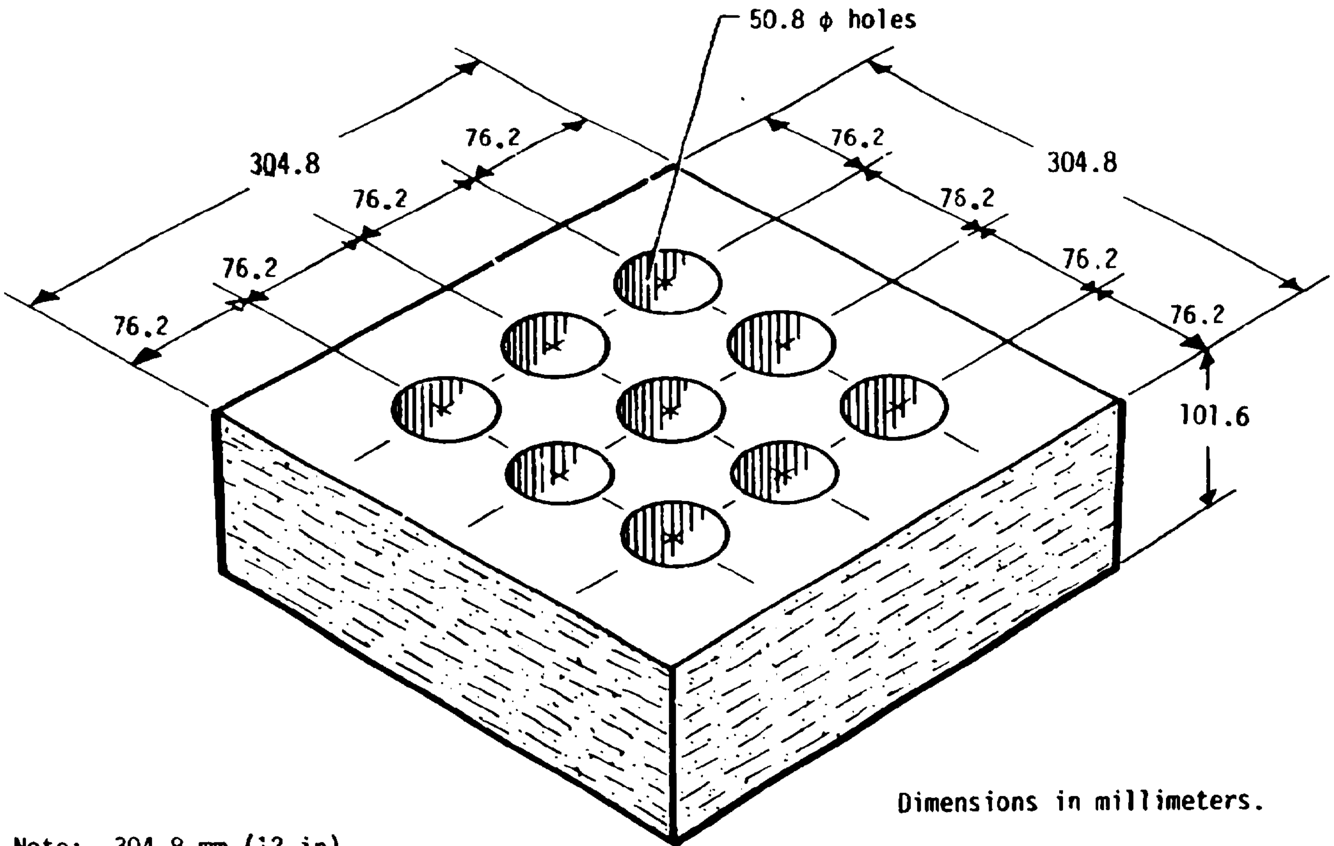

Dimensions in millimeters.

Note: 304.8 mm (12 in)
101.6 mm (4 in)
76.2 mm (3 in)
50.8 mm (2 in)

Figure 33. SIFCON slab test specimen.

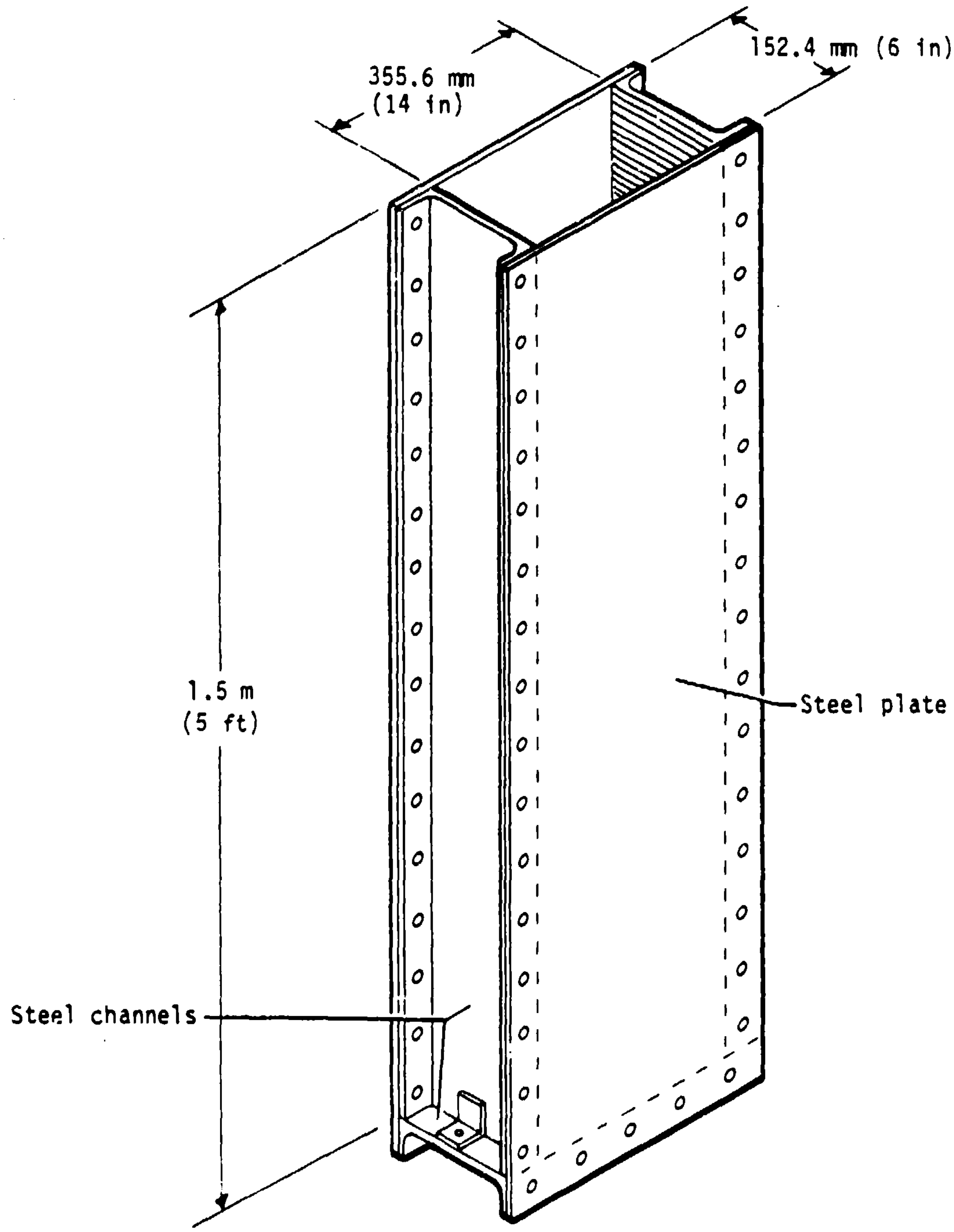

Figure 34. Special form for ISST SIFCON model test specimens.

2. On the 7th day, the 6.4-mm (0.25-in)-thick steel plates were removed and nine 50.8-mm (2-in)-diam specimens were cored out in a line from top to bottom, as shown in Figure 35, and tested in unconfined axial compression.

3. The plates were then reattached to the form and the specimen was replaced next to the model and allowed to cure.

4. On the 28th day, nine cores were again removed and tested as before.

5. The plates were again replaced and the specimen placed next to the model.

6. On test day, nine cores were removed and tested.

Several tables of graphs are given in Appendix B which show in detail the results of the SIFCON tests. Average values for each lift are summarized in Table 6. The location of each pour in the model is shown in Figure 36. Again note that many of the different specimen types and curing conditions were added later in the program so they are not listed in some of the first pours. Additional testing of similar SIFCON mixes were performed for several confined conditions as well as dynamic loadings under another subtask. The results of these tests are given in Section III.

Steel liner plates--The testing program for the steel liner consisted of obtaining test specimens corresponding to the liner sections. These specimens were tested in tension to failure with the results given in Table 7.

REVIEW AND RECOMMENDATIONS

Introduction--This portion of Section II reviews only the construction, materials testing, and field operations of the ISST structure.

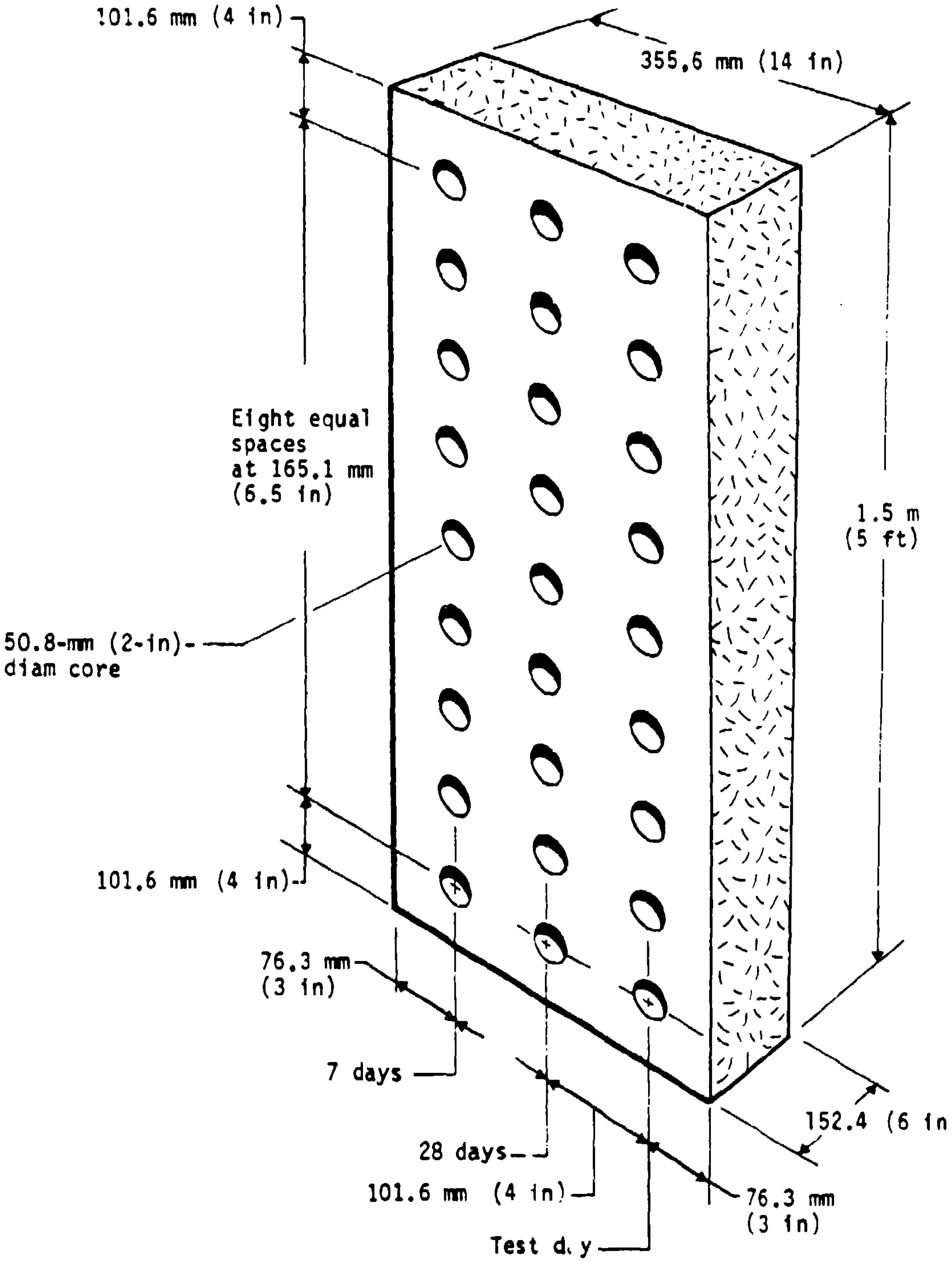

Figure 35. Core locations from wall slab.

TABLE 6. SUMMARY OF SIFCON TEST RESULTS

		Compression					Flexural					
Series	Age, days	MC air	MC wet	CCS air	CCS wet	CCW air	G air	G wet	B air	B wet	C air	C wet
6	7	6,883					7,012		2,750			
6	28	8,953					5,518		3,781			
6	Test day	9,629	10,235						2,164	3,075		
7	7	9,125		11,836			10,816		2,925		975	
7	28	12,061		12,462			13,096		1,721		825	
7	Test day	12,295	10,862						3,286	3,806	853	
8	7	5,311					6,611		2,138		867	
8	28	6,856	6,545	11,865			4,163		1,828	3,010		872
8	Test day	6,585	7,600						2,181	2,841	947	
9	7	8,369	7,507	12.048	11,841	12,813	6,556	7,222	2,355	2,306		
9	28	9,112	8,356		10.117	15,907			2,787	2,968	1,059	1,303
9	Test day	9,798	10,839			15,776			2,269	3,750		1,078
10	7	7,928	6,963		13,136	11,958			2,490	3,502	1,322	1,519
10	28	10,753	8,465		12,754	11,216			2,616	2,368	825	
10	Test day	10,455	11,459			14,232				4,210	1,491	1,059

Notes: MC = Molded Cylinder
CCS = Cored Cylinder, Slab
CCW = Cored Cylinder, Wall
G = Grout
B = Beam
C = Column
air = Ambient Curing
wet = Wetroom Curing

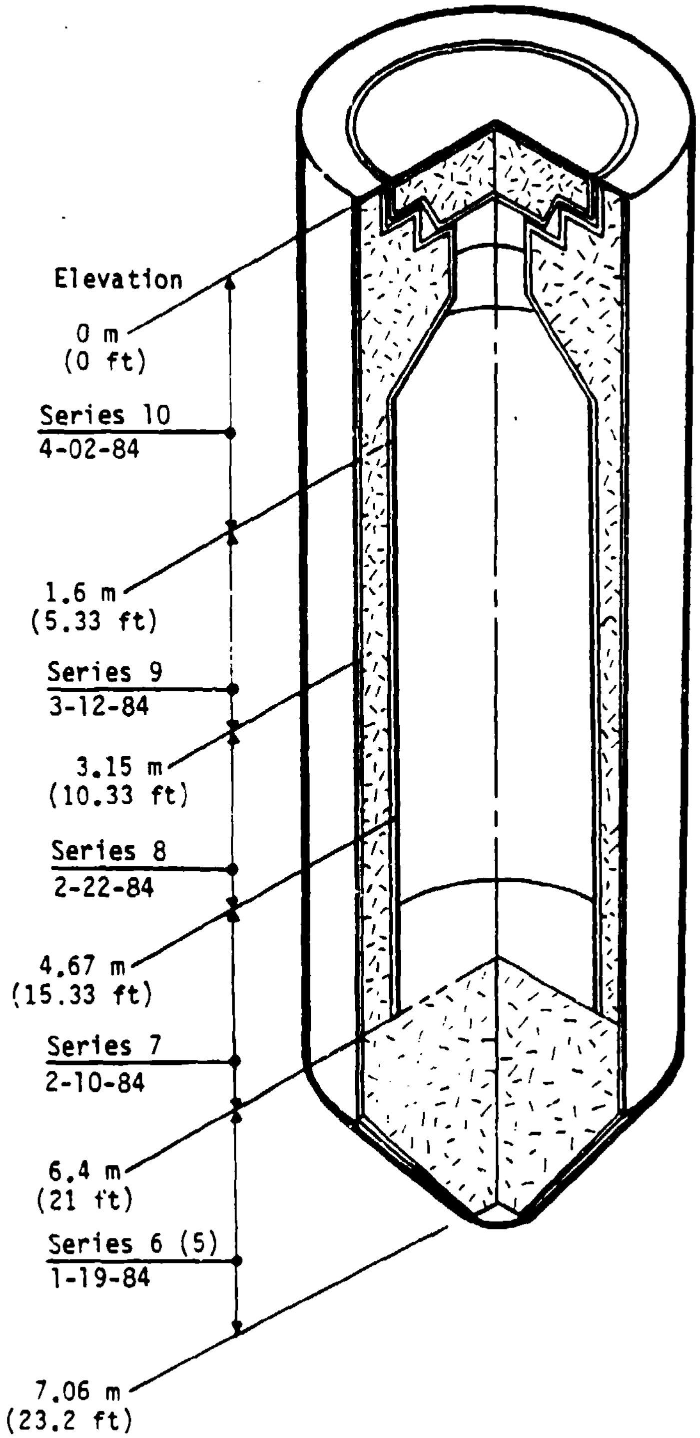

Figure 36. Location of SIFCON pours.

TABLE 7. STEEL PLATE TENSILE STRENGTHS

Item	Specimen mark	Tensile strength, MPa (lb/in²)	
		Yield	Ultimate
12.7-mm (0.5-in)-thick flat plates in headworks, closure, and gusset plates	1	379 (55,000)	508 (73,667)
	2	375 (54,333)	508 (73,667)
	3	375 (54,333)	503 (72,933)
	4	372 (54,000)	508 (73,667)
	1a	372 (54,000)	510 (74,000)
	2a	379 (55,000)	510 (74,000)
Average		375 (54,444)	508 (73,656)
9.5-mm (0.38-in)-thick inner liner plate in headworks	5	---	567 (82,222)
	6	---	555 (80,444)
	7	---	555 (80,444)
Average			559 (81,037)
6.4-mm (0.25-in)-thick inner and outer liner plate	A	403 (58,400)	524 (76,000)
	A	396 (57,400)	524 (76,000)
	B	386 (56,000)	472 (68,400)
	B	375 (54,400)	463 (67,200)
	C	403 (58,400)	521 (75,600)
	C	404 (58,600)	523 (75,800)
	D	414 (60,000)	545 (79,000)
	D	410 (59,400)	536 (77,800)
	E	378 (54,800)	483 (70,000)
	E	374 (54,200)	487 (70,600)
	O	405 (58,800)	532 (77,200)
	O	403 (58,400)	531 (77,000)
Average		396 (57,400)	512 (74,217)

Construction--In general, the construction of the ISST model using SIFCON proceeded extremely well with no major problems. The accuracy of the construction was much better than expected. As shown in Table 8 the average variation in wall thickness as measured at four locations at each liner joint was within 1.5 mm (0.06 in) of the design value of 152 mm (6 in). The overall average of all the measurements was within 0.5 mm (0.02 in) of the design value. Considering the problems inherent in rolling steel plate, this represents highly precise work on the part of the subcontractor.

The assembly of the liner sections went well with no major complications. In the future, only minor changes in some of the details would make the work even easier. Such changes would include staggering the elevations of the horizontal joint of both the inner and outer liners. The inner liner joint should be about 203 to 305 mm (8 to 12 in) above the outer liner joint. This will facilitate welding the horizontal joints of the liners and provide easier access to the interior of the model during fabrication.

A second suggestion would be a change in the detail where gusset plates intersect at the center of the model. Making good welds in the acute angle formed by the gussets was a difficult process. It is therefore suggested that a solid steel bar or pipe about 64 or 76 mm (2.5 or 3 in) in diameter be located at the center and the gussets welded to it.

TABLE 8. MEASURED WALL THICKNESSES IN CYLINDER SECTION

	Structure azimuth, deg				
Elevation	0	90	180	270	Average
[a]6096 (240)	154 (6.063)	152 (5.984)	153 (6.024)	154 (6.063)	153 (6.024)
4572 (180)	153 (6.024)	154 (6.063)	152 (5.984)	153 (6.024)	153 (6.024)
3048 (120)	153 (6.024)	152 (5.984)	151 (5.945)	154 (6.063)	152 (5.984)
1524 (60)	155 (6.102)	156 (6.142)	154 (6.063)	154 (6.063)	155 (6.102)
Average	154 (6.063)	154 (6.063)	152 (5.984)	154 (6.063)	153 (6.024)

[a]millimeters (inches)

The fiber placement was a very simple process but was quite time consuming being a hand operation. Other than designing and fabricating some sort of semiautomated fiber distribution system, no changes are planned for future work on models of this size. The quantity and location of the form vibrators seemed adequate to maintain relatively uniform fiber densities and proper infiltration of the slurry. There may be a better method for determining the vibrator location and operation frequency; however, detailed calculations and actual testing would be required to determine it. Even then, the amount of improvement achieved probably would not be significant.

The mixing and placing of the slurry was also very simple but again highly labor intensive and slow. To help speed up the process and simplify it even more, the use of a double tub grout mixer and pump is suggested. This equipment would provide a continuous, well-controlled operation of slurry mixing and placement.

The use of the small weep holes drilled in the liner proved to be very valuable in verifing slurry placement. Sometimes, however, the slurry being placed would run down the inside of the liner and exit at a hole higher than the true level of the slurry. When this happened, the hole usually became clogged and had to be cleaned out. Although a simple enough task, it was considered an annoyance and produced some doubt as to the true location of the slurry. In other instances the slurry would begin to run freely from a hole higher than one from which no slurry had begun to flow. This condition was even more confusing. Although the exact cause for this occurrence is not known, it is suspected that the slurry which was placed first had begun to thicken by the time it reached the lower hole so that it was too thick to flow out the small hole. As additional slurry was added, it had a shorter distance to flow to get to the higher hole and hence flowed out. The pressure was then increased on the thicker slurry due to the slurry above until it too finally flowed from the hole. In all lifts of the model construction, grout did eventually flow freely from all the holes.

The thickening of the slurry is generally a result of the superplasticizer losing its effectiveness. A detailed program is recommended for future study and testing on the effect of the dosage rate of the superplasticizer on the flowability of the slurry under various vibration conditions and distances traveled through fiber.

One problem encountered on the first two pours was the existance of various sized lumps of fly ash in the mix. Even extensive mixing failed to break up these lumps. When poured into the fiber the lumps appeared to clog the openings in the top surface of the fiber mass preventing subsequent buckets of slurry from flowing through the fiber. When the top surface of the fiber was raked up the clog was broken and the slurry flowed easily until it became clogged again. To remedy this situation, the technicians poured the slurry through common wire window screen laid on top of the fiber mass (Fig. 20). As the screen became clogged it was removed, cleaned, and replaced on the fiber. This method worked extremely well and no further problems were encountered. Although the wire screens worked well, they still required constant cleaning. To minimize the amount of cleaning, the fly ash was screened prior to mixing. This was quite helpful but did not totally eliminate the necessity of having to clean the screens.

Instrumentation--Weldable strain gages on the liners proved to be very easy and quick to install. Although somewhat more expensive than epoxy-bonded gages, the time saved in labor to install the weldable gages made them very economical. In addition, because they were welded, rather than glued, to the liner they should prove to be less susceptible to damage and debonding.

The strain gages mounted on bent reinforcing bars and used to monitor the response of the SIFCON were easily built and installed in the model. Because the gage is measuring the deformation of the reinforcing bar rather than the SIFCON directly, the data may require some interpretation by the analyst. Unless some laboratory tests are performed relating strain gage readings to the deformation of the SIFCON, the interpretation of the data may be inaccurate and difficult.

Some difficulty was encountered in installing certain media interface pressure gage cases through the outer liner. To prevent the gage case from being in direct contact with the liner, the hole in the liner had to be made larger than the case. This gap between the case and the liner proved very difficult to seal and prevent the slurry from leaking out while also accurately holding the case in position. Part of the problem is that the available gage cases were originally designed for use in concrete structures

without a steel outer liner. In this use the gage case could be securely mounted to concrete formwork; and when the forms were stripped, the mount would be left flush with the surface of the concrete. It is recommended that if future structures continue to use outer liners, then the gage mounts should be appropriately redesigned.

Materials testing--As mentioned earlier, the SIFCON testing program grew up as the model construction progressed. Looking back, several recommendations could be made for future work.

The 102-mm (4-in)-diam molded samples were easy to make; however, the test results seemed to have large variations in strength within a test series and were generally lower in strength than cored specimens of the same test series. Part of the variation was probably due to not knowing just how the samples should be made. In particular, the method of raining the fibers into the cylinder mold and the amount and type of vibration to provide were not known at the time. Although the same techniques for making the specimens were used in all cases, they may not have been the right ones. However, it is believed that the major reason for the variation in strengths for the 102-mm (4-in)-diam molded specimens was in the geometry of the sample itself. It appears that due to the length of the fiber and the curve of the cylinder mold, the density of the fiber in an area near the surface of the specimen is not as great as in the central portion. The possibility of this condition, designated as "edge effects," is illustrated in Figure 37. Because the fiber is straight and of a finite length, it cannot get close to the wall of the mold. This gap is filled only by the ends of other fibers. In addition the gap is also filled with fibers which preferentially align themselves vertically against the wall of the mold. These vertical fibers contribute virtually nothing to the strength of the specimens, because they usually slough off early in the test. The actual dimension of this lower density region is unknown but it is suspected to be about one-half the fiber length. It has also been suggested that the dimension is equivalent to the development length of the fiber in the particular slurry matrix. Obviously more study in this area is required if molded samples are to be used in the future.

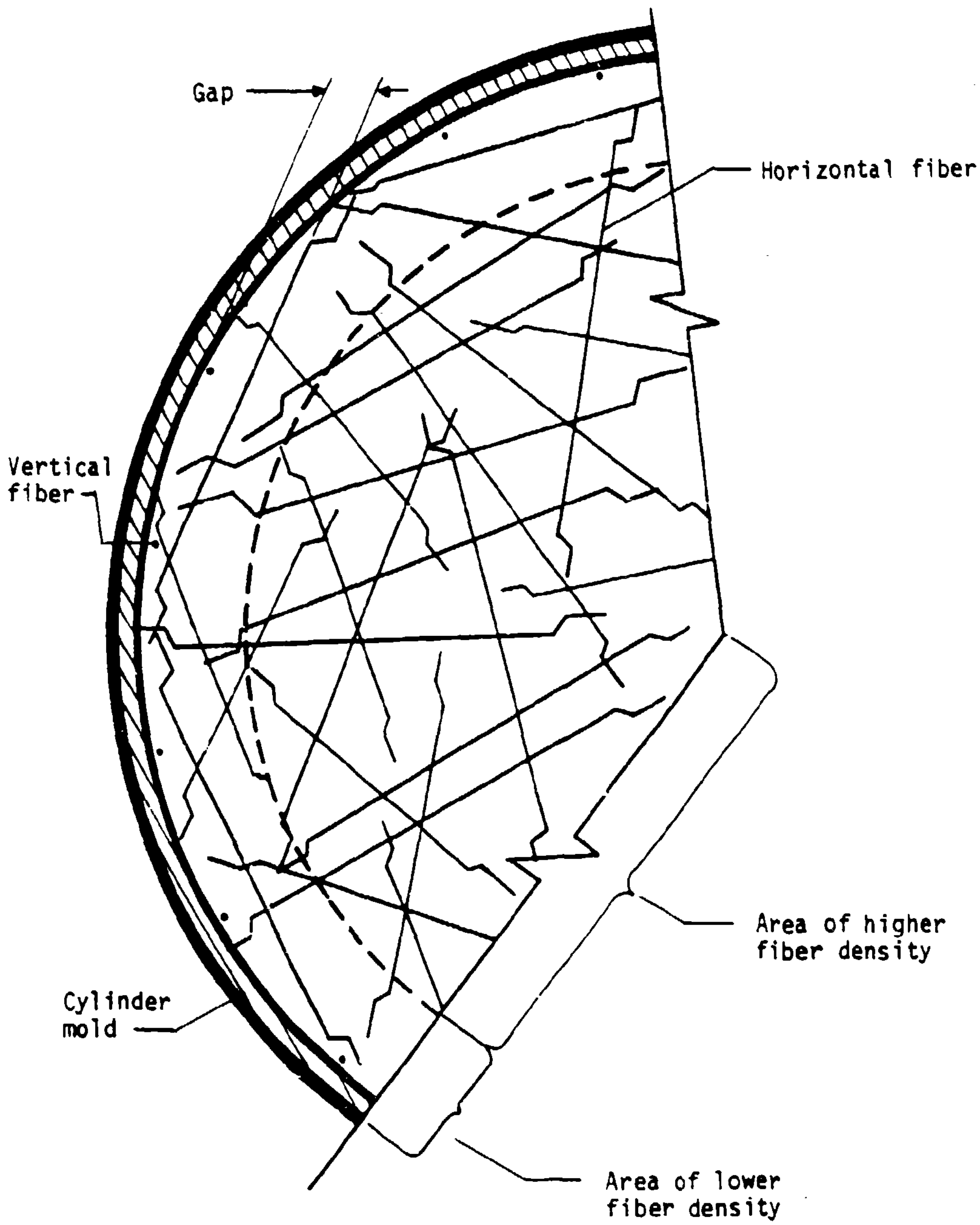

Figure 37. Edge effects in a molded cylinder specimen.

A more preferred specimen is the cored sample. These samples were drilled from small slabs made with SIFCON. When tested, the samples gave higher and more consistent results than the molded type. The lack of edge effects in the cored specimens is believed to be the major reason for the higher strengths. Although the cored samples appear to be the better type of specimen, they are also more expensive, mainly due to the time needed to drill the core. Note that even though a 305- by 305-mm (12- by 12-in) slab will yield nine 51-mm (2-in)-diam cores, leaving 80 percent of the slab as waste, it still uses much less material than 102-mm (4-in)-diam molded specimens. It is recommended that future specimens be of the cored type, either 51 or 76 mm (2 or 3 in) in diameter. The slab should be sized to allow the cores to be drilled not closer than 1.5 to 2 fiber lengths from the edge to eliminate edge effects. In addition, the slab thickness should be 25 to 38 mm (1 to 2 in) thicker than the desired length of the core to allow for trimming off the rough edges of the specimen which result during the coring process.

In most of the unconfined compression tests performed, a sulfur-based capping compound was used. When observed after the test, it was found that the cap was greatly deformed laterally and in many cases severely cracked or crushed. It is believed that this lateral deformation of the cap has little effect on the strength of the SIFCON sample with adequate fiber density in the top and bottom surfaces. The fiber in the top and bottom surfaces would prevent a tensile-type split in the specimen such as would occur in a plain concrete sample. Even so, it is recommended that a study be made to determine the actual effects of different types of capping compounds on SIFCON test specimens. As an alternate, the ends of the samples could be saw-cut square and the specimen be tested uncapped. This, of course, is more expensive than using a capping compound.

One item of particular interest is the apparent preferential direction of SIFCON under a compressive load as related to the way the fibers were placed. Only a very few tests were conducted to study this phenomenon n the early demonstration program. For those tests, it was found that a specimen molded and loaded in the same direction (i.e., the gravity vector) was about twice as strong as one molded in one direction with the load applied perpendicular to that axis (Fig. 38). More study concerning this effect is highly recommended.

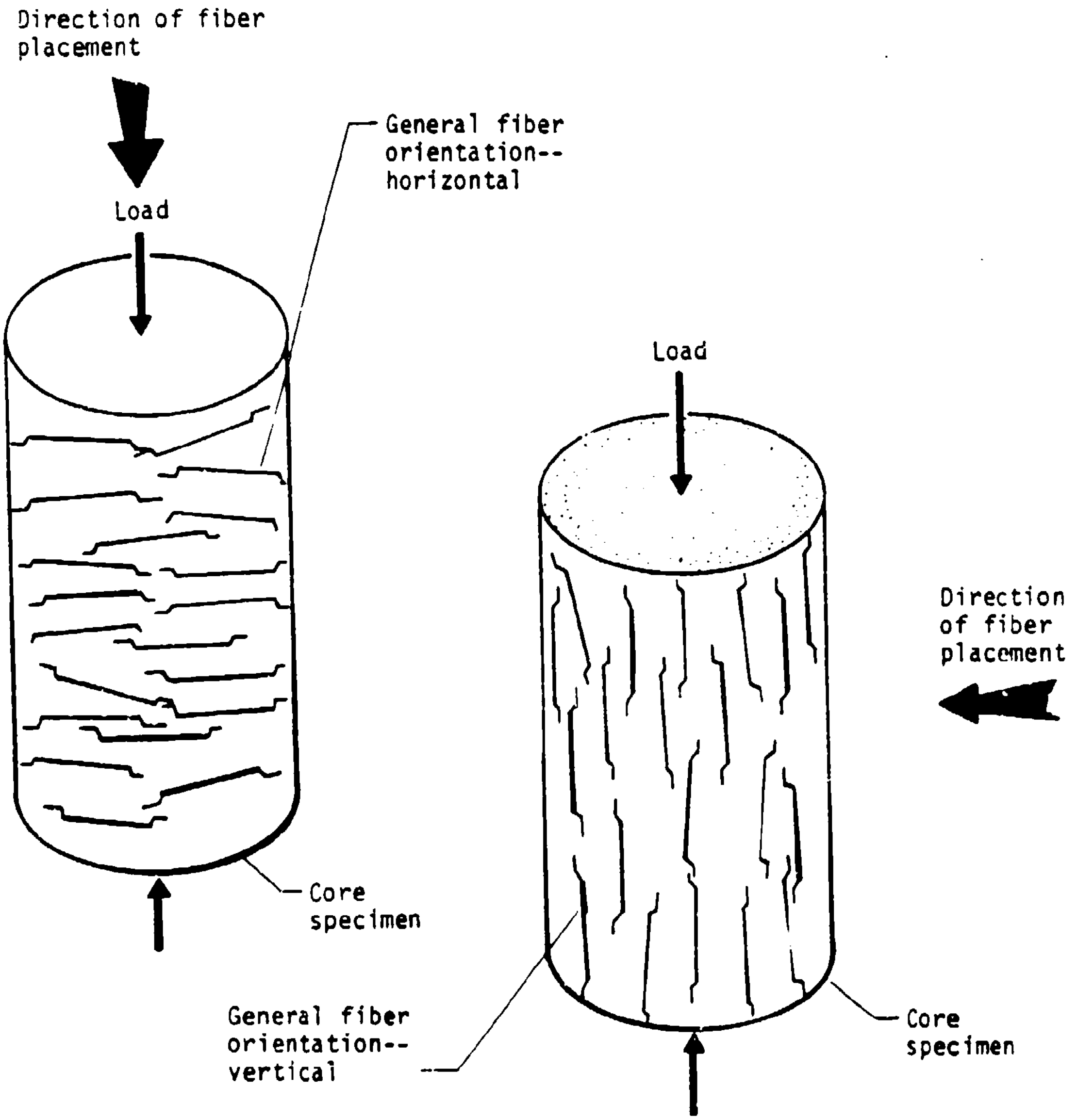

Figure 38. Effect of loading direction on fiber orientation.

As a start, NMERI has already undertaken a study to develop a type of fiber which may minimize or eliminate the preferential effects of fiber placement.

The method of curing the SIFCON when compared to its strength posed an interesting situation. In general the cylindrical specimens cured in a standard wet room environment were consistently lower in strength than those cured under ambient conditions. This situation was, of course, opposite what would be expected with regular concrete. Because of the many variables involved, even a suggestion for the cause of this phenomenon would be impossible. However, this is an important parameter and should be investigated thoroughly in future programs.

Another interesting point was that in three instances the 7-day unconfined compression strengths were higher than the 28-day strengths. Note, however, that the differences were less than 5.5 MPa (800 lb/in^2) except in one case when it was 11.7 MPa (1700 lb/in^2). The reasons for this apparent paradox are not known; however, two theories may be suggested. First, the slurry gains strength very rapidly. Perhaps in as little as 3 days it may be 98 percent or more of the 28-day strength. This is because of the use of Type III cement and an unusually large dosage rate of superplastizer. Therefore, by the time the 28-day tests are conducted, the differences are actually just standard deviations for the tests rather than an actual indication of strength differences. Secondly, one theory suggests that the strength of the SIFCON is much more dependent on the type and density of the fiber rather than on the strength of the slurry. Then, as above, the strength differences are actually only standard deviations for the tests. These theories require closer study and testing which is recommended as part of a future comprehensive testing program.

The portion of the materials testing program which included the flexural tests brought to light situations similar to the unconfined compression tests. First, about 30 percent of the tests had 7-day strengths higher than the 28-day strengths. As before, the actual reasons are unknown but one or both of the theories noted may also account for this effect. Secondly, the effect of the higher strength as a function of fiber orientation was also noted. The strength of a flexural specimen molded as a beam was 2 or 3 times higher than a flexural specimen molded as a column. The differences of the two types are

shown in Figure 39. As can be seen, the fibers in the sample molded as a beam act like tensile reinforcement, whereas the majority of fibers in the sample molded as a column are in vertical plane for the test and therefore do not function to resist tensile stresses. Note, however, that the fiber orientation for the specimen molded as a column would appear to be ideal in resisting shear-related stresses. Additional study in this area may prove to be quite usable for future applications.

One situation, opposite to that noted for the compression tests, was that the wet-room-cured specimens were consistently higher than those cured under ambient conditions.

Because SIFCON is such a new material the test results obtained in this program must be carefully studied and interpreted. Until a larger base of knowledge and understanding concerning the product is established, the dogmatic adherence or rejection of specific test results is discouraged. Instead, average values of several tests should be considered or the data used in a qualitative way. To develop this larger data base, a comprehensive testing and data acquisition program is strongly recommended, starting as soon as possible.

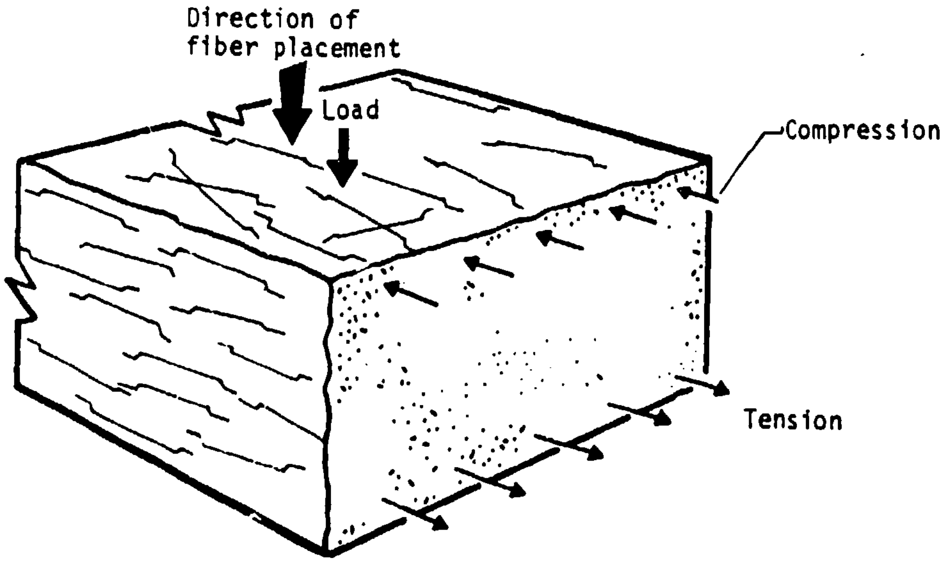

(a) Molded and tested as a beam.

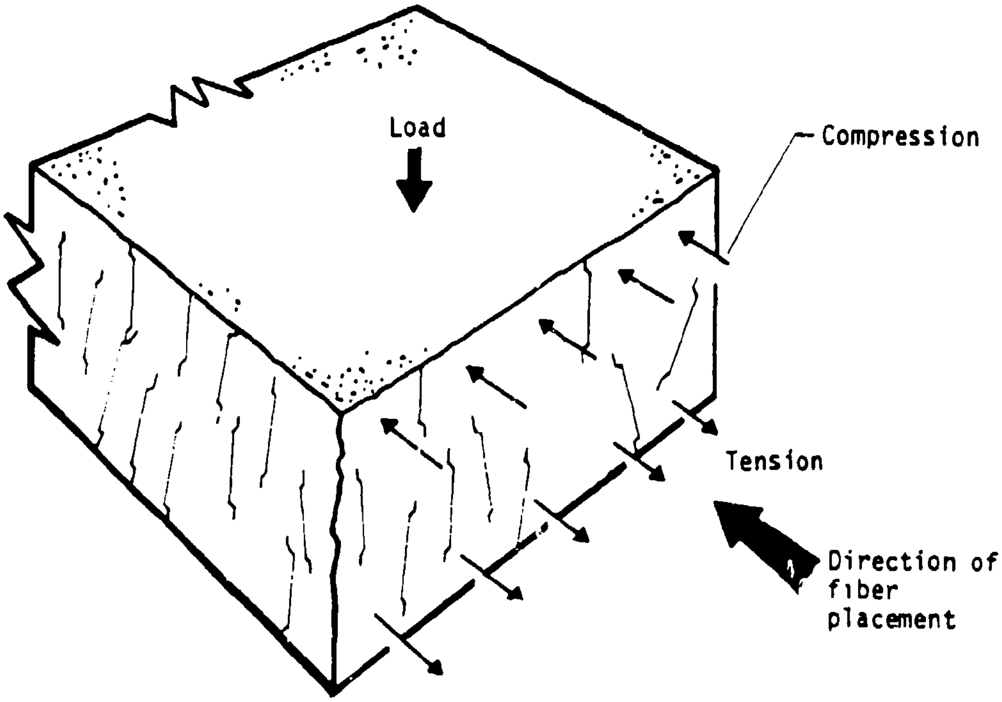

(b) Molded as a column--tested as a beam.

Figure 39. Standard flexural specimen.

III. CHARACTERIZATION OF STEEL-FIBER-REINFORCED CONCRETE

INTRODUCTION

In the fall of 1983 NMERI was tasked to conduct material characterization tests for fiber-reinforced concrete. In addition, using the data obtained from the test program, a material model was to be developed which could be used in dynamic structural analysis codes such as SAMSON2.

Lankard Materials Laboratory, Inc., provided test specimens of the fiber-reinforced concrete known specifically as Slurry Infiltrated Fiber Concrete (SIFCON).

The test program for SIFCON was designed to investigate both the dynamic and static material response characteristics. The static tests, which consisted of uniaxial compression and triaxial compression tests, were performed at Sandia National Laboratories using their equipment and test personnel. The test plan for the static tests was developed at AFWL.

The dynamic tests were performed at NMERI using a modified dual mass shock amplifier and the Monterey Research Impact 2424 HVA drop tower. Dynamic uniaxial compressive loads with strain rates from 3/s to 35/s in the SIFCON samples were obtained using this device.

SICON

Lankard Materials Laboratory provided test specimens of two different mixes of SIFCON. The primary test specimens were 51-mm (2-in)-diam by 102-mm (4-in)-long circular cylinders which were cored out of a precast 457- by 457- by 102-mm (18- by 18- by 4-in) slab. The cores were taken in a direction perpendicular to the fiber plane. The principal differences in the two mixes consisted of the length and diameter of the chopped steel wire fiber used. A summary of the two mixes is given in Table 9.

TABLE 9. SIFCON PRIMARY TEST SPECIMENS

Mix no.	Matrix material	Water/cement plus fly ash	Fiber[b] volume, %	Fiber length, mm (in)	Fiber diameter, mm (in)	Overall density[c]
ZL 30/50 Prepared 12/2/83[a]	70% Type III portland cement and 30% fly ash, shipped and stored in moist sawdust	0.3	11.4	30 (1.18)	0.5 (0.02)	158
OL 20/25 Prepared 12/8/83[d]	70% Type III portland cement and 30% fly ash, shipped and stored in moist sawdust	0.3	11.4	20 (0.79)	0.25 (0.01)	157

[a]First static tests performed at 20 days; dynamic tests performed at >28 days

[b]Bekaert Steel Wire Corporation chopped wire fiber (high carbon steel)

[c]Samples were cored out of a 457- by 457- by 102-mm (18- by 18- by 4-in) slab. The slab was prepared by pouring fibers into a wooden form with the 102-mm (4-in) dimension vertical. The form was turned 90 deg and the slurry poured into an opened 102- by 457-mm (4- by 18-in) end till full. Light external vibration was applied throughout the slurry infiltration operation to facilitate movement of slurry through the packed fiber bed

[d]All testing at >28 days

DYNAMIC TESTS

Although the principal data produced in this test series were of a static uniaxial and triaxial nature, some high strain rate information was also obtained from a series of experiments using the Monterey Research Impact 2424 HVA drop tower and a modified Dual Mass Shock Amplifier (DMSA)*.

In its normal usage the DMSA is used to subject specimens to prescribed acceleration histories. This is accomplished by mounting the specimens to the top surface of the upper mass (Fig. 40) and dropping the DMSA from a given height. When the base stops, the upper mass continues down and contacts a resilient felt programmer sandwiched between the upper mass and the base. The thickness and resilience of the felt programmer tailors the acceleration of the upper mass and subjects the mounted specimens to this acceleration history.

For this test series the DMSA had to be modified to apply a sudden axial load to the 51- by 102-mm (2- by 4-in) concrete cylinders. This was accomplished by mounting the specimen below the upper mass of the large version DMSA using a lower load platen and elastic guys (Fig. 41). In this configuration, when the DMSA is dropped from a given height and the base comes to rest, the upper mass, specimen, and lower load platen continue down until the lower load platen contacts the base mass.

To decelerate the upper mass a considerable force of short duration is generated which must act through the specimen. In practice, the load rate and peak were controlled to some degree by placing felt pads between the lower load platen and base mass. The load peak could also be controlled by changing the drop height and weight of the upper mass.

To add additional weight to the upper mass and to provide a mounting surface for the elastic guys, an upper load platen [19-mm (0.75-in) steel] was designed and attached to the upper mass. The lower load platen was a 25-mm (1-in)-thick rectangular steel plate with screw eyes for the elastic guys. A shallow 57-mm (2.25-in)-diam hole was bored into each platen for positioning the specimen and for fitting of 1.6-mm (0.06-in)-thick Teflon® friction reducers at the specimen ends.

* Monterey Reseach Laboratory, Inc. large version Dual Mass Shock Amplifier.

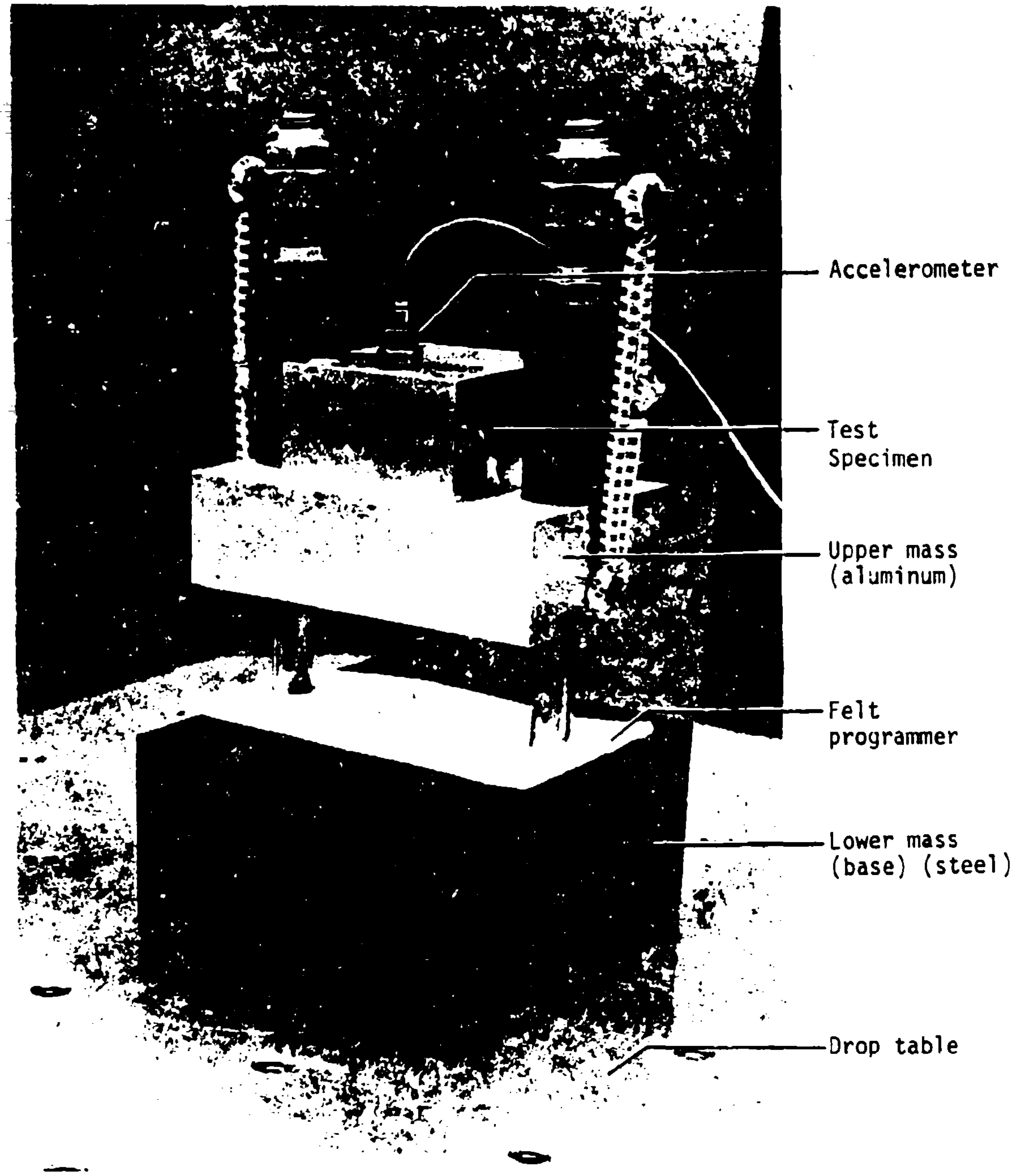

Figure 40. Dual mass shock amplifier (small version).

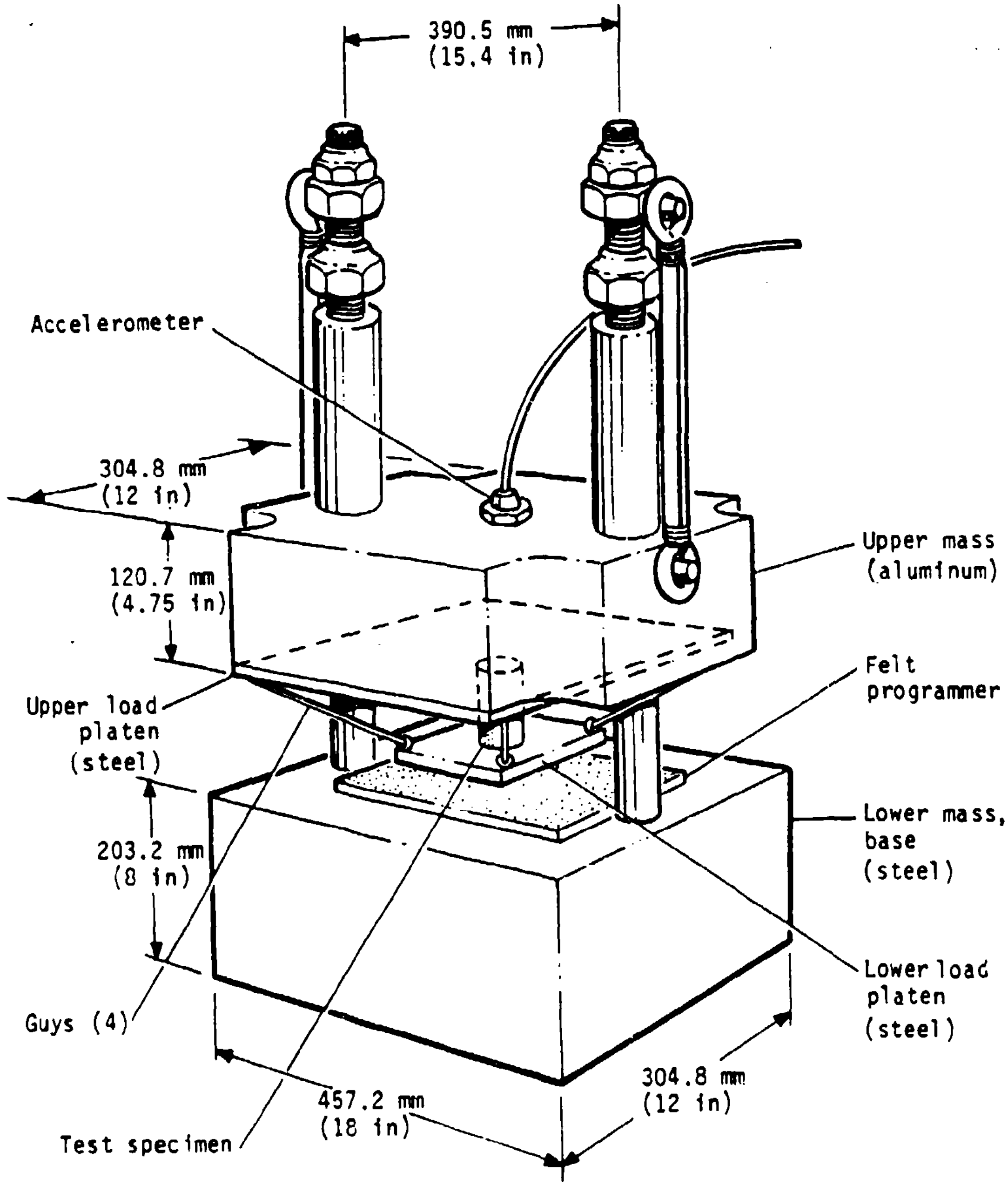

Figure 41. Modified dual mass amplifier (large version).

Loads through the specimens were measured indirectly using an accelerometer mounted to the upper surface of the upper mass in a position colinear with the specimen. By using the recorded acceleration and the known mass of the upper mass the force applied to the specimen could be calculated using Newton's 2nd Law of Motion. Due to the lack of rigidity of the upper mass and the remote mounting location of the accelerometer, only the magnitudes of loads with relatively long load wavelengths (long with respect to wave response times through the upper mass thickness) could be relied upon. The characteristic response time of the upper mass was measured to be 0.068 ms (14.6 kHz). Generally, the time to peak of the loads applied to the test specimens was greater than this by a factor of 10 or more (0.7-1 ms). Generally, to extract a smooth acceleration signal, the accelerometer data from all tests were electronically filtered at either 5 or 7 kHz. For no test did this filtering appear to affect the overall peak measured magnitude obtained.

Figures 42 through 44 are photographs depicting the test apparatus. Figure 42 shows a specimen (steel) mounted between load platens in the modified DMSA. Figure 43 shows the modified DMSA closed up with a neoprene shatter guard, and Figure 44 depicts the drop tower and mounted modified DMSA prior to a drop test.

In addition to the accelerometer data, measured with an Endevco 2225 30-kg gage, strains were also measured in the test samples as a function of time. These data were generated by M&M* strain gages attached to the specimens and recorded on a Nicolet recorder and a portable tape deck. Up to four gages were used on the samples. Generally, there were two longitudinal and two circumferential gages per specimen mounted every 90 deg around the circumference of the specimen waist. No electronic filtering was performed on strain measurements.

As a cross-check on the test method, three successive drops were made on a 51-mm (2-in)-diam by 102-mm (4-in)-long steel specimen which stressed the sample from 275.8 to 330.9 MPa (40,000 to 48,000 lb/in) within 0.8 ms. Assuming linearity, and by using the average measured peak strain and

---

* Micro-Measurement, Romulus, Michigan (gage type EA06-500BH-120).

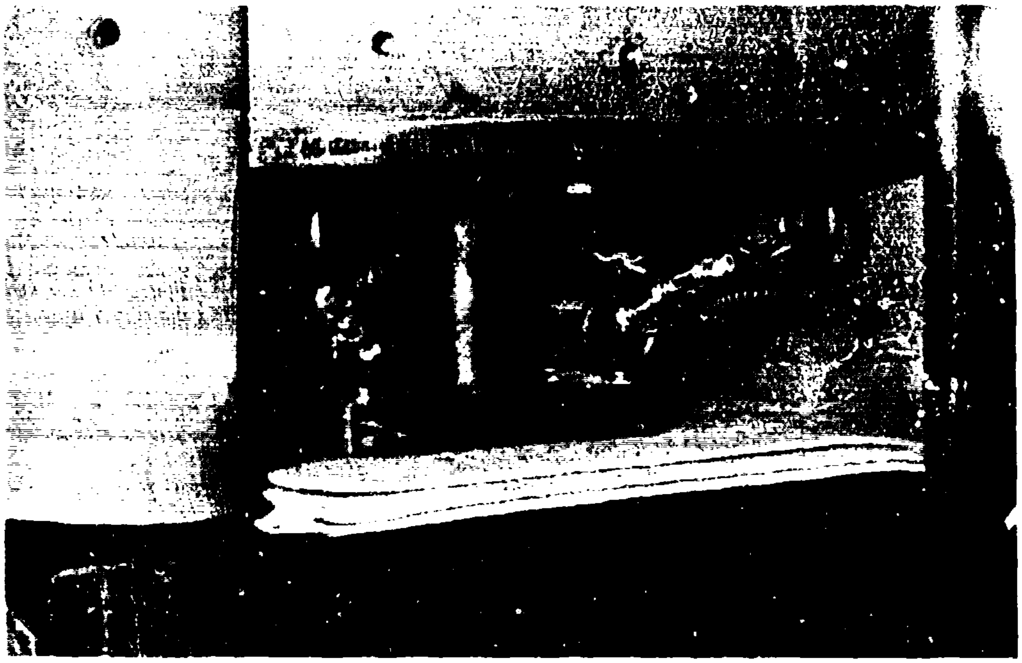

Figure 42. Steel specimen mounted between load platens in modified DMSA.

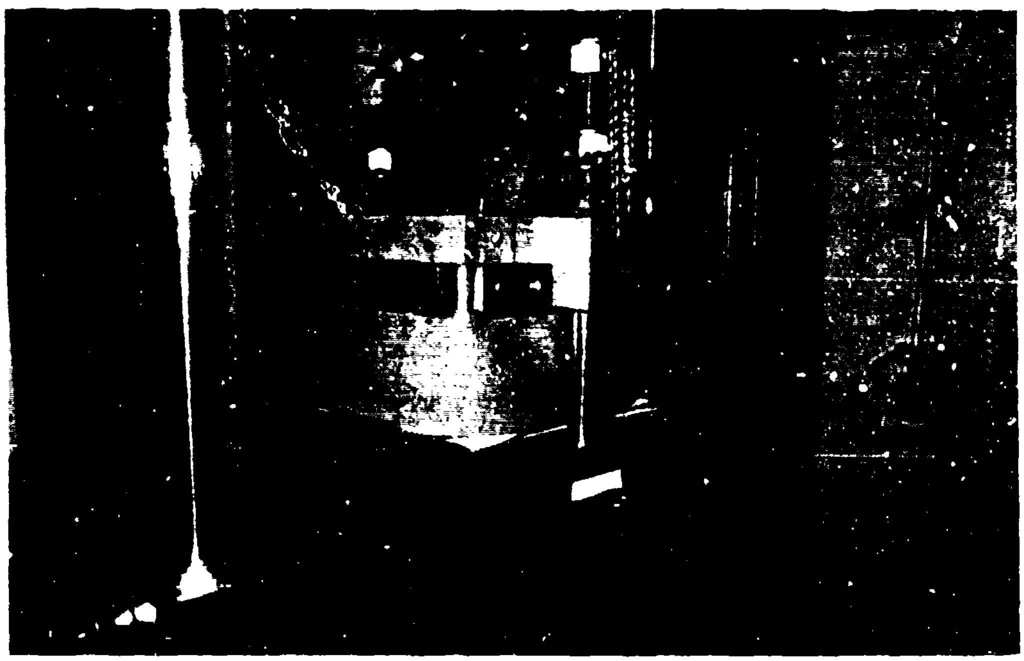

Figure 43. Modified DMSA with neoprene shatter guard in place.

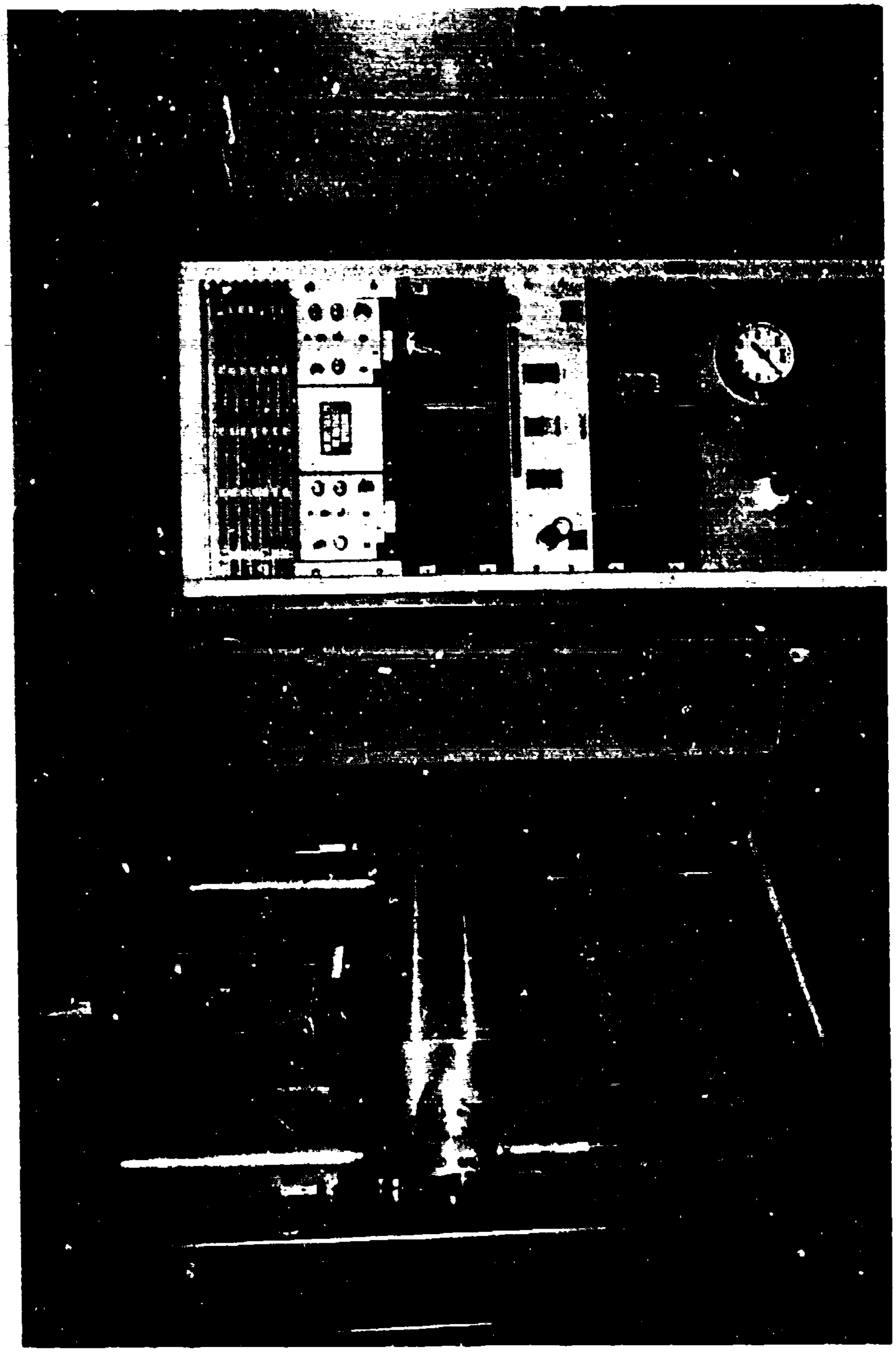

Figure 44. Drop tower and modified DMSA prior to drop test.

acceleration, values of the elastic modulus were calculated for the three tests. These values are

0.219 x 10 MPa (31.70 x 10 lb/in)
0.215 x 10 MPa (31.24 x 10 lb/in) = 0.216 x 10 MPa
(31.28 x 10 lb/in) mean
0.213 x 10 MPa (30.90 x 10 lb/in)

The static modulus of the steel sample was measured in an Instron testing machine; the tests gave a value of 0.211 x 10 (30.6 x 10 lb/in) (Fig. 45).

The difference in the mean dynamic modulus and the mean static modulus is 2.2 percent. There is some indication that the elastic modulus of steel is not significantly rate sensitive (Ref. 9). If so, the difference between the static and dynamic moduli is probably due to systematic error in the system although the few tests performed may not be sufficient to indicate any statistical difference between the two measured mean values.

Preparation of SIFCON samples consisted of cutting parallel flat end surfaces on the samples with a concrete cutoff saw and by locally grinding any rough surfaces where strain gages were to be mounted. Each specimen was installed between load platens using a 1.6-mm (0.06-in)-thick disk of Teflon® to reduce end friction effects. Several felt programming pads were used below the lower load platen to tailor the strain rate and peaks achieved during the tests. The drop height was also varied to change peak loads and rates of loading. If a specimen broke catastrophically, the normal bell-shaped character of the accelerometer response changed markedly, indicating the peak load achieved. In these types of failures the strain gages usually broke also.

---

9. Mainstone, R. J., "Part 4, Properties of Materials at High Rates of Straining or Loading," Materials and Structures, Vol. 8, No. 44, March-April 1975, p. 102-106.

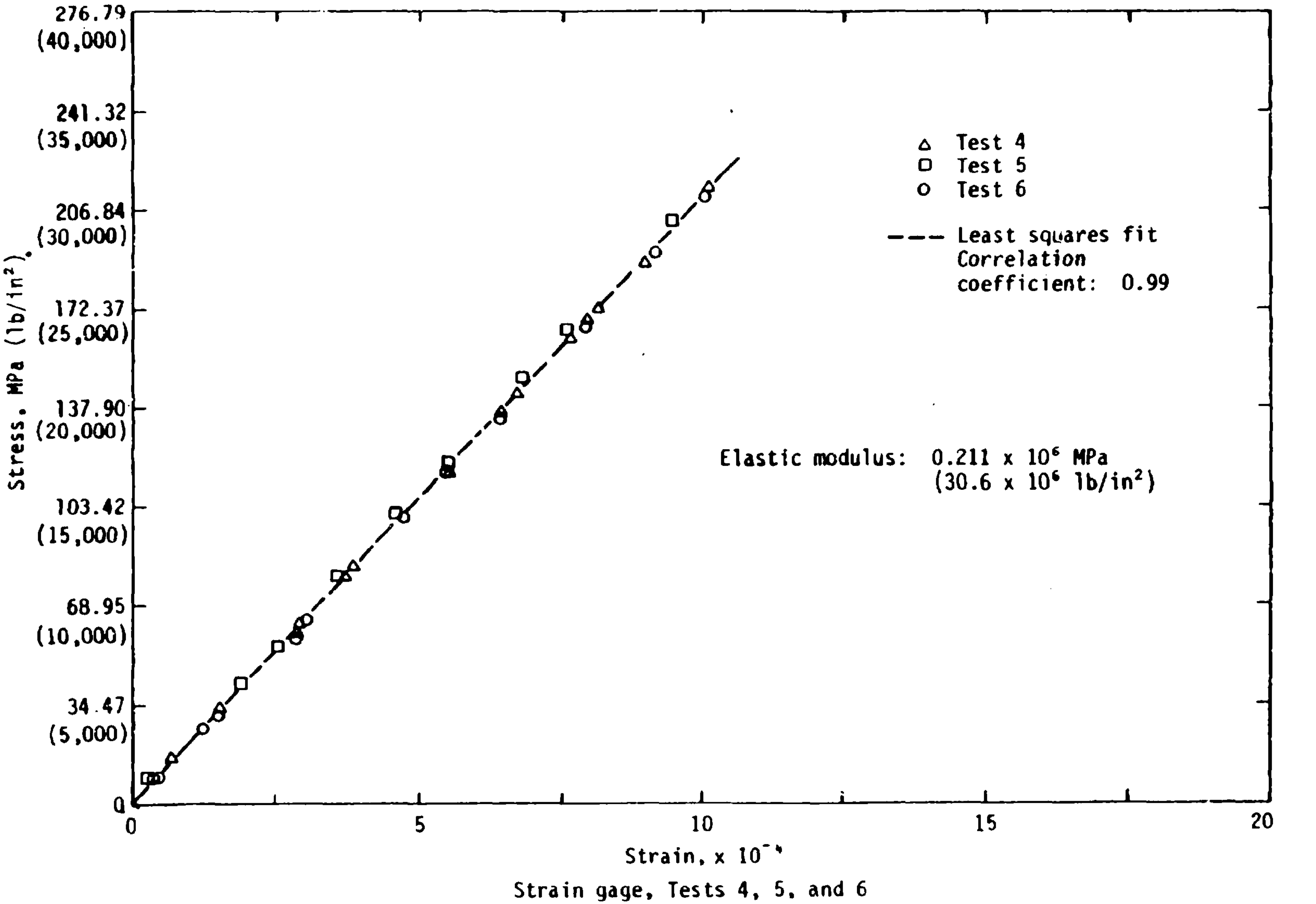

Figure 45. Static tests of steel specimen (uniaxial stress).

The SIFCON samples performed exceptionally well. Except for one test which was a multiple reload of a specimen, the most external damage observed in a specimen consisted of a surface spallation around the specimen waist (Fig. 46). This minor damage was observed in the majority of SIFCON samples. One SIFCON sample (Test 15) suffered no damage. This specimen was subsequently reloaded twice with minor damage on the second drop (Test 25) and a complete shear failure on the third drop (Test 26) (Fig. 47).

A summary of the results from the dynamic tests is given in Table 10. Where possible, elastic moduli E and Poisson's ratio ν are calculated from the data.

STATIC TESTS

Static testing of the SIFCON samples was performed at Sandia National Laboratories. A series of uniaxial stress, uniaxial strain, and triaxial tests of the 51-mm (2-in)-diam by 102-mm (4-in)-long specimens of the SIFCON samples was performed using a servo-controlled MTS 453,592-kg (1,000,000-lb) load frame for the uniaxial unconfined stress tests and a 2-kbar SBEL testing machine for the triaxial tests. Axial and transverse deformation of the unconfined samples was measured by Schaevitz LVDTs using a fixed gage length between mounting rings for axial response. The transverse LVDT was mounted in the center of the sample. All samples were end-ground to within ±0.025 mm (±0.001 in) flatness. Teflon® friction reducers [3.2 mm (0.125 in)] were used on the ends (Fig. 48).

For the triaxial tests, samples were covered with a polyolefin shrink tube to prevent oil from penetrating the samples. Steel caps were used on the ends of the samples. The test matrix is shown in Table 11.

TABLE 11. NUMBER OF STATIC TESTS

	Sample series	Unconfined compression	Triaxial ~4.14 MPa (~0.6 k/in^2)	Triaxial ~13.9 MPa (~2 k/in^2)	Triaxial ~68.9 MPa (~10 k/in^2)	Uniaxial strain
SIFCON	RF	4	1	1	1	1
	B	3	1	1	1	1

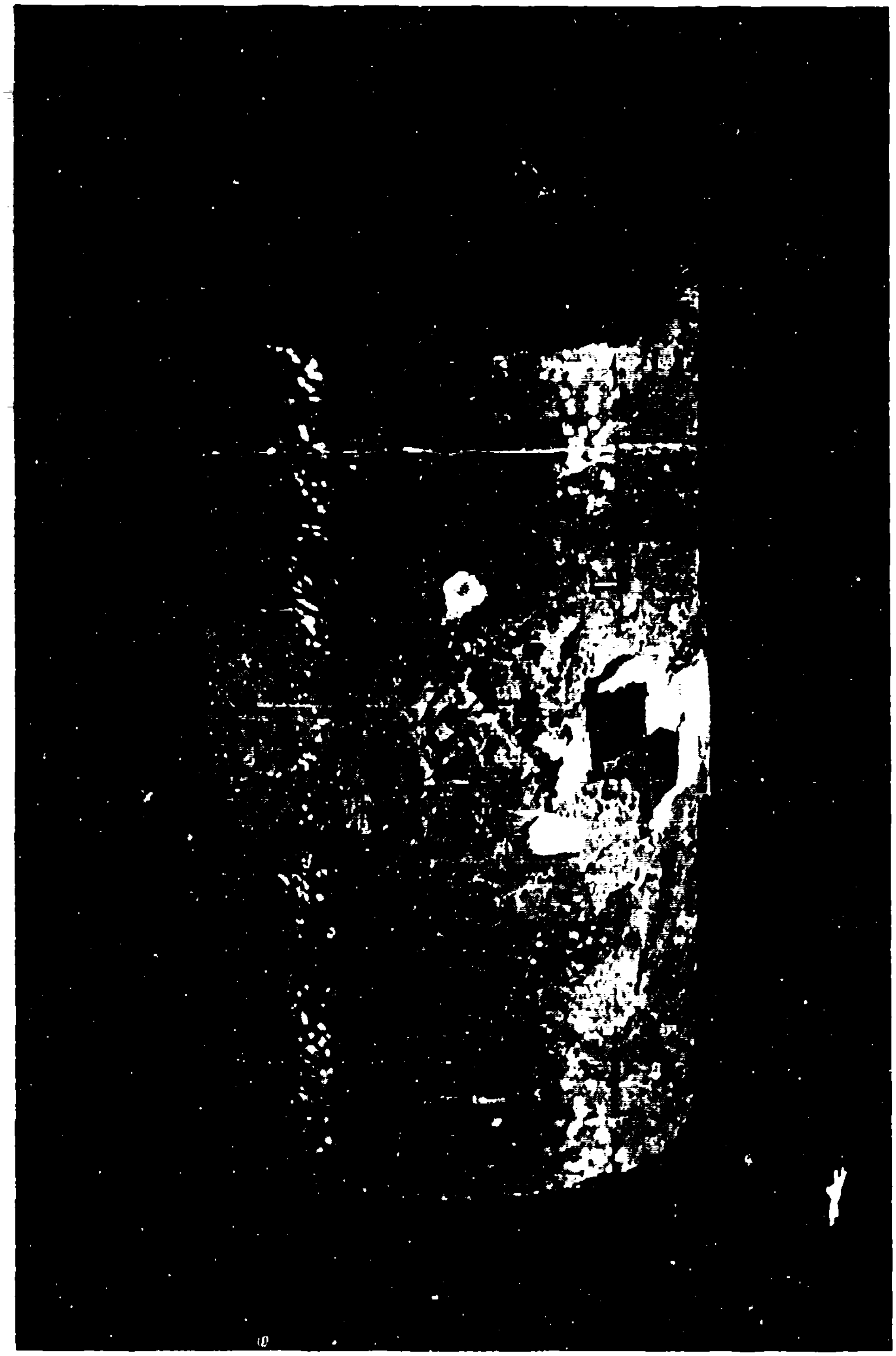

Figure 46. Typical surface spallation pattern of SIFCON specimens after drop testing. (Corresponds to "Minor Damage" in Table 2.)

Figure 47. Shear failure of SIFCON specimen FR24-30/50 after third drop test.

TABLE 10. DROP TOWER--TEST SUMMARY

SIFCON	Specimen No.	Test No.	E, MPa (lb/in^2)	ν	Peak stress, MPa (lb/in^2)	$\dot{\varepsilon}$	Comments	Drop height, mm (in)
30/50	RF24	1	12.1×10^6 (1.76×10^6)	0.29	160 (23,222)	14.6	No damage	1143 (45)
	RF22	2	16.7×10^6 (2.42×10^6)	0.29	149 (21,673)	16.8	Minor damage	1372 (54)
	RF17	3			179 (25,937)	31.2	Minor damage	1372 (54)
	RF?	4			138 (19,966)	24.3	Minor damage	1524 (60)
20/25	B-20	5	8.6×10^6 (1.25×10^6)		149 (21,630)	17.0	Minor damage	1524 (60)
	B-21	6	9.6×10^6 (1.39×10^6)		165 (23,888)	21.2	Minor damage	1829 (72)
	B-22	7			189 (27,343)	35.7	Minor damage	2134 (72)
	B-23	8			1[illegible]3 (26,474)	30.0	Minor damage	2134 (84)
	B-24	9			178 (25,780)	31.2	No damage	2134 (84)
	B-24	10			191 (27,680)		No damage	2134 (84)
30/50	RF24	11			176 (25,508)		Minor damage (retest)	2134 (84)
	RF24	12			159 (23,063)		Broke (retest)	2134 (84)

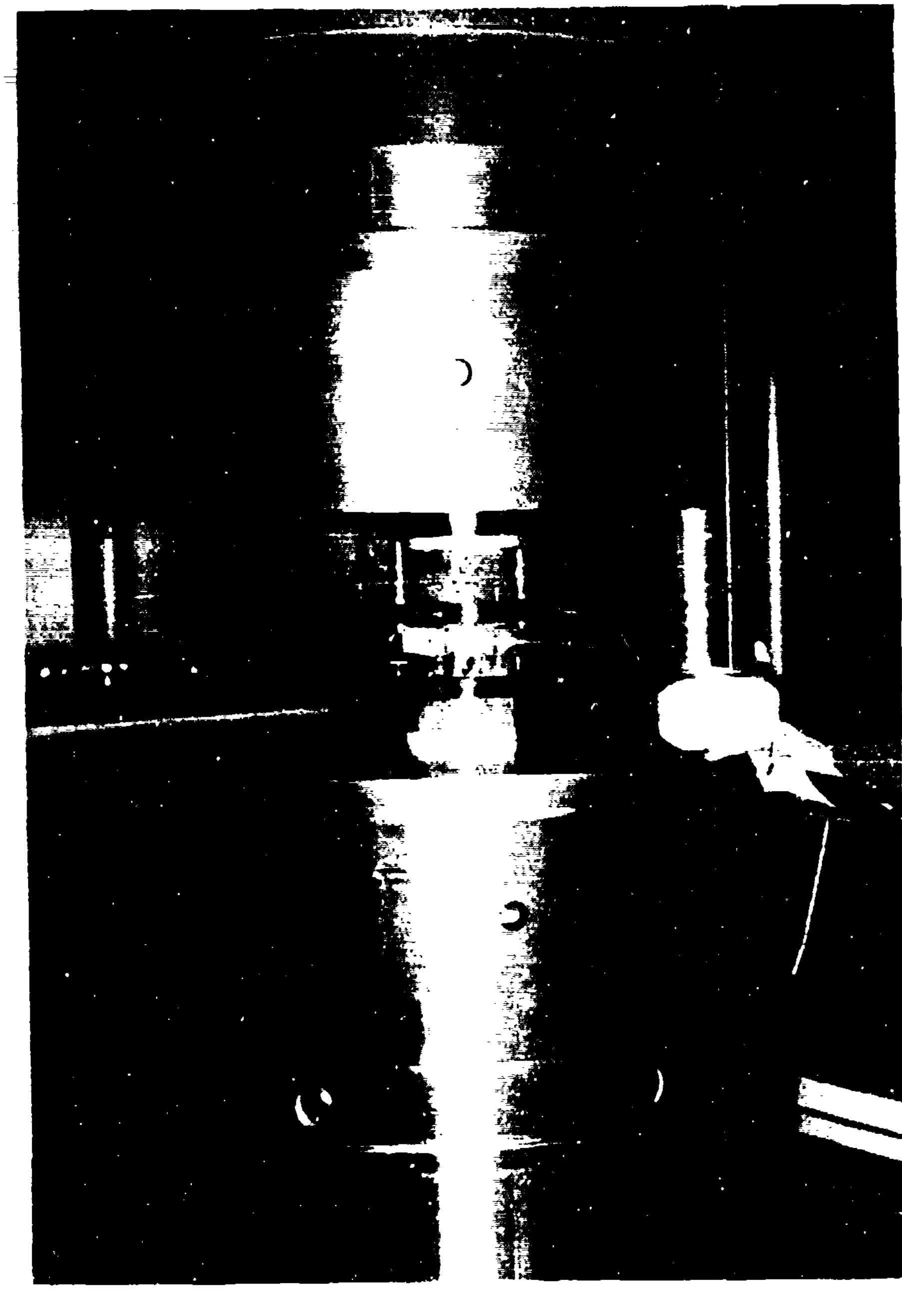

Figure 48. Specimen with LVDT gages mounted in 453,592-kg load frame for uniaxial stress test (Teflon friction reducers on ends).

Data from the tests were recorded and plotted using a PDP 11-23 and a Tektronics 4010 data acquisition system with floppy disk storage. Data plots were digitized and replotted for analysis. The results of the uniaxial stress tests are shown together for each material species in Figures 49 and 50 as axial stress versus axial strain. Similarly, triaxial data are shown in Figures 51 and 52 for three confining pressures. Here again axial stress is plotted versus axial strain for the various test specimens.

The data for the uniaxial strain test are presented in Figures 53 and 54 and include axial stress versus axial strain and axial stress versus confining pressure respectively.

A summary of results for static uniaxial stress tests is shown in Table 12.

MATERIAL MODELS

The principal purpose of the effort expended on this portion of the task was to develop material models which can be used in dynamic structural analysis codes such as SAMSON2. It is important, therefore, to provide models which are reliable and readily usable in such codes. Mathematical models using endochronic and viscoplastic theory are available which can match the unloading and dilatational behavior of concrete-like materials. Experience has shown, however, that matching these models to experimental data can be a time consuming process, with the endochronic model perhaps the worst in this respect of the two mentioned theories. Moreover, when these models are run in large deformation dynamic codes they tend to be very tempermental and much care must be exercised in their use. An early attempt was made to use the data from this test series to produce a viscoplastic model. Subsequently, the model was used in a severly loaded test simulation calculation. The calculation was not successful, possibly because the tensile region of the viscoplastic model currently available at NMERI is poorly defined. Certainly, since the viscoplastic model can be made to match important aspects of material response, work in improving such modeling techniques should continue. However, in the interest of time, and the need to run calculations immediately, the reliable AFWL engineering modeling approach was chosen as the basis for the models in this report.

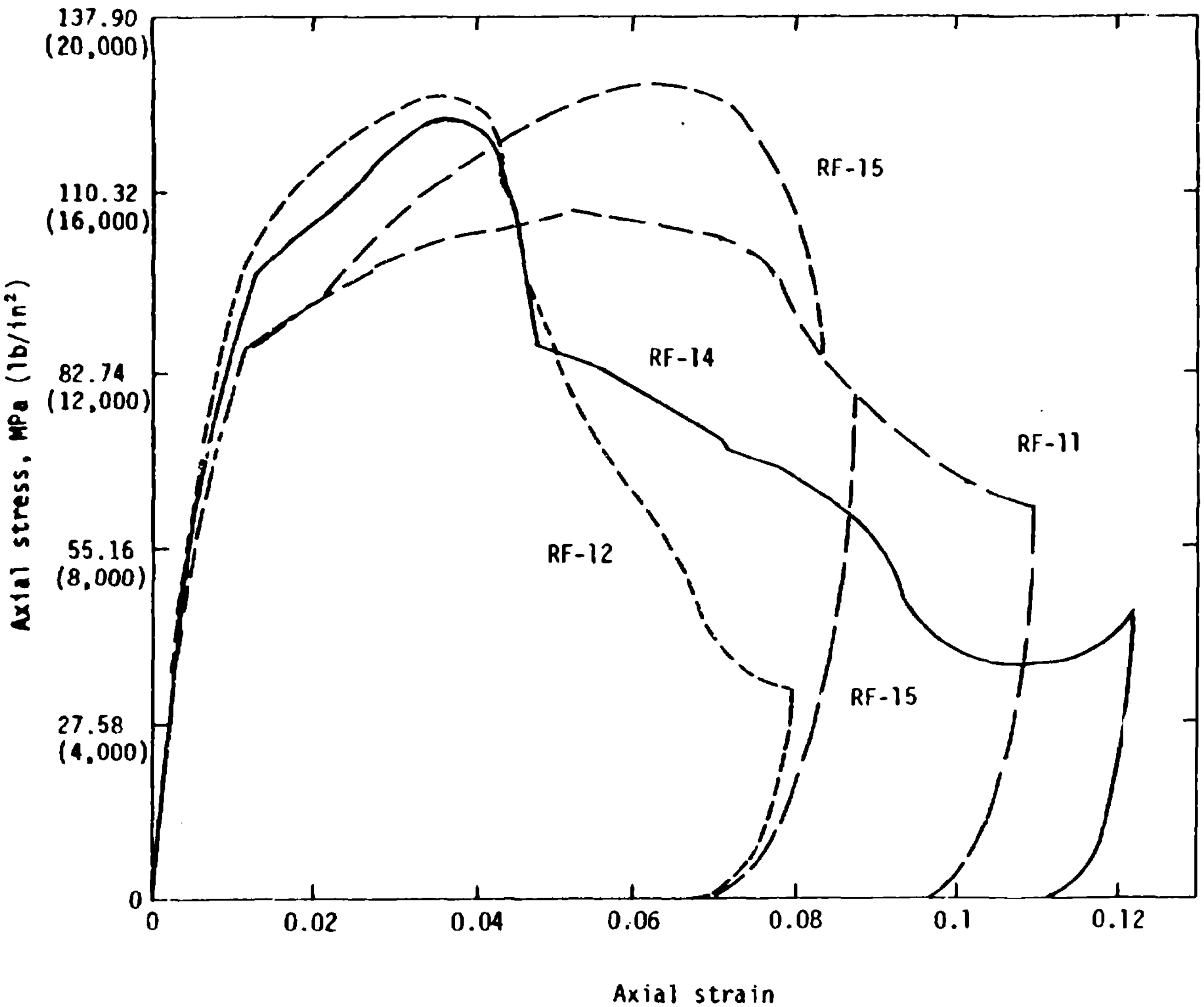

Figure 49. Uniaxial stress data for SIFCON 30/50.

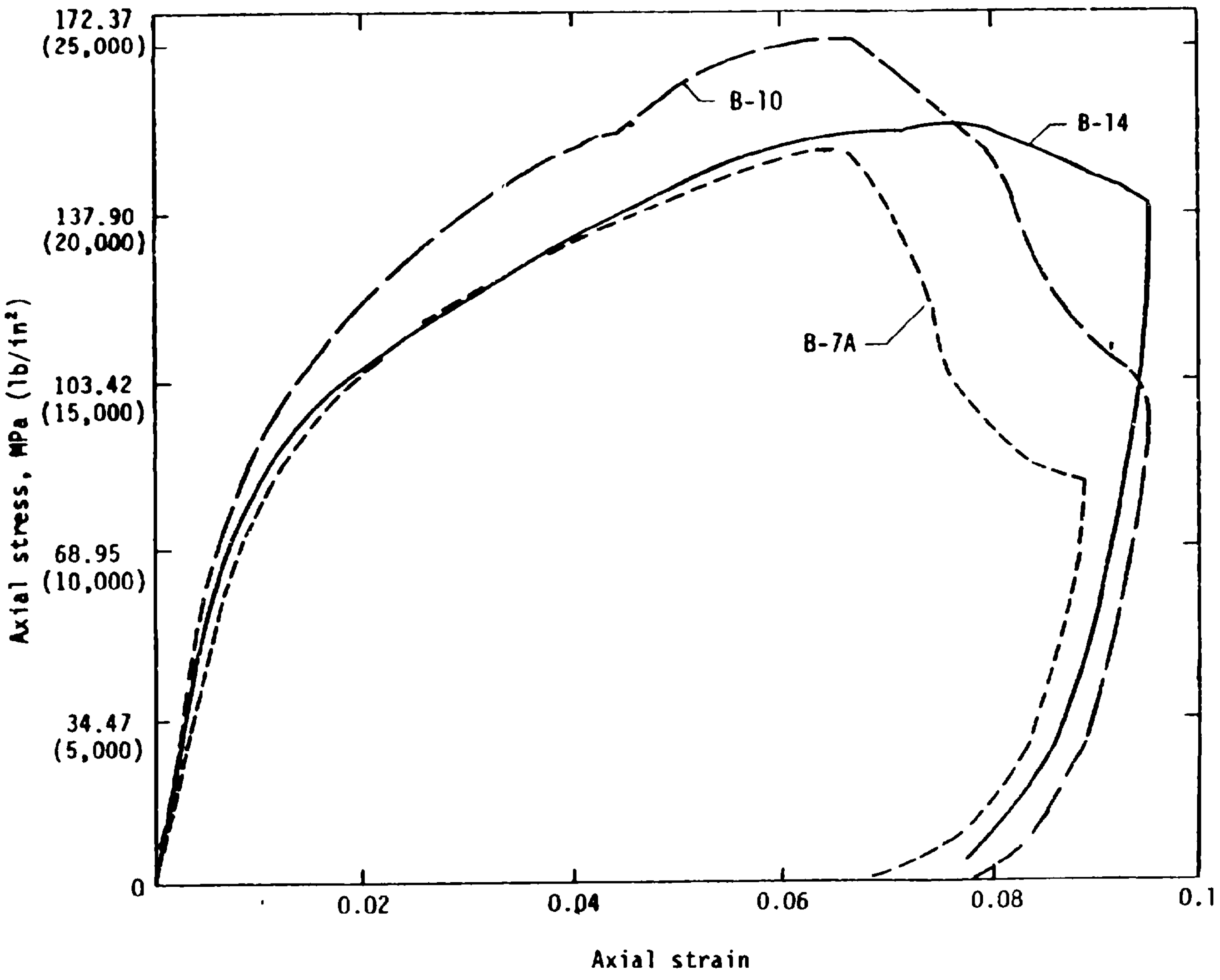

Figure 50. Uniaxial stress data for SIFCON 20/25.

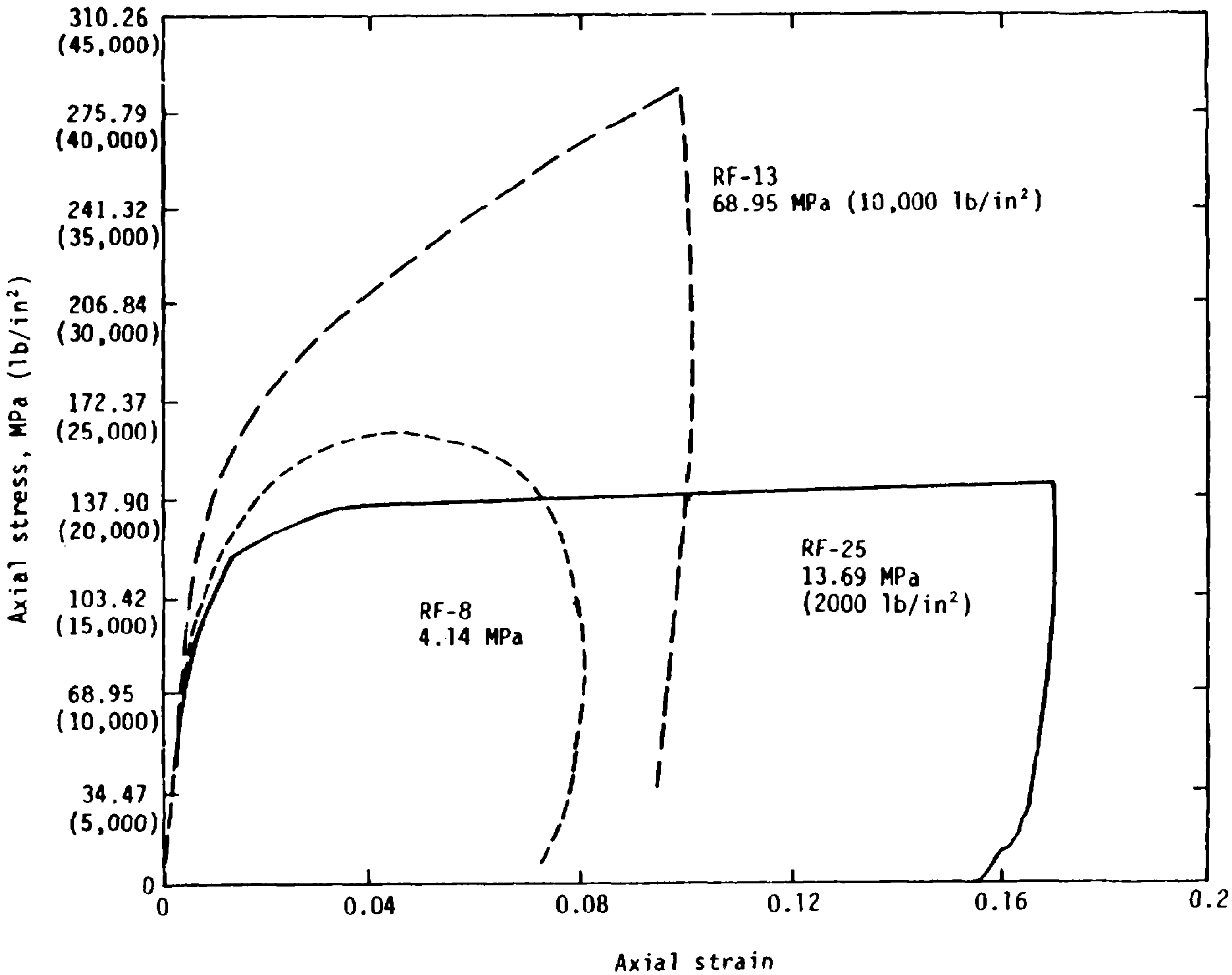

Figure 51. Triax data for SIFCON 30/50.

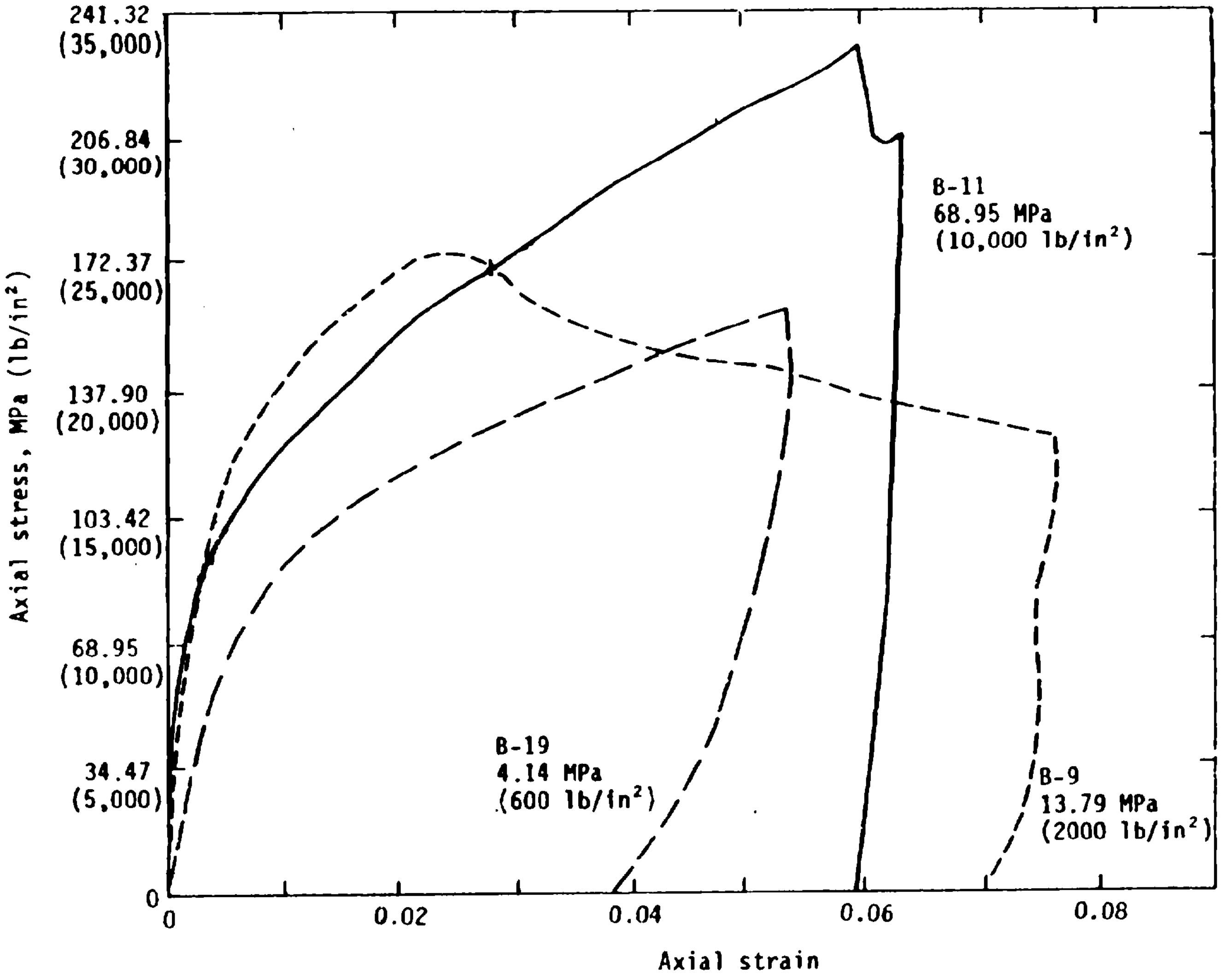

Figure 52. Triax data for SIFCON 20/25.

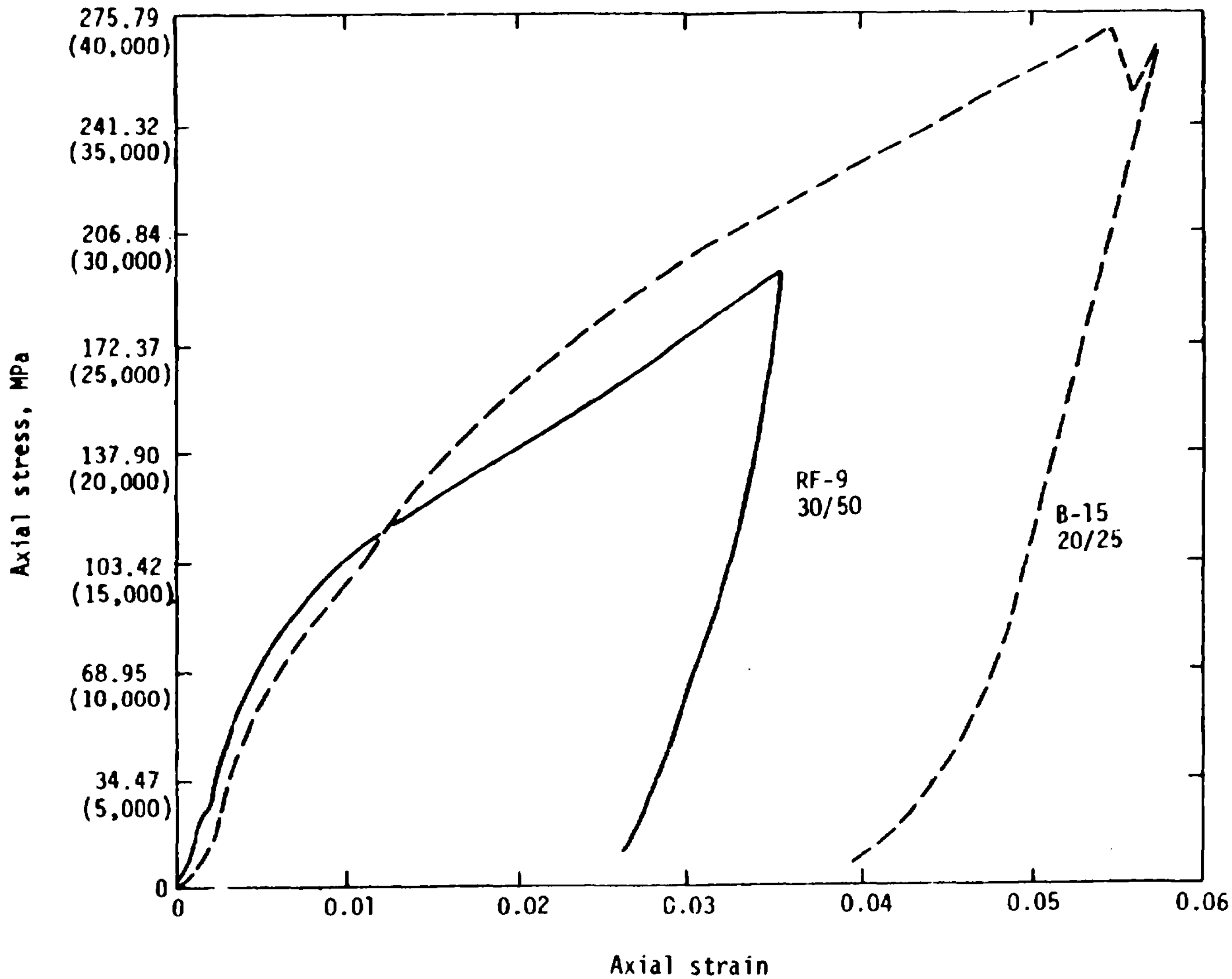

Figure 53. Uniaxial strain data for SIFCON--axial stress versus axial strain.

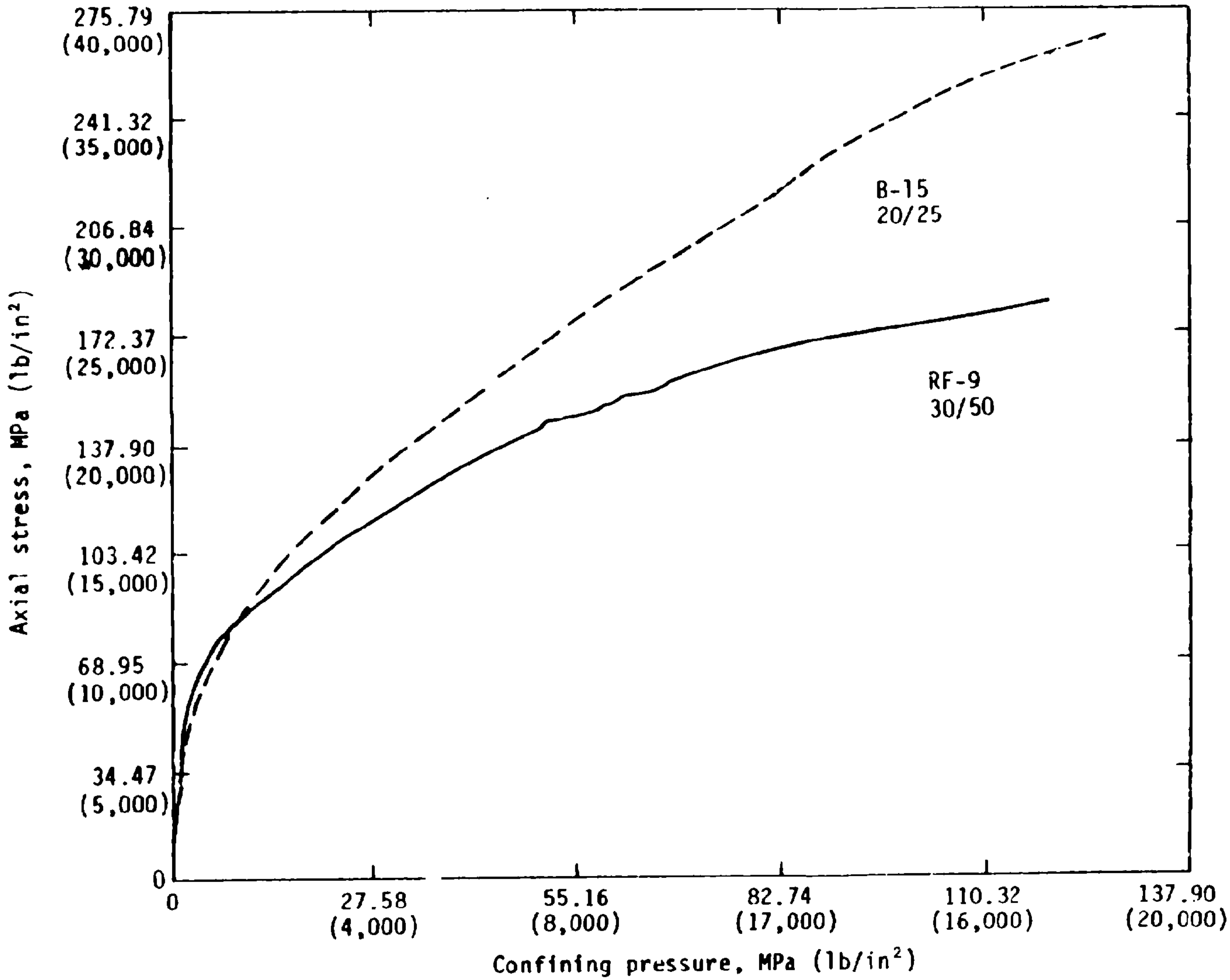

Figure 54. Uniaxial strain data for SIFCON--axial stress versus confining pressure.

TABLE 12. STATIC UNIAXIAL STRESS RESULTS

SIFCON	Specimen No.	E, MPa (lb/in²)	ν	Peak stress, MPa (lb/in²)	Peak strain
30/50	RF-11	10.7×10^6 (1.55×10^6)	0.213	108 (15,600)	0.051
	RF-12	17.0×10^6 (2.47×10^6)	0.216	125 (18,200)	0.039
	RF-15	10.3×10^6 (1.49×10^6)	0.176	127 (18,400)	0.065
	RF-14			123 (17,900)	~0.04
20/25	B7A	9.2×10^6 (1.34×10^6)	0.156	151 (21,900)	0.066
	B10	13.9×10^6 (2.01×10^6)	0.179	174 (25,300)	0.0675
	B14	12.0×10^6 (1.74×10^6)	0.224	157 (22,800)	0.0763

AFWL ENGINEERING MODEL

The AFWL engineering model is fully defined for the purpose of code calculations based upon two functional relationships--a yield function and a hydrostat. The yield function is a plot of $\sqrt{J_2'}$ (square root of the 2nd invariant of the stress deviator tensor) versus pressure at failure. This is also know as a failure surface. The hydrostat is a plot of bulk behavior of the material, i.e., a pressure-volume relationship.

In principal stress space $\sqrt{J_2'}$ and the pressure P can be written

$$\sqrt{J_2'} = \left\{\frac{1}{6}\left[(\sigma_1 - \sigma_2)^2 + (\sigma_1 - \sigma_3)^2 + (\sigma_2 - \sigma_2)\right]\right\}^{1/2} \qquad (1)$$

$$P = \frac{1}{3}(\sigma_1 + \sigma_2 + \sigma_3) \qquad (2)$$

where σ_i = 1, 2, 3 are the principal stresses. Points on the failure surface can be obtained by performing static tests that follow different stress paths.

For example, in an unconfined uniaxial stress test at failure, $\sigma_1 = f'_c$, $\sigma_2 = 0$, $\sigma_3 = 0$, and

$$\sqrt{J'_2} = \left\{\frac{1}{6}\left[(f'_c - 0)^2 + (f'_c - 0)^2 + (0 - 0)^2\right]\right\}^{1/2} \tag{3}$$

$$= 0.5774\ f'_c$$

$$P = \frac{1}{3}\ (f'_c + 0 + 0)$$

$$= \frac{1}{3}\ f'_c \tag{4}$$

Triaxial tests have shown that failure in concrete (and in the SIFCON materials) increases as a function of confining stress. Rather than finding specific points on the failure surface, an entire section of the surface can be found if the failure strength increases in a known manner as a function of confining stress. Assume that a linear relationship exists between confining stress and axial strength. Then at failure

$$\sigma_1 = f'_c + C\sigma \tag{5}$$

where $\sigma_2 = \sigma_3 = \sigma$ is the confining stress and C is a constant. The slope of the yield function beyond $P = 1/3\ f'_c$ can therefore be calculated as

$$\text{slope} = \frac{\Delta(\sqrt{J'_2})}{\Delta P}$$

$$= \frac{\left\{\frac{1}{6}\left[(f'_c + C\sigma - \sigma)^2 + (f'_c + C\sigma - \sigma)^2\right]\right\}^{1/2} - 0.5774\ f'_c}{\frac{1}{3}\ (f'_c + C\sigma + \sigma + \sigma) - \frac{1}{3}\ f'_c}$$

$$= \frac{\left\{\frac{2}{6}\left[(f'_c + C\sigma - \sigma)^2\right]\right\}^{1/2} - 0.5774\ f'_c}{\frac{C\sigma}{3} + \frac{2\sigma}{3}}$$

$$= \frac{0.5774\ (f'_c + C\sigma - \sigma) - 0.5774\ f'_c}{\frac{\sigma}{3}\ (C + 2)} = \frac{0.5774\ (C - 1)\sigma}{(C + 2)\ \frac{\sigma}{3}}$$

$$= \sqrt{3}\ \frac{(C - 1)}{(C + 2)} \qquad (6)$$

Another point on the failure surface can be determined from the tensile strength of the material. For uniaxial tension, $\sigma_1 = \sigma_T$, $\sigma_2 = \sigma_3 = 0$. Using these values in Equations 1 and 2 yields

$$\sqrt{J'_2} = 0.5774\ \sigma_T \qquad (7)$$

$$P = \frac{1}{3}\ \sigma_T$$

where σ_T is the tensile strength of the material. Between the points of uniaxial stress failure in tension and compression, a straight line is assumed.

The hydrostat describes the bulk or volume response of the material to the action of an hydrostatic pressure. The best kind of test to obtain this kind of response is the application of a hydrostatic pressure to the material. In the absence of such a test, other types of test data can be used. For the SIFCON material the uniaxial strain test is used to obtain the hydrostat.

Material models were developed from the available data for both of the materials tested. These are

SIFCON 30/50 Series RF
SIFCON 20/25 Series B

From Table 11 the unconfined compressive failure stress f'_c of the SIFCON can be estimated by averaging the peak stresses observed in the several tests. In addition, an estimate of failure at elevated confining

pressures can be obtained from Figures 50 and 51. Unfortunately, only one test was performed at each confining pressure, introducing considerable uncertainty into the confined failure stresses. Nevertheless, estimates of these failure stresses along with the unconfined compressive failure stress are shown in Table 13.

TABLE 13. COMPRESSIVE FAILURE STRESSES

Failure stress	f'_c, MPa (lb/in^2)	f'_c 600, MPa (lb/in^2)	f'_c 2000, MPa (lb/in^2)	f'_c 1000, MPa (lb/in^2)
SIFCON 30/50, Series RF	121 (17,520)	159 (23,000)	145 (21,000)	> 286 (>41,500)
SIFCON 20/25, Series B	161 (23,330)	159 (23,000)	172 (25,000)	> 228 (>33,000)

The tensile strengths of the samples were not tested in this program. However, flexure tests of some samples to be used in the ISST test program suggest values of σ_T of 20.7 MPa (3000 lb/in^2) for the SIFCON RF series. This value was also used for the SIFCON B series.

Using these values and Equations 3 through 7, plots of the yield functions are shown in Figures 55 and 56.

Hydrostatic behavior of the SIFCON material was obtained from the uniaxial strain tests. Using Figures 53 and 54, the hydrostatic response can be calculated. For unloading, the initial slope (approximately) is used (Figs. 57 and 58).

Note that these material models are based upon static test data only. At high strain rates (3/s to 35/s) the strengths observed in the dynamic uniaxial stress tests were greater than the static strengths by 33 percent and 9 percent for SIFCON 30/50 series RF and SIFCON 20/25 series B, respectively. Moreover, the capacity limitations of the DMSA and drop table

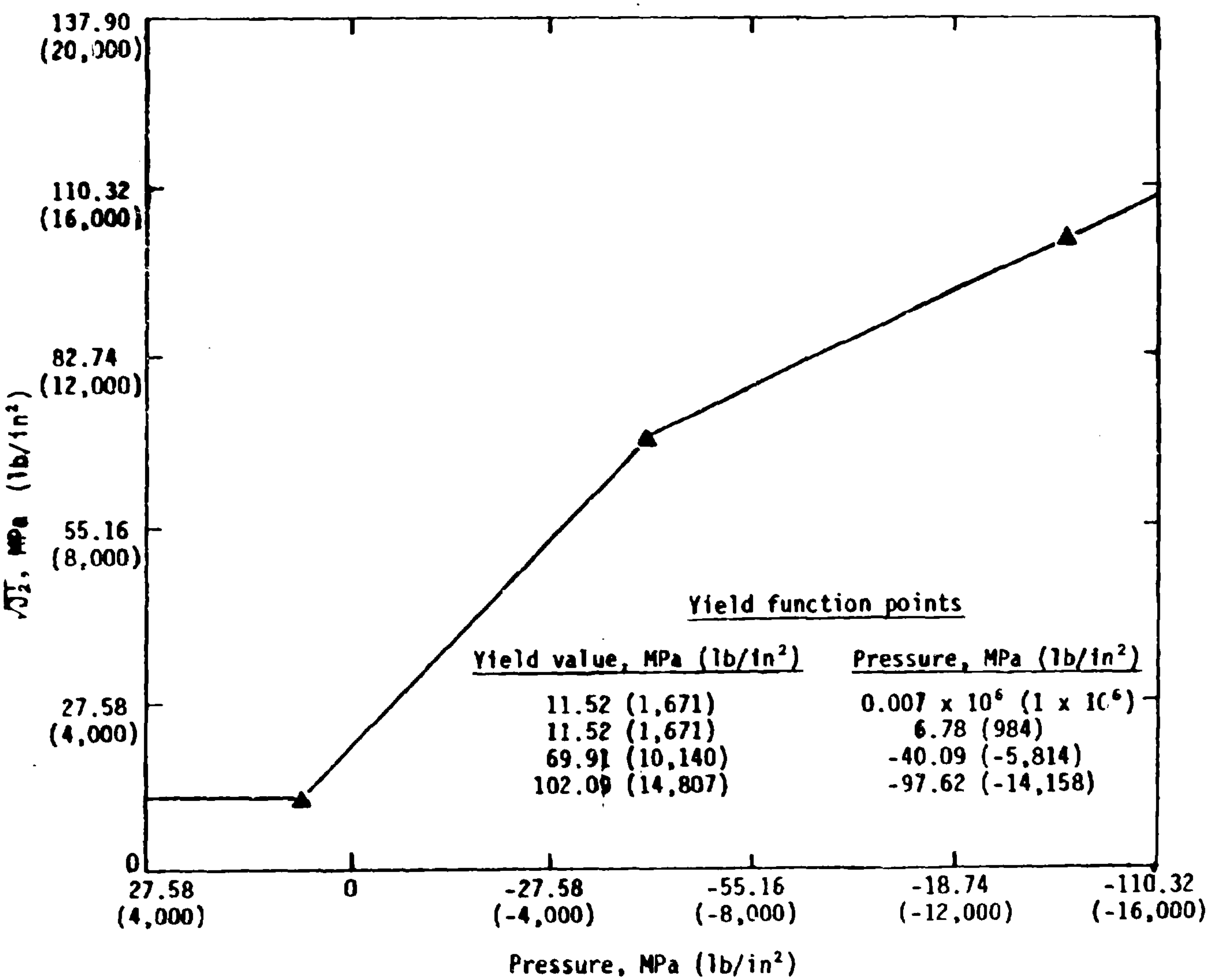

Figure 55. SIFCON 30/50 RF series yield surface.

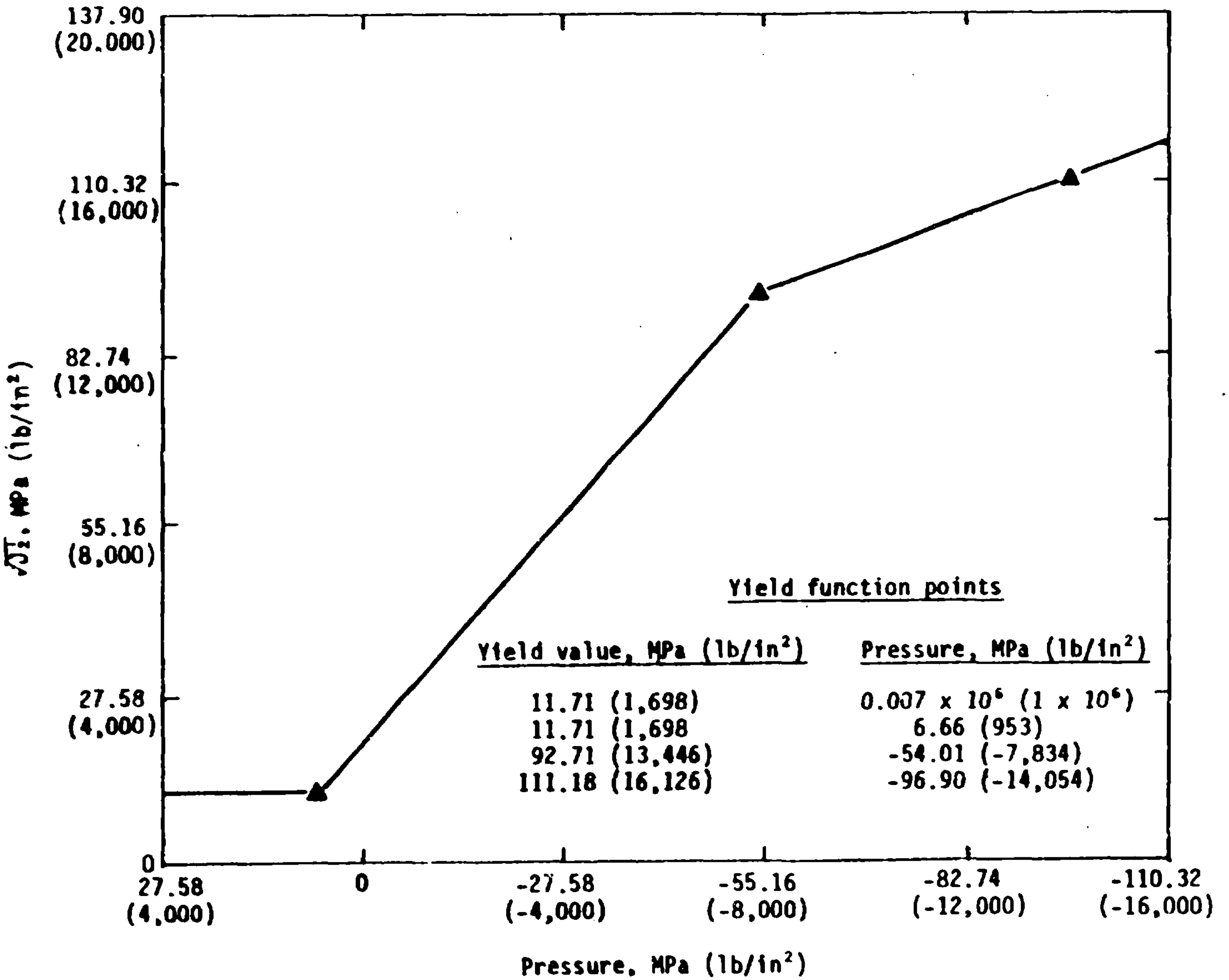

Figure 56. SIFCON 20/25 B series yield surface.

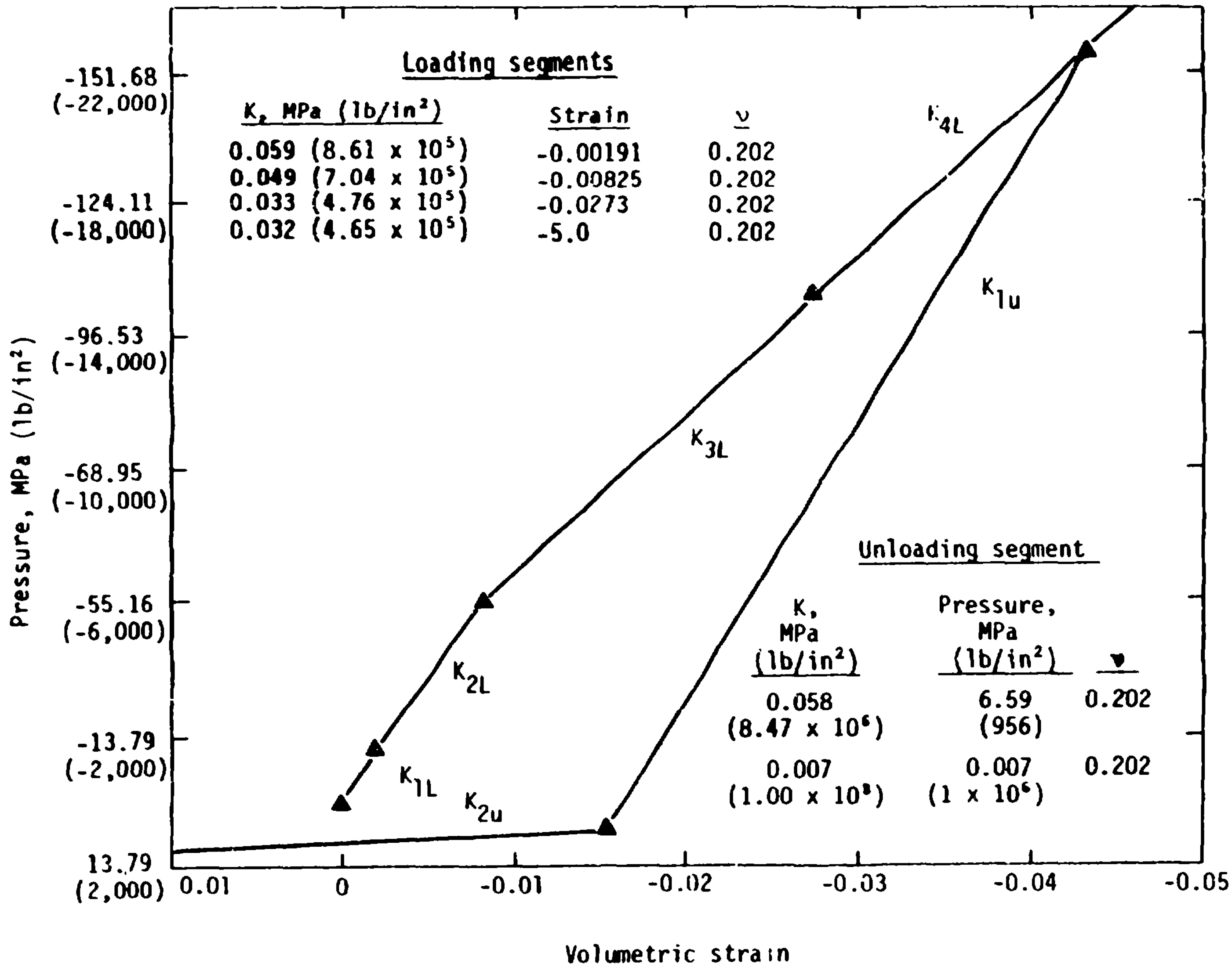

Figure 57. SIFCON 30/50 RF series hydrostat.

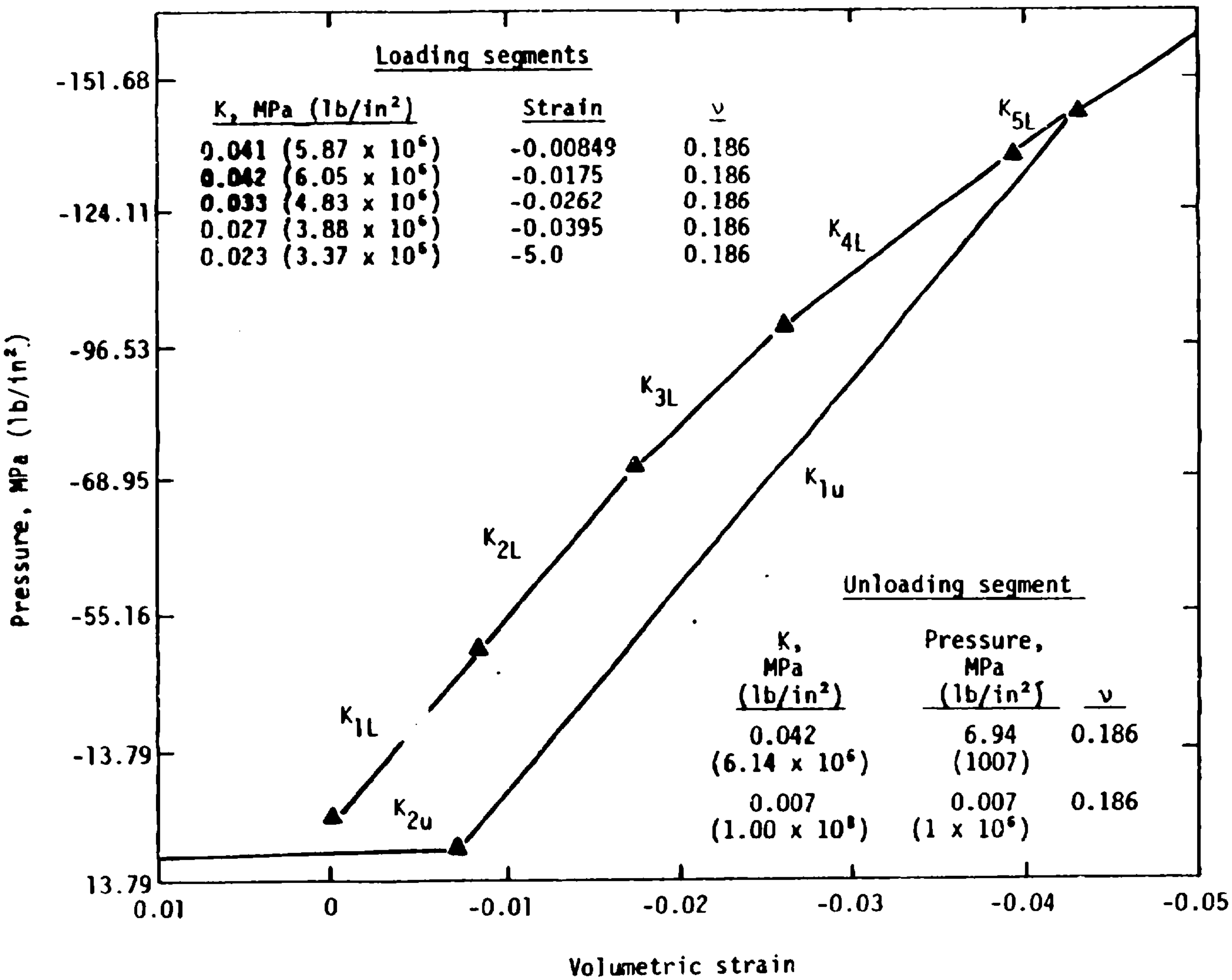

Figure 58. SIFCON 20/25 B series hydrostat.

prevented the attainment of a well-defined failure in the SIFCON specimens on the first drop. The most severe damage level achieved in the test of a virgin SIFCON specimen corresponded to a condition of surface spallation around the waist of the specimen (Fig. 46). This was arbitrarily defined as failure though the specimens were otherwise quite sound and could support additional load. It is quite possible therefore that the dynamic strength of the SIFCON was actually greater than that indicated by the 33 percent and 9 percent increases indicated above.

It must also be emphasized that the SIFCON samples tested in this series were loaded in a direction perpendicular to the fiber plane The fiber plate is generated by the process of fabrication of the SIFCON material. Prior to the injection of the slurry matrix, the fibers are generally rained into the form under the action of gravity and tend to come to rest in a horizontal position. This process tends to create a SIFCON material away from the form boundaries that is anisotropic, or more precisely, transversely isotropic. The direction of greatest strength in the SIFCON material is in the direction perpendicular to the fiber plane.

For loads parallel to the fiber plane the strength of the SIFCON is considerably reduced. Although not specifically reported herein, several drop tests were performed on SIFCON samples for a different batch, some of which were loaded parallel to the fiber planes. On average, these parallel-loaded specimens failed at a stress level 45 percent below that for those loaded perpendicular to the fiber plane.

IV. POSTTEST OBSERVATIONS

INTRODUCTION

This section reviews the qualitative observations made by NMERI of the generic silo model following the test. The analysis of the gage data was done by AFWL and will be reported in a separate document.

The two areas of obvious interest following the test were the condition of the SIFCON walls and the steel liner plates. In addition, observations were made of the newly designed instrumention cable protection system and the mounting system for the high-speed camera to determine if there were any problems with their operation.

MODEL RESPONSE

Closure--Examination of the closure following the test found it to be still securely anchored in the headworks. The closure bolts were easily removed; however, the lid was jammed in the headworks. When the lid was eventually removed, it was discovered that the gypsum-based slurry used to seal the gap between the lid and the headworks had been deformed in the gap from the airblast loading. The slurry material was so tightly compressed between the lid and the headworks that it apparently jammed the lid.

Virtually no deformation of the steel side liner of the lid was observed and only a slight dishing of the bottom steel plate was noted. Only slight surface blemishes were observed in the SIFCON material in the lid. The lead seal was severely deformed from its original 6-mm (0.25-in) thickness to less than 3 mm (0.125 in) thick. In addition, it appeared some of the lead material had been squeezed inward and fallen to the bottom of the model. No discernible deformation of the closure bolts was observed.

Inner liner--Two horizontal ripples, running all around the circumference, were noted in the vertical headworks liner plate. One was at a point directly under the closure bearing plate, about 280 mm (11.0 in) from the top of the model. The second was at a point just above the start of

the transition plate, or about 550 mm (21.5 in) from the top of the model. It was estimated that the ripples protruded into the opening no more than 3 mm (0.125 in).

Further down, at a point about 1.08 m (42.5 in) from the top of the model, another very small ripple or buckle was observed in the wall liner plate. While not as pronounced as the ripple in the headworks liner plate, it too ran completely around the circumference. The location of this ripple was just below the end of the transition gusset plates in the wall of the model.

A large buckle was observed in the wall liner plate at a point about 1.4 m (55.0 in) from the top of the model as shown in Figure 59. This buckle ran all around the circumference of the plate and uniformly protruded inside about 60 mm (2.25 in). The projected vertical dimension of the buckle was estimated to be about 85 mm (3.3 in). This seemed to indicate a vertical compression at this point of about 65 mm (2.5 in).

The largest buckle in the wall liner plate was observed at a point 3.0 m (120.0 in) from the top of the model as shown in Figure 60. This location corresponded with the horizontal weld between two liner plates. This buckle, which also ran completely around the circumference of the liner plate, protruded into the model an average of 75 mm (3.0 in) and a maximum of 120 mm (4.75 in) at one point. The projected vertical dimension of the buckle was estimated at about 90 mm (4.0 in), or an average compression of about 85 mm (3.4 in). As can be seen in Figure 60, this buckle has the same appearance of a classic buckling failure of a thin-walled cylinder under an axial load.

Despite the large deformations in the inner liner plate, no tears in the plate or exposed SIFCON was observed.

Outer liner plate--The soil around the outside of the model had been excavated to a depth of about 5.1 m (200 in) below the top of the model. Two major deformations in the outer liner plate were observed in that length. One was just below the first horizontal weld, or at a point about 1.57 m (62.0 in) below the top of the model. At that point, the liner plate

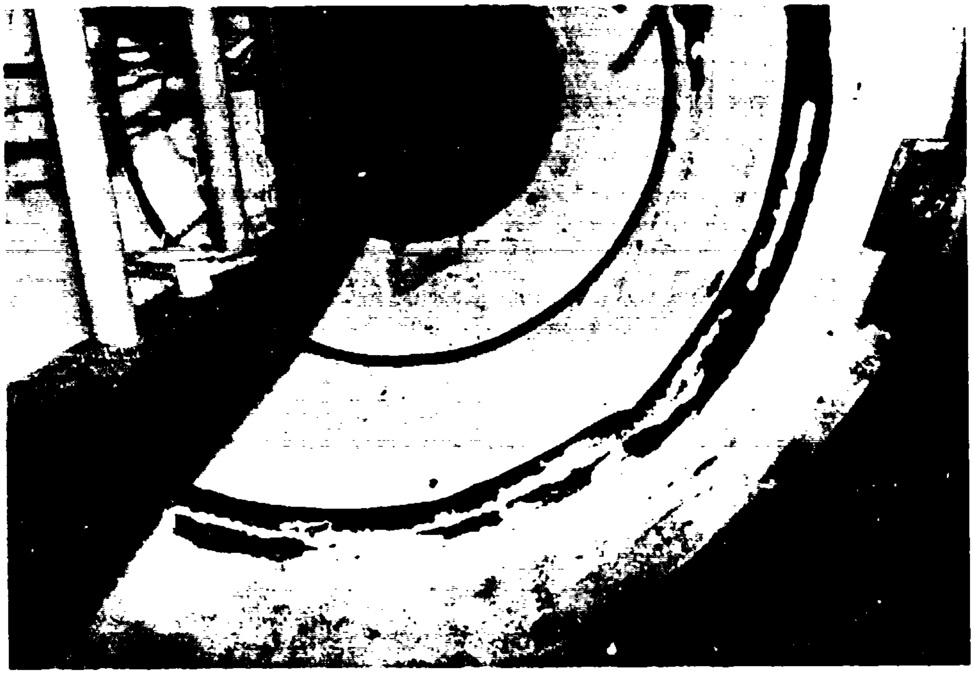

Figure 59. Large buckle in wall liner plate 1.4 m from top of model.

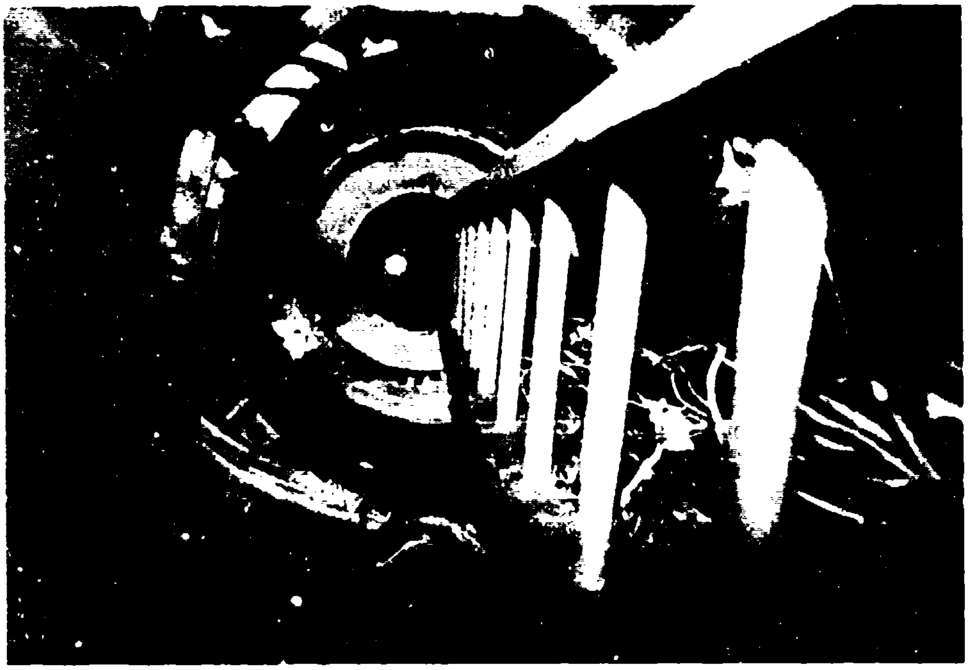

Figure 60. Buckle in liner plate at 3.0 m from top of model.

appeared to have been torn horizontally just below the weld and peeled downward, as shown in Figure 61. This condition generally existed all around the circumference of the model in a fairly uniform manner. Closer examination showed that the exposed SIFCON was not crushed or cracked in any way. Also, all tears in the plate occurred in the base metal rather than in the weld.

The second major deformation was noted at a point just below the second horizontal liner joint, or about 3.2 m (125 in) below the top of the model. The buckle was very similar in appearance to the one above near the first horizontal joint. As before, the liner was torn and buckled, exposing the SIFCON. In general, the deformation consisted of a single fold or buckle. However, in a few locations around the circumference, the deformation was made up of two smaller folds.

Examination of the outside of the structure, down past the third liner joint at 4.5 m (180 in) below the top of the model, showed no additional folds or buckles in the liner plate.

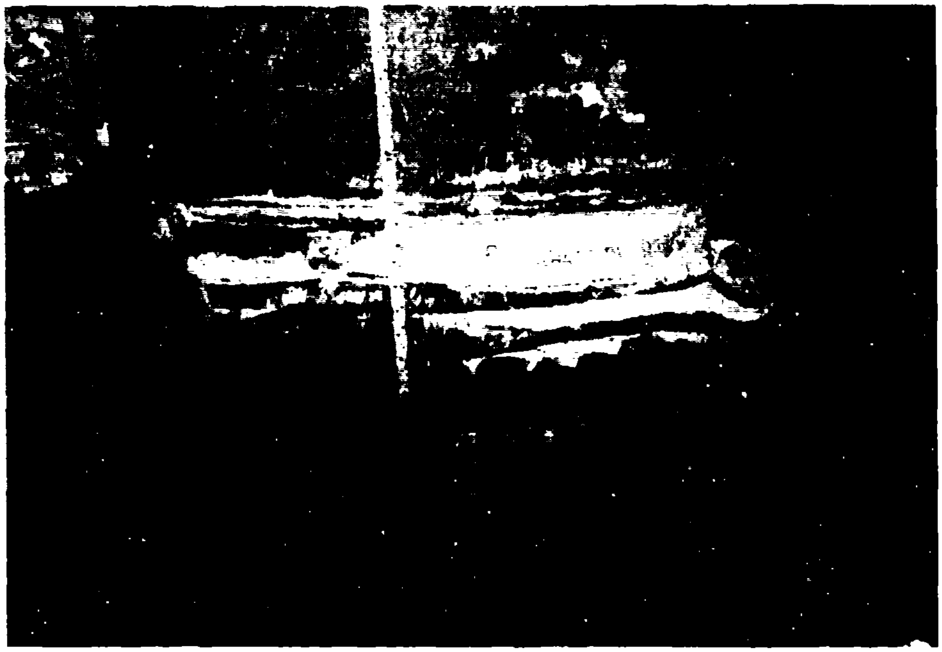

Figure 61. Deformation of outer liner plate below first horizontal weld 1.57 m from top of model.

Cable egress--During the excavation of the model, approximately 5.0 m (15.0 ft) of the cable protection piping was exposed. The examination of the system found that piping had not pulled apart at the model wall or at any of the two exposed joints. However, it had been pulled to its full extension at the second joint from the wall. A look inside the model showed that the bundle of instrumentation cable was still in the pipe but had been torn from the gages' lead wires.

High-speed camera mounting--The mounting system worked as expected since the protective box was found in the catch net. The camera was recovered intact from inside the protective box. The only damage noted was a broken lens, apparently caused by a fragement of the lead seal on the closure. A review of the film showed in excess of 100 ms of excellent quality documentation. Even though the camera continued to operate for much longer, dust and debris flying about inside the model made later time documentation quite difficult. The camera stopped when the power cord was severed at the camera motor.

PASSIVE PUNCH GAGES

Because of the harsh environment to which the structure would be subjected, some concern was expressed before the test about the length of time the active instrumentation would function before the cables were severed. In an attempt to have some sort of low-cost backup system, NMERI installed a series of punch marks on the outer liner of the model. The system used was a set of 10 vertical pairs of punch marks at various locations on the outer liner plate. The distance between the punch marks in each of the 10 pairs was measured with a vernier caliper before the model was backfilled prior to the test. Following the test, the measurements were taken again, and compared to the original measurements, providing a rough approximation of vertical strains in the structure. Table 14 presents the data obtained from the punch gages.

While a precise quantative analysis of such data is meaningless, one can detect a general pattern. An ever increasing strain can be seen as the distance from the top of the model increases. This pattern exists up to the first horizontal liner joint where the large buckle in the liner plate

TABLE 14. PASSIVE PUNCH GAGE RESULTS

Location	Distance from top, mm (in)	Pretest dimension, mm (in)	Posttest dimension, mm (in)	Change, mm (in)	Percent change
90° Azimuth					
A	171 (6.75)	81.79 (3.220)	81.08 (3.192)	0.71 (0.028)	0.87
B	572 (22.50)	103.66 (4.081)	101.88 (4.011)	0.78 (0.070)	1.69
C	1048 (41.25)	127.05 (5.002)	124.38 (4.897)	2.67 (0.105)	2.10
D	[a]1514 (59.63)	109.45 (4.309)	N/A[b]	--- -----	----
E	2131 (83.91)	106.04 (4.175)	106.09 (4.177)	-0.05 (-0.002)	-0.05
F	2426 (95.53)	126.80 (4.992)	126.67 (4.987)	0.13 (0.005)	0.10
G	[c]3050(120.06)	94.89 (3.736)	N/A[b]	--- -----	----
270° Azimuth					
H	127 (5.00)	102.39 (4.031)	101.98 (4.015)	0.41 (0.016)	0.40
I	502(19.75)	65.86 (2.593)	61.65 (2.427)	4.21 (0.166)	6.40
L	[a]1514(59.63)	86.51 (3.406)	86.08 (3.389)	0.43 (0.017)	0.50

[a]Liner weld at 243 mm (59.56 in) from top.

[b]Liner buckled.

[c]Liner weld at 3035 mm (119.50 in) from top.

occurred. Although not as clear as in the upper 1.5 m (60.0 in), there is some evidence that the pattern begins to repeat itself in the next lower 1.5 m (60.0 in).

REVIEW AND RECOMMENDATIONS

The condition observed which would be considered a detriment to the proper functioning of the structure is obviously the large deformations and buckles in both the inner and outer liner plates. Following is a theory that might be considered as a possible explanation to the problem.

It is suspected that the root of the problem is the construction method used for the fabrication of the joints between the several lifts of slurry. The method described earlier in Section II had been shown to produce an adequate horizontal joint ONLY if the fibers from the higher lift interlock with those in the adjacent lower lift. This did not seem to be the case in this model. When placing the slurry, it was observed that the slurry eventually had to be poured over most of the entire surface of the fiber bed as the specified pouring locations became clogged with fly ash lumps. Even though the level of the slurry did not submerge the top of the fiber bed as specified, the top fibers still became coated with the slurry. This coating of slurry on the fibers caused the top surface of the fiber bed to be stuck together in a semirigid condition. When the next lift of fibers was placed they could not properly interlock with the coated fibers in the lift below. In addition to not having the fibers properly interlocked, the coated fibers would also present smaller openings for the slurry to infiltrate. If the openings were too small the slurry could not penetrate and a series of small voids would be formed. As a result, a discontinuity of some thickness was formed in the SIFCON wall at every lift. During the test, the discontinuity provided an ideal location for the SIFCON to crush. The liner plate buckled, being unrestrained by the crushed SIFCON and under a high strain.

The basis for this theory is that the major liner buckles are located only at the construction joints. In addition, the large amount of vertical compression witnessed at the buckled liner and the large amount of liner material protruding into the model seemed to indicate a much weaker material at the joints, possibly filled with voids, than in the rest of the model.

It is believed that, if cores were taken at each joint location, one might find a section of unreinforced or lightly reinforced slurry that had been crushed due to the axial load.

A solution to the problem would be to pump the slurry up from the bottom of the structure. In fact, this method would probably solve many of the difficulties reported with the slurry placement in Section II. First, it would eliminate the question of fibers interlocking between lifts, as all the fibers could be placed before any of the slurry was installed. Second, it would minimize the problem of knowing if the wall was completely full of slurry because it would always be installed under some pressure head.

A second condition is the liner plates. Under load, the SIFCON can experience large strains and yet still remain intact and functional. The liner plate on the other hand may buckle under the same load. The size and location of the buckle is a function of the liner thickness, curvature, and anchor stud spacing. In addition, the condition of the SIFCON as a supporting medium also contributes to the way in which the liner will buckle. Because SIFCON is different than conventional concrete, the techniques used to design the liner plate in a SIFCON structure may not necessarily be the same as for a concrete structure. The procedures to determine the design of the liner plate need to be established.

It is recommended that the liner plate design should be such that a series of many "small" buckles are formed rather than one or two large buckles. Probably a very thin cylindrical plate or a corrugated plate would meet the criteria.

Finally, it is recommended that future tests on SIFCON silo models be designed so that the results can be directly compared with other designs. For example, the question "Would the large buckles in the inner liner plate have formed under the less harsh environment used on the other concrete structures?" cannot really be answered without a comparable test.

In summary, this testing program has demonstrated the potential of SIFCON as a future material for hardened structures. Like most first-time tests, many questions were raised. With an adequate research and development effort, an economical design for a superhard missile silo should be achievable in the near future.

APPENDIX A

INSTRUMENTATION MEASUREMENT LIST AND WIRING DIAGRAMS

MEASUREMENT LIST

Measurement Number Assignment

Acceleration	
Radial	1601-1603
Vertical	1701-1708
Steel Strain	3601-3625
Concrete Strain	4601-4613
Relative Displacement	
Passive	P001-P002
Developmental Gages (from AFWL)	E001-E007

General Location

CW - Generic Silo Concrete Wall

LD - Generic Silo Lid

LN - Generic Silo Liner

FL - Generic Silo Floor

Structure Coordinate System

Y Axis - The Y-axis is positive in a direction, starting at the top, moving toward the bottom of the fixture.

R Axis - 0 at the center of the structure, positive in the direction from the center toward the outside.

Θ Axis - The angle of rotation is positive in the clockwise position.

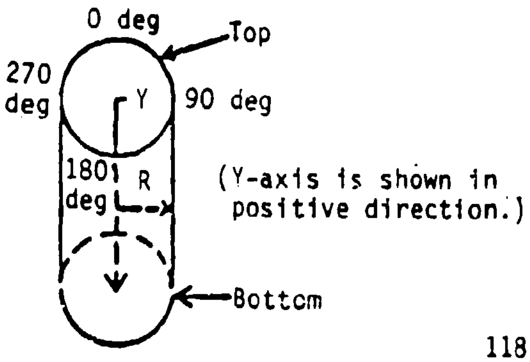

Sensing Axis

Y - Vertical, parallel to longitudinal silo axis.

R - Radial, perpendicular to vertical axis.

C - Circumferential, horizontal and normal to the radial vector.

θ - Angle of rotation of a radial vector from 0-deg reference point.

Sensing Polarity

Concrete Strain, Steel Strain

+ Compression
- Tension

Accelerometers

+ Motion in + Sensing axis direction

- Motion in - Sensing axis direction

Transducers

Accelerometers - 11

Concrete Strain - 13

Steel Strain - 25

Relative Displacement (Passive) - 2

Developmental Gages (from AFWL) - 7 (includes measurement numbers 1707 and 1708)

MEASUREMENT LIST | DATE MAY 29, 1984 | PAGE 1 OF 7 PAGES

TEST EVENT SIFCON ISST/HFC-2 (SS 8.36) | IPO KIRST

MEAS. NO.	LOCATION GEN	Y	R	θ	SENS. AXIS	PRED. MAX.	REQ. RESP.	TRANSDUCER MODEL	RANGE			CHANGES ITEM	AUTH.	DATE
3601	LN	1.375	21.250	270	Y			Alltech SG159-11-10-65	±20,000 με	Weldable	Welded to liner			
3602	LN	5.750	21.250	0	Y			Alltech SG159-11-10-65	±20,000 με	Weldable	Welded to liner			
3603	LD	5.750	13.625	195	Y			Alltech SG159-11-10-65	±20,000. με	Weldable	Welded to liner			
3604	LD	8.500	13.375	15	Y			Alltech SG159-11-10-65	±20,000 με	Weldable	Welded to liner			
3605	LD	8.500	13.375	255	Y			Alltech SG159-11-10-65	±20,000 με	Weldable	Welded to liner			
3606	LN	8.750	21.250	180	Y			Alltech SG159-11-10-65	±20,000 με	Weldable	Welded to liner			
3607	LN	8.750	21.250	270	Y			Alltech SG159-11 10-65	±20,000 με	Weldable	Welded to liner			
3608	LN	9.750	9.750	0	Y			Alltech SG159-11-10-65	±20,000 με	Weldable	Welded to liner			
3609	LN	9.750	9.750	270	Y			Alltech SG159-11-10-65	±20,000 με	Weldable	Welded to liner			
3610	LN	15.750	9.750	180	Y			Alltech SG159-11-10-65	±20,000 με	Weldable	Welded to liner			
3611	LN	23.000	9.970	180	Y			Alltech SG159-11-10-65	±20,000 με	Weldable	Welded to liner			
3612	LN	23.000	9.970	270	Y			Alltech SG159-11-10-65	±20,000 με	Weldable	Welded to liner			

MEASUREMENT LIST

DATE MAY 29, 1984 | PAGE 2 OF 7 PAGES

TEST EVENT: SIFCON ISST/HFC-2 (SS 8.36) | IPO: KIRST

MEAS. NO.	LOCATION				SENS. AXIS	PRED. MAX	REQ. RESP.	TRANSDUCER				CHANGES		
	GEN	Y	R	θ				MODEL	RANGE			ITEM	AUTH.	DATE
3613	LN	28.500	12.375	0	Y			Alltech SG159-11-10-65	±20,000 με	Weldable	Welded to liner			
3614	LN	28.500	21.250	0	Y			Alltech SG159-11-10-65	±20,000 με	Weldable	Welded to liner			
3615	LN	34.000	14.780	180	Y			Alltech SG159-11-10-65	±20,000 με	Weldable	Welded to liner			
3616	LN	35.000	15.000	0	Y			Alltech SG159-11-10-65	±20,000 με	Weldable	Welded to liner			
3617	LN	35.000	21.250	180	Y			Alltech SG159-11-10-65	±20,000 με	Weldable	Welded to liner			
3618	LN	35.000	15.000	270	Y			Alltech SG159-11-10-65	±20,000 με	Weldable	Welded to liner			
3619	LN	90.000	15.000	180	Y			Alltech SG159-11-10-65	±20,000 με	Weldable	Welded to liner			
3620	LN	90.000	21.250	270	C			Alltech SG159-11-10-65	±20,000 με	Weldable	Welded to liner			
3621	LN	125.000	15.000	0	Y			Alltech SG159-11-10-65	±20,000 με	Weldable	Welded to liner			
3622	LN	175.000	21.250	180	Y			Alltech SG159-11-10-65	±20,000 με	Weldable	Welded to liner			
3623	LN	175.000	15.000	270	Y			Alltech SG159-11-10-65	±20,000 με	Weldable	Welded to liner			
3624	LN	250.000	21.250	0	Y			Micro Measurements CEA-06-125UW-350	±5%	Epoxy	Epoxied to liner			

MEASUREMENT LIST

DATE MAY 29, 1984

TEST EVENT SIFCON ISST/HFC-2 (SS 8.36)

IPO KIRST

MEAS. NO.	LOCATION GEN	Y	R	Θ	SENS. AXIS	PRED. MAX.	REQ. RESP.	TRANSDUCER MODEL	RANGE			CHANGES ITEM	AUTH.	DATE
3625	LN	250.000	15.000	270	Y			Micro Measurements CEA-06-125UW-350	±5%	Epoxy	Epoxied to liner			
4601	CW	3.750	18.250	270	Y			Micro Measurements EA-06-5006	±5%	Epoxy	Rebar suspended in concrete			
4602	CW	8.500	18.250	270	Y			Micro Measurements EA-06-5006	±5%	Epoxy	Rebar suspended in concrete			
4603	CW	12.000	12.125	270	Y			Micro Measurements EA-06-5006	±5%	Epoxy	Rebar suspended in concrete			
4604	CW	23.000	18.250	0	Y			Micro Measurements EA-06-5006	±5%	Epoxy	Rebar suspended in concrete			
4605	CW	34.500	18.250	180	Y			Micro Measurements EA-06-5006	±5%	Epoxy	Rebar suspended in concrete			
4606	CW	35.000	18.250	0	Y			Micro Measurements EA-06-5006	±5%	Epoxy	Rebar suspended in concrete			
4607	CW	35.000	18.250	270	Y			Micro Measurements EA-06-5006	±5%	Epoxy	Rebar suspended in concrete			
4608	CW	47.250	18.250	0	Y			Micro Measurements EA-06-5006	±5%	Epoxy	Rebar suspended in concrete			
4609	CW	90.000	18.250	0	Y			Micro Measurements EA-06-5006	±5%	Epoxy	Rebar suspended in concrete			
4610	CW	125.000	18.250	0	Y			Micro Measurements EA-06-5006	±5%	Epoxy	Rebar suspended in concrete			

MEASUREMENT LIST

DATE MAY 29, 1984

TEST EVENT SIFCON 1SST/HFC-2 (SS 8.36)

IPO KIRST

MEAS. NO.	LOCATION GEN	Y	R	θ	SENS. AXIS	PRED. MAX.	REQ. RESP.	TRANSDUCER MODEL	RANGE			CHANGES ITEM	AUTH.	DATE
4611	CW	150.000	18.250	0	Y			Micro Measurements EA-06-5006	±5%	Epoxy	Rebar suspended in concrete			
4612	CW	210.000	18.250	0	Y			Micro Measurements EA-06-5006	±5%	Epoxy	Rebar suspended in concrete			
4613	CW	250.000	18.250	180	Y			Micro Measurements EA-06-5006	±5%	Epoxy	Rebar suspended in concrete			
1601	CW	6.875	14.875	180	R	8 Kg		Endevco 2264A	50 Kg		Epoxy mounting block			
1602	LN	20.750	9.750	180	R	7 Kg		Endevco 2264A	20 Kg	NMERI Mount				
1603	LN	125.000	15.000	270	R	2.5 Kg		Endevco 2264A	5 Kg	NMERI Mount				
1701	LD	9.000	0	--	Y	30 Kg		Endevco 2664A	50 Kg		Directly bolted to lid			
1702	LN	8.750	14.875	180	Y	15 Kg		Endevco 2264A	50 Kg	NMERI Mount				
1703	LN	20.750	9.750	180	Y	9 Kg		Endevco 2264A	20 Kg	NMERI Mount				
1704	LN	47.500	15.000	180	Y	7.5 Kg		Endevco 2264A	20 Kg	NMERI Mount				

MEASUREMENT LIST												DATE MAY 29, 1984	PAGE 5 OF 7 PAGES		
TEST EVENT SIFCON ISST/HFC-2 (SS 8.36)									IPO KIRST						
MEAS. NO.	LOCATION				SENS. AXIS	PRED. MAX.	REQ. RESP.	TRANSDUCER					CHANGES		
	GEN	Y	R	Θ				MODEL	RANGE				ITEM	AUTH.	DATE
1705	LN	125.000	15.000	270	Y	6.5 Kg		Endevco 2264A	20 Kg	NMERI Mount					
1706	FL	252.000	0	--	Y	3.5 Kg		Endevco 2264A	20 Kg	NMERI Mount	Directly bolted to floor				
P001	LN	90.000	15.000	180	Y										
P002	LN	175.000	15.000	270	Y										
E001	CW	--	18.875	0	Y			ISG			Air blast load				
E002											Not used				
E003	LN	15.750	21.250	150				NS	25 K	NS Gage Mount					
E004	LN	15.750	21.250	300				¼ Bridge ISG			Air blast load				
E005	LN	90.000	21.250	90				NS	25 K	NS Gage Mount					
E006	LN	90.000	21.500	135	R			SMI Normal							

MEASUREMENT LIST

DATE MAY 29, 1984

TEST EVENT SIFCON ISST/HFC-2 (SS 8.36)

IPO KIRST

MEAS. NO.	LOCATION GEN	Y	R	Θ	SENS. AXIS	PRED. MAX.	REQ. RESP.	TRANSDUCER MODEL	RANGE			CHANGES ITEM	AUTH.	DATE
E006A	LN	90.000	21.500	135	Y			SMI Vertical						
E007											Not used			

MEASUREMENT LIST												DATE MAY 31, 1984	PAGE 7 OF 7 PAGES		
TEST EVENT SIFCON ISST/HFC-2 (SS 8.36)										ITPO KIRST					
MEAS.	LOCATION				SENS.	PRED.	REQ.	TRANSDUCER					CHANGES		
NO.	GEN	Y	R	Θ	AXIS	MAX.	RESP.	MODEL	RANGE				ITEM	AUTH.	DATE
1707	LN	47.500	15.000	180 + 1"	Y	7.5 Kg		Endevco 2264A	20 Kg	"Soft" Mount					
1708	LN	47.500	15.000	180 - 1"	y	7.5 Kg		Endevco 7270	70 Kg	NMERI Mount					

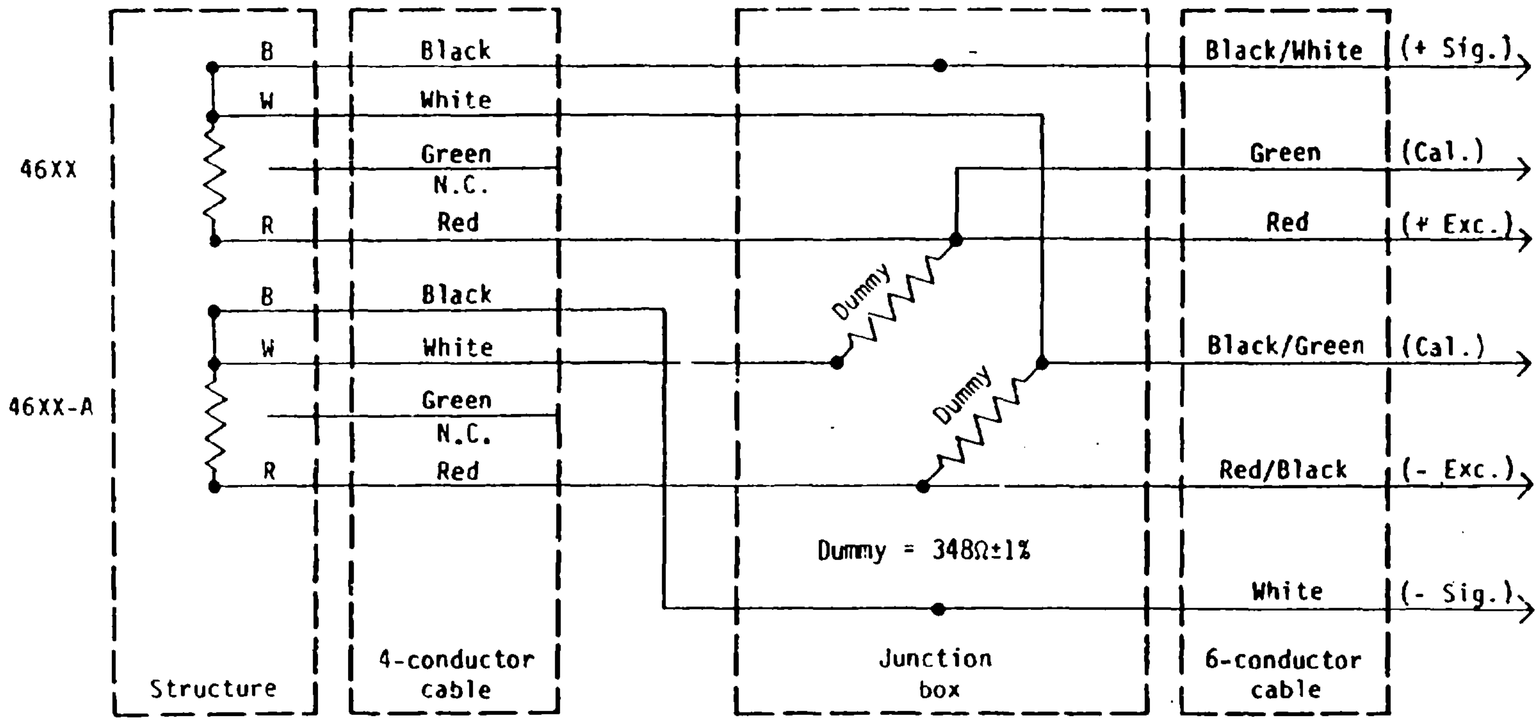

Figure A-1. Concrete strain wiring.

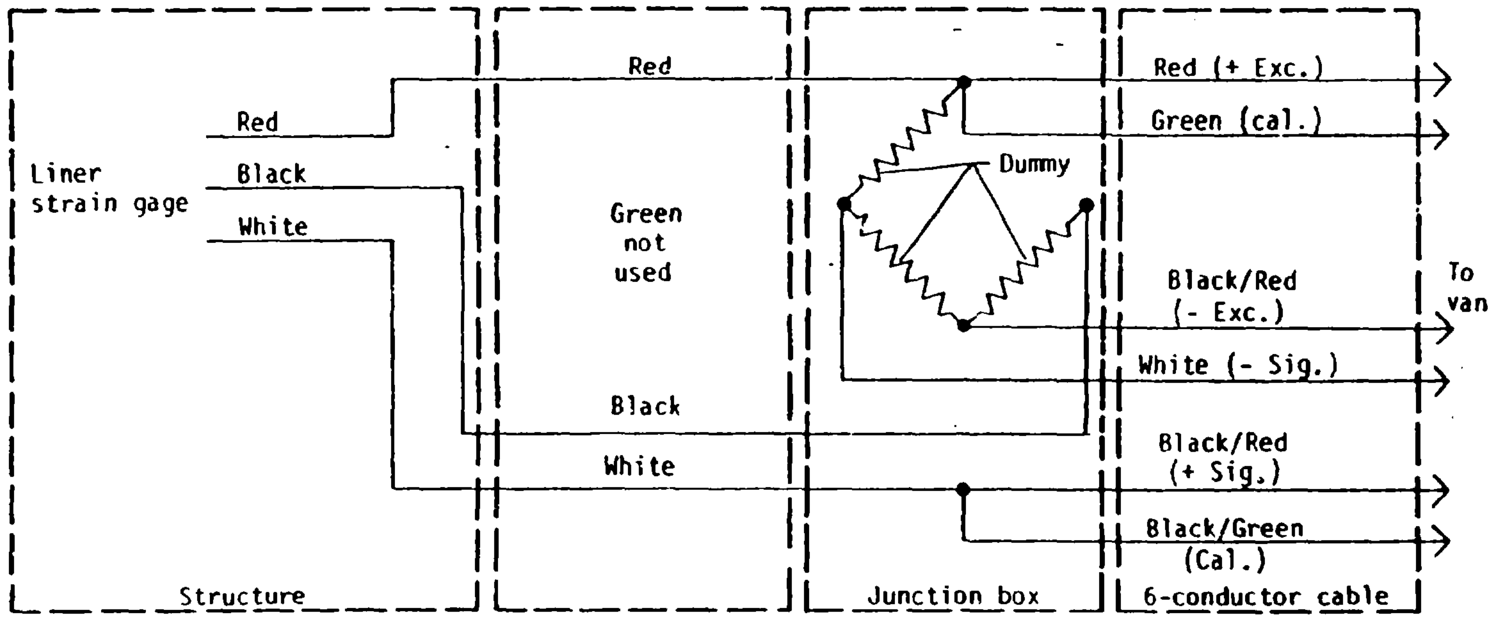

Dummy = 350Ω±1% precision resistor

Figure A-2. Liner strain wiring.

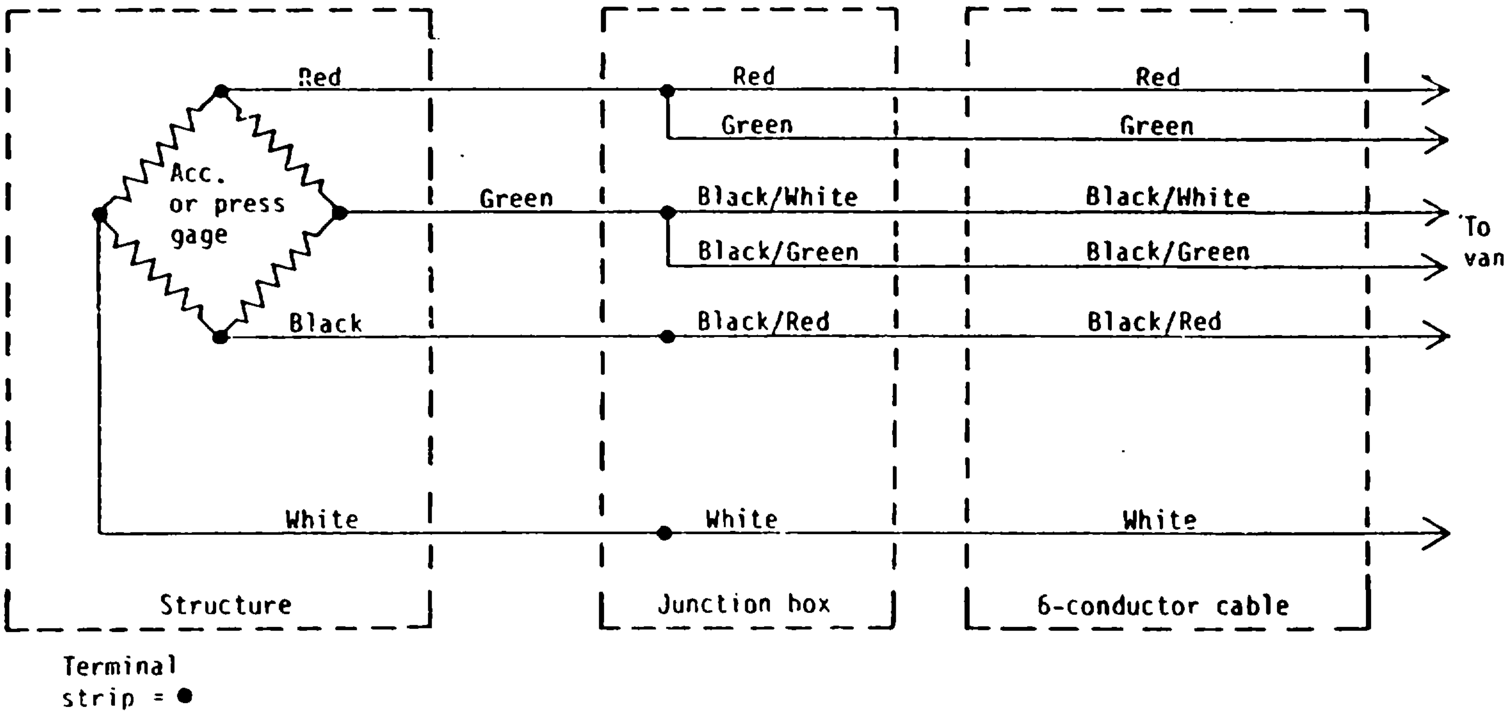

Figure A-3. Accelerometer or pressure gage wiring.

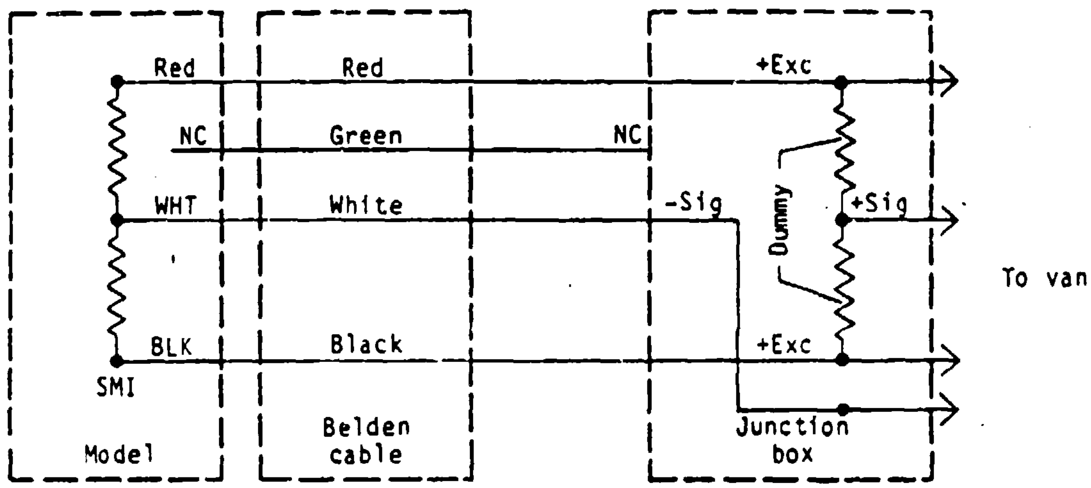

Figure A-4. SMI vertical axis wiring.

APPENDIX B

RESULTS OF MATERIAL TESTING PROGRAMS

SIFCON STRENGTH TESTS

NOTES

1. Failure of SIFCON material is not clearly defined. Therefore, for uniformity the results noted in the following tables represent the strengths at the peak loadings recorded.

2. All results are in lb/in^2 (1000 lb/in^2 = 6.895 MPa)

3. All test results are included. In calculating averages no test results were thrown out because there were not enough results to accurately determine if a sample may have defective.

TABLE EXPLANATION

Air--Sepcimens listed under columns noted with this designation represent samples that were entirely air-cured.

Wet--Specimens listed under columns noted with this designation represent samples that were at least partially, but usually, entirely wet-cured.

MC--Molded SIFCON cylinders formed in 4-in-diam by 8-in-deep plastic molds.

CCS--Cored SIFCON cylinders removed from 1- by 1-ft by 4-in slabs.

CCW--Cored SIFCON cylinders removed from 5-ft by 14-in by 6-in slabs that were molded in steel plate forms simulating the model wall.

G--Grout samples that were cubically molded without any fiber.

B--Beam specimens molded horizontally in 4- by 4- by 20-in molds.

C--Beam specimens molded vertically as columns in 4- by 4- by 20-in molds but tested as beams.

Compression--Uniaxial compressive stress calculated using original pretest dimensions of specimen.

Flexural--Maximum tensile or compressive stress calculated using original uncracked cross section of specimen.

SERIES: 6
POURED: 1/19/84
AGE: 7 DAYS

MARK	AGE (DAYS)	COMPRESSION							FLEXURAL			
		MC AIR	MC WET	CCS AIR	CCS WET	CCW AIR	G AIR	G WET	B AIR	B WET	C AIR	C WET
6-1	7	6,883										
6-10	7								2,632			
6-11	7								3,445			
6-13	7								2,226			
6-20	7								2,696			
CUBE*	8						8,237					
CUBE*	8						5,944					
CUBE*	8						6,856					
AVERAGE		6,883					7,012		2,750			

MC - Molded Cylinder
CCS - Cored Cylinder, Slab
CCW - Cored Cylinder, Wall
G - Grout
B - Beam
C - Column
*1 9/16 by 2 by 1 7/16 in

SERIES: 6
POURED: 1/19/84
AGE: 28 DAYS

		COMPRESSION							FLEXURAL			
MARK	AGE (DAYS)	MC AIR	MC WET	CCS AIR	CCS WET	CCW AIR	G AIR	G WET	B AIR	B WET	C AIR	C WET
6-5	28	9,629										
6-6	28	8,674										
6-7	28	8,316										
6-9	28	9,191										
6-17	28								4,090			
6-18	28								2,923			
6-19	28								4,335			
6-21	28								3,776			
CUBE*	28						6,778					
CUBE*	28						4,333					
CUBE*	28						5,444					
AVERAGE		8,953					5,518		3,781			

MC - Molded Cylinder
CCS - Cored Cylinder, Slab
CCW - Cored Cylinder, Wall
G - Grout
B - Beam
C - Column
*1 1/2 by 1 1/2 by 2 in

SERIES: 6
POURED: 1/19/84
AGE: TEST DAY

		COMPRESSION							FLEXURAL			
MARK	Age (DAYS)	MC AIR	MC WET	CCS AIR	CCS WET	CCW AIR	G AIR	G WET	B AIR	B WET	C AIR	C WET
6-2	175		8,838									
6-4	174		9,788									
6-12	174		11,897									
6-14	175		10,942									
6-16	174		9,708									
6-3	174	9,350										
6-15	174	9,907										
6-22	175								2,357			
6-23	175								1,971			
6-24	174									2,786		
6-25	174									3,364		
AVERAGE		9,629	10,235						2,164	3,075		

MC = Molded Cylinder
CCS = Cored Cylinder, Slab
CCW = Cored Cylinder, Wall
G = Grout
B = Beam
C = Column

SERIES: 7
POURED: 2/4/84
AGE: 7 DAYS

		COMPRESSION							FLEXURAL			
MARK	AGE (DAYS)	MC AIR	MC WET	CCS AIR	CCS WET	CCW AIR	G AIR	G WET	B AIR	B WET	C AIR	C WET
7-1	7	8,555										
7-2	7	9,987										
7-3	7	8,833										
7-14	7								3,413			
7-15	7								2,550			
7-16	7								2,813			
7-27 CUBE*	7						10,453					
7-27 CUBE*	7						11,179					
7-31	7										975	
7-28-1	12			11,777								
7-28-2	12			12,685								
7-28-4	12			11,045								
AVERAGE		9,125		11,836			10,816		2,925		975	

MC - Molded Cylinder
CCS - Cored Cylinder, Slab
CCW - Cored Cylinder, Wall
G - Grout
B - Beam
C - Column
*1 1/2 by 1 9/16 by 2 in

SERIES: 7
POURED: 2/4/84
AGE: 28 DAYS

		COMPRESSION							FLEXURAL			
MARK	AGE (DAYS)	MC AIR	MC WET	CCS AIR	CCS WET	CCW AIR	G AIR	G WET	B AIR	B WET	C AIR	C WET
7-4	27	13,071										
7-5	27	11,976										
7-7	27	12,215										
7-8	27	10,982										
7-18	27								2,841			
7-19	27								981			
7-20	27								1,781			
7-21	27								1,280			
7-25 CUBE*	27						14,222					
7-25 CUBE*	27						12,089					
7-25 CUBE*	27						12,978					
7-29	27										825	
7-28-5	30			13,289								
7-28-6	30			11,300								
				----CONTINUED----								

MC - Molded Cylinder
CCS - Cored Cylinder, Slab
CCW - Cored Cylinder, Wall
G - Grout
B - Beam
C - Column
*1 1/2 by 1 1/2 by 2 in

SERIES: 7
POURED: 2/4/84
AGE: 28 DAYS

		COMPRESSION							FLEXURAL			
MARK	AGE (DAYS)	MC AIR	MC WET	CCS AIR	CCS WET	CCW AIR	G AIR	G WET	B AIR	B WET	C AIR	C WET
7-28-8	30			12,796								
AVERAGE		12,061		12,462			13,096		1,721		825	

MC - Molded Cylinder
CCS - Cored Cylinder, Slab
CCW - Cored Cylinder, Wall
G - Grout
B - Beam
C - Column

SERIES: 7
POURED: 2/4/84
AGE: TEST DAY

		COMPRESSION							FLEXURAL			
MARK	AGE (DAYS)	MC AIR	MC WET	CCS AIR	CCS WET	CCW AIR	G AIR	G WET	B AIR	B WET	C AIR	C WET
7-6	158		10,862									
7-10	158	11,777										
7-12	158	12,812										
7-17	159								3,244			
7-24	153								3,328			
7-13	158									3,769		
7-22	158									2,934		
7-23	158									4,716		
7-32	159										853	
AVERAGE		12,295	10,862						3,286	3,806	853	

MC = Molded Cylinder
CCS = Cored Cylinder, Slab
CCW = Cored Cylinder, Wall
G = Grout
B = Beam
C = Column

SERIES: 8
POURED: 2/22/84
AGE: 7 DAYS

		COMPRESSION							FLEXURAL			
MARK	AGE (DAYS)	MC AIR	MC WET	CCS AIR	CCS WET	CCW AIR	G AIR	G WET	B AIR	B WET	C AIR	C WET
8-1	7	5,212										
8-2	7	5.391										
8-3	7	5,395										
8-4	7	5,247										
8-13	7								3,094			
8-14	7								1,076			
8-15	7								2,063			
8-16	7								2,320			
8-25	7										867	
8-30-1 CUBE*	7						6,000					
8-30-2 CUBE*	7						6,989					
8-30-3 CUBE*	7						6,844					
AVERAGE		5,311					6,611		2,138		867	

MC - Molded Cylinder
CCS - Cored Cylinder, Slab
CCW - Cored Cylinder, Wall
G - Grout
B - Beam
C - Column
*1 1/2 by 1 1/2 by 2 in

SERIES: 8
POURED: 2/22/84
AGE: 28 DAYS

MARK	AGE (DAYS)	COMPRESSION							FLEXURAL			
		MC. AIR	MC WET	CCS AIR	CCS WET	CCW AIR	G AIR	G WET	B AIR	B WET	C AIR	C WET
8-5	28	6,883										
8-8	28		6,147									
8-11	28	6,828										
8-12	28		6,943									
8-18	28									3,356		
8-21	28								2,475			
8-22	28								1,181			
8-24	28									2,663		
8-27	28											872
8-32 CUBE*	28						5,111					
8-32 CUBE**	28						3,111					
8-32 CUBE***	28						4,267					
8-S5	28			11,459								
8-S6	28			12,271								
AVERAGE		6,856	6,545	11,865			4,163		1,828	3,010		872

MC - Molded Cylinder
CCS - Cored Cylinder, Slab
CCW - Cored Cylinder, Wall
G - Grout
B - Beam
C - Column
*1 1/2 by 1 1/2 by 1 3/4 in
**1 1/2 by 1 1/2 by 1 3/4 in
***1 1/2 by 1 1/2 by 2 3/8 in

SERIES: 8
POURED: 2/22/84
AGE: TEST DAY

		COMPRESSION							FLEXURAL			
MARK	AGE (DAYS)	MC AIR	MC WET	CCS AIR	CCS WET	CCW AIR	G AIR	G WET	B AIR	B WET	C AIR	C WET
8-6	140		8,037									
8-9	141		7,162									
8-7	140	5,332										
8-10	140	7,838										
8-19	141								3,141			
8-20	141								1,221			
8-17	139									3,038		
8-23	139									2,644		
8-26	139										1,163	
8-28	141										731	
AVERAGE		6,585	7,600						2,181	2,841	947	

MC = Molded Cylinder
CCS = Cored Cylinder, Slab
CCW = Cored Cylinder, Wall
G = Grout
B = Beam
C = Column

SERIES: 9
POURED: 3/12/84
AGE: 7 DAYS

MARK	AGE (DAYS)	COMPRESSION							FLEXURAL			
		MC AIR	MC WET	CCS AIR	CCS WET	CCW AIR	G AIR	G WET	B AIR	B WET	C AIR	C WET
9-1	7		8,196									
9-5	7		7,878									
9-6	7		6,446									
9-22	7									2,057		
9-24	7								2,663			
9-36 CUBE*	7							7,222				
9-38 CUBE*	7						6,556					
9-23	8								2,046			
9-26	8									2,555		
9-S1-4	8			12,048								
9-S1-5	8				11,841							
9-S2-1	8					10,122						
9-S2-2	8					13,592						
9-S2-3	8					13,210						
				----CONTINUED----								

MC - Molded Cylinder
CCS - Cored Cylinder, Slab
CCW - Cored Cylinder, Wall
G - Grout
B - Beam
C - Column
*1 1/2 by 1 1/2 by 2 in

SERIES: 9
POURED: 3/12/84
AGE: 7 DAYS

MARK	AGE (DAYS)	COMPRESSION							FLEXURAL			
		MC AIR	MC WET	CCS AIR	CCS WET	CCW AIR	G AIR	G WET	B AIR	B WET	C AIR	C WET
9-S2-4	8					13,608						
9-S2-5	9					12,987						
9-S2-6	9					12,064						
9-S2-7	9					13,130						
9-S2-8	9					14,746						
9-S2-9	9					11,857						
9-12	9	8,614										
9-13	9	8,654										
9-15	9	7,838										
AVERAGE		8,369	7,507	12,048	11,841	12,813	6,556	7,222	2,355	2,306		

MC - Molded Cylinder
CCS - Cored Cylinder, Slab
CCW - Cored Cylinder, Wall
G - Grout
B - Beam
C - Column

SERIES: 9
POURED: 3/12/84
AGE: 28 DAYS

		COMPRESSION							FLEXURAL			
MARK	AGE (DAYS)	MC AIR	MC WET	CCS AIR	CCS WET	CCW AIR	G AIR	G WET	B AIR	B WET	C AIR	C WET
9-2	28		8,555									
9-3	28		8,157									
9-27	28								2,620			
9-29	28								2,953			
9-11	29	8,952										
9-14	29	9,271										
9-19	29									3,544		
9-25	29									2,391		
9-32	29										1,059	
9-34	29											1,303
9-S1-1	31				11,523							
9-S1-2	31				11,602							
9-S1-3	31				7,226							
9-S2-10	31					16,234						
AVERAGE				----CONTINUED----								

MC - Molded Cylinder
CCS - Cored Cylinder, Slab
CCW - Cored Cylinder, Wall
G - Grout
B - Beam
C - Column

SERIES: 9
POURED: 3/12/84
AGE: 28 DAYS

		COMPRESSION							FLEXURAL			
MARK	AGE (DAYS)	MC AIR	MC WET	CCS AIR	CCS WET	CCW AIR	G AIR	G WET	B AIR	B WET	C AIR	C WET
9-S2-11	31					18,080						
9-S2-12	31					16,329						
9-S2-13	31					14,961						
9-S2-14	31					15,693						
9-S2-15	31					17,357						
9-S2-16	31					14,069						
9-S2-17	31					13,608						
9-S2-18	31					16,329						
AVERAGE		9,112	8,356		10,117	15,907			2,787	2,968	1,059	1,303

MC - Molded Cylinder
CCS - Cored Cylinder, Slab
CCW - Cored Cylinder, Wall
G - Grout
B - Beam
C - Column

SERIES: 9
POURED: 3/12/84
AGE: TEST DAY

		COMPRESSION							FLEXURAL			
MARK	AGE (DAYS)	MC AIR	MC WET	CCS AIR	CCS WET	CCW AIR	G AIR	G WET	B AIR	B WET	C AIR	C WET
9-4	121		9,947									
9-7	120		12,852									
9-8	120		10,982									
9-9	120		10,305									
9-10	120		9,151									
9-35	120		12,414									
9-16	120		10,226									
9-17	119	9,549										
9-18	119	10,027										
9-39	119	9,510										
9-40	122	10,106										
				----CONTINUED----								

MC = Molded Cylinder
CCS = Cored Cylinder, Slab
CCW = Cored Cylinder, Wall
G = Grout
B = Beam
C = Column

SERIES: 9
POURED: 3/12/84
AGE: TEST DAY

		COMPRESSION							FLEXURAL			
MARK	AGE (DAYS)	MC AIR	MC WET	CCS AIR	CCS WET	CCW AIR	G AIR	G WET	B AIR	B WET	C AIR	C WET
1-9-1B	123					15,136						
1-9-2B	123					15,565						
1-9-3B	123					15,502						
1-9-4B	123					16,218						
1-9-5B	123					16,839						
1-9-6B	123					17,603						
1-9-7B	123					15,247						
1-9-8B	123					14,483						
1-9-9B	123					15,056						
1-9-10B	123					16,106						
9-20	120									3,928		
				----CONTINUED----								

MC = Molded Cylinder
CCS = Cored Cylinder, Slab
CCW = Cored Cylinder, Wall
G = Grout
B = Beam
C = Column

SERIES: 9
POURED: 3/12/84
AGE: TEST DAY

		COMPRESSION							FLEXURAL			
MARK	AGE (DAYS)	MC AIR	MC WET	CCS AIR	CCS WET	CCW AIR	G AIR	G WET	B AIR	B WET	C AIR	C WET
9-21	120									3,572		
9-28	119								2,522			
9-30	119								2,016			
9-33	120											947
9-37	119											1,209
AVERAGE		9,798	10,839			15,776			2,269	3,750		1,078

MC = Molded Cylinder
CCS = Cored Cylinder, Slab
CCW = Cored Cylinder, Wall
G = Grout
B = Beam
C = Column

SERIES: 10
POURED: 4/2/84
AGE: 7 DAYS

		COMPRESSION							FLEXURAL			
MARK	AGE (DAYS)	MC AIR	MC WET	CCS AIR	CCS WET	CCW AIR	G AIR	G WET	B AIR	B WET	C AIR	C WET
10-15	7		7,122									
10-17	7		6,804									
10-19	7								2,616			
10-20	7								2,363			
10-6	8	5,610										
10-8	8	10,246										
10-23	8									2,934		
10-24	8									3,169		
10-32	8											1,519
10-34	8										1,322	
10-S2-1	11					11,555						
10-S2-2	11					12,350						
10-S2-3	11					11,364						
10-S2-4	11					11,236						
				----CONTINUED----								

MC - Molded Cylinder
CCS - Cored Cylinder, Slab
CCW - Cored Cylinder, Wall
G - Grout
B - Beam
C - Column

SERIES: 10
POURED: 4/2/84
AGE: 7 DAYS

		COMPRESSION							FLEXURAL			
MARK	AGE (DAYS)	MC AIR	MC WET	CCS AIR	CCS WET	CCW AIR	G AIR	G WET	B AIR	B WET	C AIR	C WET
10-S2-5	11					10,154						
10-S2-6	11					12,955						
10-S2-7	11					11,777						
10-S2-8	11					11,841						
10-S2-9	11					14,388						
10-S1-1	14				12,637							
10-S1-2	14				13,560							
10-S1-3	14				13,210							
AVERAGE		7,928	6,963		13,136	11,958			2,490	3,052	1,322	1,519

MC - Molded Cylinder
CCS - Cored Cylinder, Slab
CCW - Cored Cylinder, Wall
G - Grout
B - Beam
C - Column

SERIES: 10
POURED: 4/2/84
AGE: 28 DAYS

		COMPRESSION							FLEXURAL			
MARK	AGE (DAYS)	MC AIR	MC WET	CCS AIR	CCS WET	CCW AIR	G AIR	G WET	B AIR	B WET	C AIR	C WET
10-9	30	10,405										
10-10	30	11,101										
10-13	30		9,569									
10-16	30		7,361									
10-S1-4	31				11,205							
10-S1-5	31				13,051							
10-S1-6	31				14,006							
10-25	31								2,606			
10-27	31								2,625			
10-28	31									938		
10-29	31									3,797		
10-33	31										825	
10-S2-10	31					9,518						
10-S2-11	31					11,300						
				----CONTINUED----								

MC - Molded Cylinder
CCS - Cored Cylinder, Slab
CCW - Cored Cylinder, Wall
G - Grout
B - Beam
C - Column

SERIES: 10
POURED: 4/2/84
AGE: 28 DAYS

		COMPRESSION							FLEXURAL			
MARK	AGE (DAYS)	MC AIR	MC WET	CCS AIR	CCS WET	CCW AIR	G AIR	G WET	B AIR	B WET	C AIR	C WET
10-S2-12	31					9,359						
10-S2-13	31					10,791						
10-S2-14	31					11,332						
10-S2-15	31					11,364						
10-S2-16	31					11,969						
10-S2-17	31					12,924						
10-S2-18	31					12,383						
AVERAGE		10,753	8,465		12,754	11,216			2,616	2,368	825	

MC - Molded Cylinder
CCS - Cored Cylinder, Slab
CCW - Cored Cylinder, Wall
G - Grout
B - Beam
C - Column

SERIES: 10
POURED: 4/2/84
AGE: TEST DAY

		COMPRESSION							FLEXURAL			
MARK	AGE (DAYS)	MC AIR	MC WET	CCS AIR	CCS WET	CCW AIR	G AIR	G WET	B AIR	B WET	C AIR	C WET
10-2	99		12,533									
10-4	99		11,340									
10-11	98		12,136									
10-12	98		10,663									
10-14	98		10,942									
10-18	99		11,141									
10-1	98	10,743										
10-3	98	9,629										
10-5	98	10,186										
10-7	99	11,250										
				----CONTINUED----								

----CONTINUED----

MC = Molded Cylinder
CCS = Cored Cylinder, Slab
CCW = Cored Cylinder, Wall
G = Grout
B = Beam
C = Column

SERIES: 10
POURED: 4/2/84
AGE: TEST DAY

		COMPRESSION							FLEXURAL			
MARK	AGE (DAYS)	MC AIR	MC WET	CCS AIR	CCS WET	CCW AIR	G AIR	G WET	B AIR	B WET	C AIR	C WET
1-10-1	101					14,961						
1-10-2	101					13,528						
1-10-3	101					11,555						
1-10-4	101					14,929						
1-10-5	101					14,897						
1-10-6	101					15,311						
1-10-7	101					14,547						
1-10-8	102					12,446						
1-10-9	102					15,915						
10-30	98									4,397		
10-31	98									4,022		
10-35	98											1,059
AVERAGE		10,455	11,459			14,232				4,210		1,059

MC = Molded Cylinder CCW = Cored Cylinder, Wall B = Beam
CCS = Cored Cylinder, Slab G = Grout C = Column

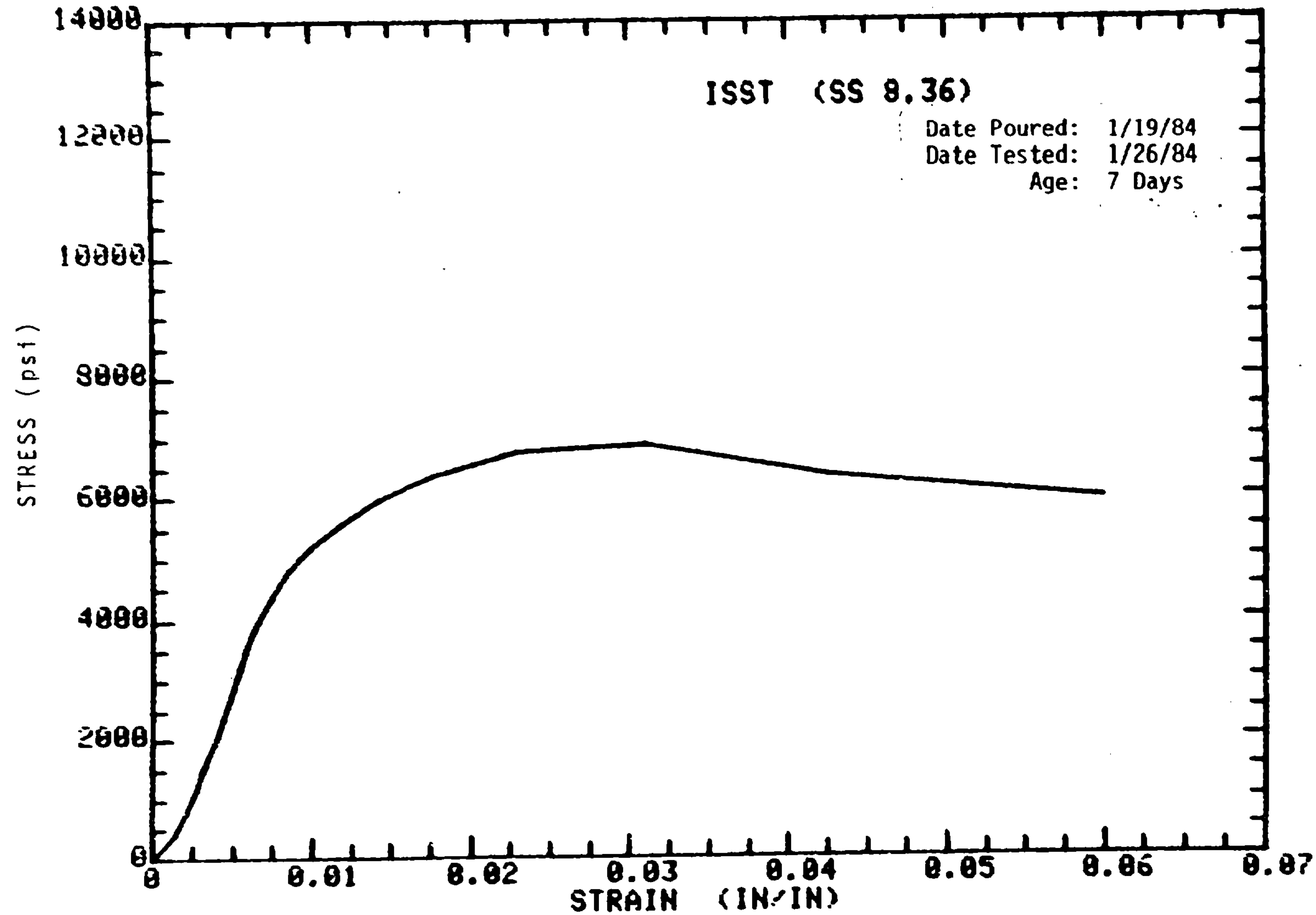

SAMPLE: FIBER 6-1 MOLDED: 4in DIA x 8in
CONCRETE SAMPLE

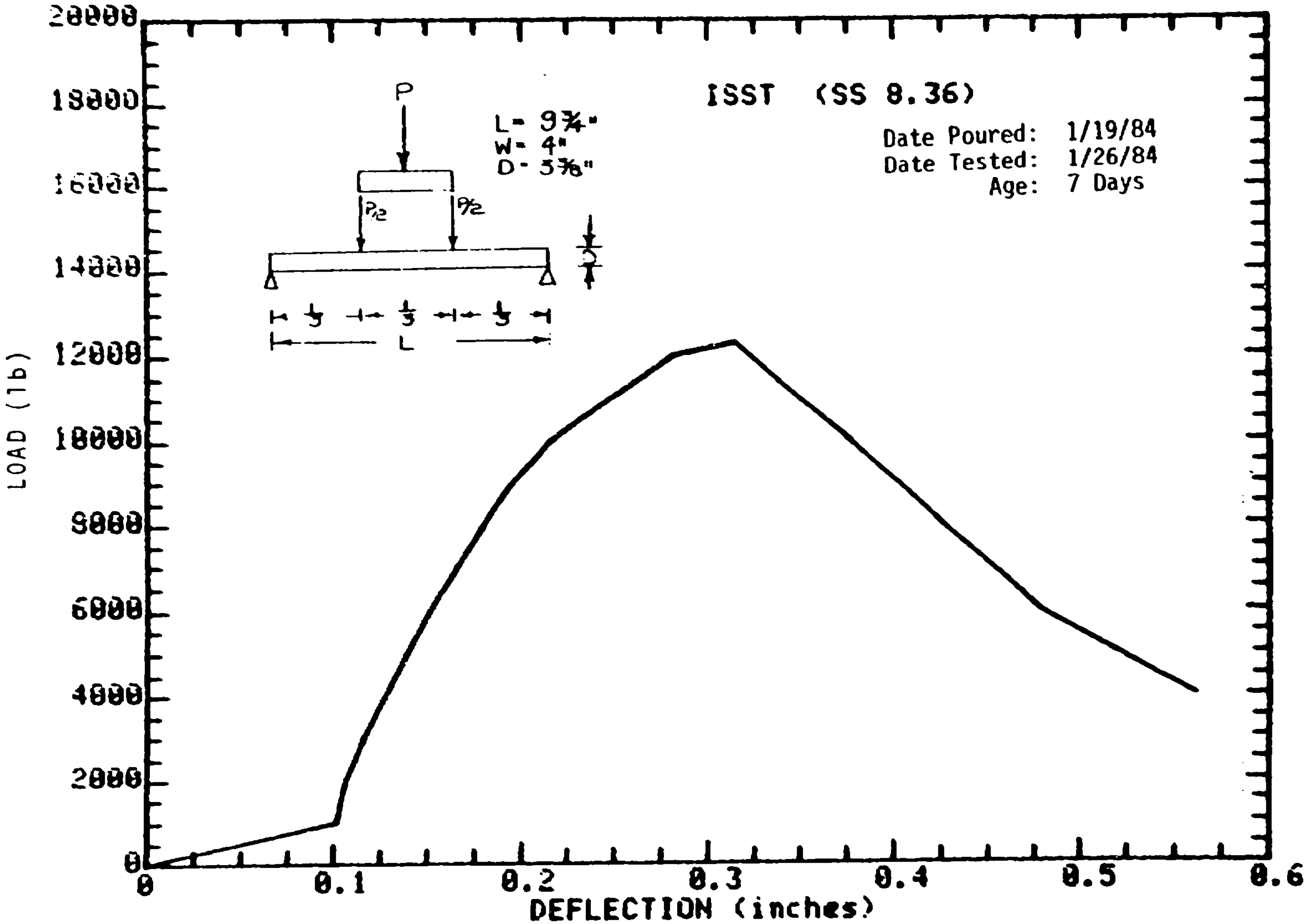

SAMPLE: BEAM 6-10
CONCRETE SAMPLE

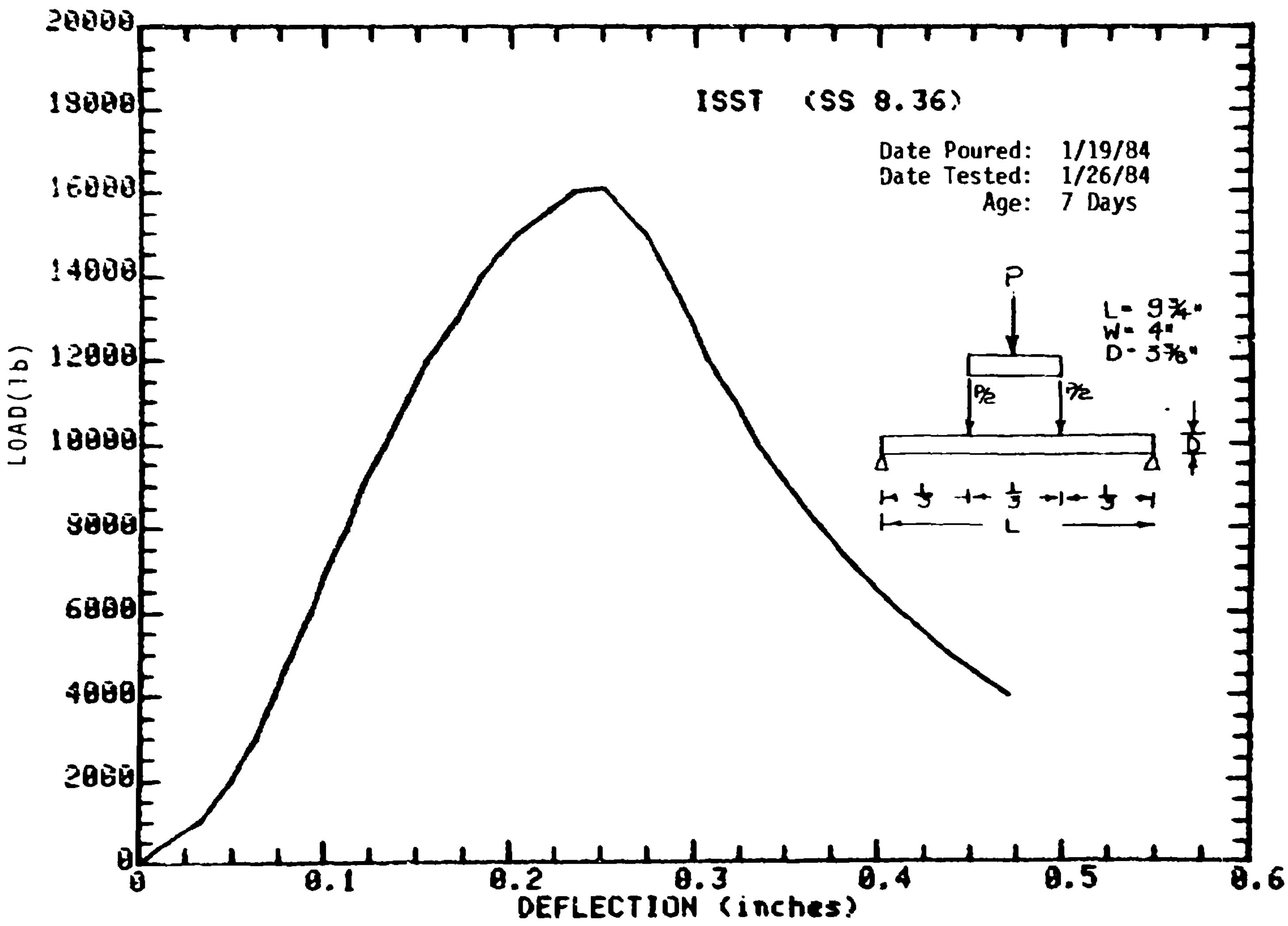

SAMPLE: BEAM 6-11
CONCRETE SAMPLE

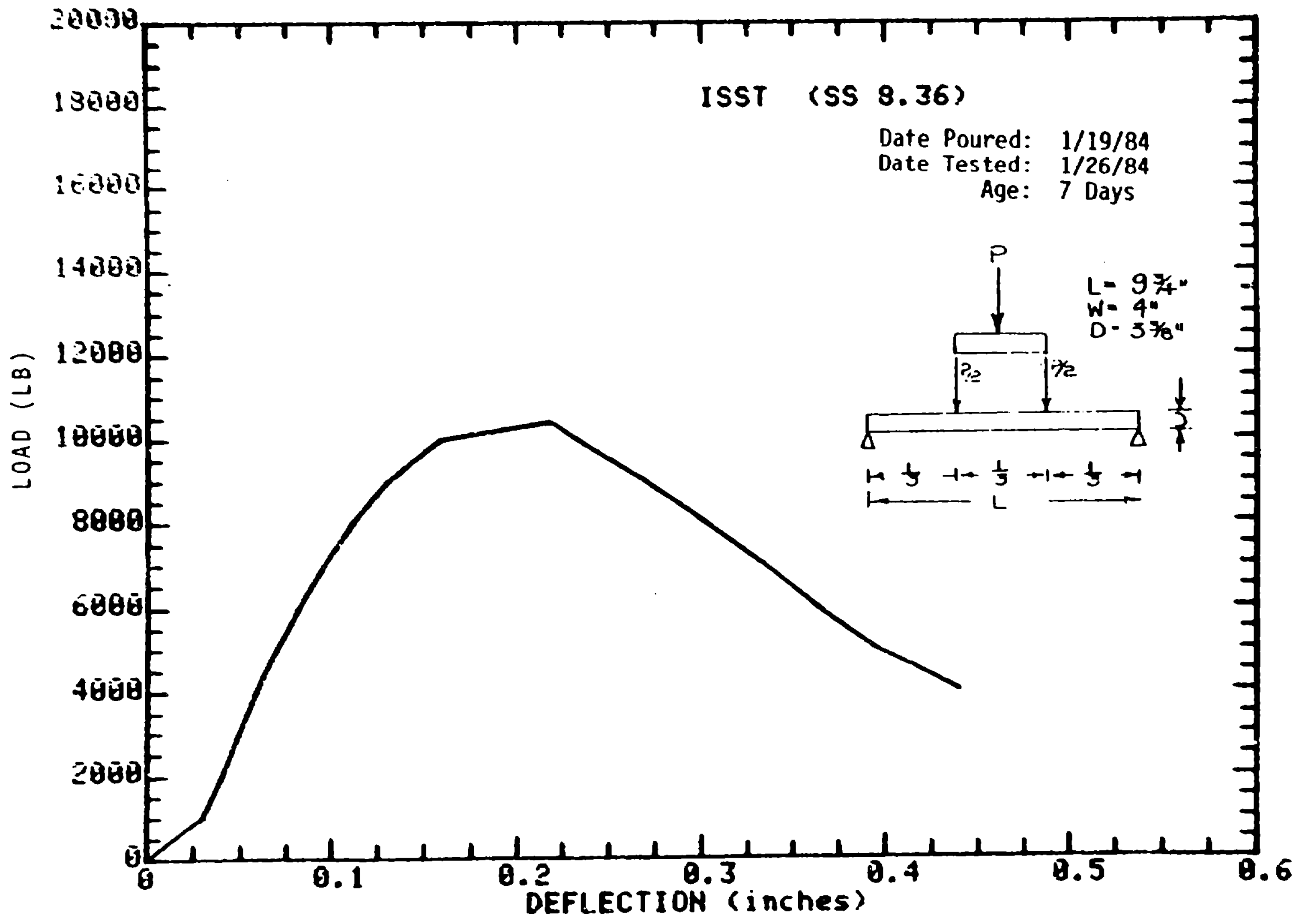

SAMPLE: BEAM 6-13
CONCRETE SAMPLE

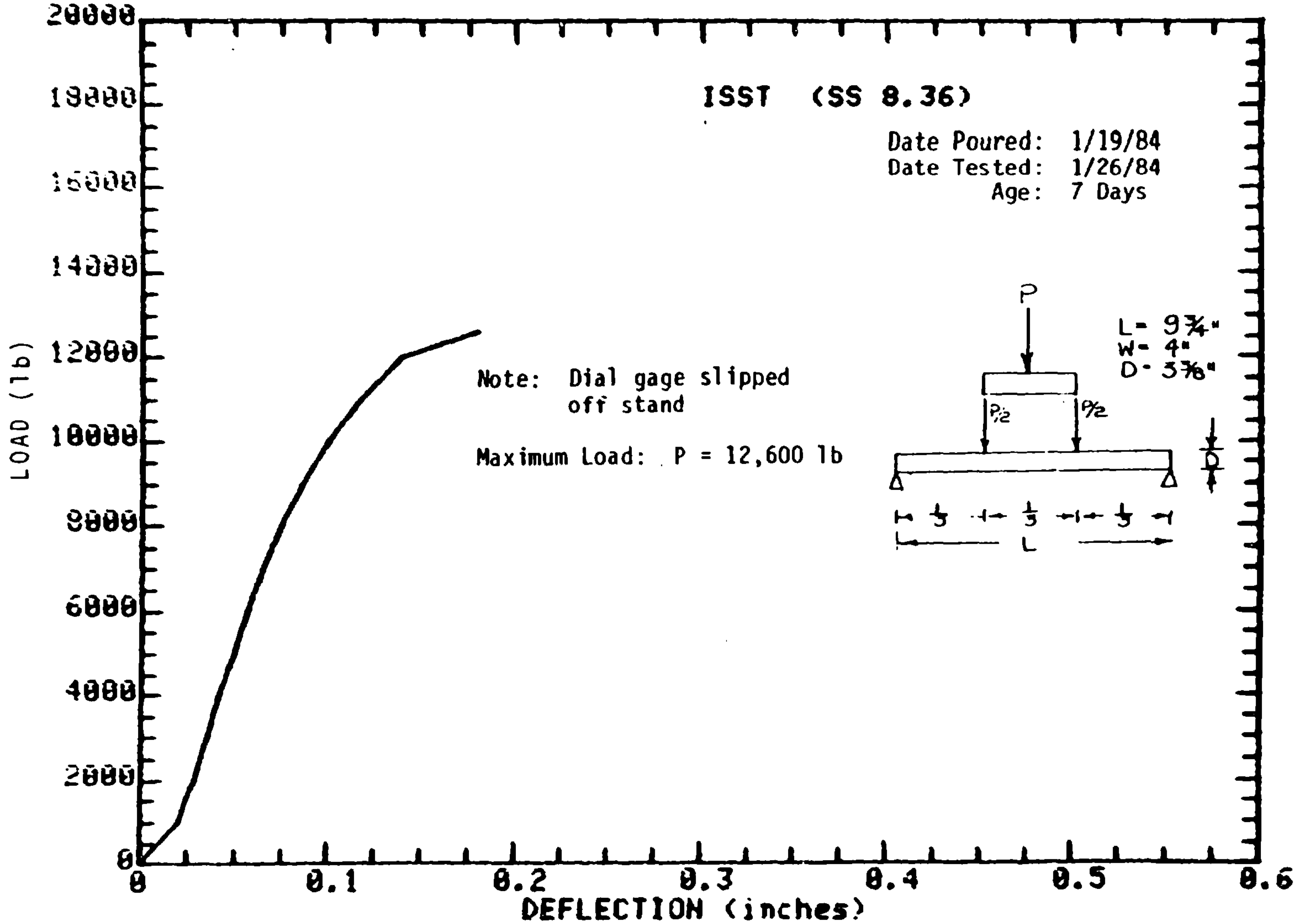

SAMPLE: BEAM 6-20
CONCRETE SAMPLE

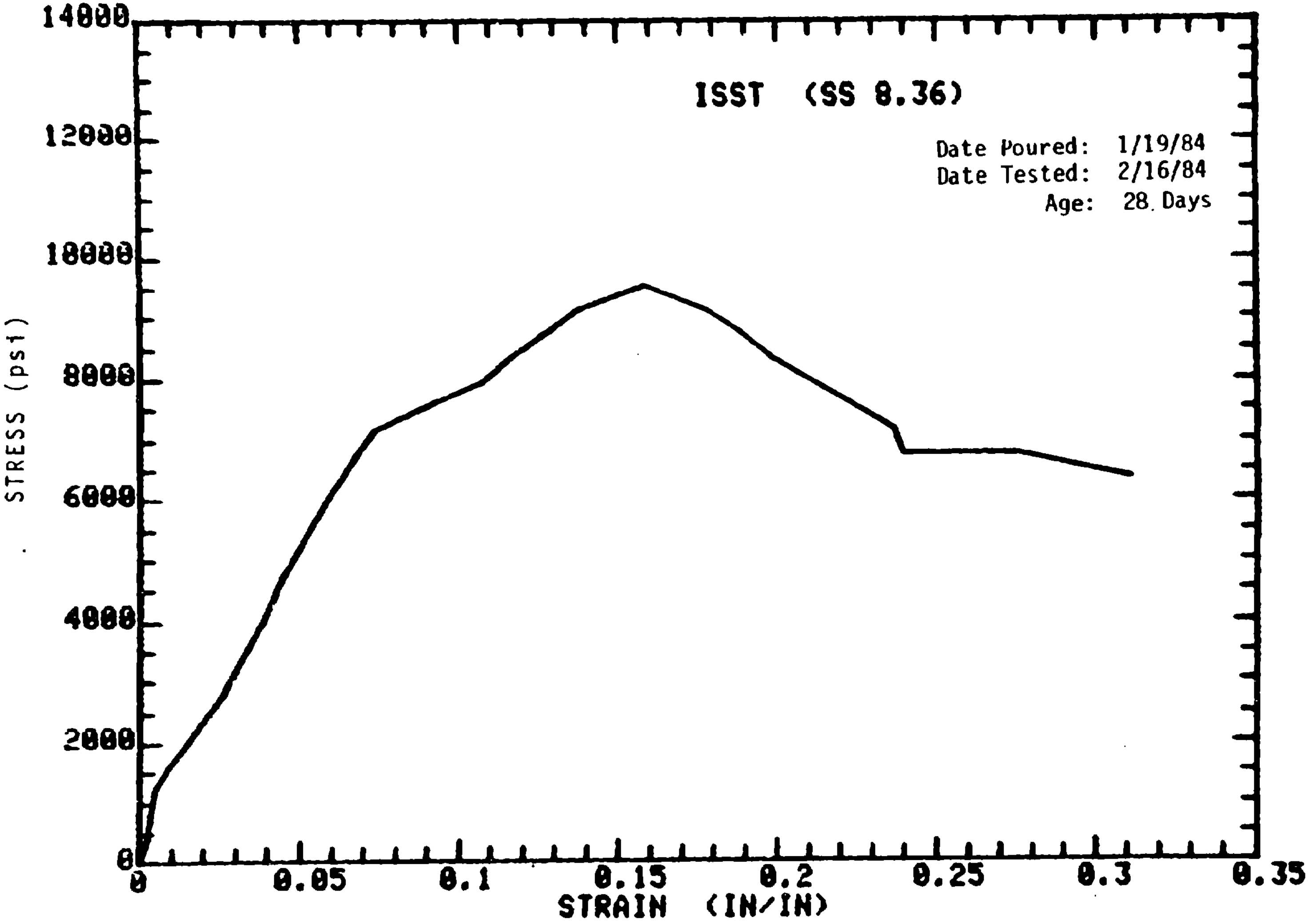

SAMPLE: FIBER 6-5 MOLDED: 4in DIA x 8in
CONCRETE SAMPLE

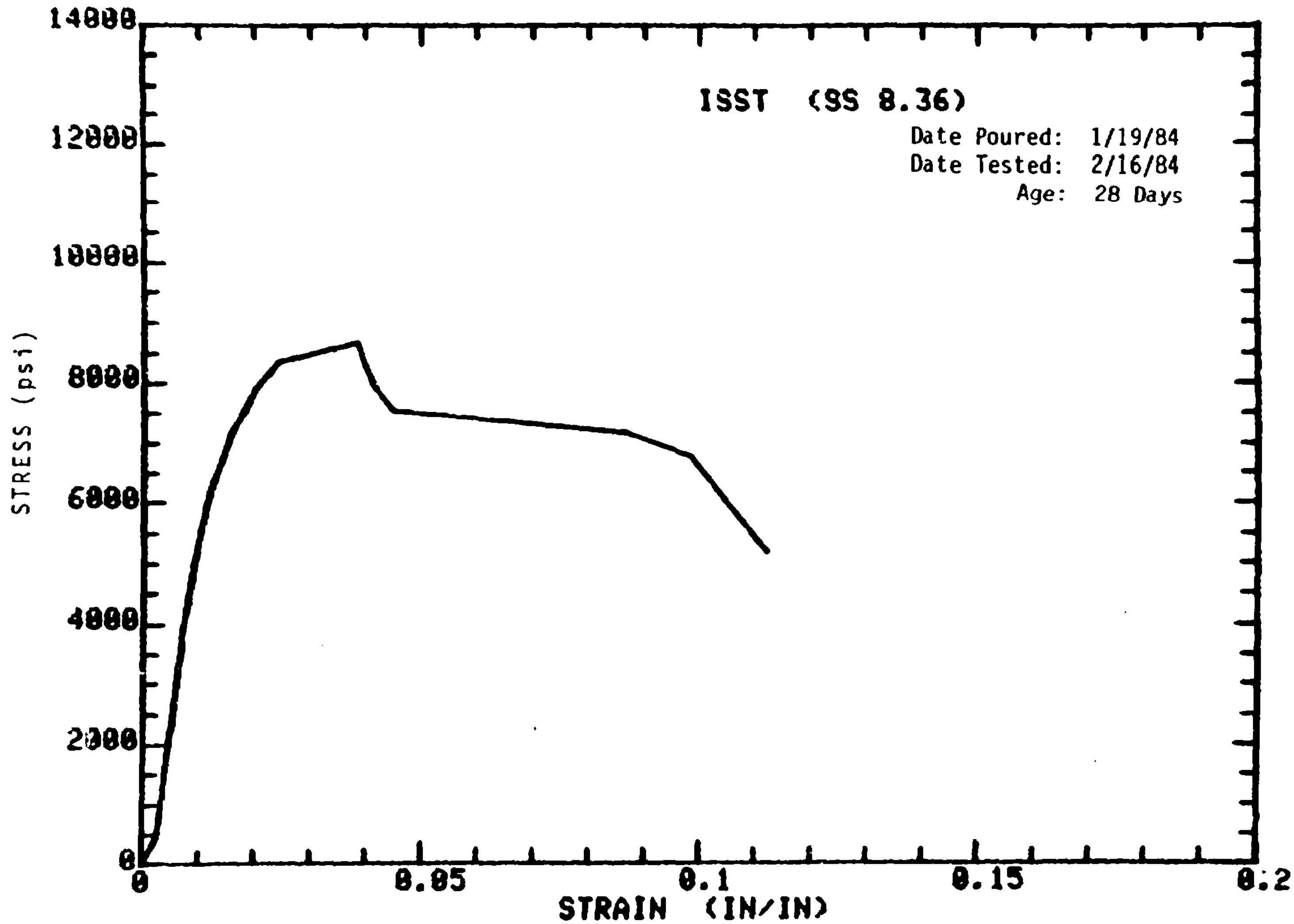

SAMPLE: FIBER 6-6 MOLDED: 4in DIA x 8in
CONCRETE SAMPLE

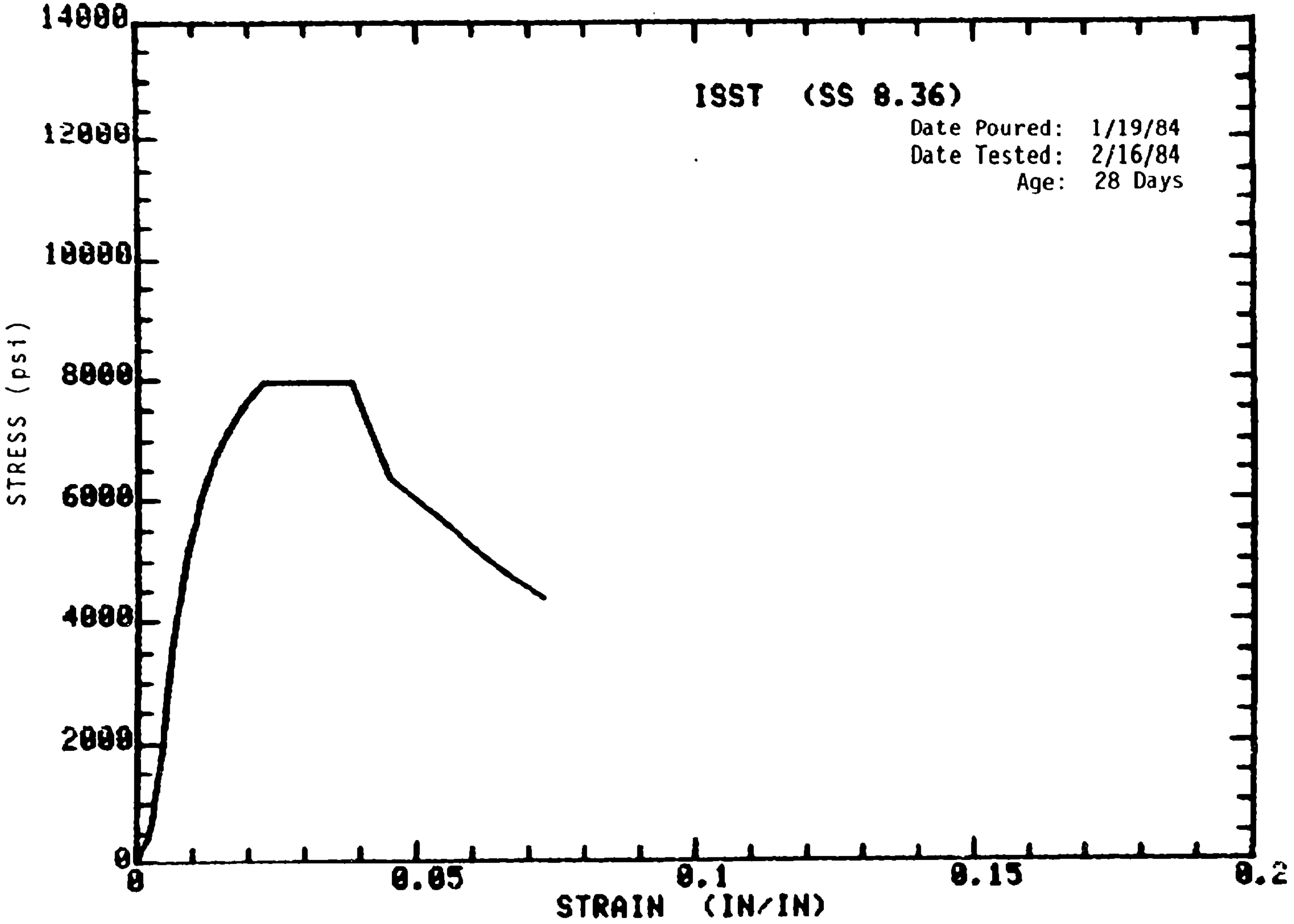

SAMPLE: FIBER 6-7 MOLDED: 4in DIA x 8in
CONCRETE SAMPLE

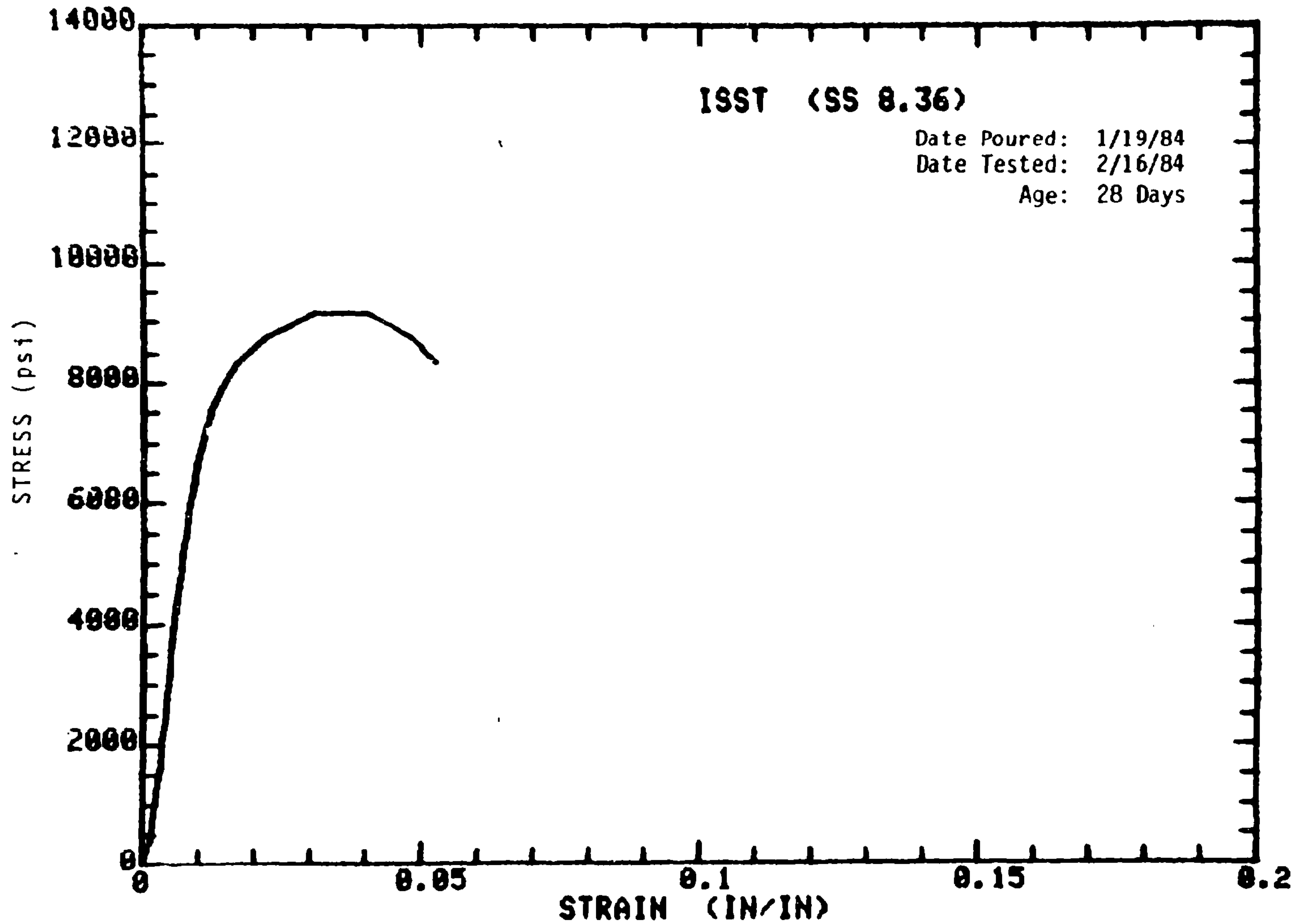

SAMPLE: FIBER 6-9 MOLDED: 4in DIA x 8in
CONCRETE SAMPLE

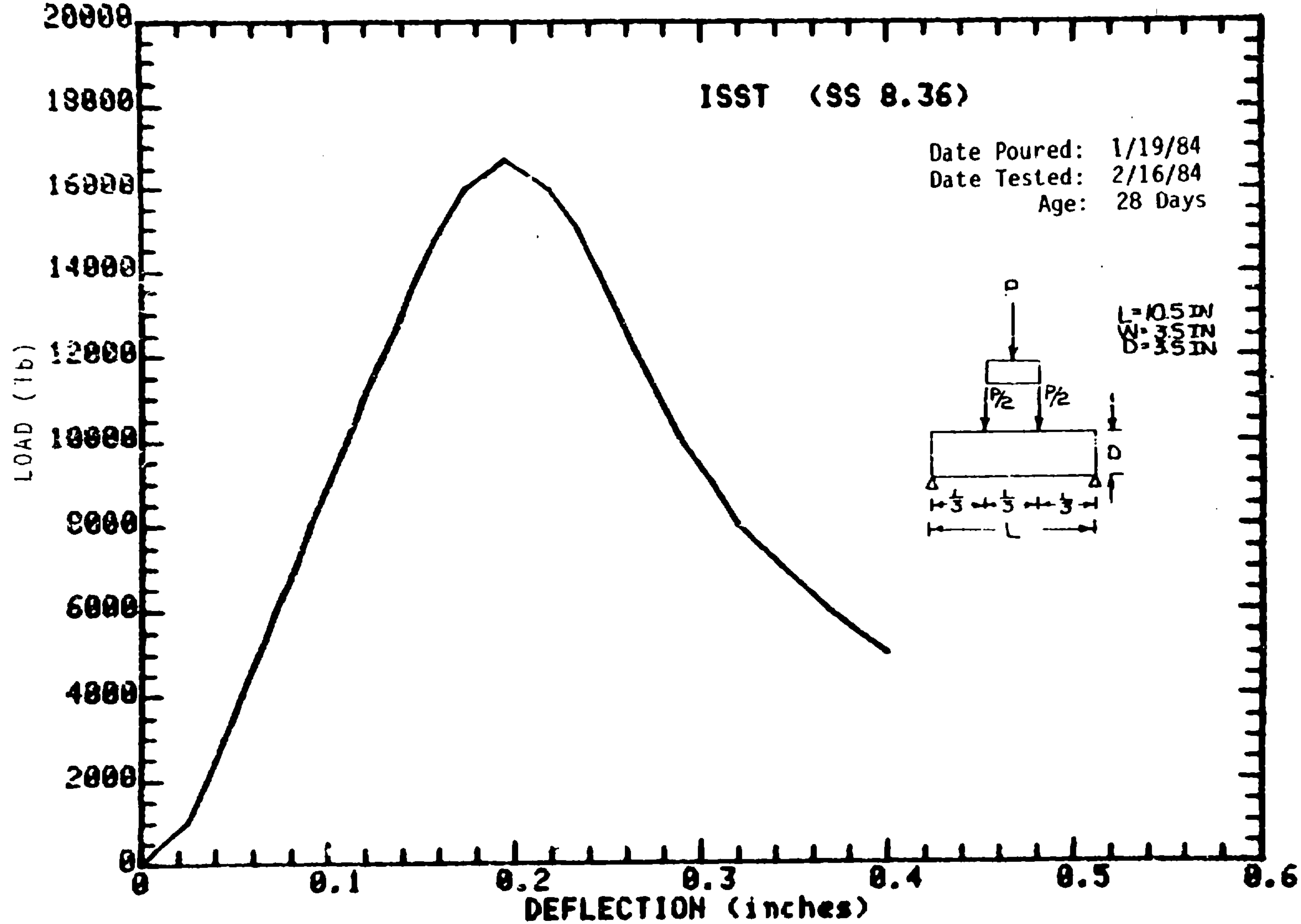

SAMPLE: BEAM 6-17
CONCRETE SAMPLE

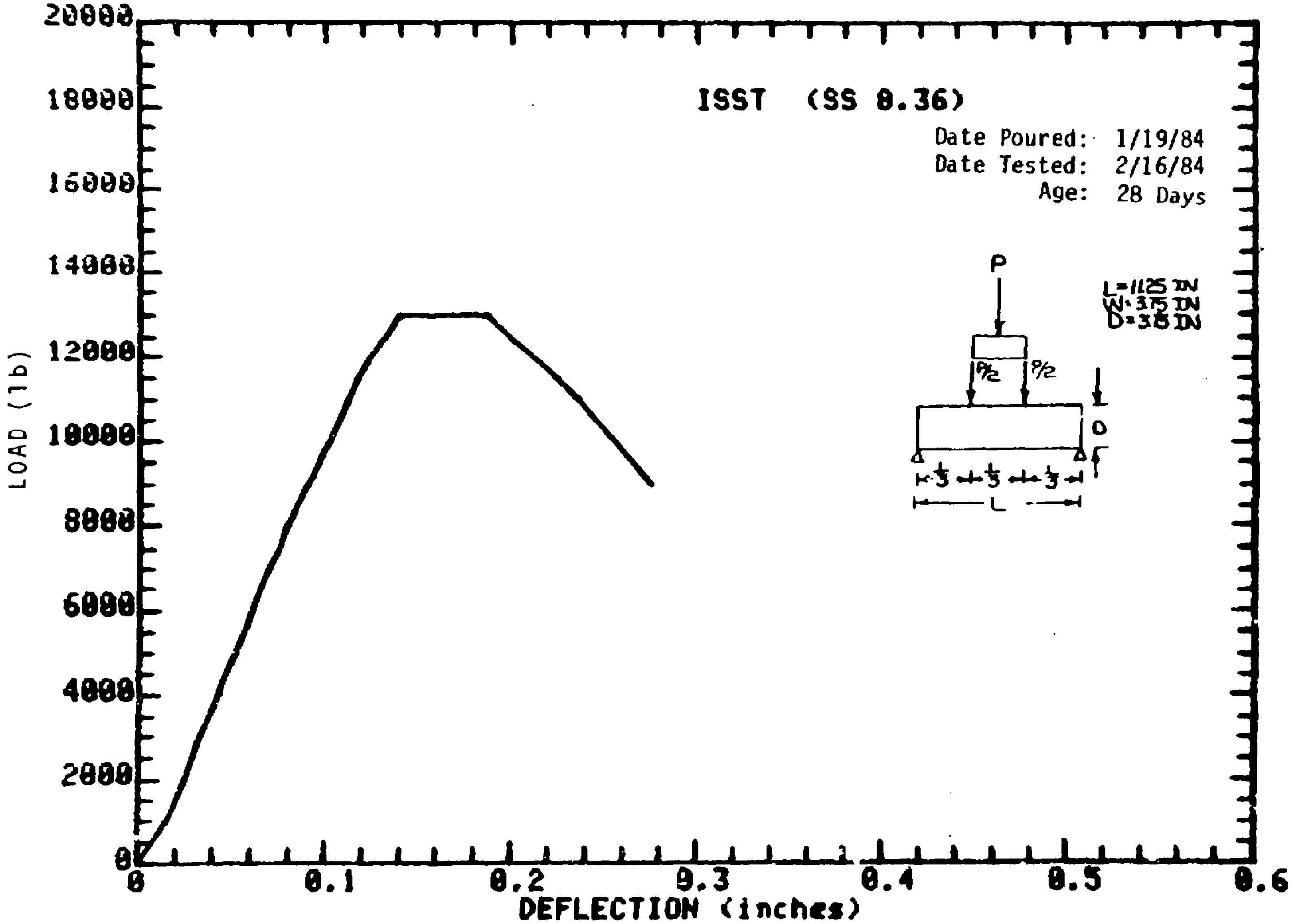

SAMPLE: BEAM 6-10
CONCRETE SAMPLE

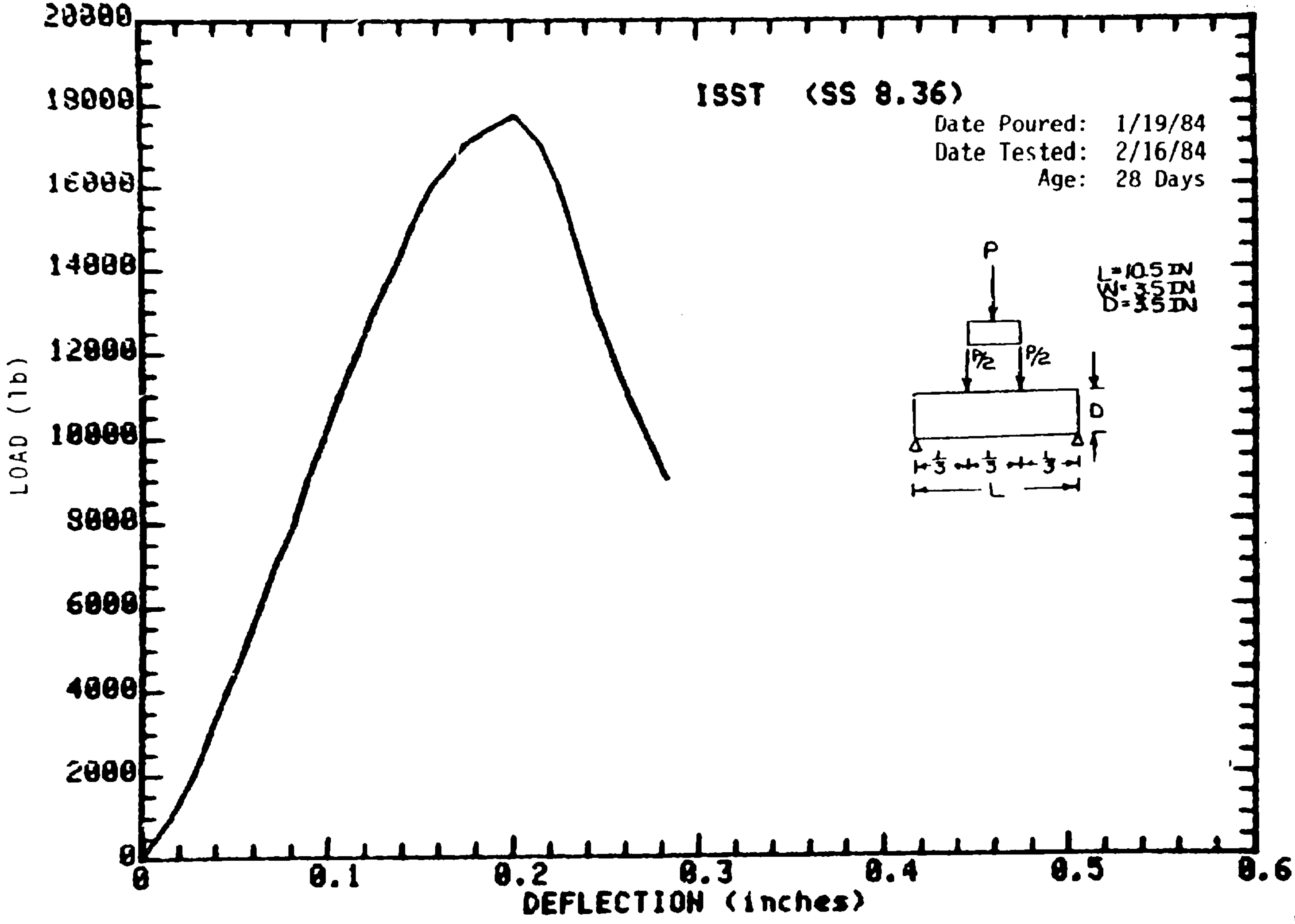

SAMPLE: BEAM 6-19
CONCRETE SAMPLE

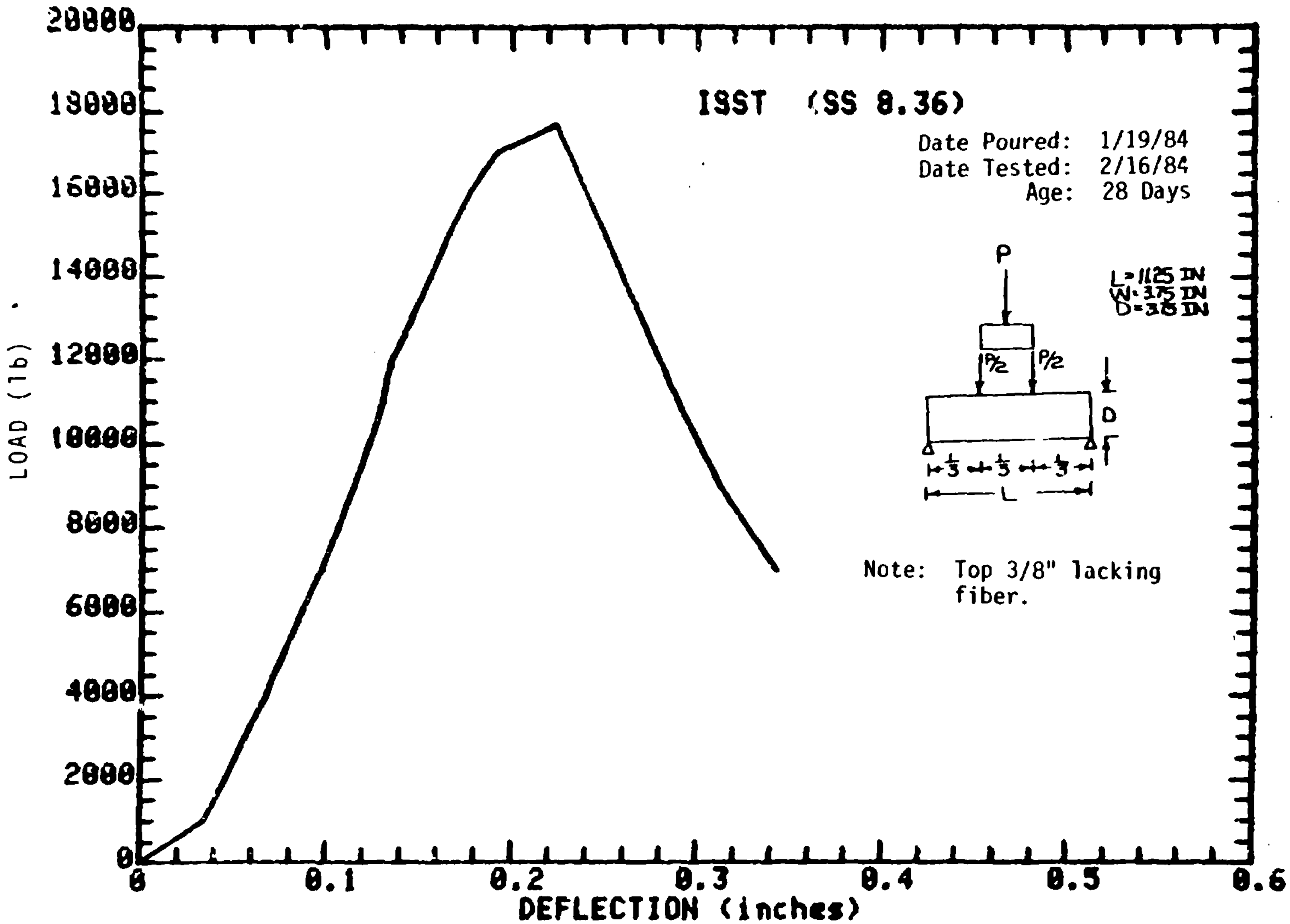

SAMPLE: BEAM 6-21
CONCRETE SAMPLE

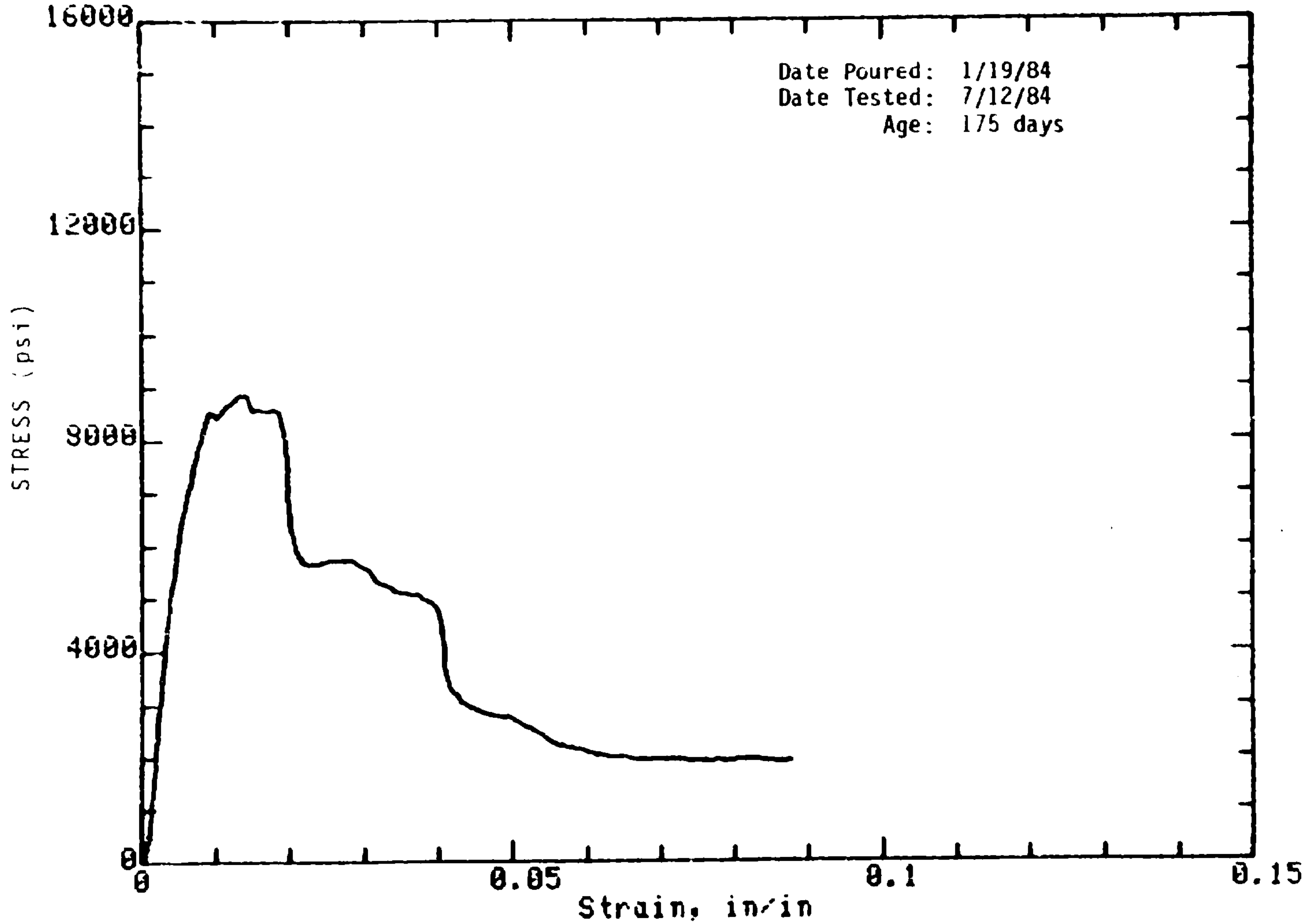

Mark: 6-2 Molded: 4in dia × 8in Cure: Wet
Concrete Sample

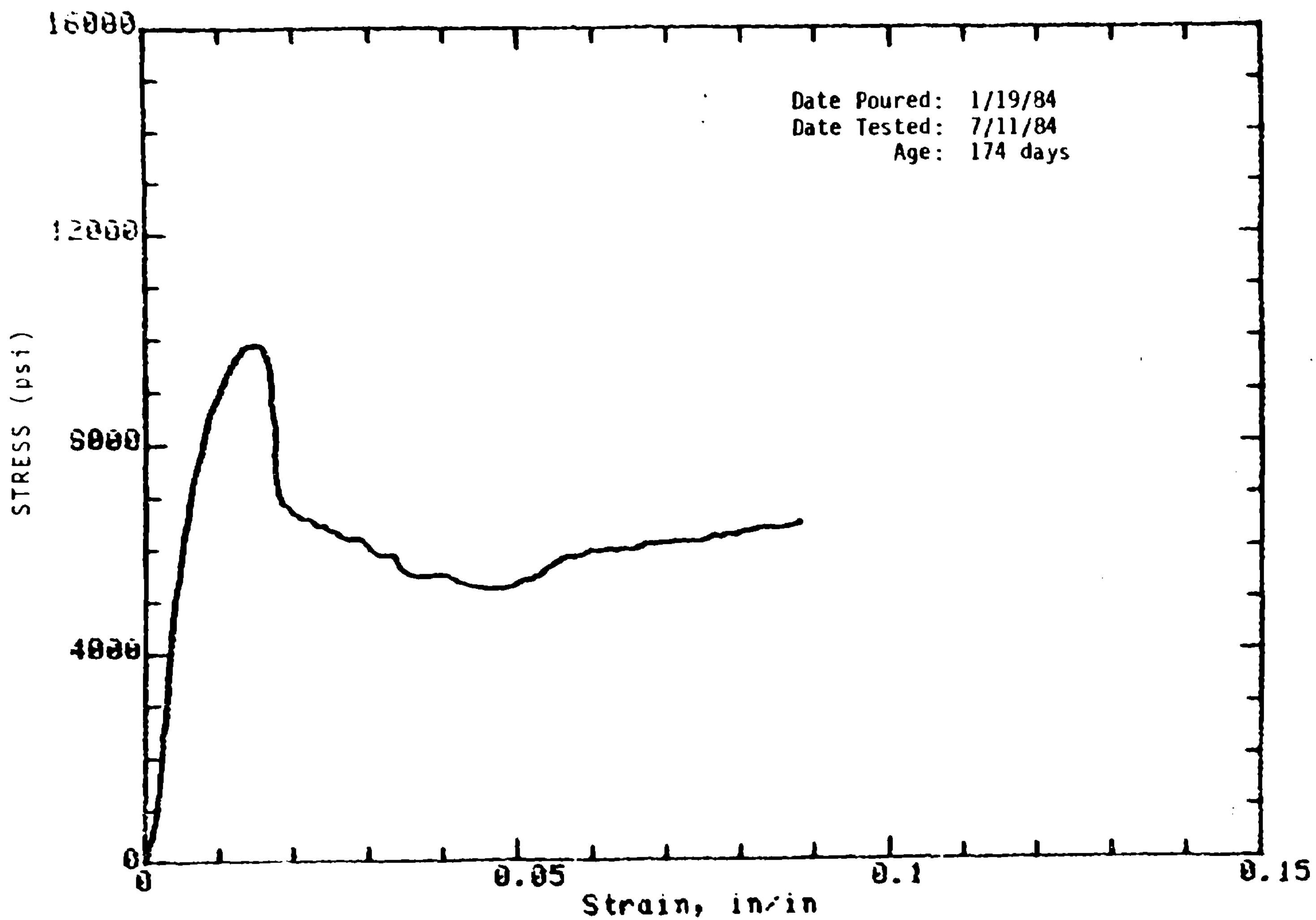

Mark: 6-4 Molded: 4in dia x 8in Cure: Wet
Concrete Sample

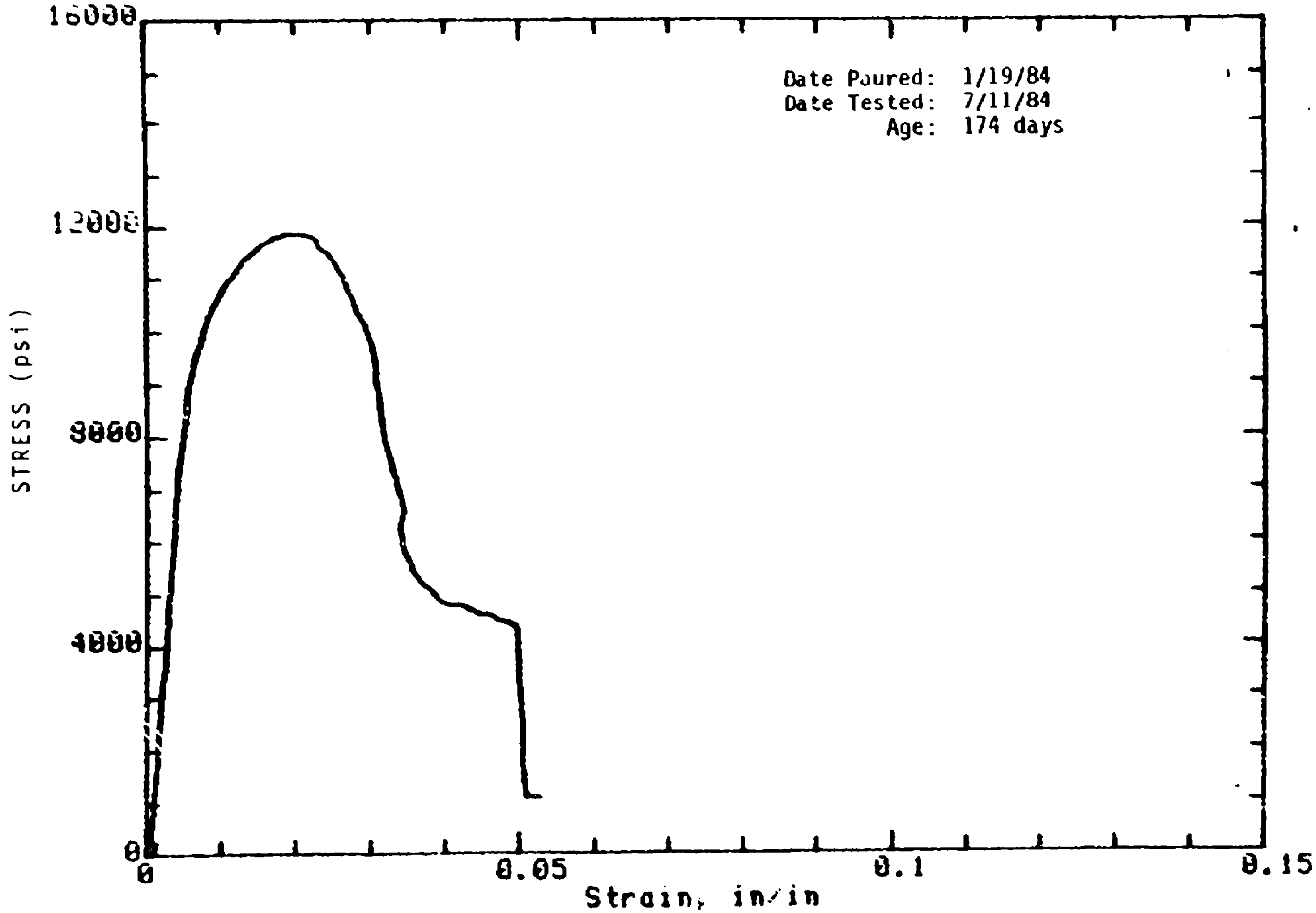

Mark: 6-12 Molded: 4in dia x 8in Cure: Wet
Concrete Sample

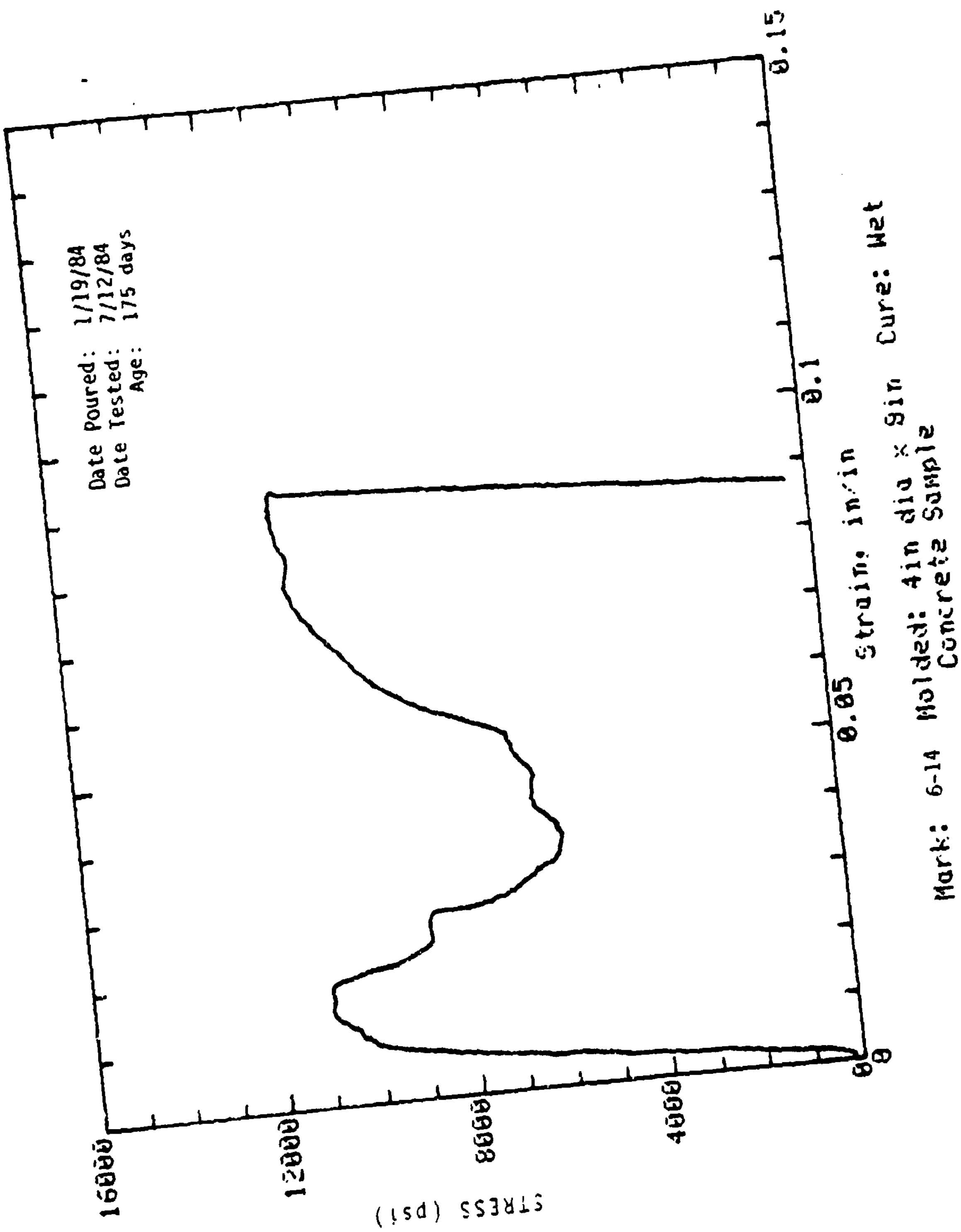

Date Poured: 1/19/84
Date Tested: 7/12/84
Age: 175 days
16000
12000
8000
4000
0
STRESS (psi)
0
0.05
0.1
0.15
Strain in/in
Mark: 6-14 Molded: 4in dia x 9in Cure: Wet
Concrete Sample

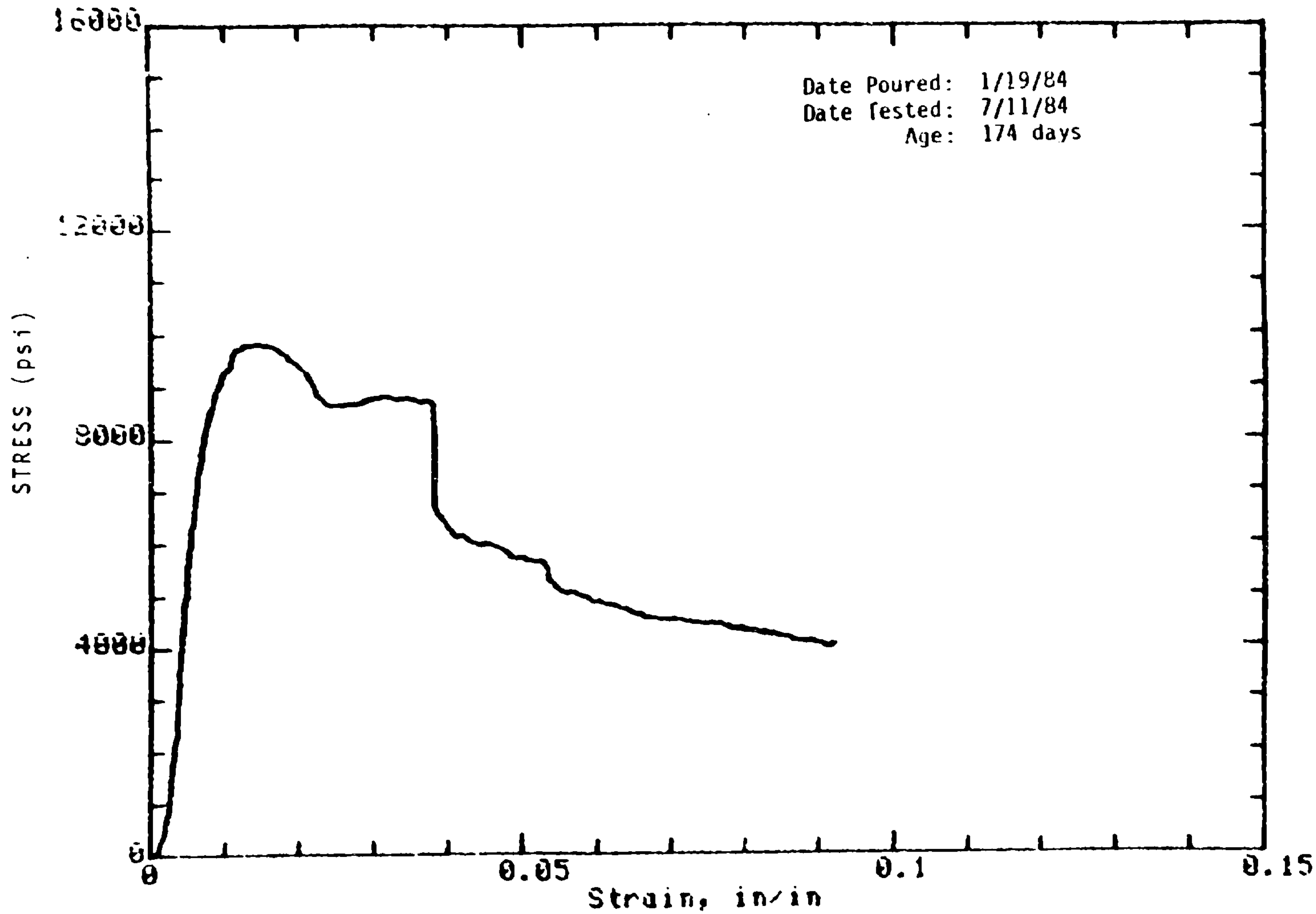

Mark: 6-16 Molded: 4in dia x 8in Cure: Wet
Concrete Sample

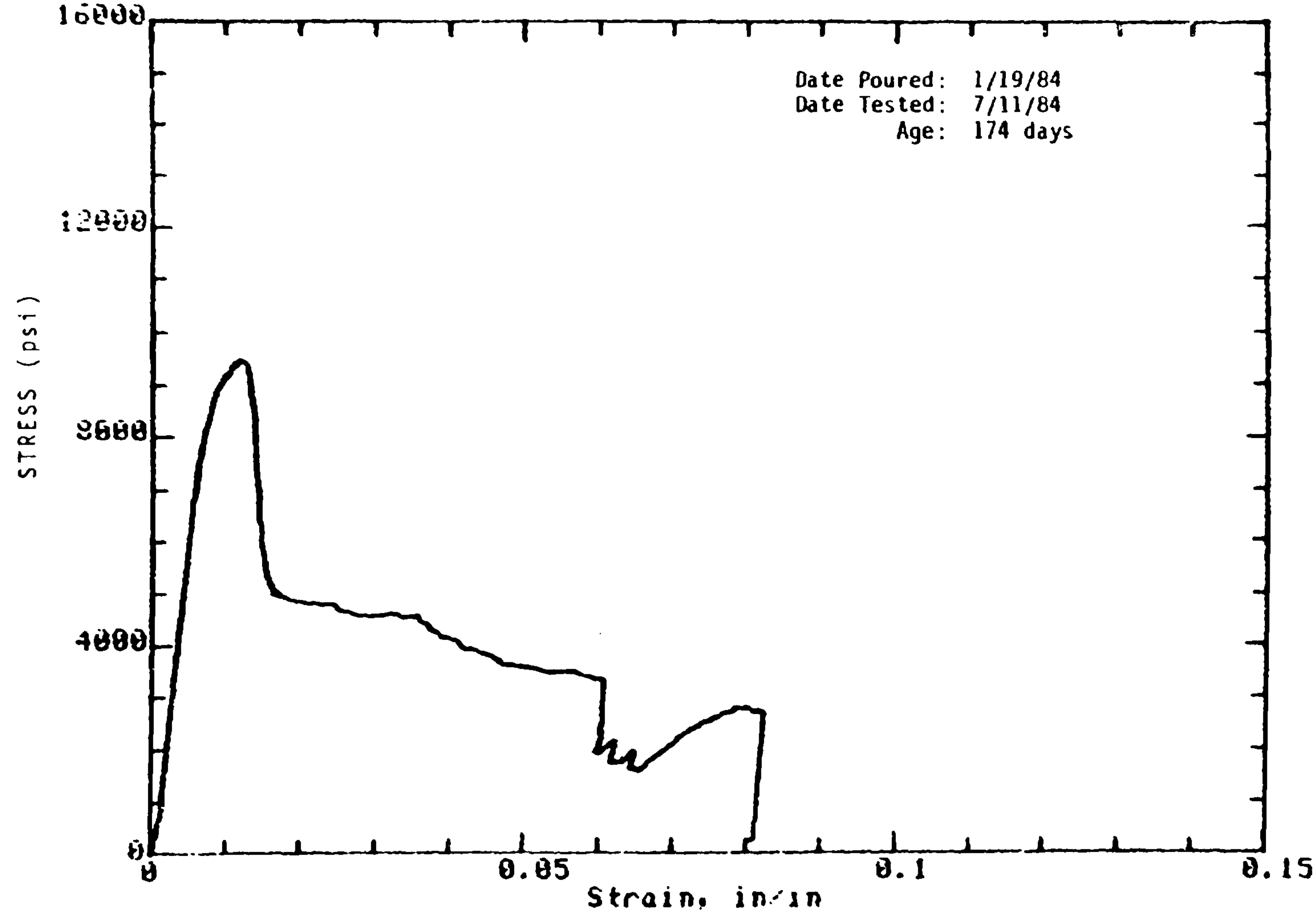

Mark: 6-3 Molded: 4in dia x 8in Cure: Dry
Concrete Sample

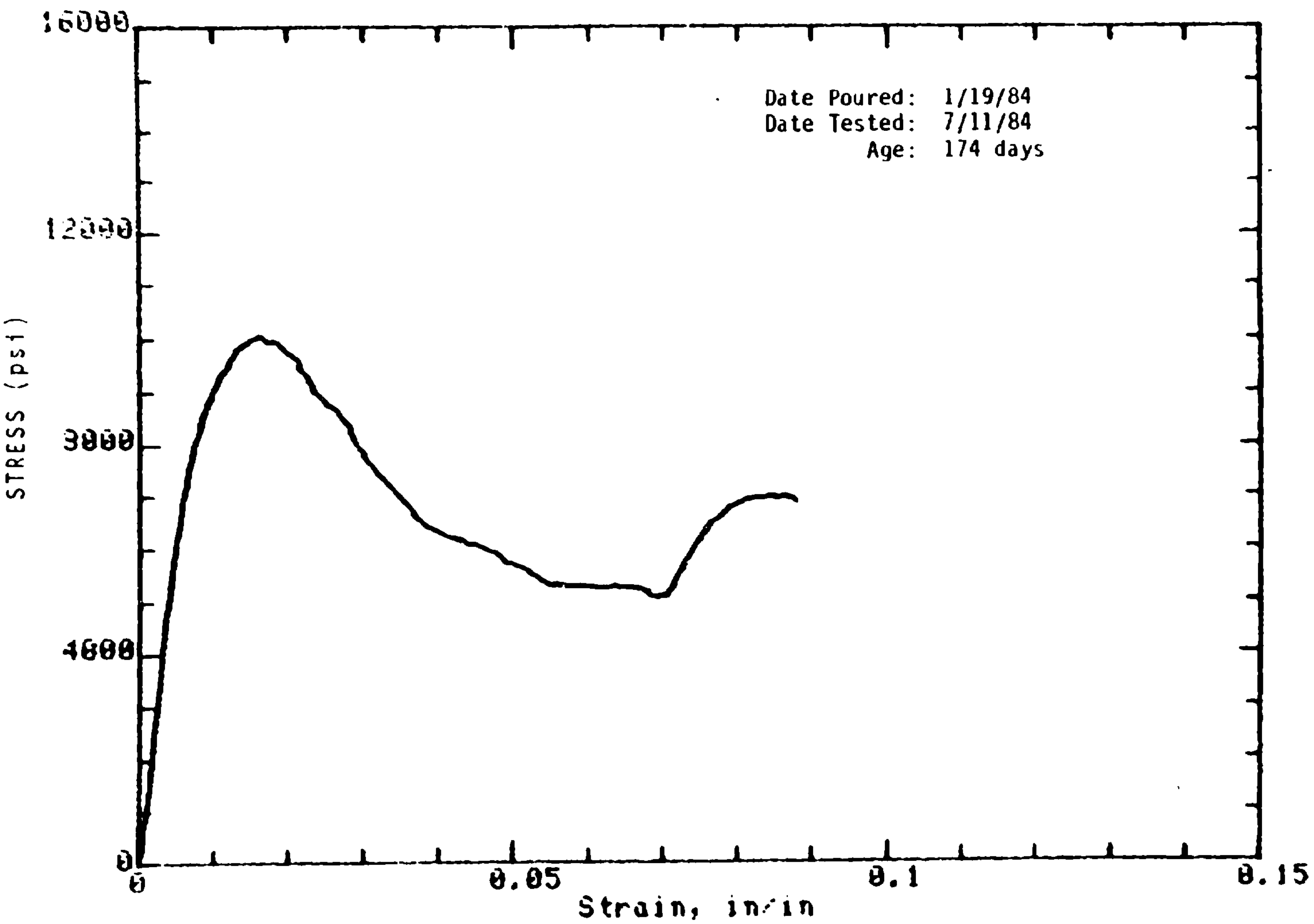

Mark: 6-15 Molded: 4in dia x 8in Cure: Dry
Concrete Sample

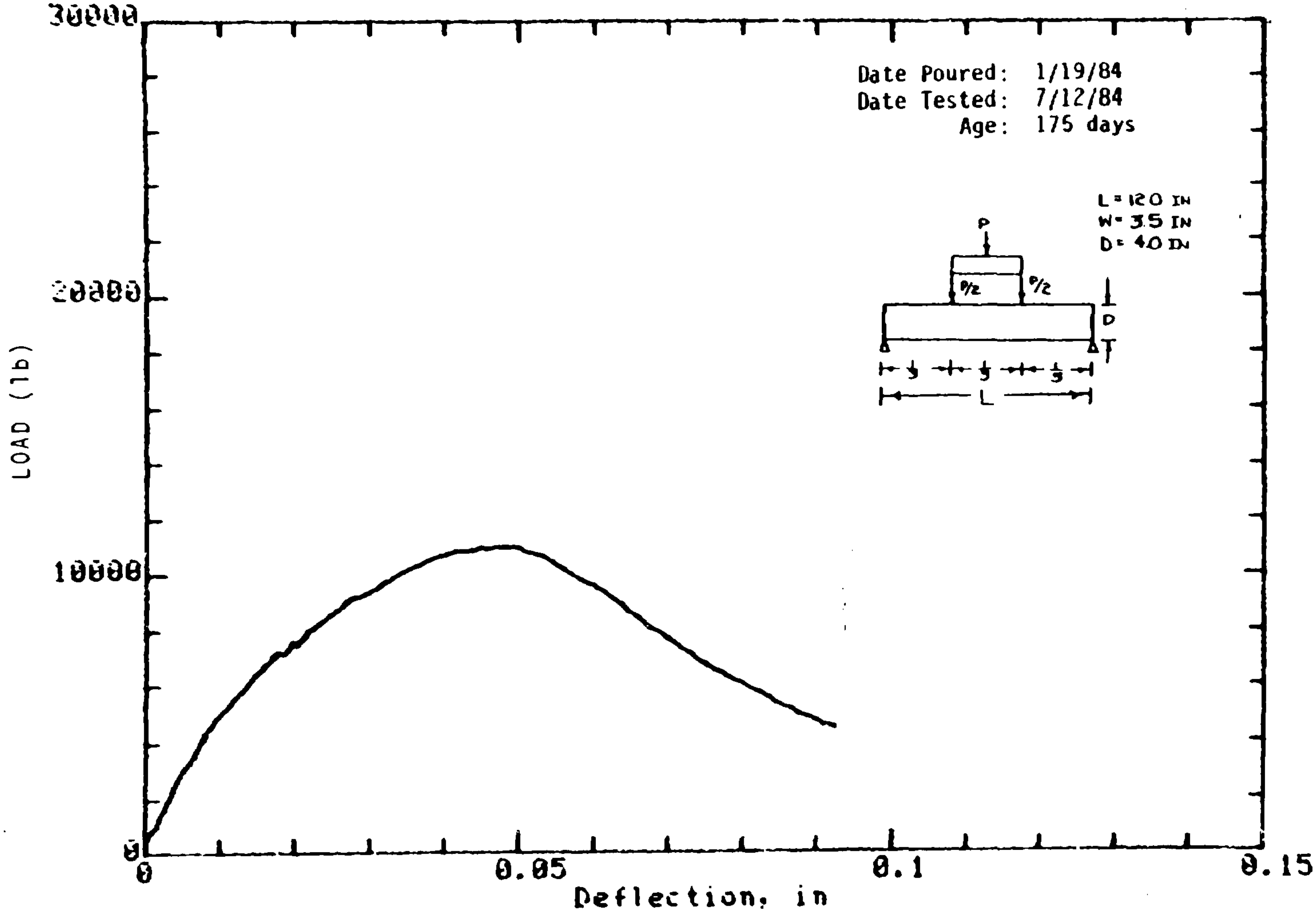

Mark: 6-22 Beam: 4in x 3.5in Cure: Dry
Concrete Sample

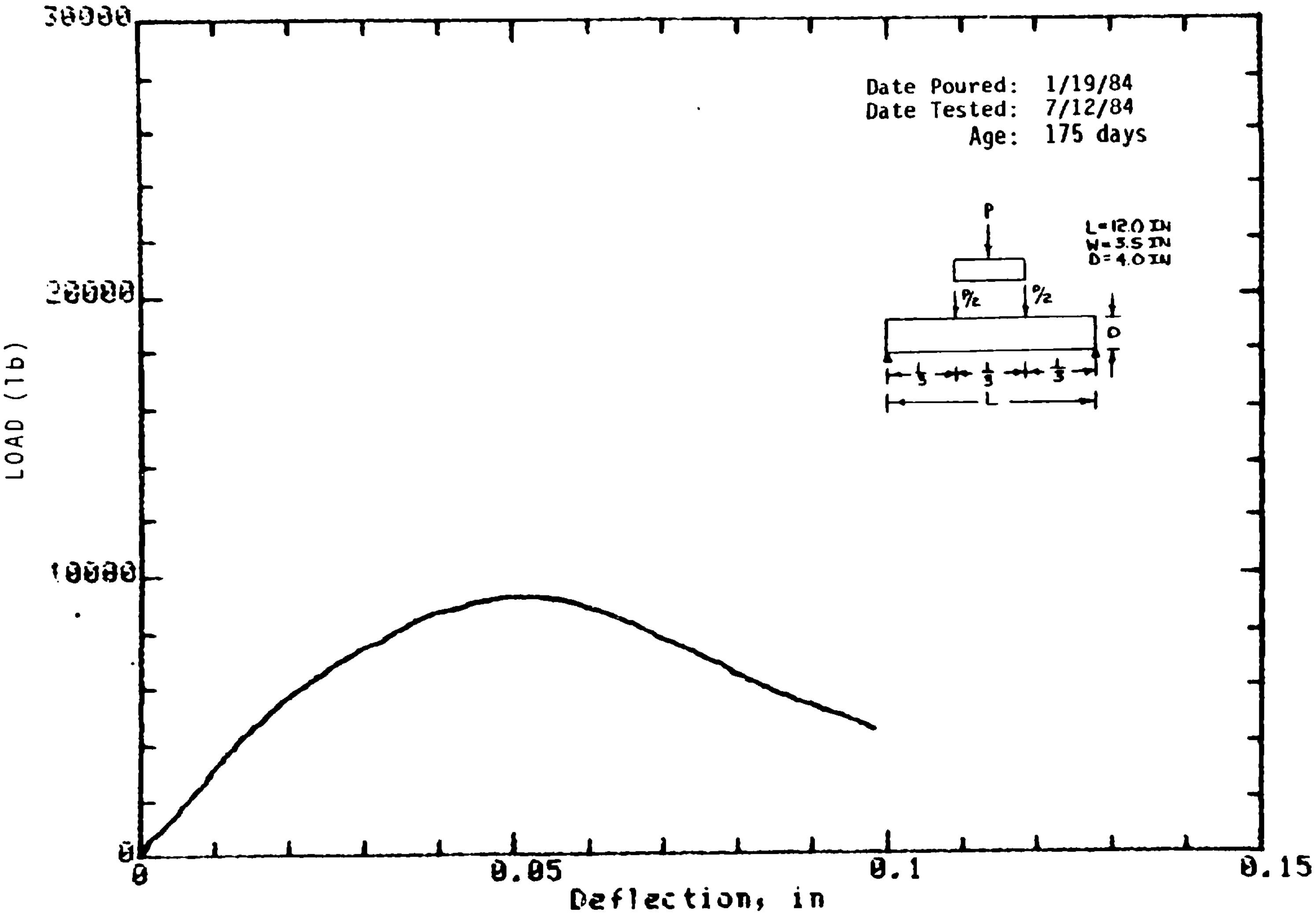

Mark: 6-23 Beam: 4in x 3.5in Cure: Dry
Concrete Sample

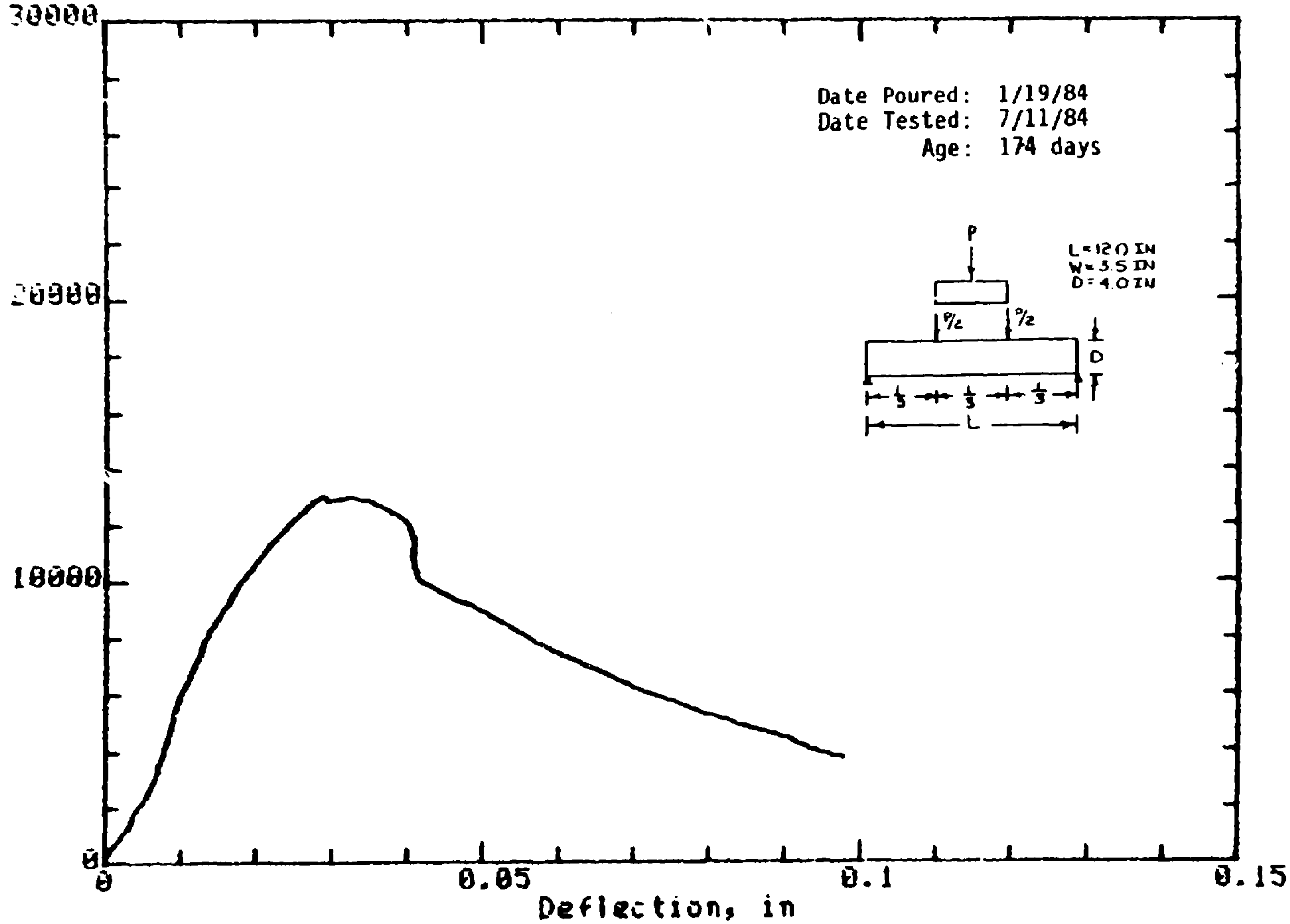

Mark: 6-24 Beam: 4in x 3.5in Cure: Wet
Concrete Sample

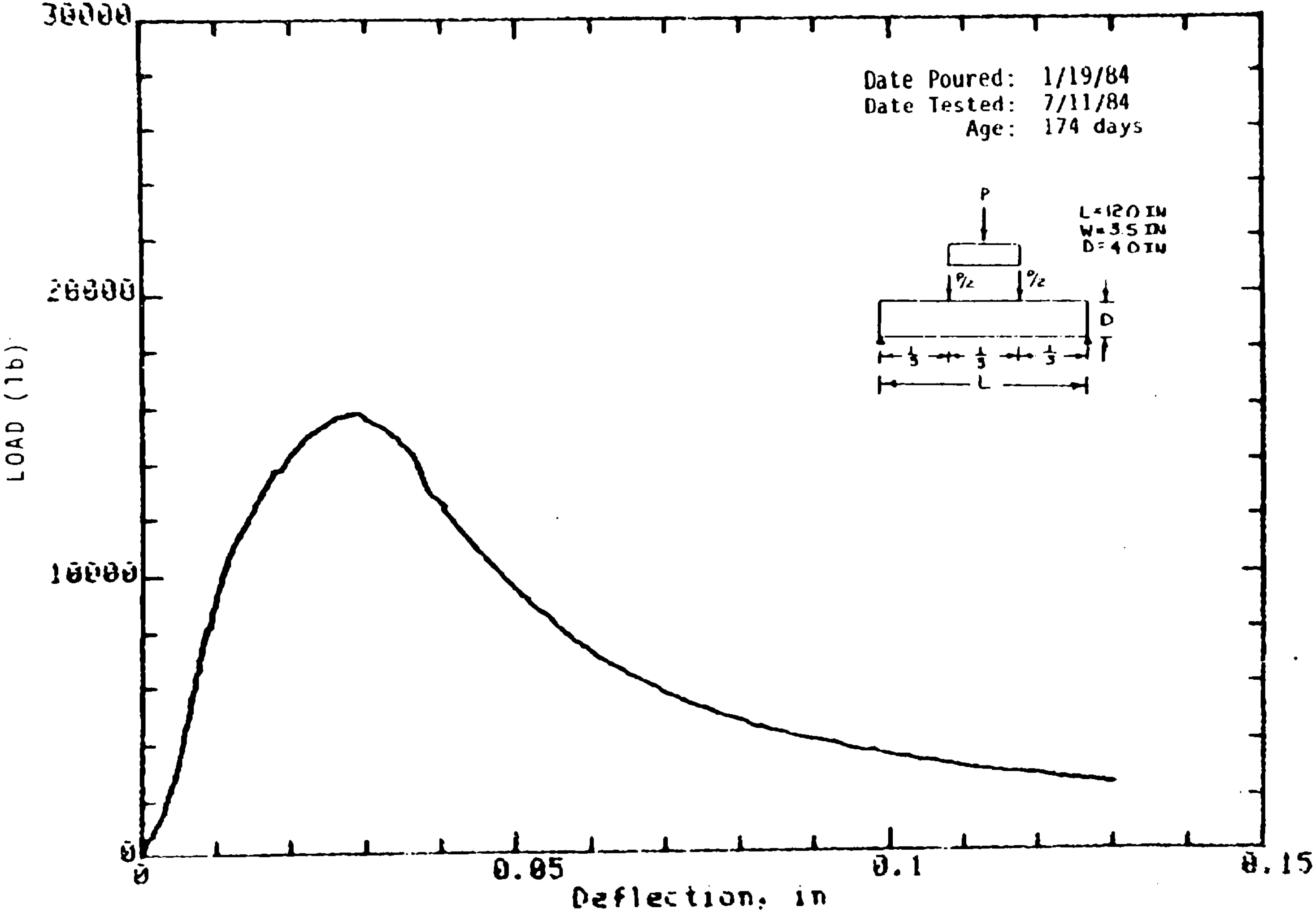

Mark: 6-25 Beam: 4in x 3.5in Cure: Wet
Concrete Sample

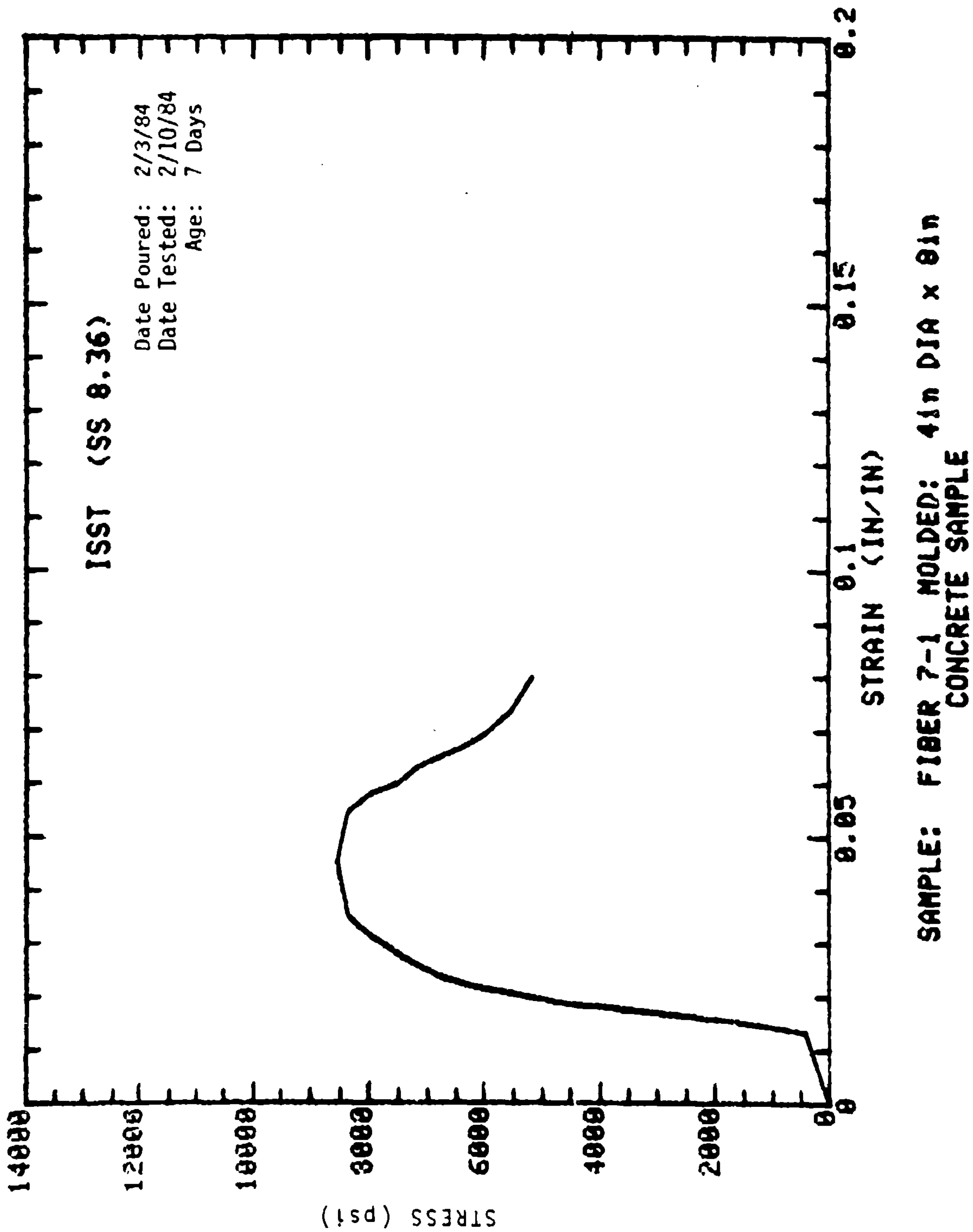
ISST (SS 8.36)
Date Poured: 2/3/84
Date Tested: 2/10/84
Age: 7 Days
STRESS (psi)
0
2000
4000
6000
8000
10000
12000
14000
0
0.05
0.1
0.15
0.2
STRAIN (IN/IN)
SAMPLE: FIBER 7-1 MOLDED: 4in DIA x 8in
CONCRETE SAMPLE

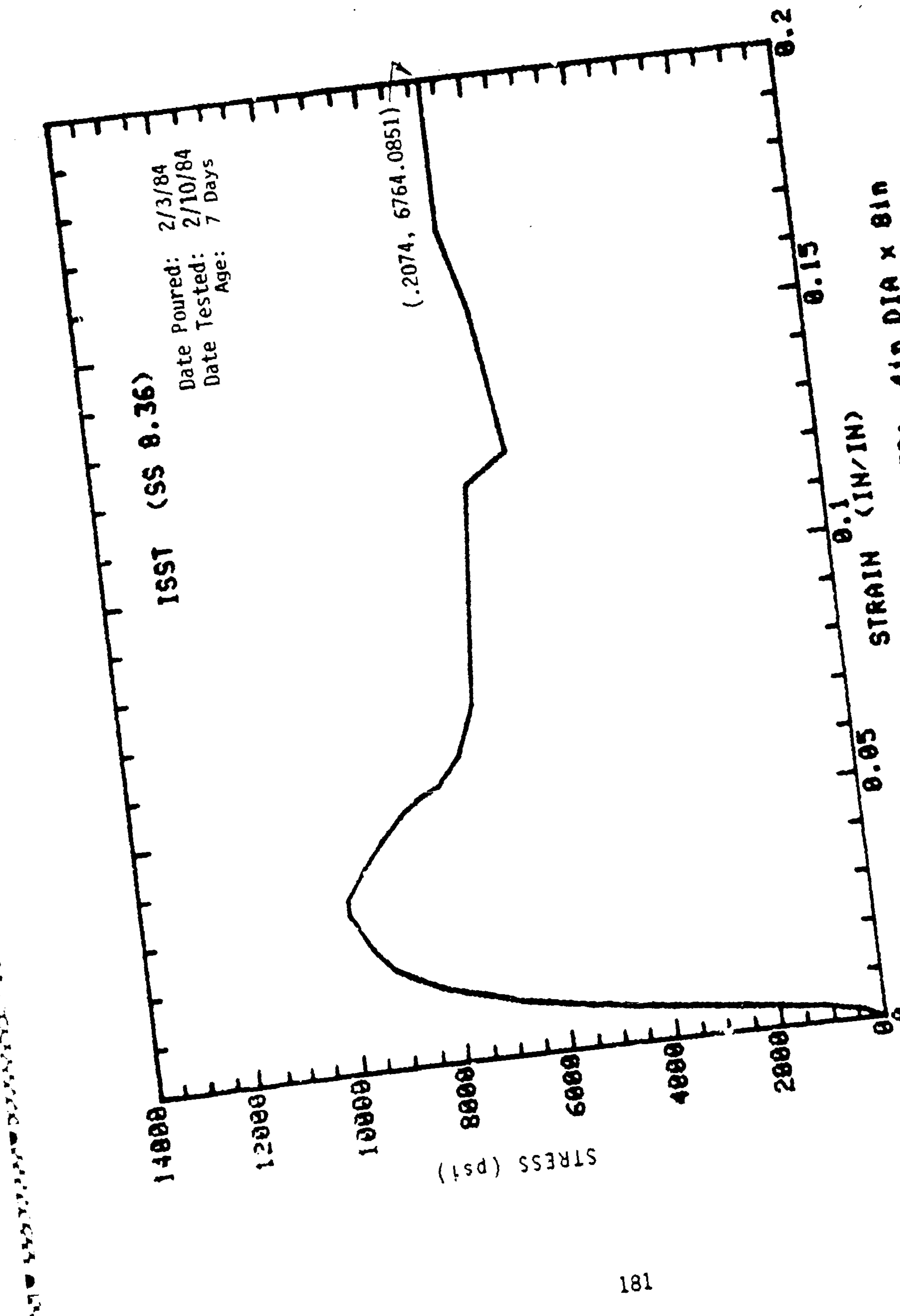

SAMPLE: FIBER 7-2 MOLDED: 4in DIA x 8in
CONCRETE SAMPLE

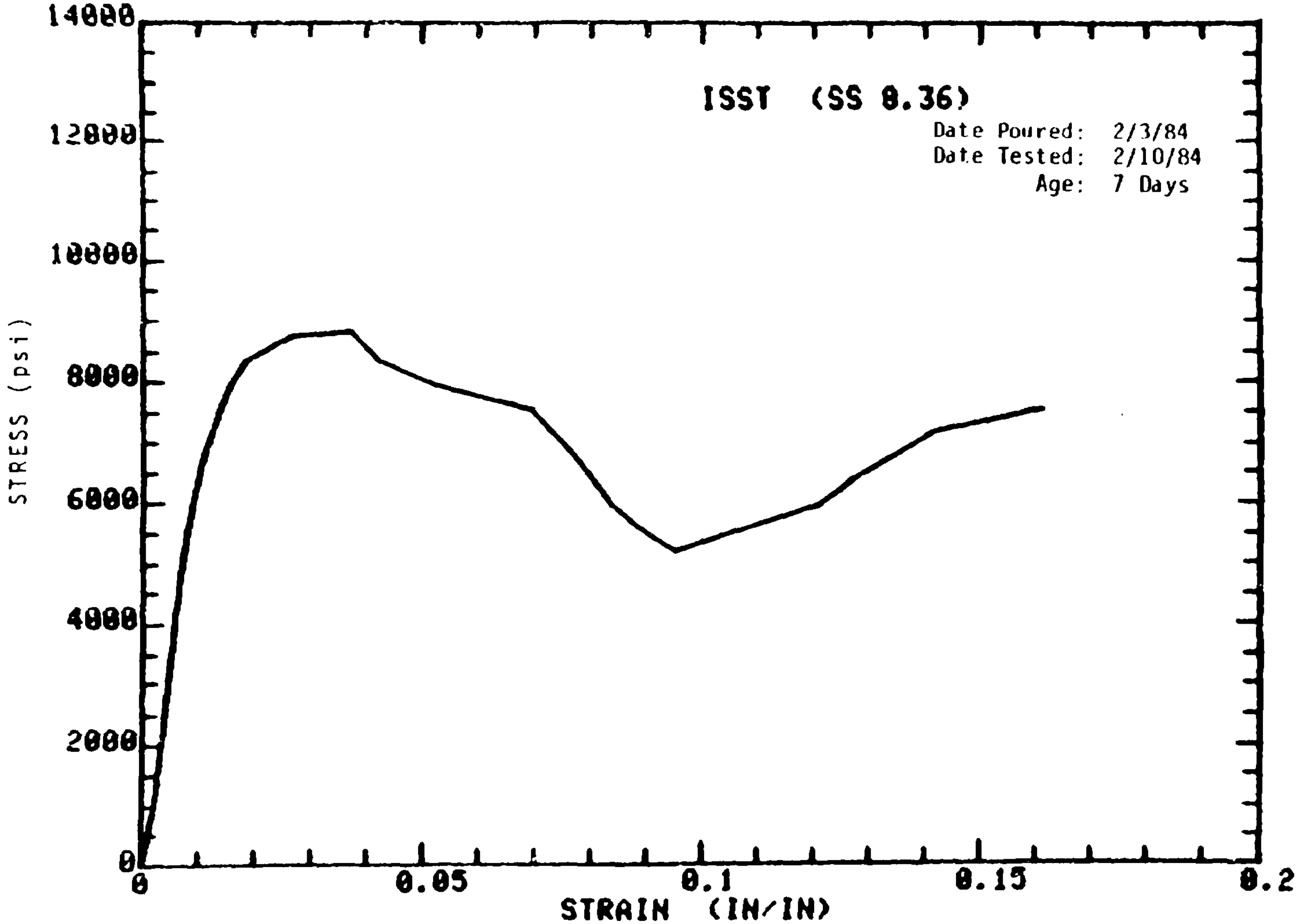

SAMPLE: FIBER 7-3 MOLDED: 4in DIA x 8in
CONCRETE SAMPLE

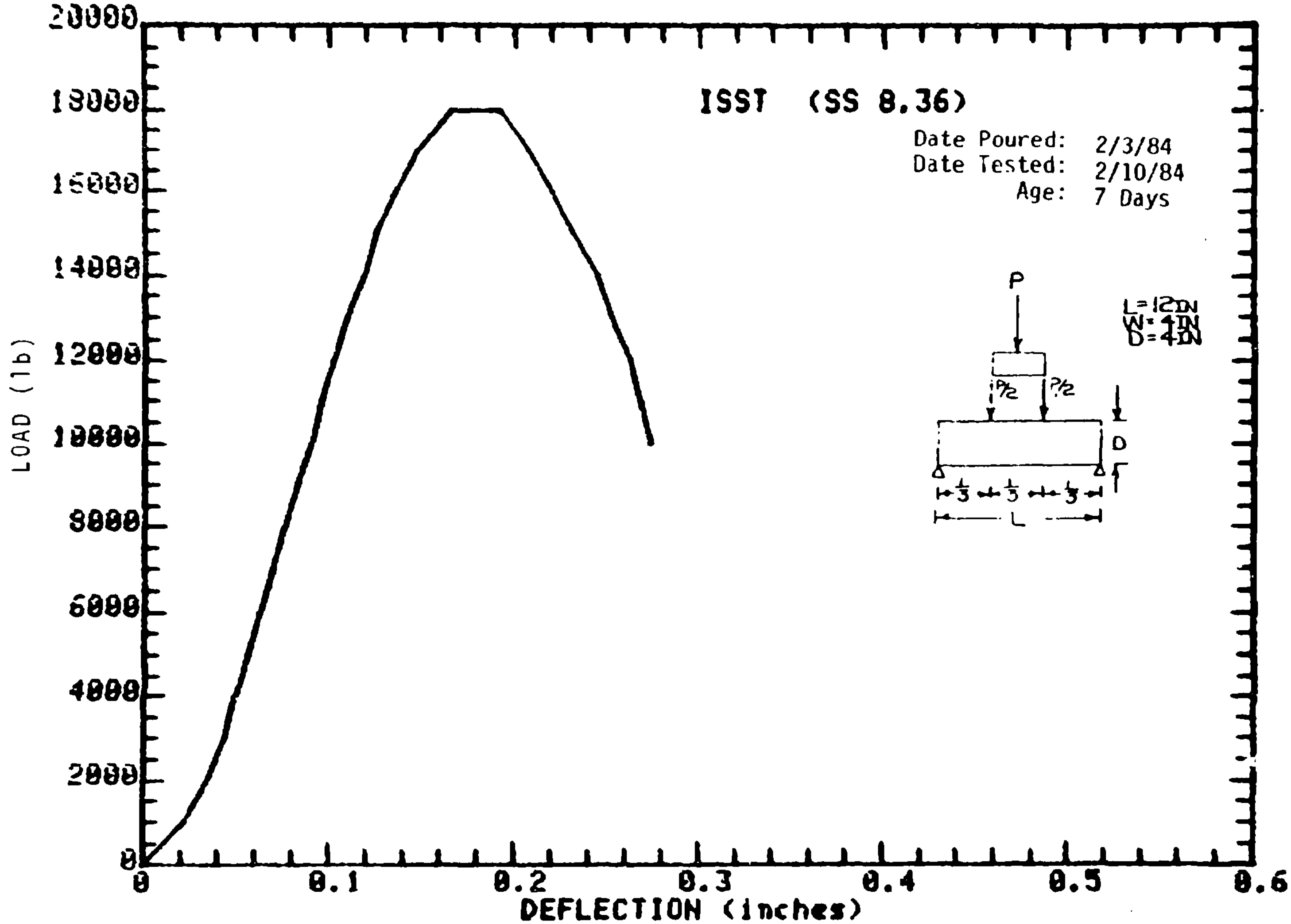

SAMPLE: BEAM 7-14
CONCRETE SAMPLE

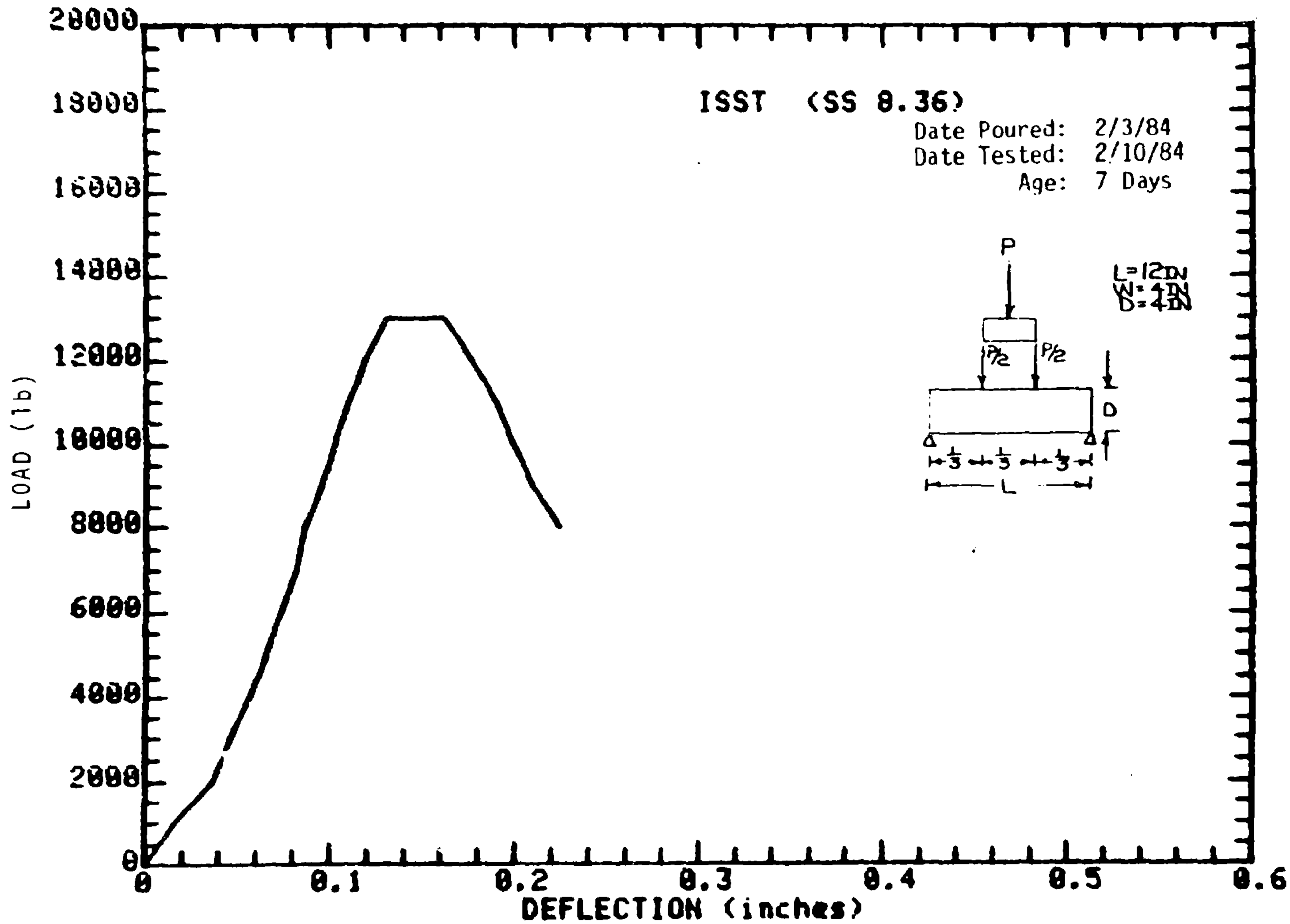

SAMPLE: BEAM 7-15
CONCRETE SAMPLE

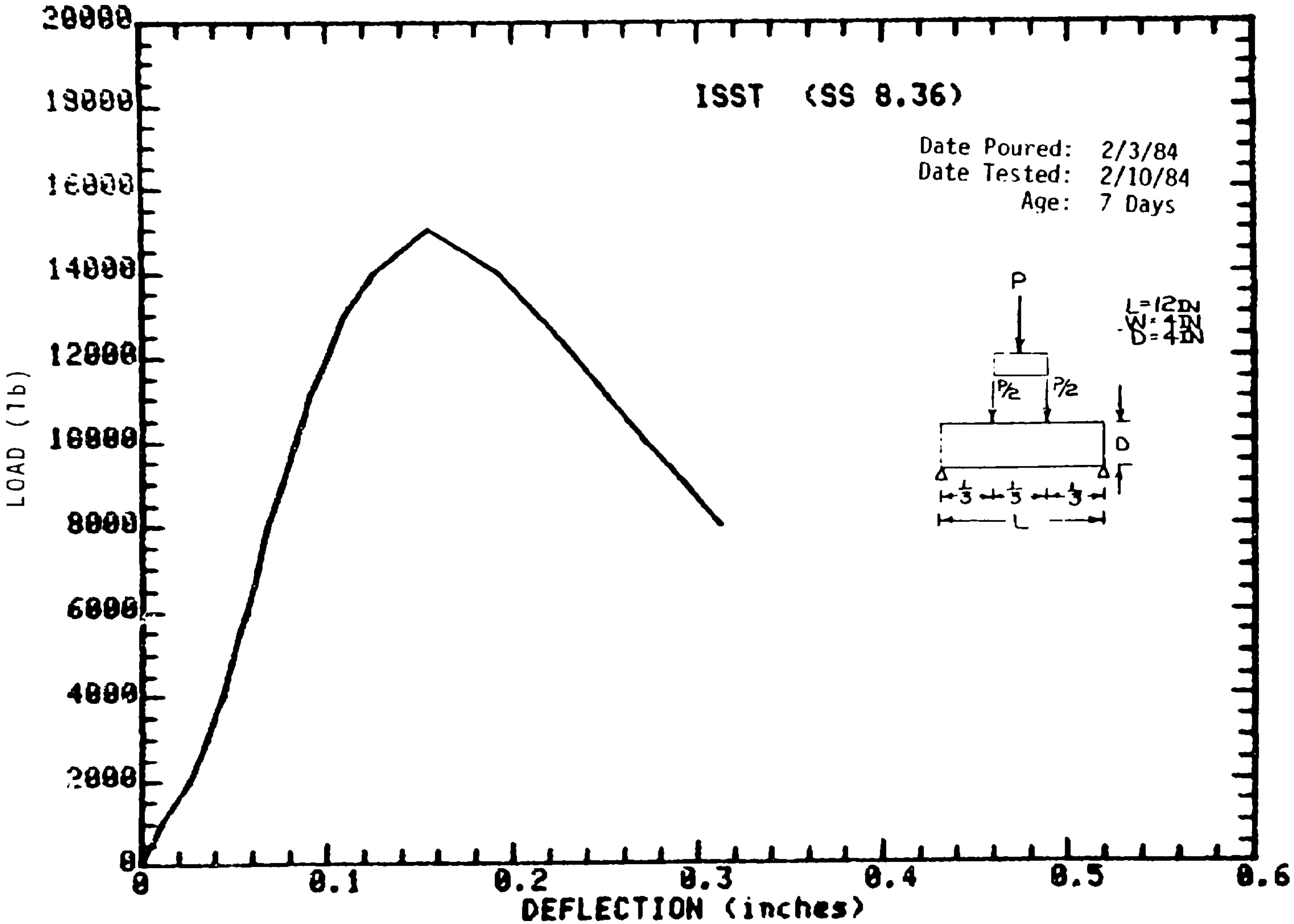

SAMPLE: BEAM 7-16
CONCRETE SAMPLE

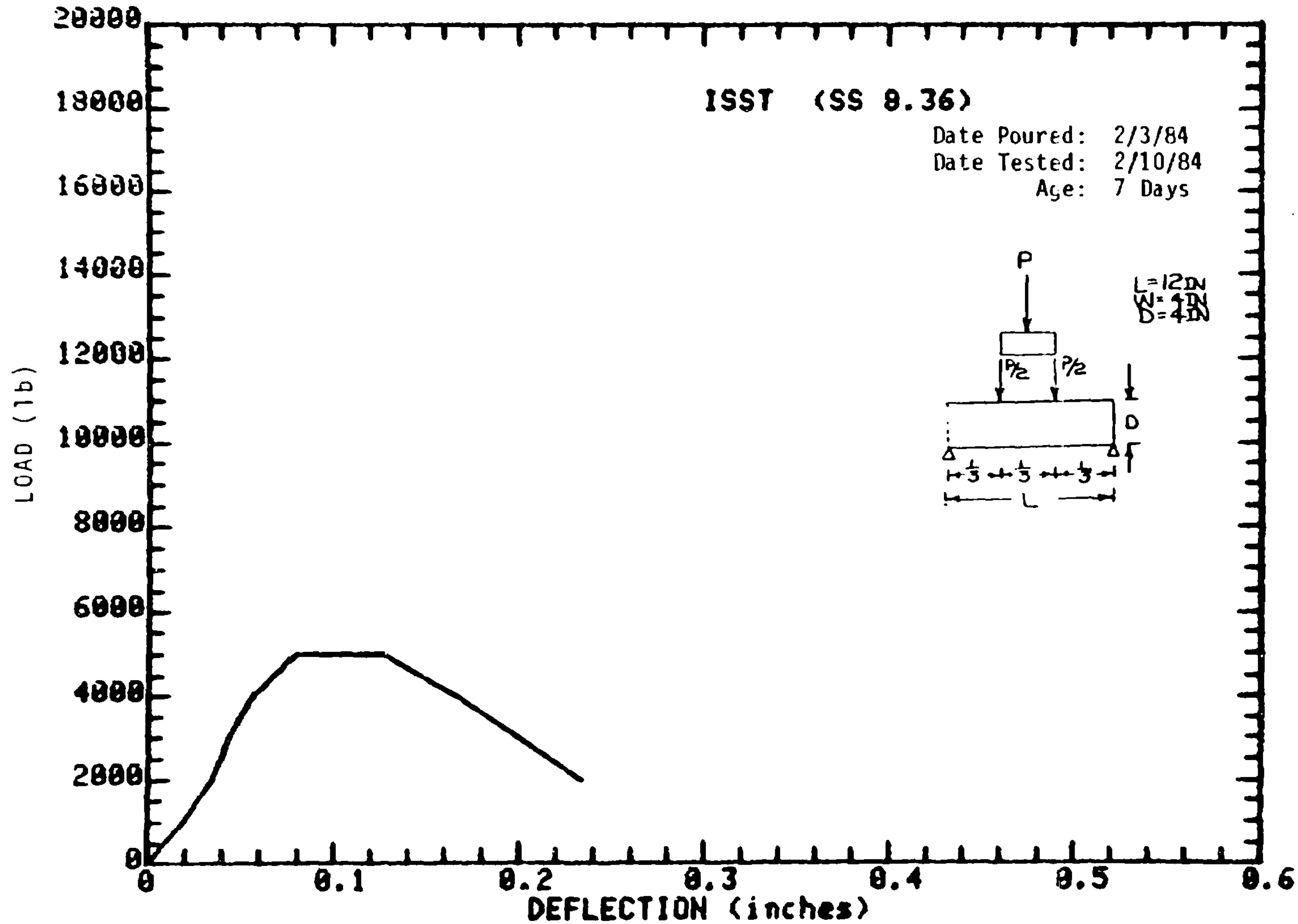

SAMPLE: BEAM (COLUMN) 7-31
CONCRETE SAMPLE

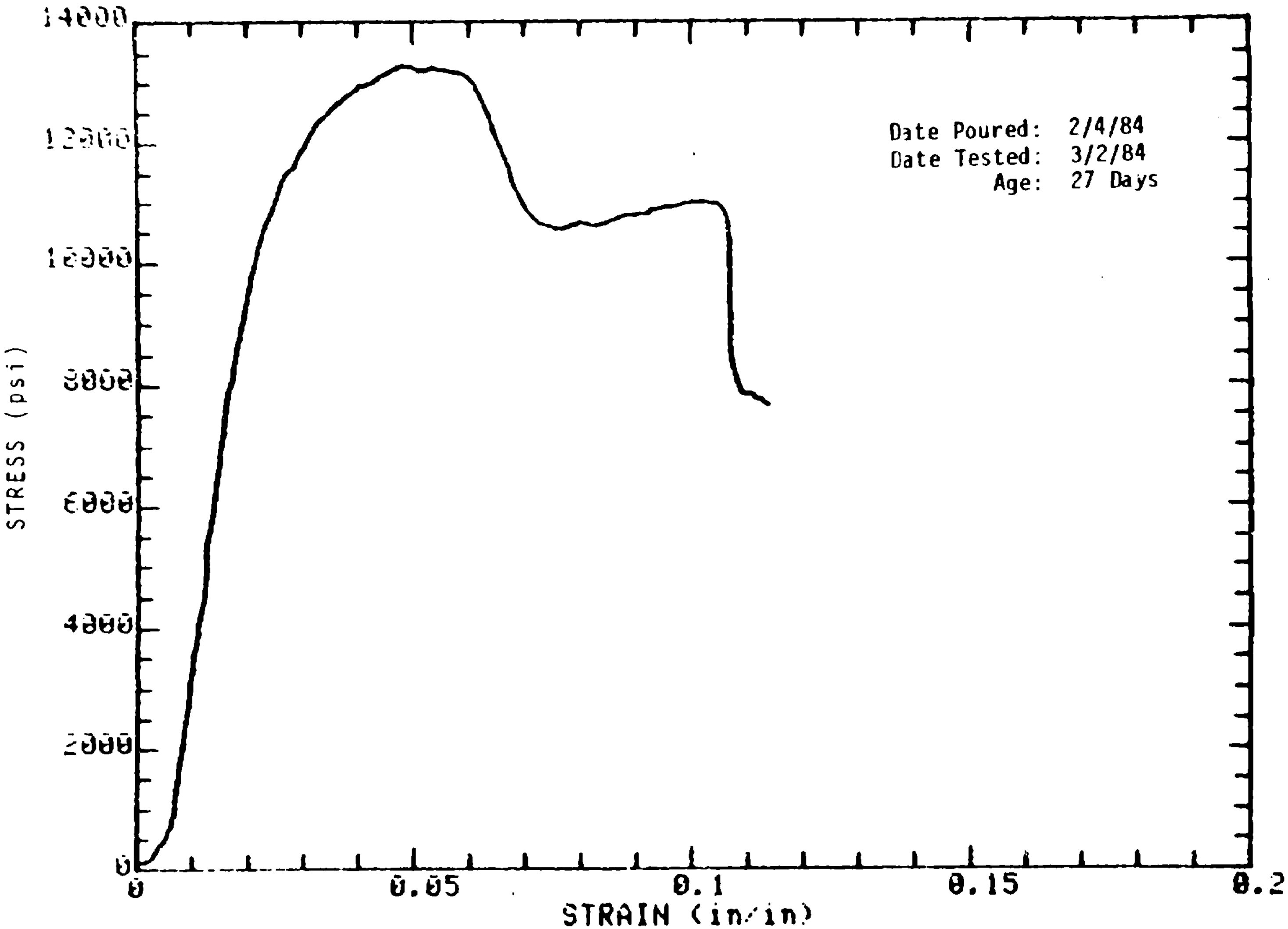

SAMPLE: 7-4 MOLDED: 4in DIA x 8in
CONCRETE SAMPLE

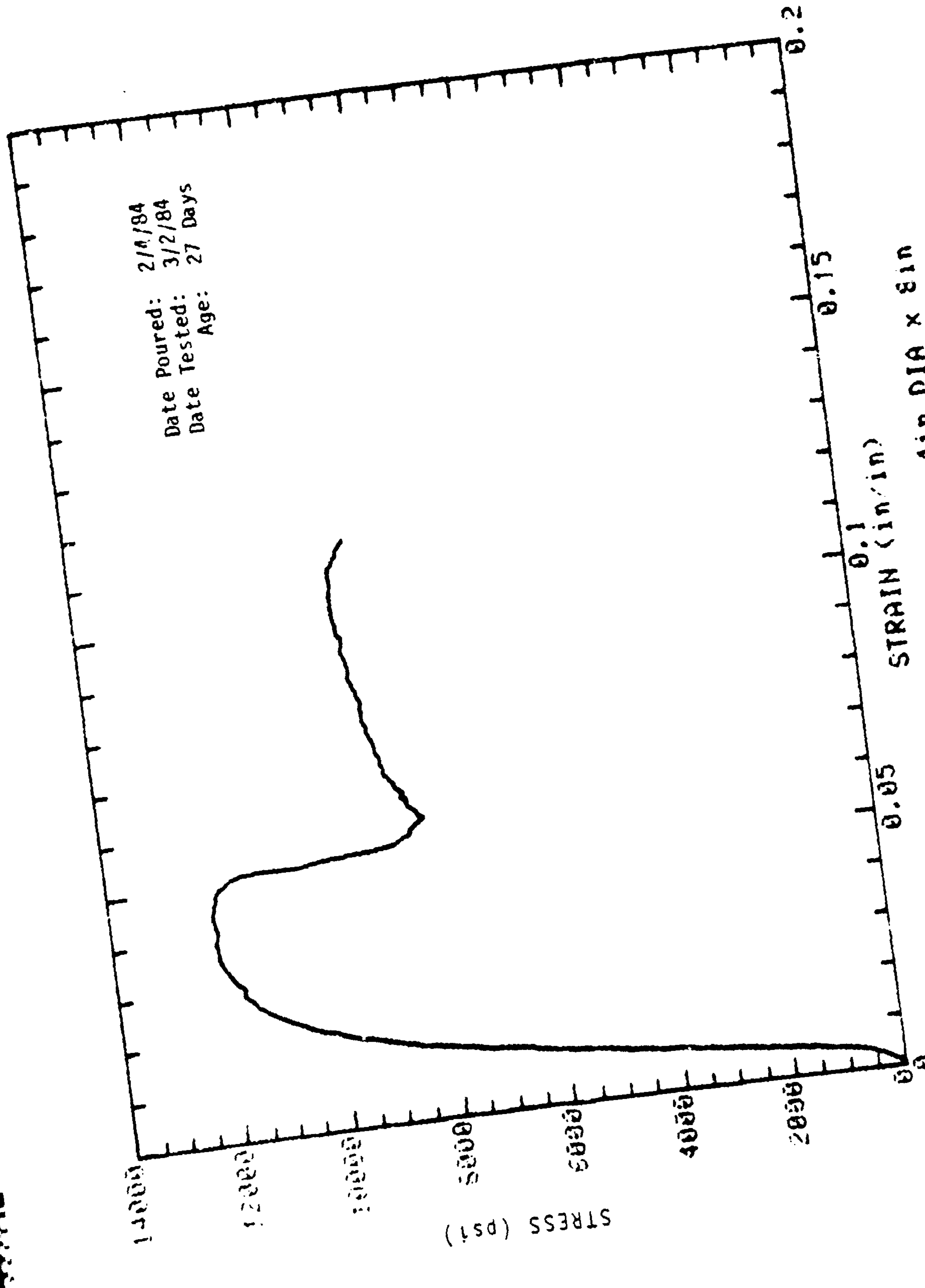

SAMPLE: 7-5 MOLDED: 4in DIA x 8in
CONCRETE SAMPLE

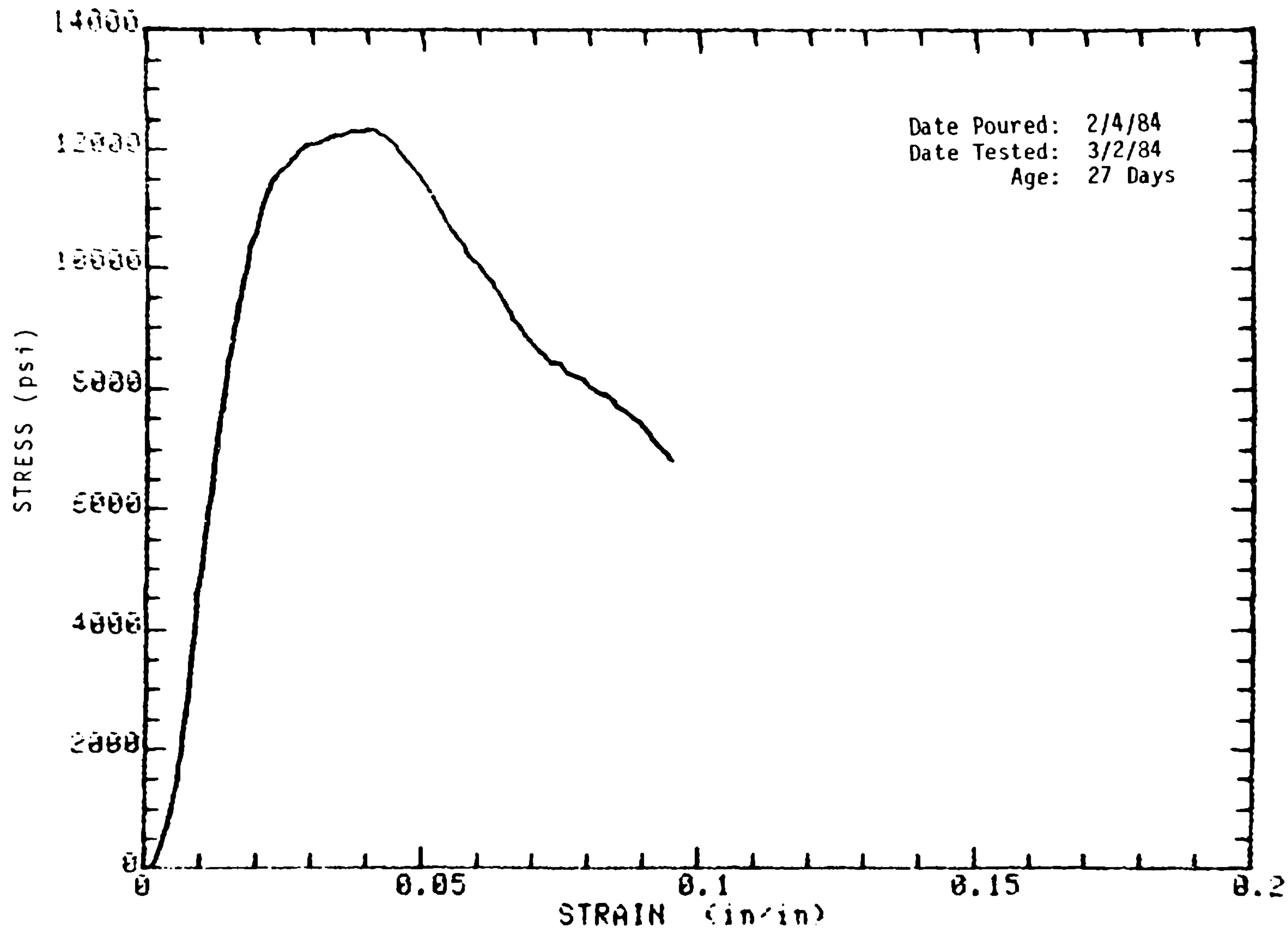

SAMPLE: 7-7 MOLDED: 4in DIA x 8in
CONCRETE SAMPLE

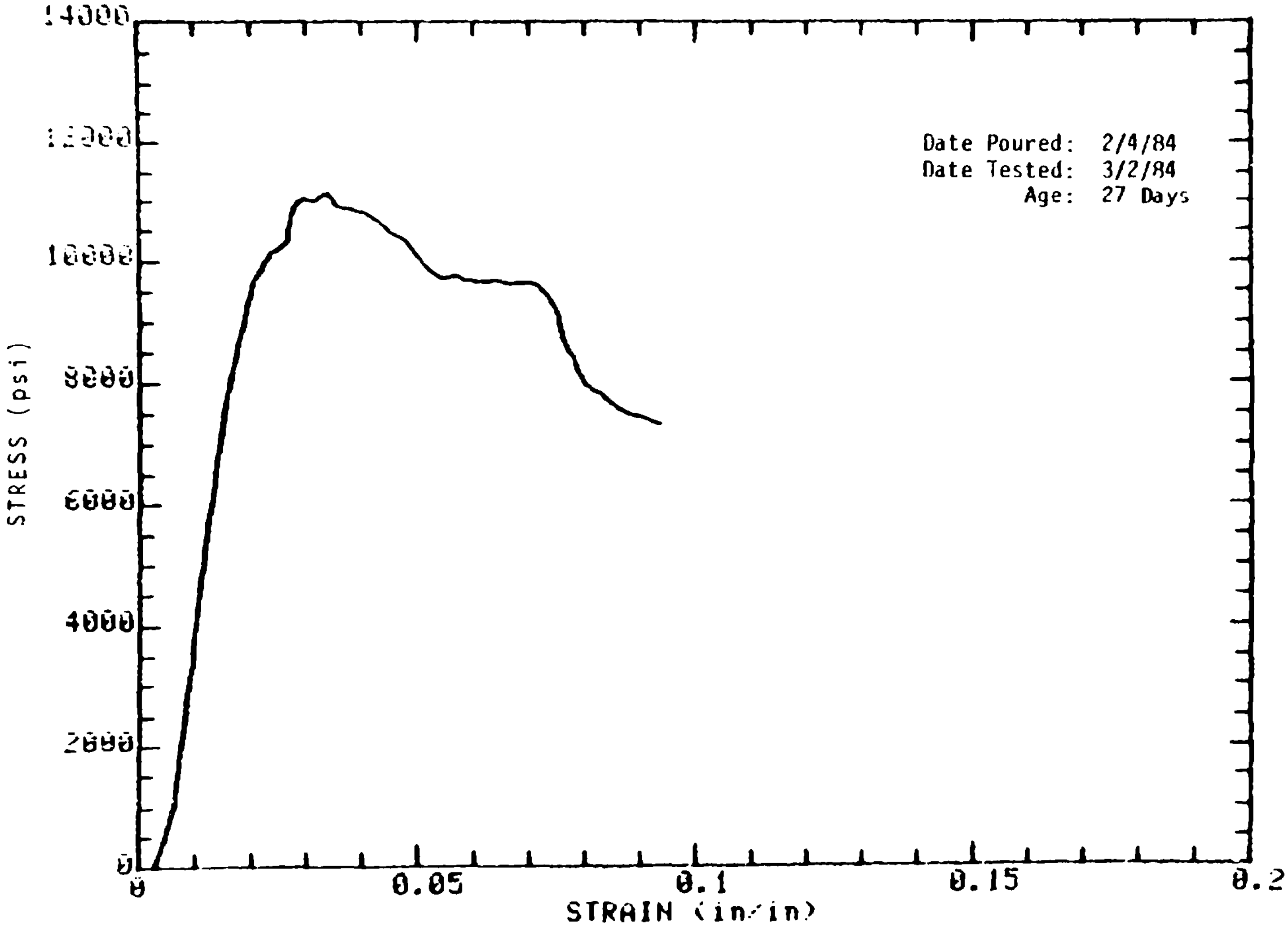

SAMPLE: 7-8 MOLDED: 4in DIA x 8in
CONCRETE SAMPLE

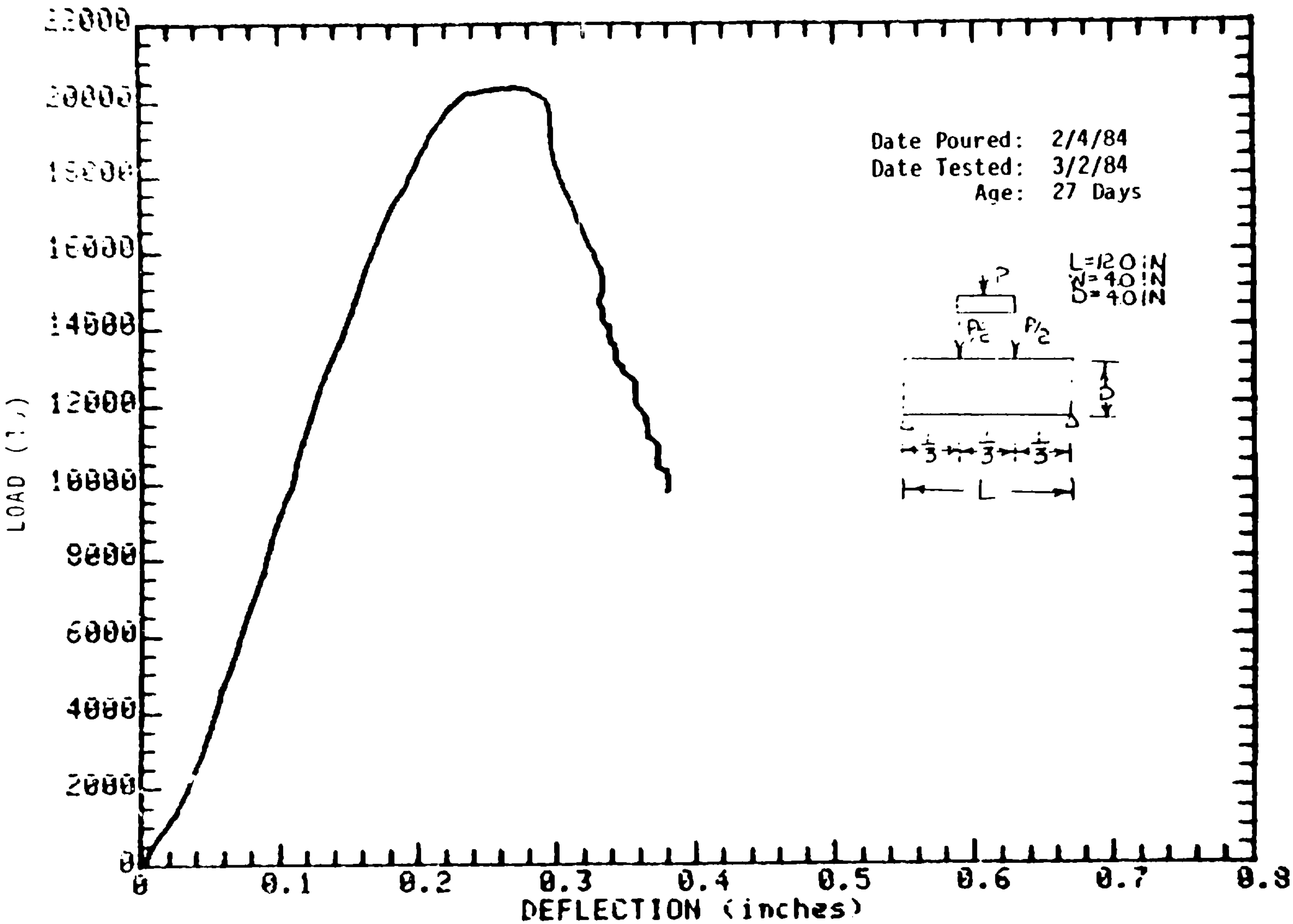

SAMPLE: BEAM 7-18
CONCRETE SAMPLE

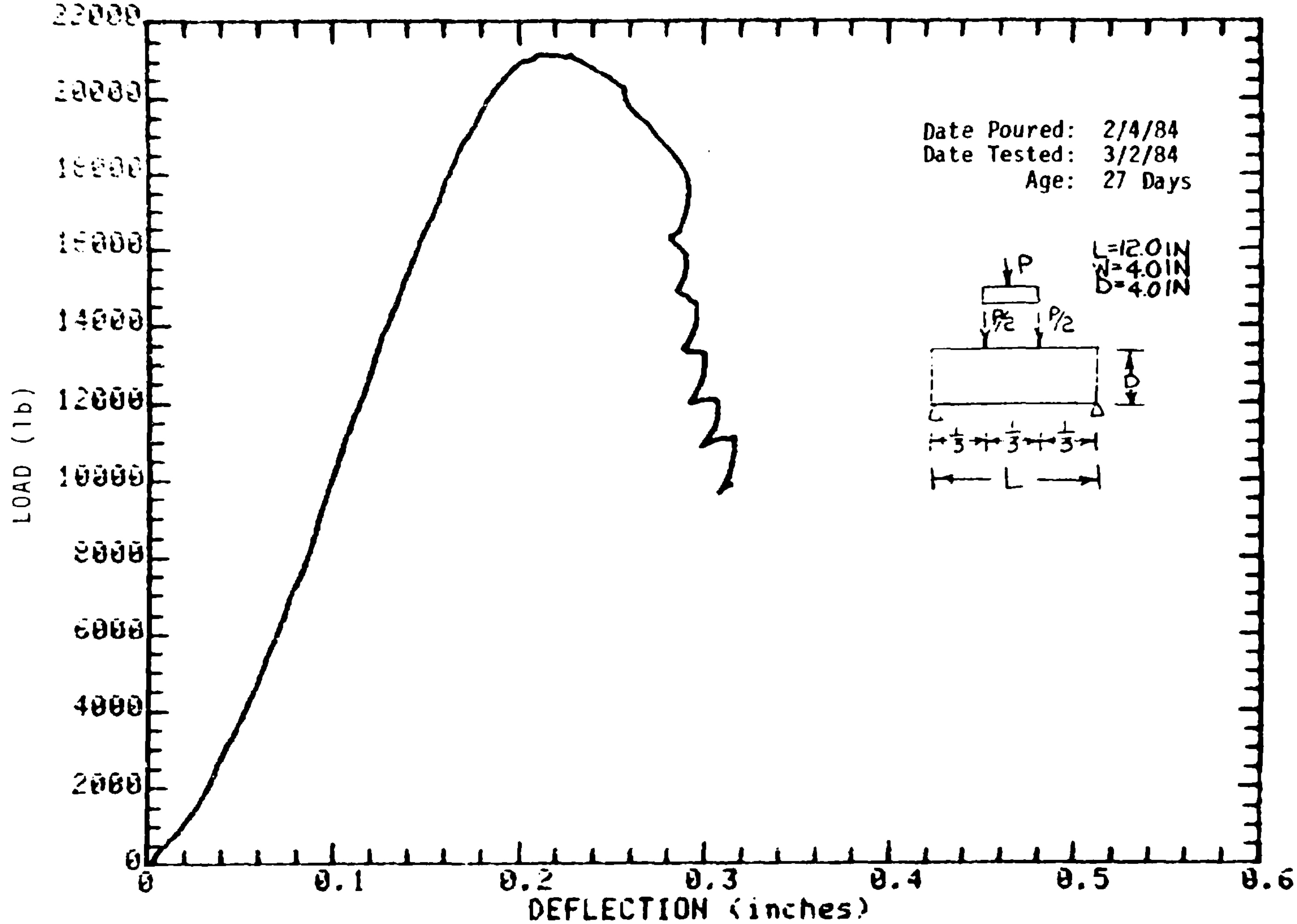

SAMPLE: BEAM 7-19
CONCRETE SAMPLE

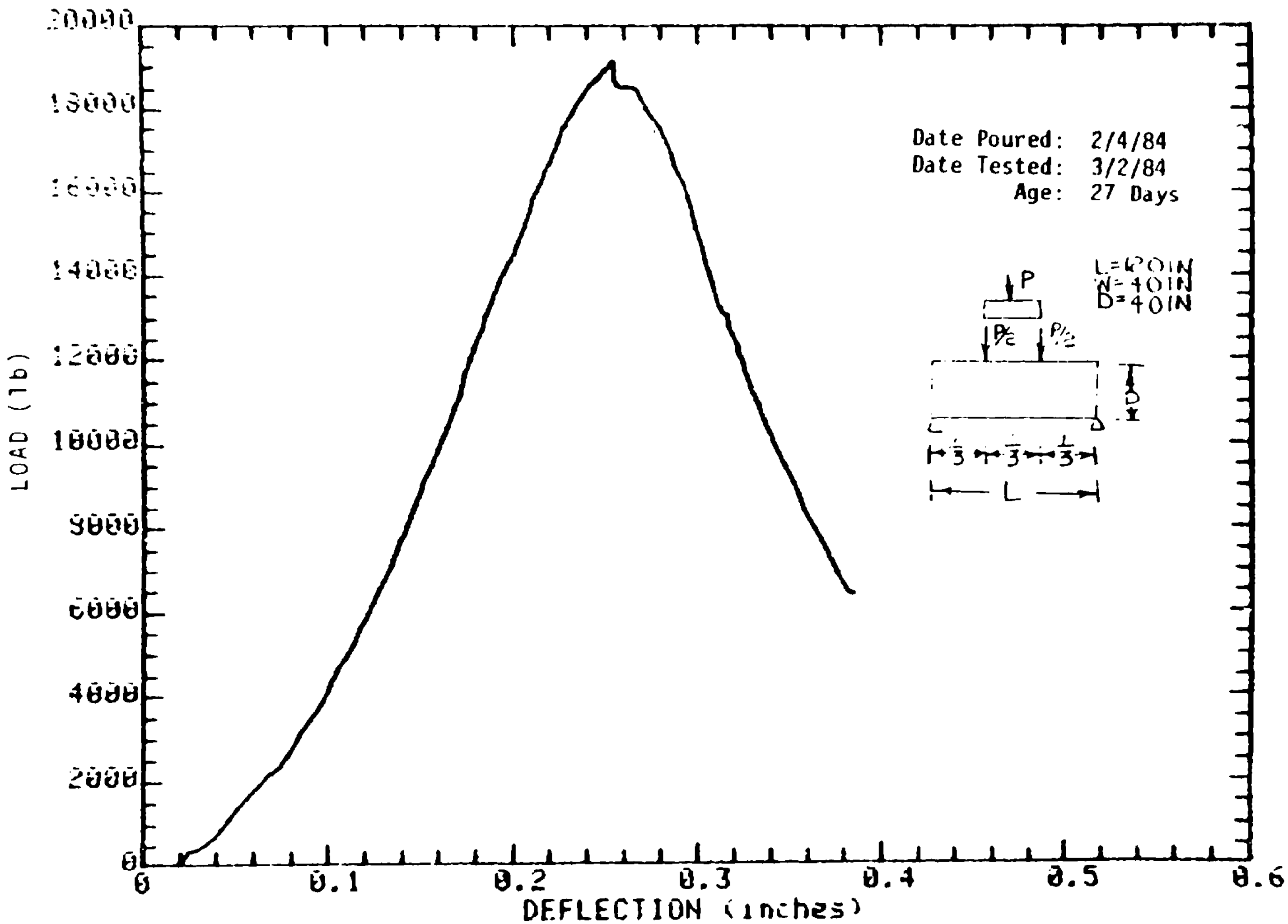

SAMPLE: BEAM 7-20
CONCRETE SAMPLE

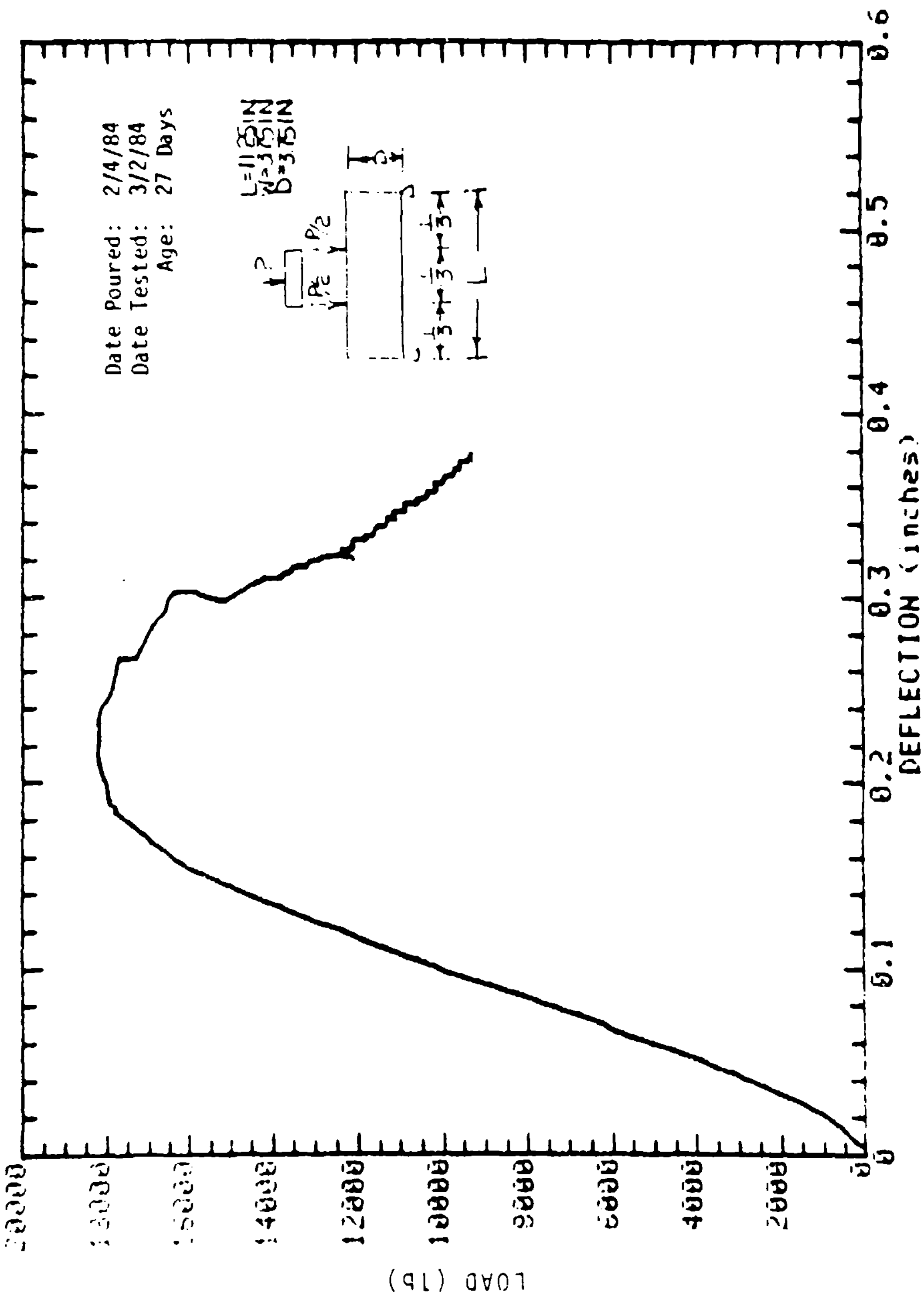

SAMPLE: BEAM 7-21
CONCRETE SAMPLE

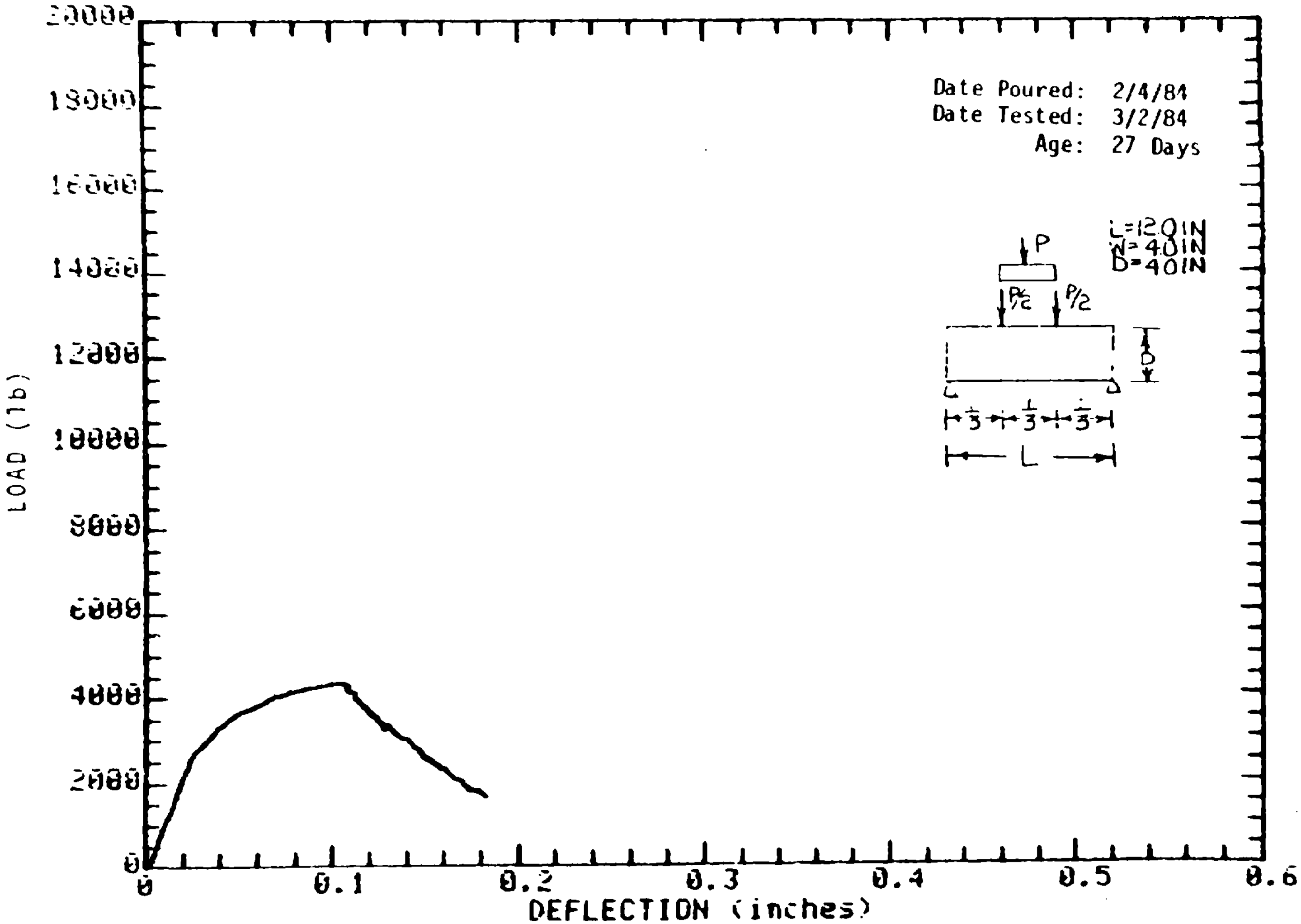

SAMPLE: COLUMN 7-29
CONCRETE SAMPLE

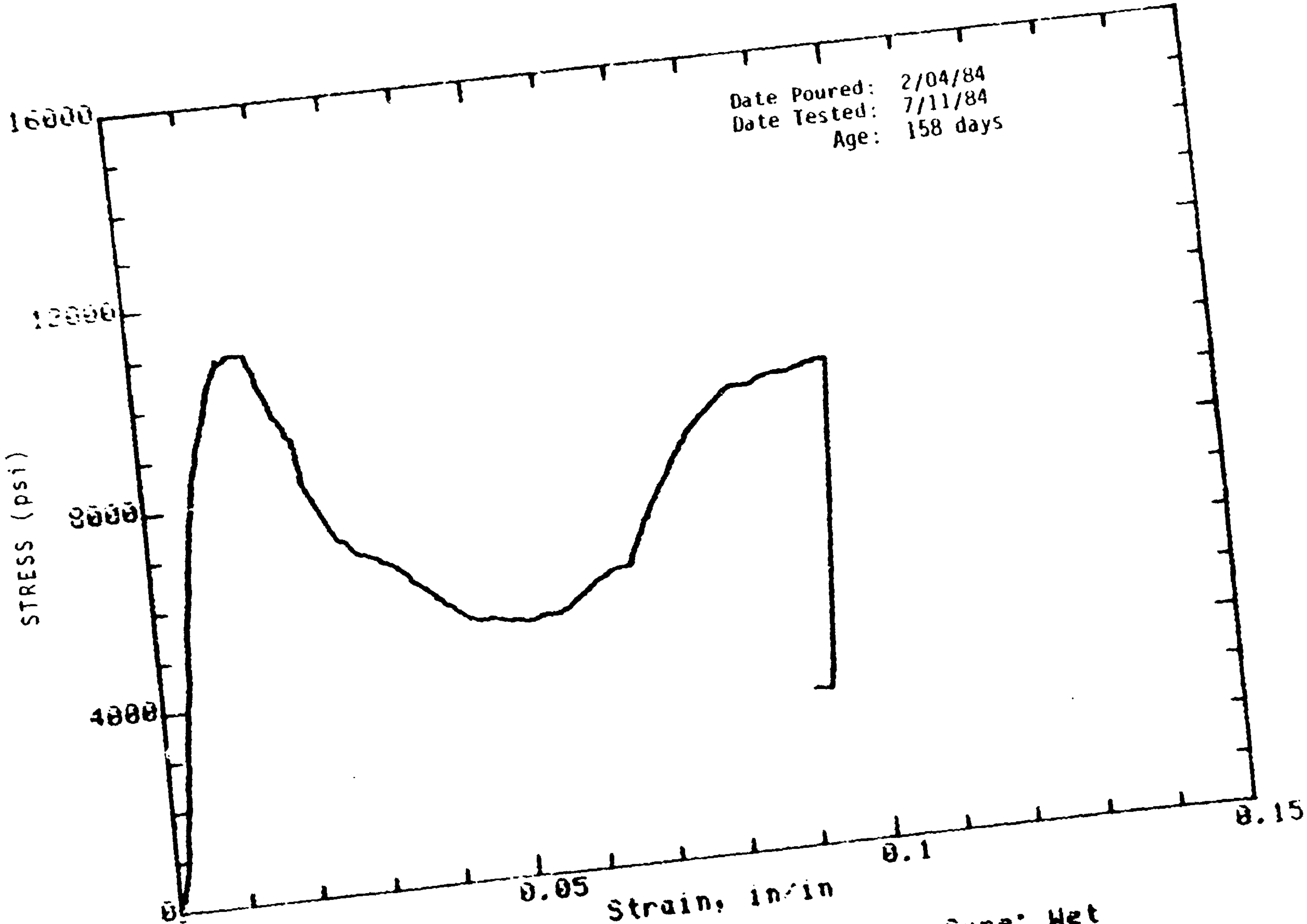

Mark: 7-6 Molded: 4in dia x 8in Cure: Wet
Con_rete Sample

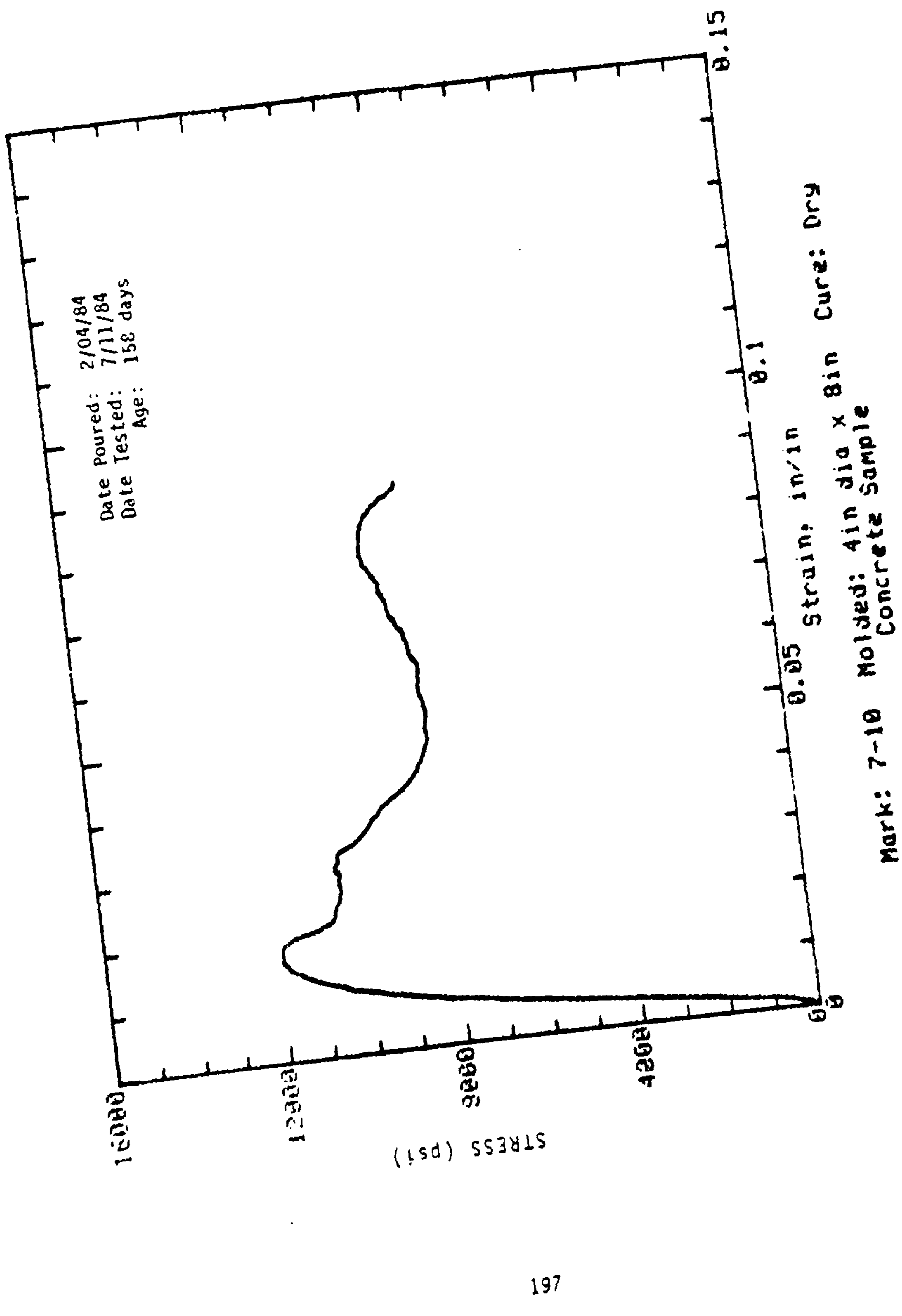

Date Poured: 2/04/84
Date Tested: 7/11/84
Age: 158 days
STRESS (psi)
16000
12000
8000
4000
0
0
0.05
0.1
0.15
Strain, in/in
Mark: 7-10 Molded: 4in dia x 8in Cure: Dry
Concrete Sample

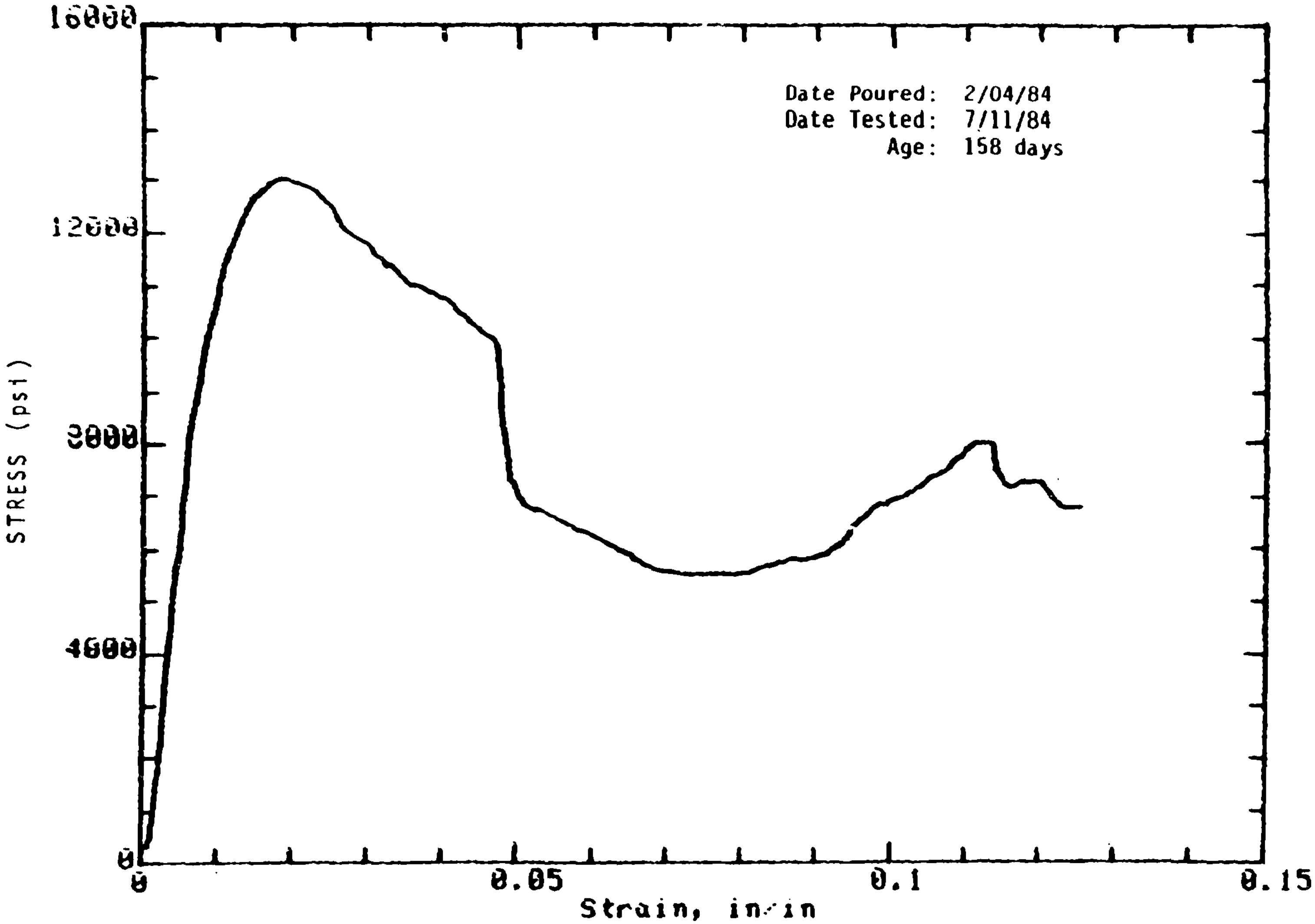

Mark: 7-12 Molded: 4in dia x 8in Cure: Dry
Concrete Sample

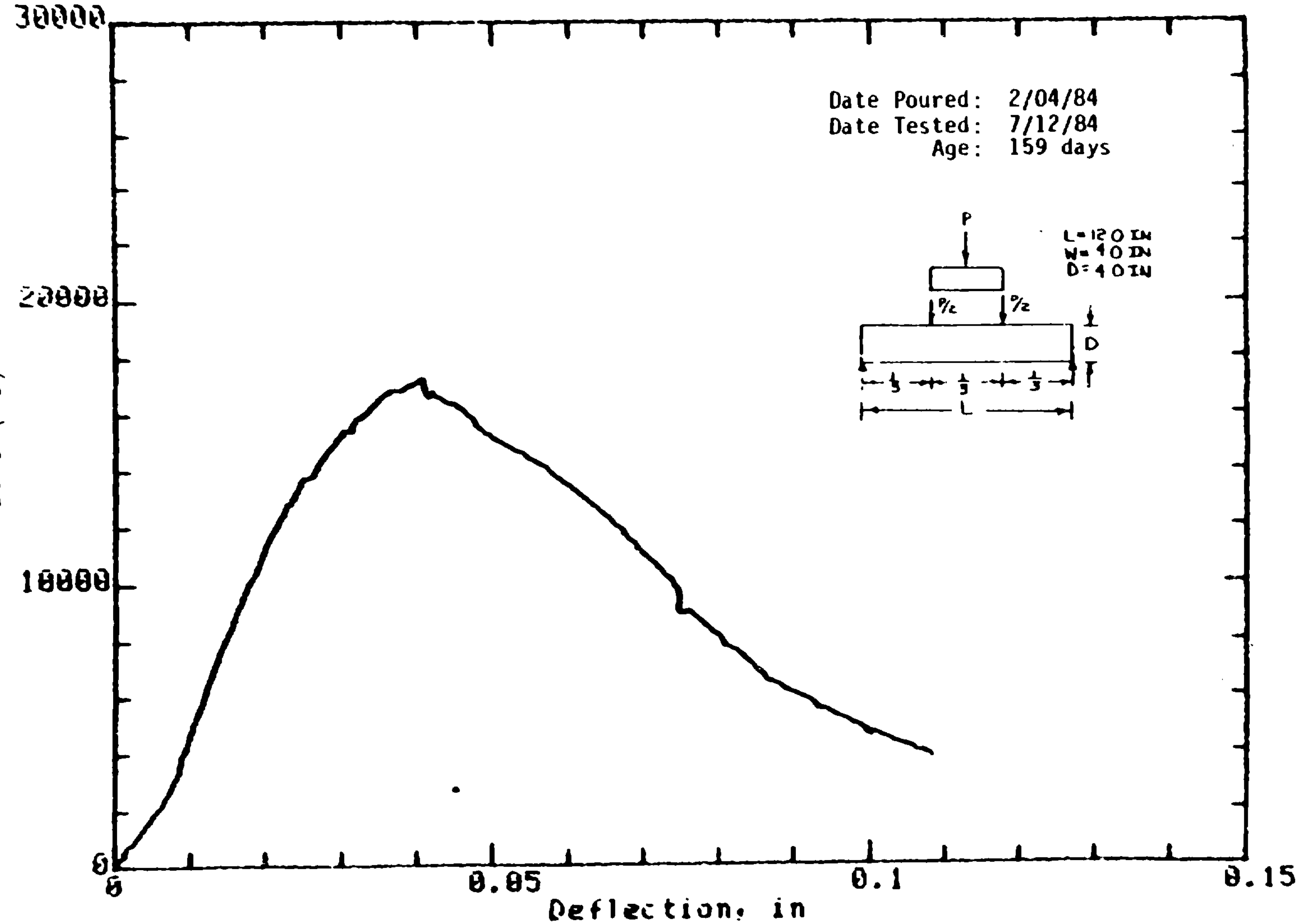

Mark: 7-17 Beam: 4in x 4in Cure: Dry
Concrete Sample

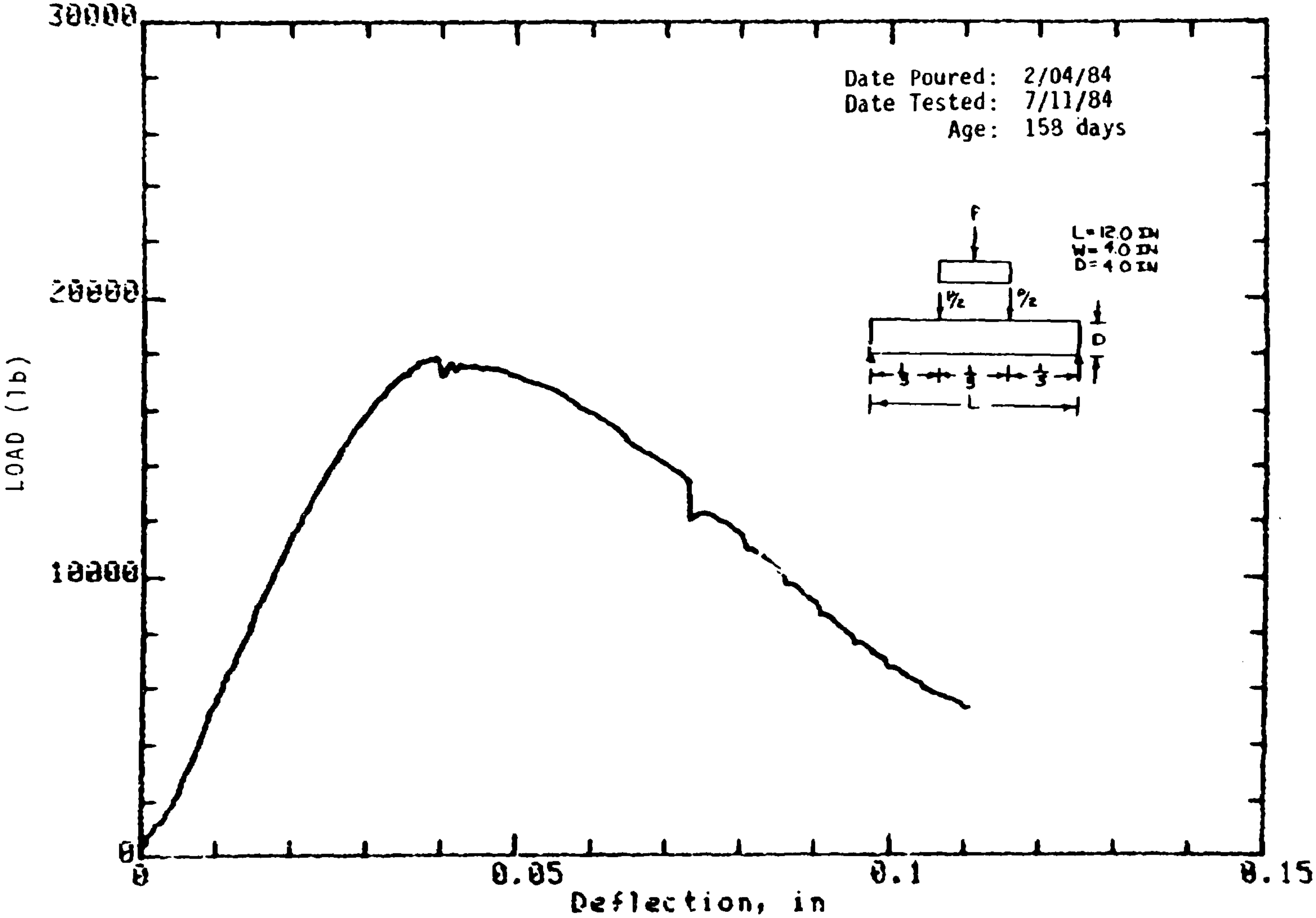

Mark: 7-24 Beam: 4in x 4in Cure: Dry
Concrete Sample

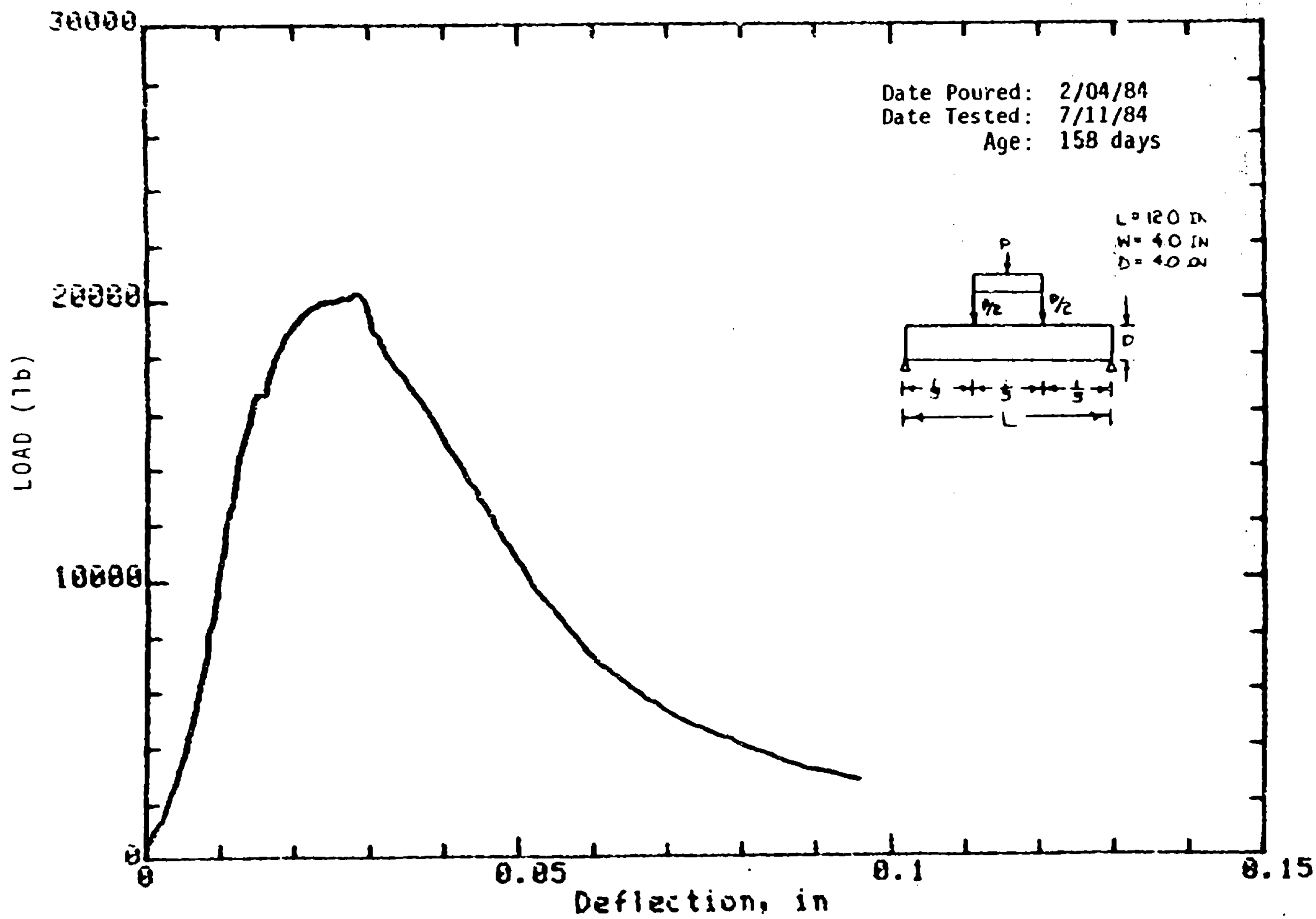

Mark: 7-13 Beam: 4in x 4in Cure: Wet
Concrete Sample

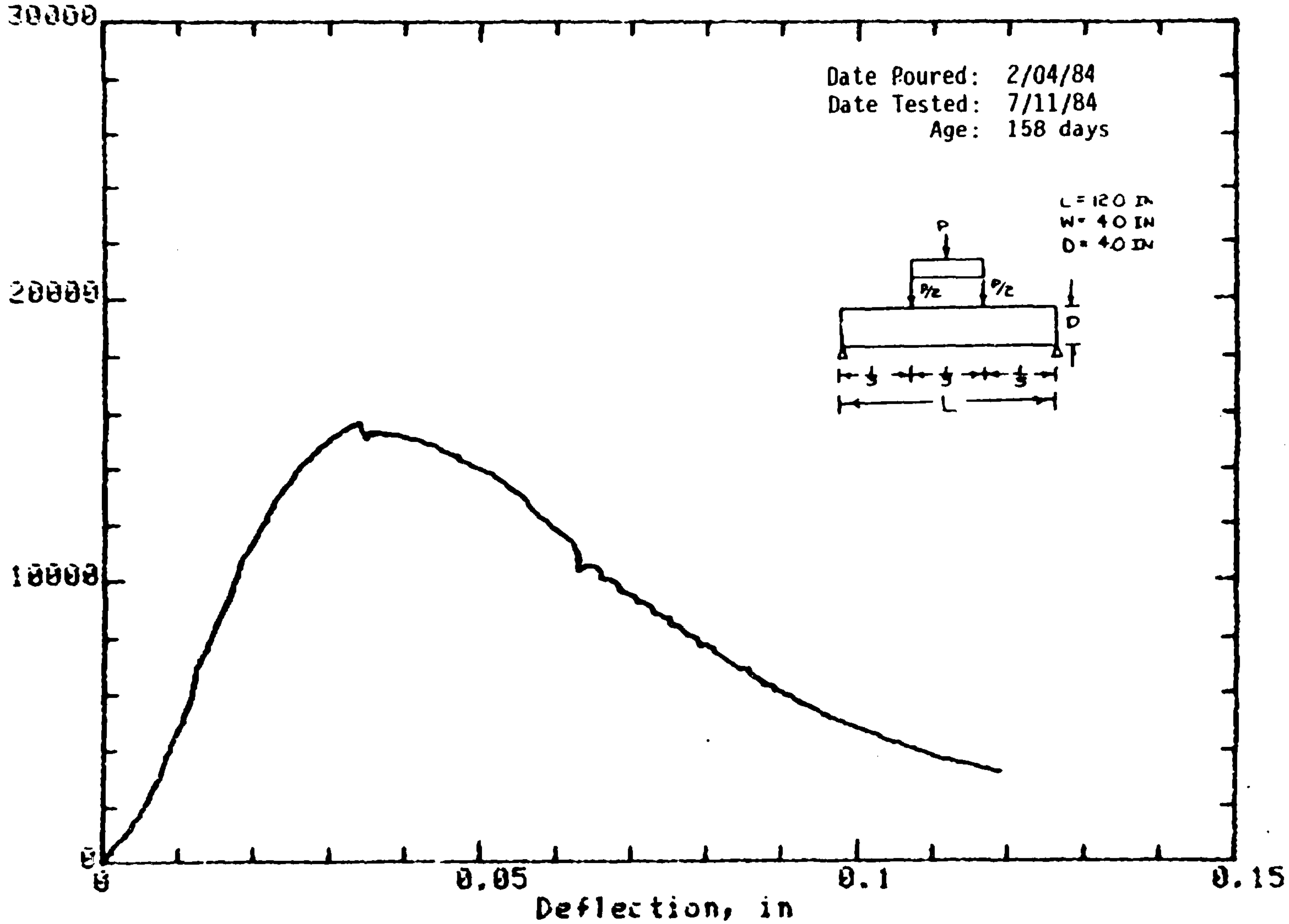

Mark: 7-22 Beam: 4in x 4in Cure: Dry
Concrete Sample

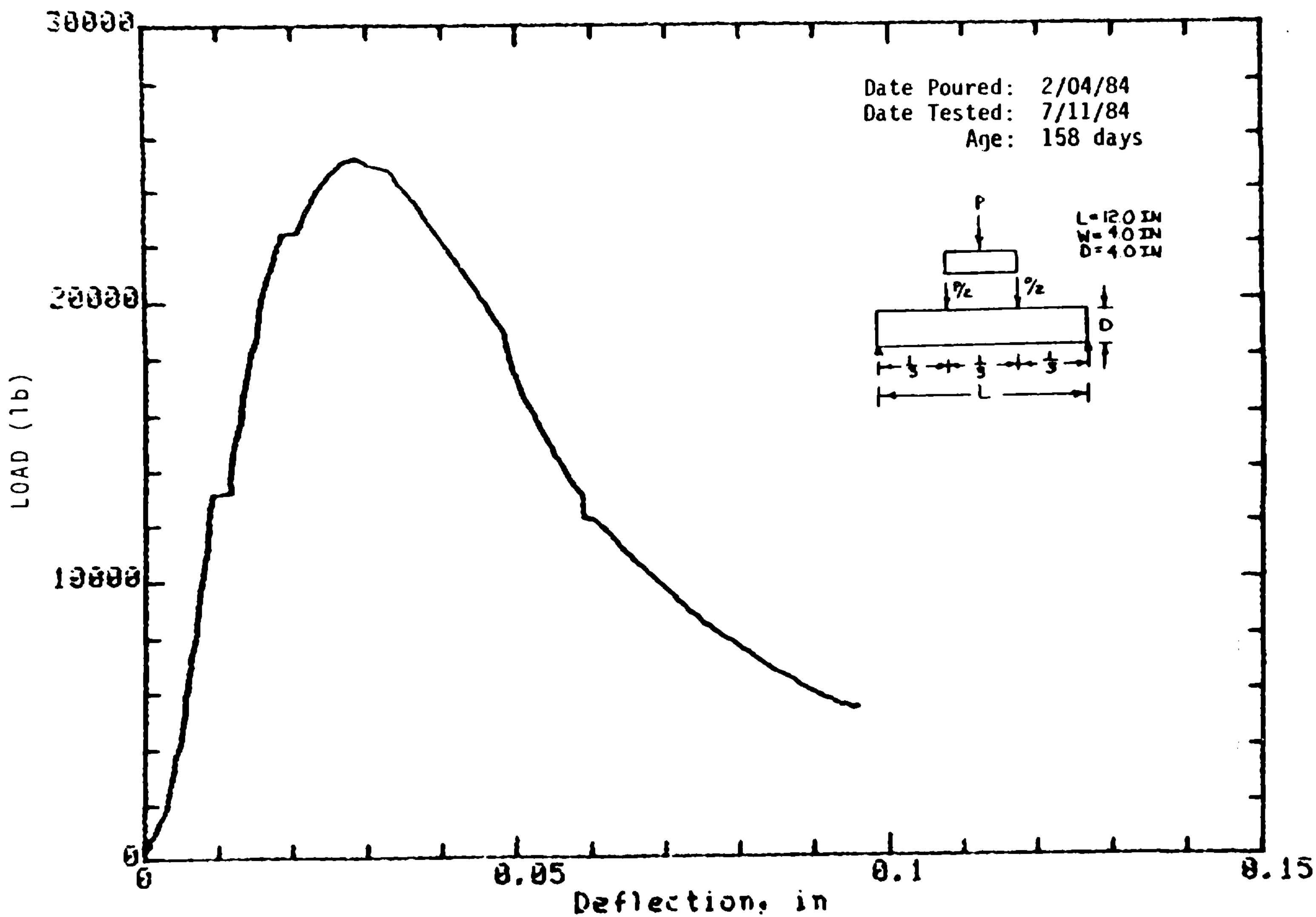

Mark: 7-23 Beam: 4in x 4in Cure: Wet
Concrete Sample

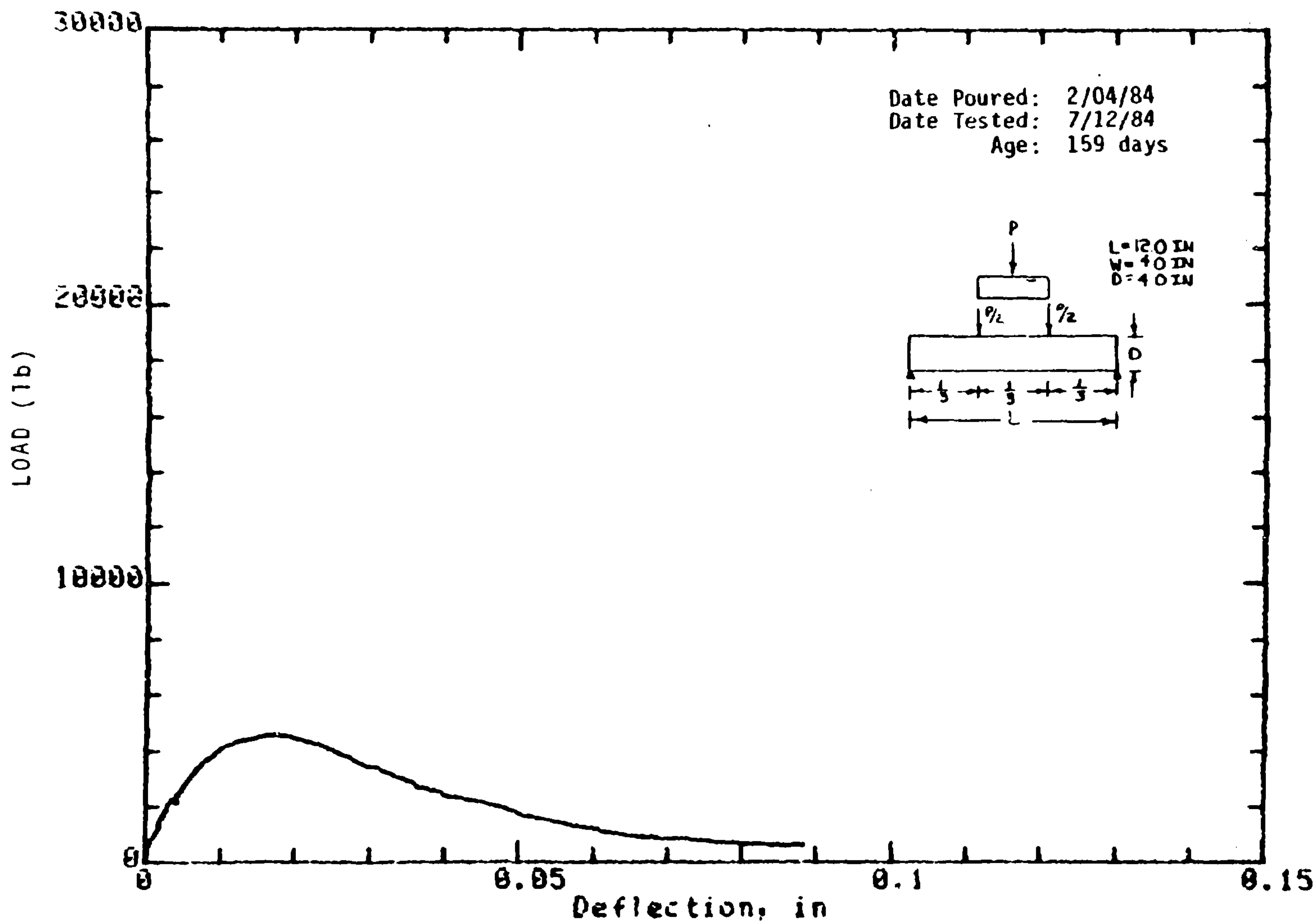

Mark: 7-32 Column: 4in x 4in Cure: Dry
Concrete Sample

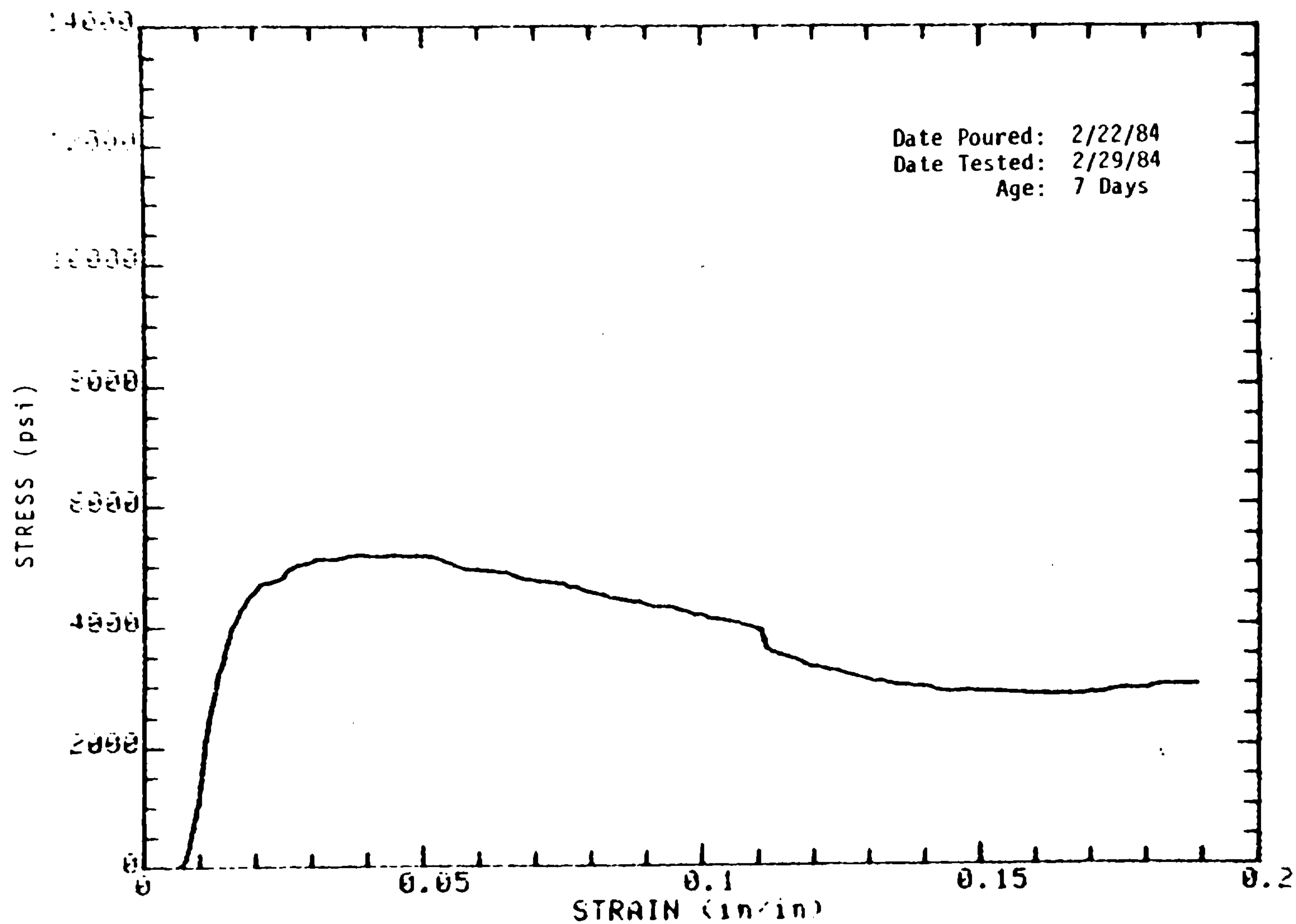

SAMPLE: 8-1 MOLDED: 4in DIA x 8in
CONCRETE SAMPLE

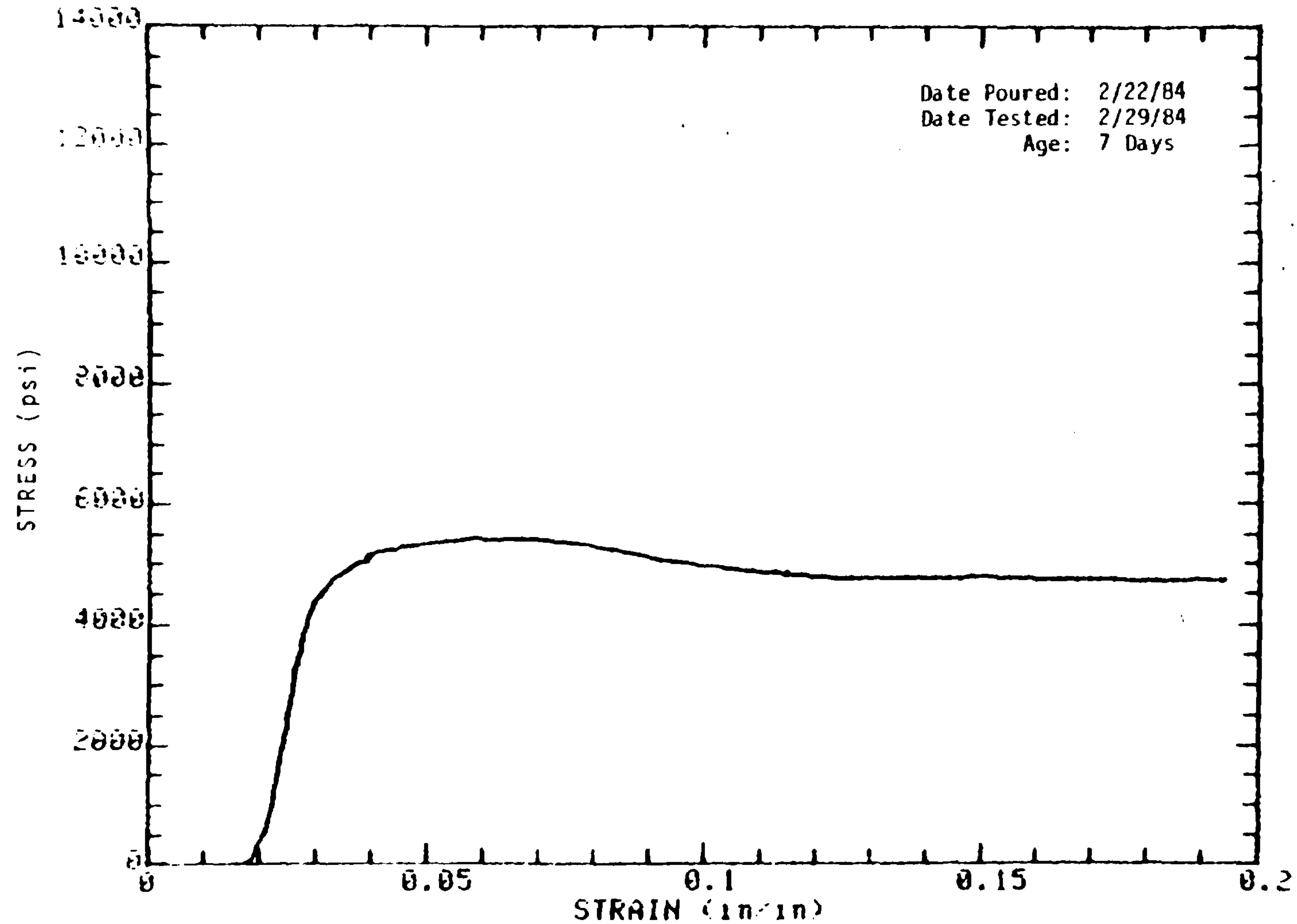

SAMPLE: 8-2 MOLDED: 4in DIA x 8in
CONCRETE SAMPLE

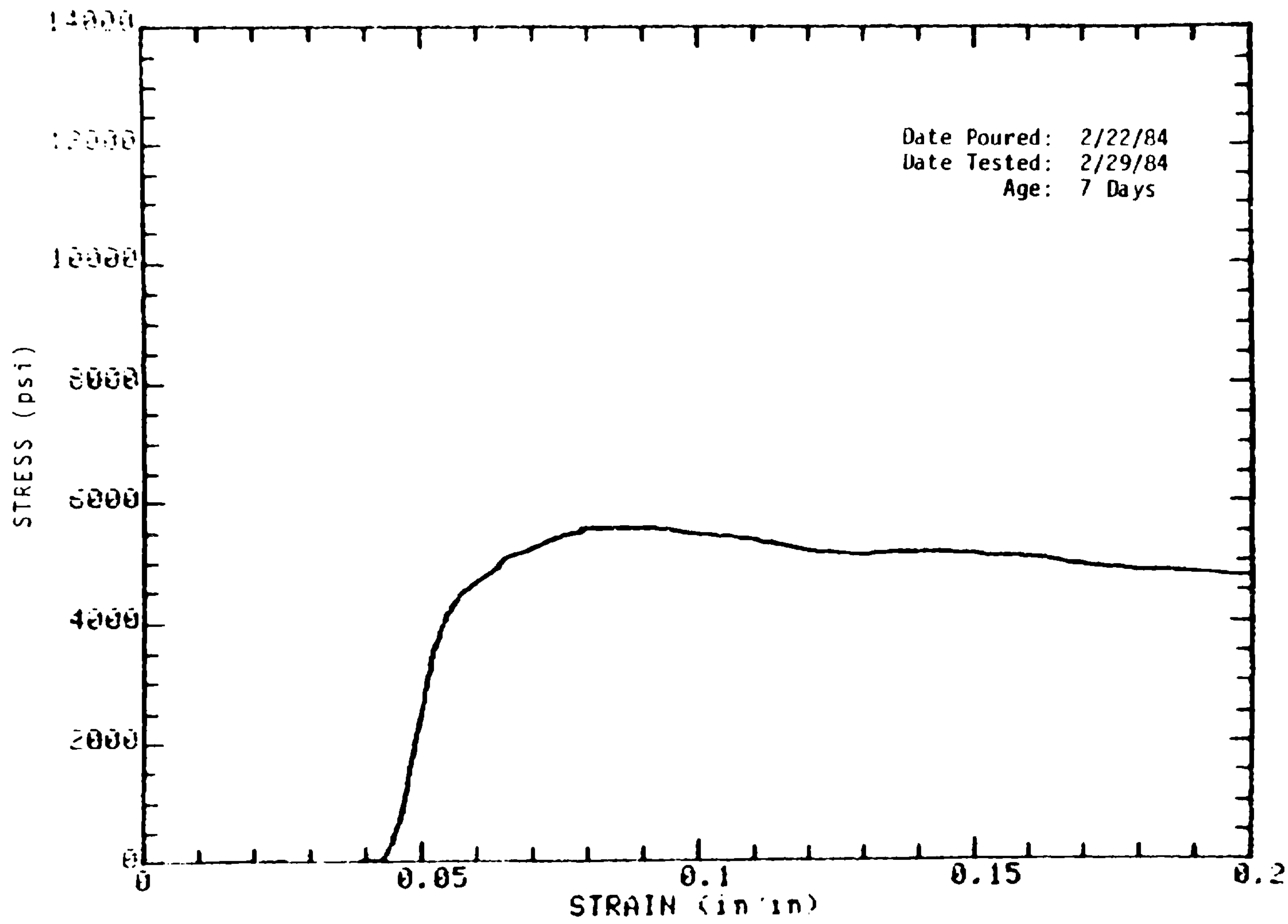

SAMPLE: 8-3 MOLDED: 4in DIA x 8in
CONCRETE SAMPLE

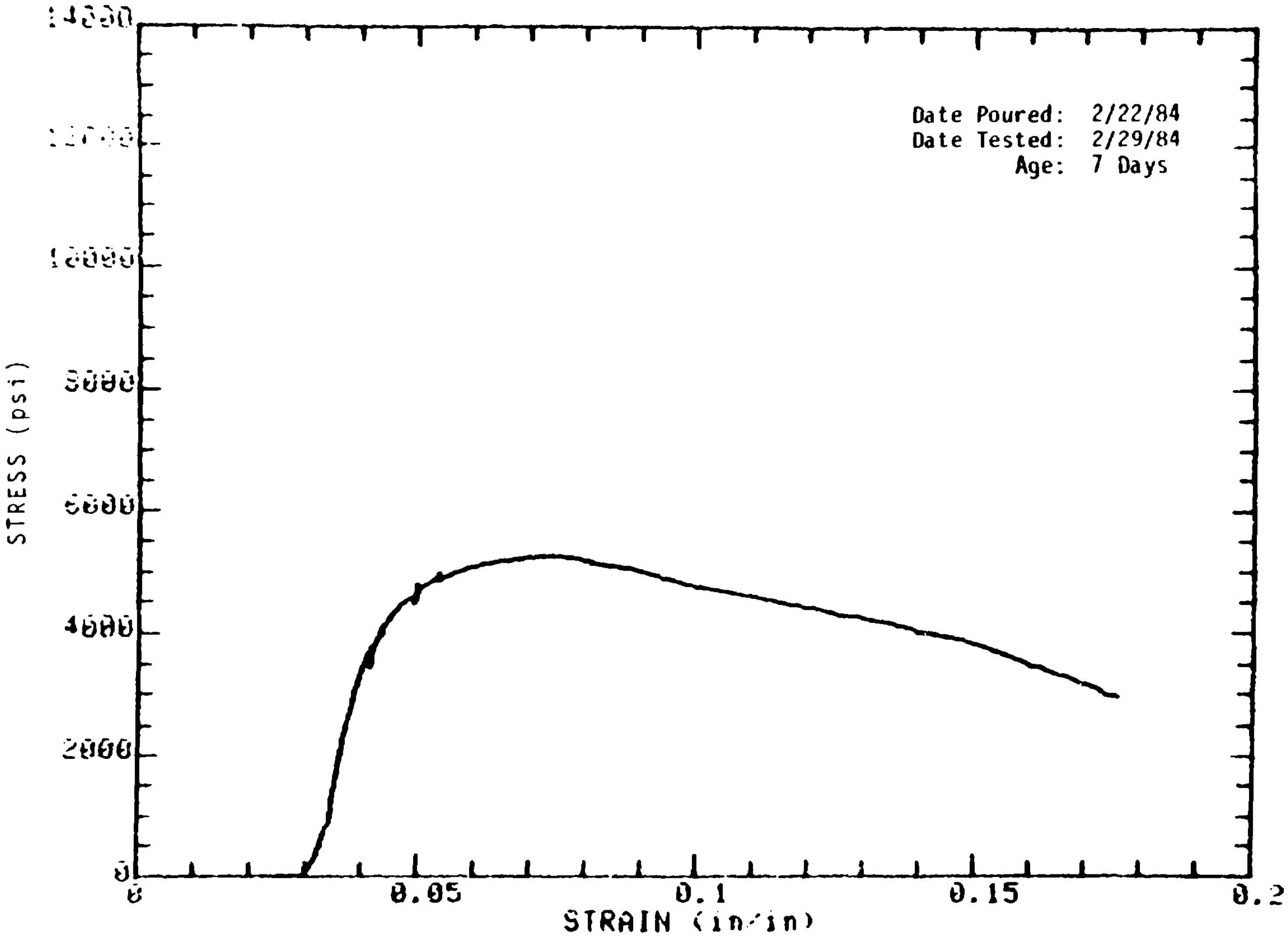

SAMPLE: 9-4 MOLDED: 4in DIA x 8in
CONCRETE SAMPLE

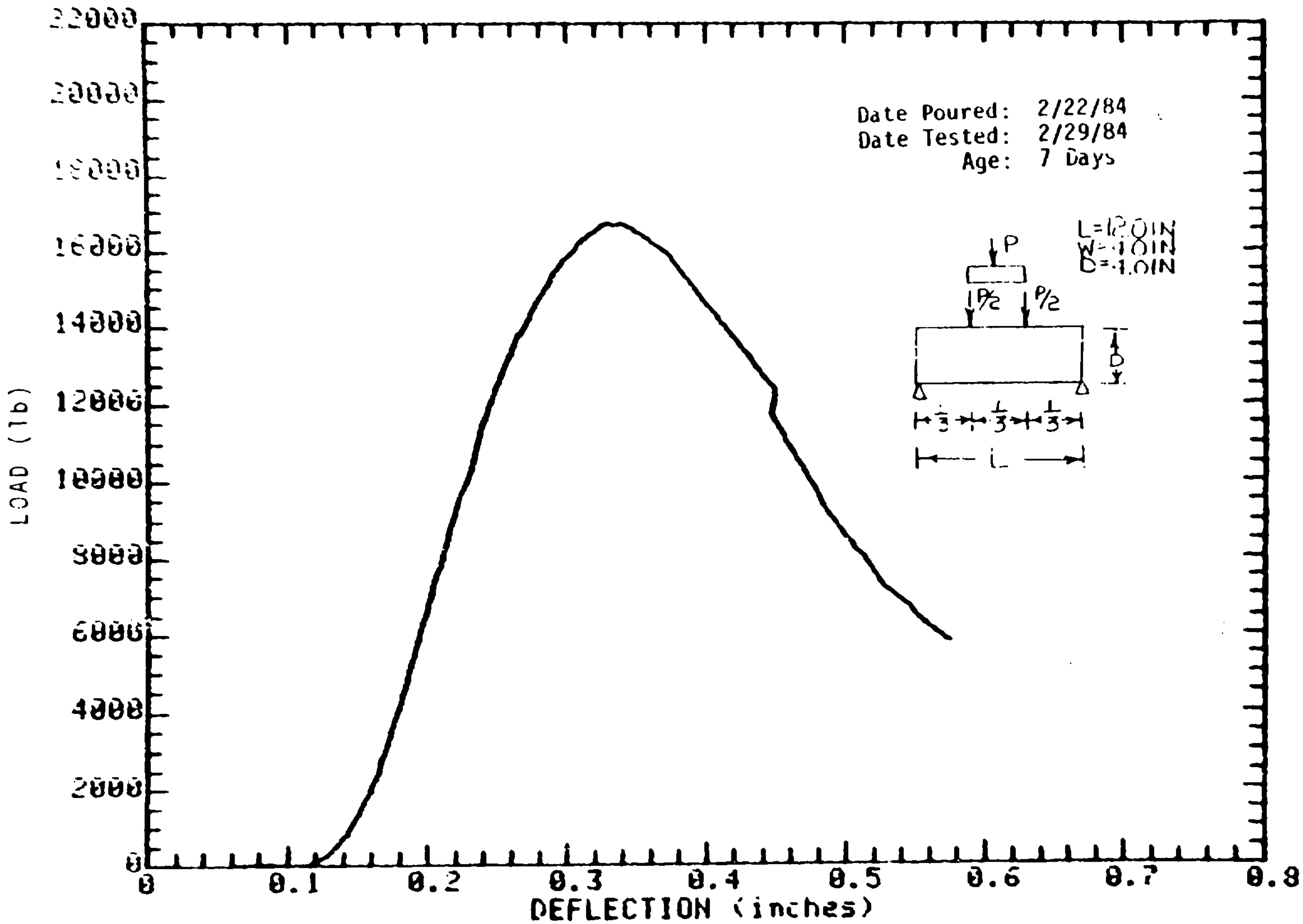

SAMPLE: BEAM 9-13
CONCRETE SAMPLE

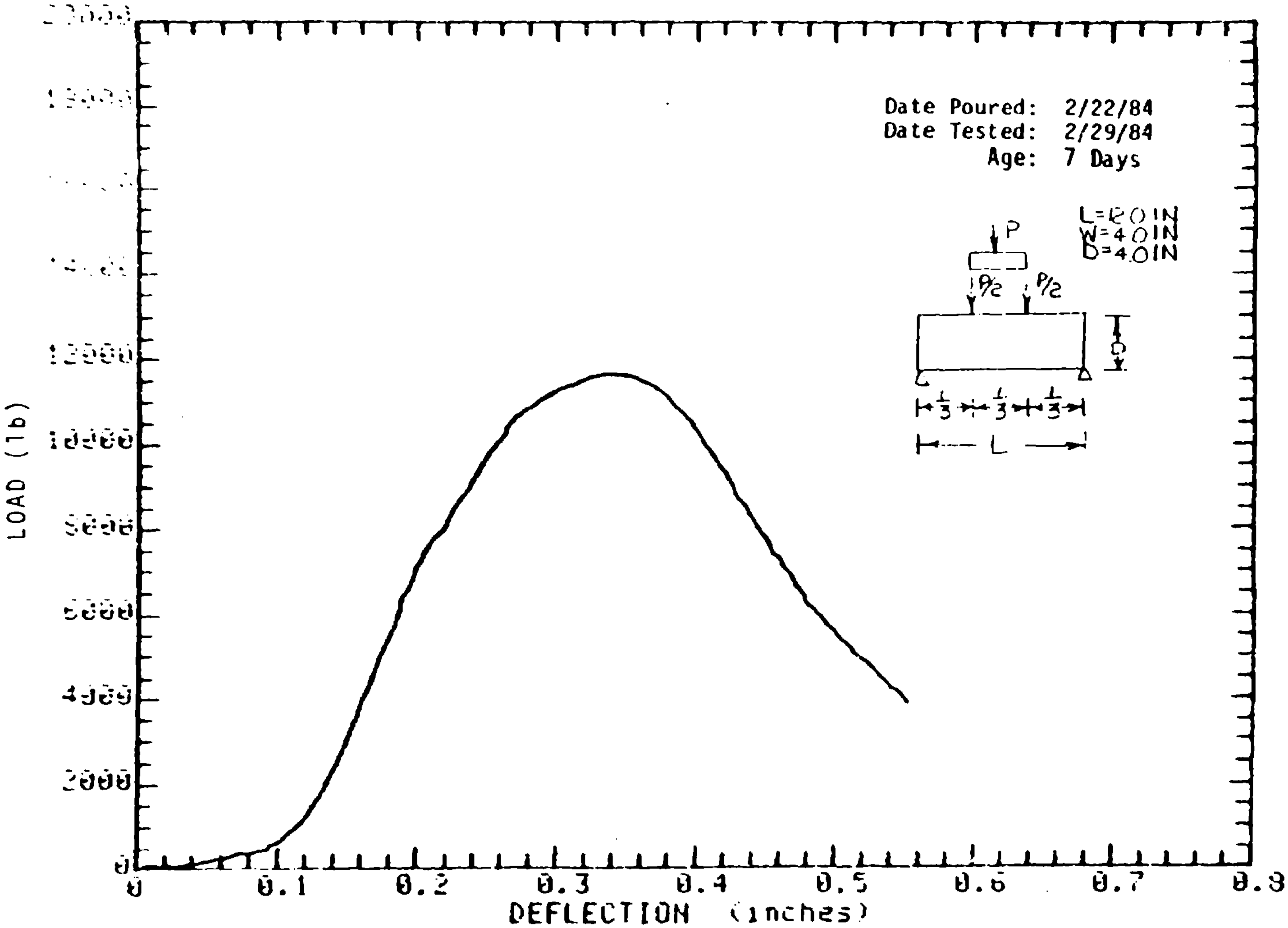

SAMPLE: BEAM 8-14
CONCRETE SAMPLE

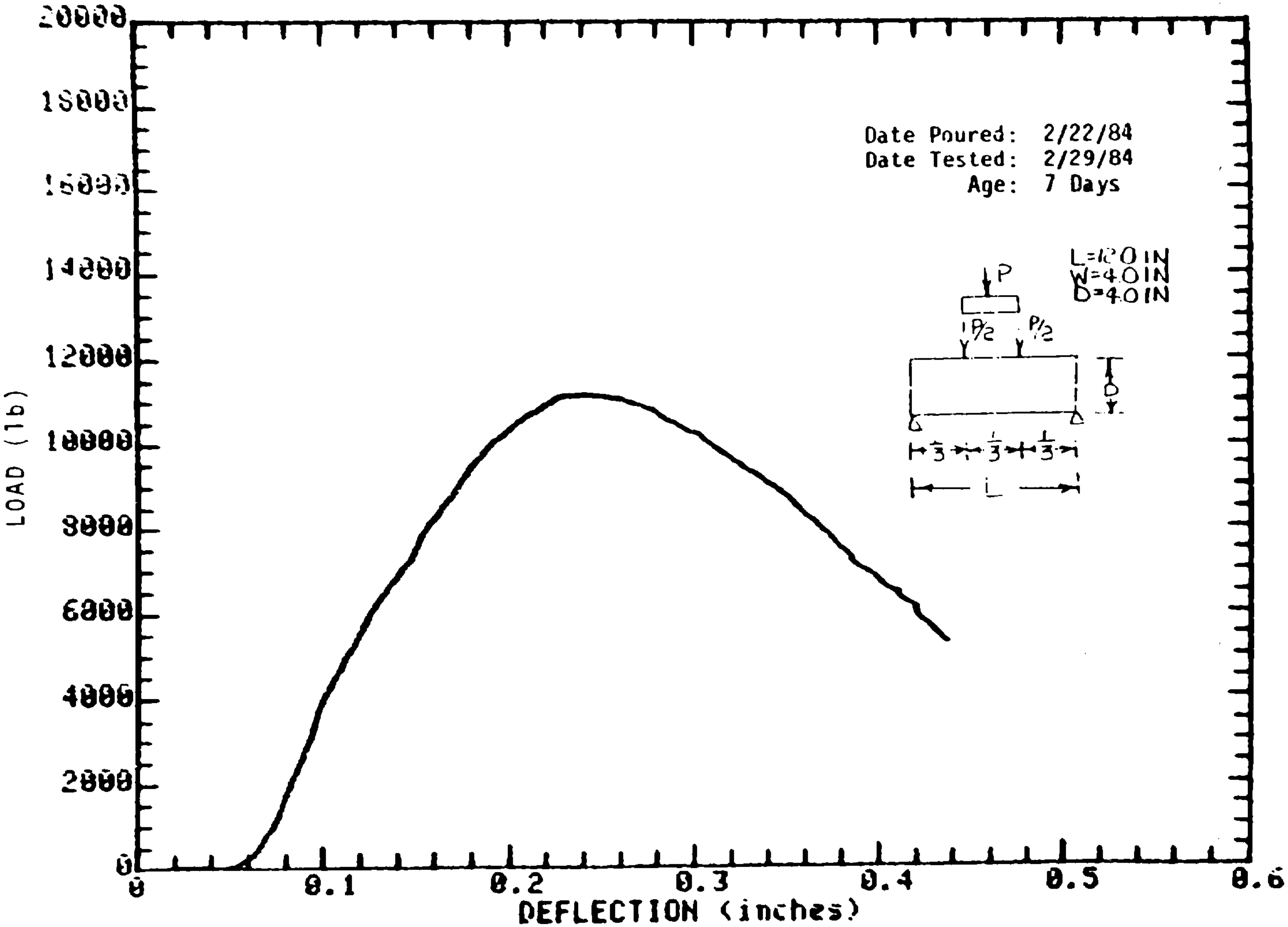

SAMPLE: BEAM 8-15
CONCRETE SAMPLE

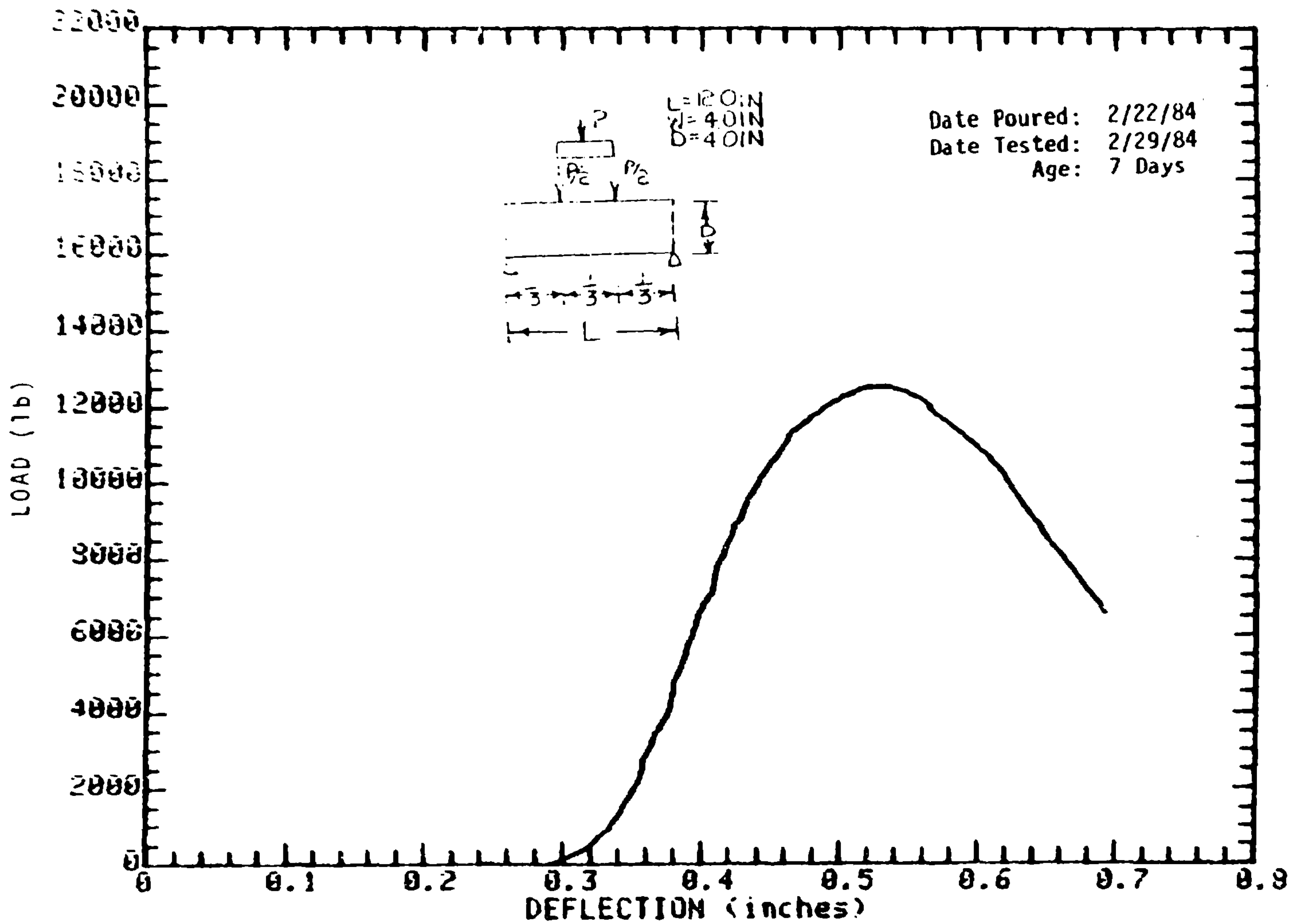

SAMPLE: BEAM 8-16
CONCRETE SAMPLE

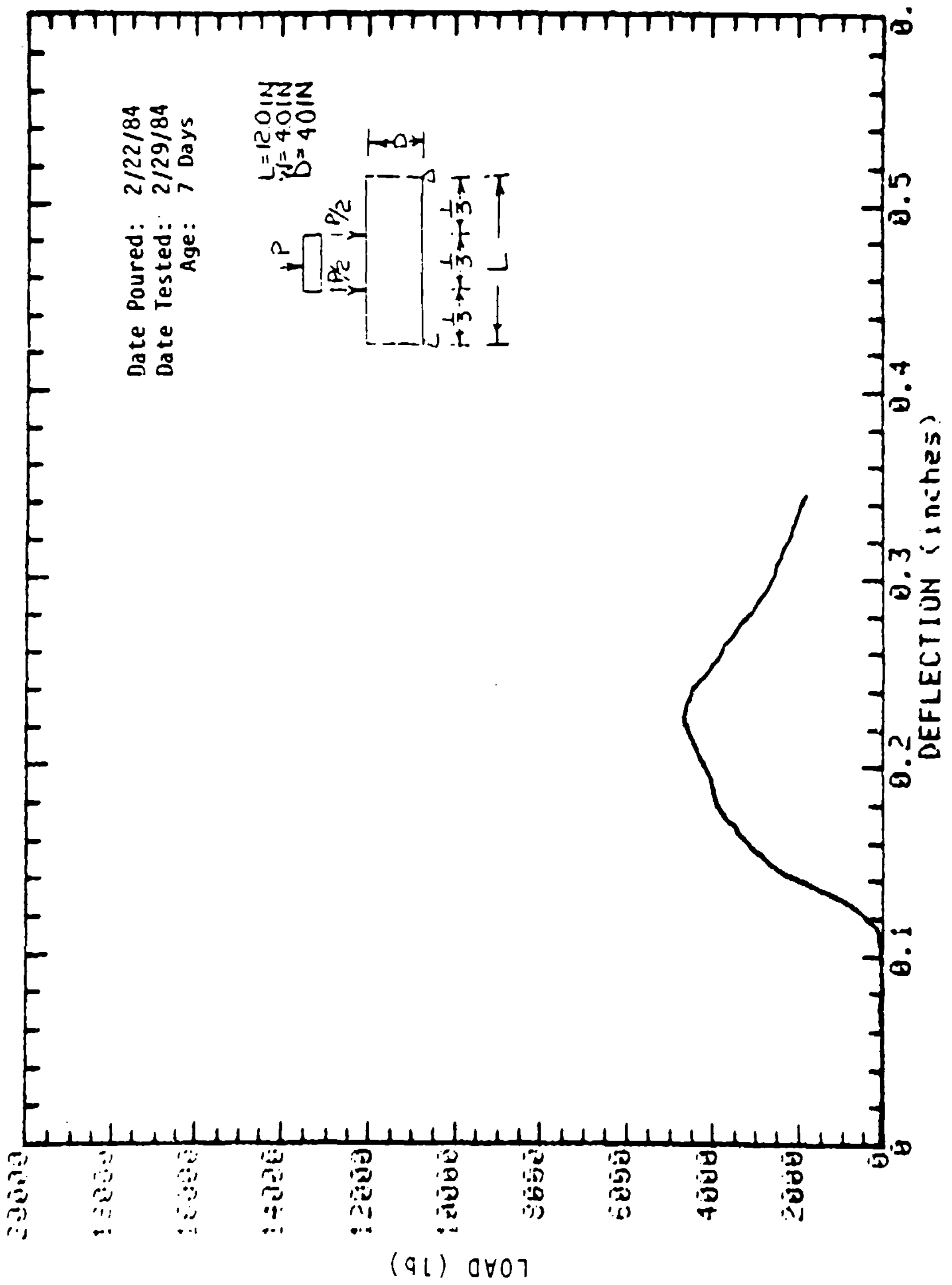

SAMPLE: COLUMN 3-25
CONCRETE SAMPLE

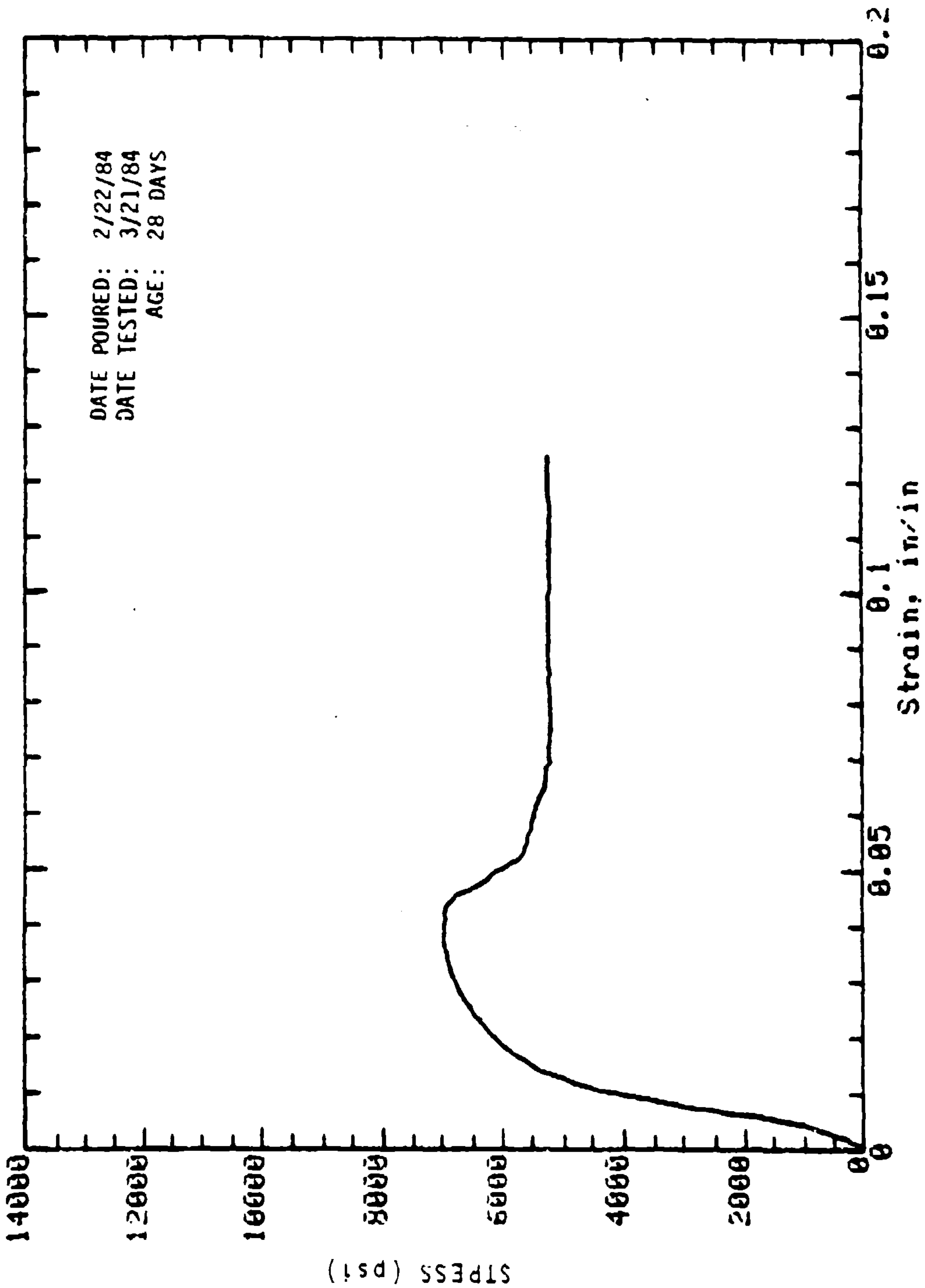

Mark: B-5 Molded: 4in dia x 8in Cure: Dry
Concrete Sample

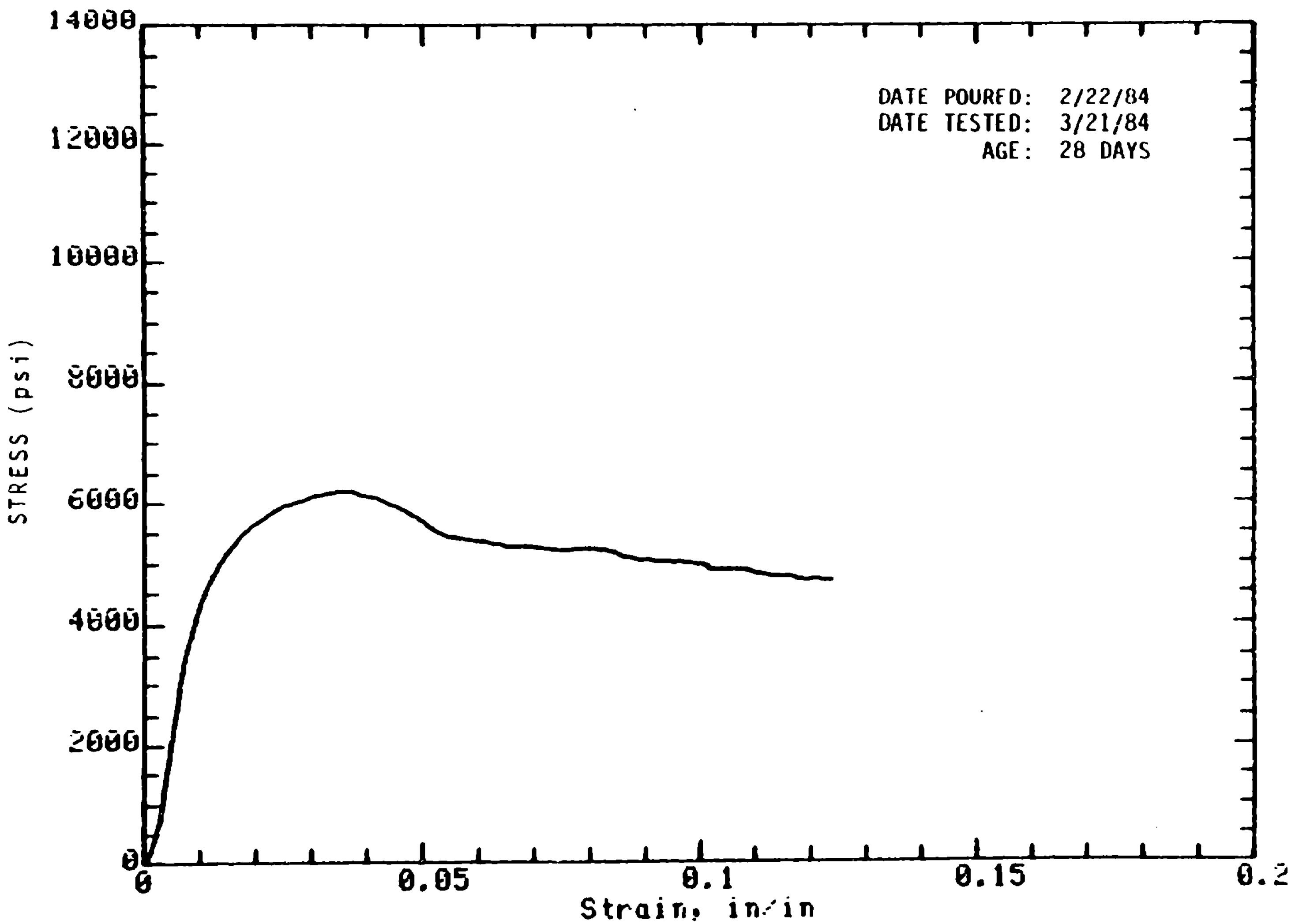

Mark: 8-8 Molded: 4in dia × 8in Cure: Wet
Concrete Sample

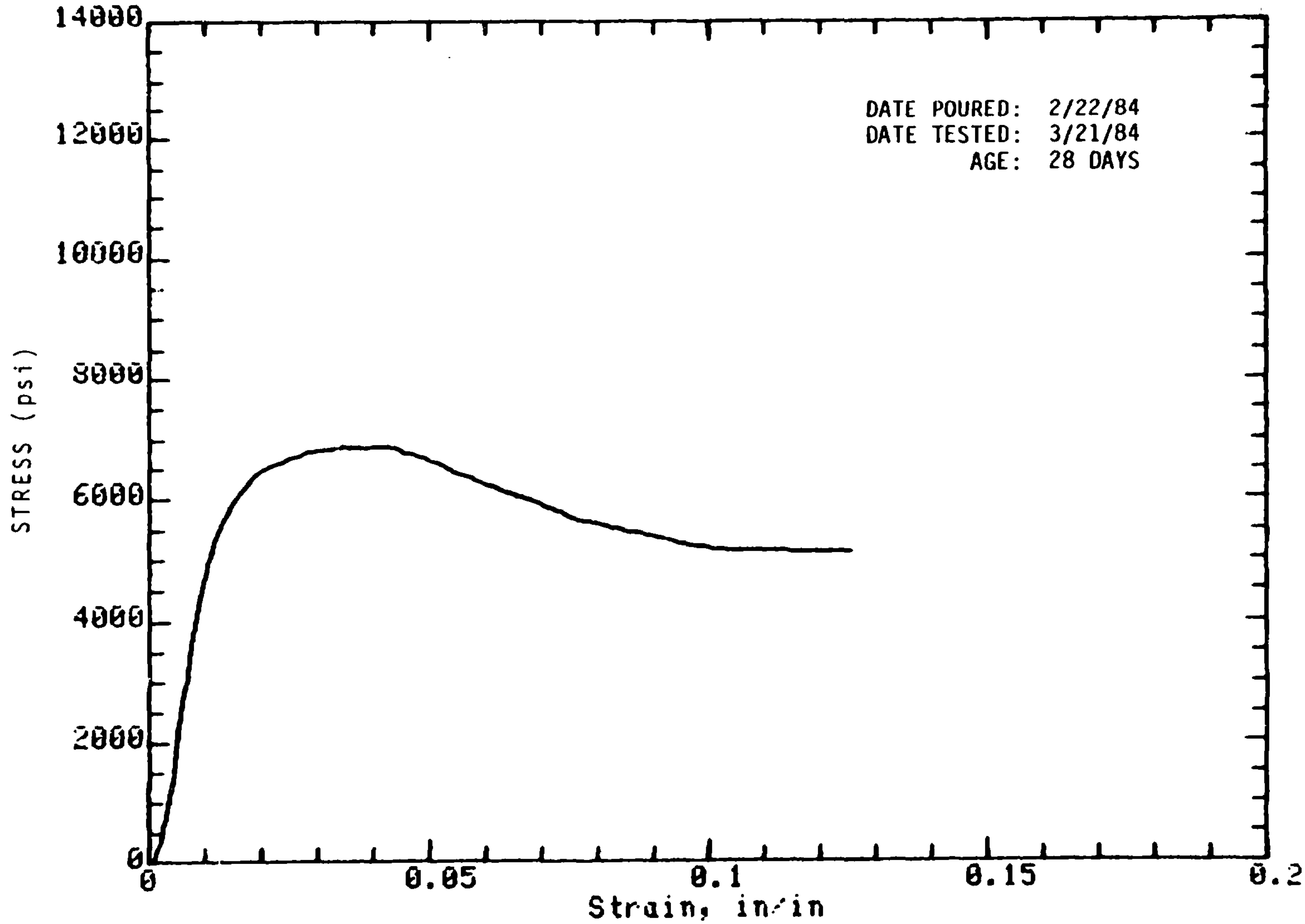

Mark: 8-11 Molded: 4in dia x 8in Cure: Dry
Concrete Sample

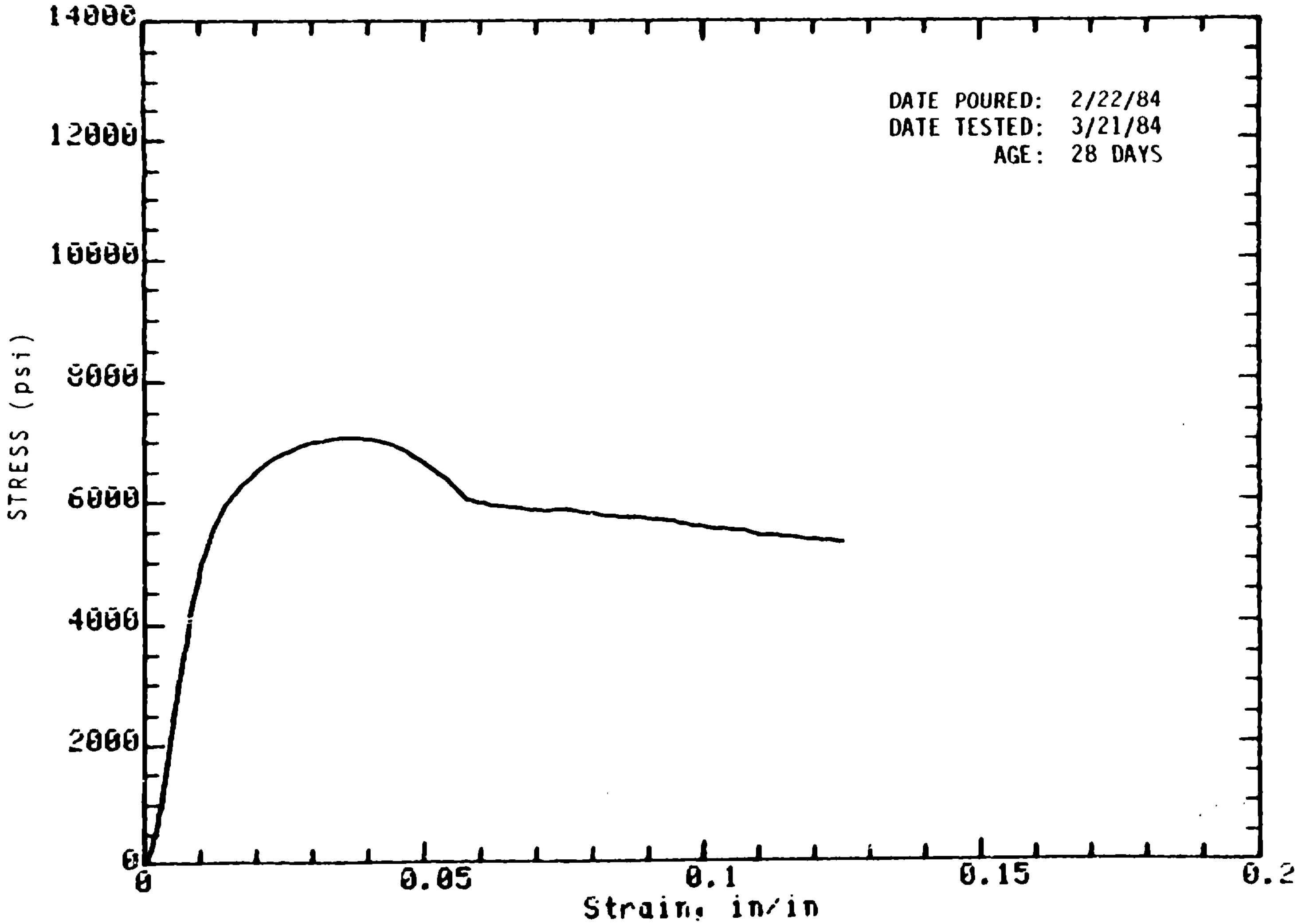

Mark: 9-12 Molded: 4in dia x 8 in Cure: Wet
Concrete Sample

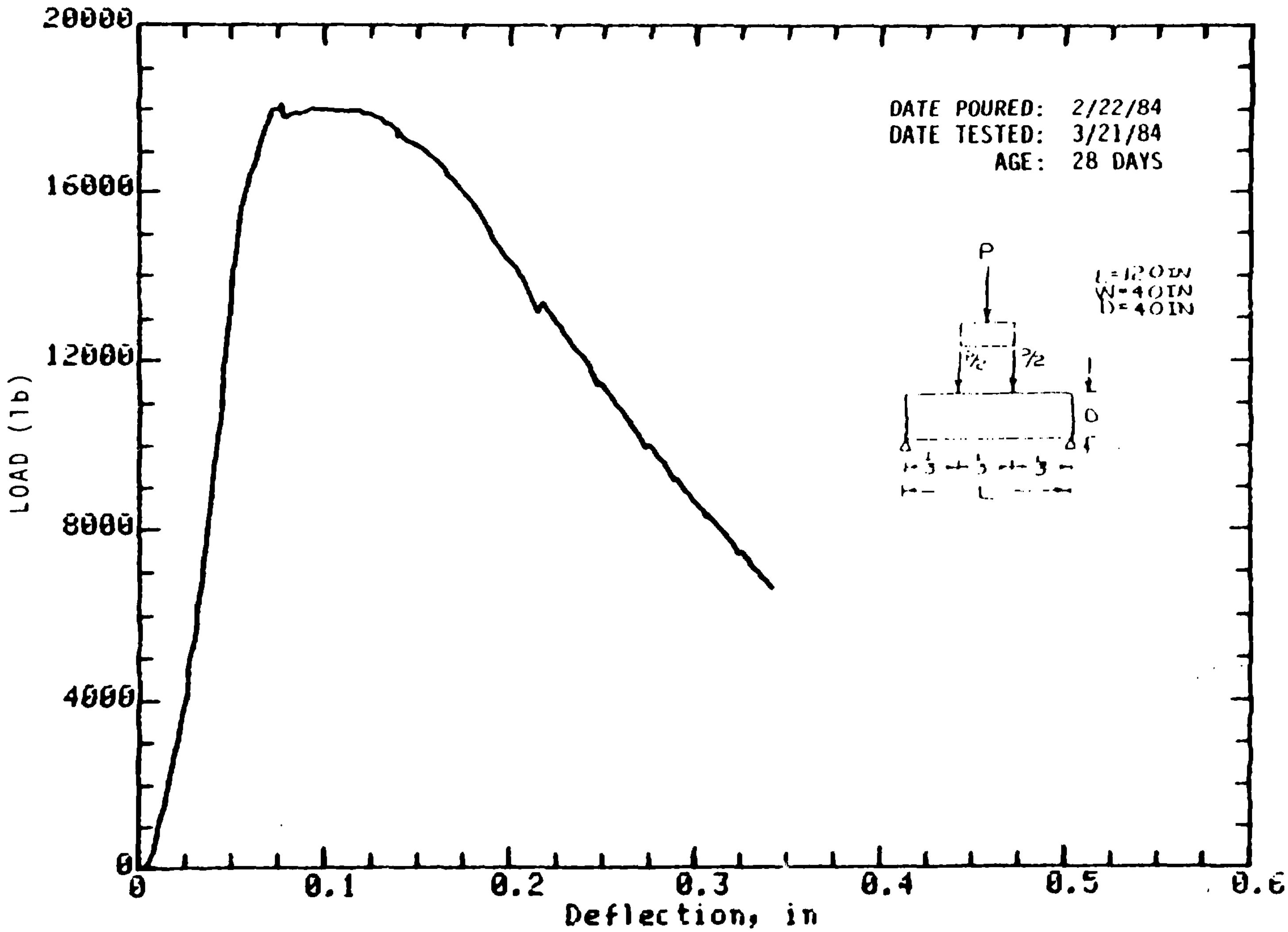

Mark: 8-18 Beam: 4in x 4in Cure: Wet
Concrete Sample

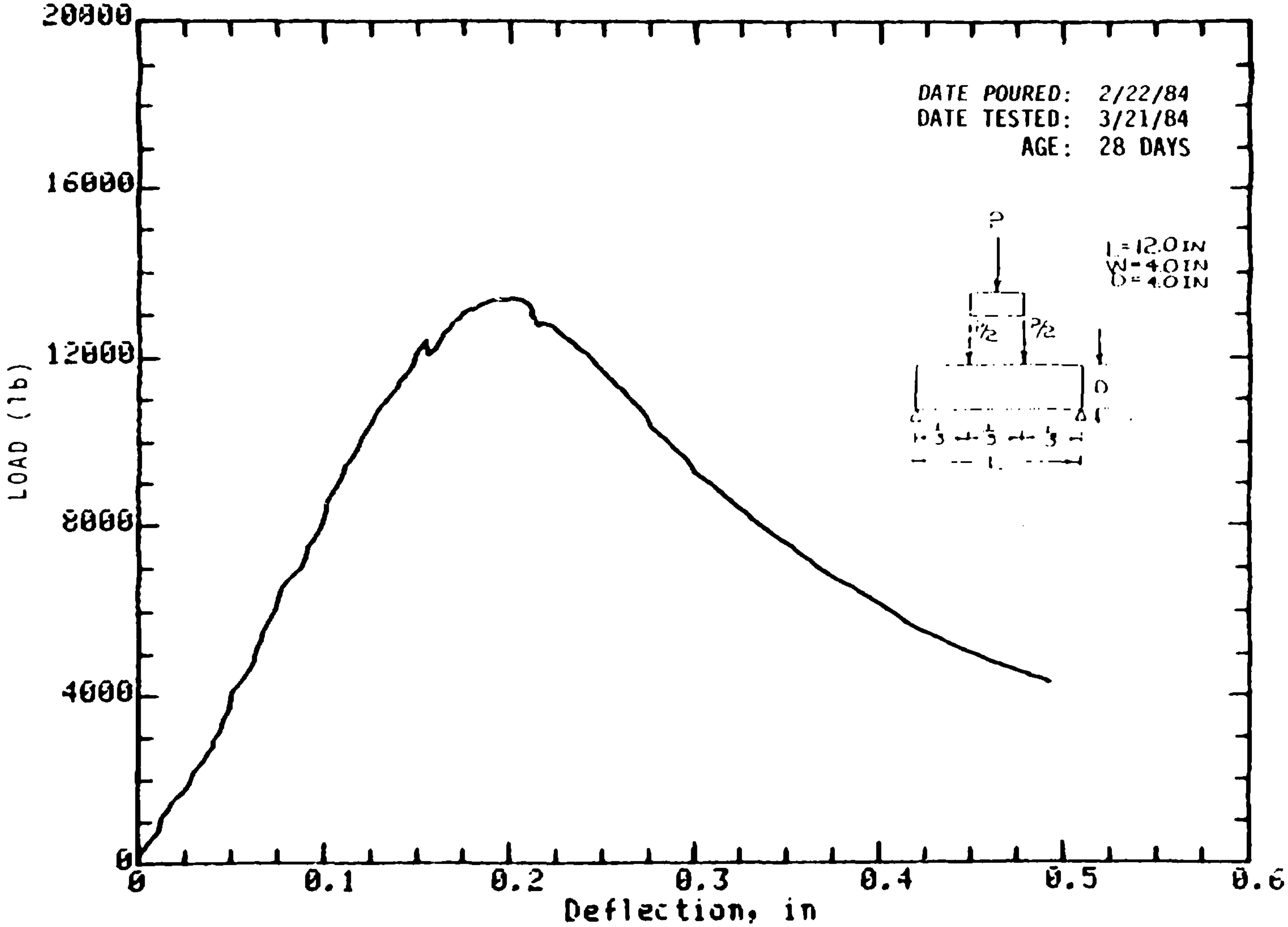

Mark: 8-21 Beam: 4in x 4in Cure: Dry
Concrete Sample

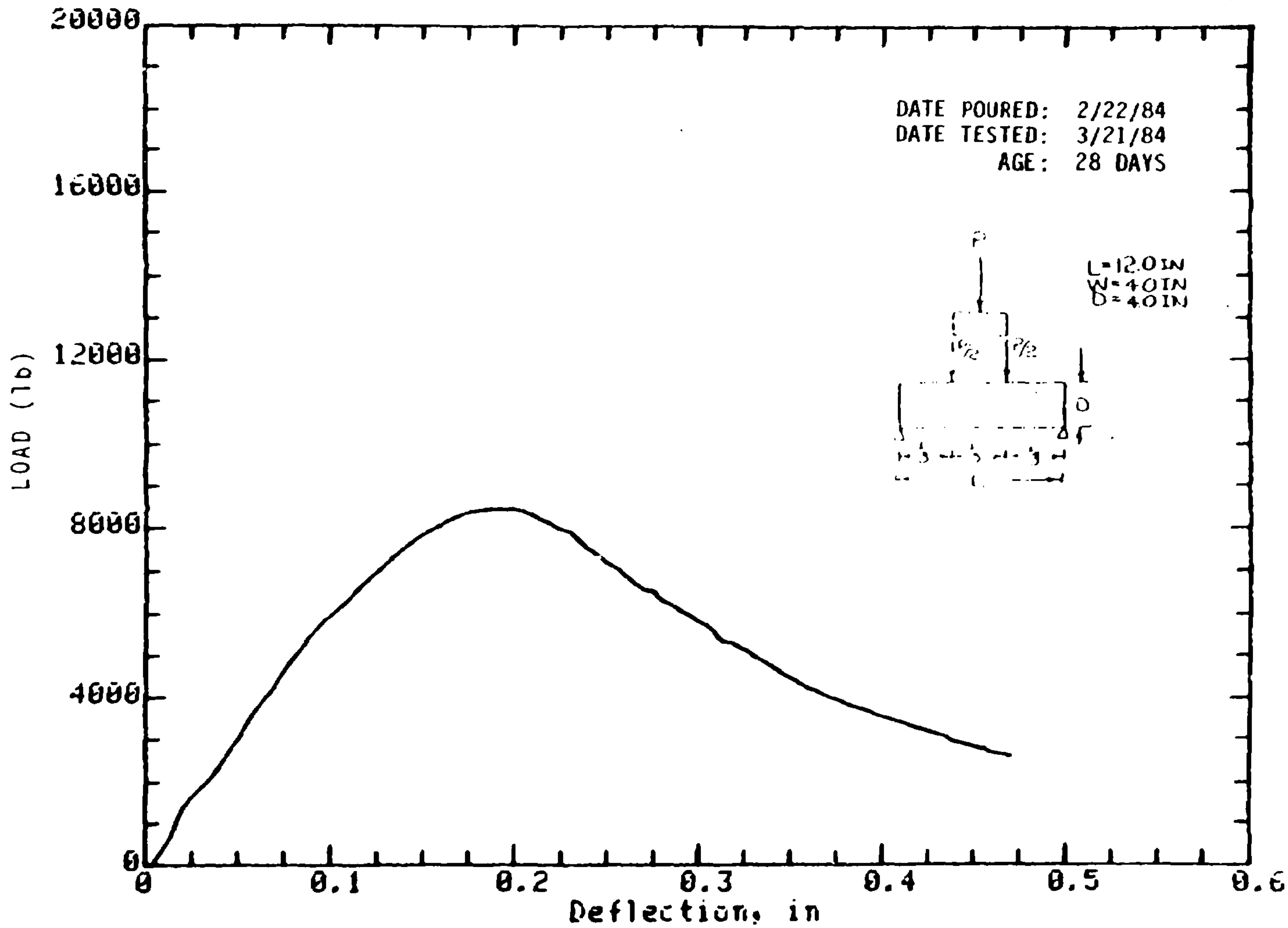

Mark: 8-22 Beam: 4in x 4in Cure: Dry
Concrete Sample

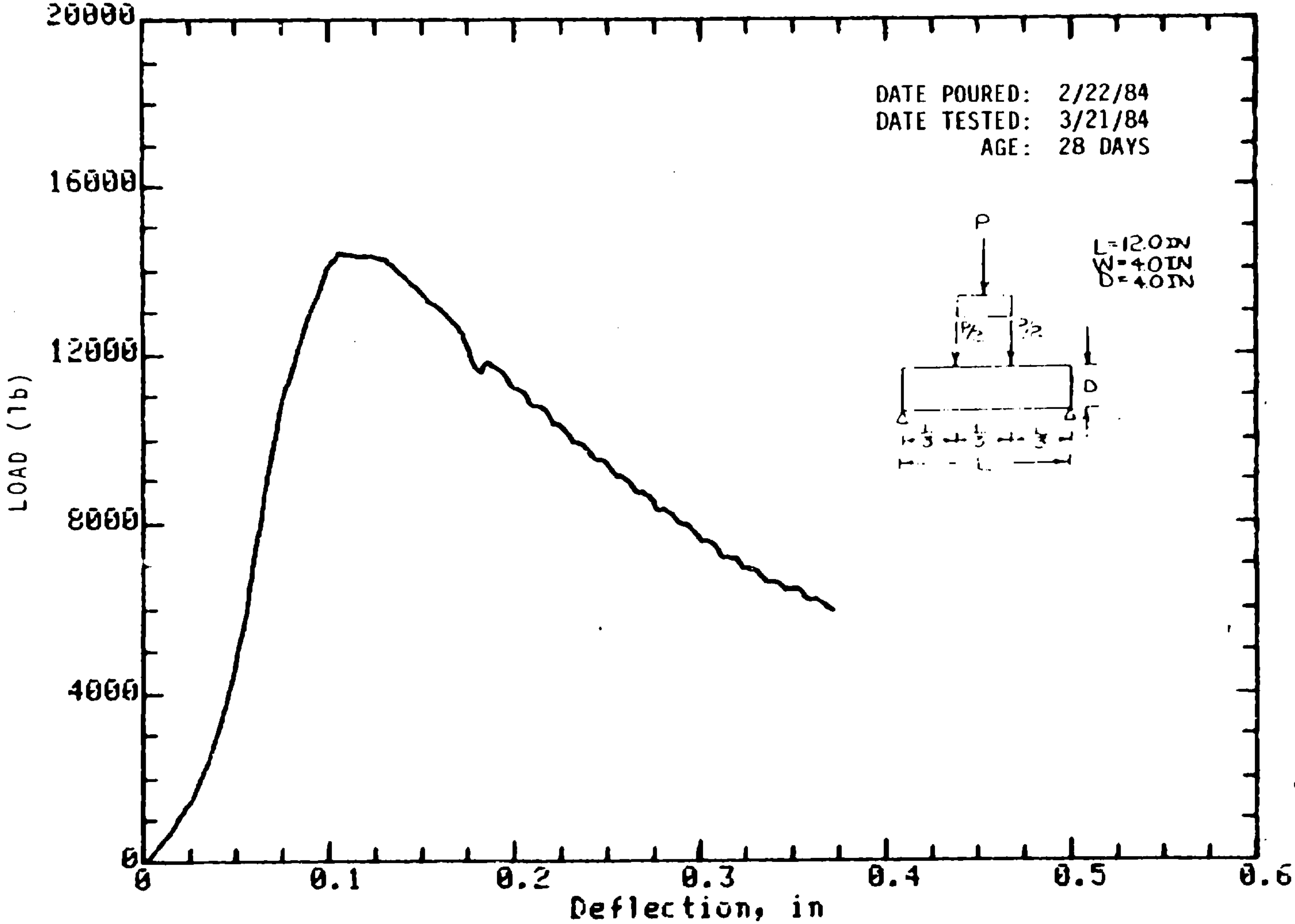

Mark: 8-24 Beam: 4in x 4in Cure: Wet
Concrete Sample

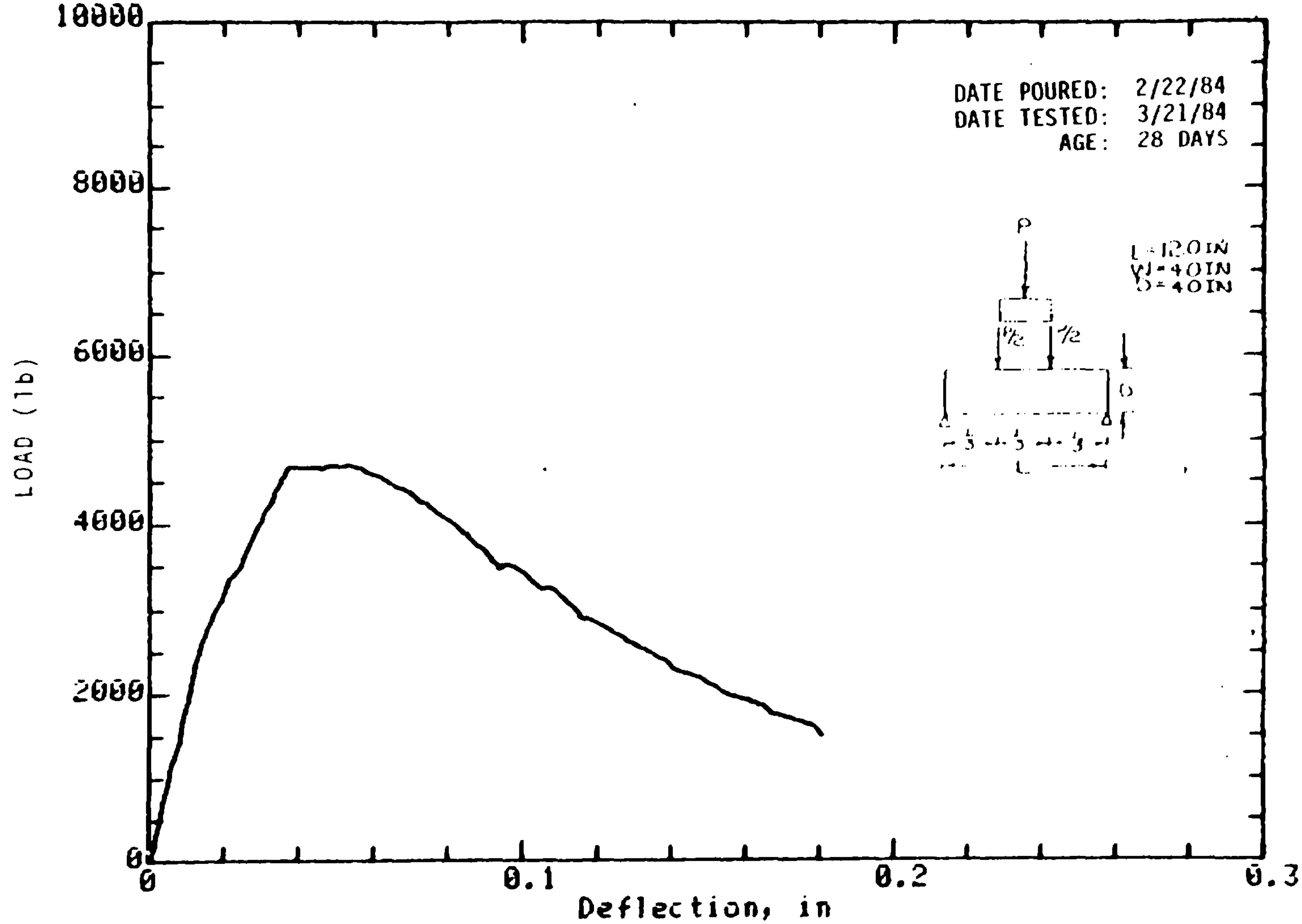

Mark: 8-27 Column: 4in x 4in Cure: Wet
Concrete Sample

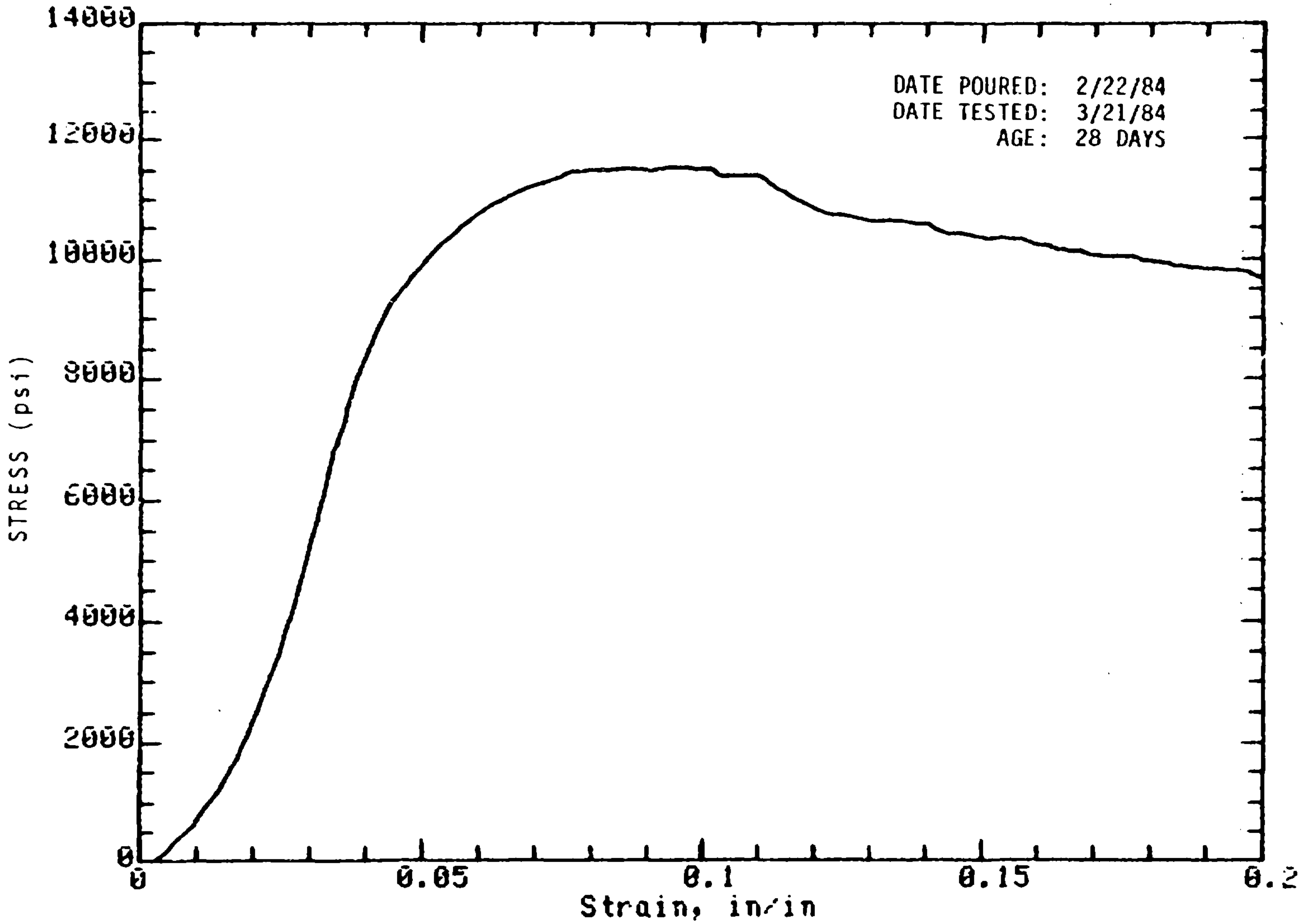

Mark: 8-S5 Cored (slab): 2in dia x 3.5in Cure: Dry
Concrete Sample

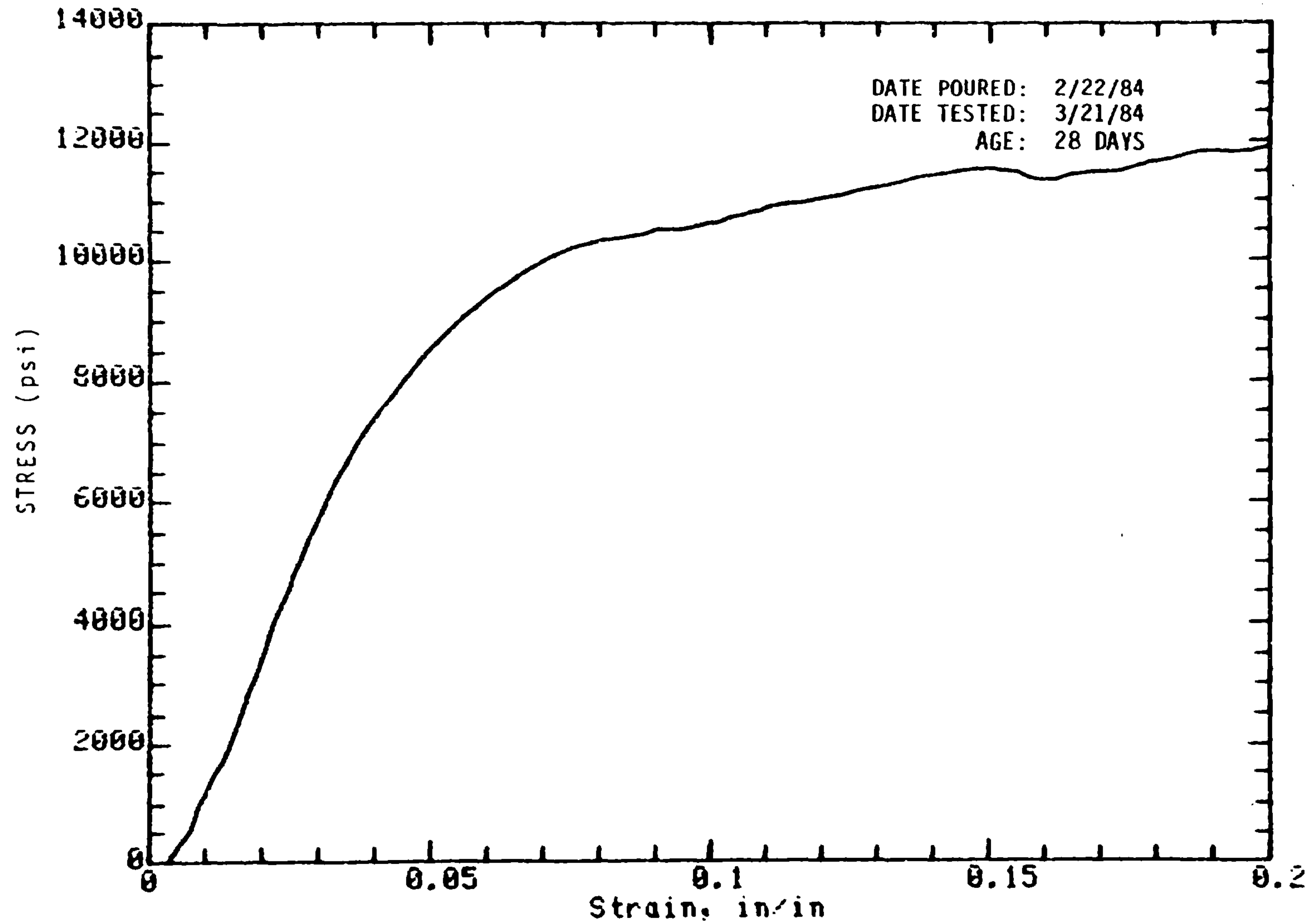

Mark: 8-S6 Cored (slab): 2in dia x 3.5in Cure: Dry
Concrete Sample

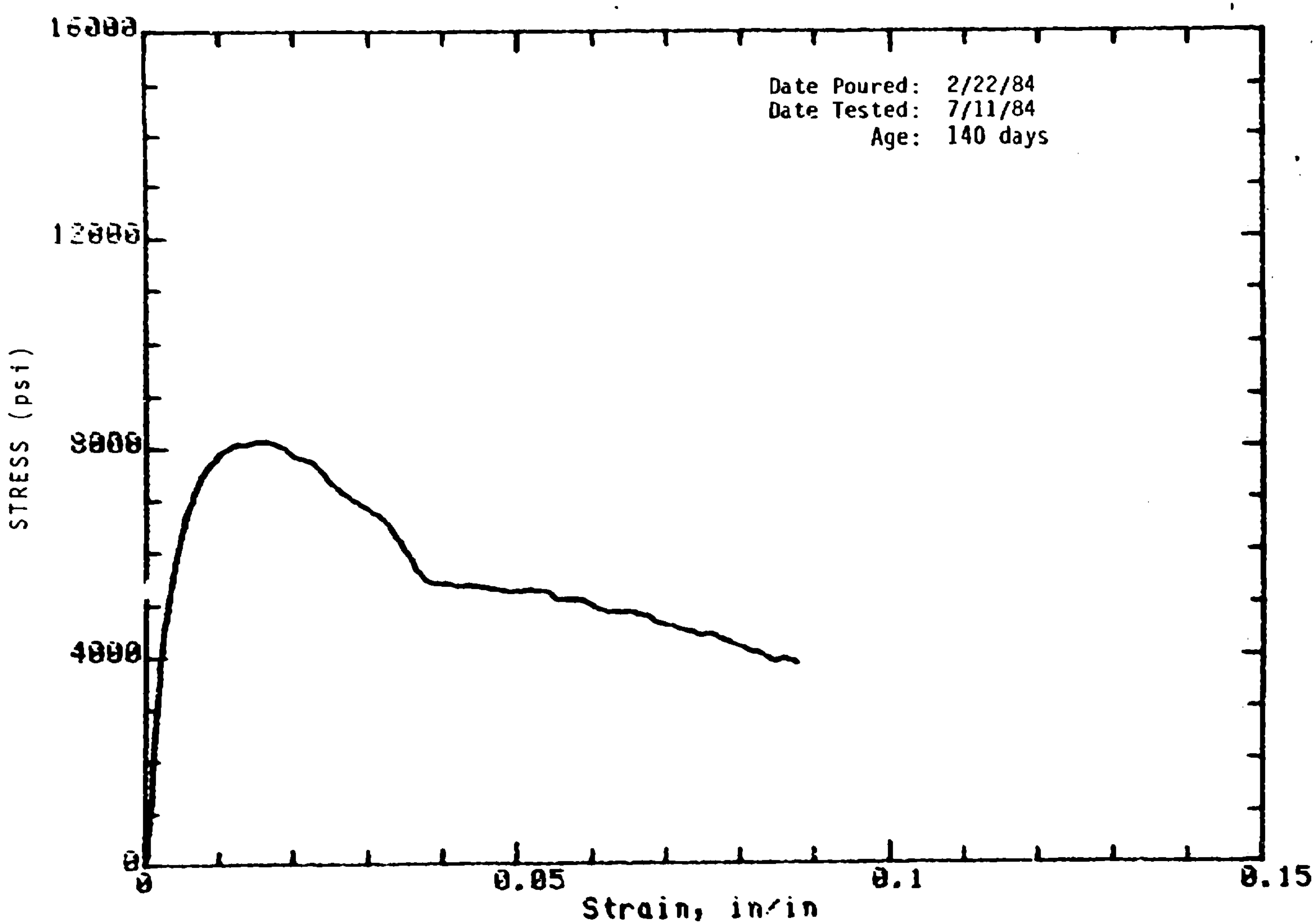

Mark: 8-6 Molded: 4in dia x 8in Cure: Wet
Concrete Sample

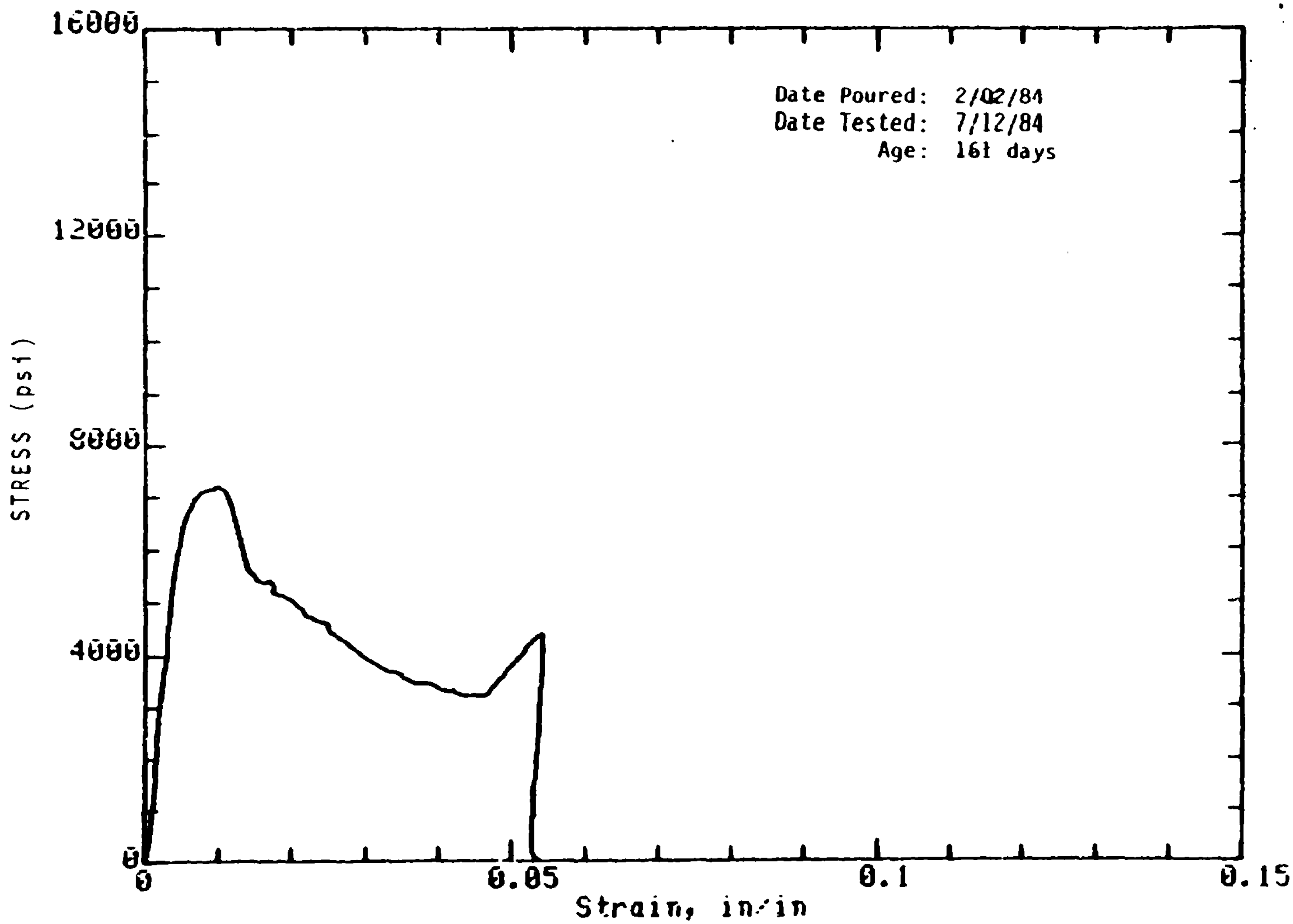

Mark: 8-9 Molded: 4in dia x 8in Cure: Wet
Concrete Sample

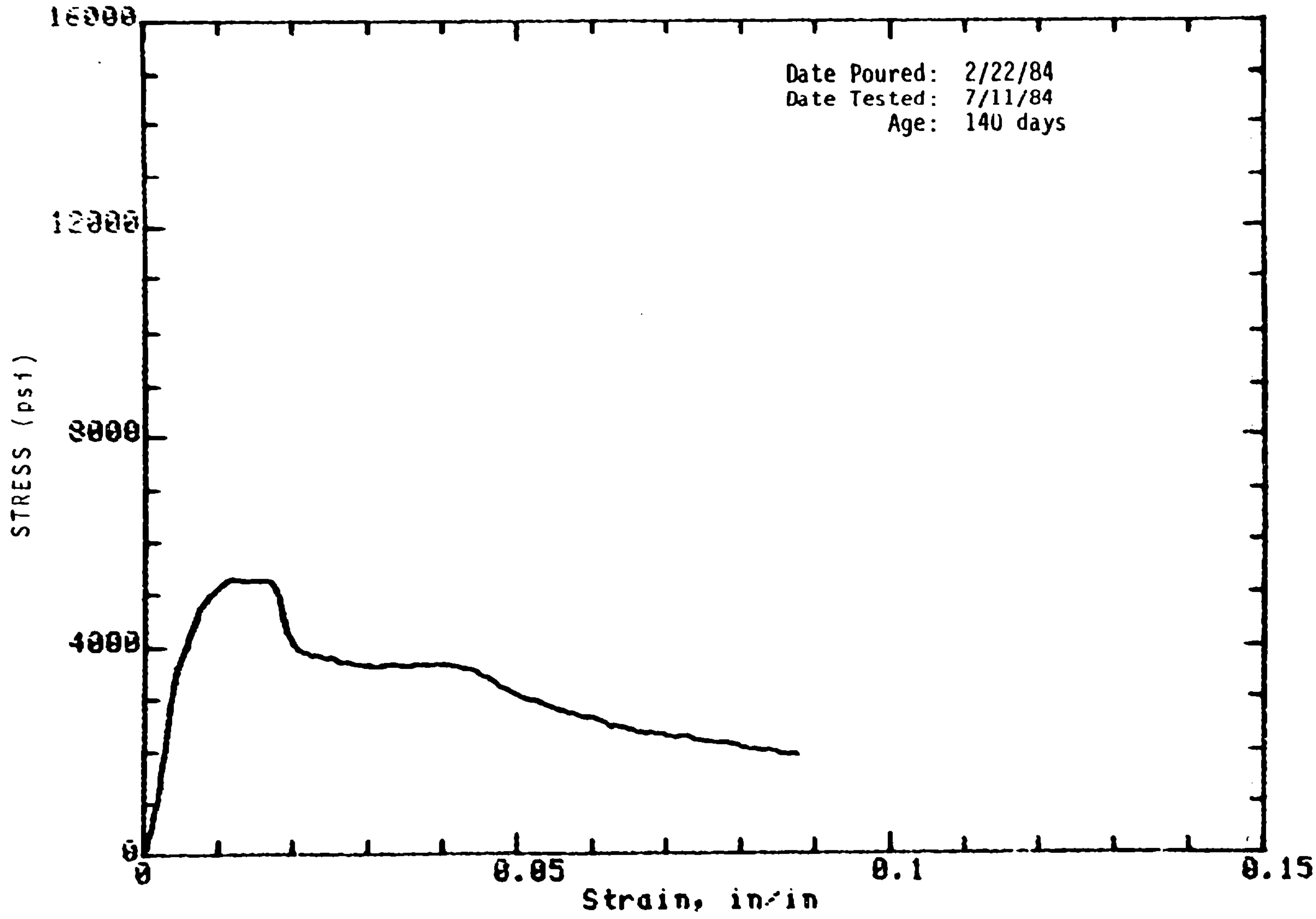

Mark: 8-7 Molded: 4in dia x 8in Cure: Dry
Concrete Sample

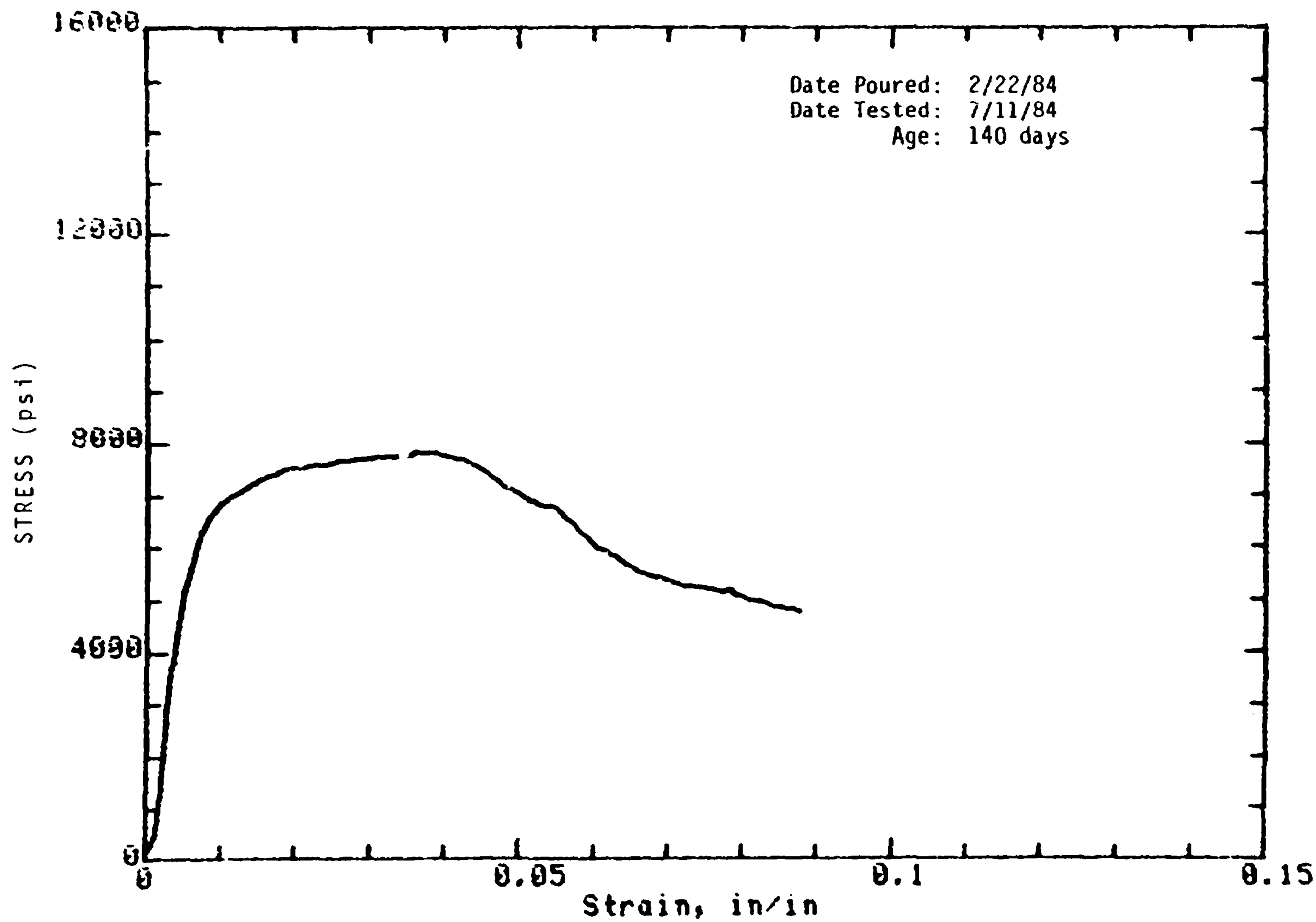

Mark: 8-10 Molded: 4in dia x 8in Cure: Dry
Concrete Sample

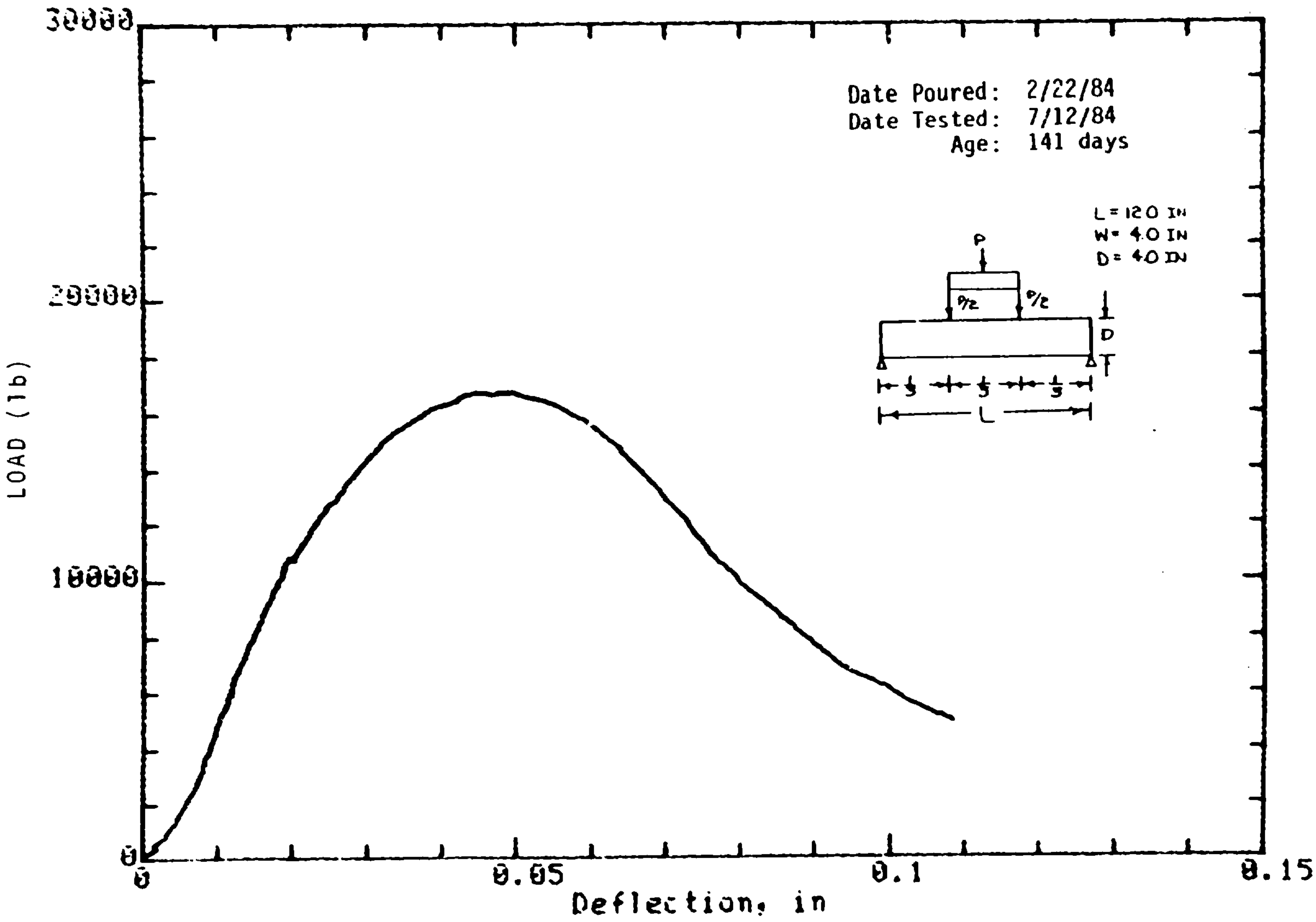

Mark: 8-19 Beam: 4in x 4in Cure: Dry
Concrete Sample

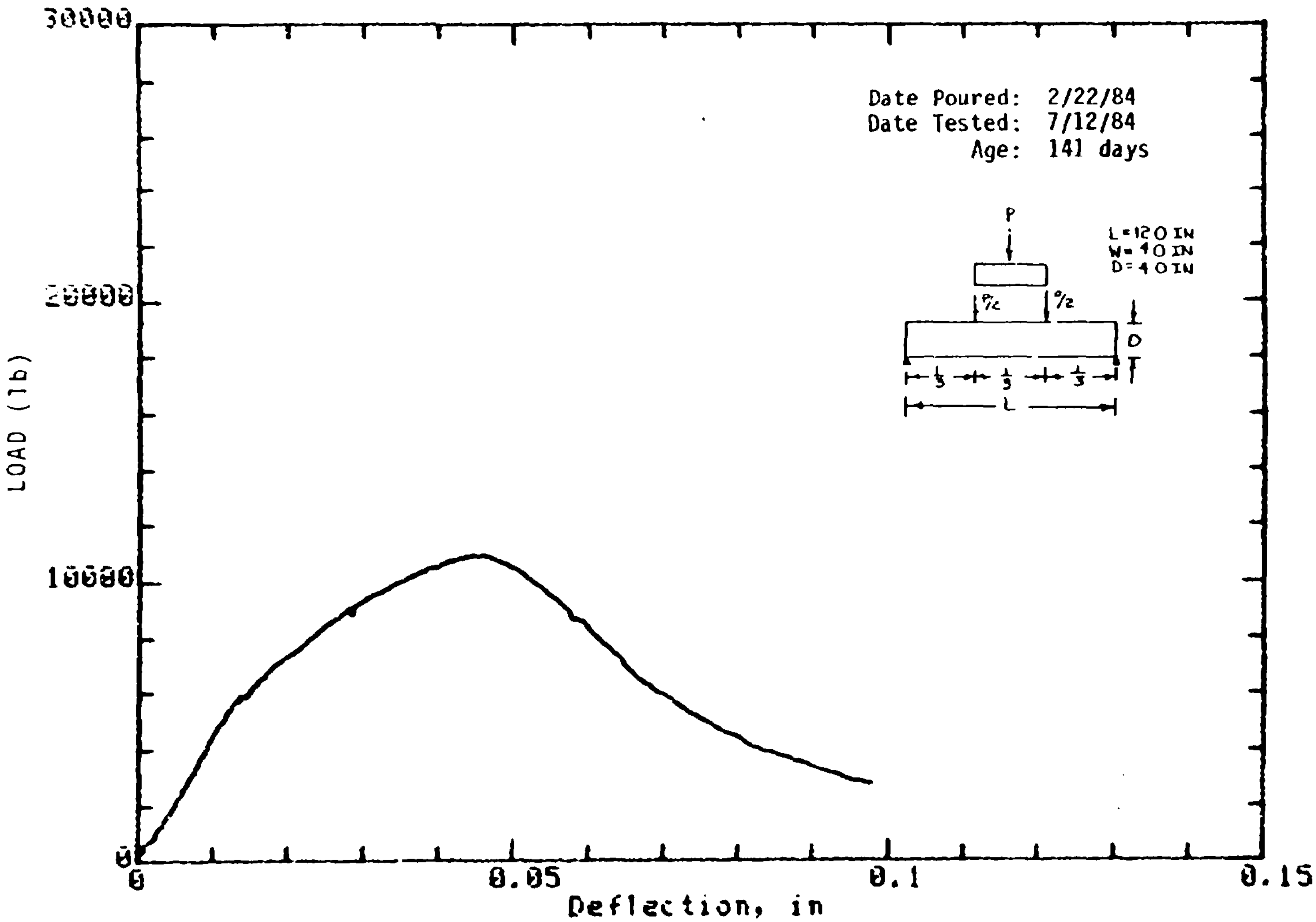

Mark: 8-20 Beam: 4in x 4in Cure: Dry
Concrete Sample

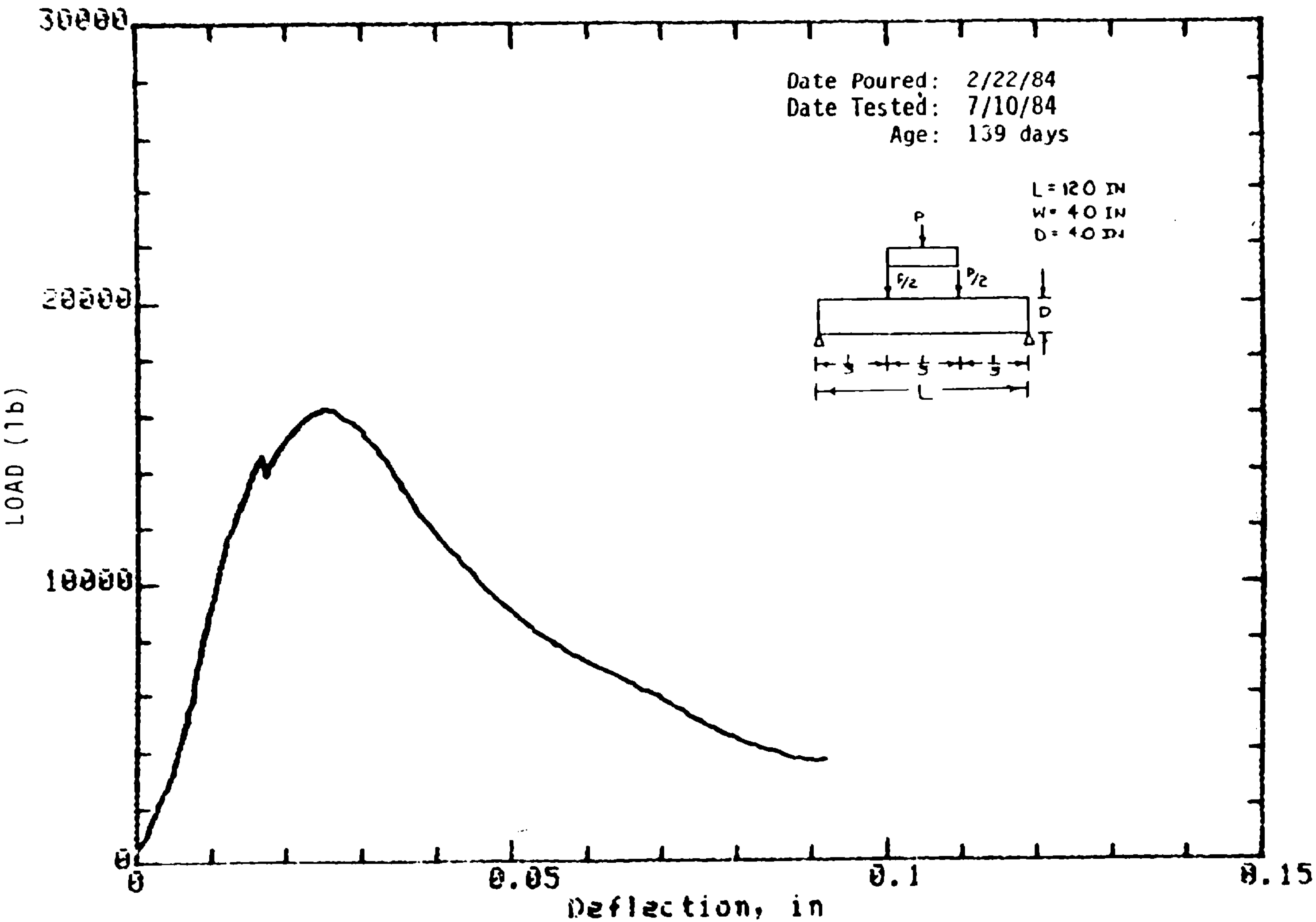

Mark: 8-17 Beam: 4in x 4in Cure: Wet
Concrete Sample

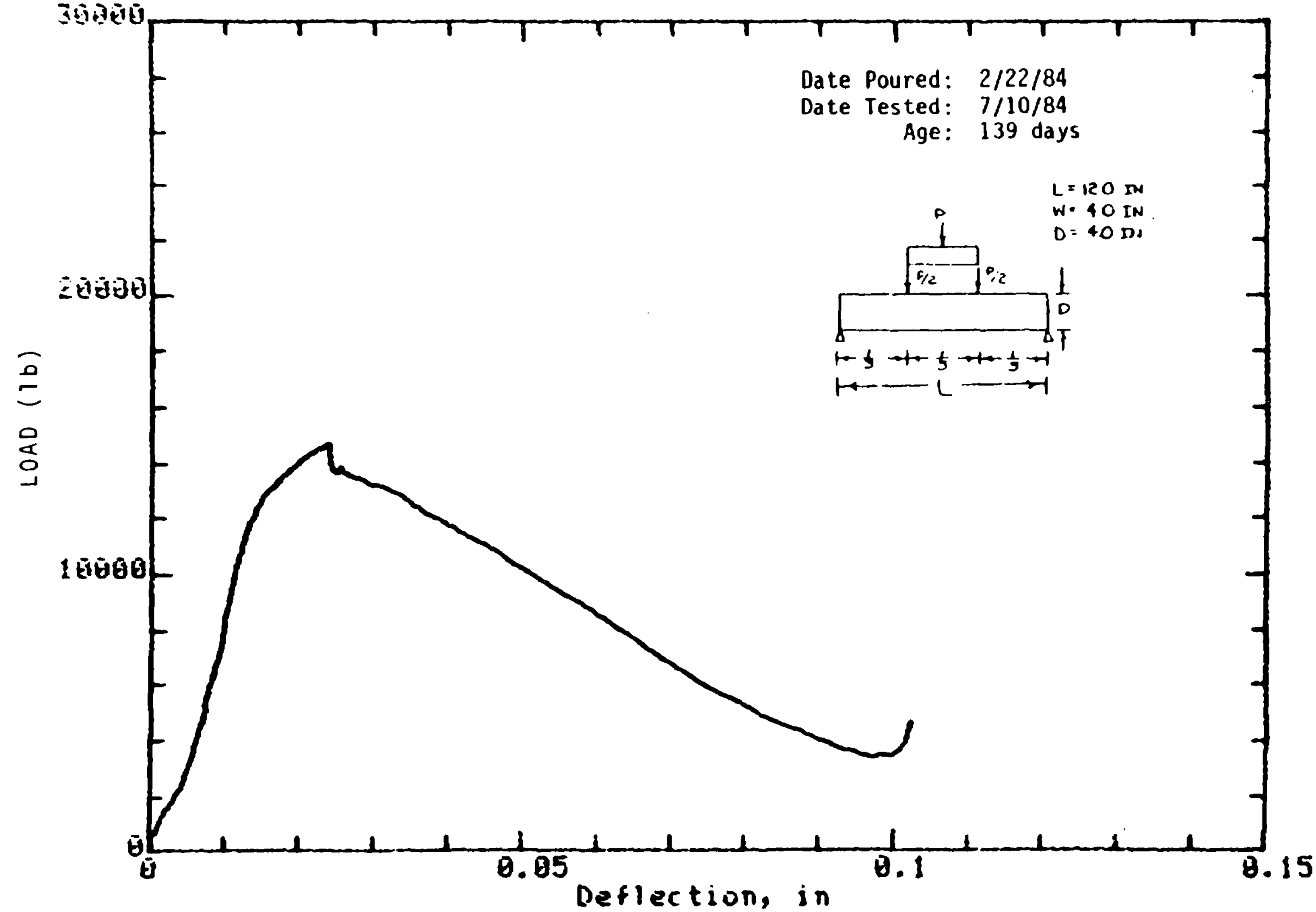

Mark: 8-23 Beam: 4in x 4in Cure: Wet
Concrete Sample

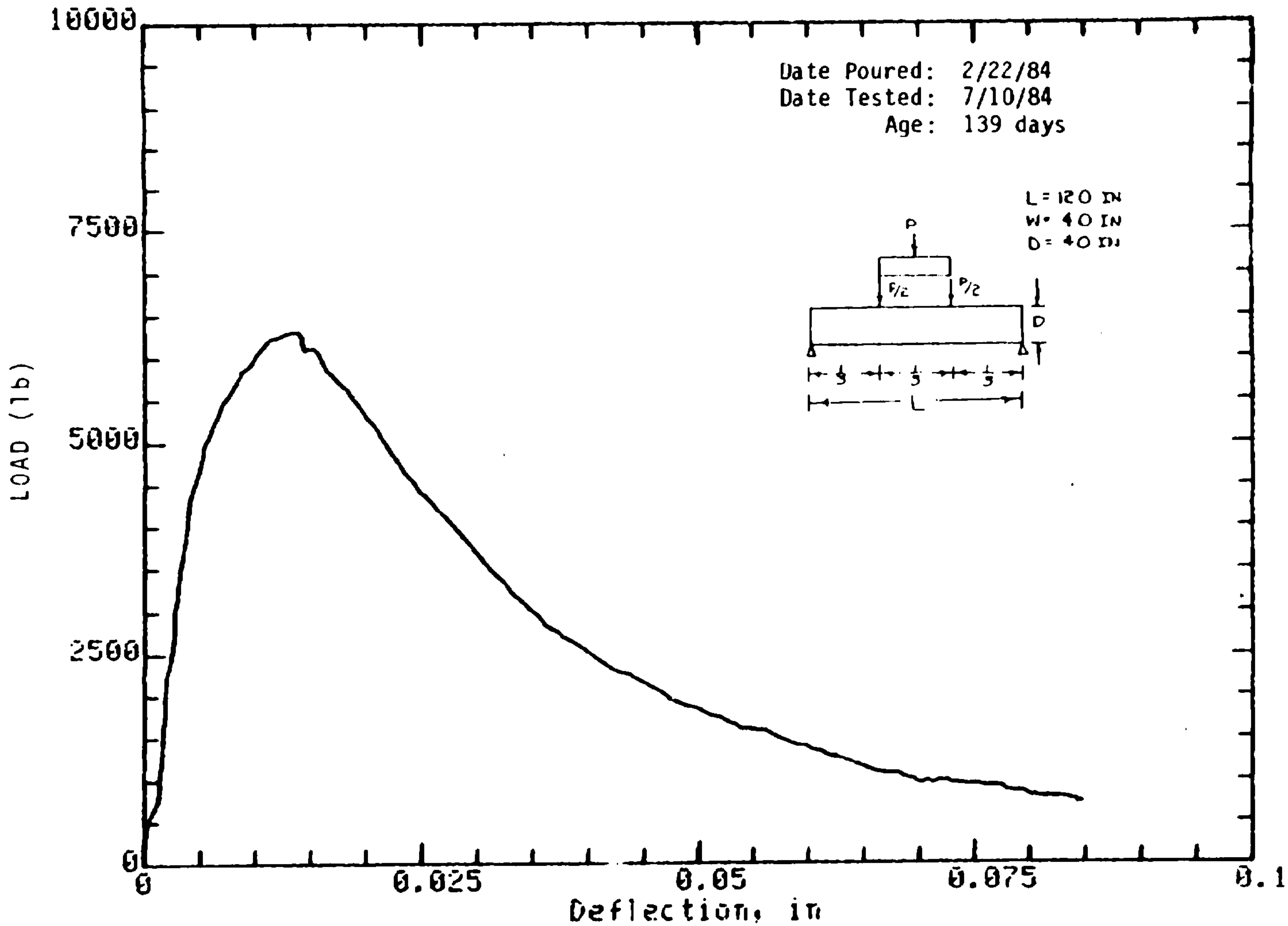

Mark: 8-26 Column: 4in x 4in Cure: Wet
Concrete Sample

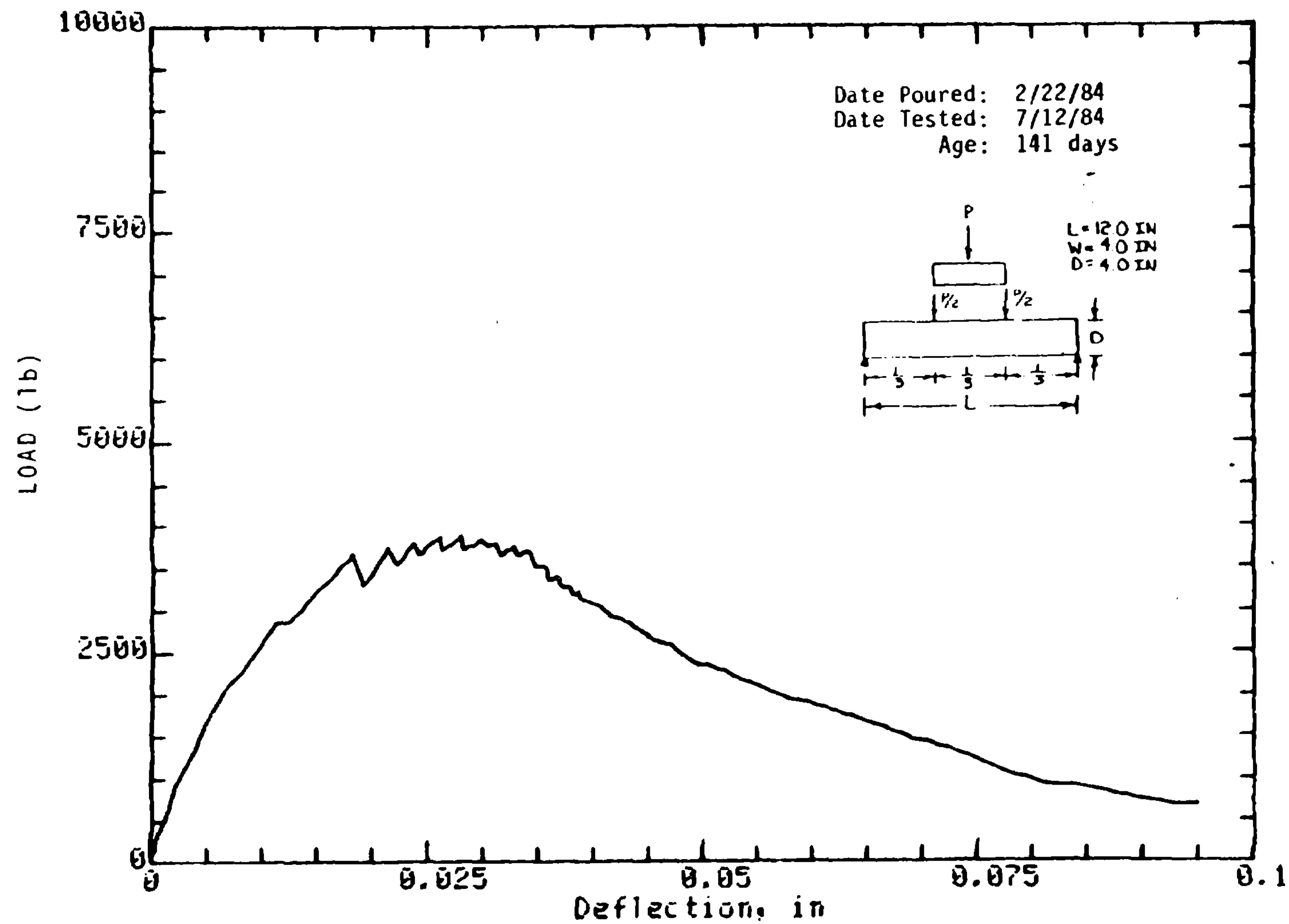

Mark: 8-28 Column: 4in x 4in Cure: Dry
Concrete Sample

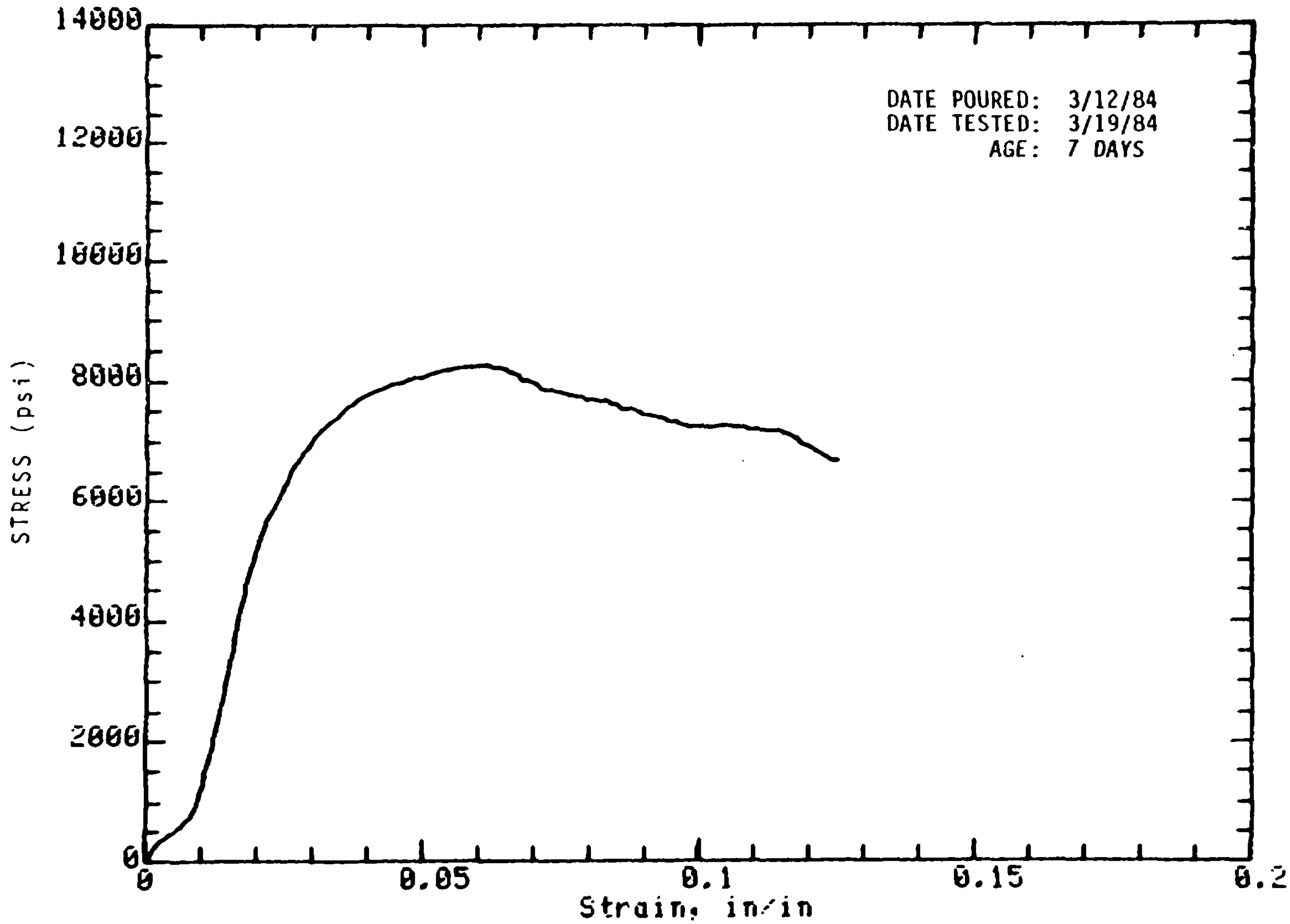

Mark: 9-1 Molded: 4in dia x 8in Cure: Wet
Concrete Sample

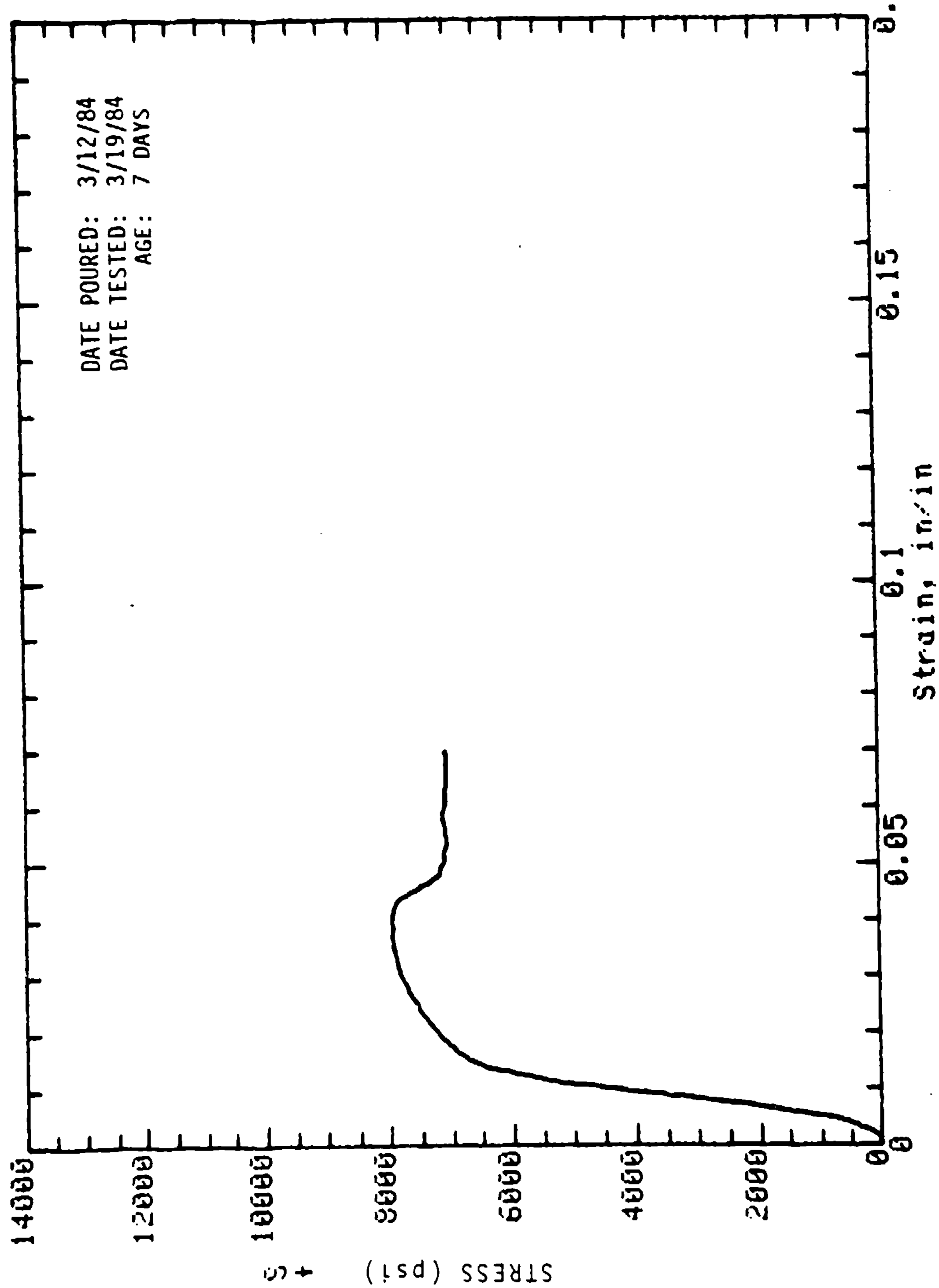

Mark: 9-5 Molded: 4in dia x 8in Cure: Wet
Concrete Sample

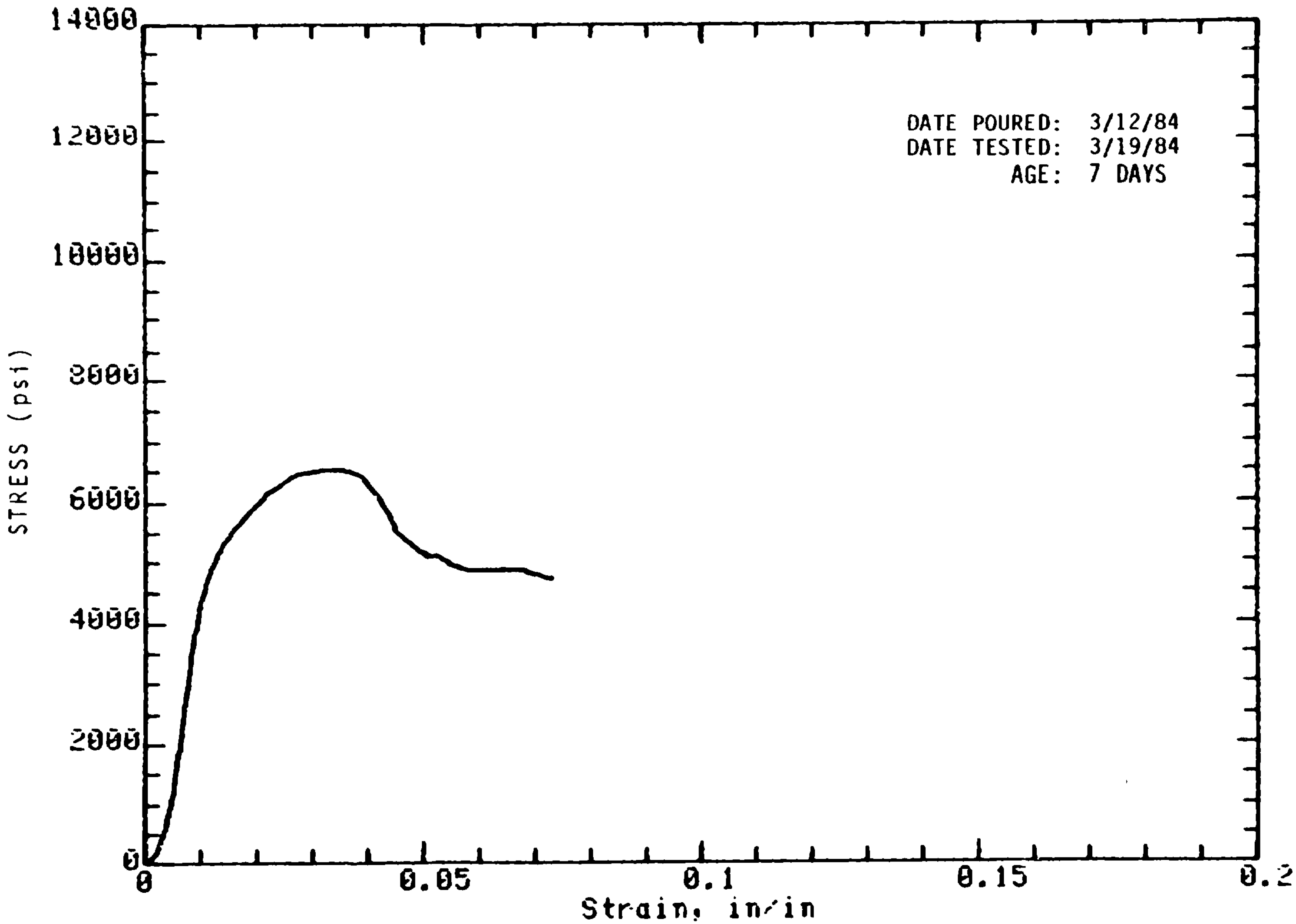

Mark: 9-6 Molded: 4in dia x 8in Cure: Wet
Concrete Sample

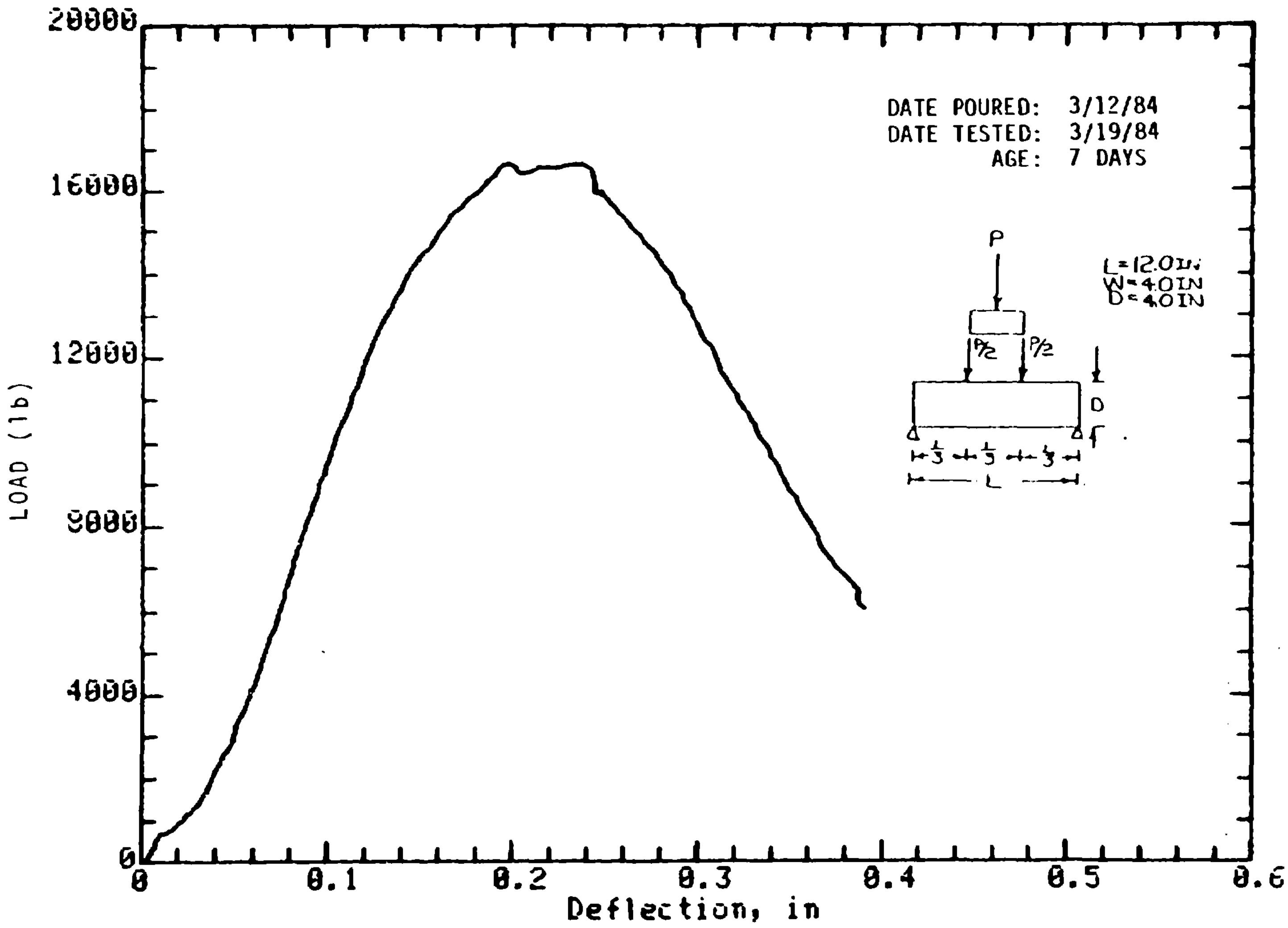

Mark: 9-22 Beam: 4in x 4in Cure: Wet
Concrete Sample

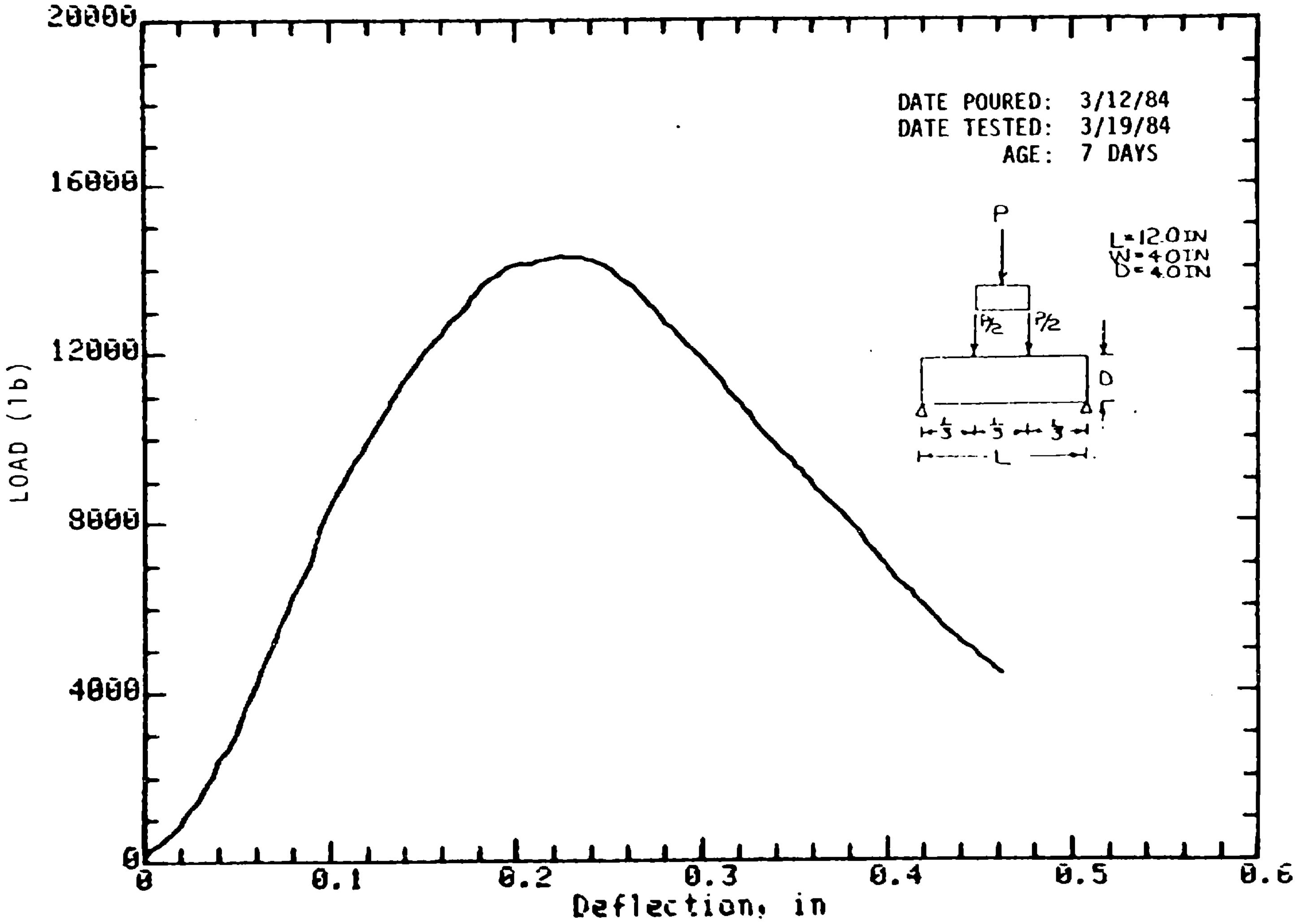

Mark: 9-24 Beam: 4in x 4in Cure: Dry

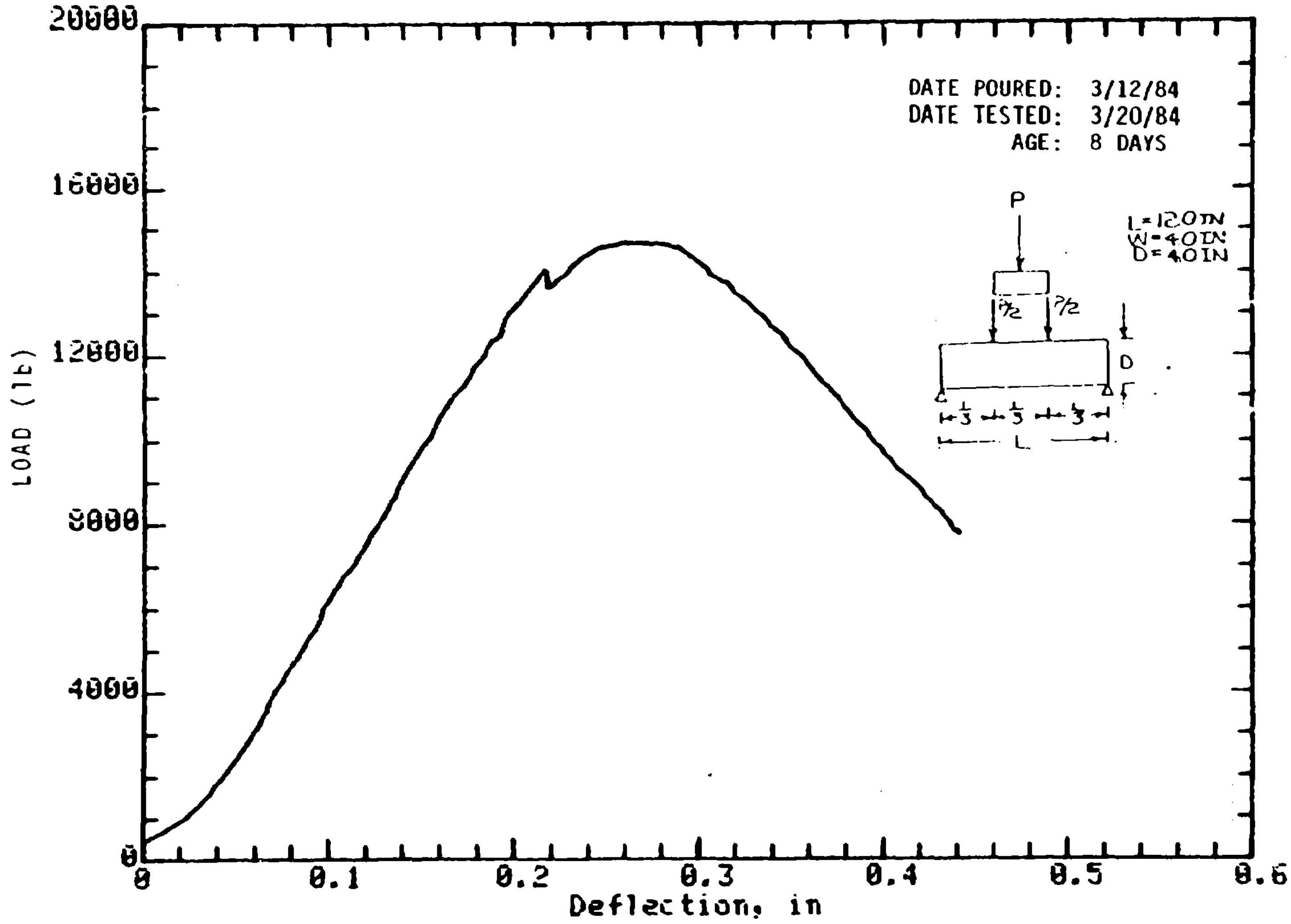

Mark: 9-23 Beam: 4in x 4in Cure: Dry
Concrete Sample

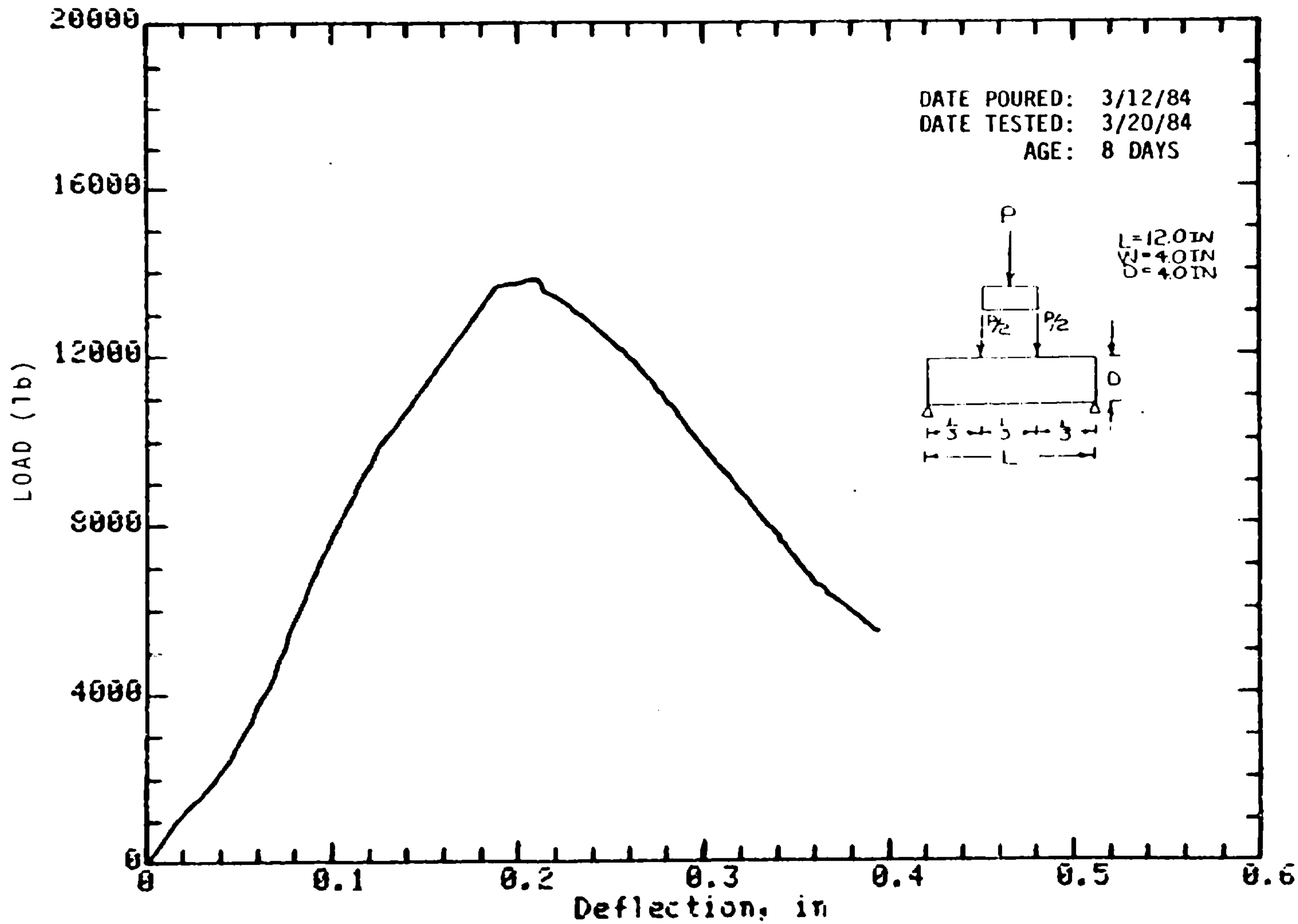

Mark: 9-26 Beam: 4in x 4in Cure: Wet
Concrete Sample

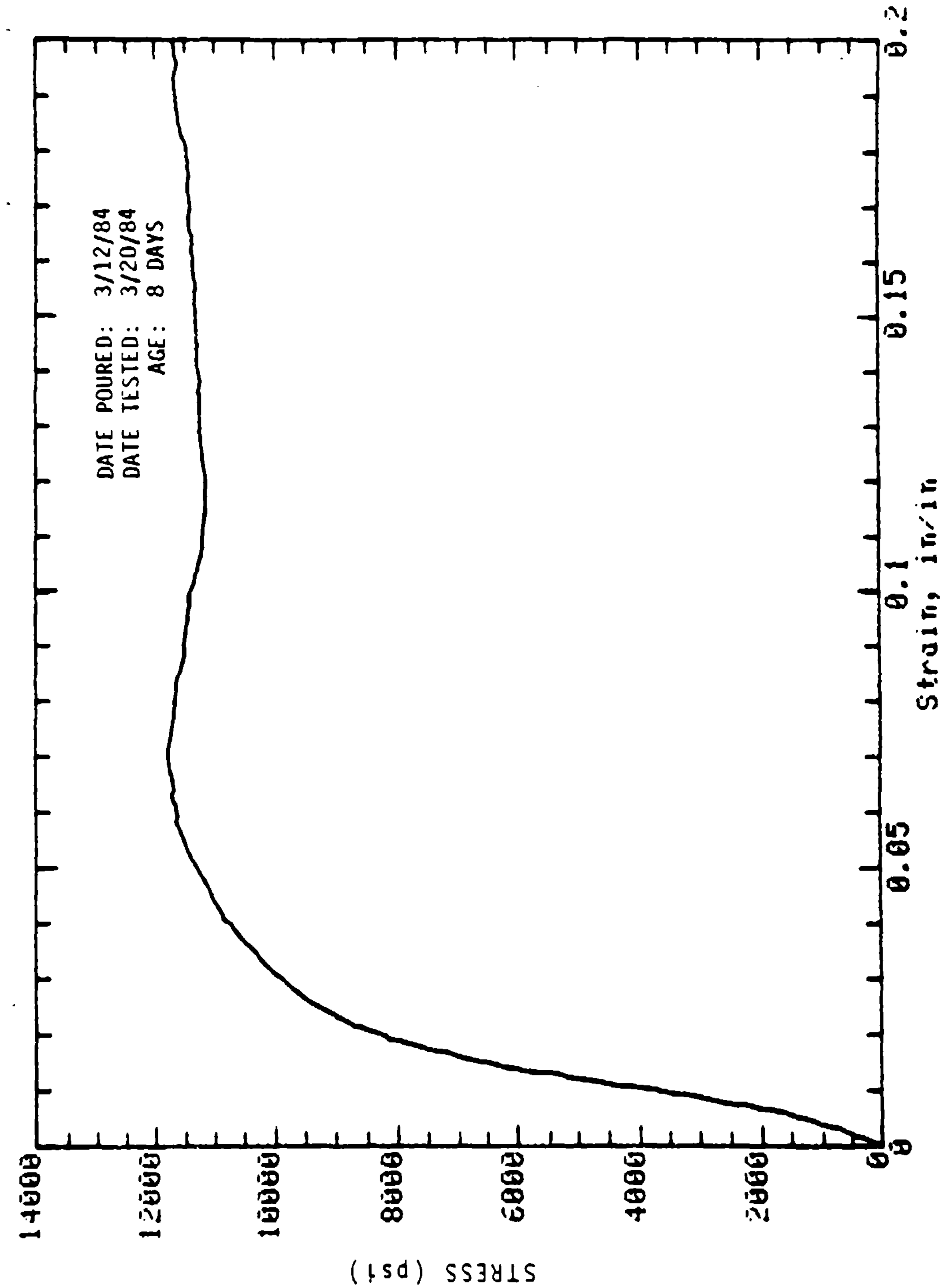

Mark: 9-S1-4 Cored (slab): 2in dia x 3.5in Cure: Dry

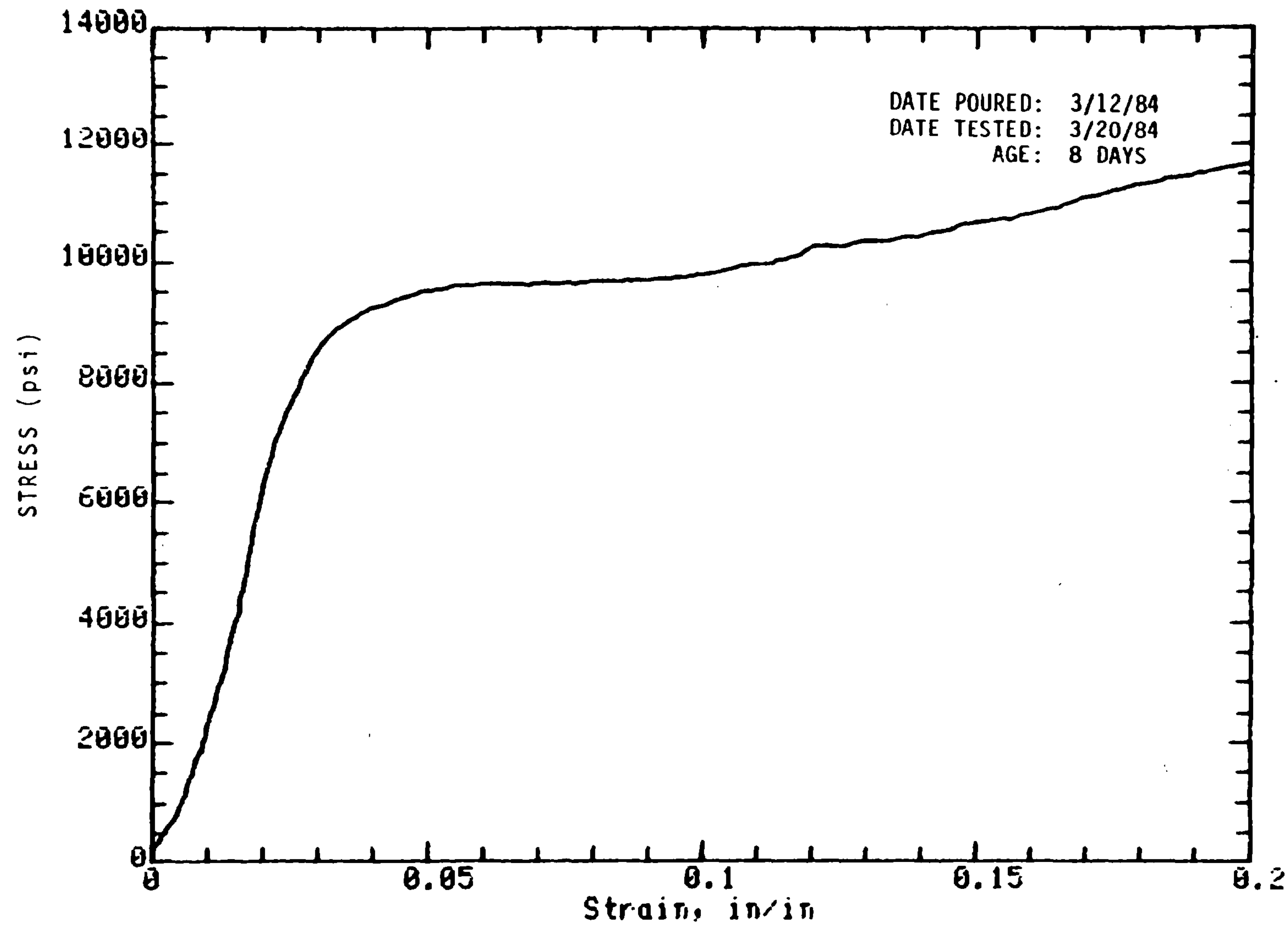

Mark: 9-S1-5 Cored (slab): 2in dia x 3.5in Cure: Wet

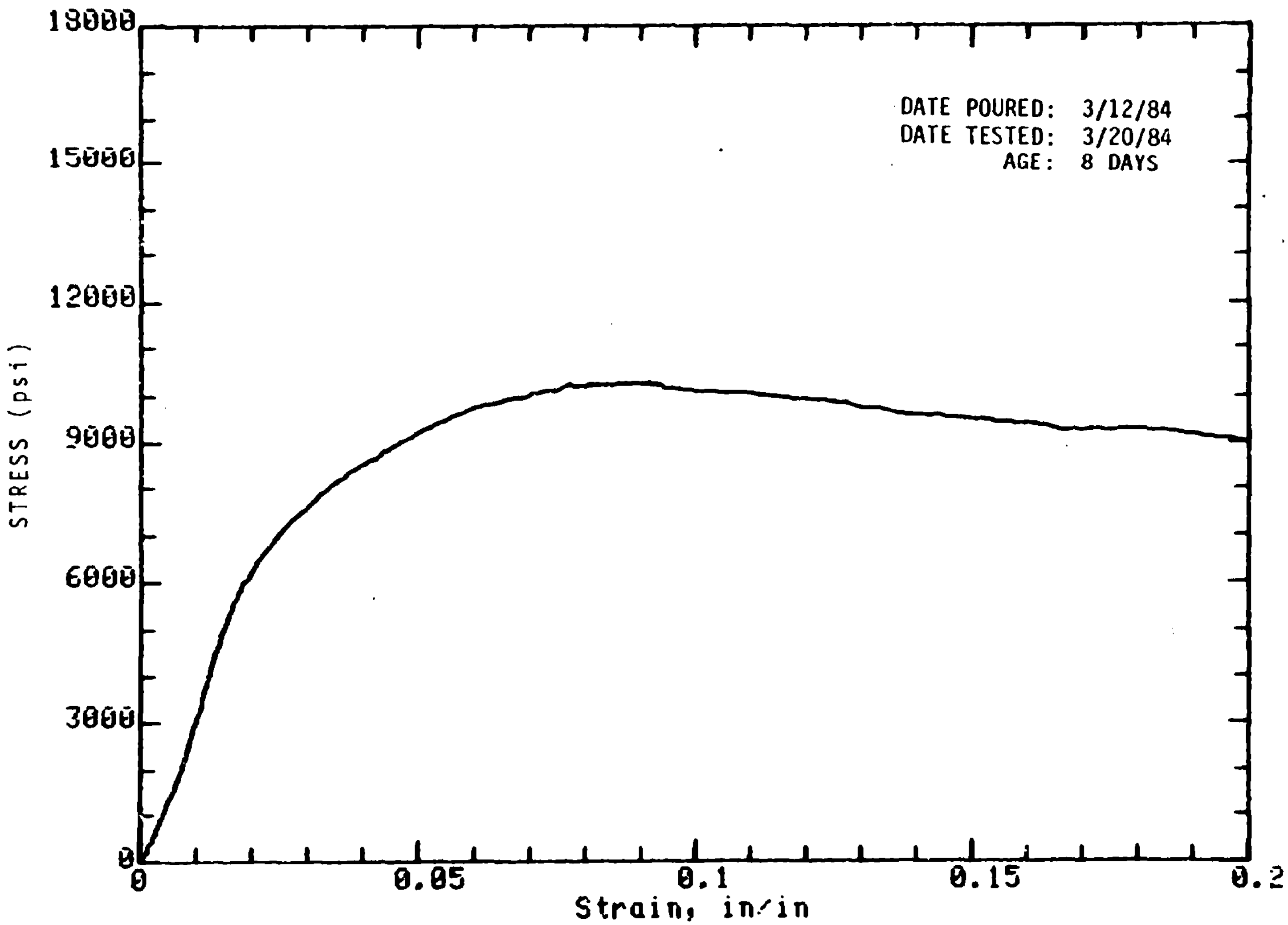

Mark: 9-S2-1 Cored (wall): 2in dia x 4in Cure: Dry
Concrete Sample

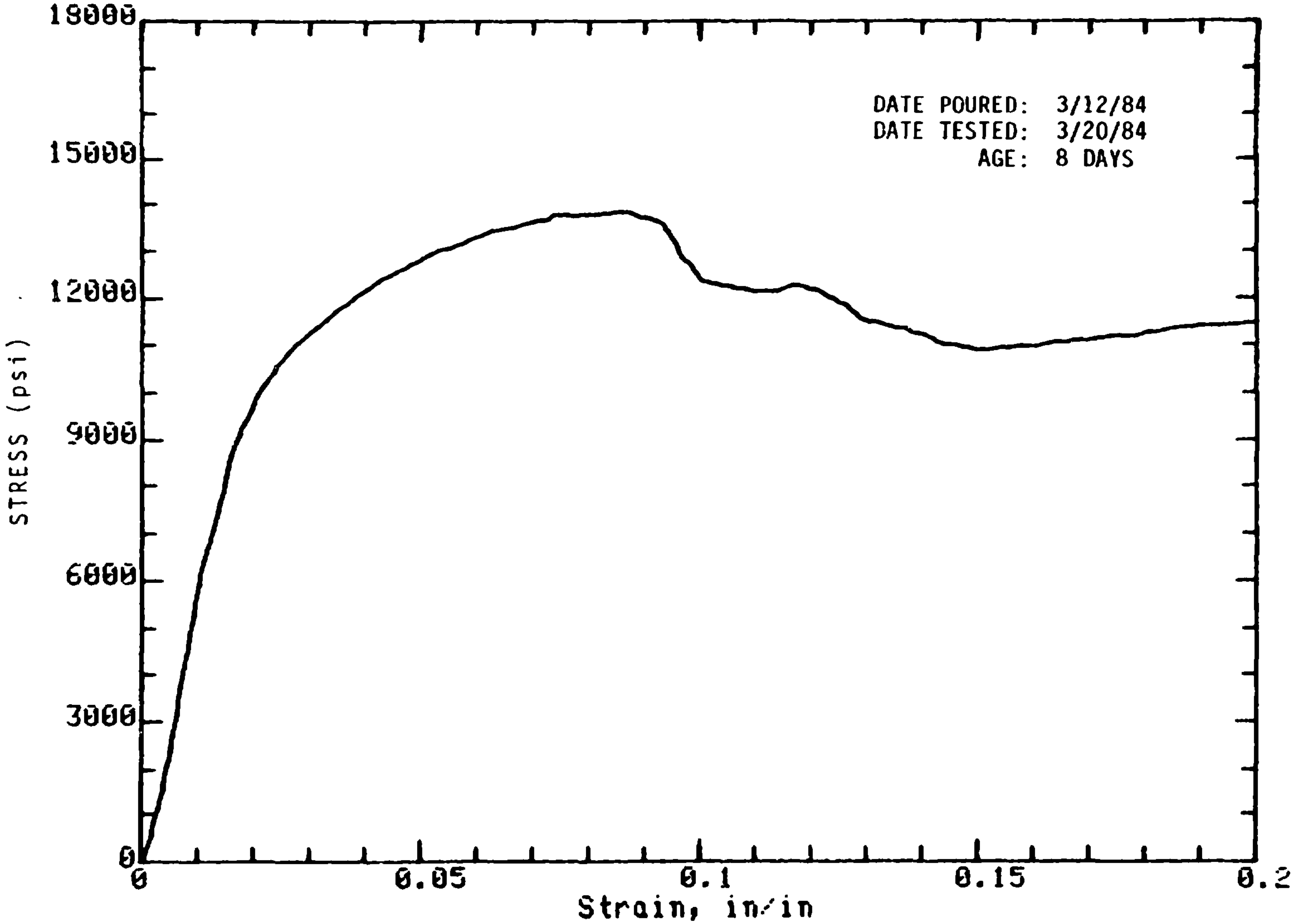

Mark: 9-S2-2 Cored (wall): 2in dia x 4in Cure: Dry
Concrete Sample

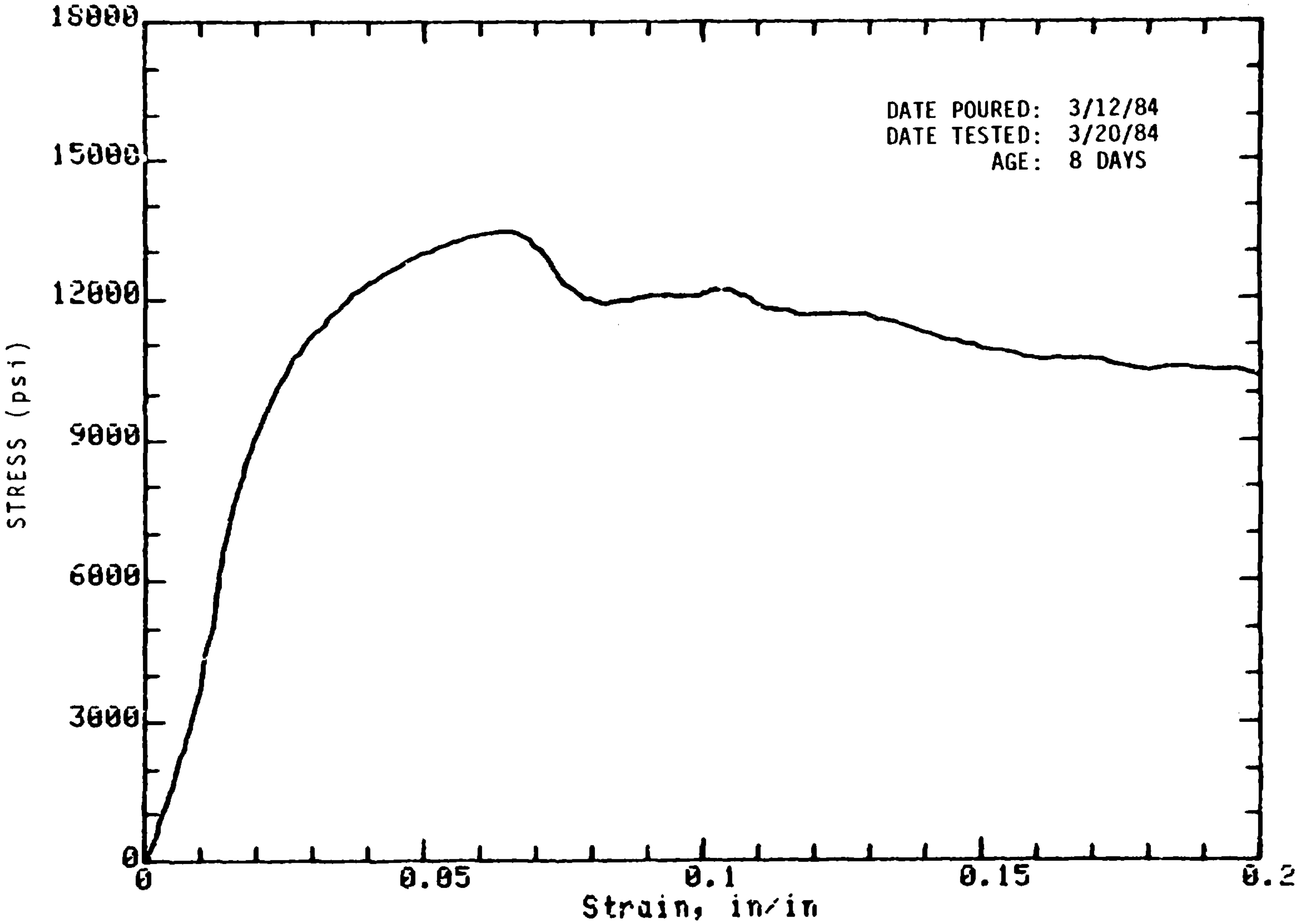

Mark: 9-S2-3 Cored (wall): 2in dia x 4in Cure: Dry
Concrete Sample

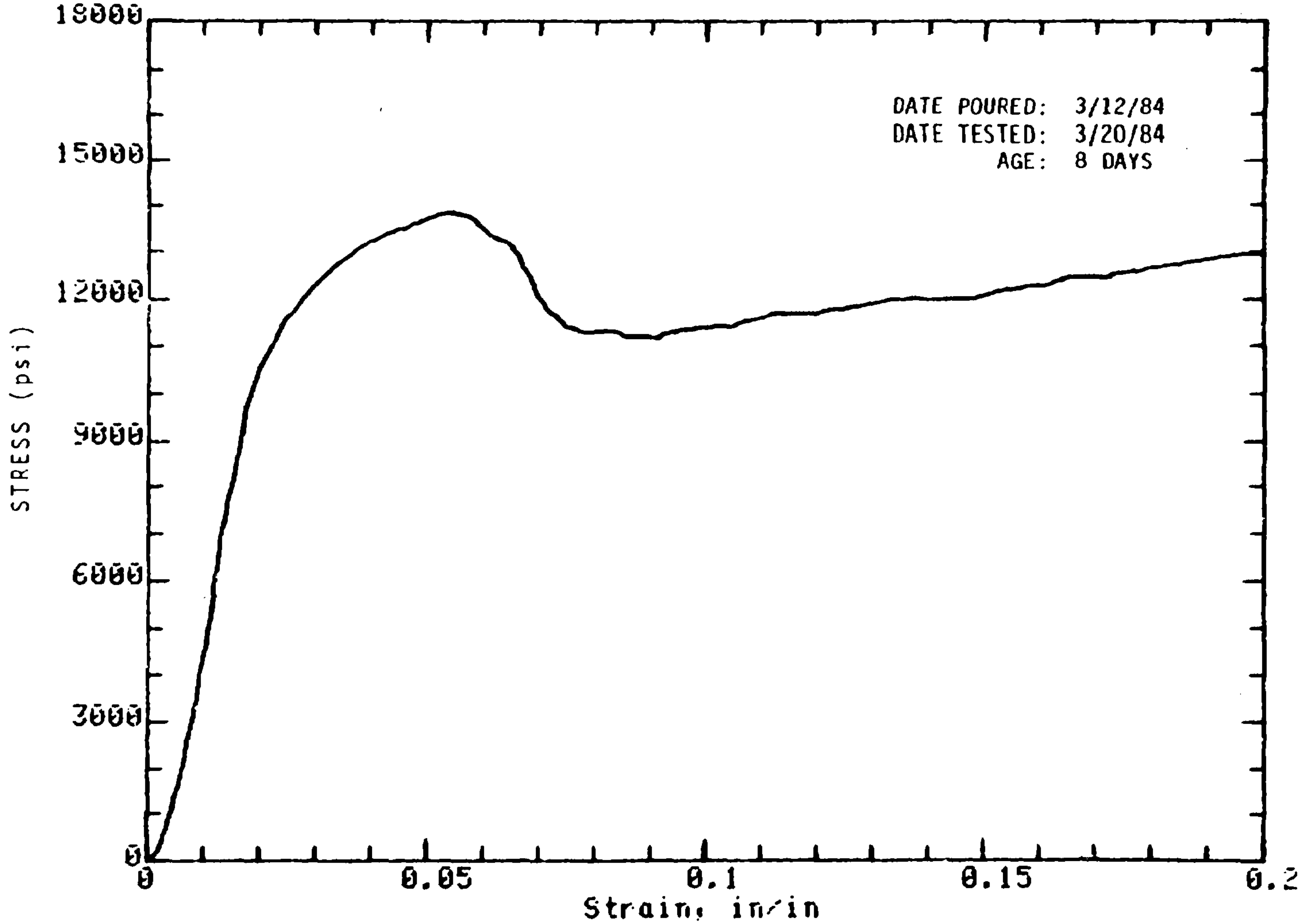

Mark: 9-S2-4 Cored (wall): 2in dia x 4in Cure: Dry
Concrete Sample

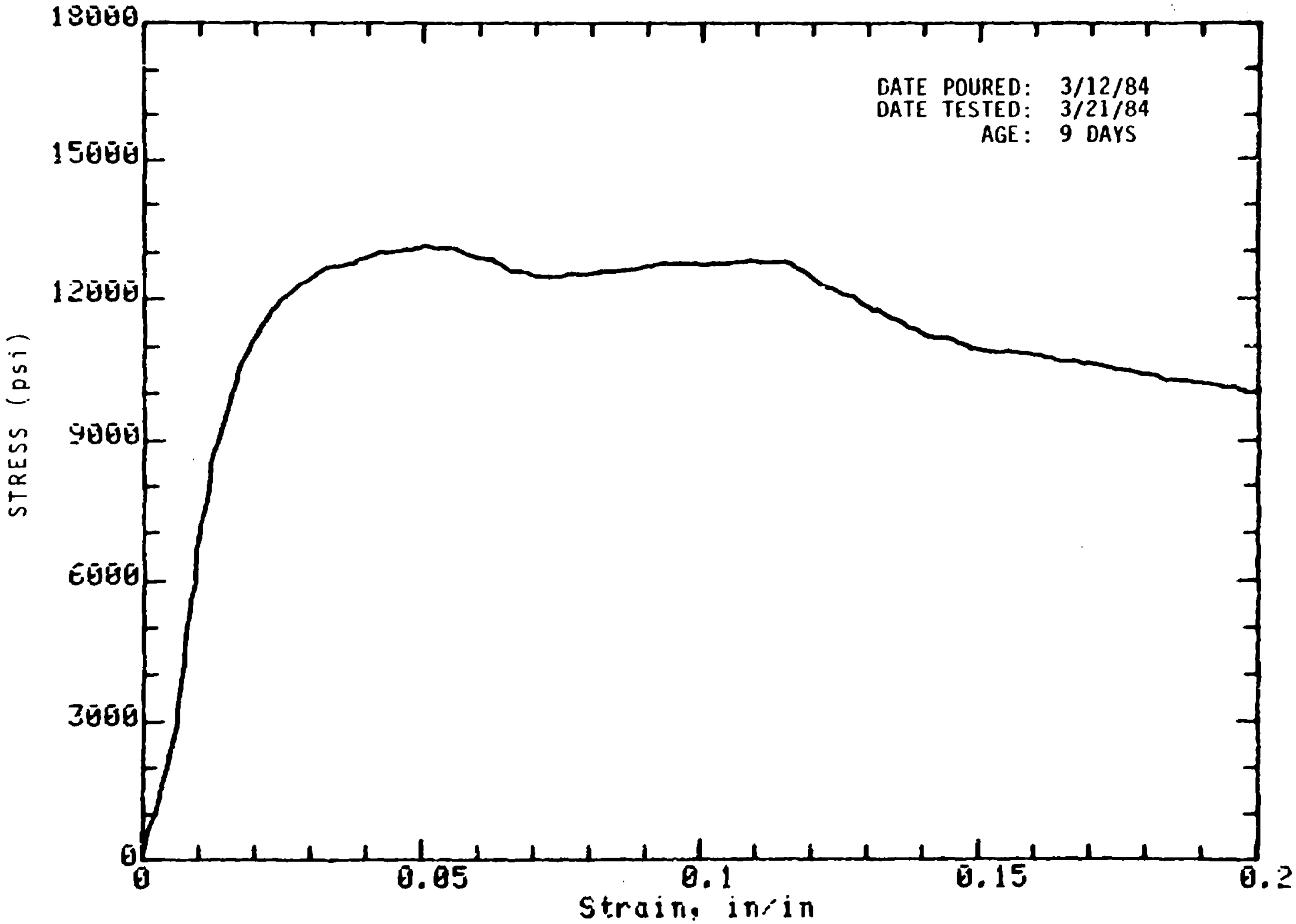

Mark: 9-S2-5 Cored (wall): 2in dia x 4in Cure: Dry
Concrete Sample

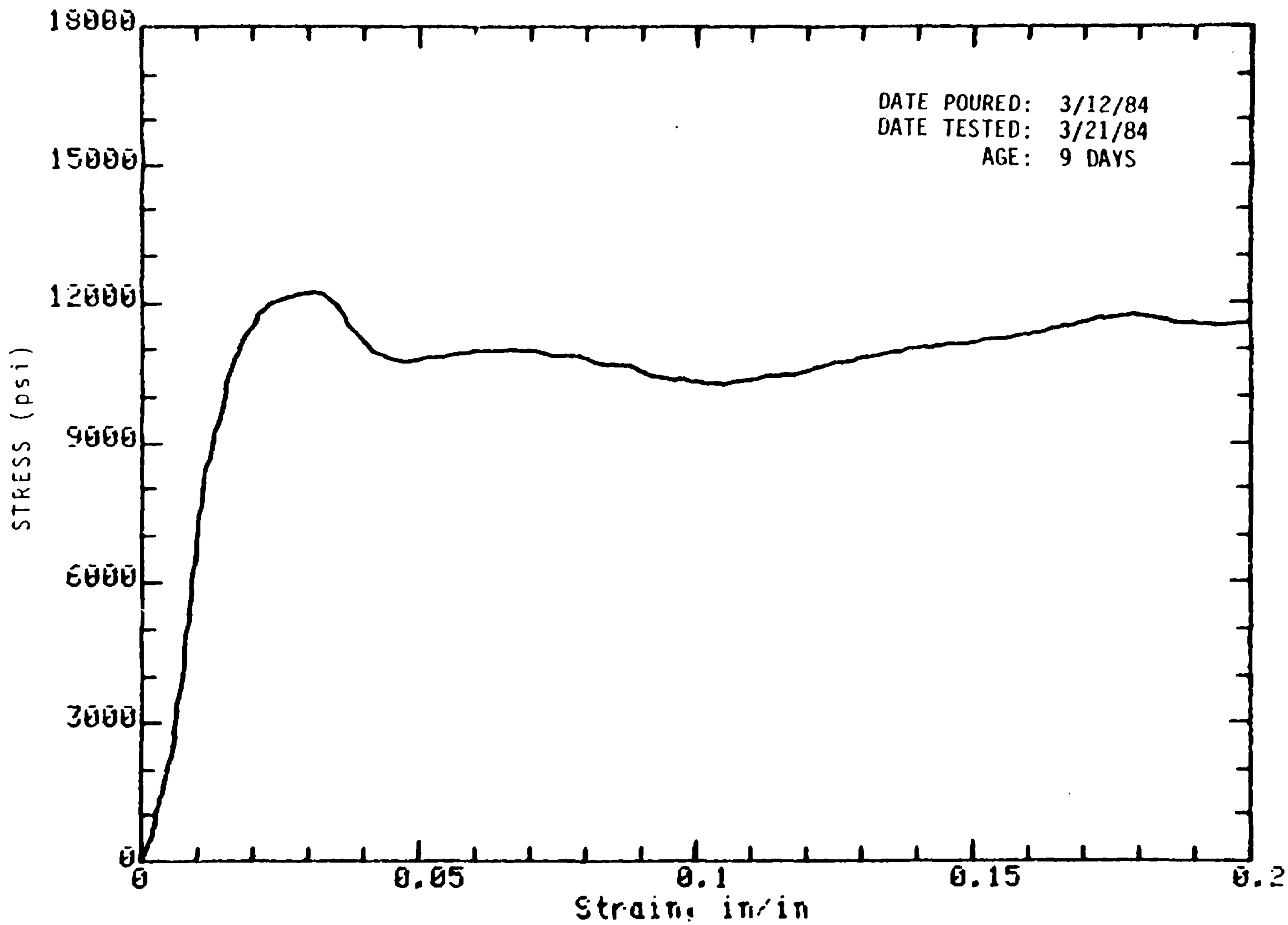

Mark: 9-S2-6 Cored (wall): 2in dia x 4in Cure: Dry
Concrete Sample

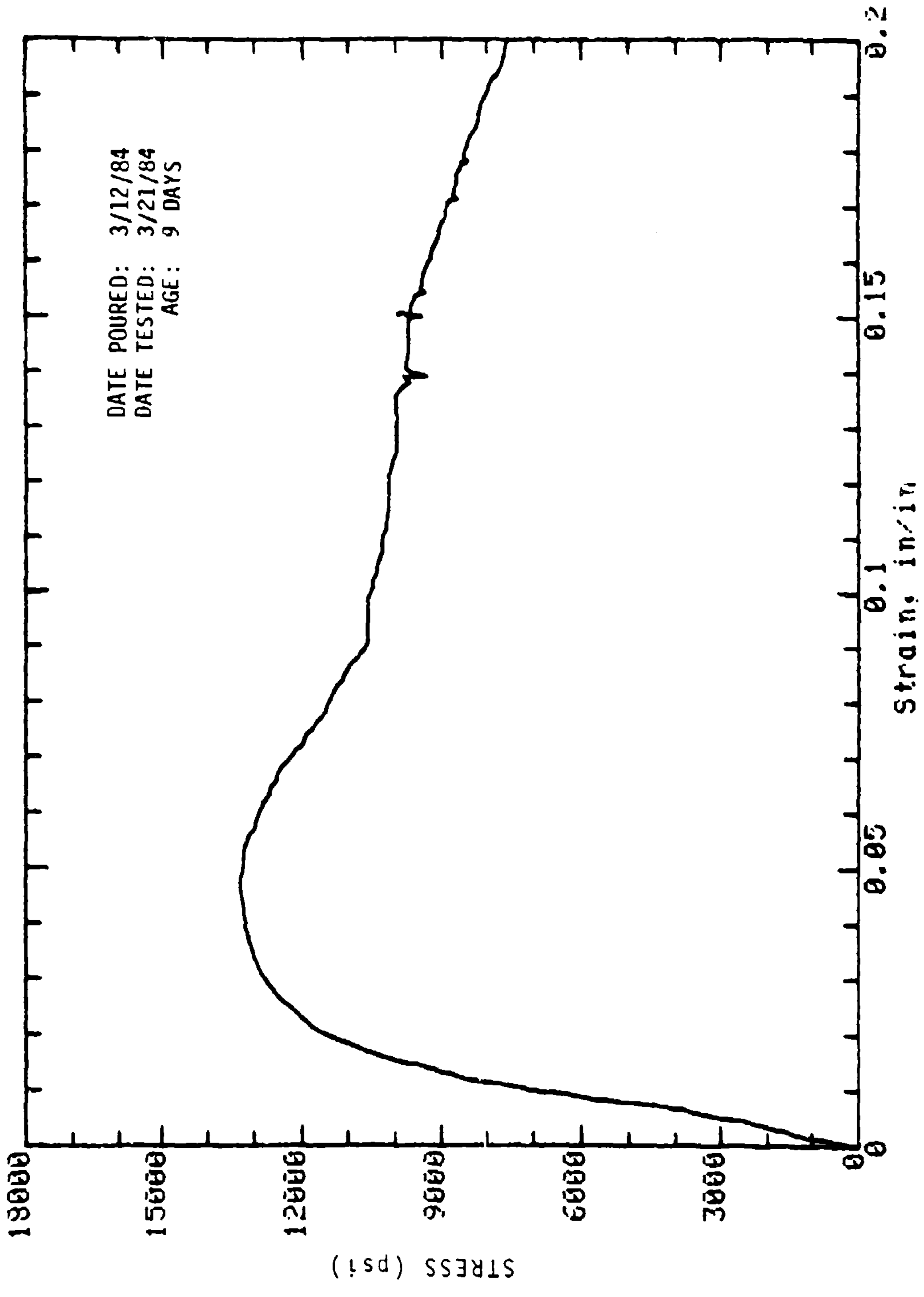

Mark: 9-S2-7 Cored (wall): 2in dia x 4in Cure: Dry
Concrete Sample

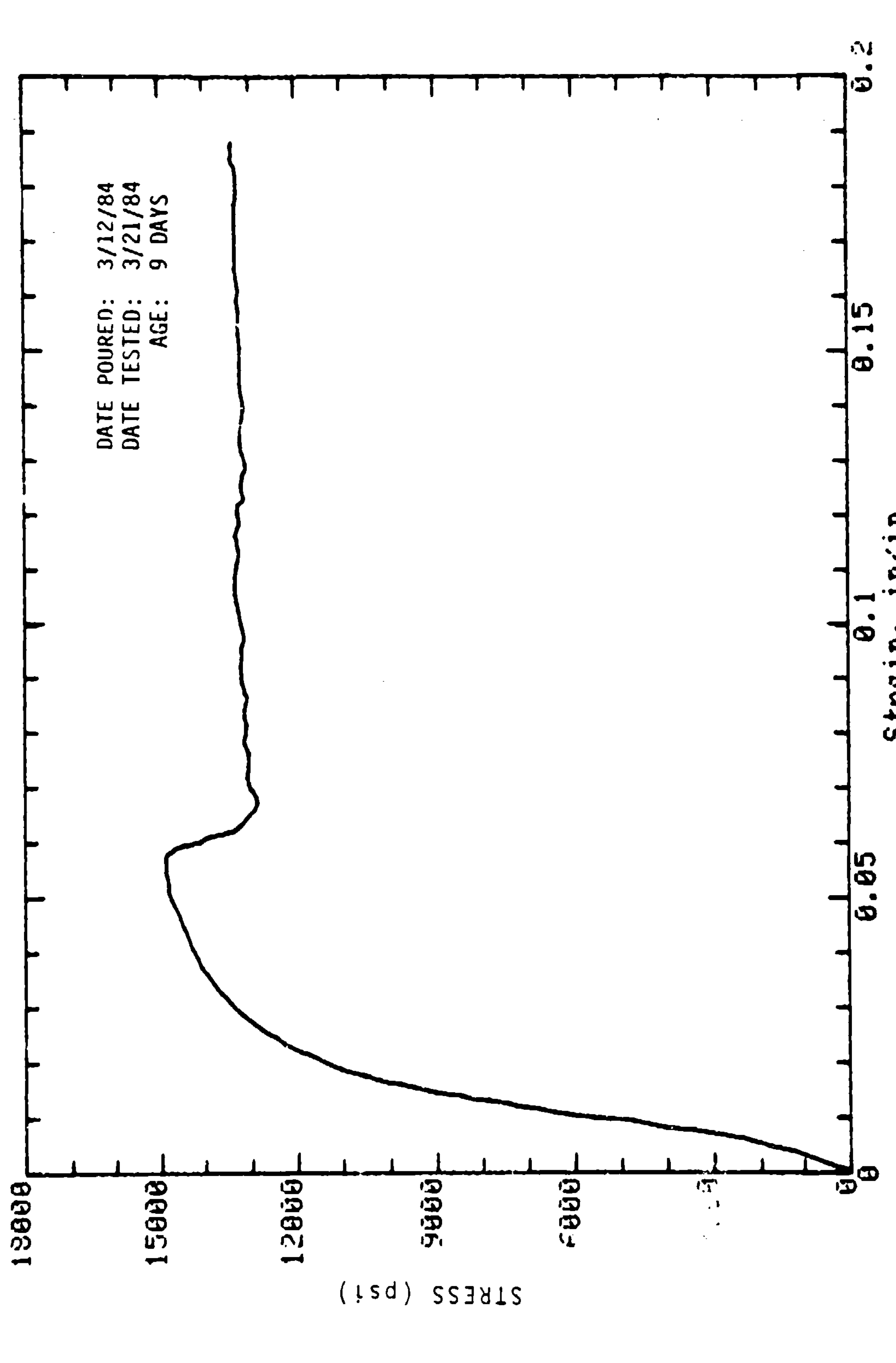

Mark: 9-S2-8 Cored (wall): 2in dia x 4in Cure: Dry
Concrete Sample

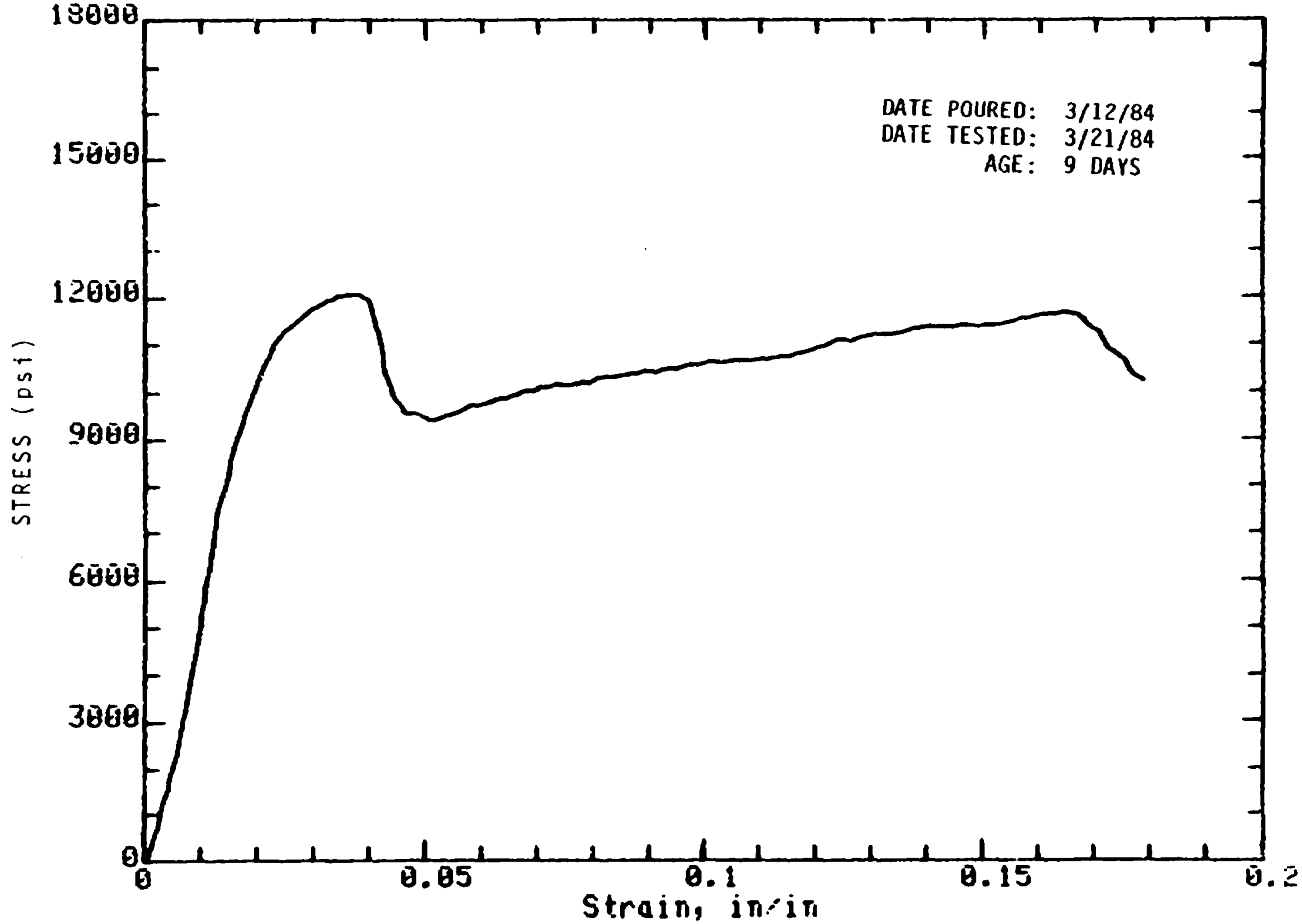

Mark: 9-S Cored (wall): 2in dia x 4in Cure: Dry
Concrete Sample

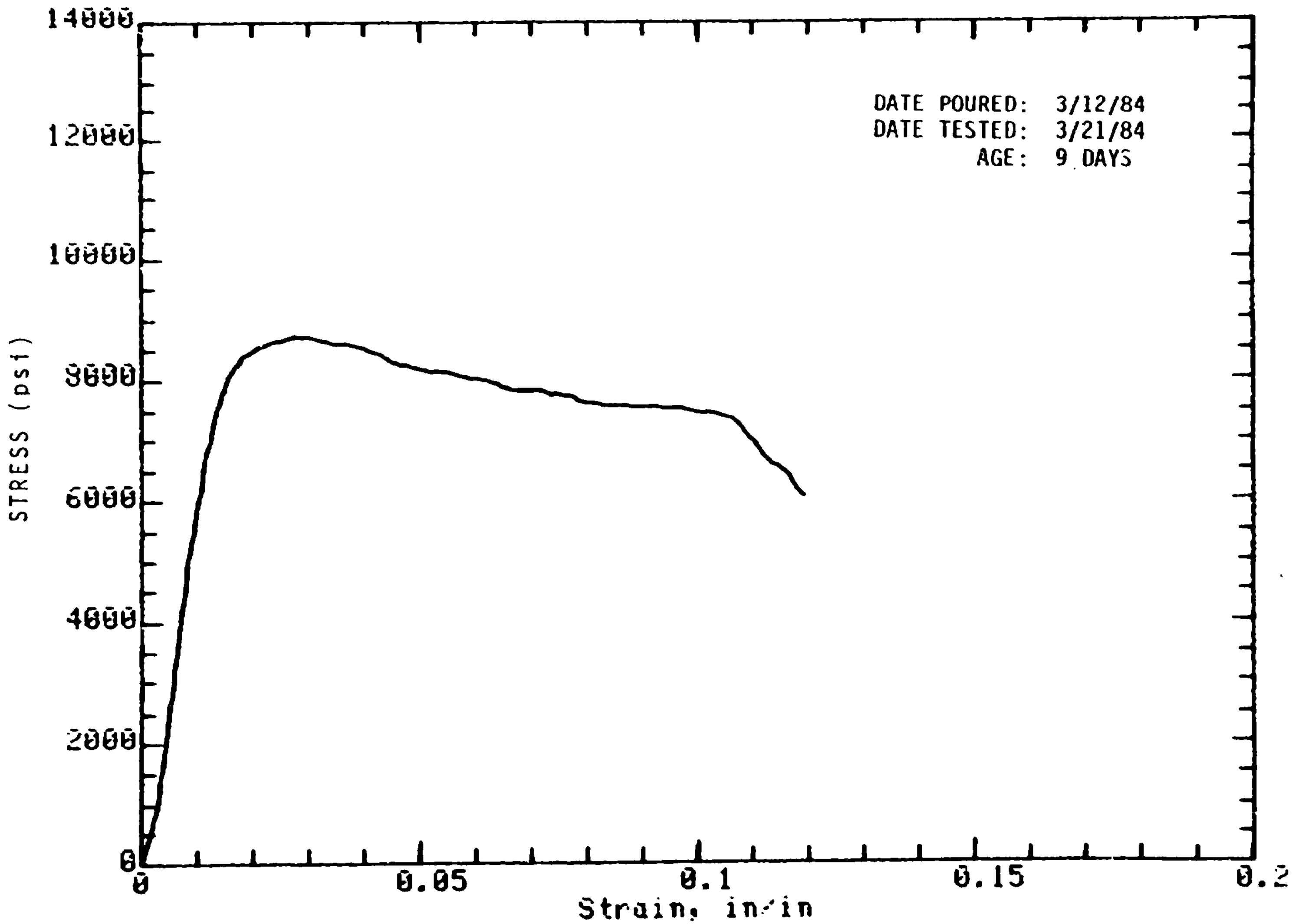

Mark: 9-12 Molded: 4in dia x 8in Cure: Dry
Concrete Sample

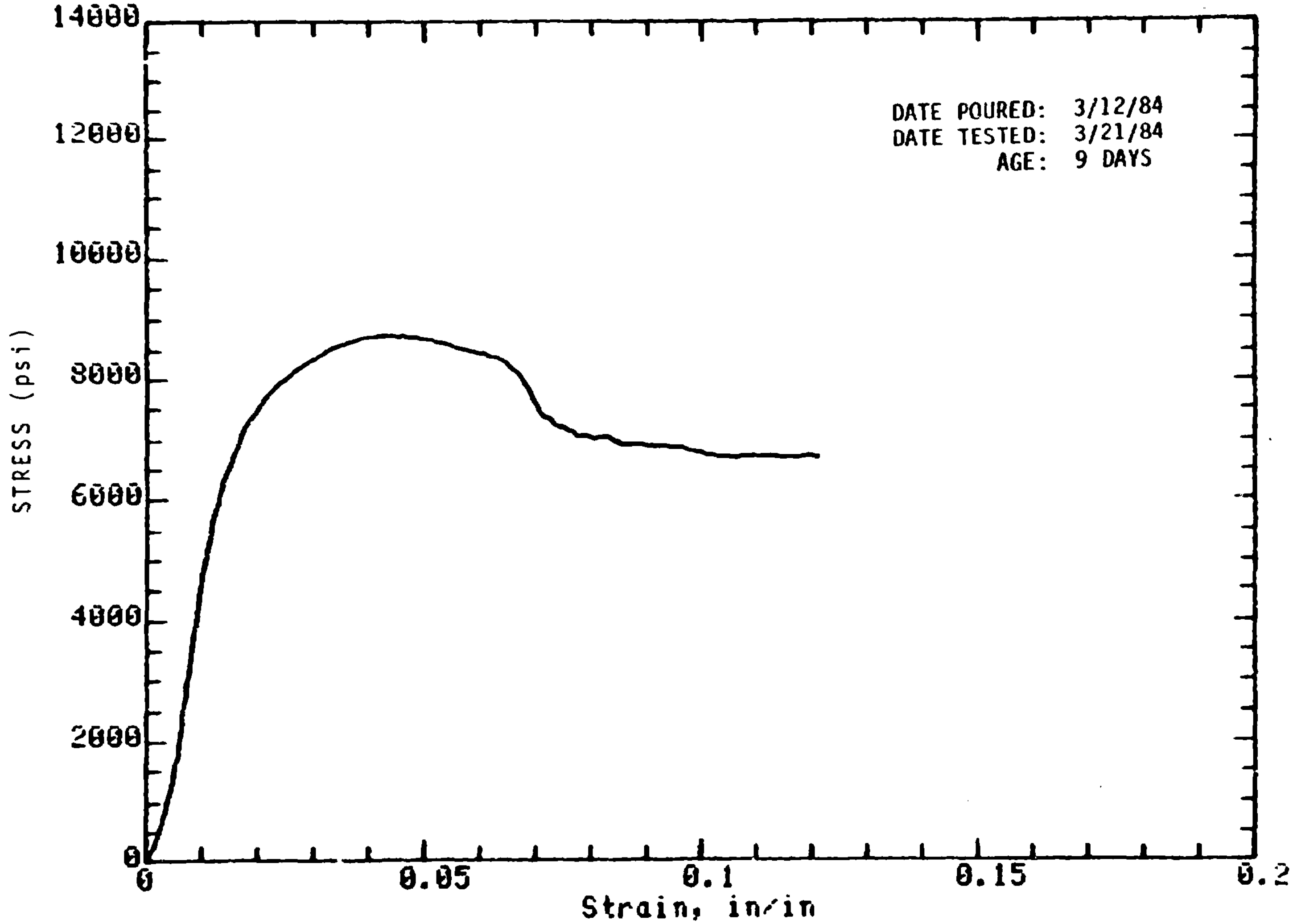

Mark: 9-13 Molded: 4in dia x 8in Cure: Dry
Concrete Sample

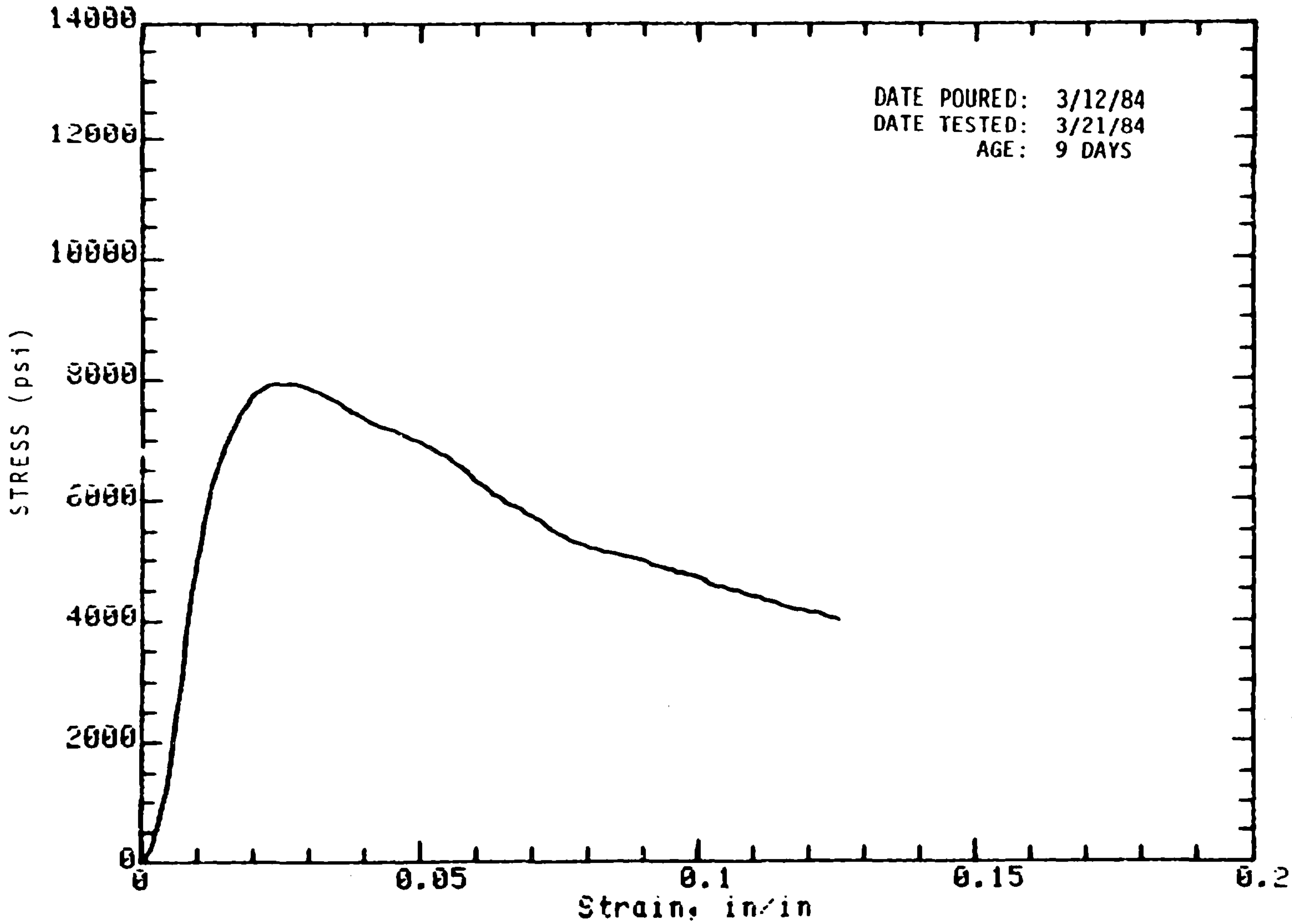

Mark: 9-15 Molded: 4in dia x 8in Cure: Dry
Concrete Sample

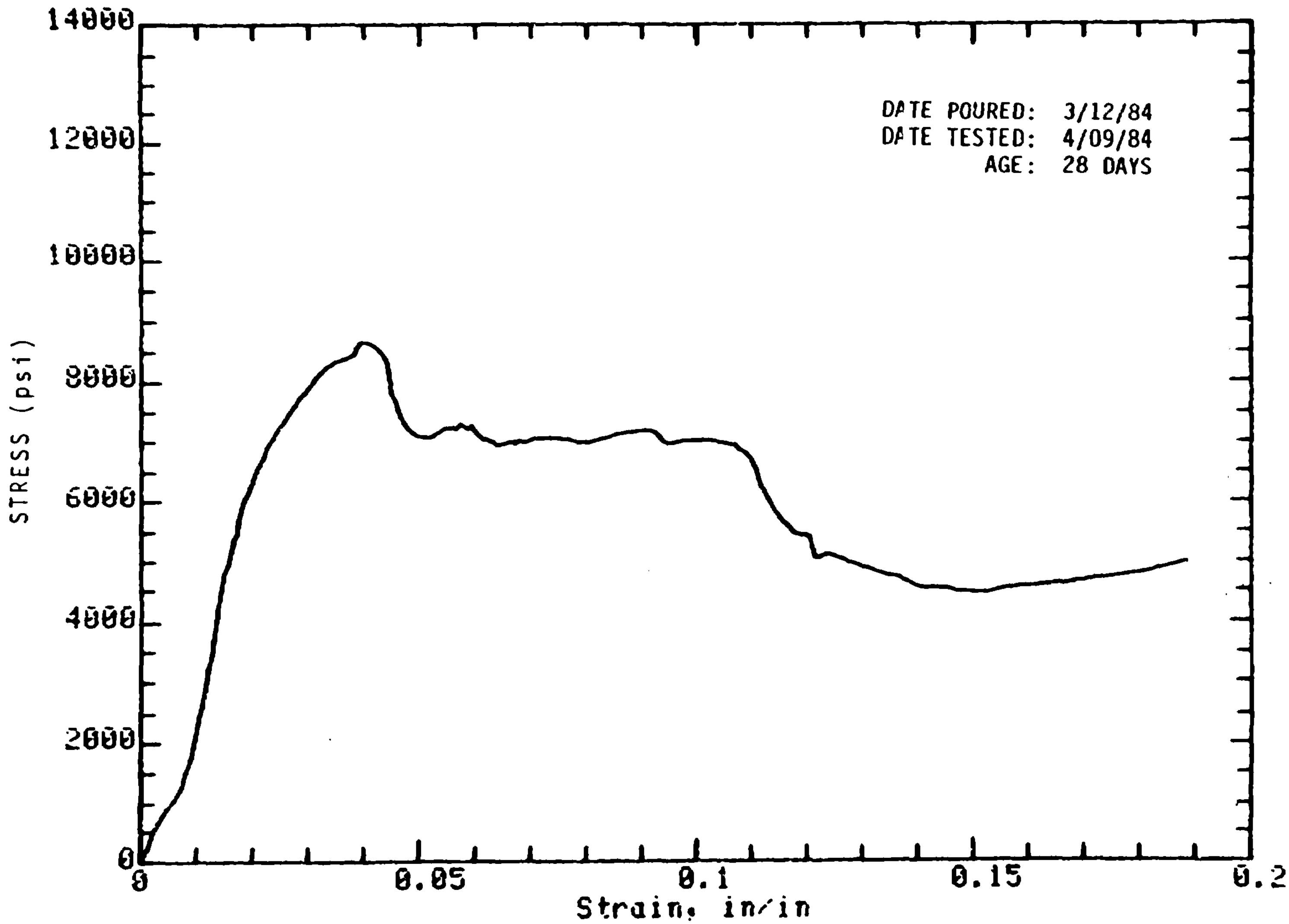

Mark: 9-2 Molded: 4in dia × 8in Cure: Wet
Concrete Sample

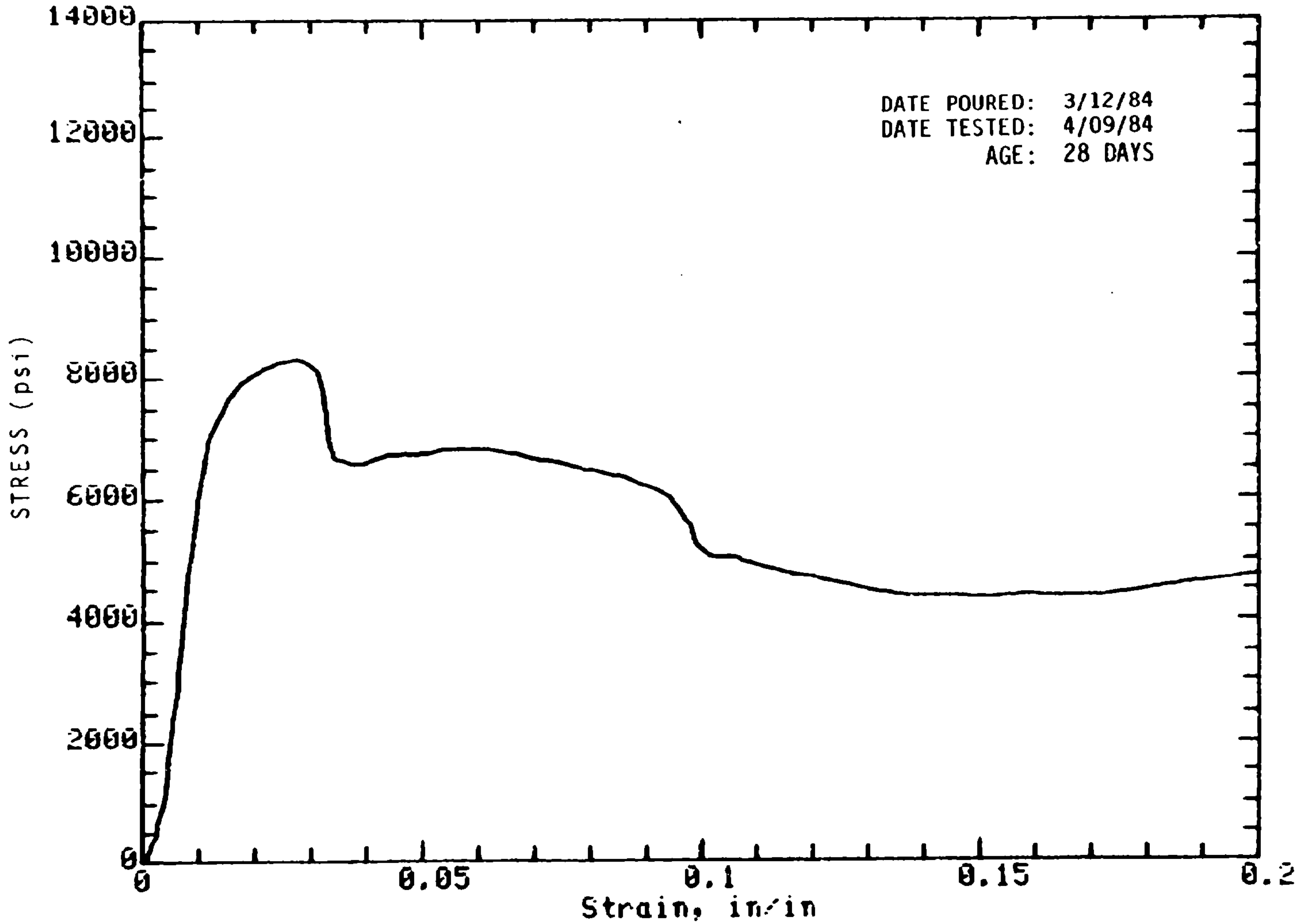

Mark: 9-3 Molded: 4in dia × 8in Cure: Wet
Concrete Sample

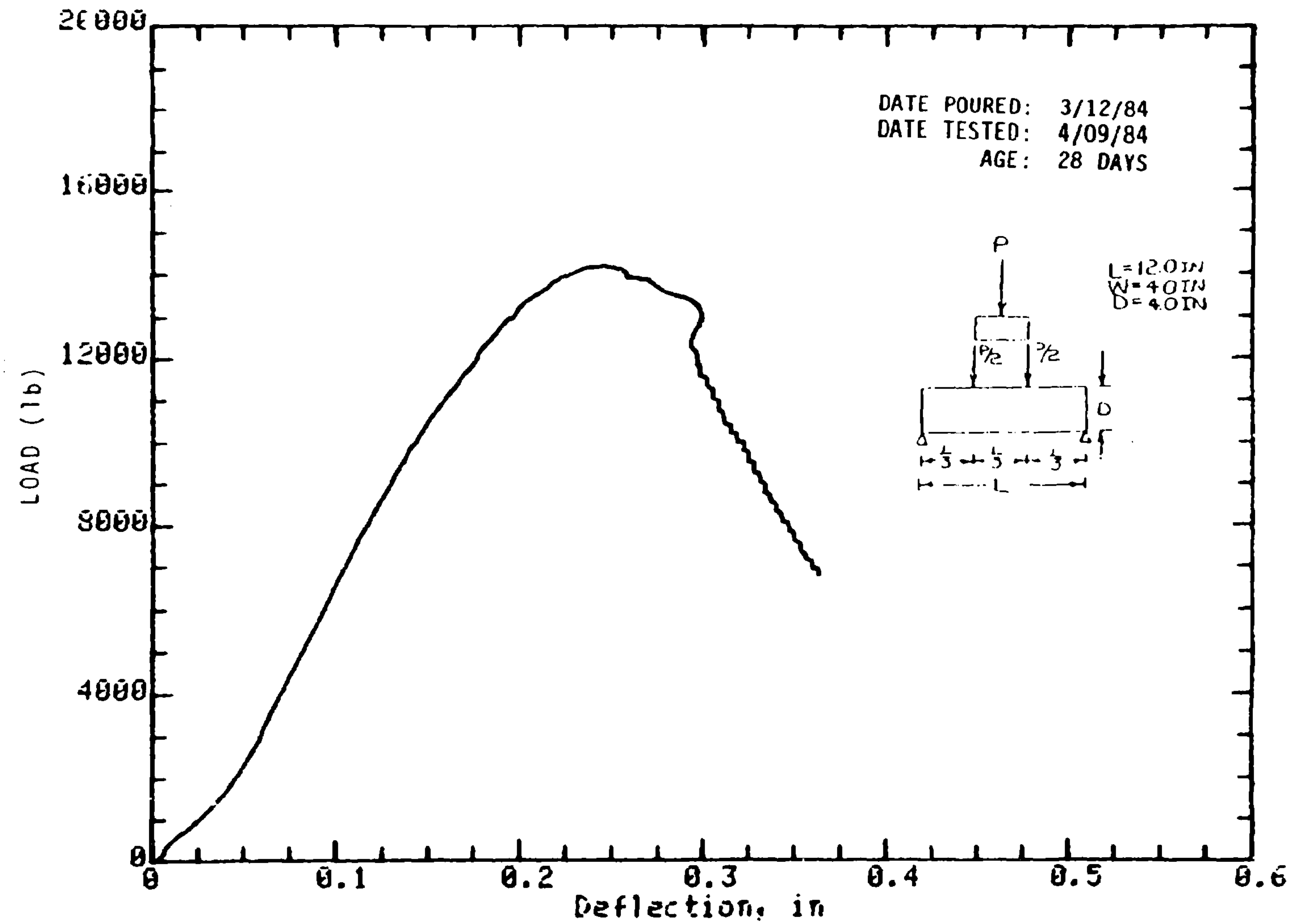

Mark: 9-27 Beam: 4in x 4in Cure: Dry
Concrete Sample

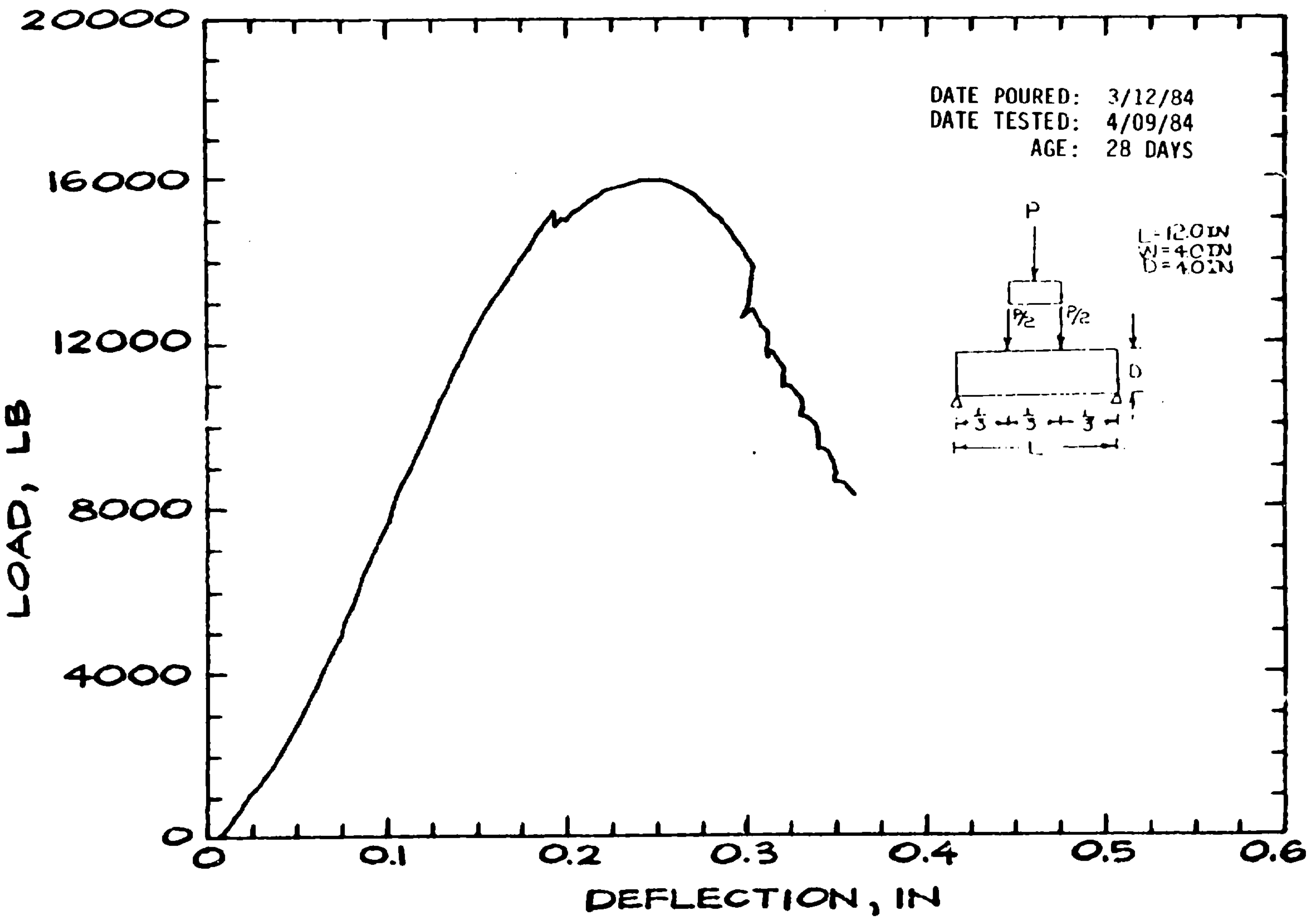

MARK: 9-29 BEAM: 4 IN x 4IN CURE:
DRY CONCRETE SAMPLE

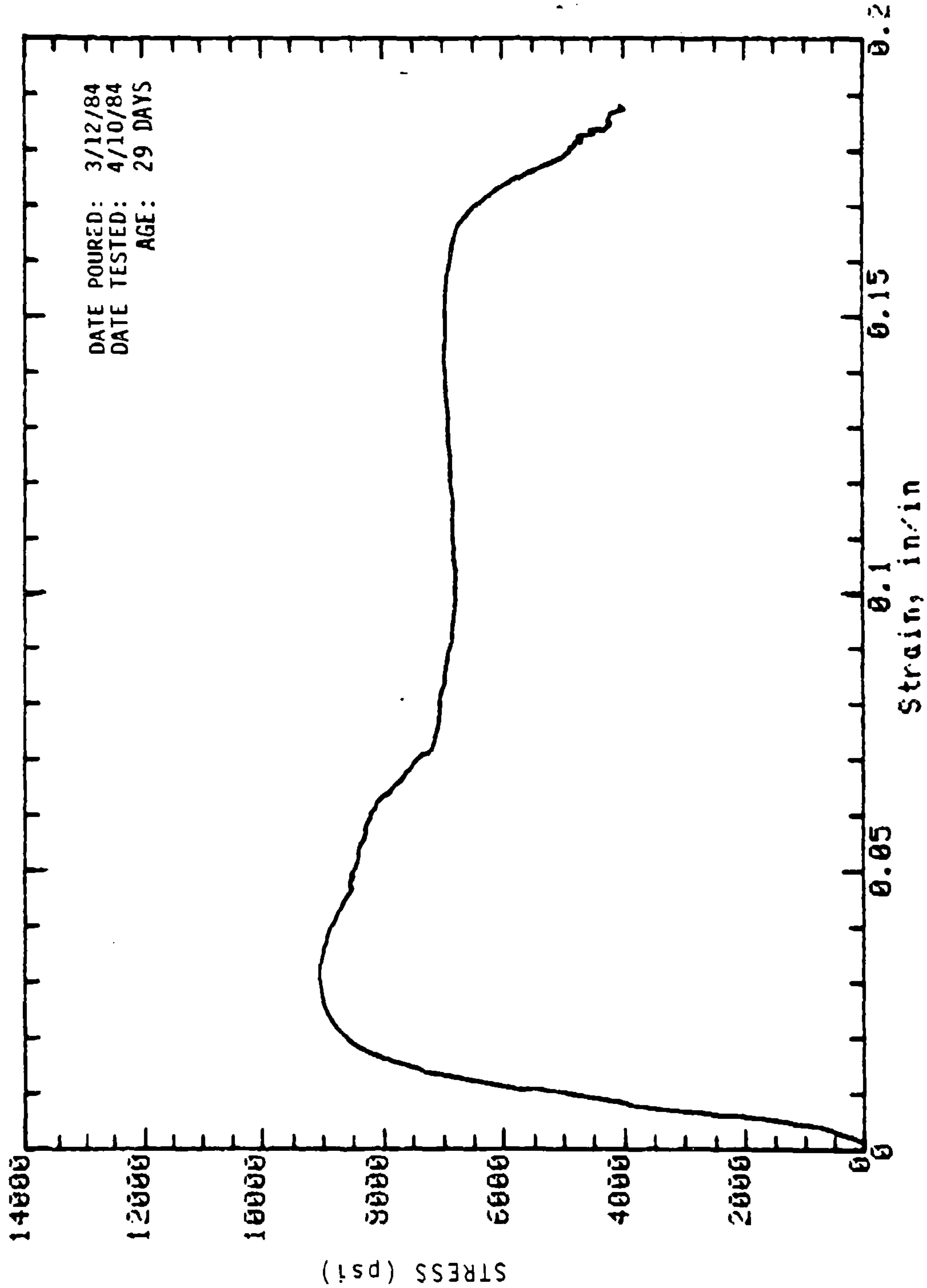

Mark: 9-11 Molded: 4in dia x 8in Cure: Dry
Concrete Sample

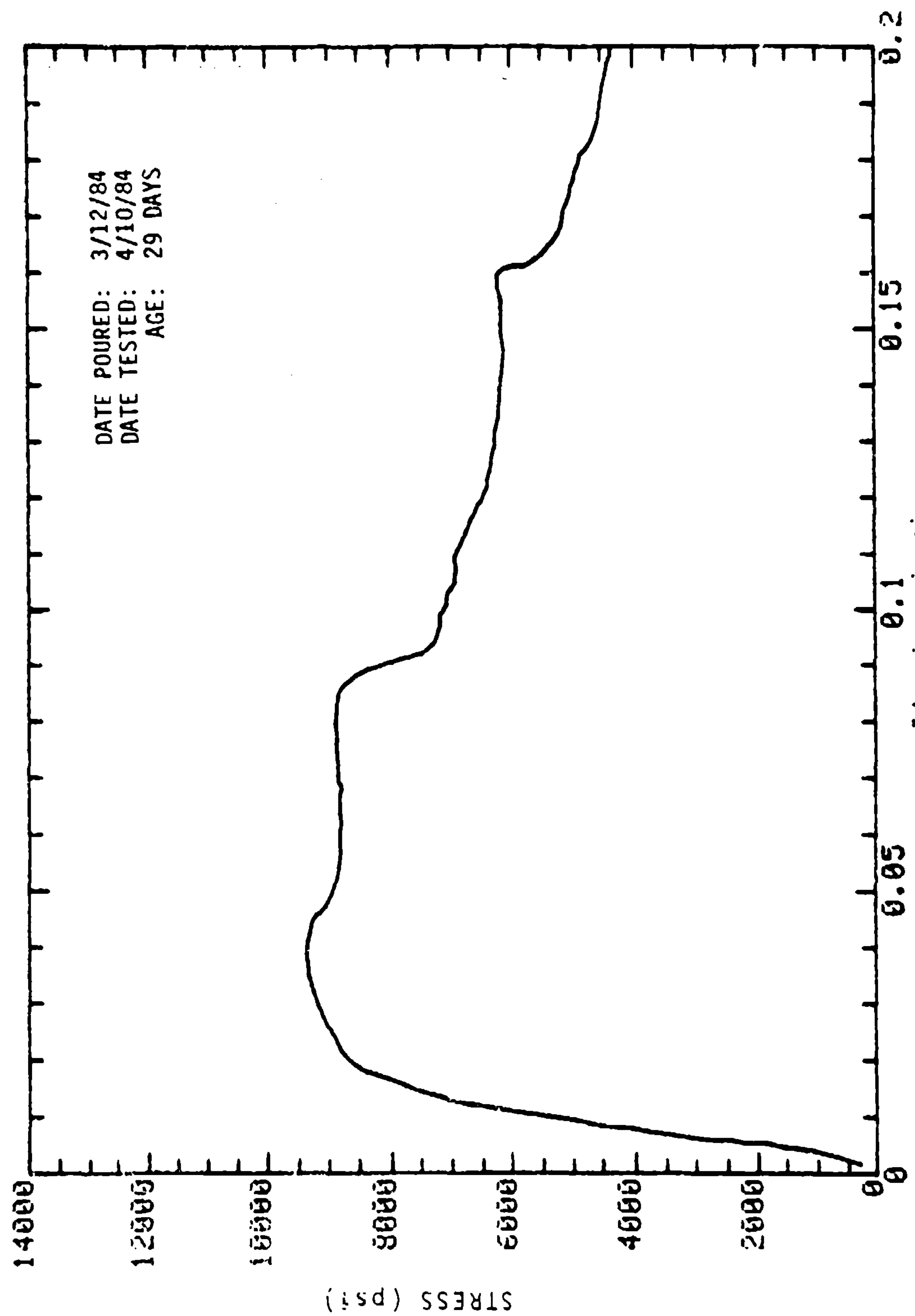

Mark: 9-14 Molded: 4in dia x 8in Cure: Dry
Concrete Sample

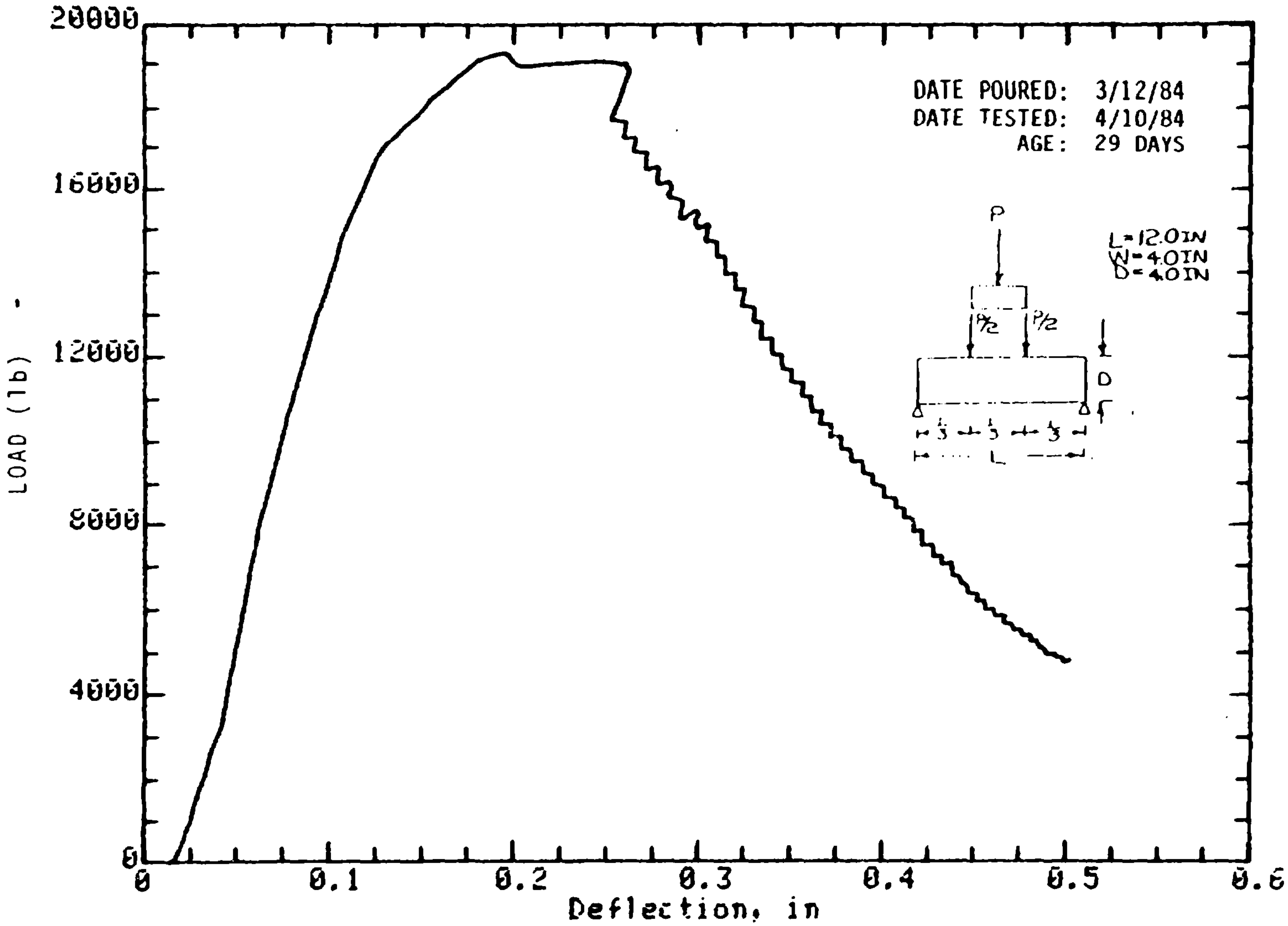

Mark: 9-19 Beam: 4in x 4in Cure: Wet
Concrete Sample

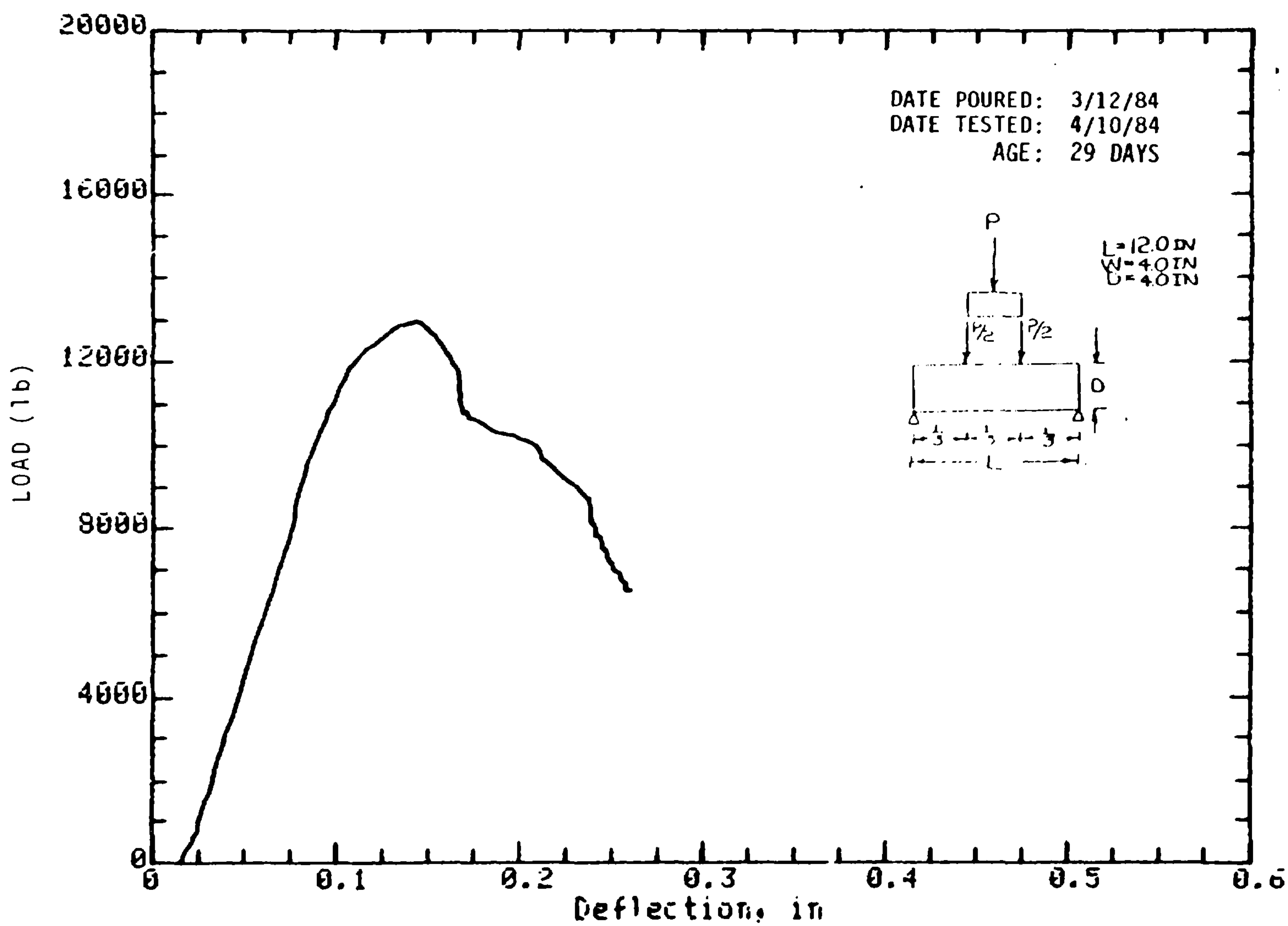

Mark: 9-25 Beam: 4in x 4in Cure: Wet
Concrete Sample

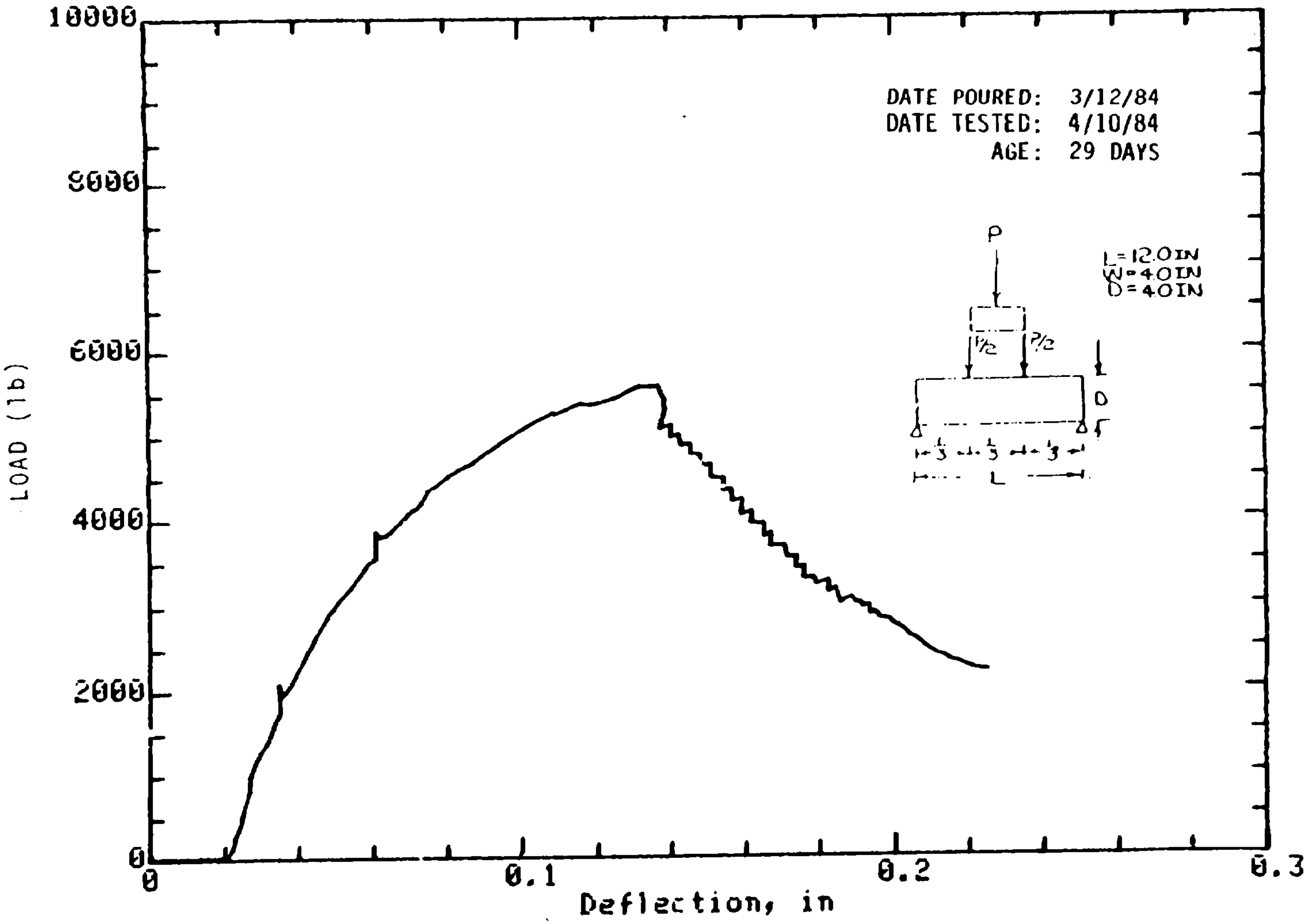

Mark: 9-32 Column: 4in x 4in Cure: Dry
Concrete Sample

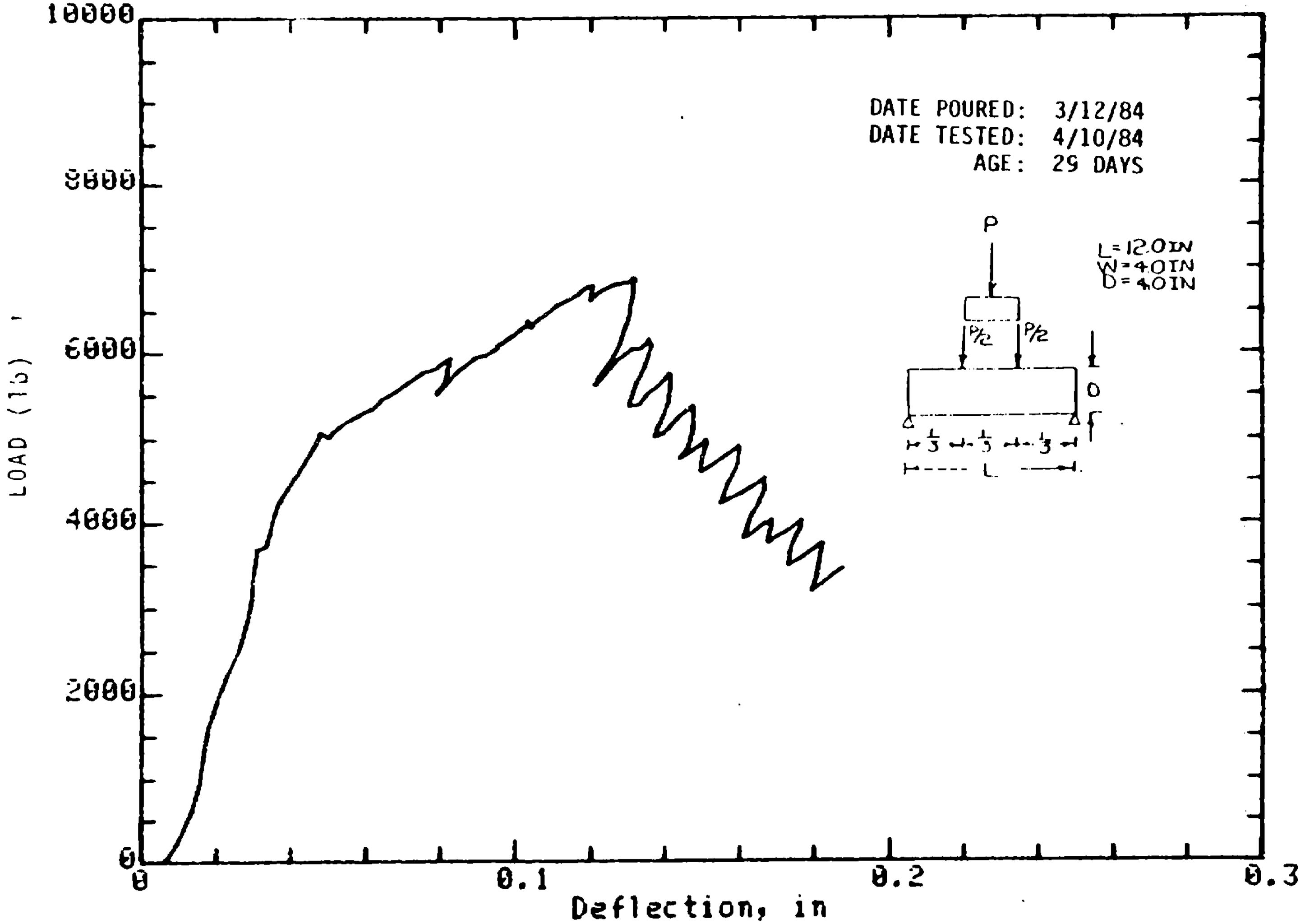

Mark: 9-34 Column: 4in x 4in Cure: Wet
Concrete Sample

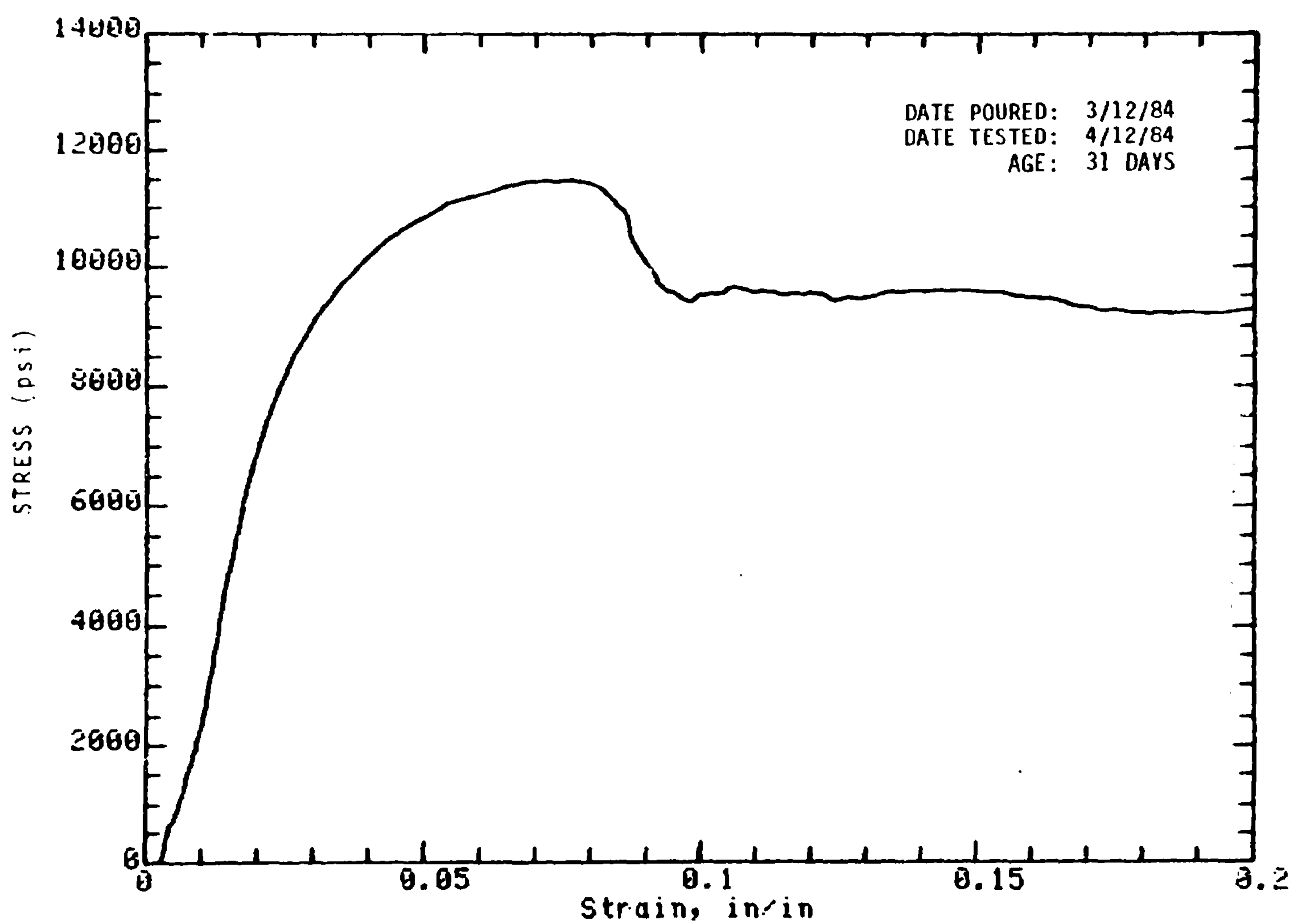

Mark: 9-S1-1 Cored (slab): 2in dia x 4in Cure: Wet
Concrete Sample

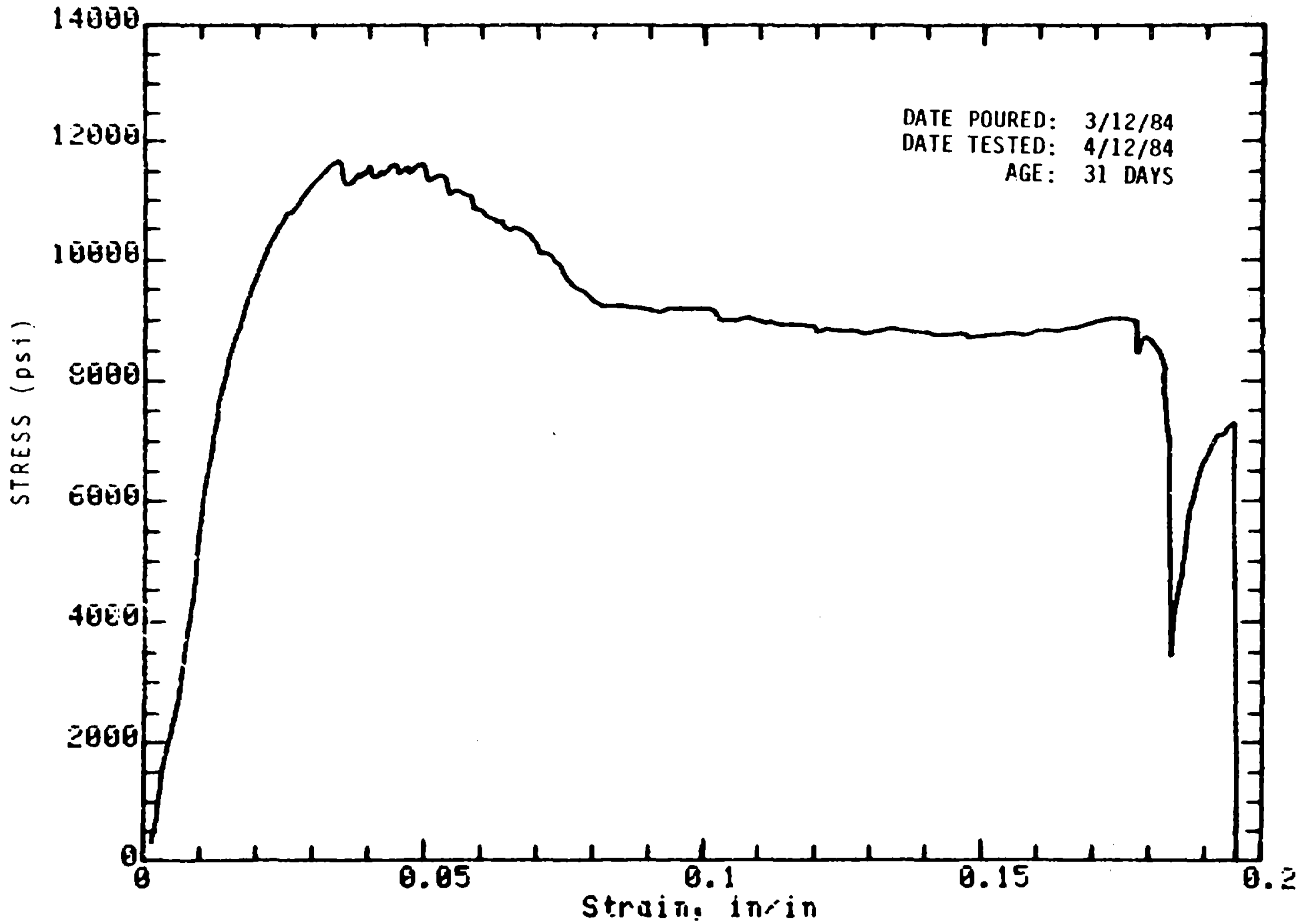

Mark: 9-S1-2 Cored (slab): 2in dia x 4in Cure: Wet
Concrete Sample

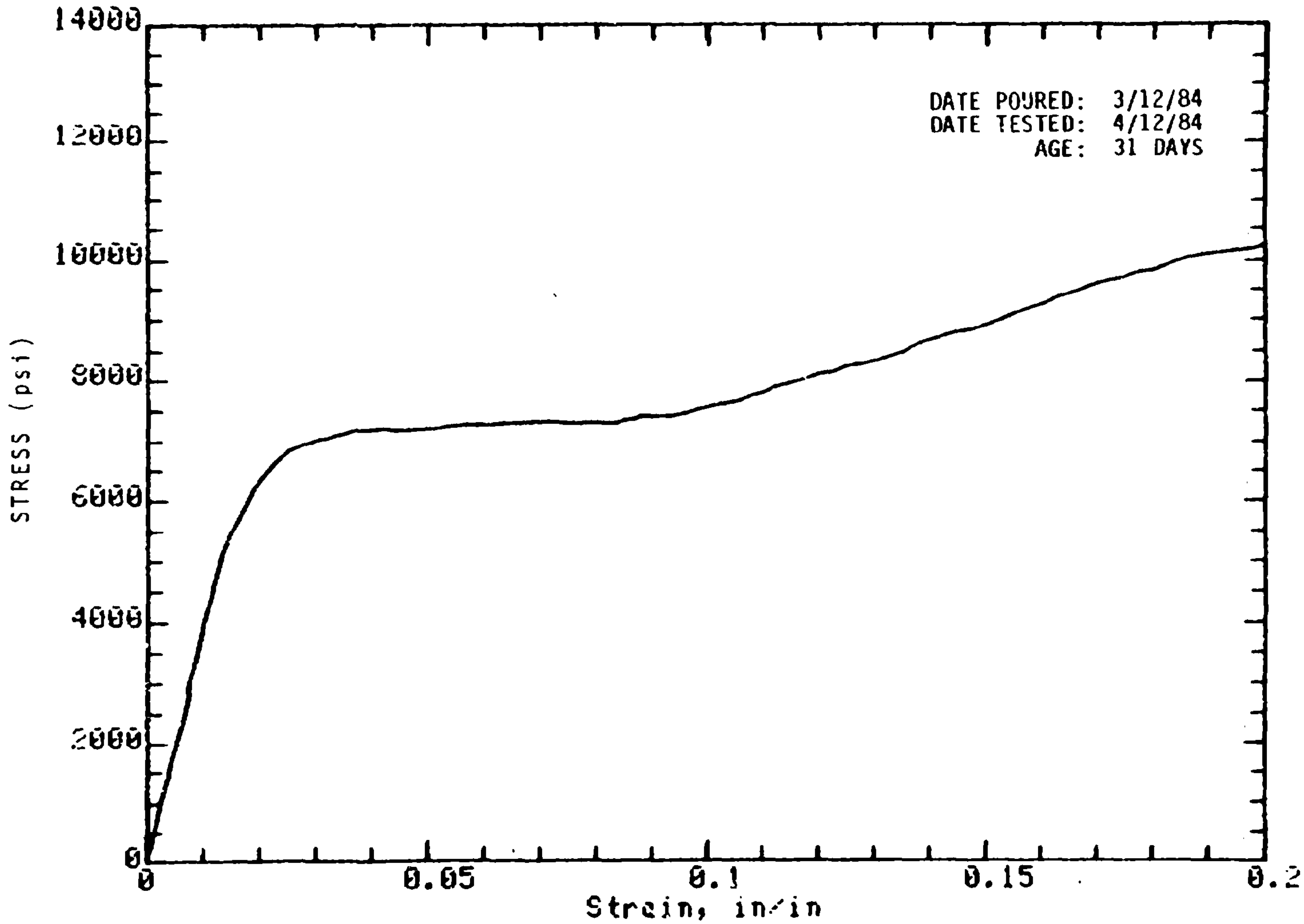

Mark: 9-S1-3 Cored (slab): 2in dia × 4in Cure: Wet
Concrete Sample

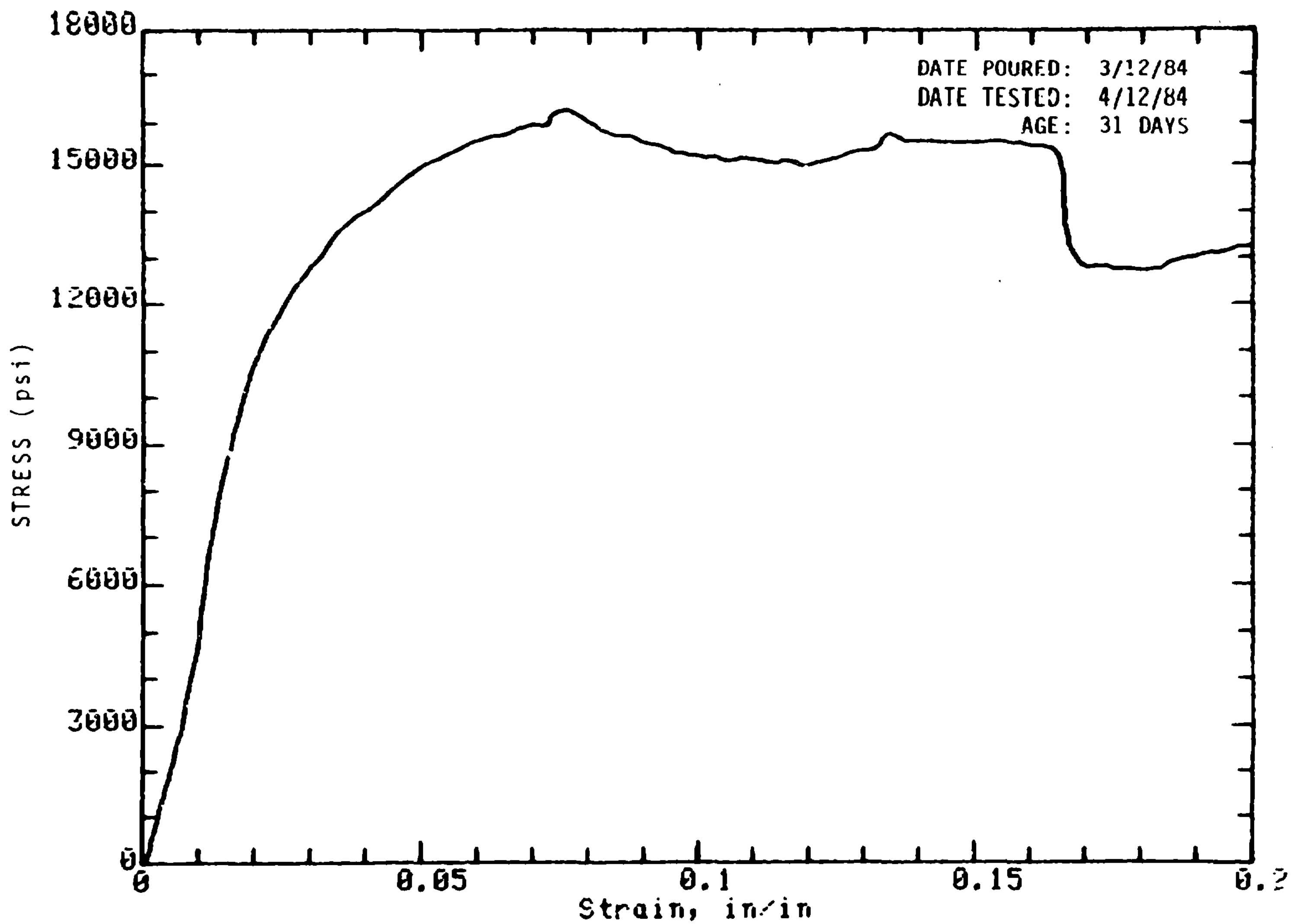

Mark: 9-S2-10 Cored (wall): 2in dia x 4in Cure: Dry
Concrete Sample

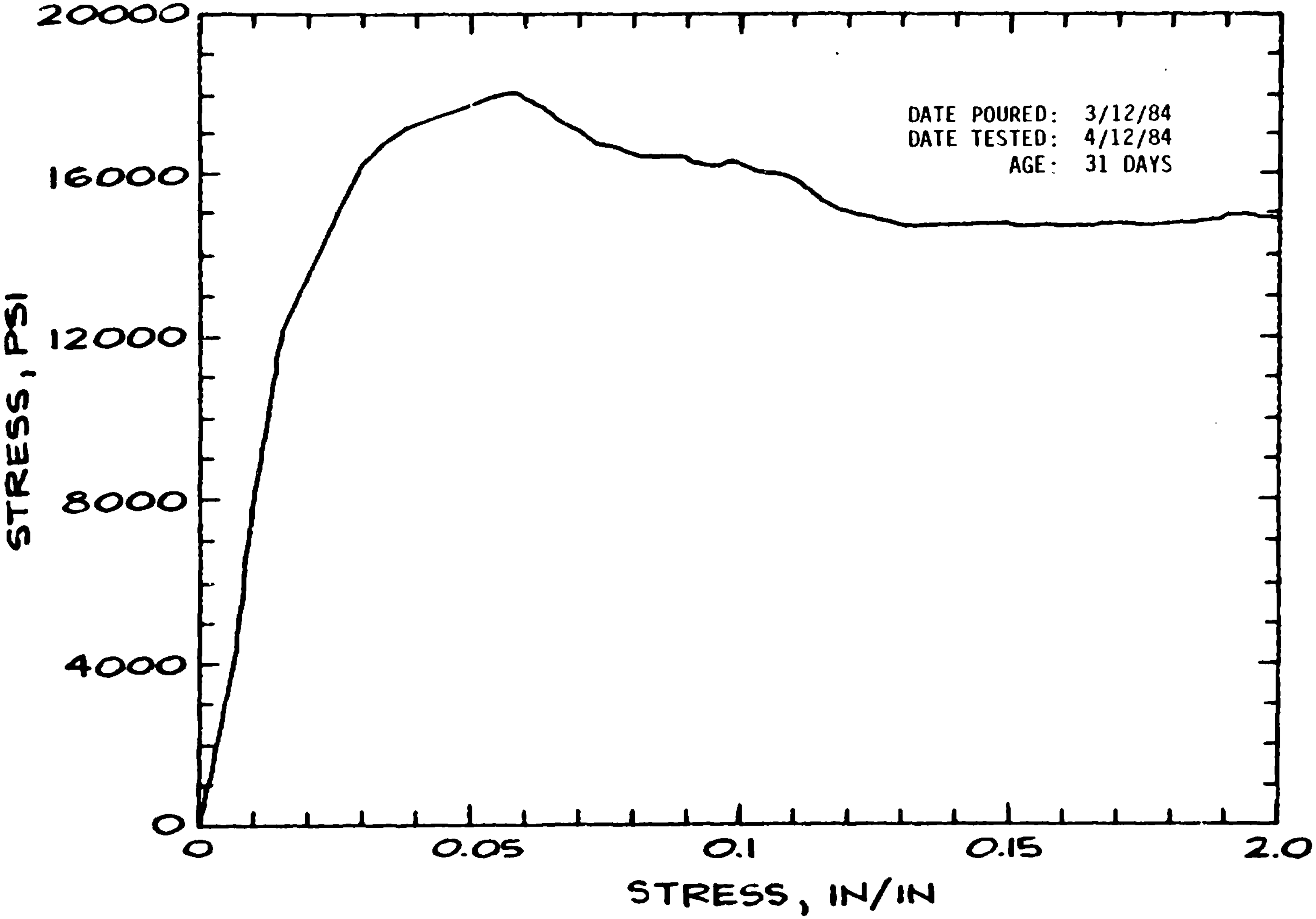

MARK: 9-52-11 CORED (WALL): 2 IN DIA. x 4 IN CURE: DRY CONCRETE SAMPLE

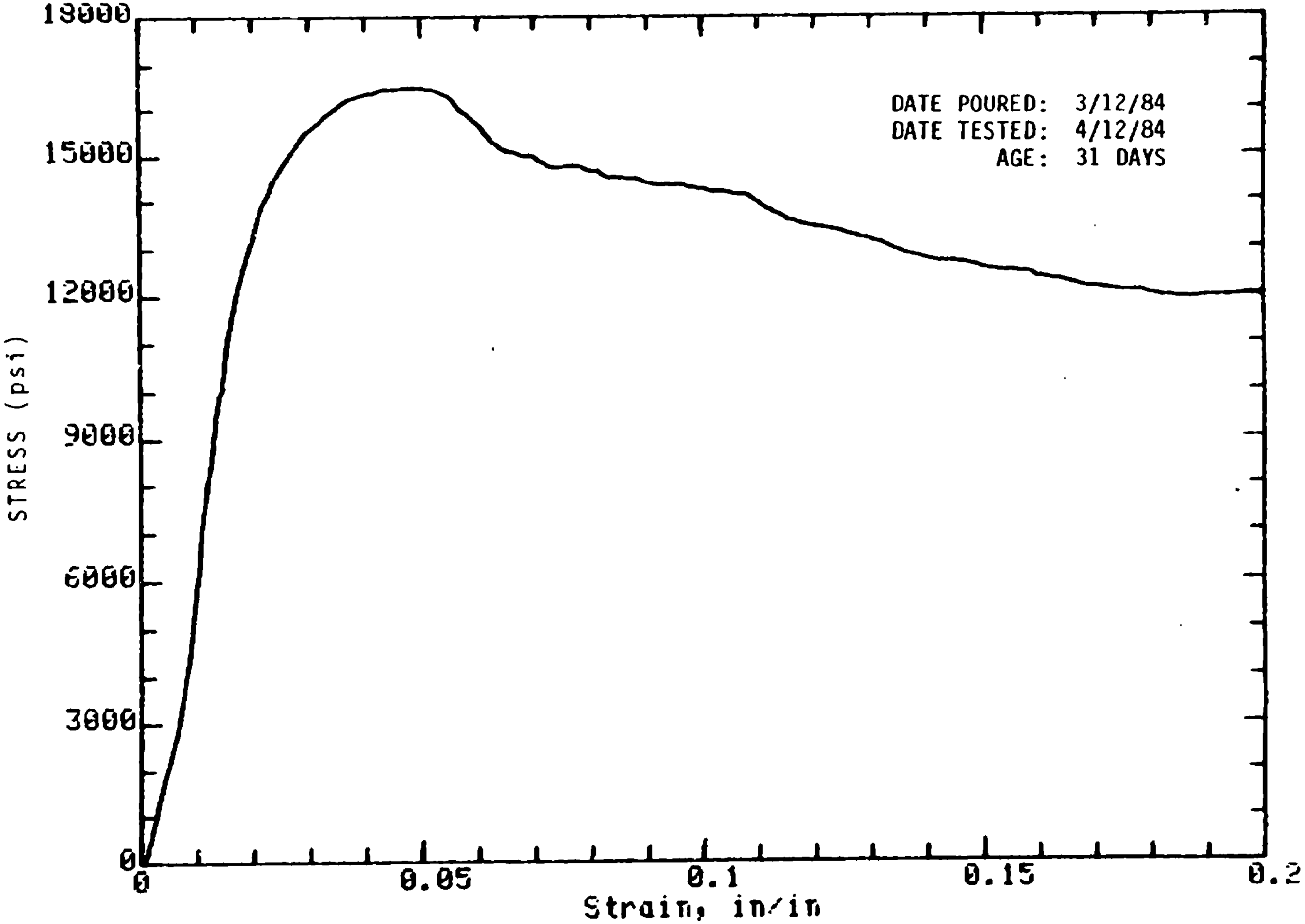

Mark: 9-S2-12 Cored (wall): 2in dia x 4in Cure: Dry
Concrete Sample

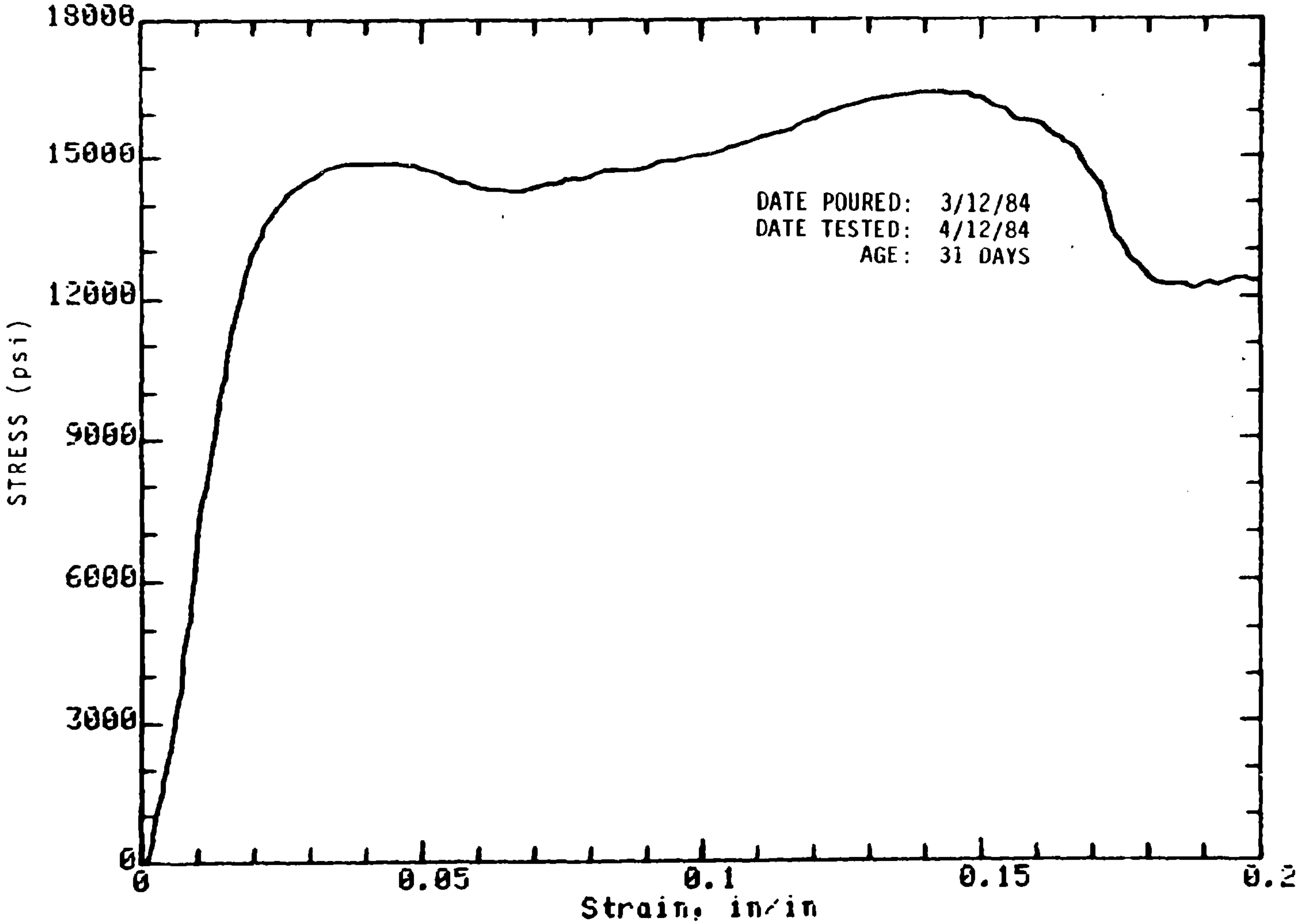

Mark: 9-S2-13 Cored (wall): 2in dia x 4in Cure: Dry
Concrete Sample

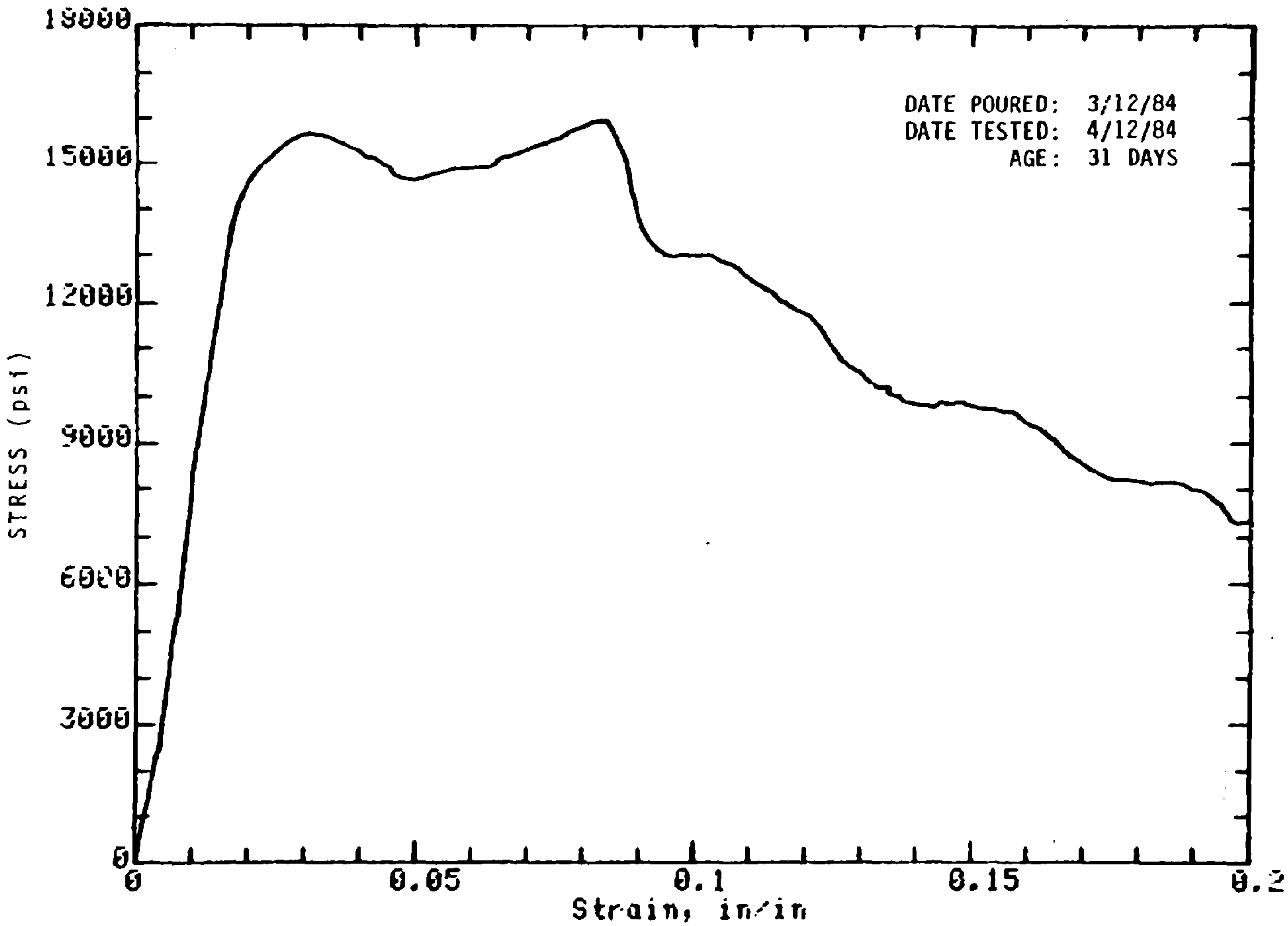

Mark: 9-S2-14 Cored (wall): 2in dia × 4in Cure: Dry
Concrete Sample

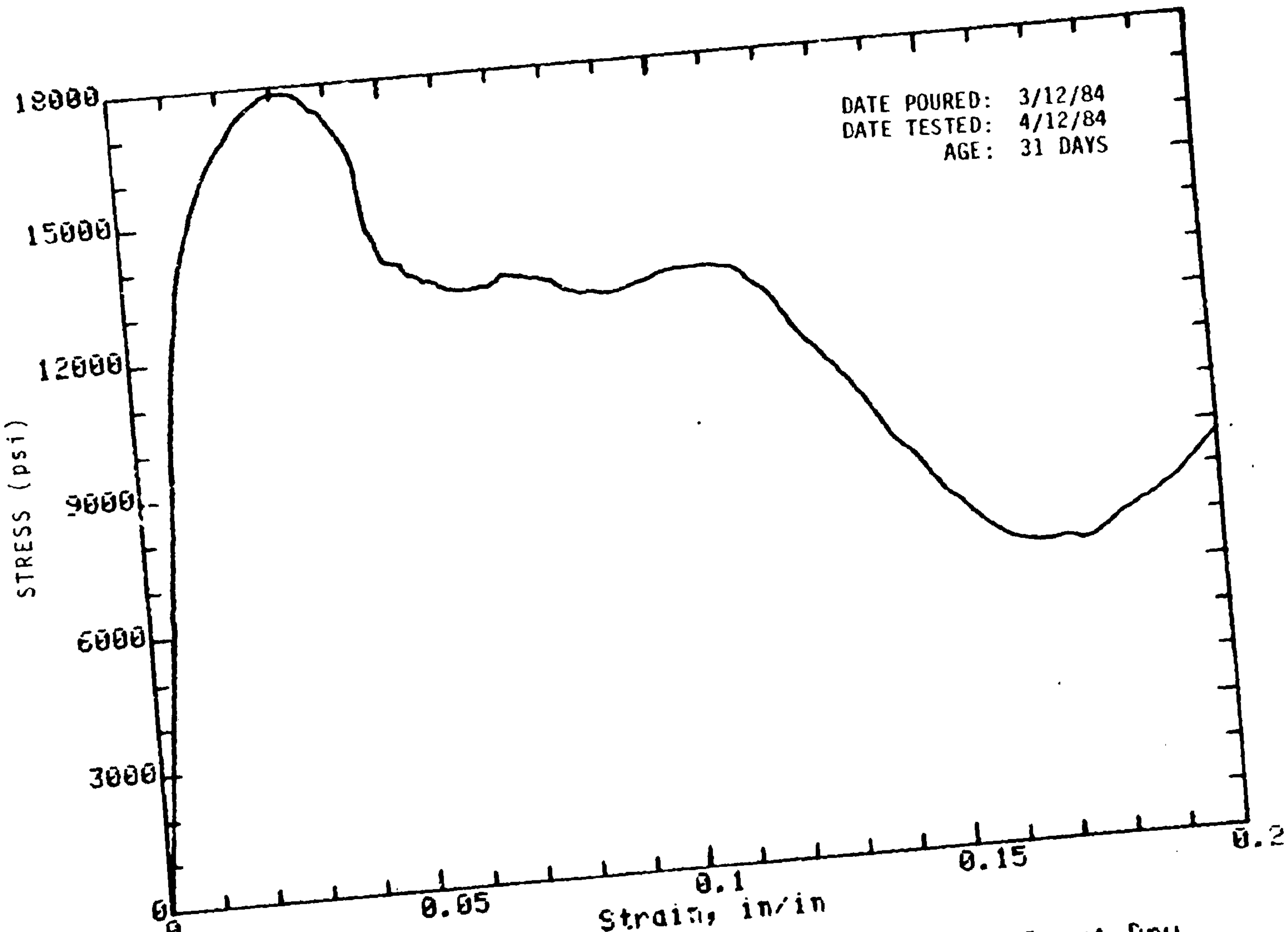

Mark: 9-S2-15 Cored (wall): 2in dia × 4in Cure: Dry
Concrete Sample

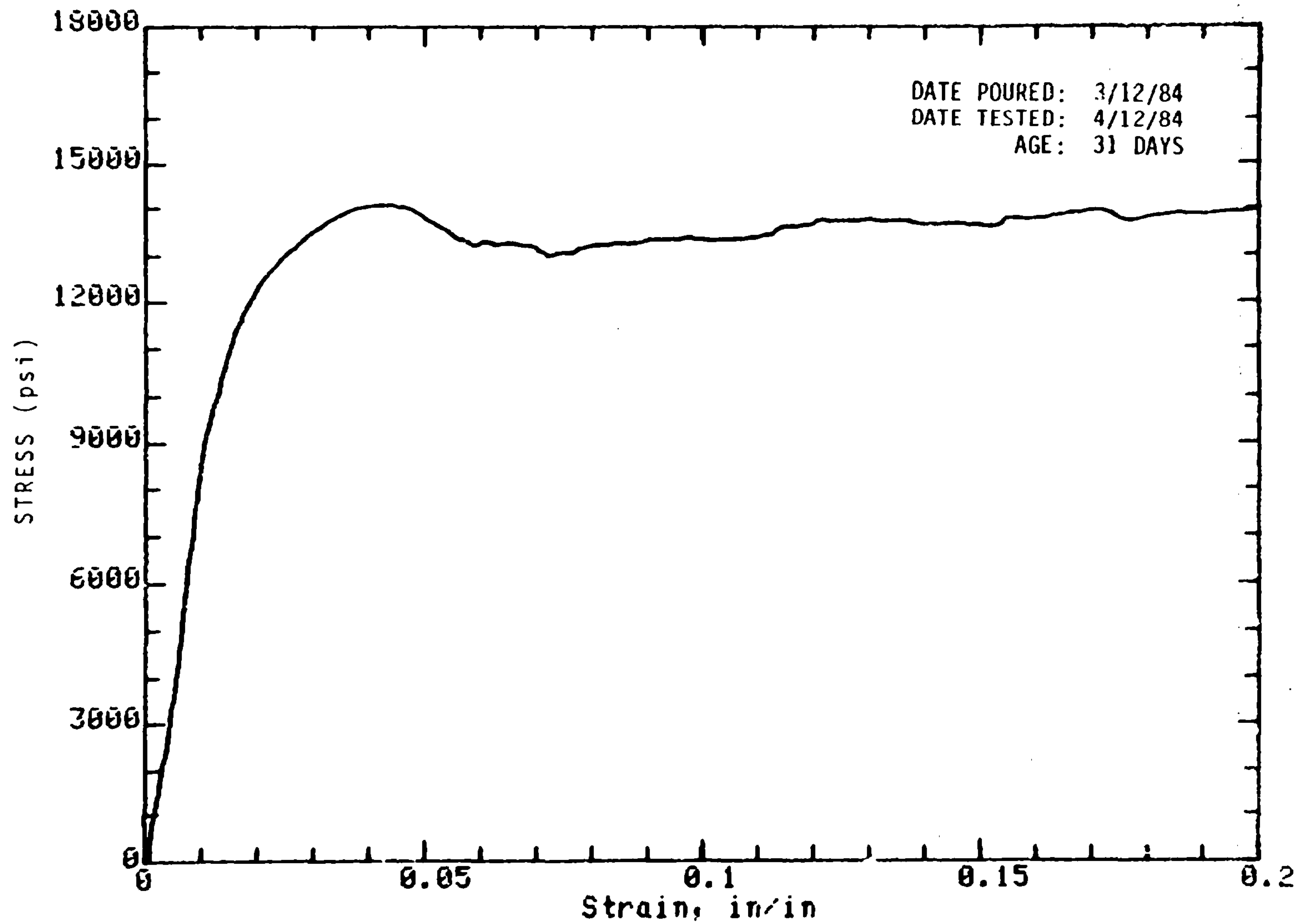

Mark: 9-92-16 Cored (wall): 2in dia x 4in Cure: Dry
Concrete Sample

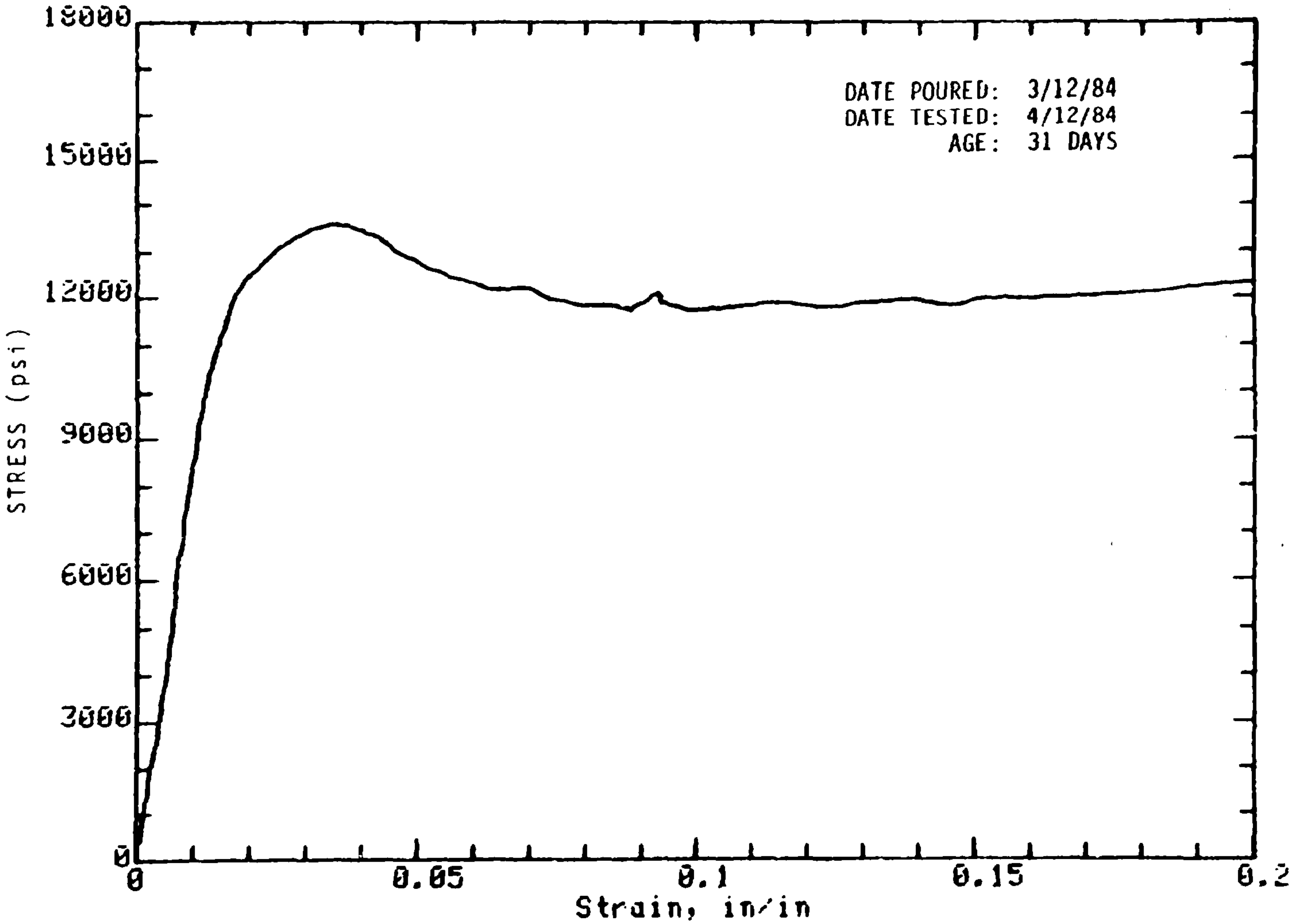

Mark: 9-S2-17 Cored (wall): 2in dia x 4in Cure: Dry
Concrete Sample

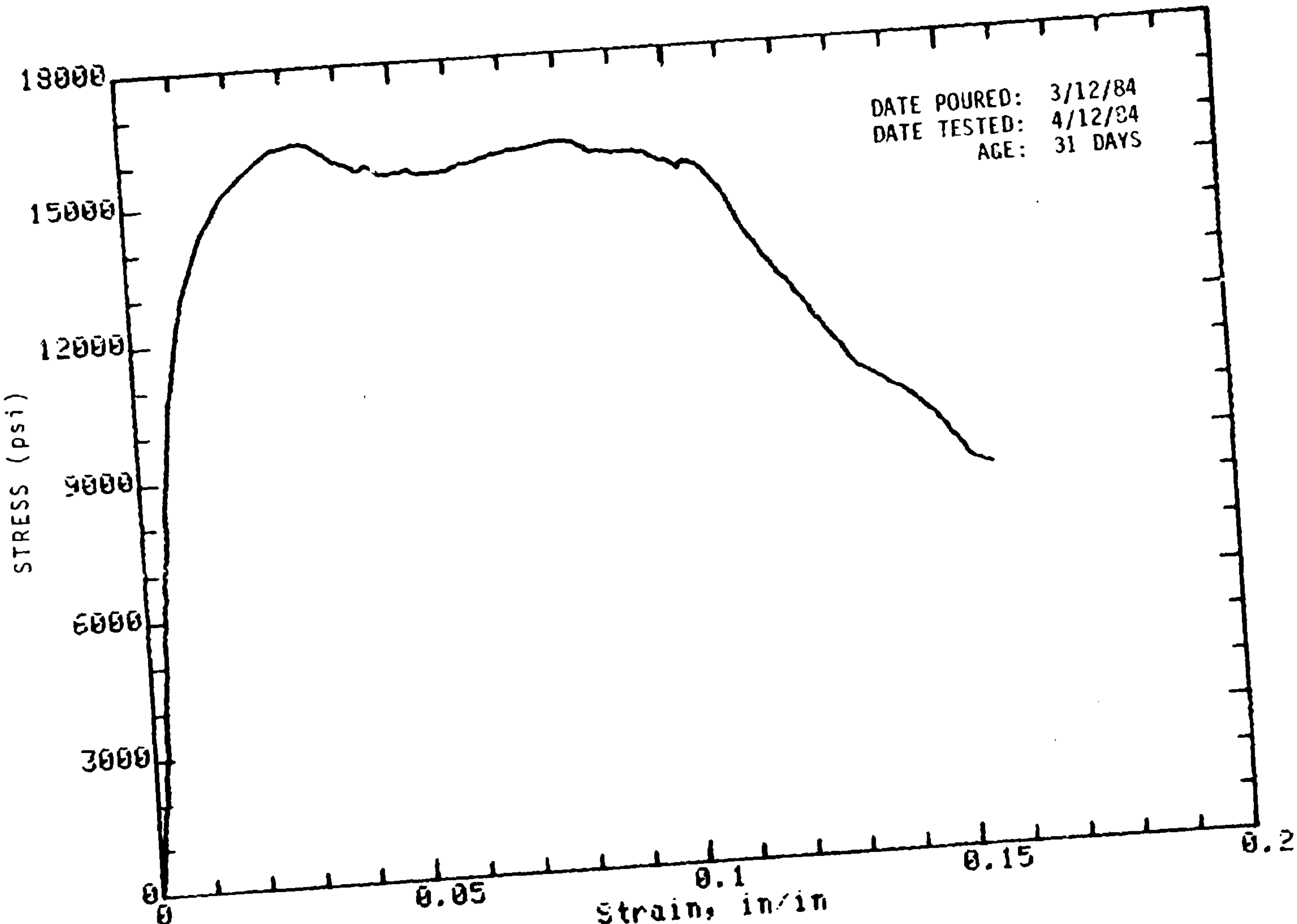

Mark: 9-S2-18 Cored (wall): 2in dia x 4in Cure: Dry
Concrete Sample

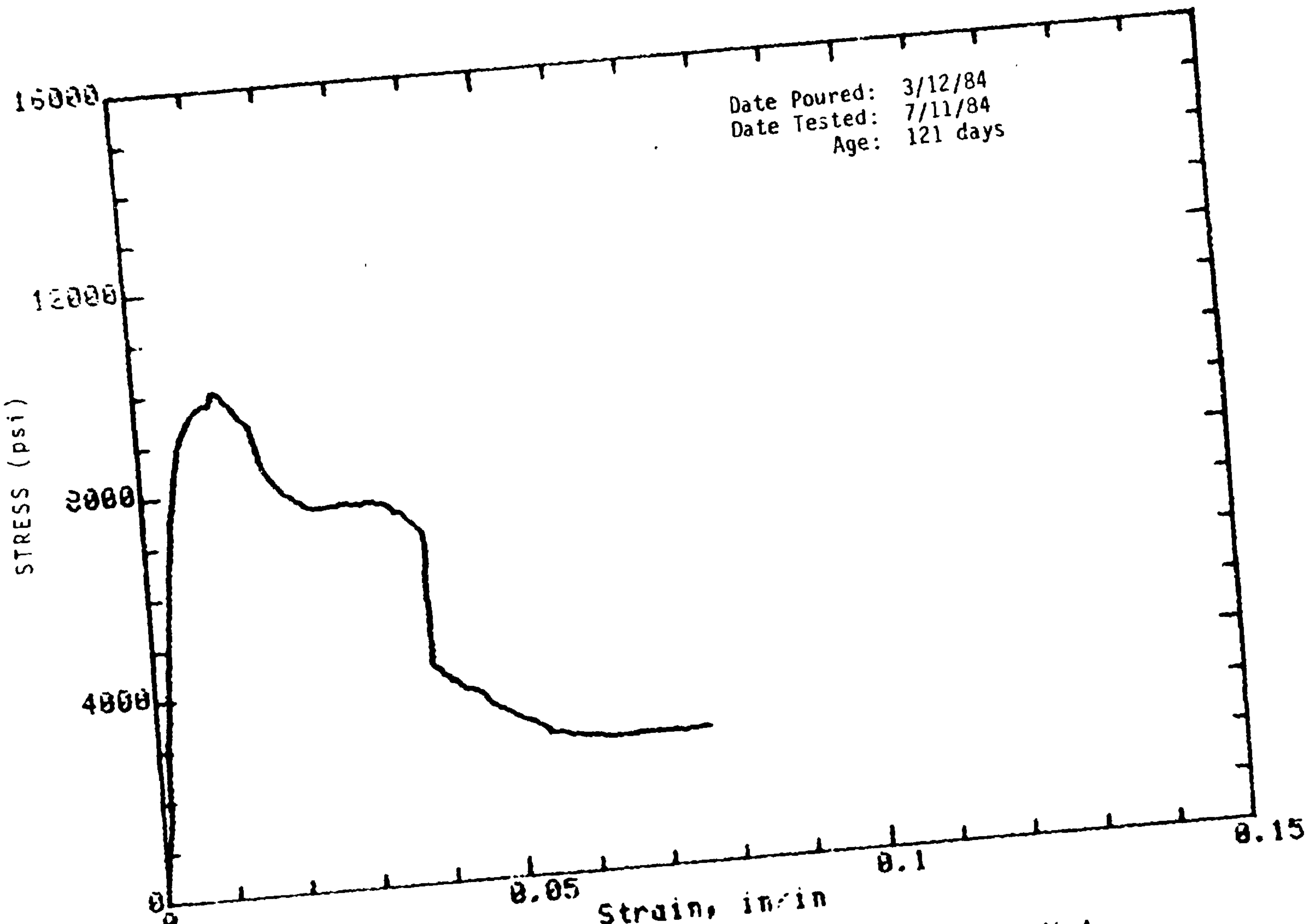

Mark: 9-4 Molded: 4in dia x 8in Cure: Wet
Concrete Sample

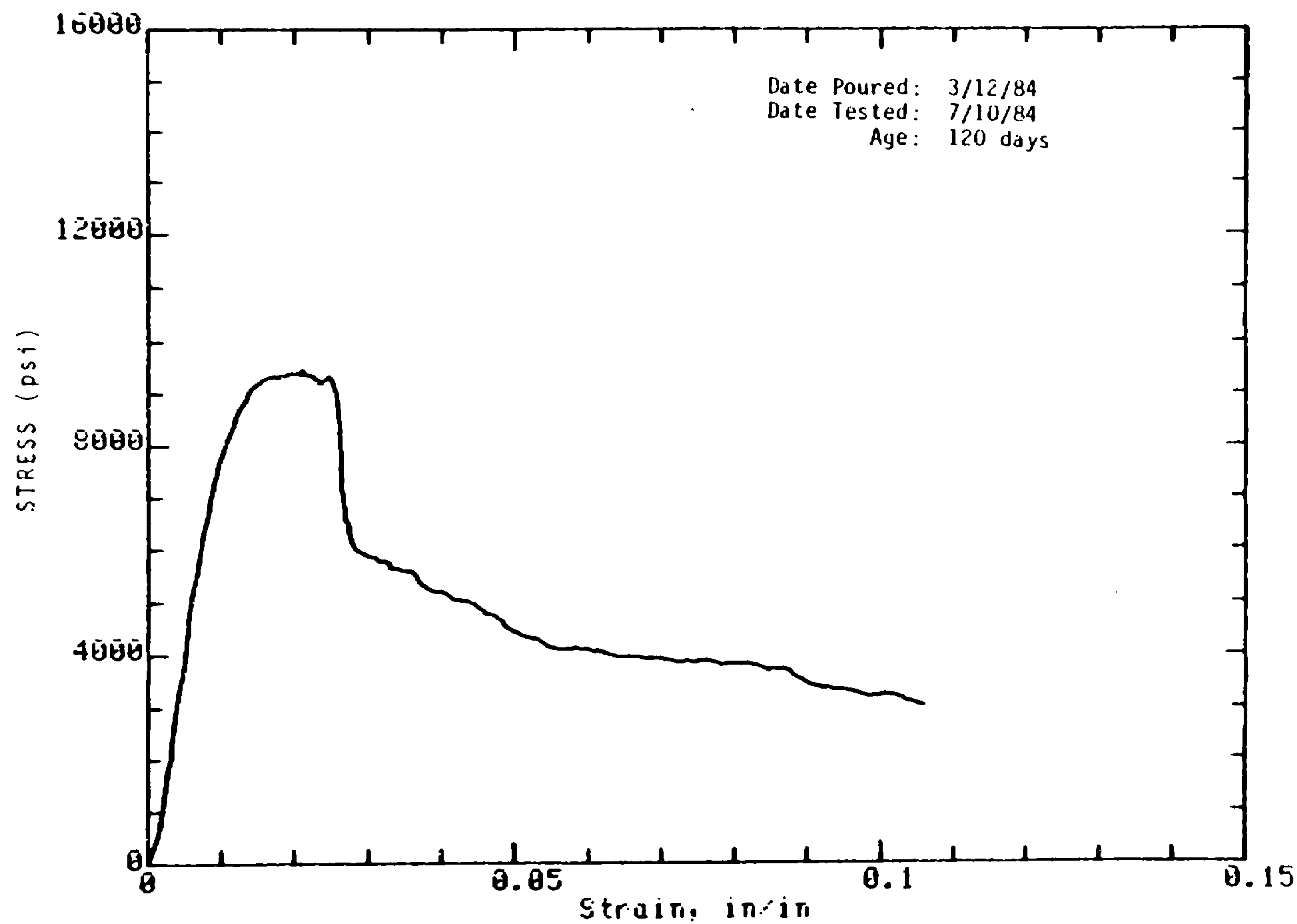

Mark: 9-7 Molded: 4in dia x 8in Cure: Wet
Concrete Sample

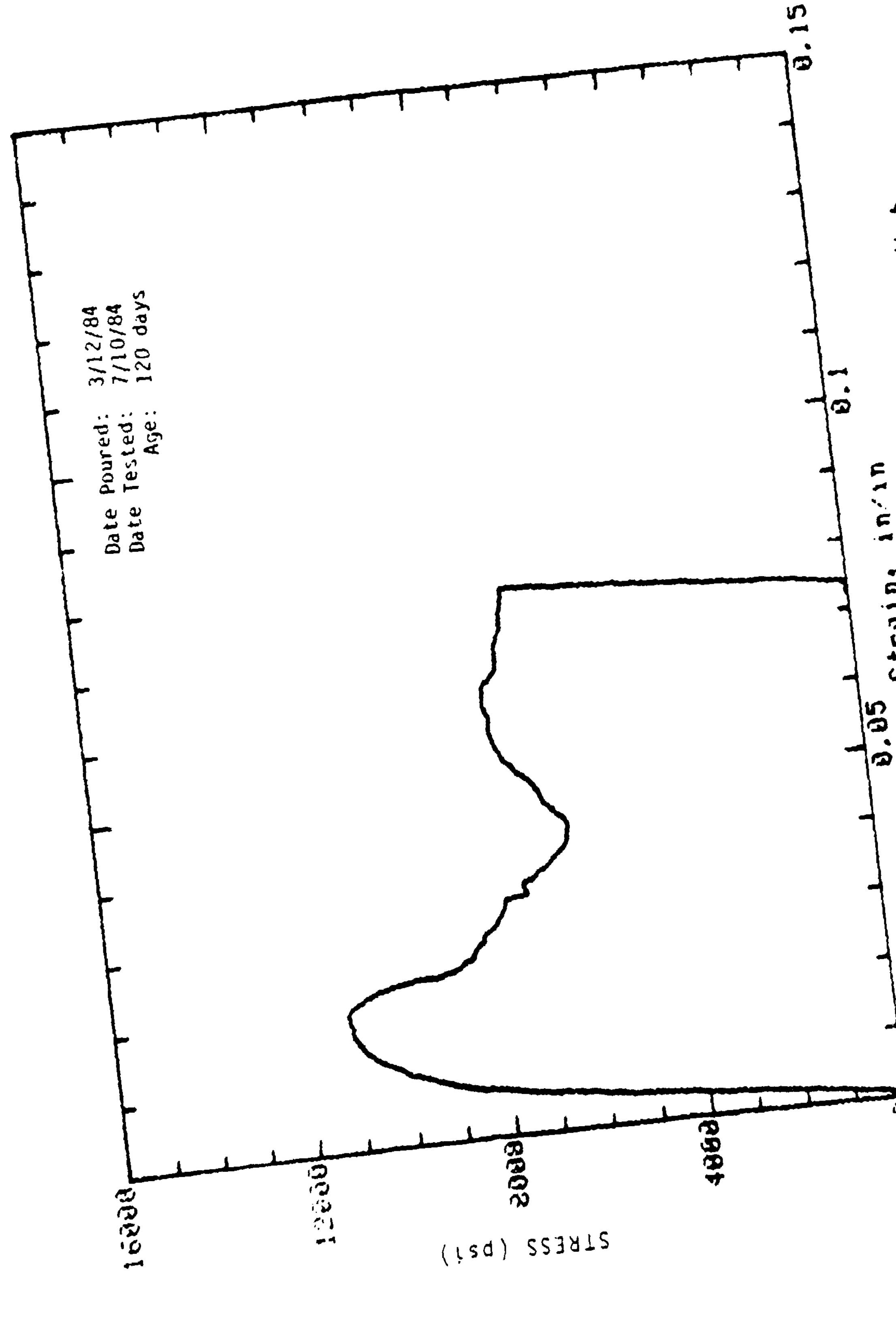

Mark: 9-8 Molded: 4in dia x 8in Cure: Wet
Concrete Sample

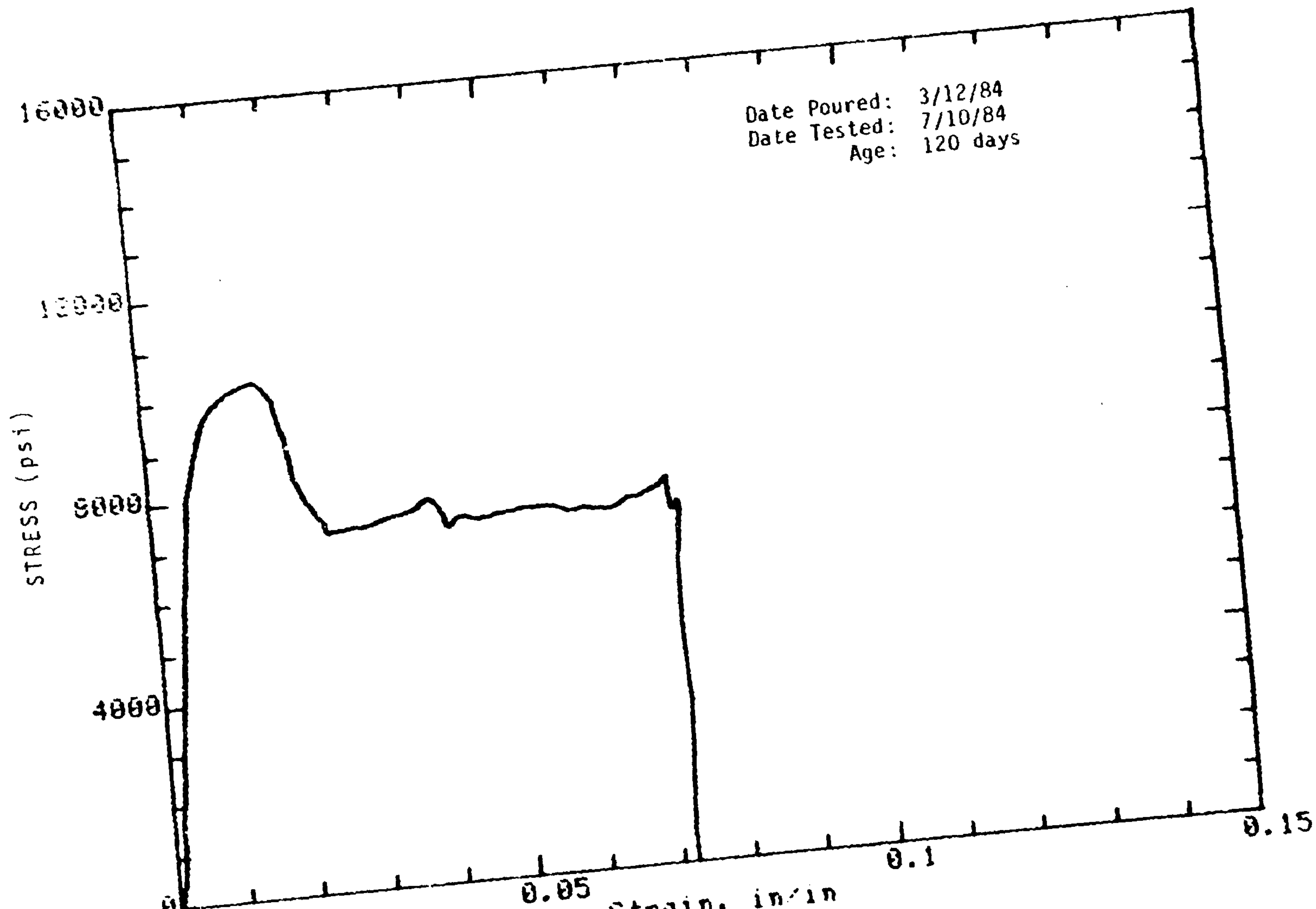

Mark: 9-9 Molded: 4in dia x 8in Cure: Wet
Concrete Sample

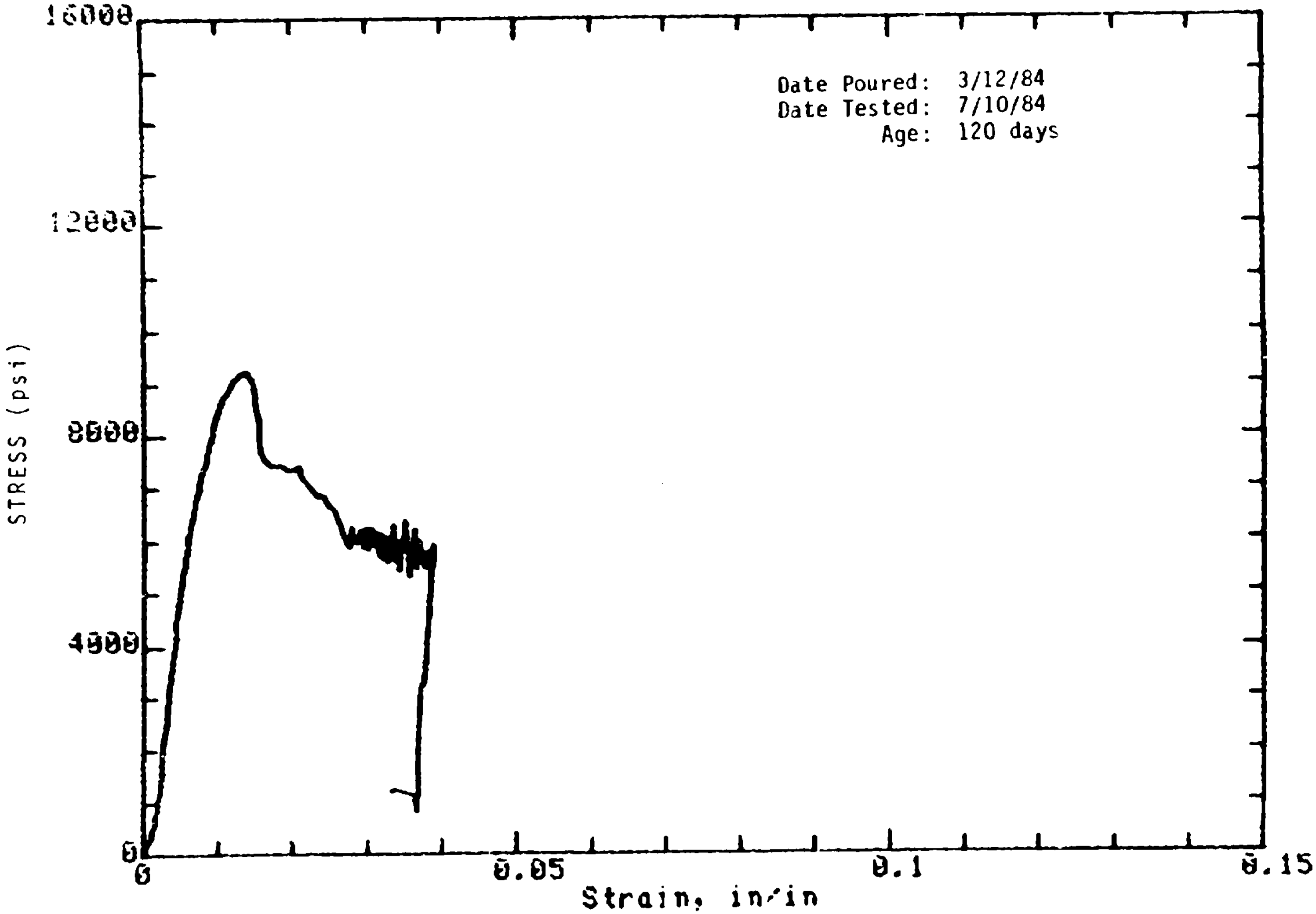

Mark: 9-10 Molded: 4in dia x 8in Cure: Wet
Concrete Sample

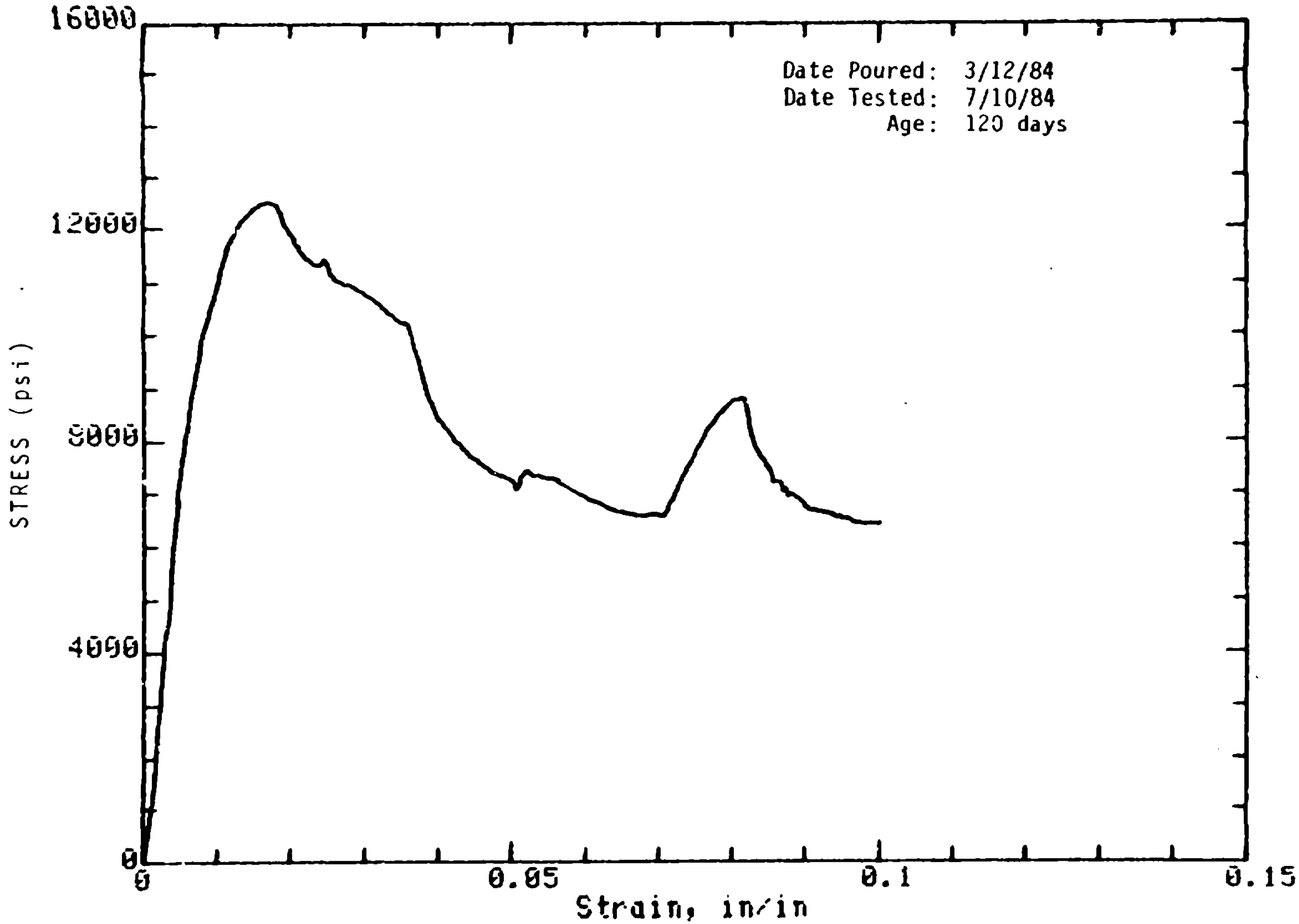

Mark: 9-35 Molded: 4in dia x 8in Cure: Wet
Concrete Sample

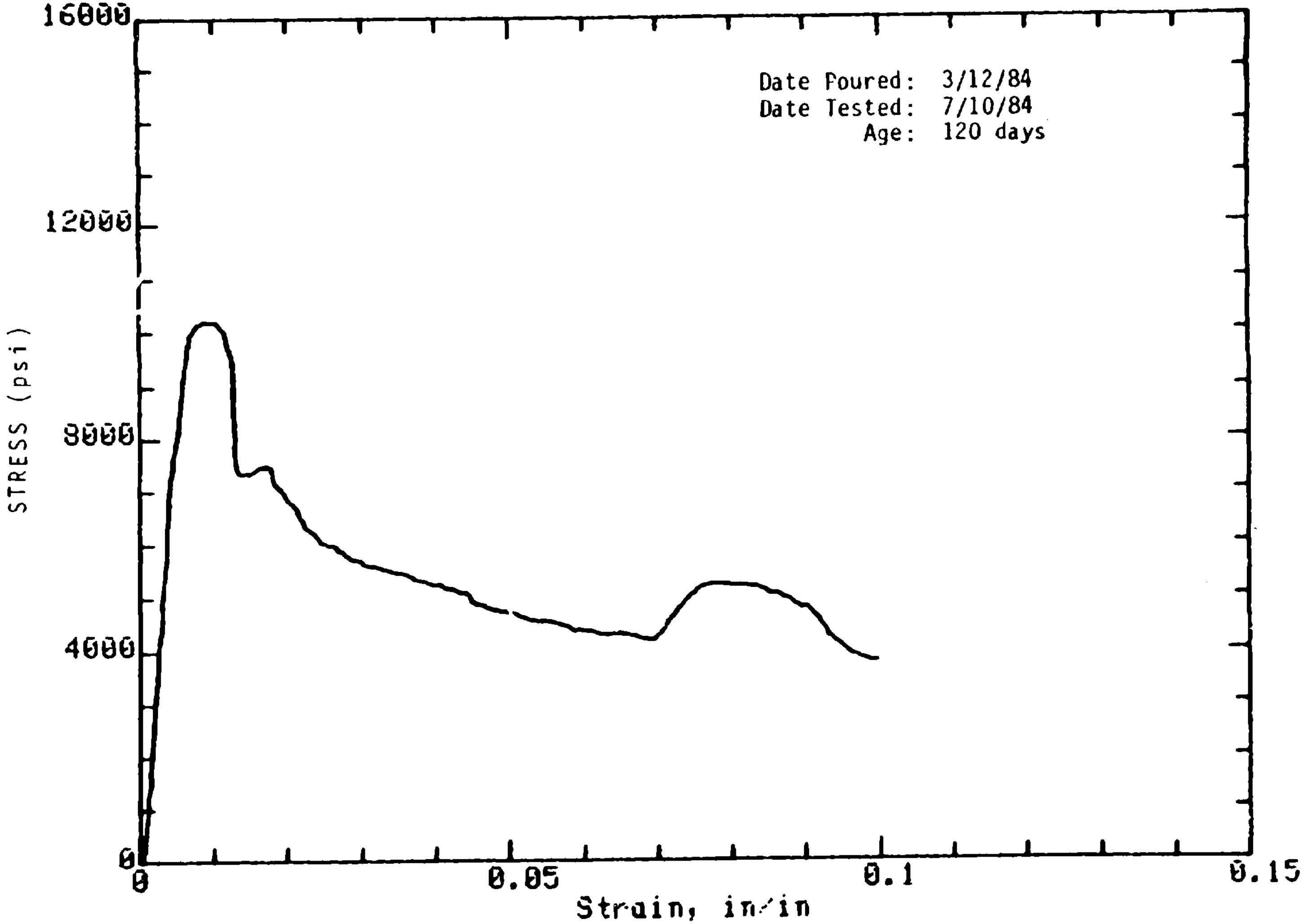

Mark: 9-16 Molded: 4in dia x 8in Cure: Wet
Concrete Sample

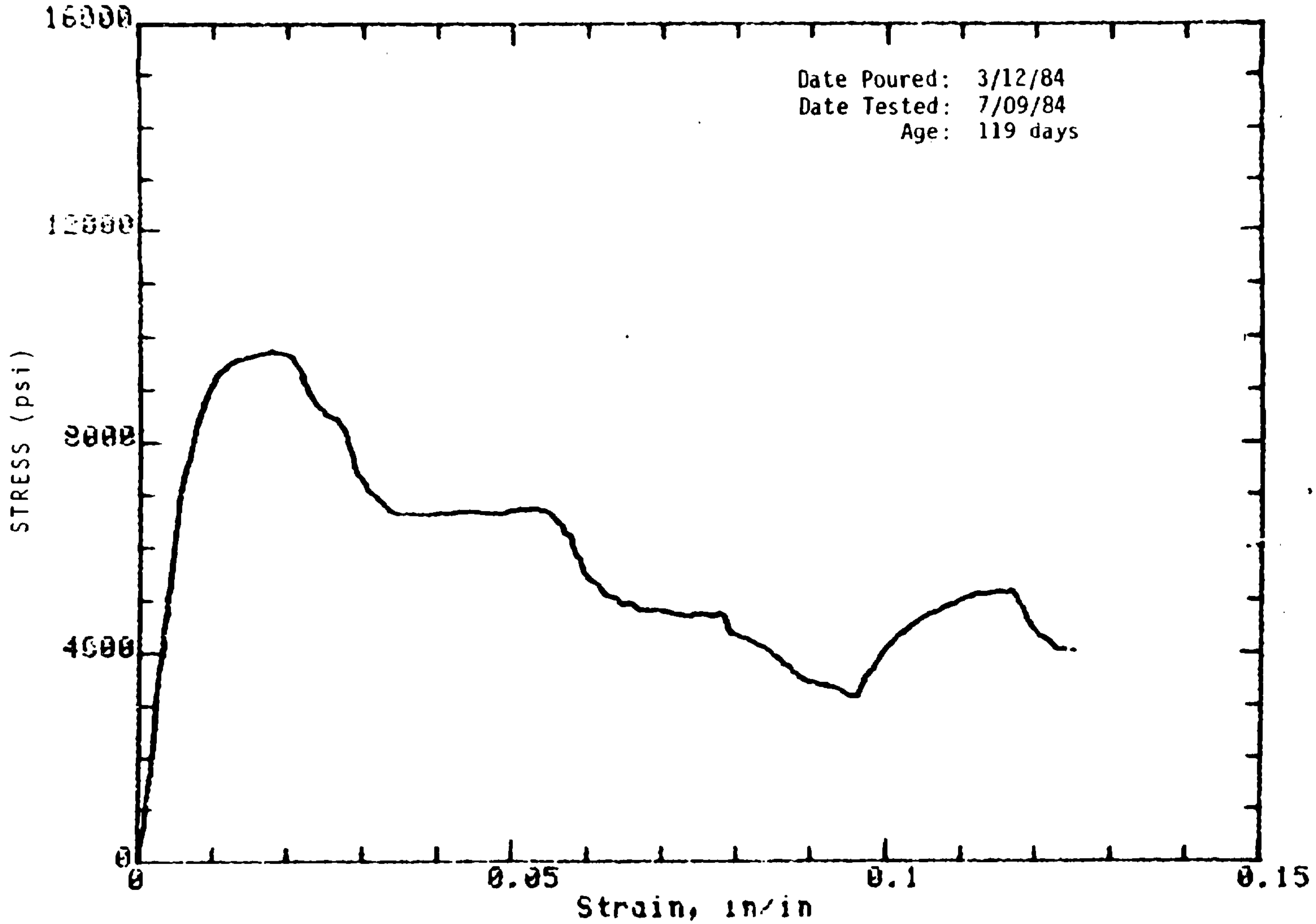

Mark: 9-17 Molded: 4in dia x 8in Cure: Dry
Concrete Sample

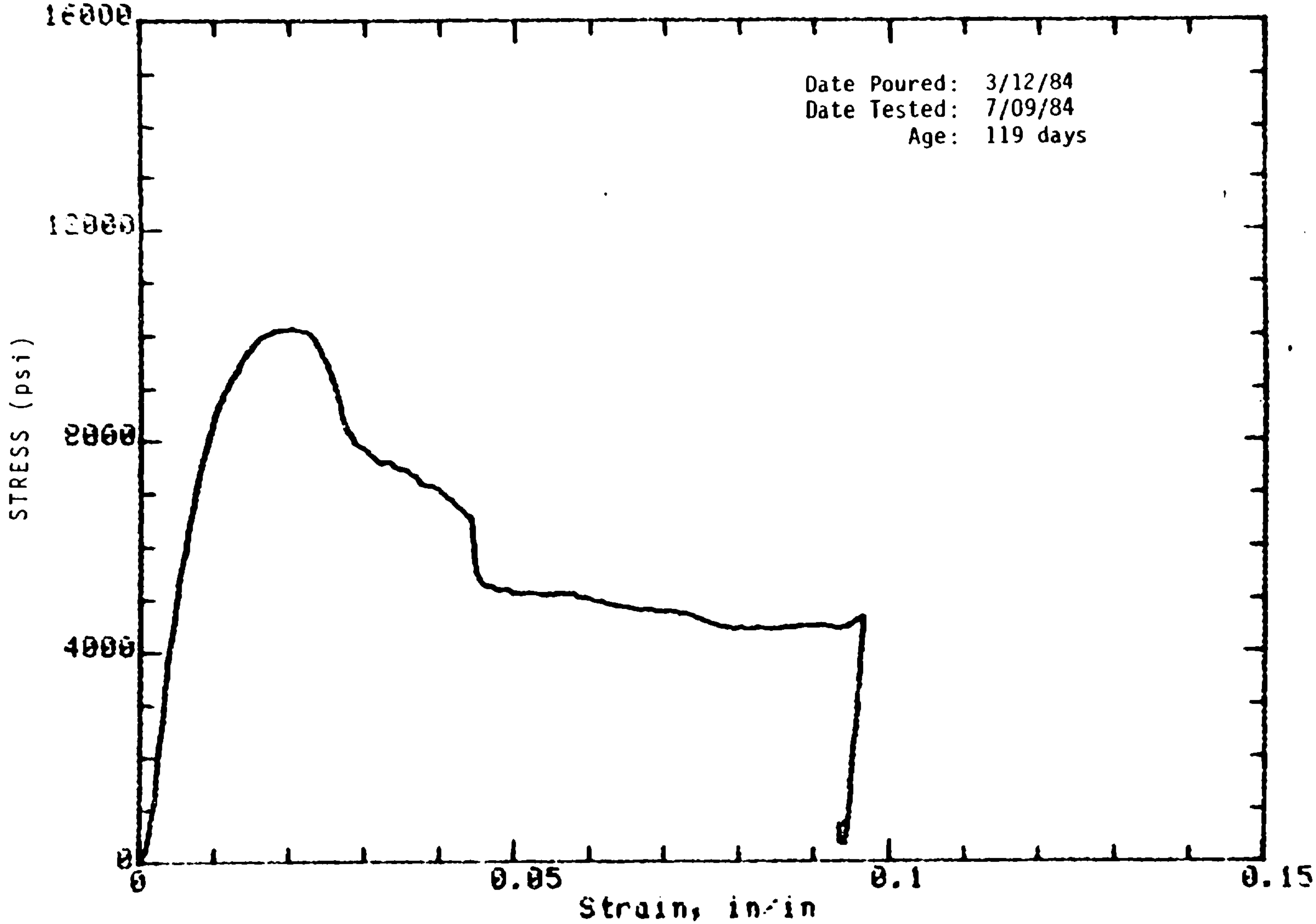

Mark: 9-18 Molded: 4in dia x 8in Cure: Dry
Concrete Sample

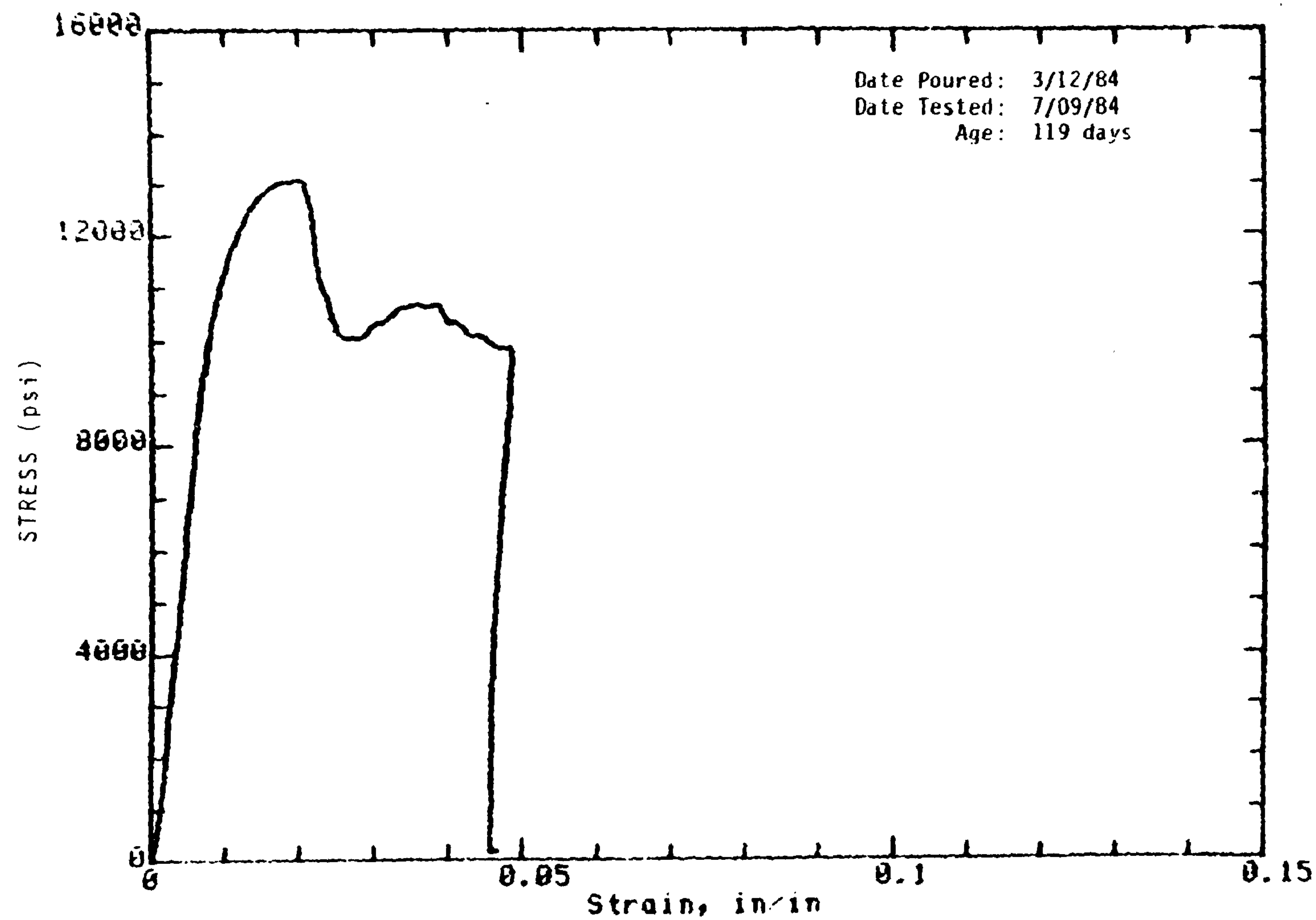

Mark: 9-39 Molded: 4in dia x 8in Cure: Dry
Concrete Sample

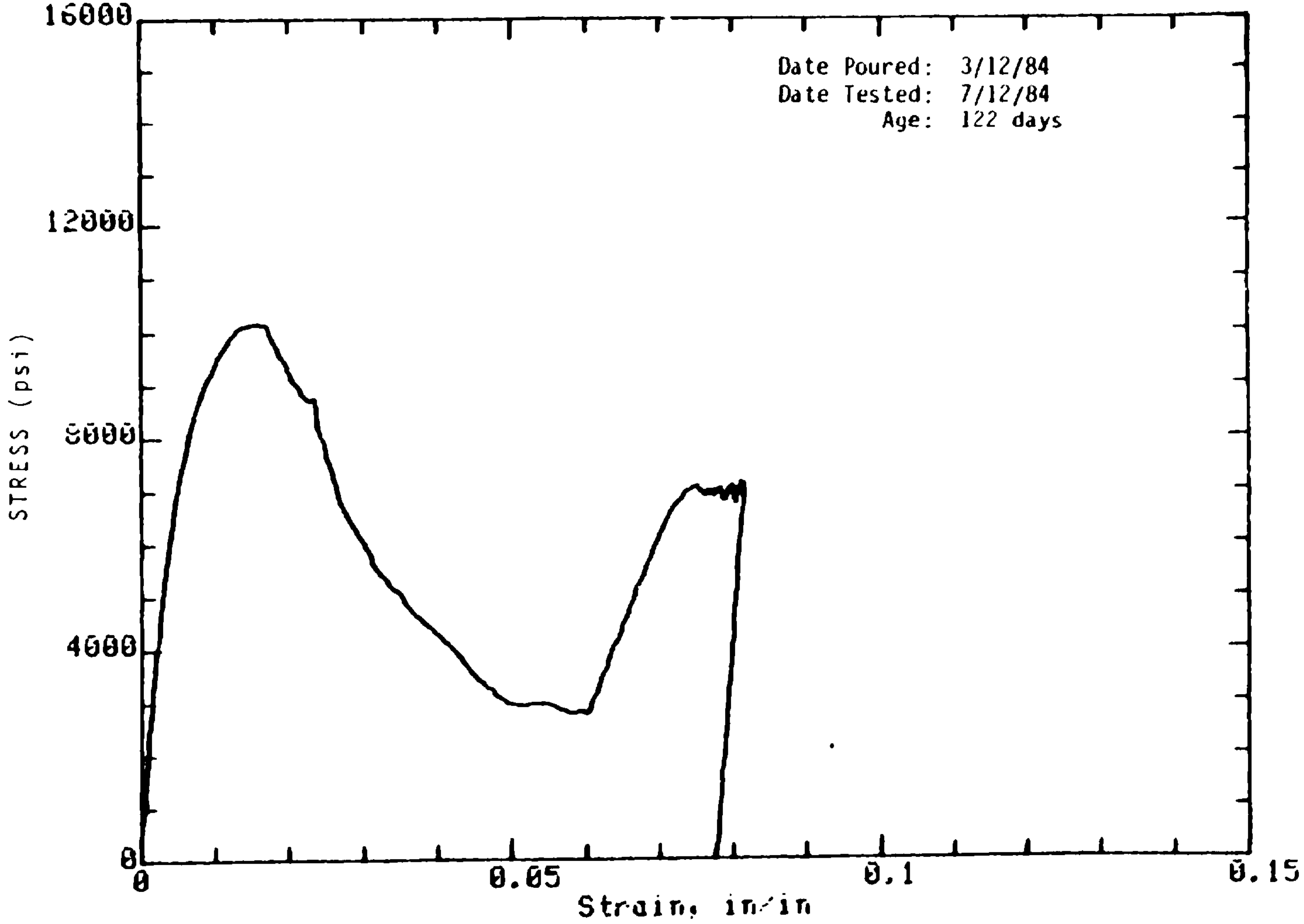

Mark: 9-40 Molded: 4in dia × 8in Cure: Dry
Concrete Sample

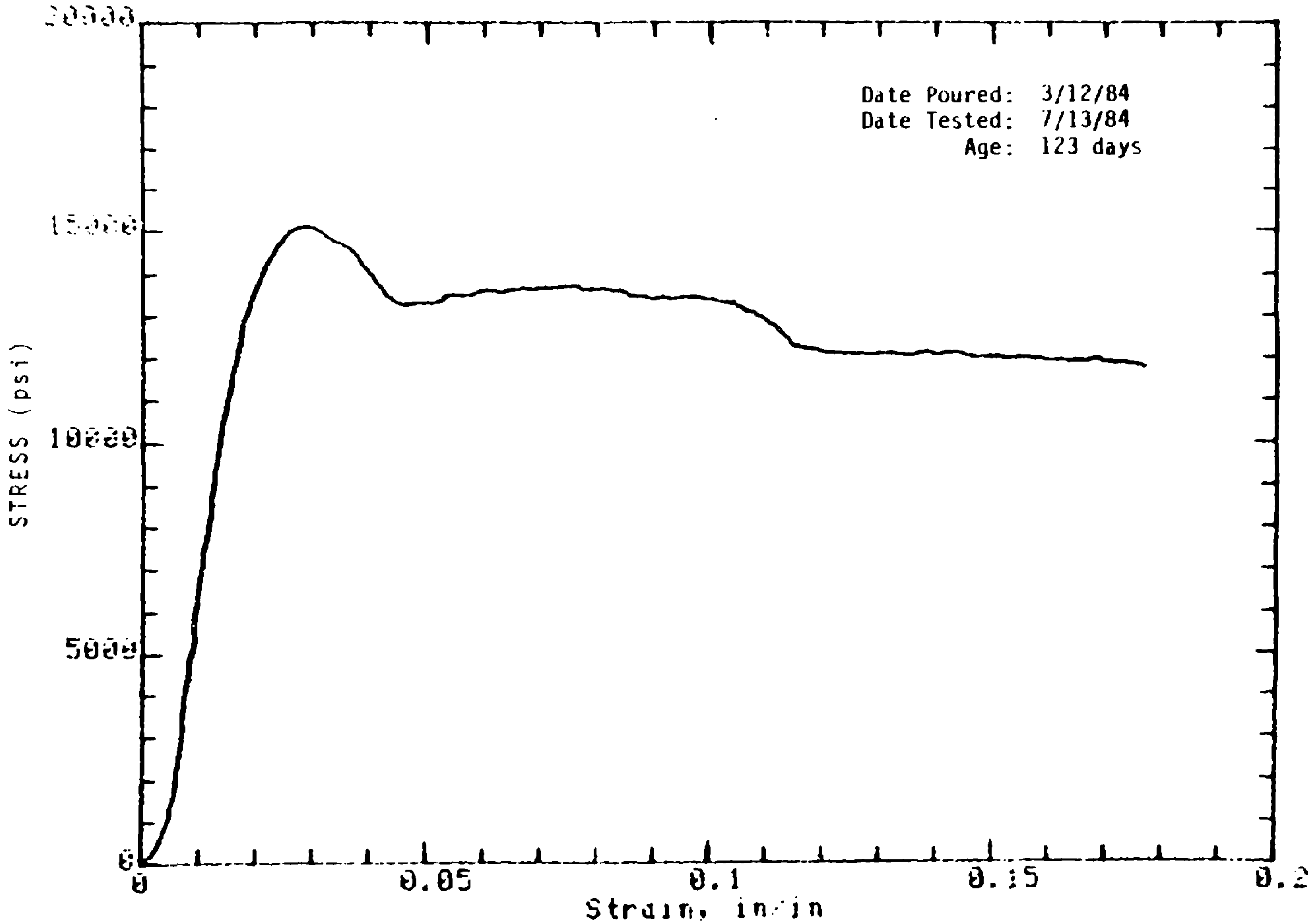

Mark: 1-9-1B Cored (Wall): 2in dia x 4in Cure: Dry
Concrete Sample

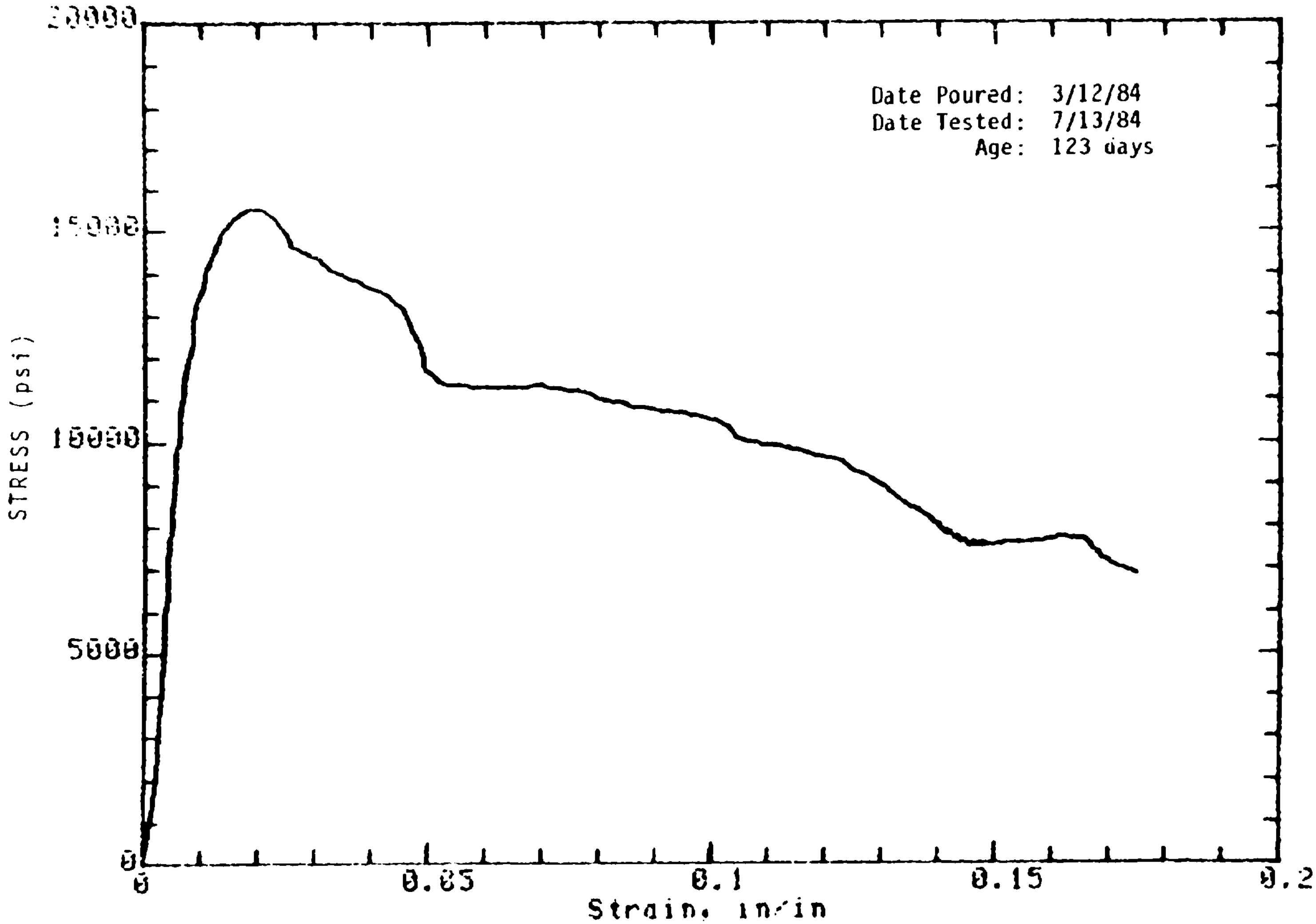

Mark: 1-9-2B Cored (Wall): 2in dia x 4in Cure: Dry
Concrete Sample

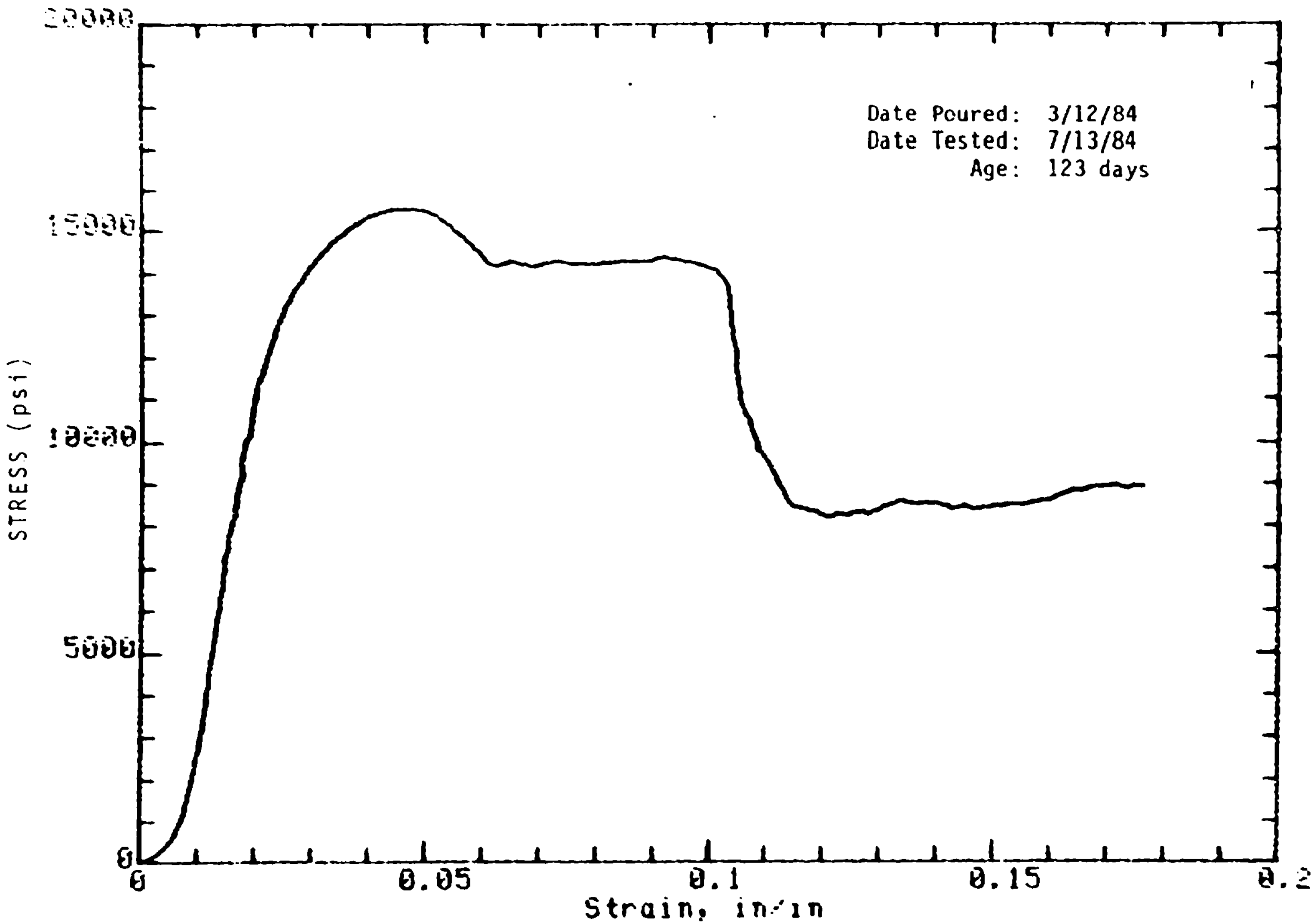

Mark: 1-9-3B Cored (Wall): 2in dia x 4in Cure: Dry
Concrete Sample

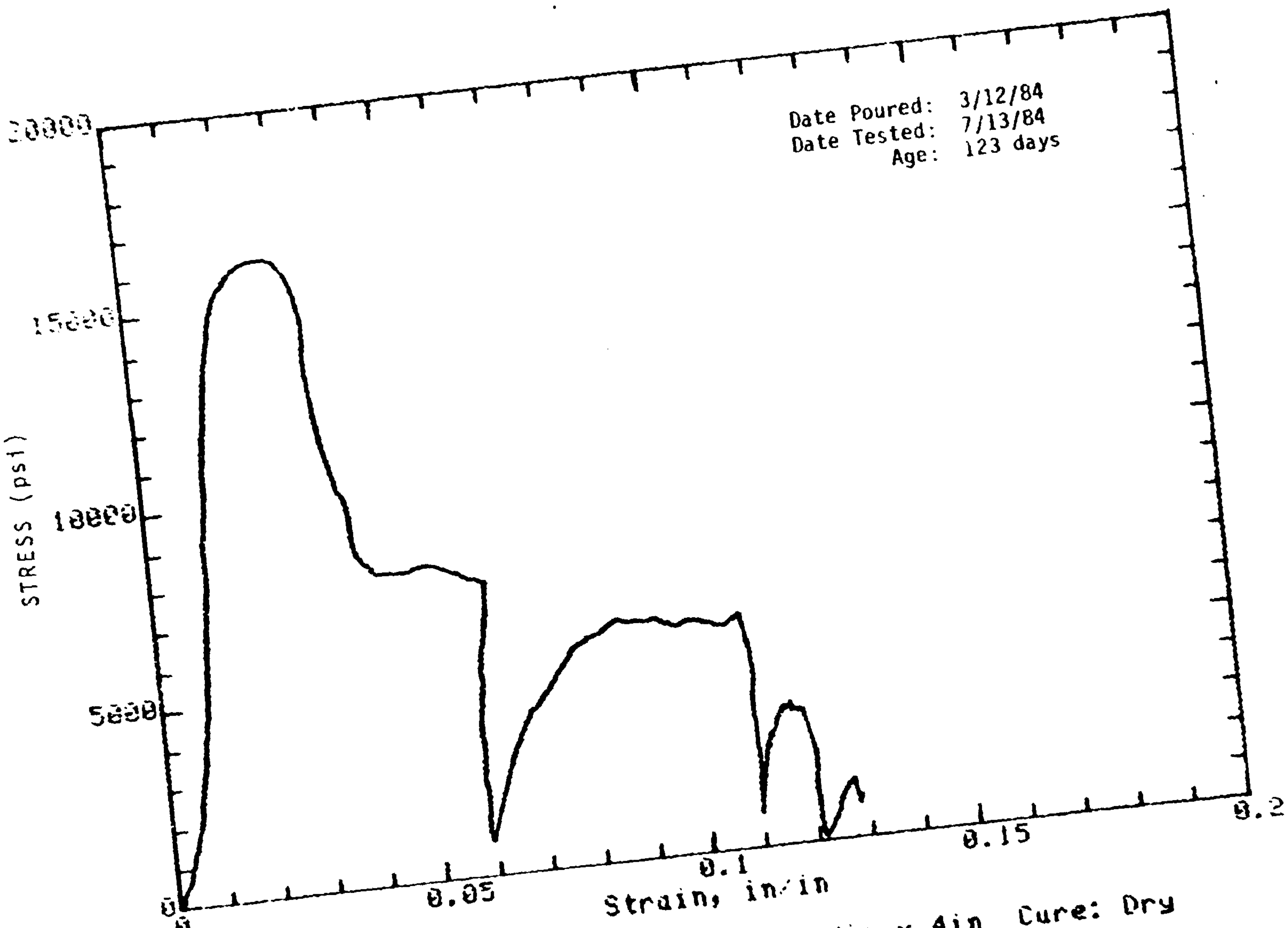

Mark: 1-9-4B Cored (Wall): 2in dia x 4in Cure: Dry
Concrete Sample

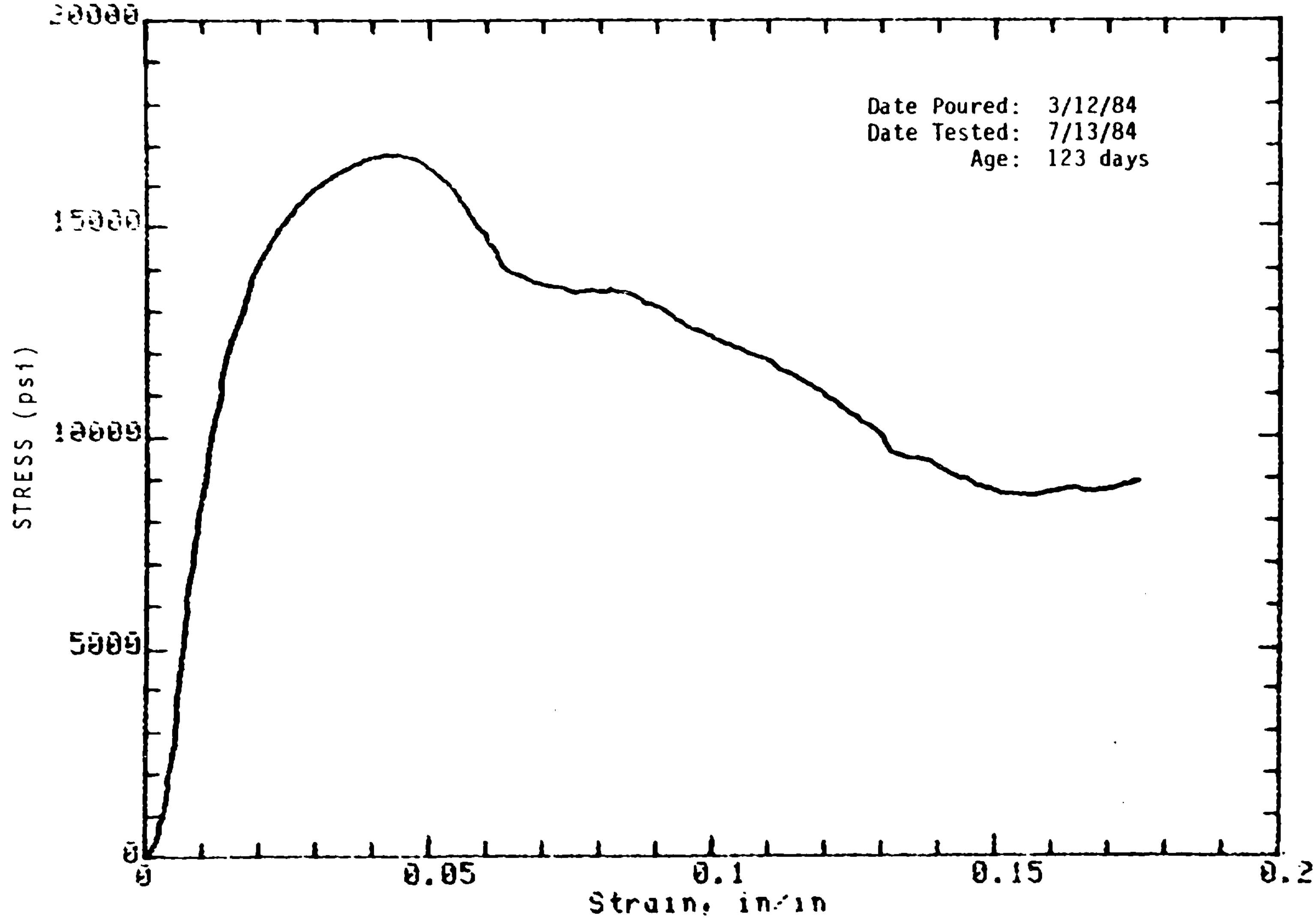

Mark: 1-9-5B Cored (Wall): 2in dia x 4in Cure: Dry
Concrete Sample

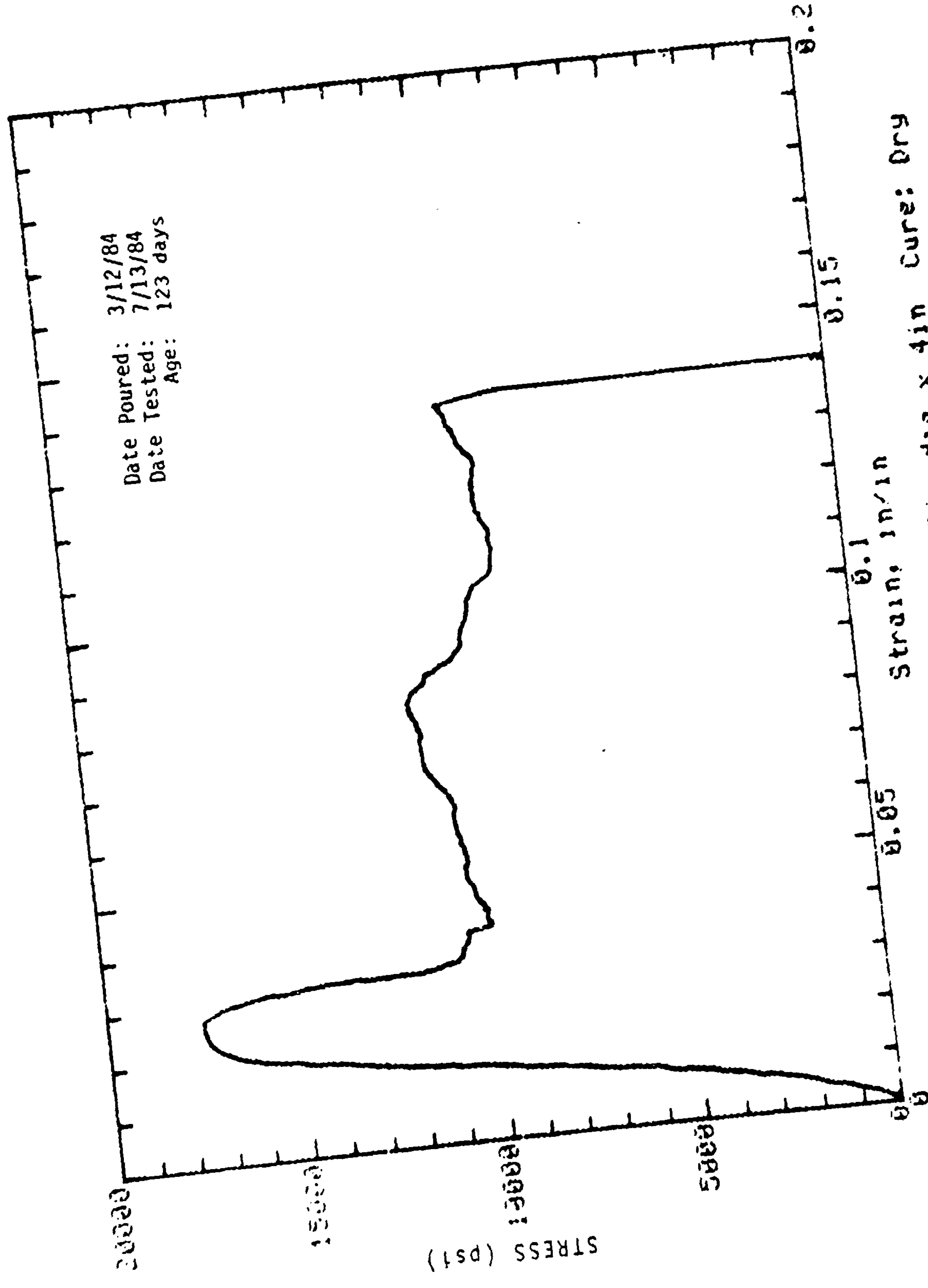

Mark: 1-9-6B Cored (Wall); 2in dia x 4in Cure: Dry
Concrete Sample

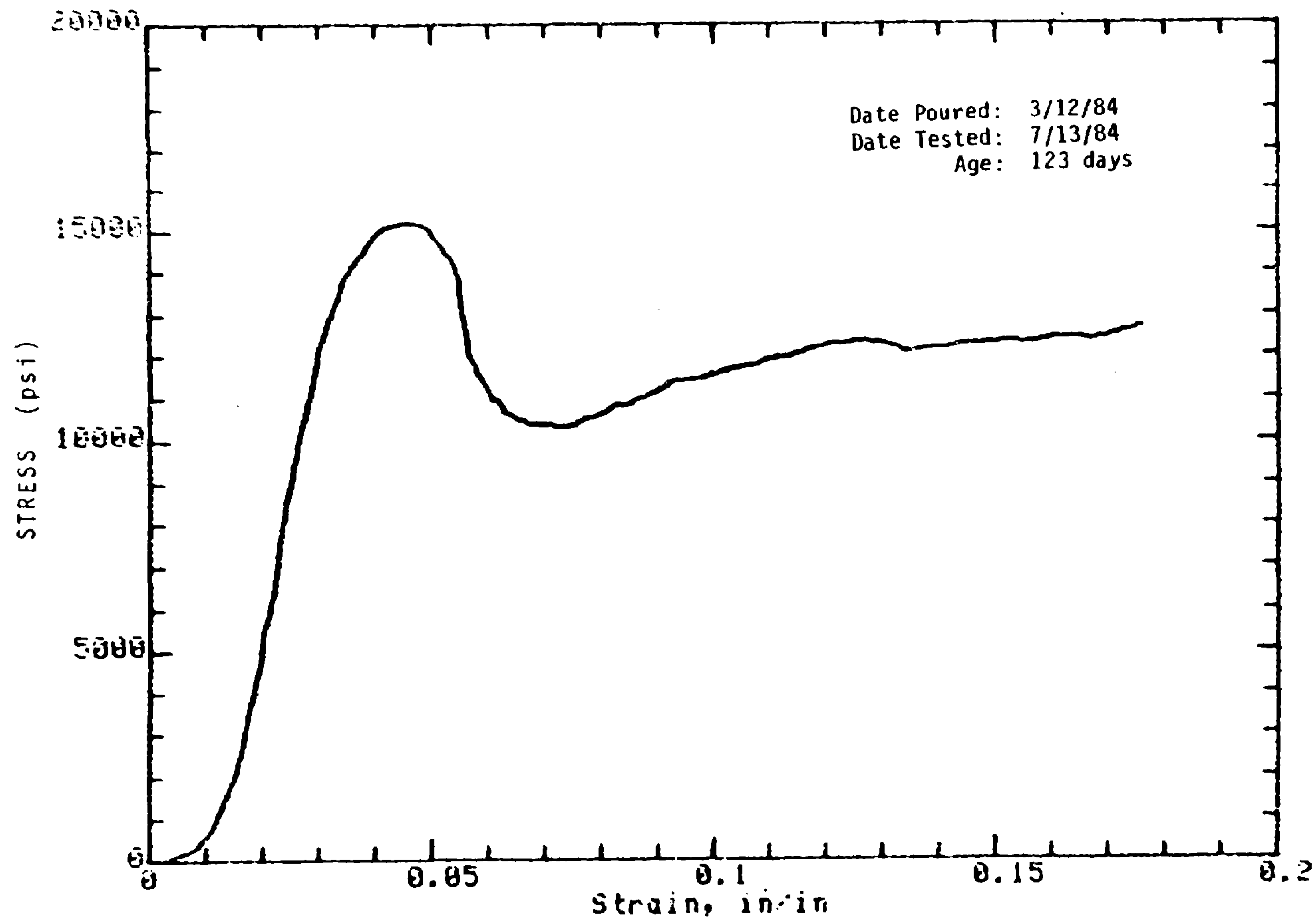

Mark: 1-9-7B Cored (Wall): 2in dia x 4in Cure: Dry
Concrete Sample

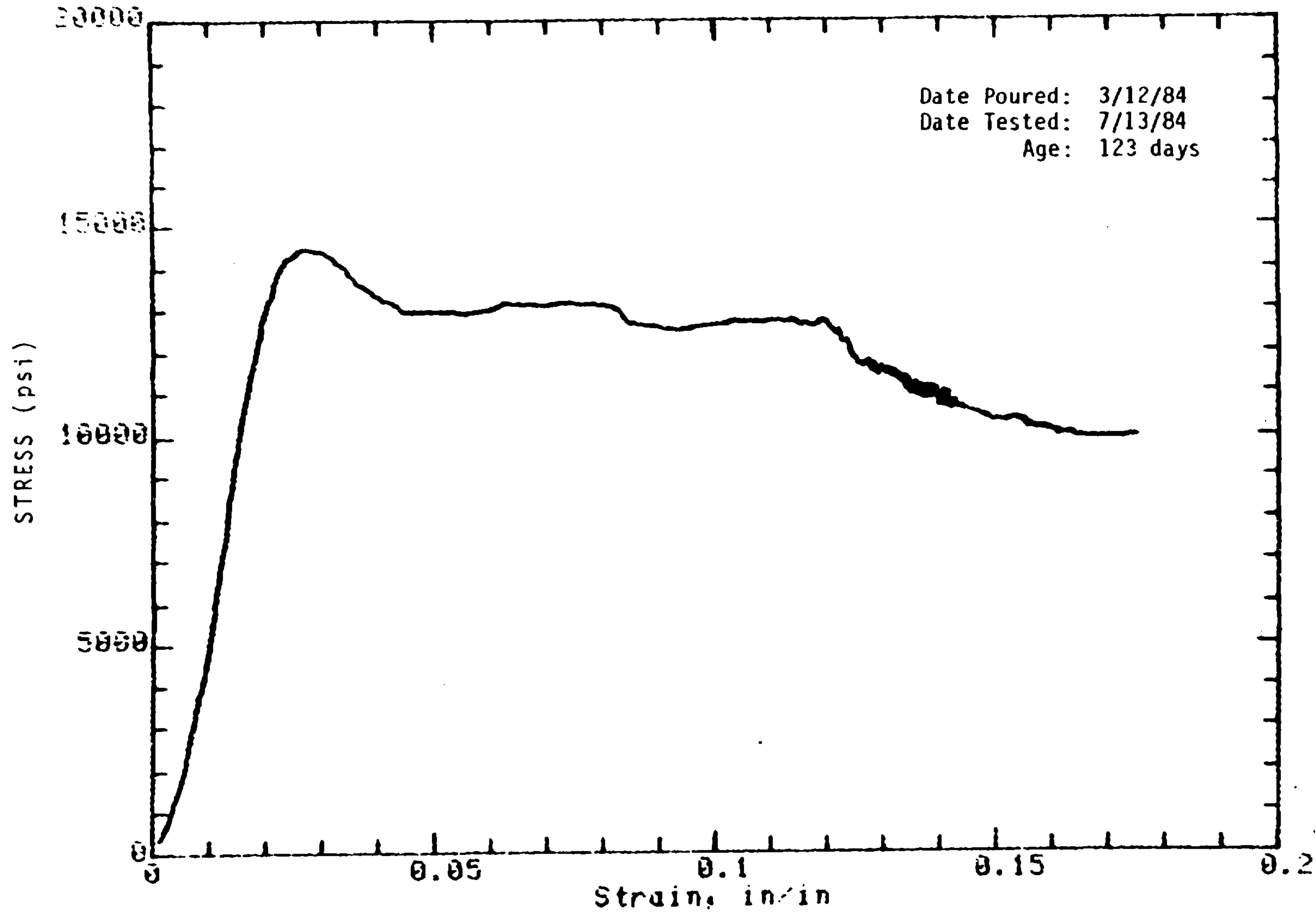

Mark: 1-9-88 Cored (Wall): 2in dia x 4in Cure: Dry
Concrete Sample

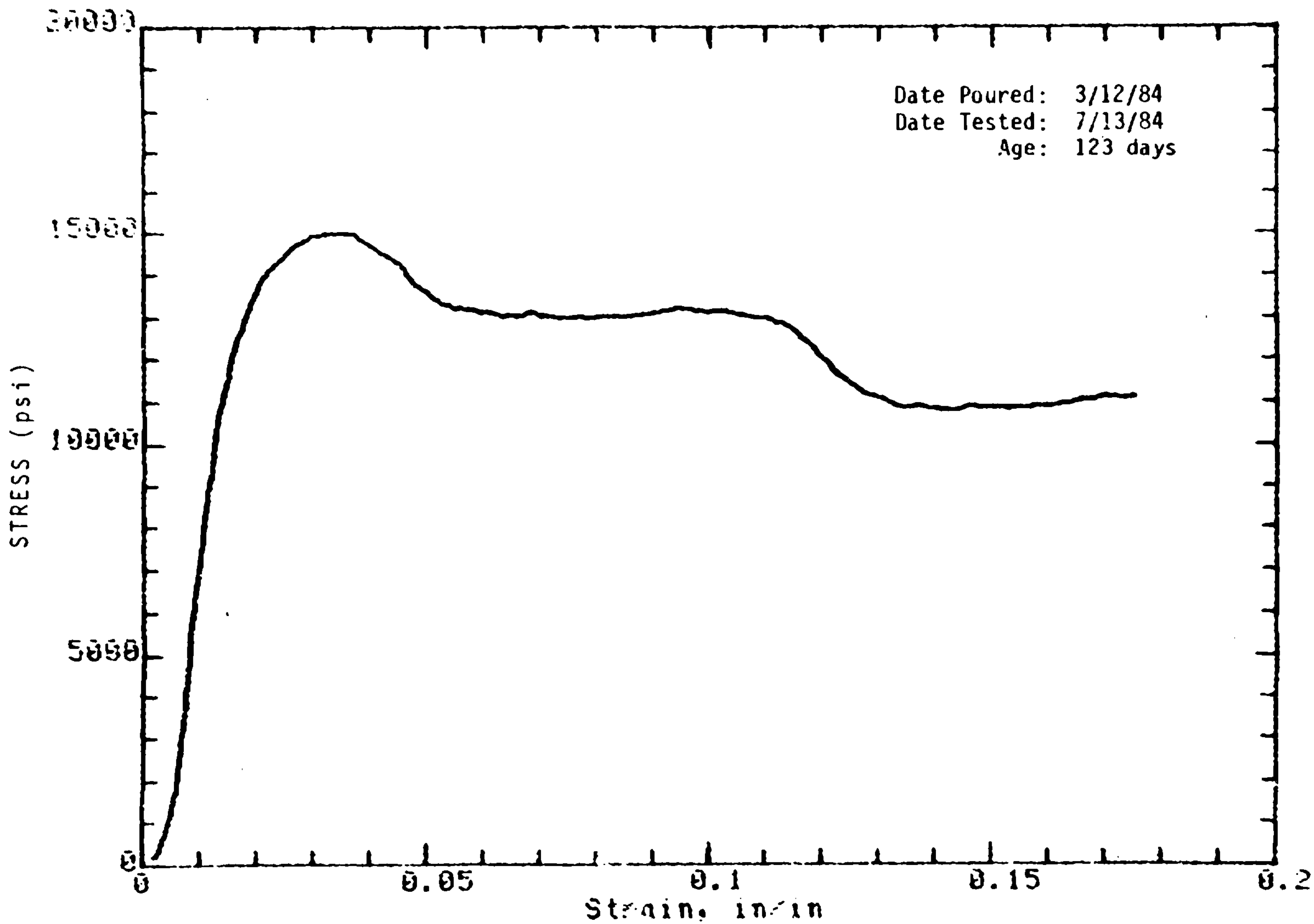

Mark: 1-9-9B Cored (Wall): 2in dia x 4in Cure: Dry
Concrete Sample

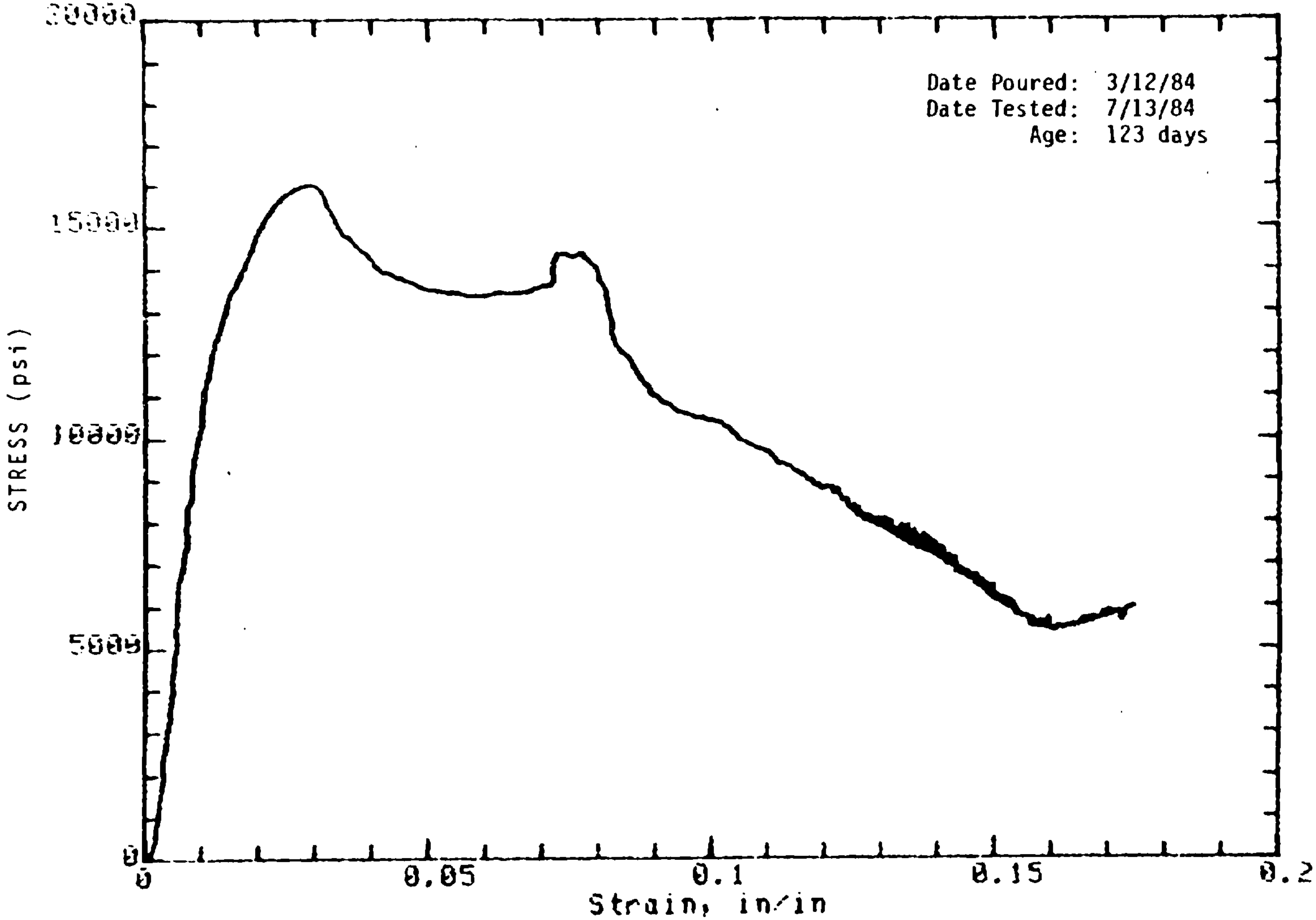

Mark: 1-9-10B Cored (Wall): 2in dia x 4in Cure: Dry
Concrete Sample

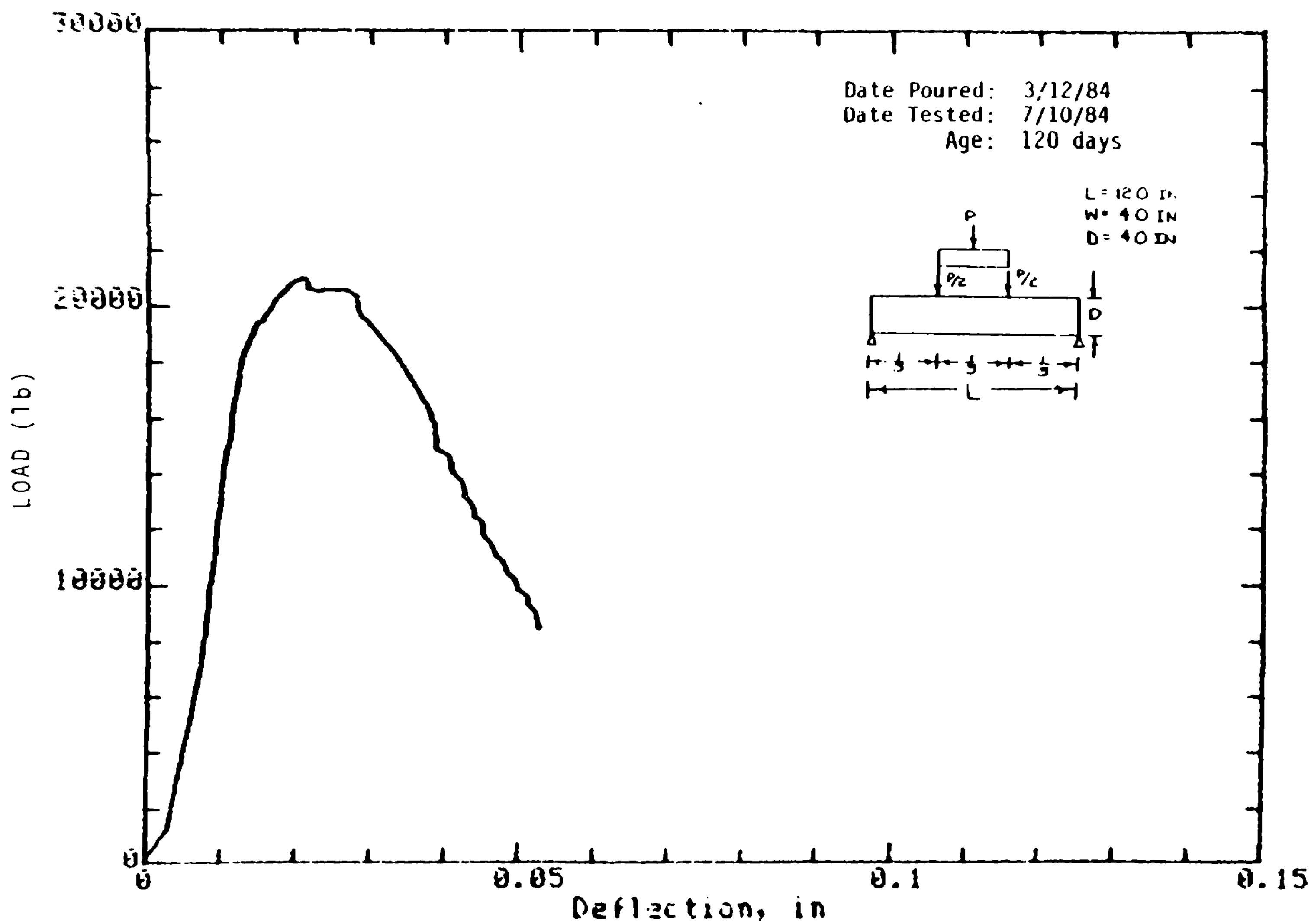

Mark: 9-20 Beam: 4in x 4in Cure: Wet
Concrete Sample

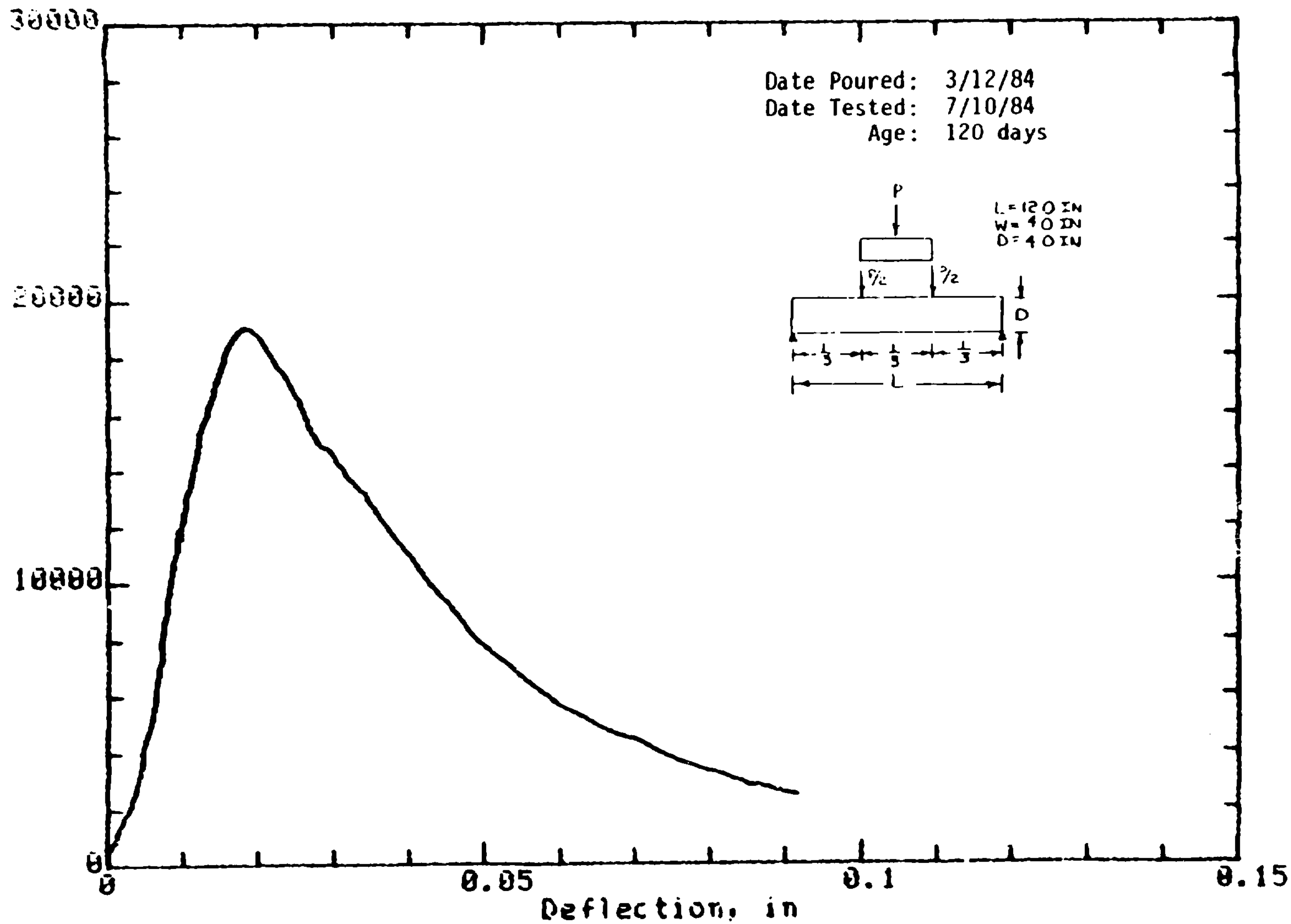

Mark: 9-21 Beam: 4in x 4in Cure: Wet
Concrete Sample

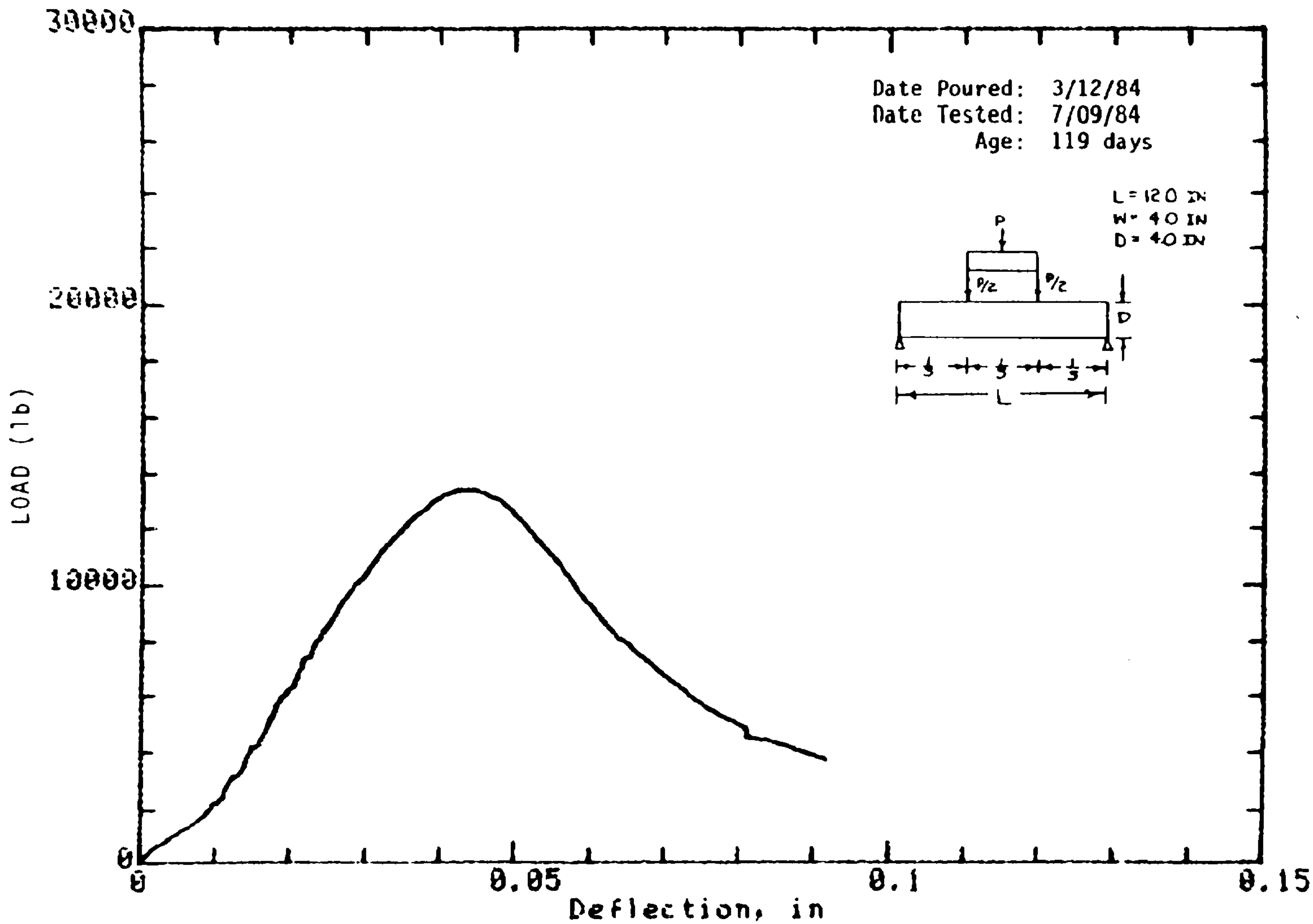

Mark: 9-28 Beam: 4in x 4in Cure: Dry
Concrete Sample

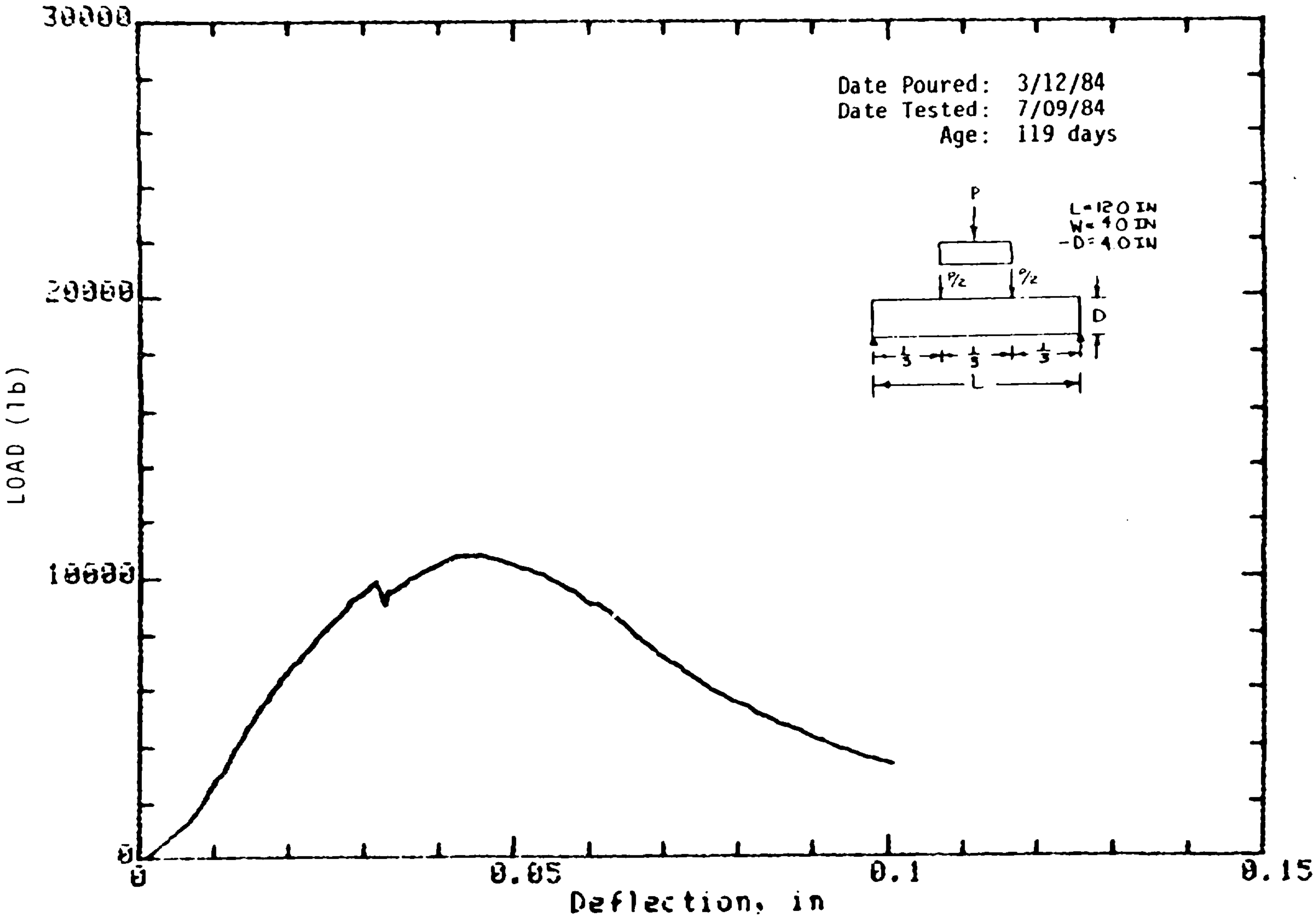

Mark: 9-30 Beam: 4in x 4in Cure: Dry
Concrete Sample

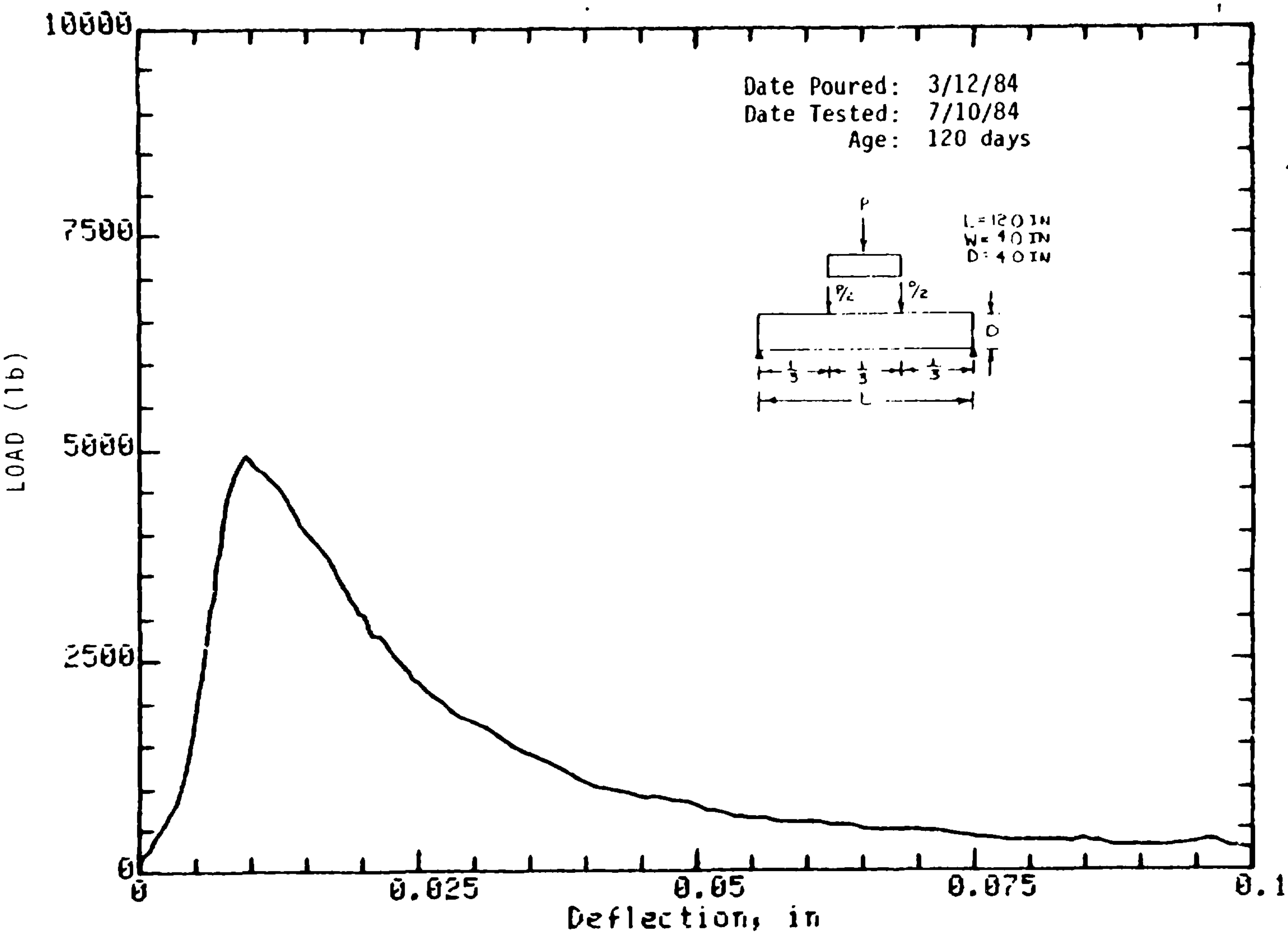

Mark: 9-33 Column: 4in × 4in Cure: Wet
Concrete Sample

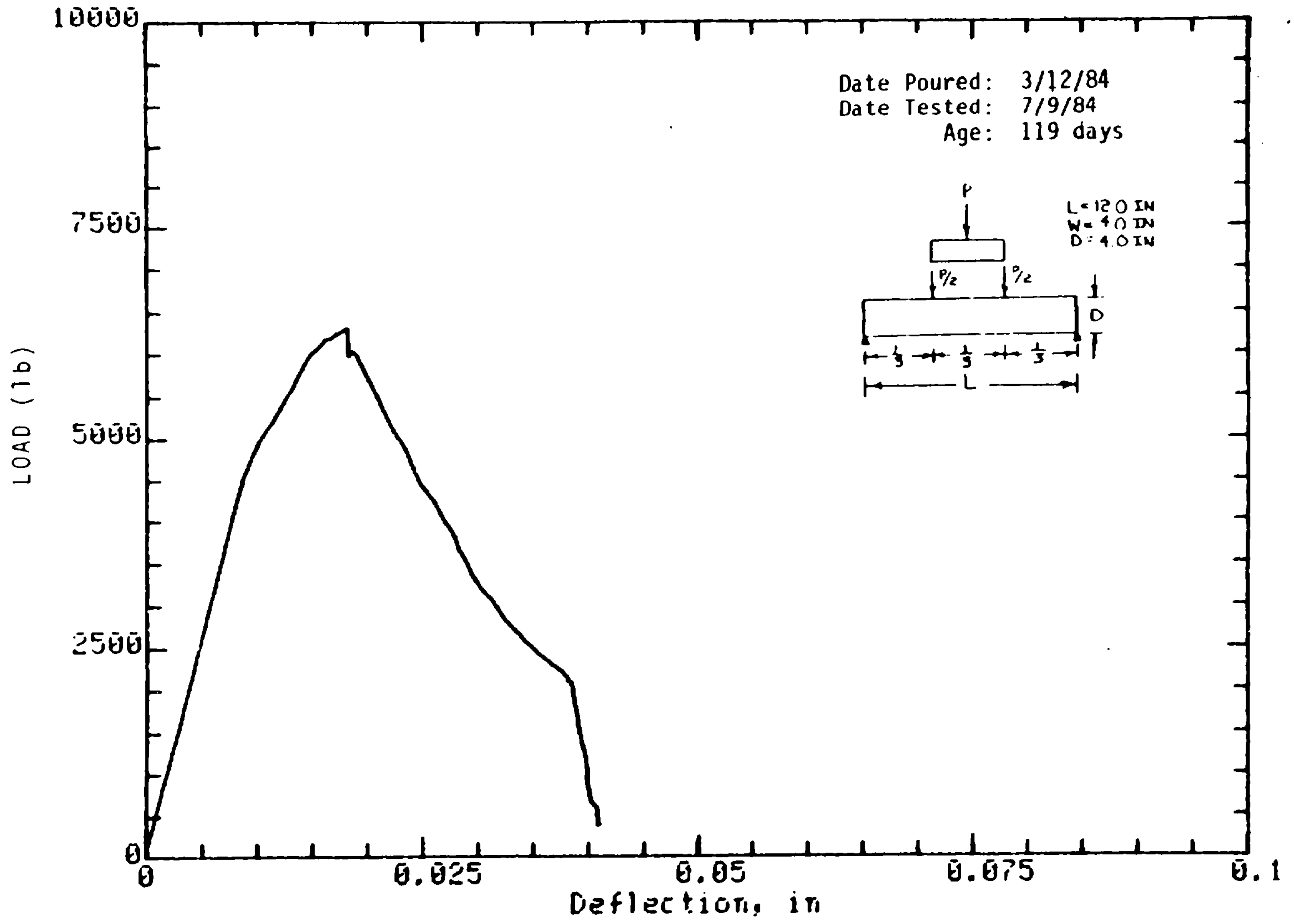

Mark: 9-37 Column: 4in × 4in Cure: Wet
Concrete Sample

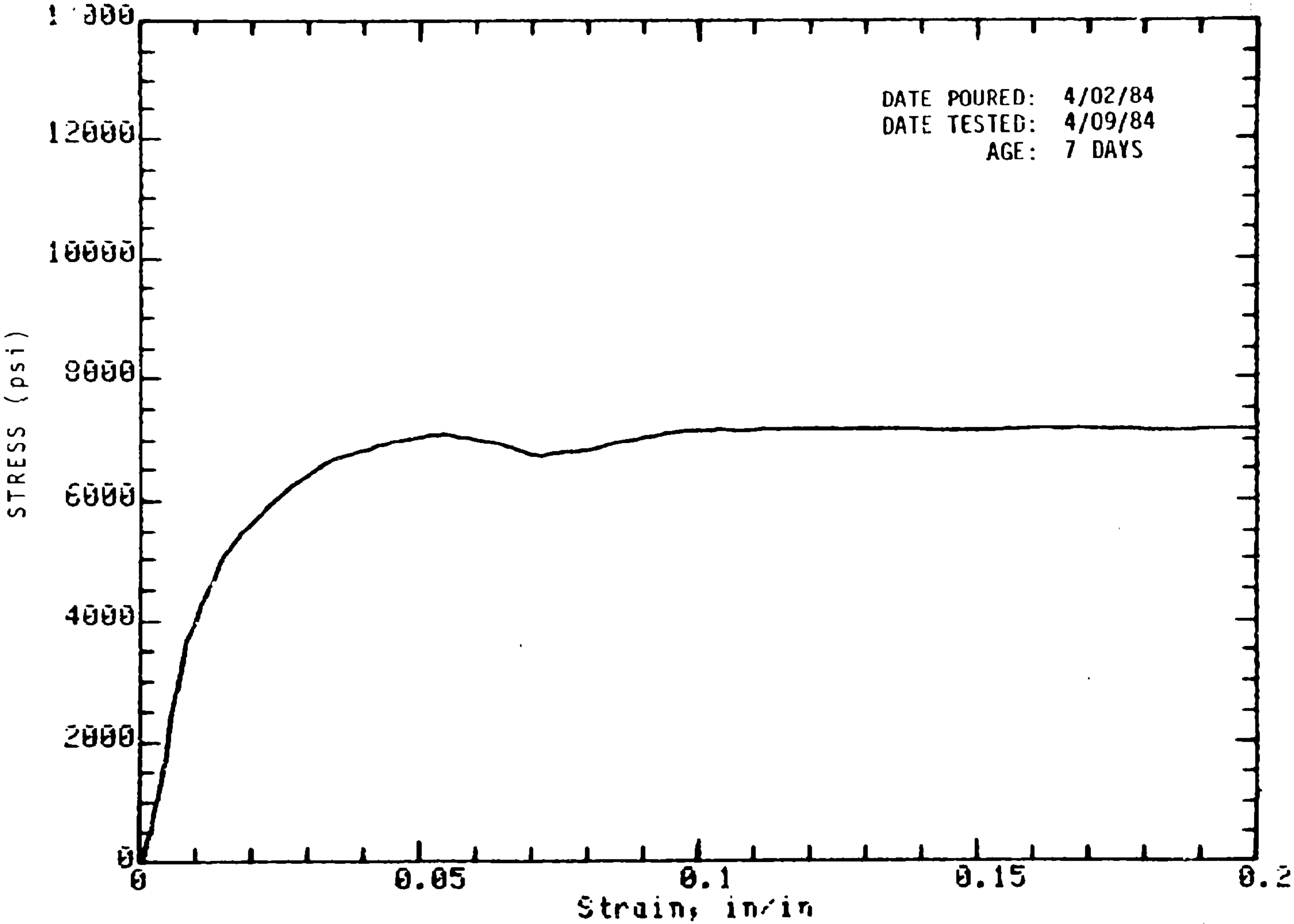

Mark: 10-15 Molded: 4in dia x 8in Cure: Wet
Concrete Sample

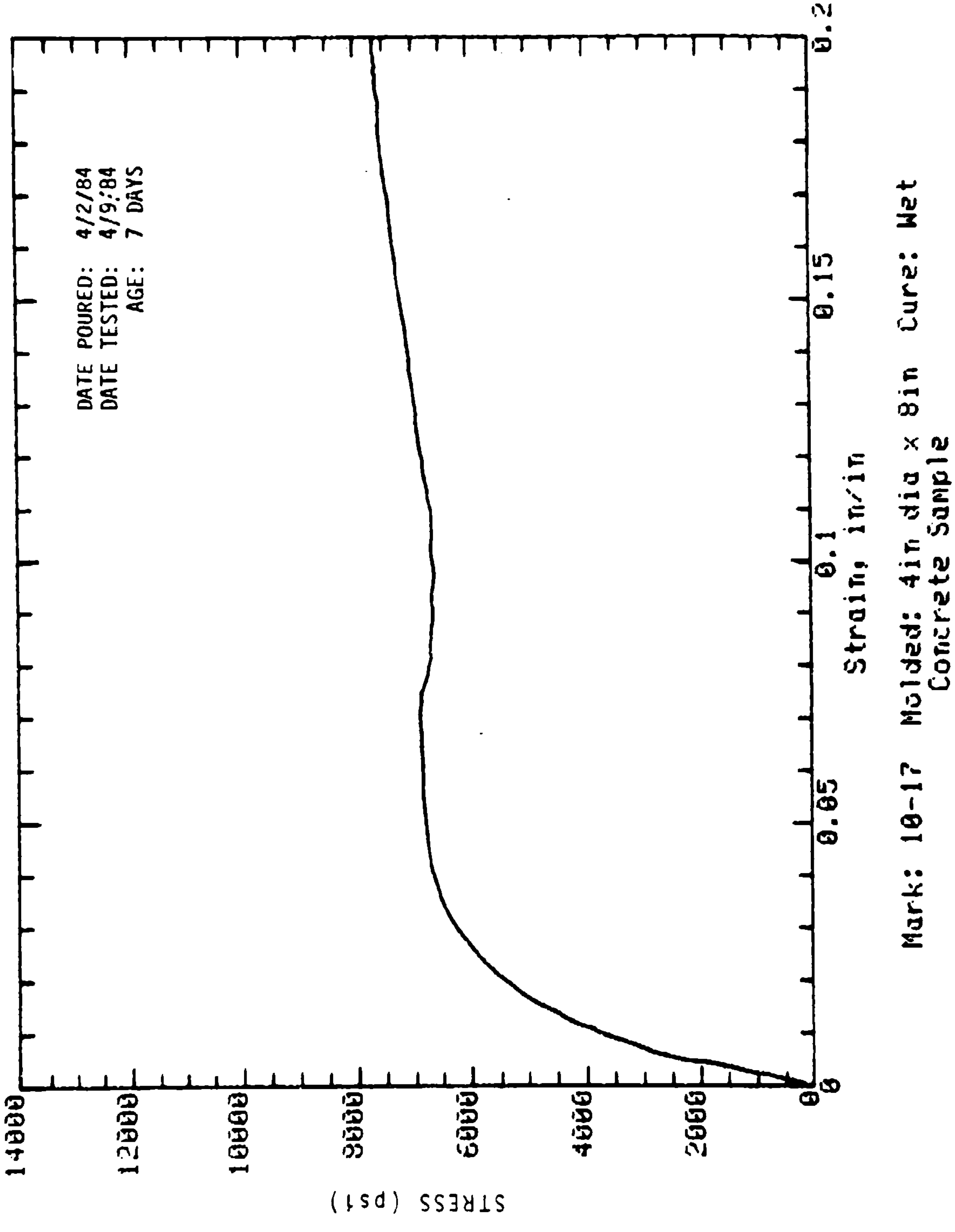

DATE POURED: 4/2/84
DATE TESTED: 4/9/84
AGE: 7 DAYS
STRESS (psi)
14000
12000
10000
8000
6000
4000
2000
0
0
0.05
0.1
0.15
0.2
Strain, in/in
Mark: 10-17 Molded: 4in dia x 8in Cure: Wet
Concrete Sample

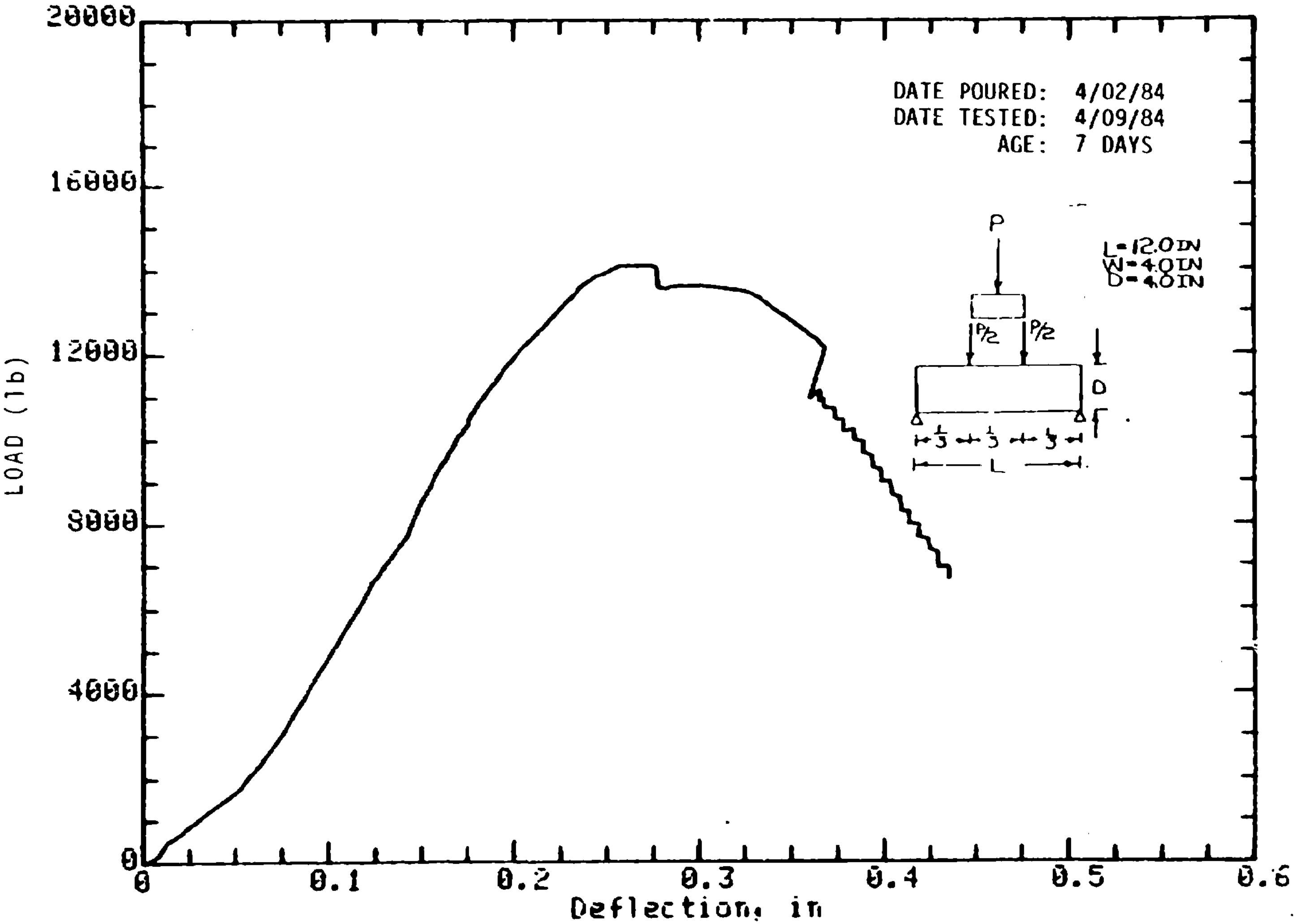

Mark: 10-19 Beam: 4in x 4in Cure: Dry
Concrete Sample

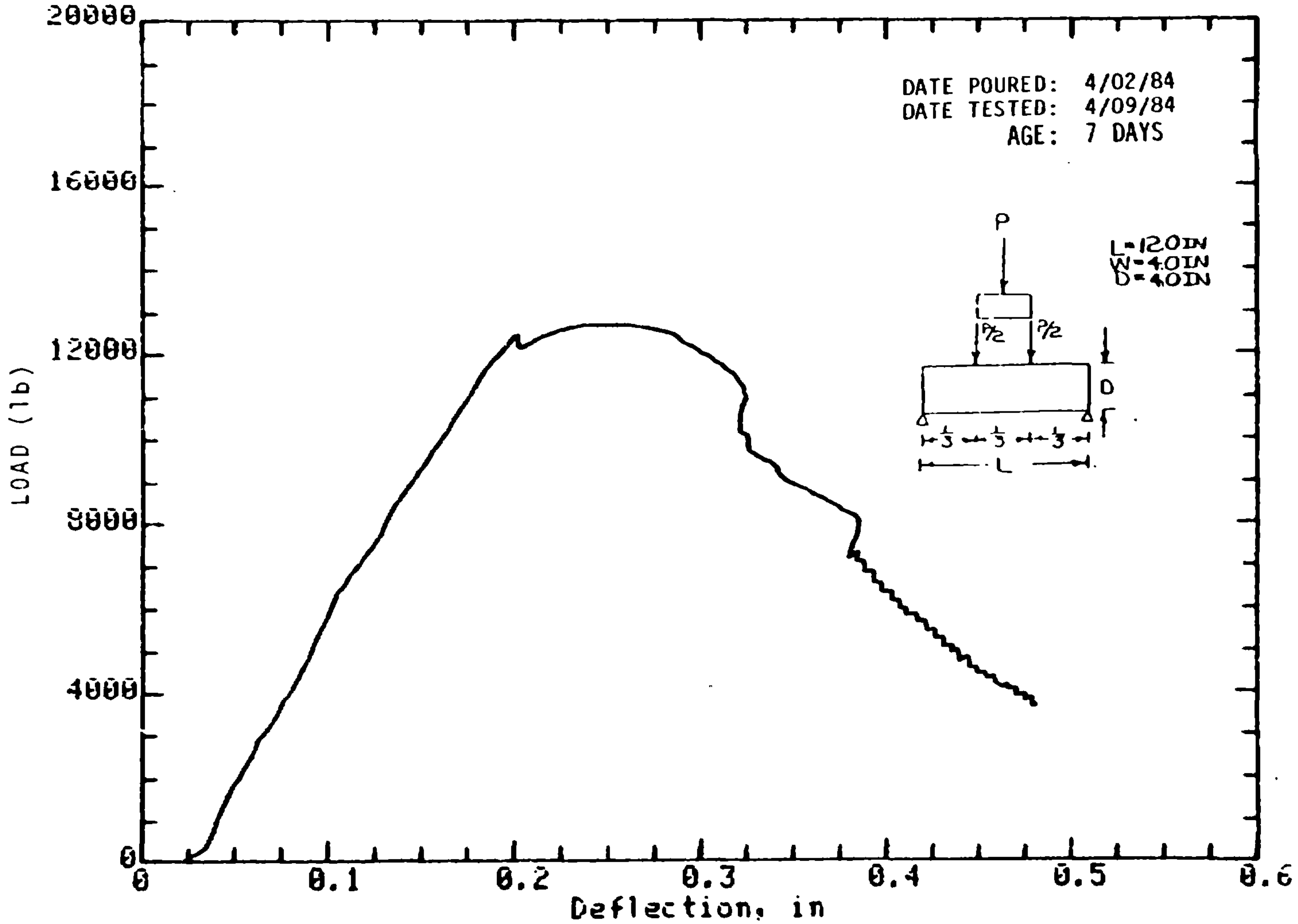

Mark: 10-20 Beam: 4in x 4in Cure: Dry
Concrete Sample

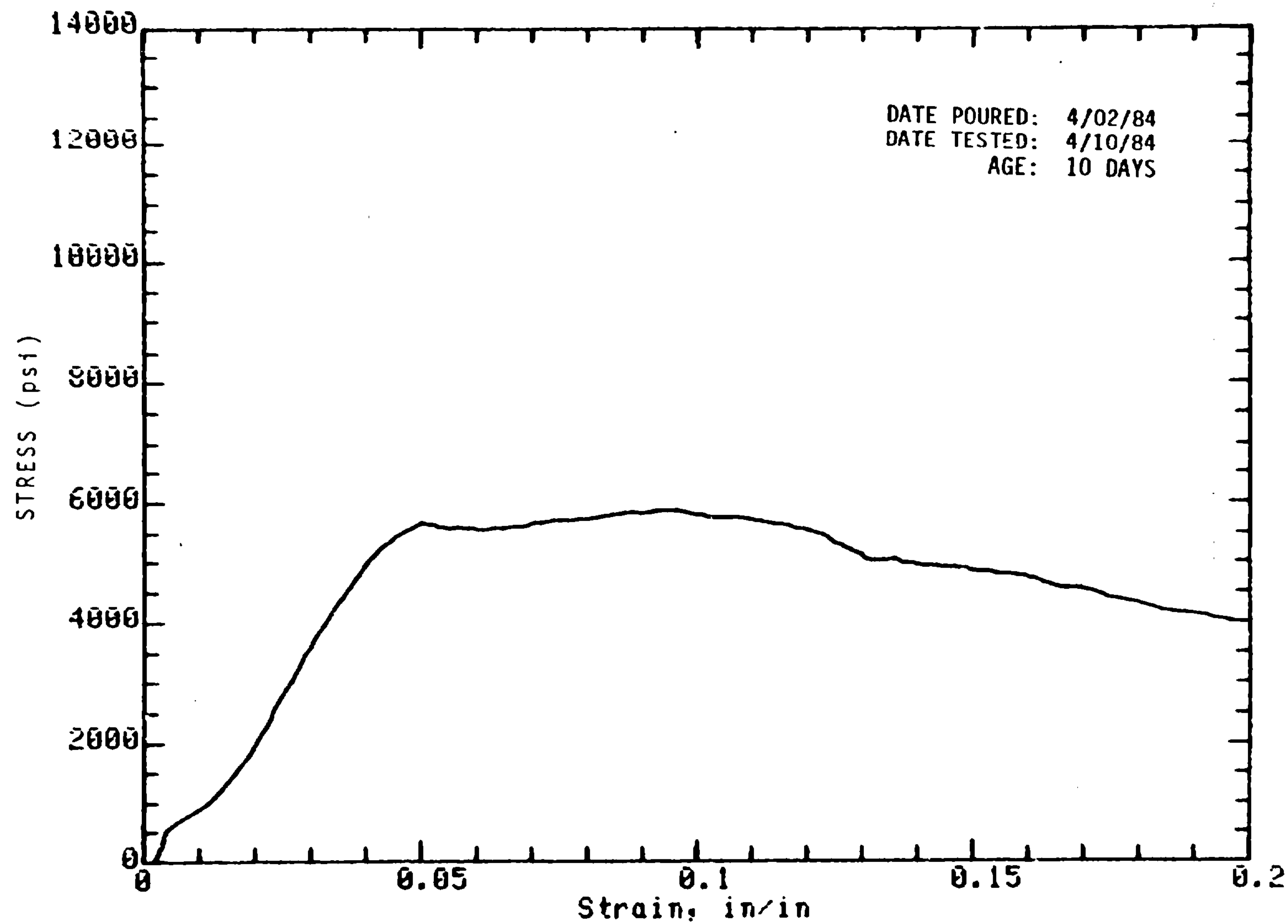

Mark: 10-6 Molded: 4in dia x 8in Cure: Dry
Concrete Sample

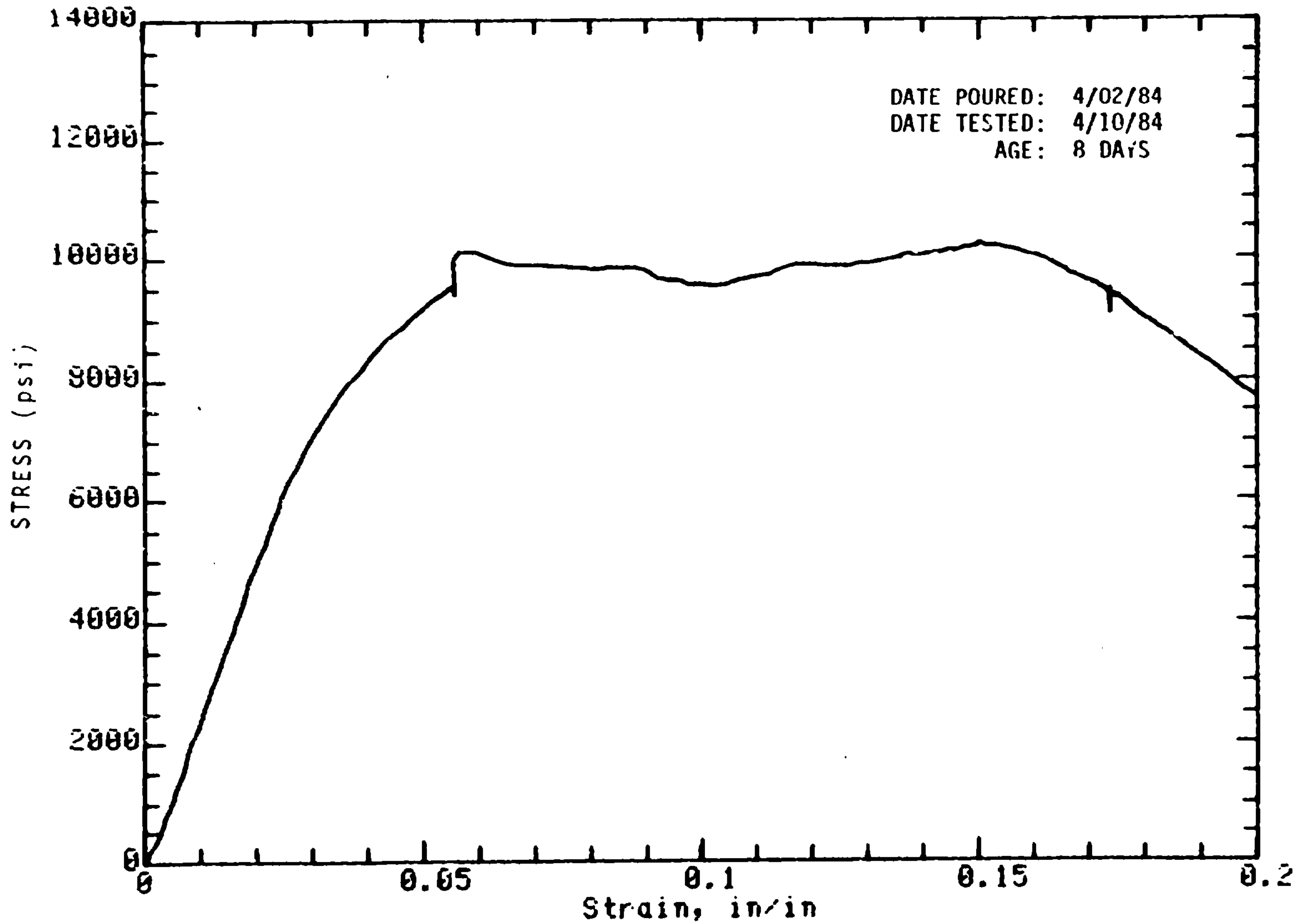

Mark: 10-8 Molded: 4in dia × 8in Cure: Dry
Concrete Sample

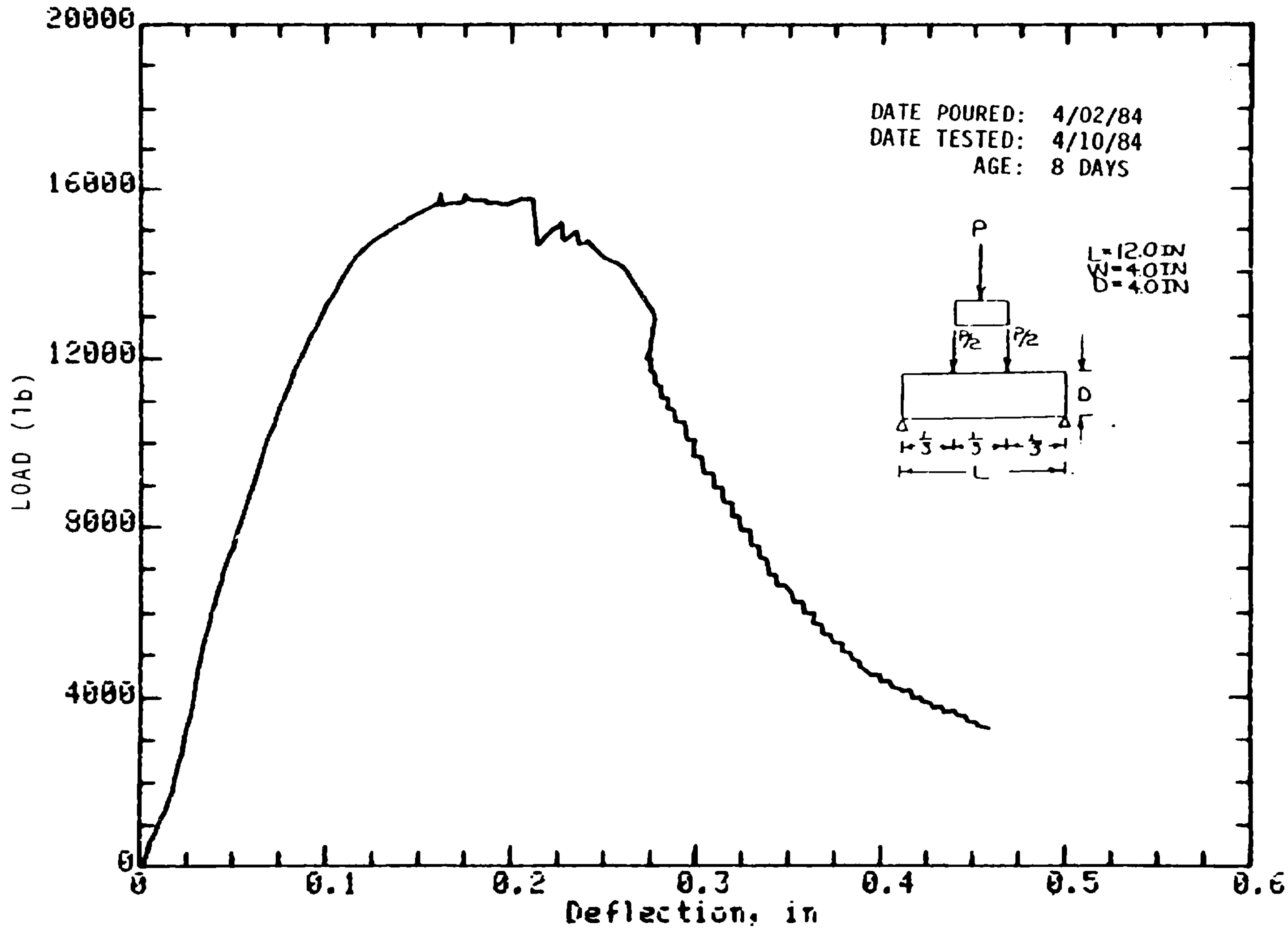

Mark: 10-23 Beam: 4in x 4in Cure: Wet
Concrete Sample

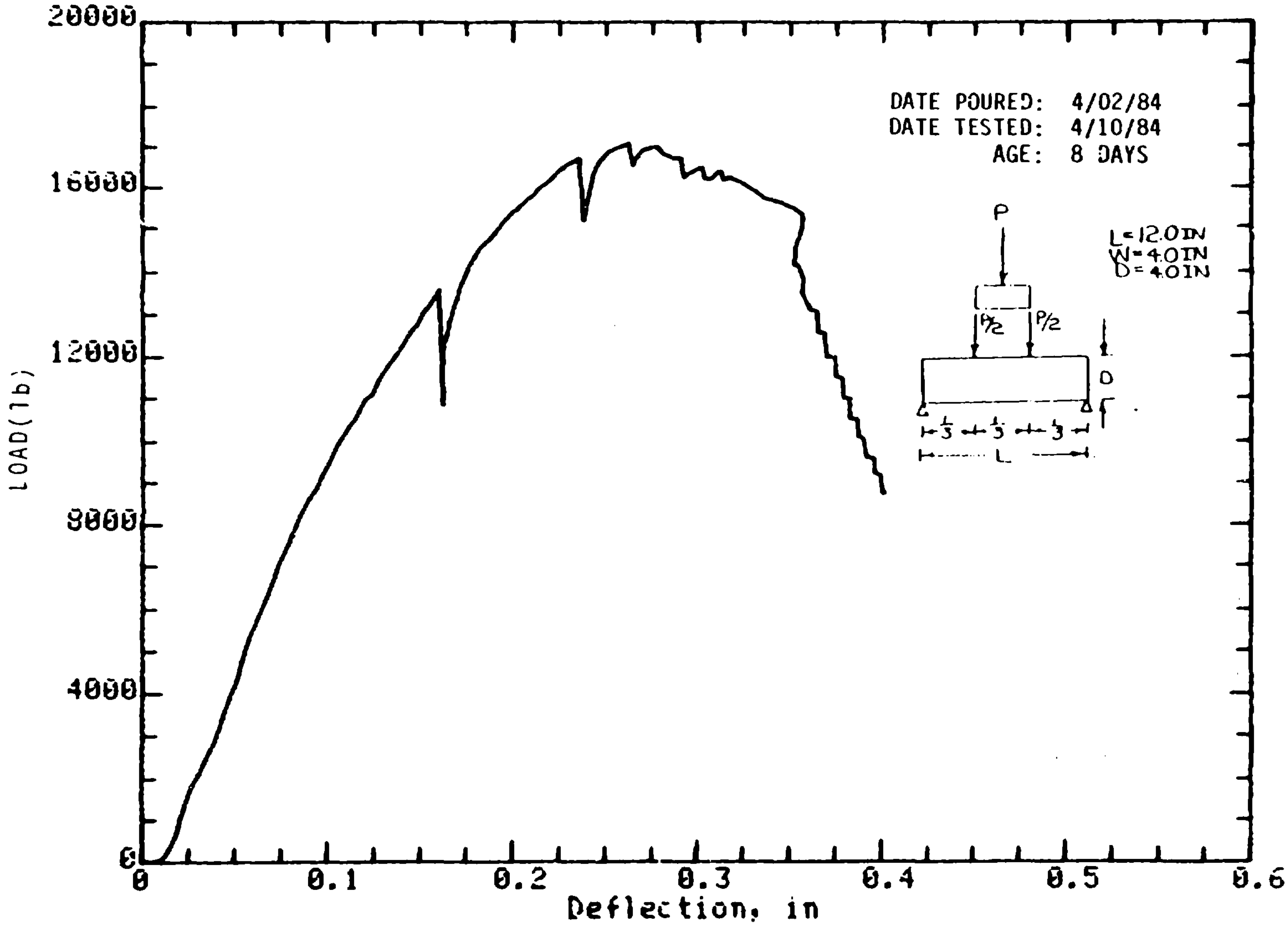

Mark: 10-24 Beam: 4in x 4in Cure: Wet
Concrete Sample

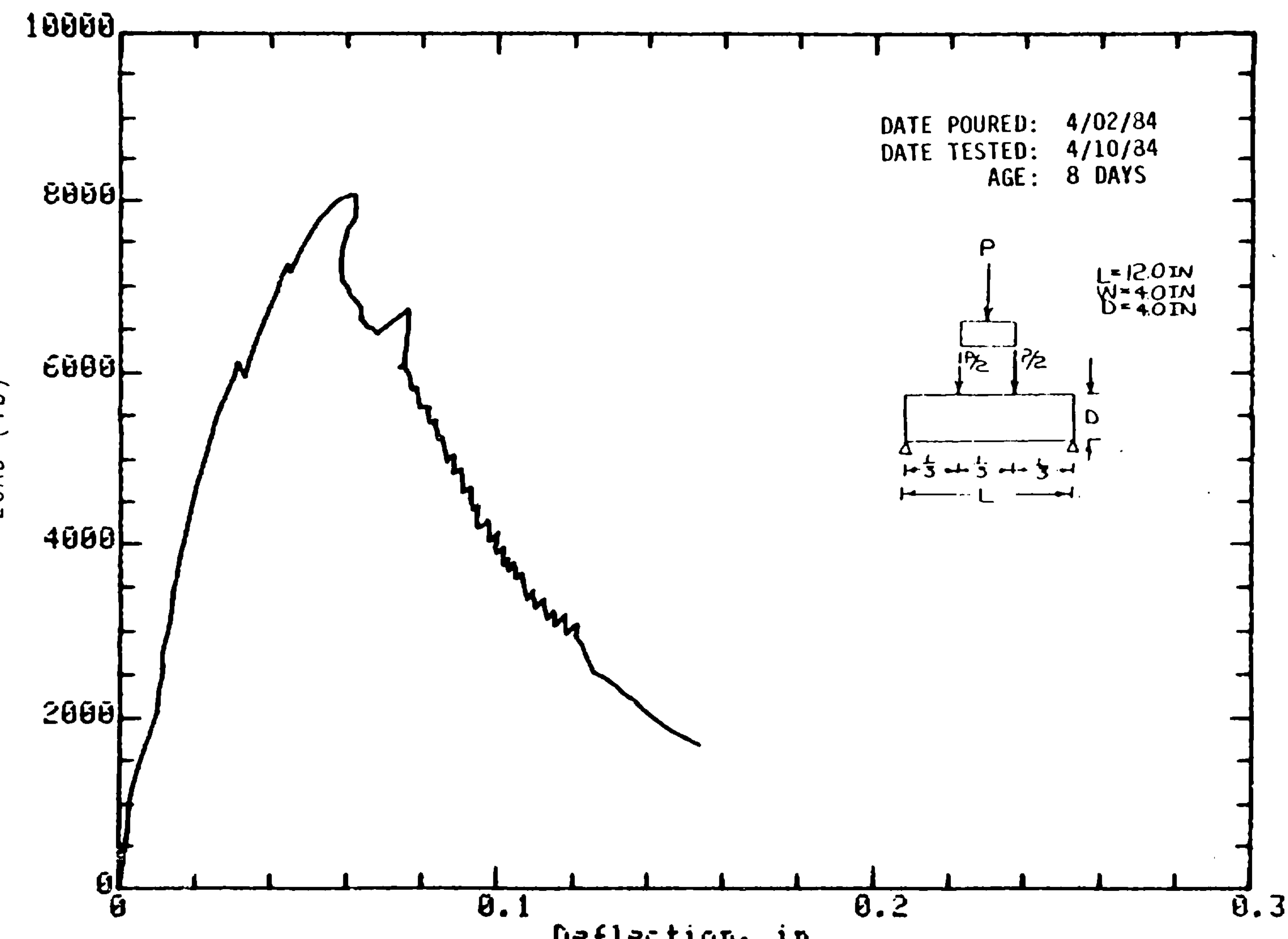

Mark: 10-32 Column: 4in x 4in Cure: Wet
Concrete Sample

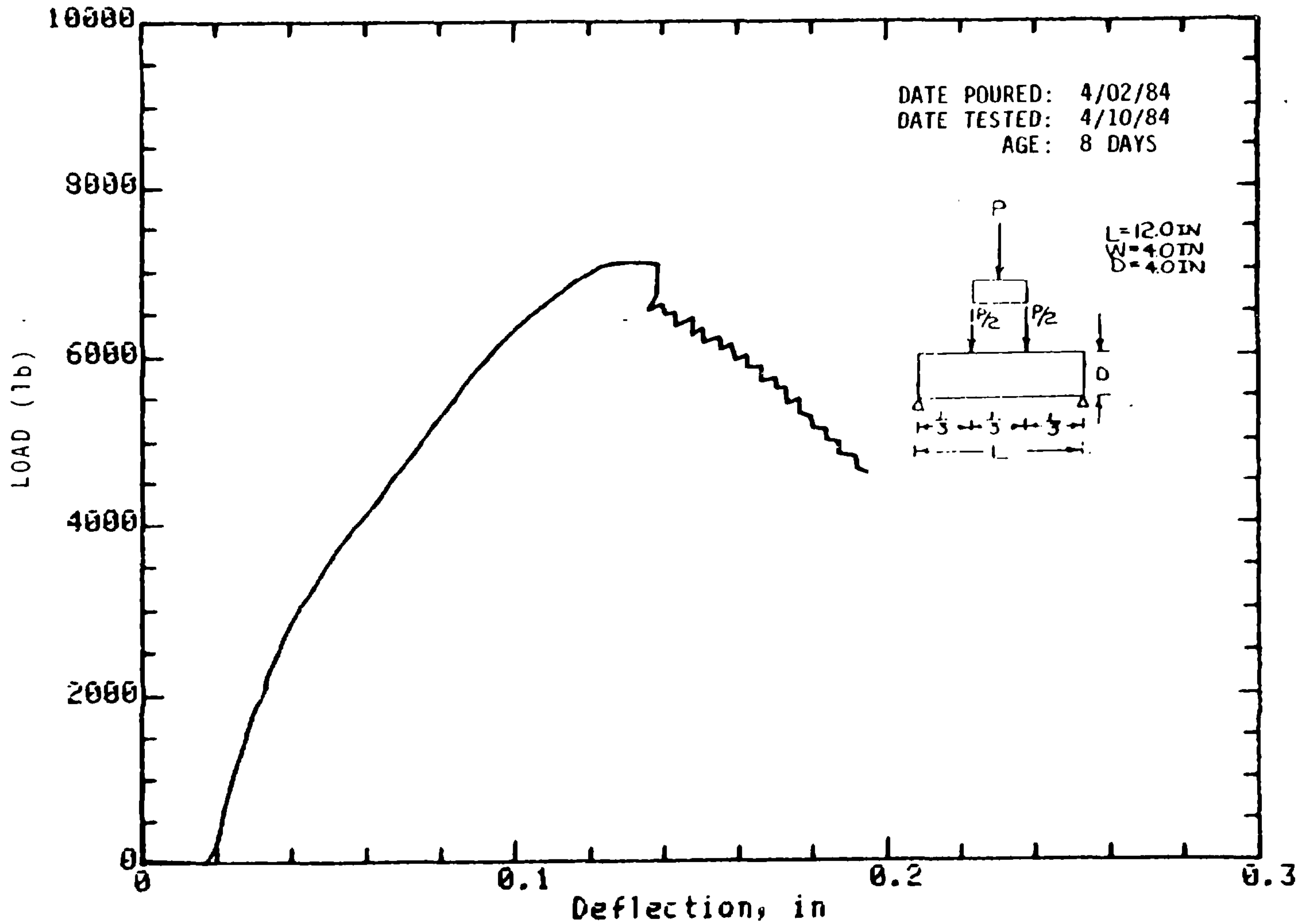

Mark: 10-34 Column: 10-34 Cure: Dry
Concrete Sample

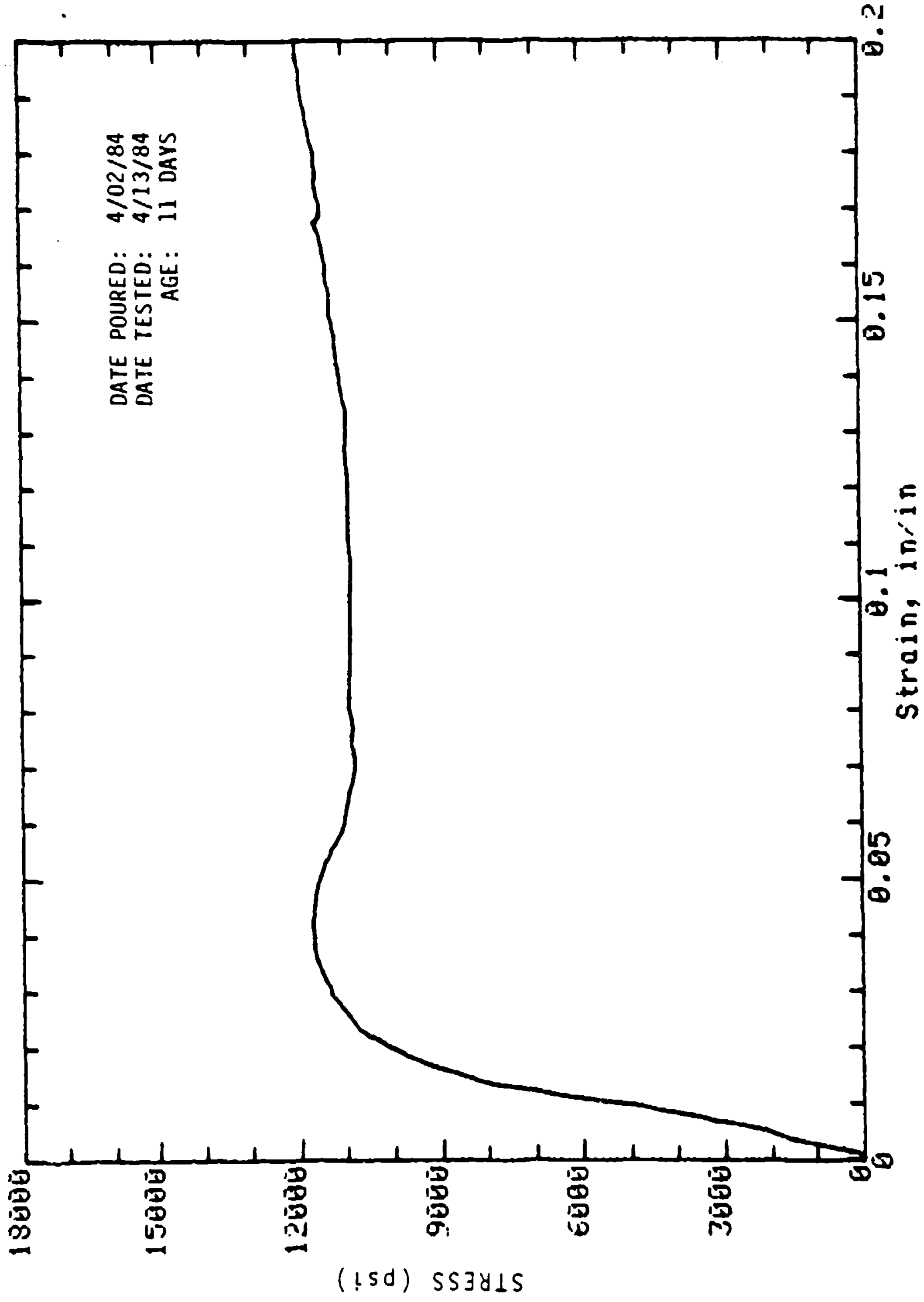

Mark: 10-S2-1 Cored (wall): 2in dia x 4in Cure: Dry
Concrete Sample

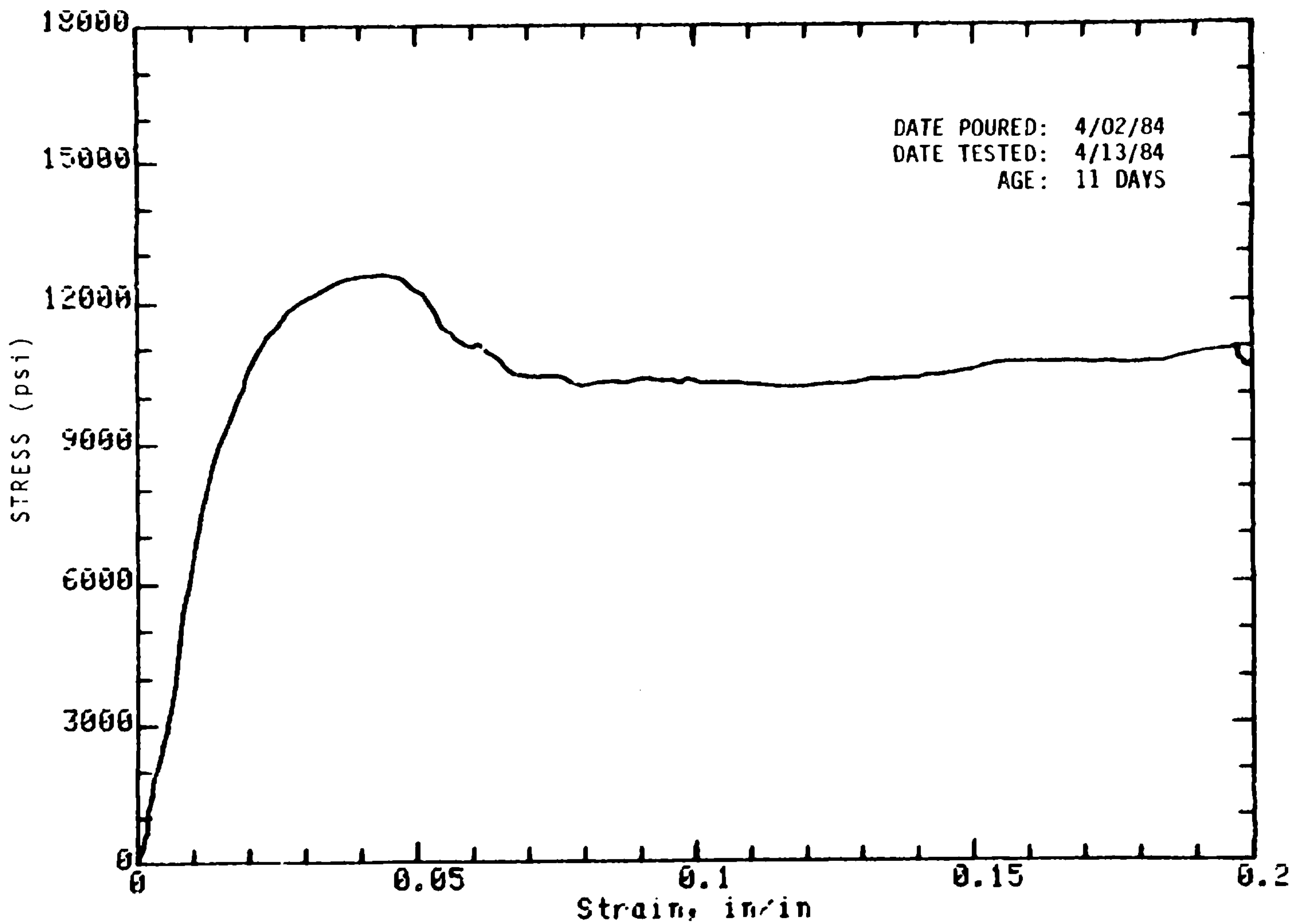

Mark: 10-S2-2 Cored (wall): 2in dia x 4in Cure: Dry
Concrete Sample

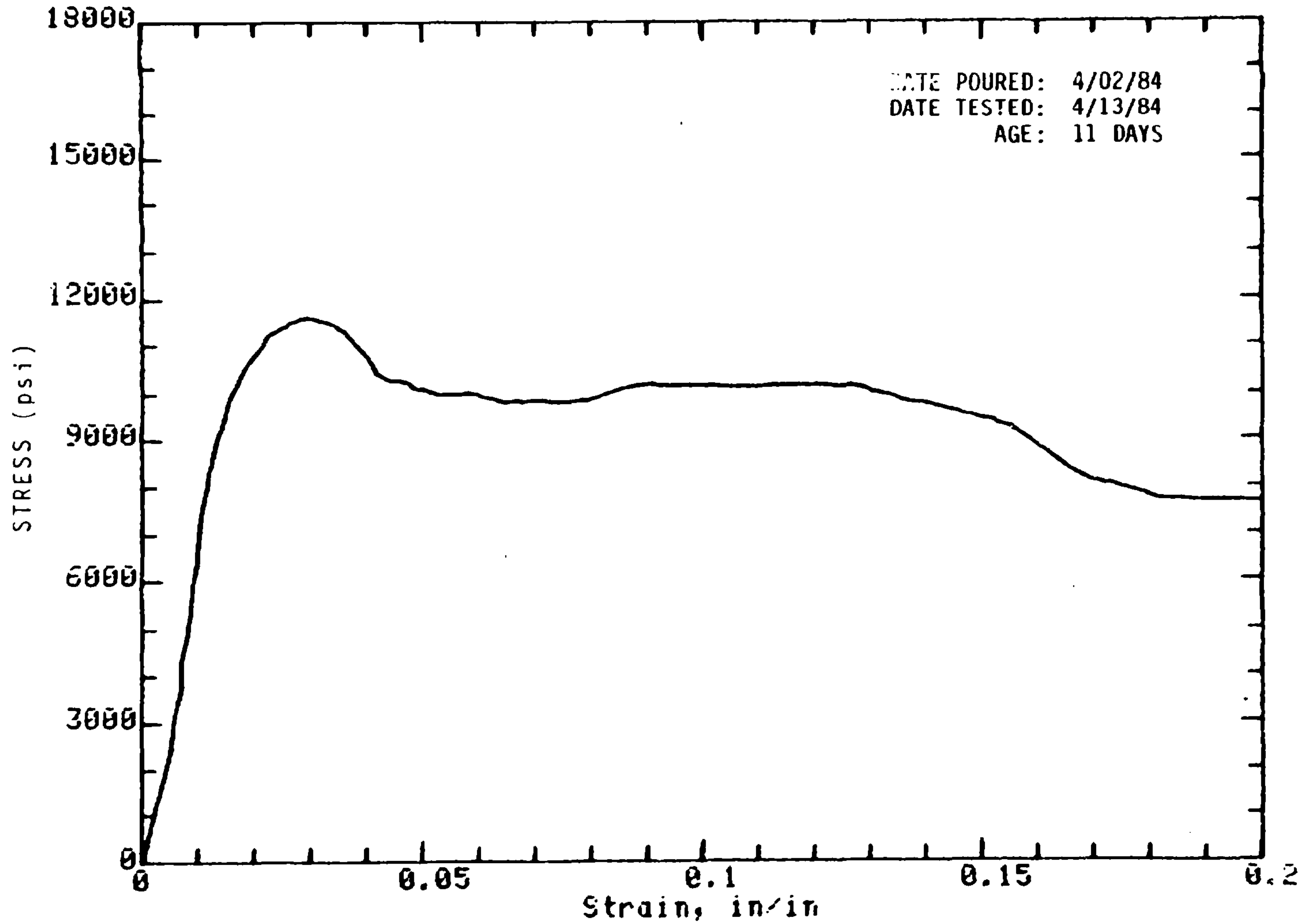

Mark: 10-S2-3 Cored (wall): 2in dia x 4in Cure: Dry
Concrete Sample

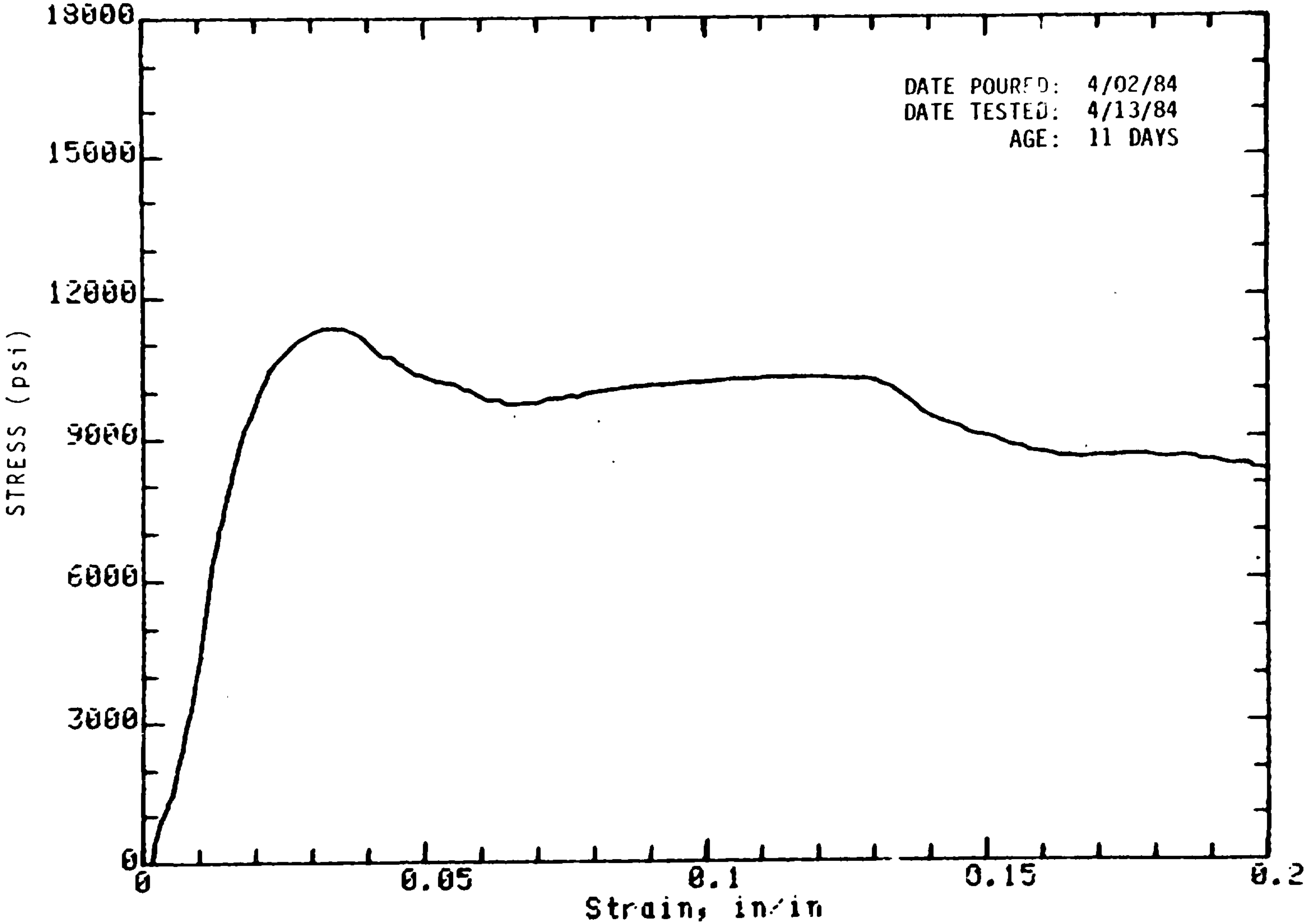

Mark: 10-S2-4 Cored (wall): 2in dia x 4in Cure: Dry
Concrete Sample

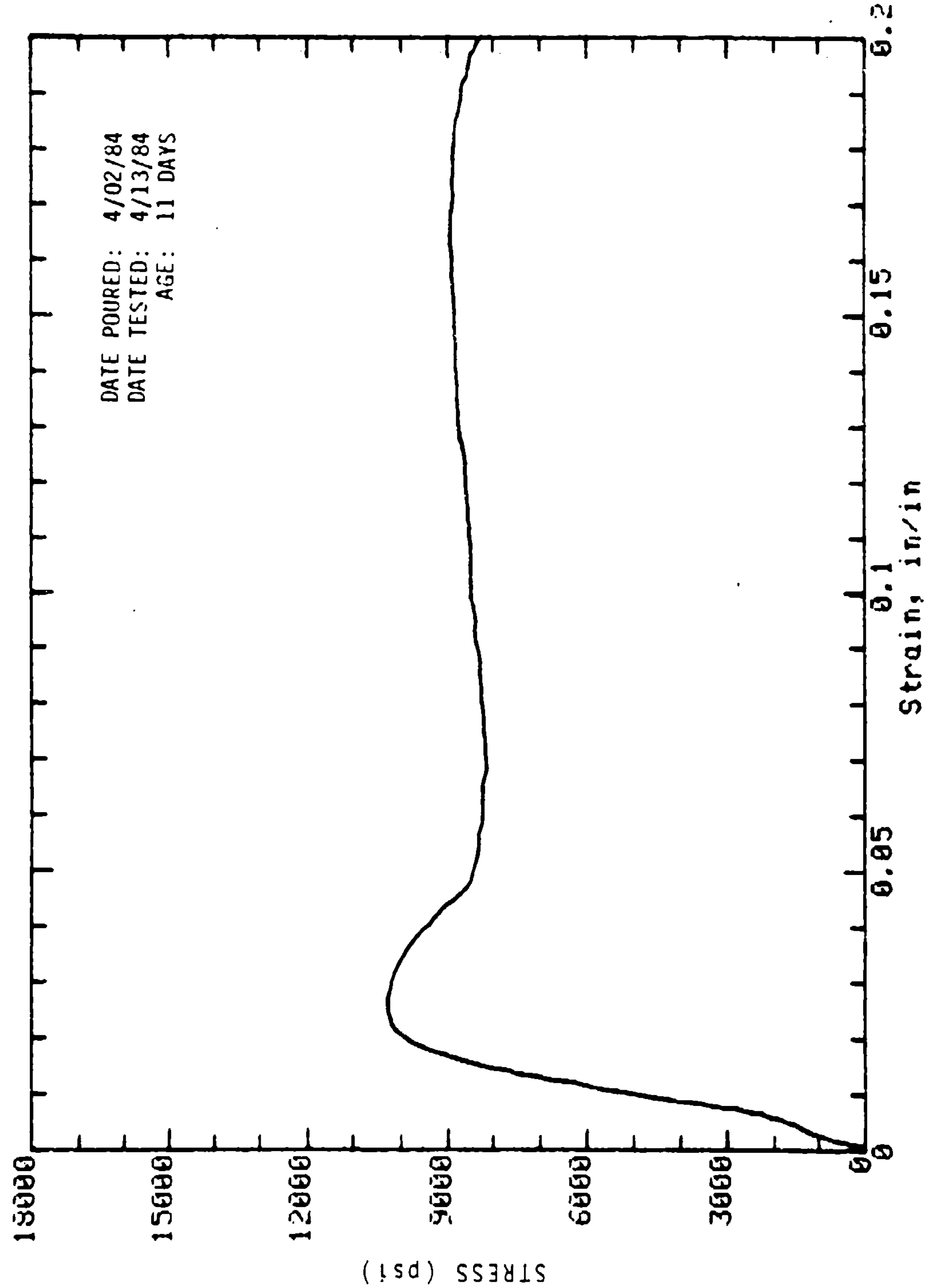

Mark: 10-S2-5 Cored (wall): 2in dia x 4in Cure: Dry
Concrete Sample

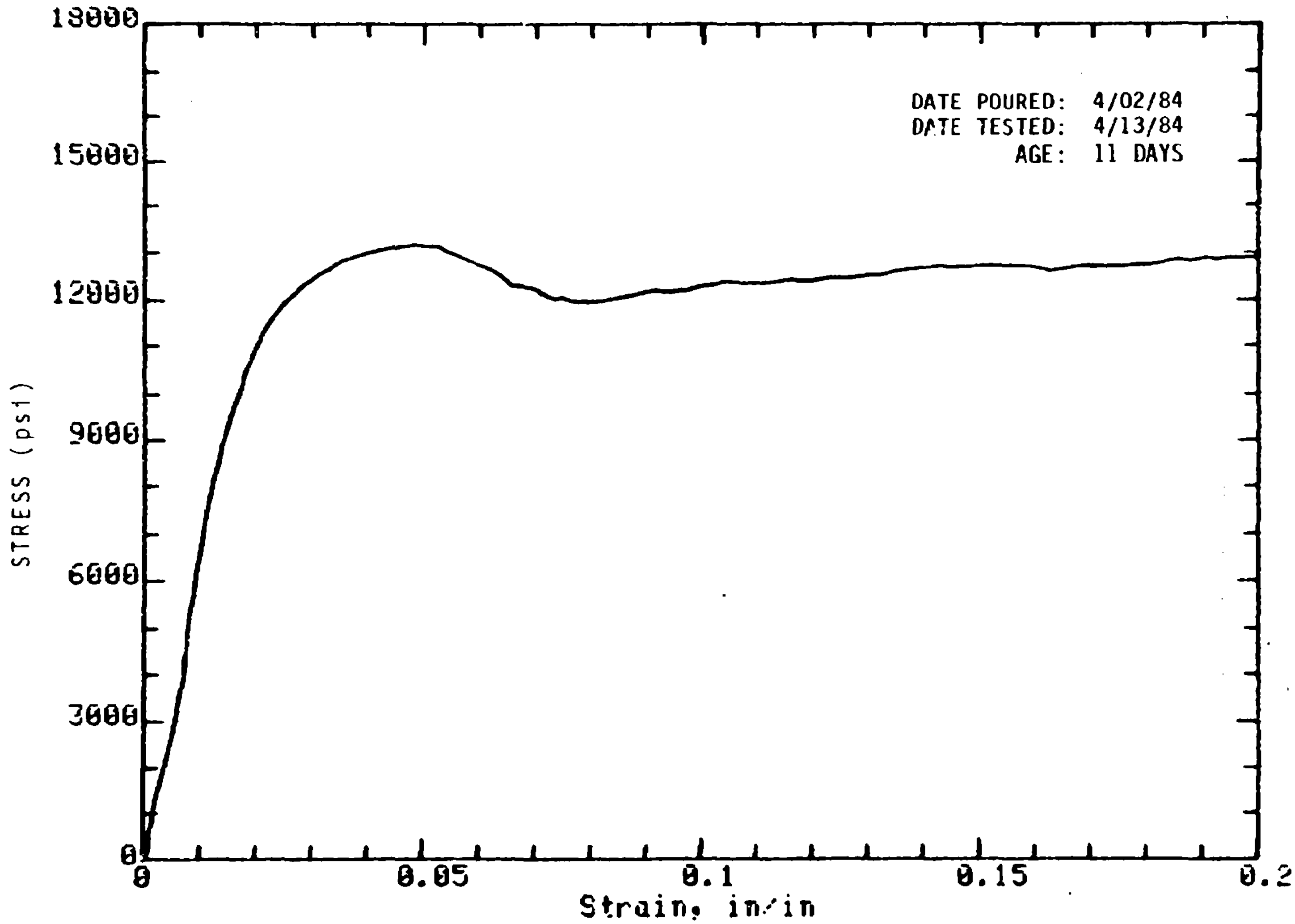

Mark: 10-S2-6 Cored (wall): 2in dia x 4in Cure: Dry
Concrete Sample

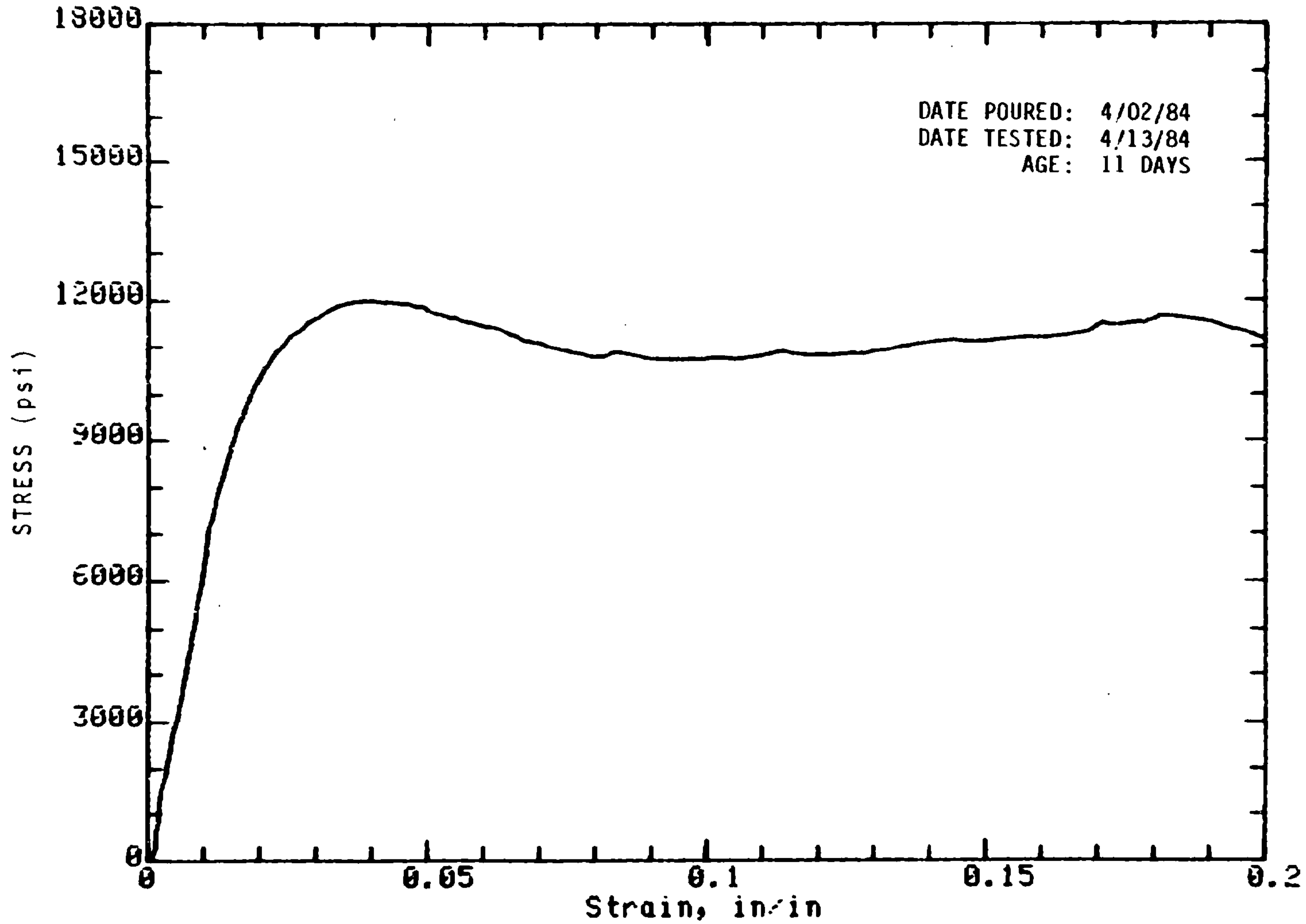

Mark: 10-S2-7 Cored (wall): 2in dia x 4in Cured: Dry
Concrete Sample

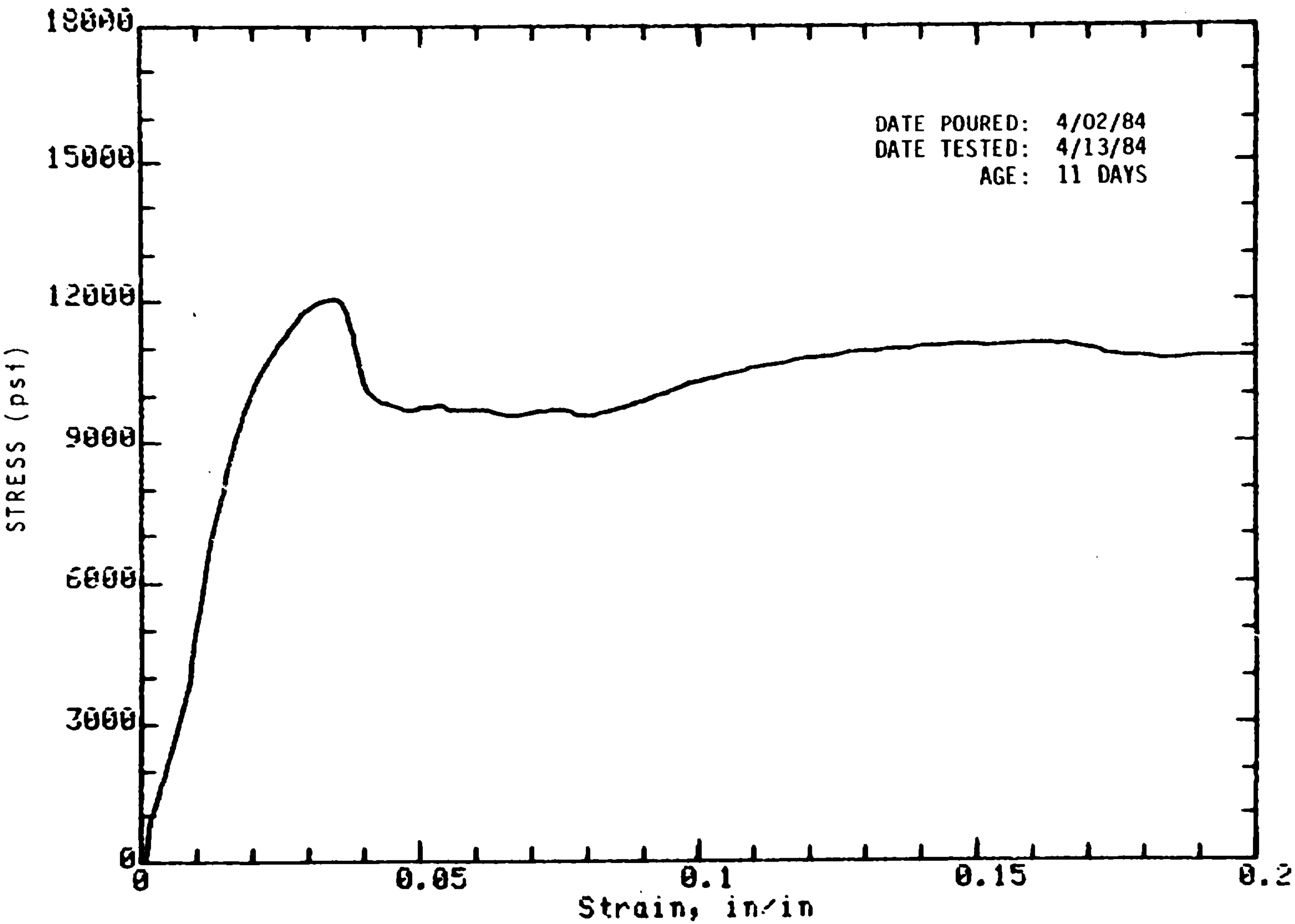

Mark: 10-52-8 Cored (wall): 2in dia x 4in Cured: Dry
Concrete Sample

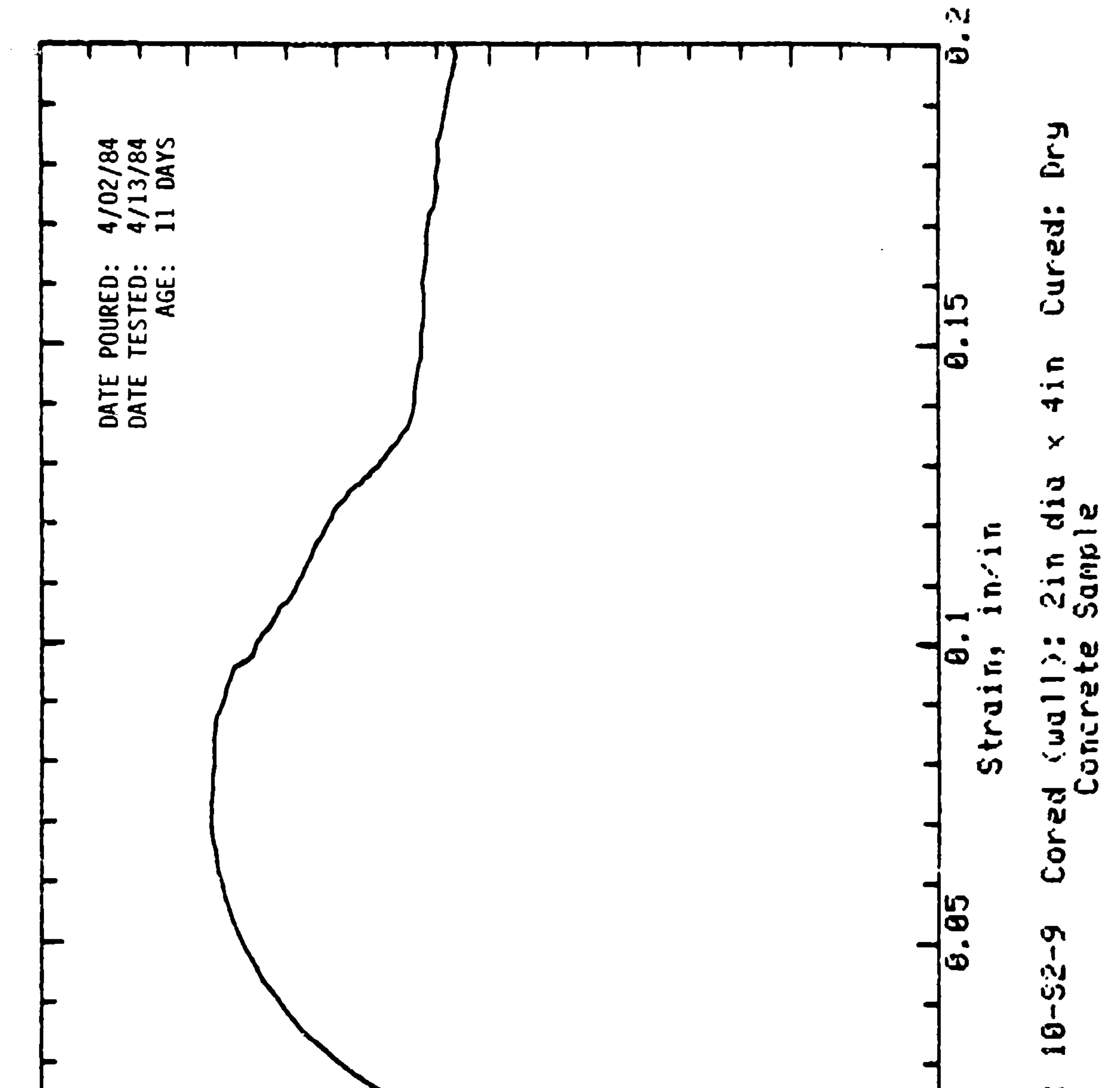
DATE POURED: 4/02/84
DATE TESTED: 4/13/84
AGE: 11 DAYS
STRESS (psi)
18000
15000
12000
9000
6000
3000
0
0
0.05
0.1
0.15
0.2
Strain, in/in
Mark: 10-S2-9 Cored (wall): 2in dia x 4in Cured: Dry
Concrete Sample

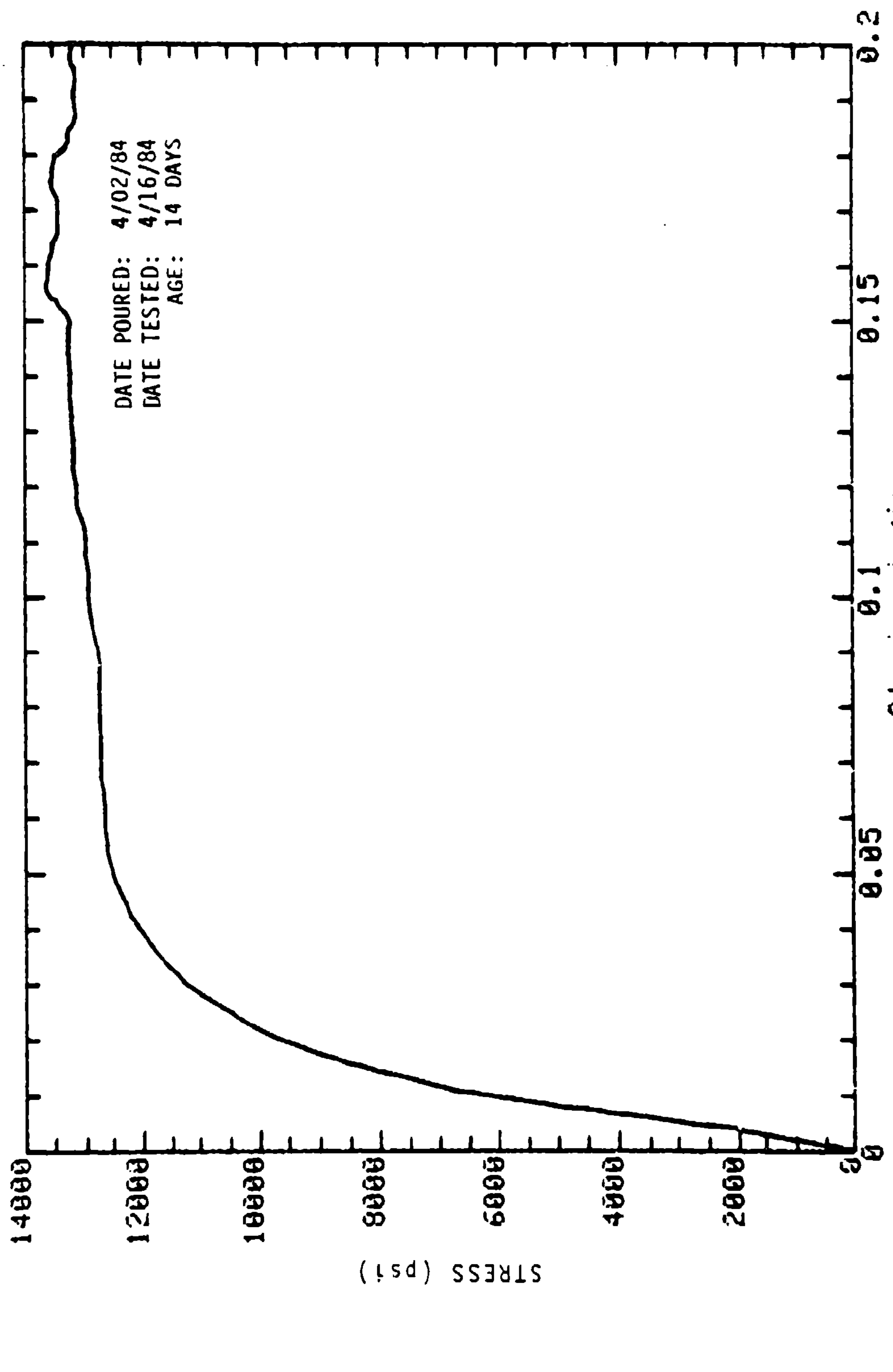

Mark: 10-S1-1 Cored (slab): 2in dia x 4in Cure: Wet
Concrete Sample

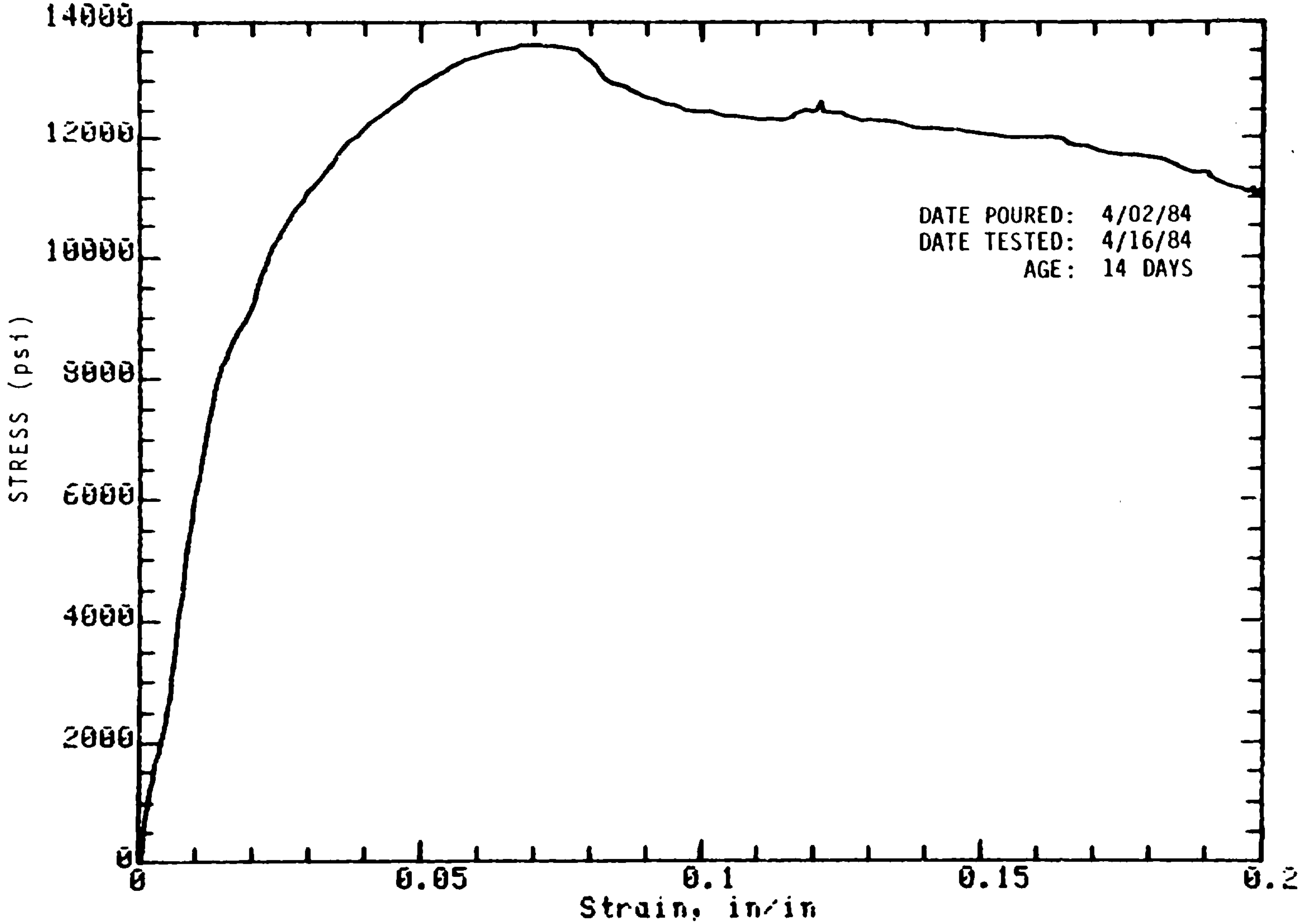

Mark: 10-S1-2 Cored (slab): 2in dia x 4in Cure: Wet
Concrete Sample

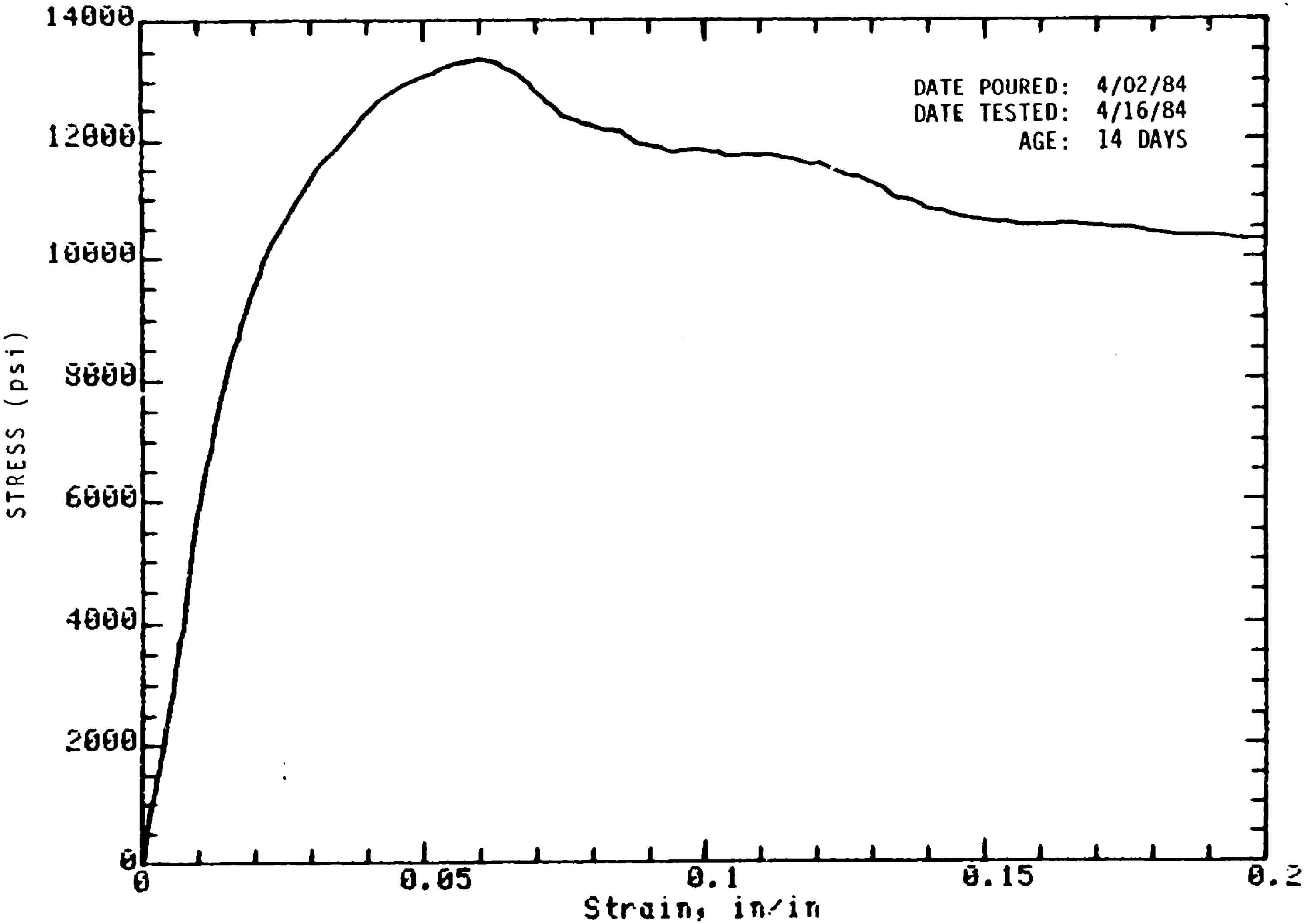

Mark: 10-S1-3 Cored (slab): 2in dia × 4in Cure: Wet
Concrete Sample

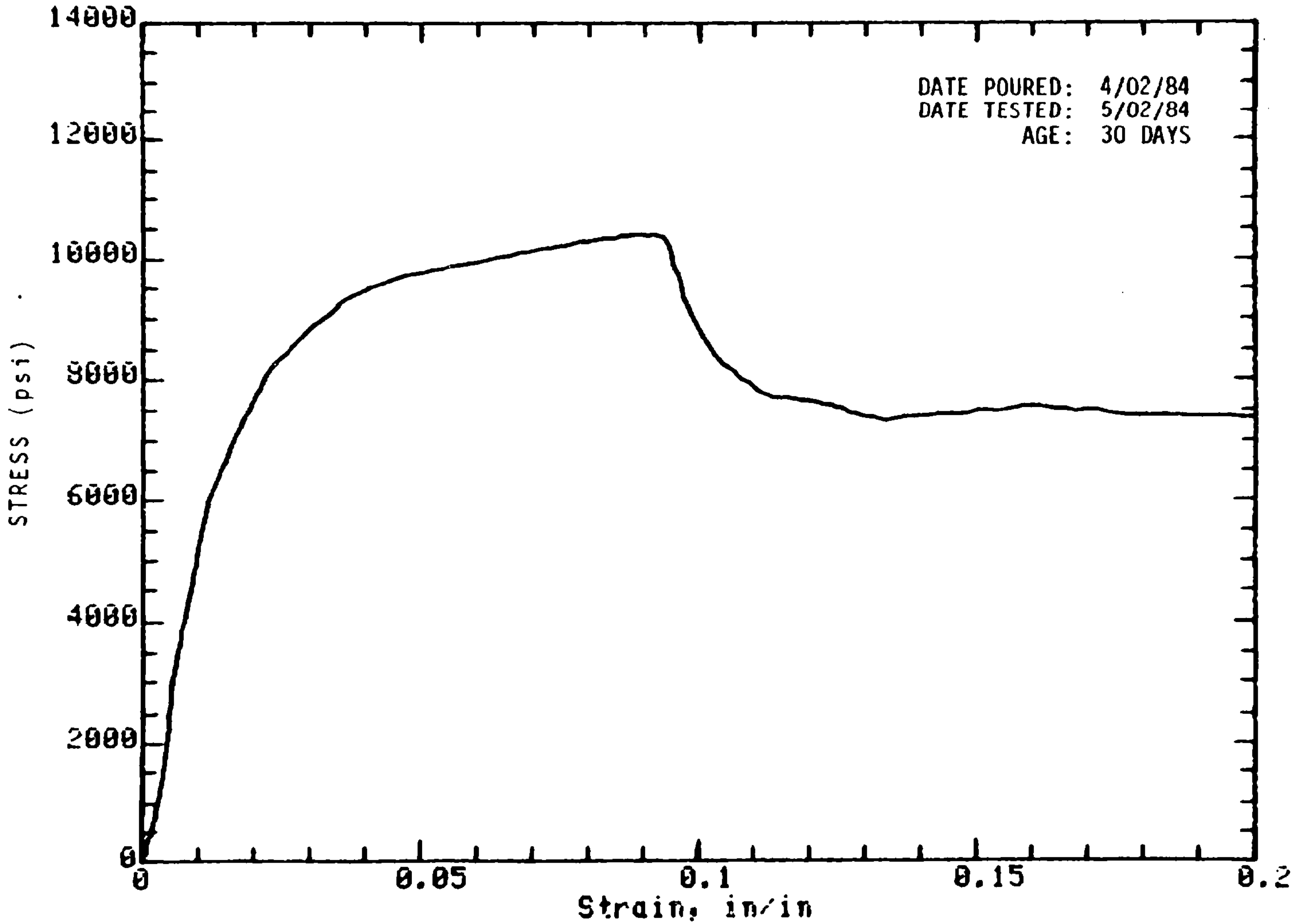

Mark: 10-9 Molded: 4in dia x 8in Cure: Dry
Concrete Sample

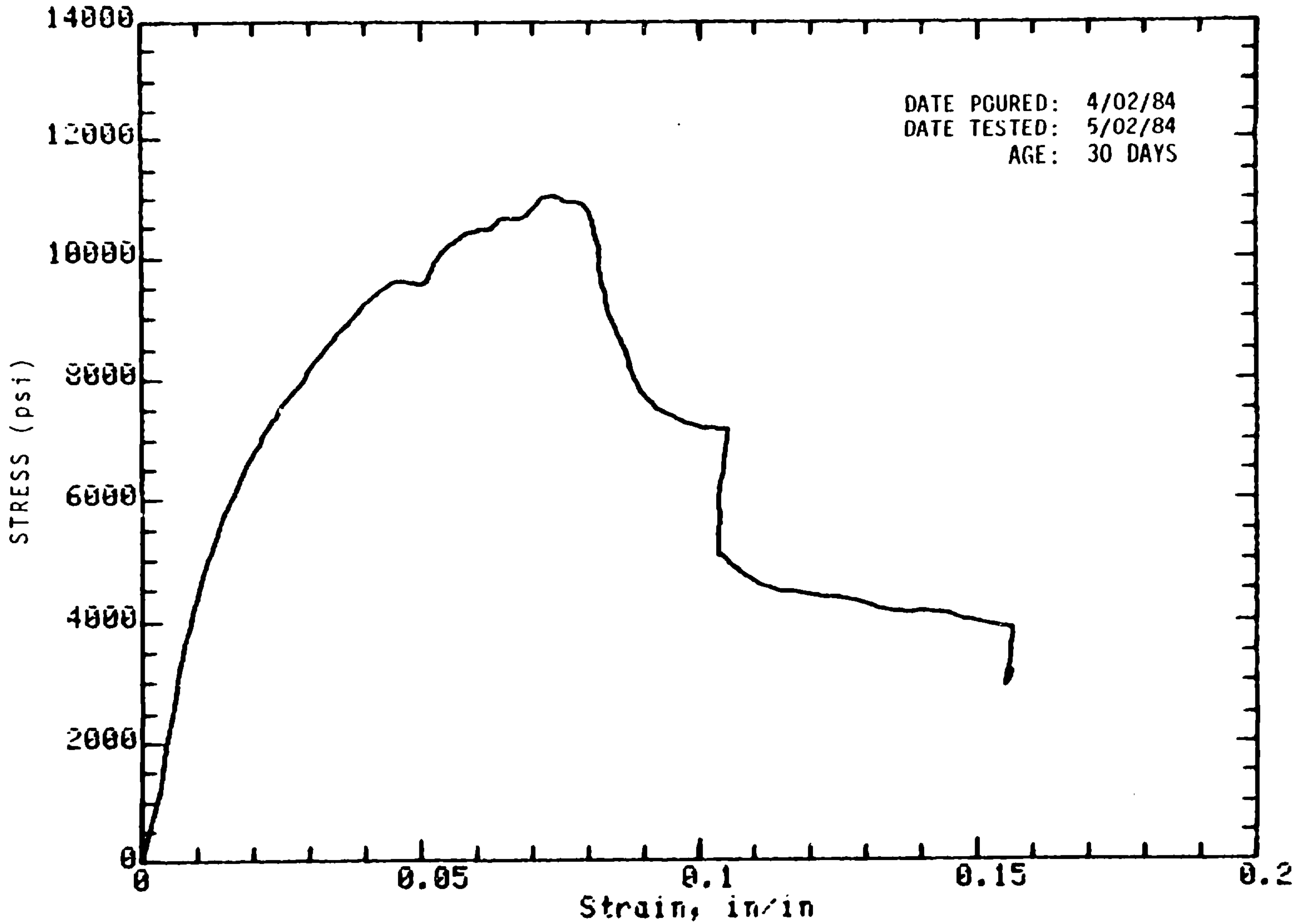

Mark: 10-10 Molded: 4in dia x 8in Cure: Dry
Concrete Sample

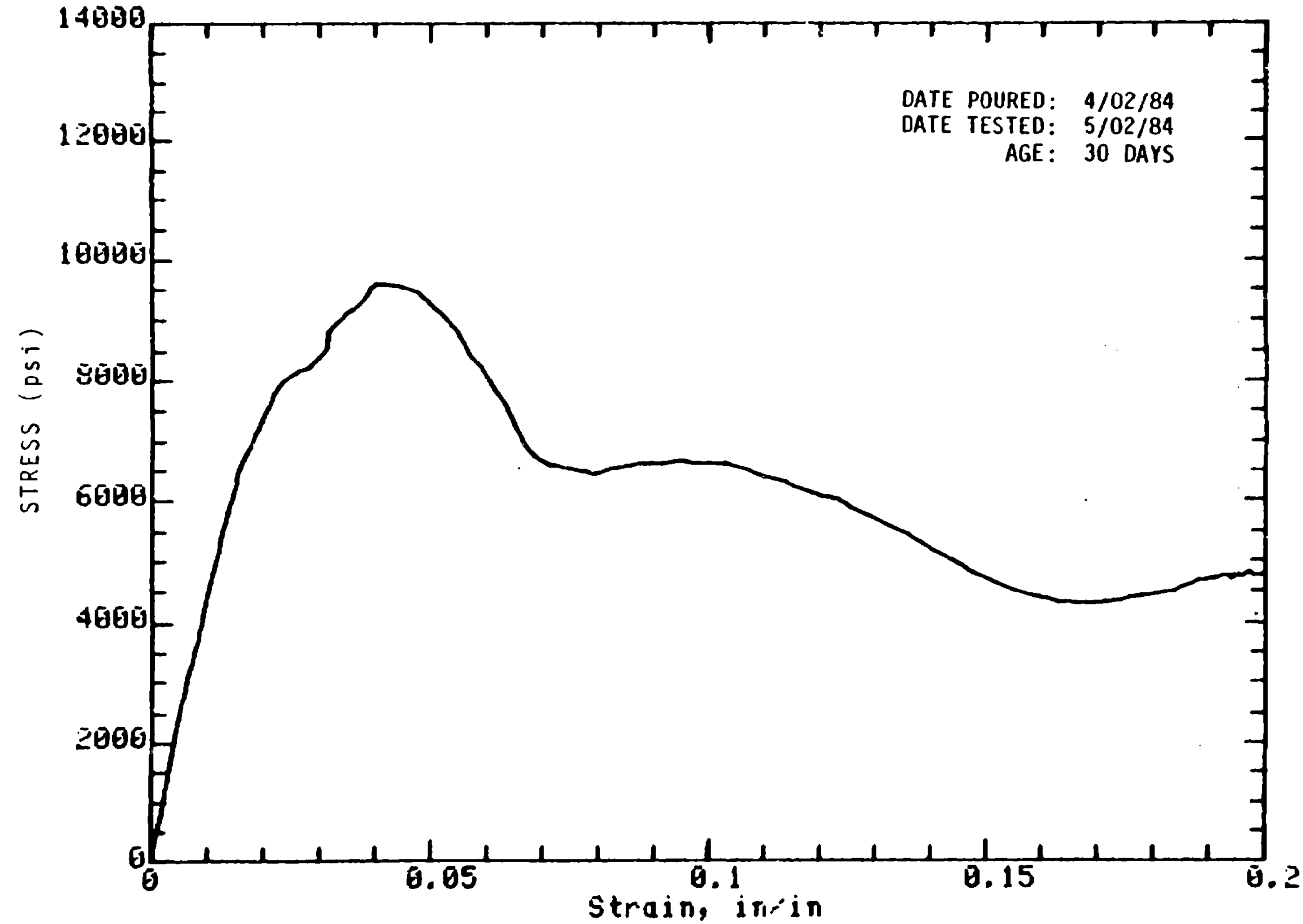

Mark: 10-13 Molded: 4in dia x 8in Cure: Wet
Concrete Sample

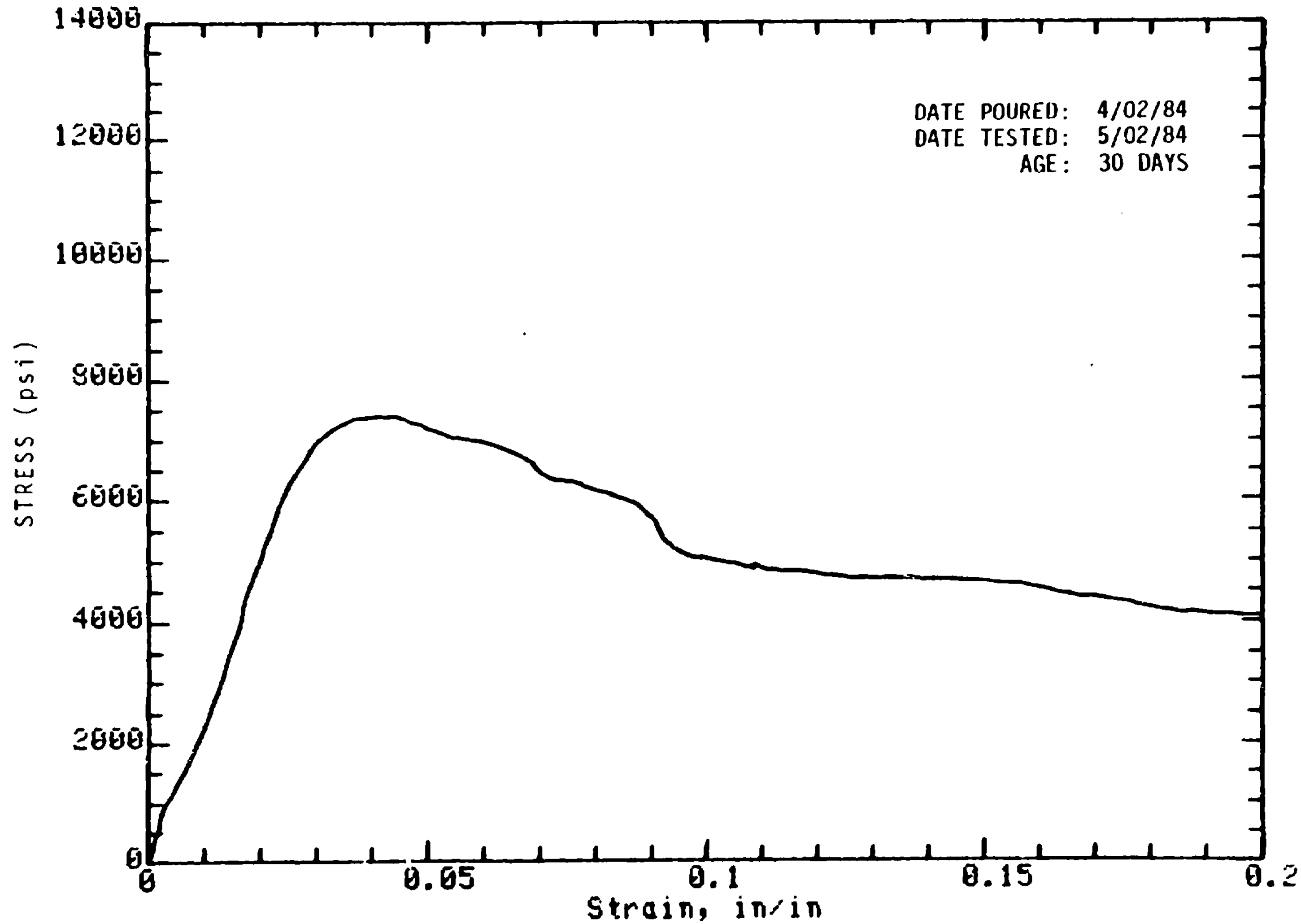

Mark: 10-16 Molded: 4in dia x 8in Cure: Wet
Concrete Sample

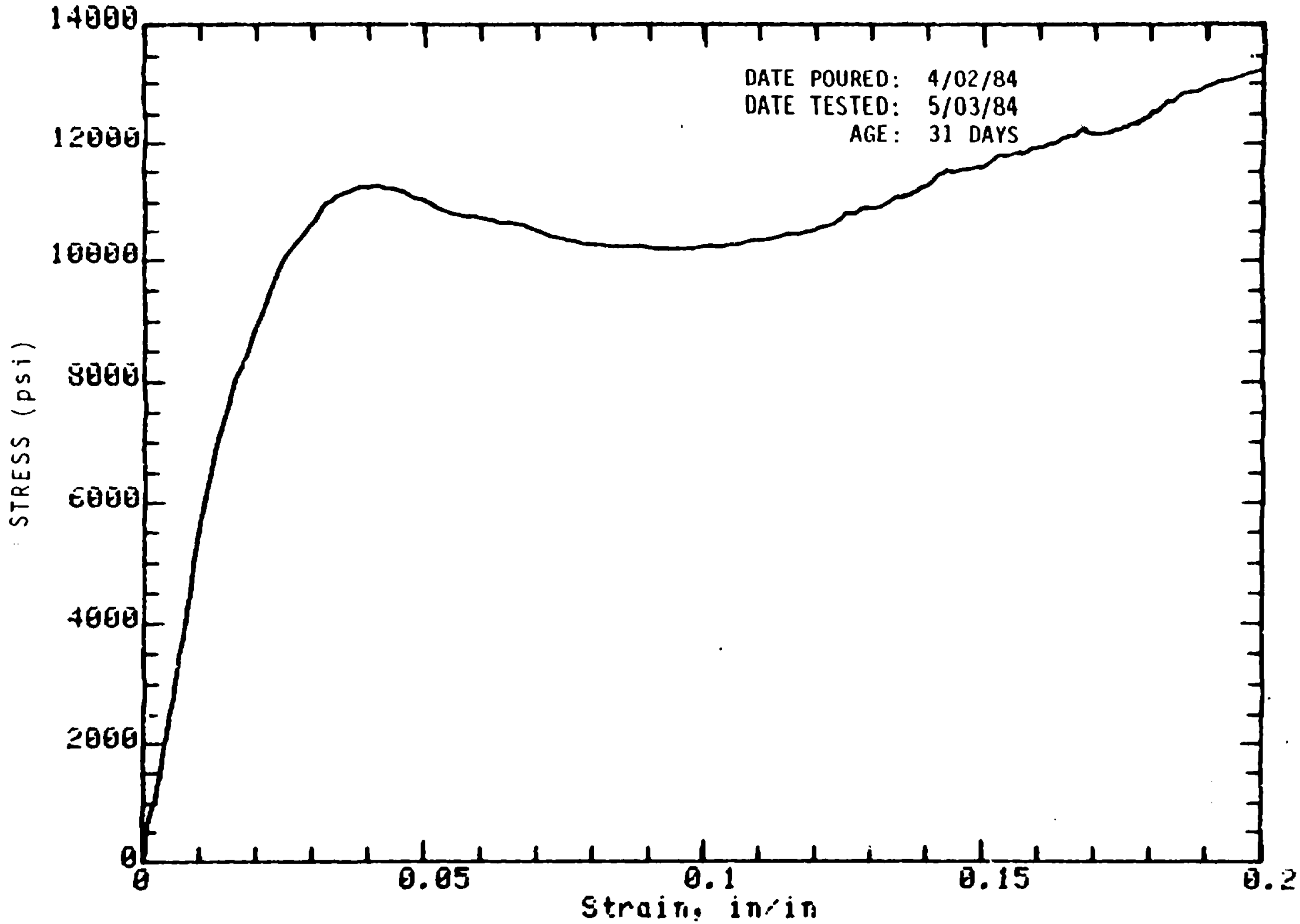

Mark: 10-S1-4 Cored (slab): 2in dia x 4in Cure: Wet
Concrete Sample

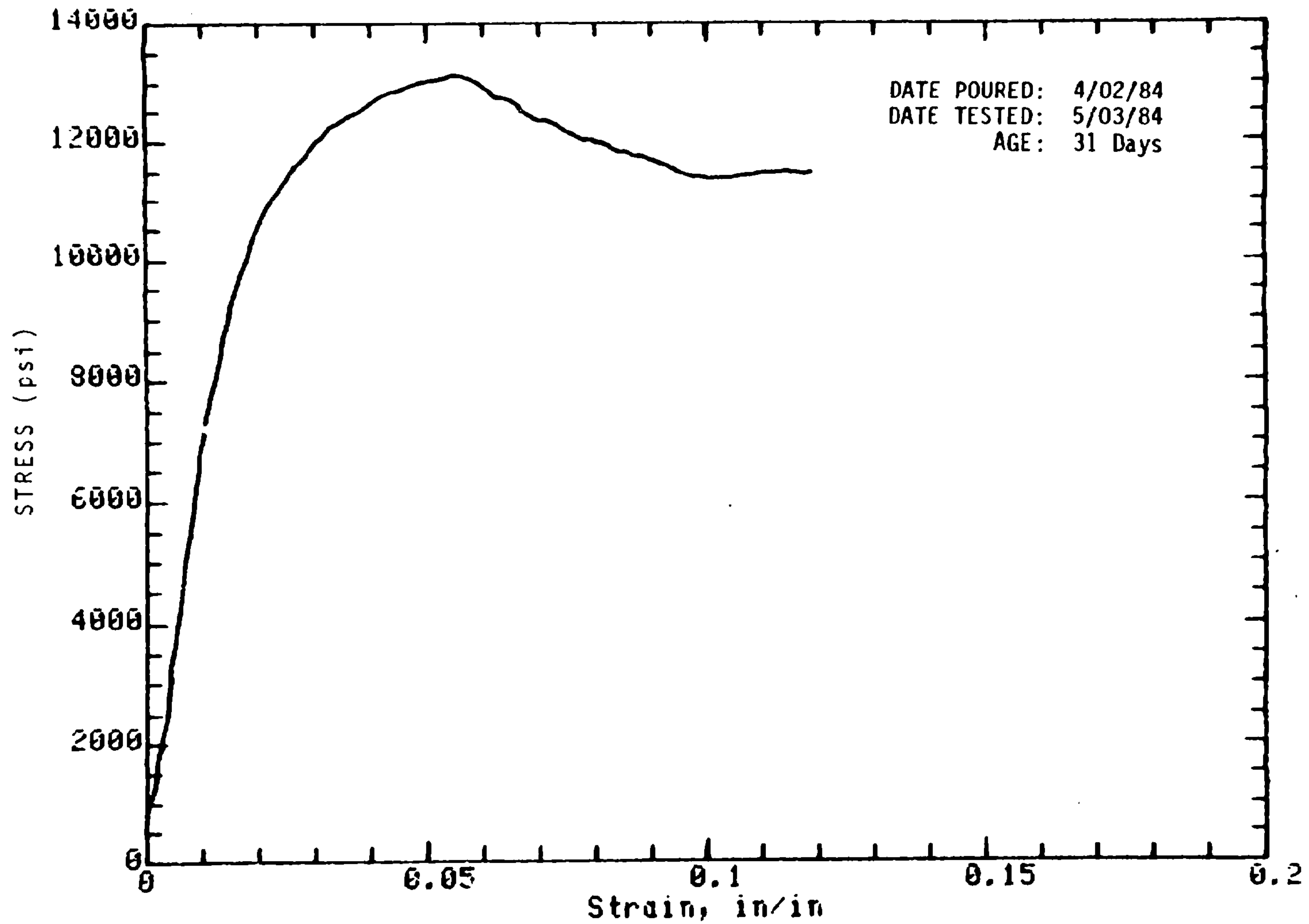

Mark: 10-S1-5 Cored (slab): 2in dia × 4in Cure: Wet
Concrete Sample

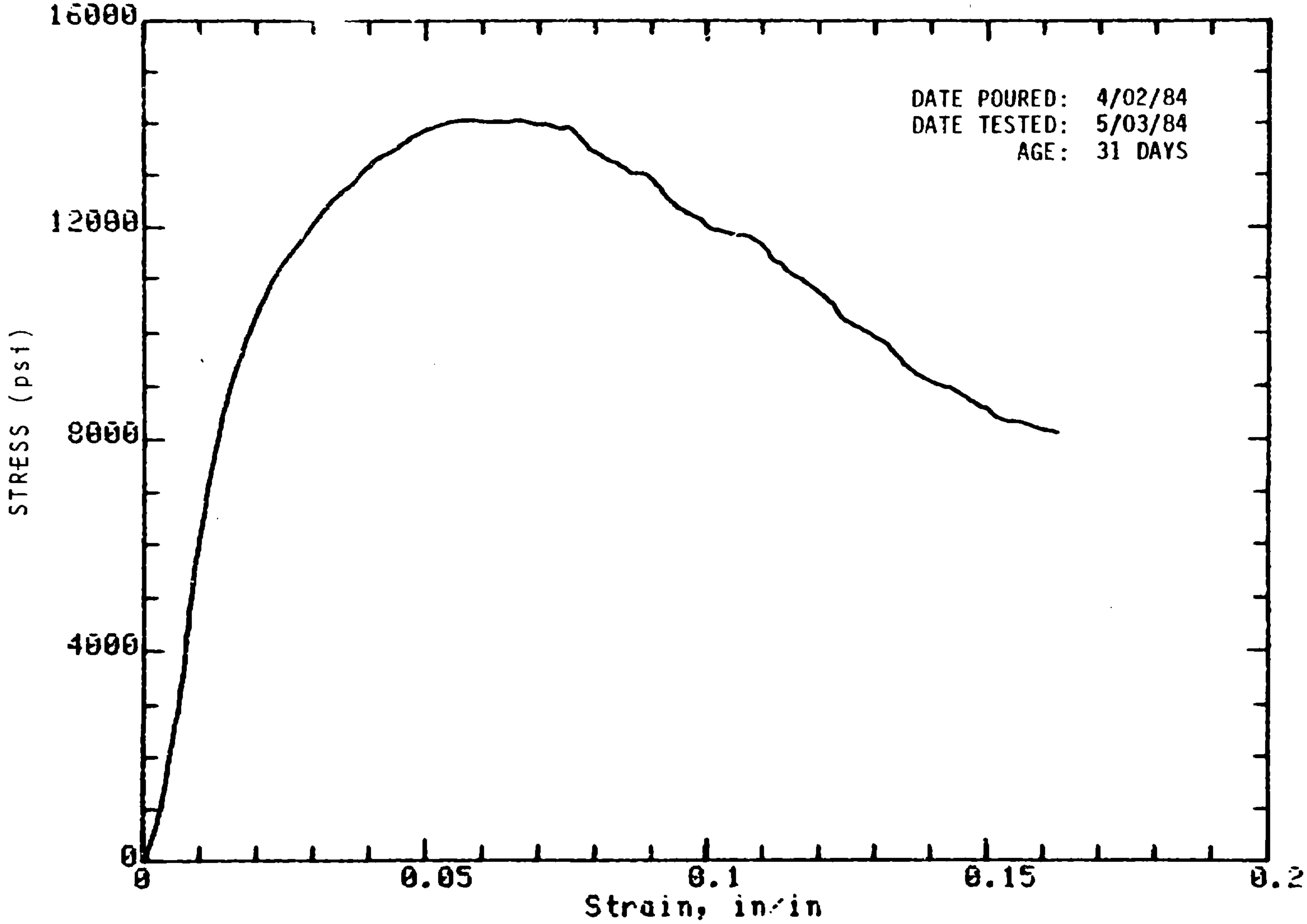

Mark: 10-S1-6 Cored (slab): 2in dia x 4in Cure: Wet
Concrete Sample

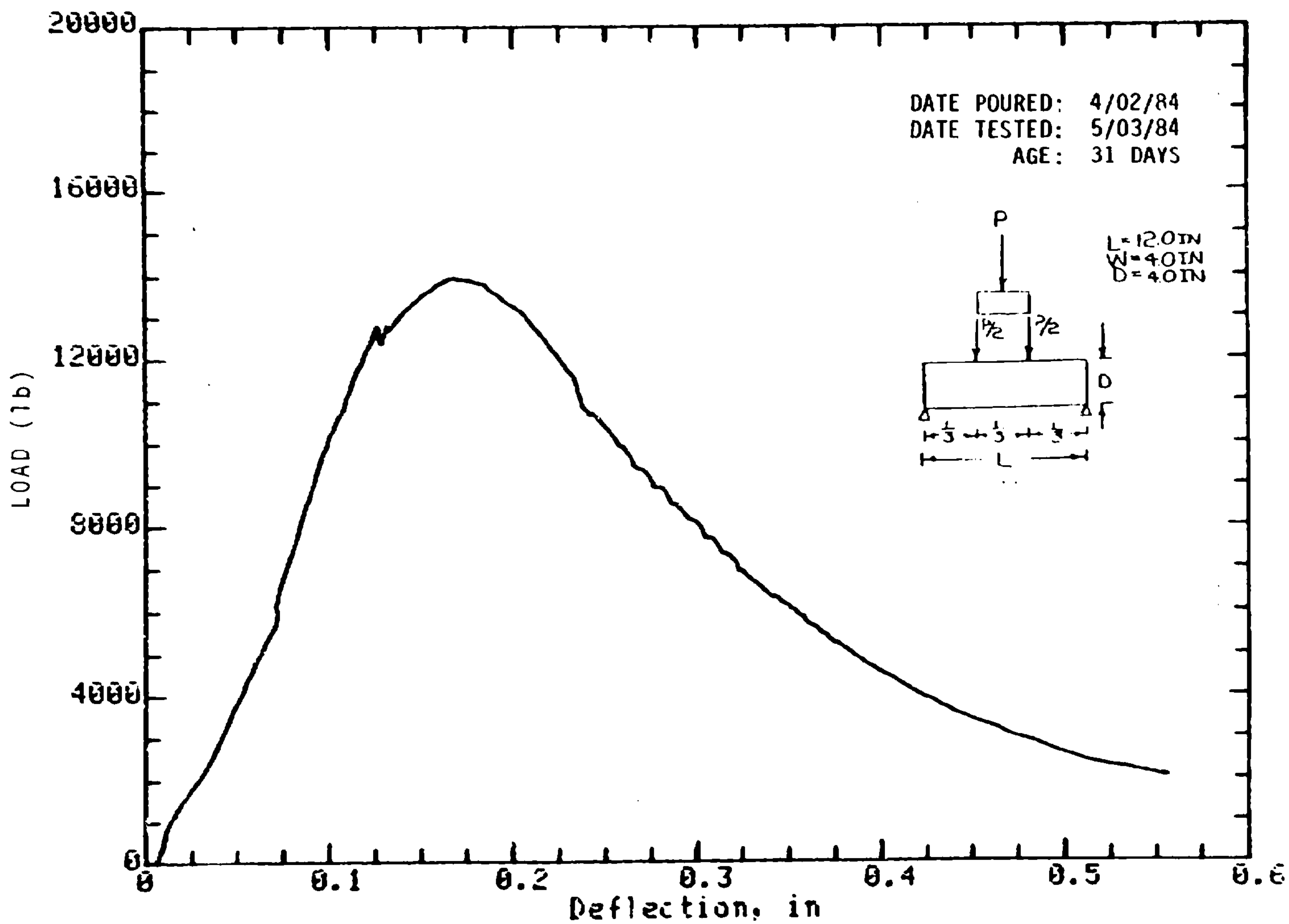

Mark: 10-25 Beam: 4in x 4in Cure: Dry
Concrete Sample

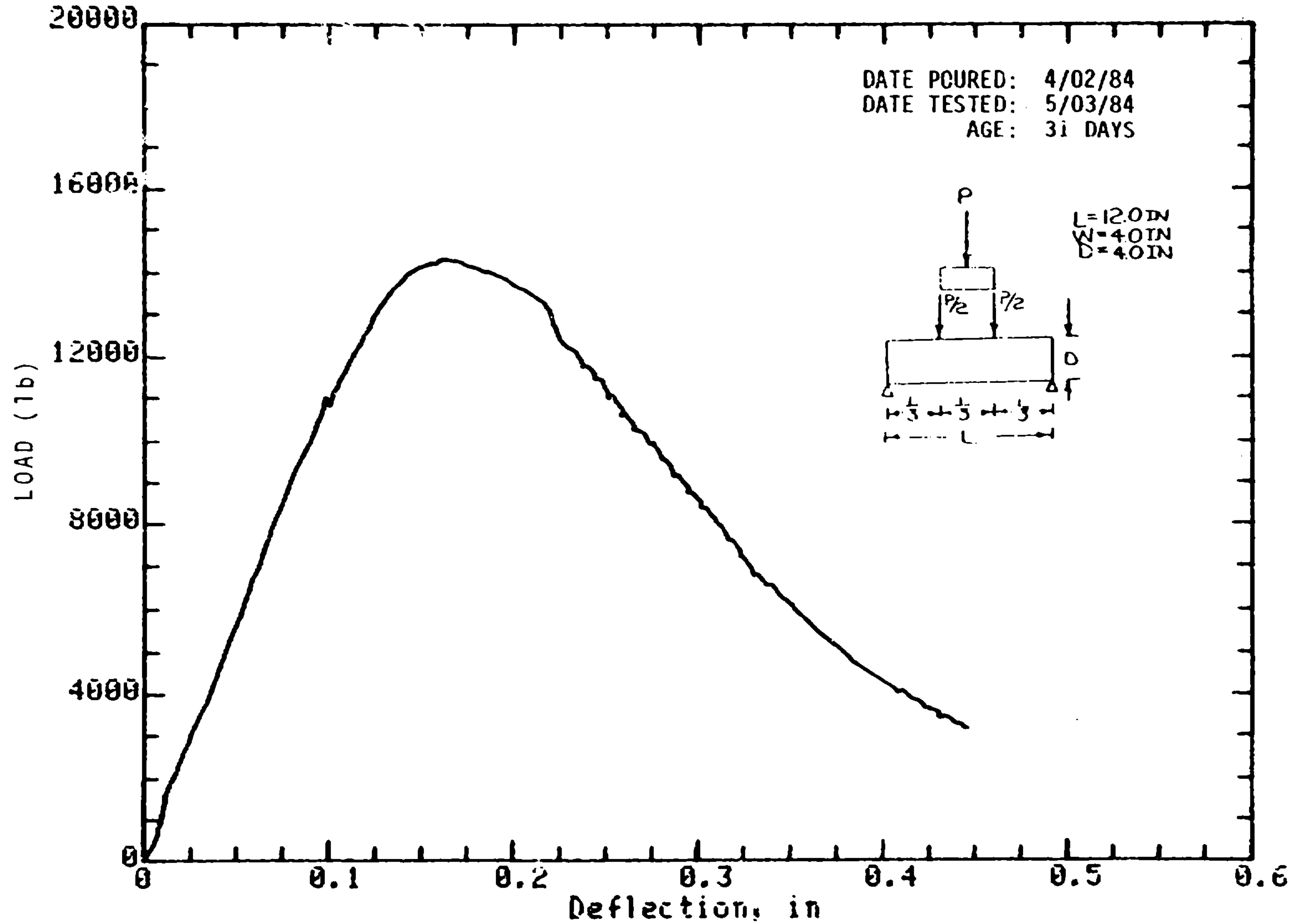

Mark: 10-27 Beam: 4in x 4in Cure: Dry
Concrete Sample

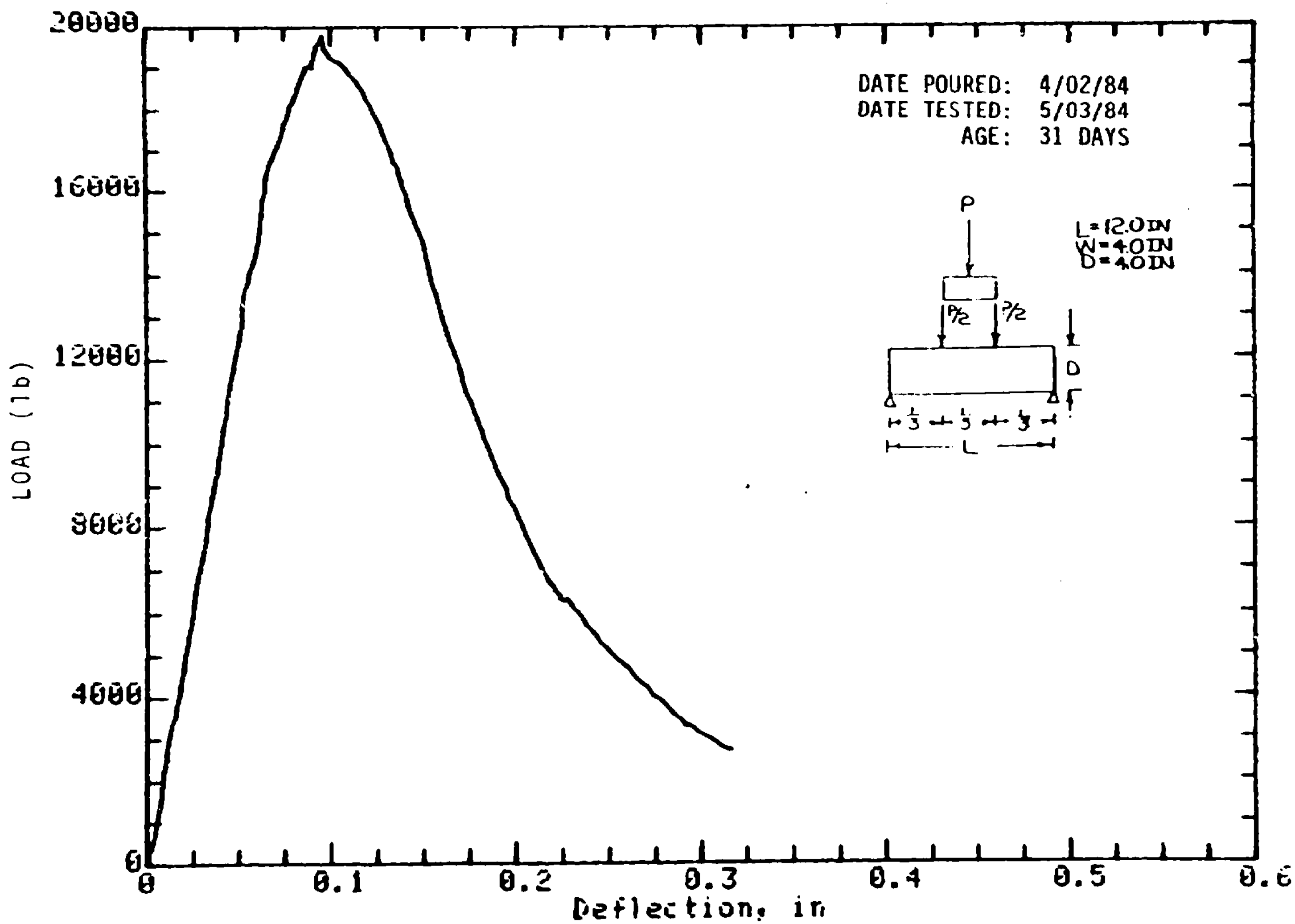

Mark: 10-28 Beam: 4in x 4in Cure: Wet
Concrete Sample

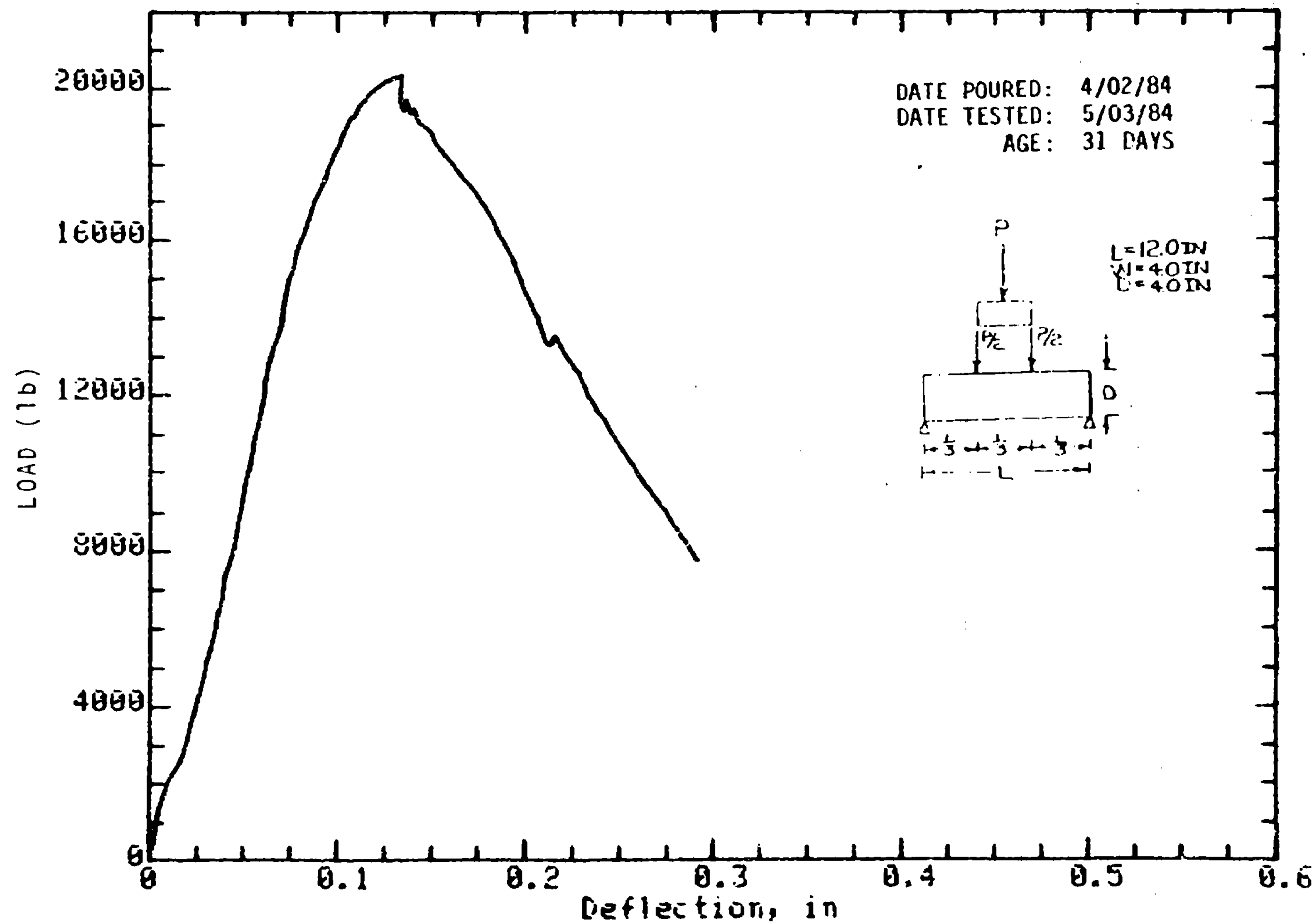

Mark: 10-29 Beam: 4in x 4in Cure: Wet
Concrete Sample

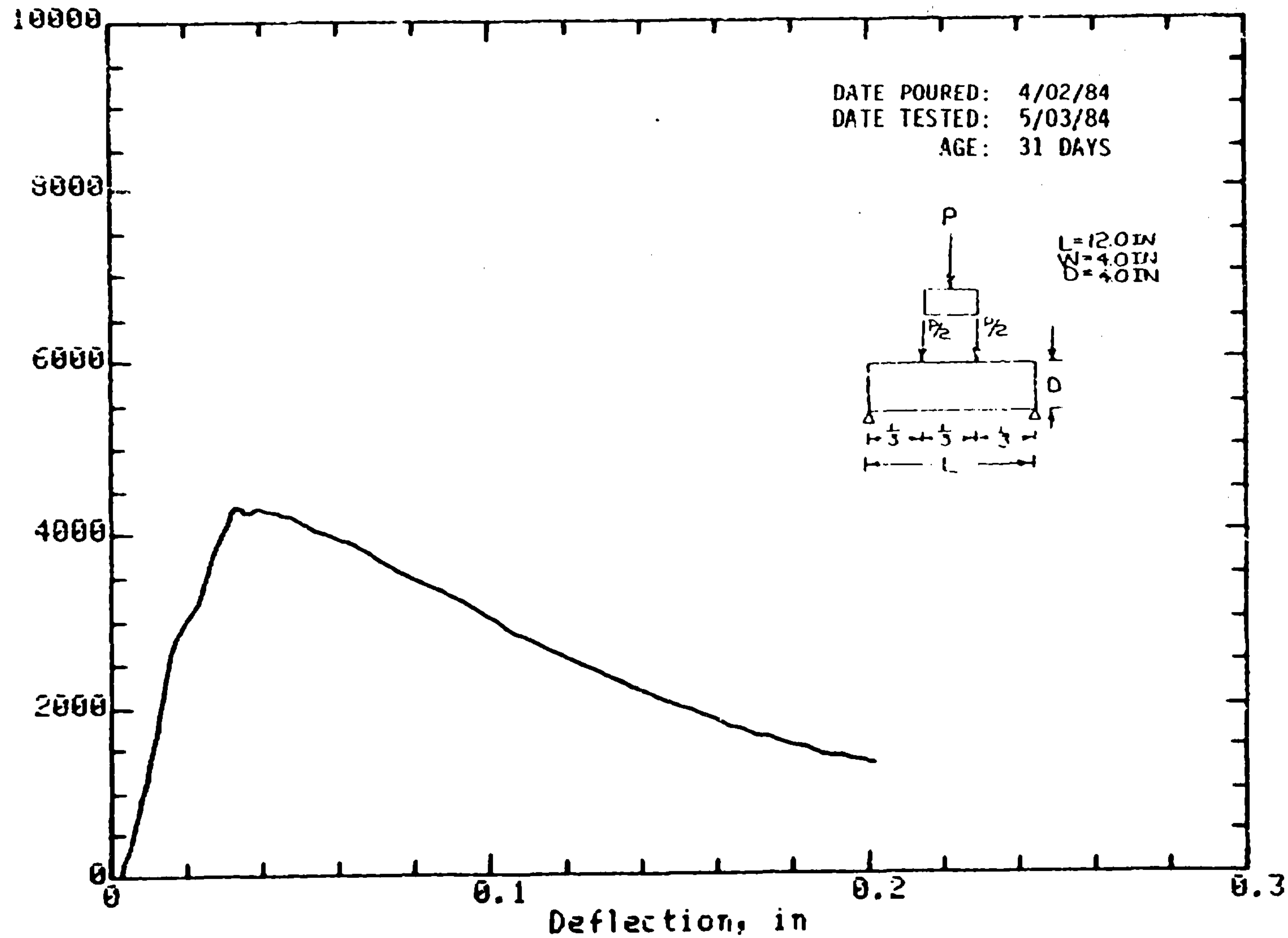

Mark: 10-33 Column: 4in x 4in Cure: Dry
Concrete Sample

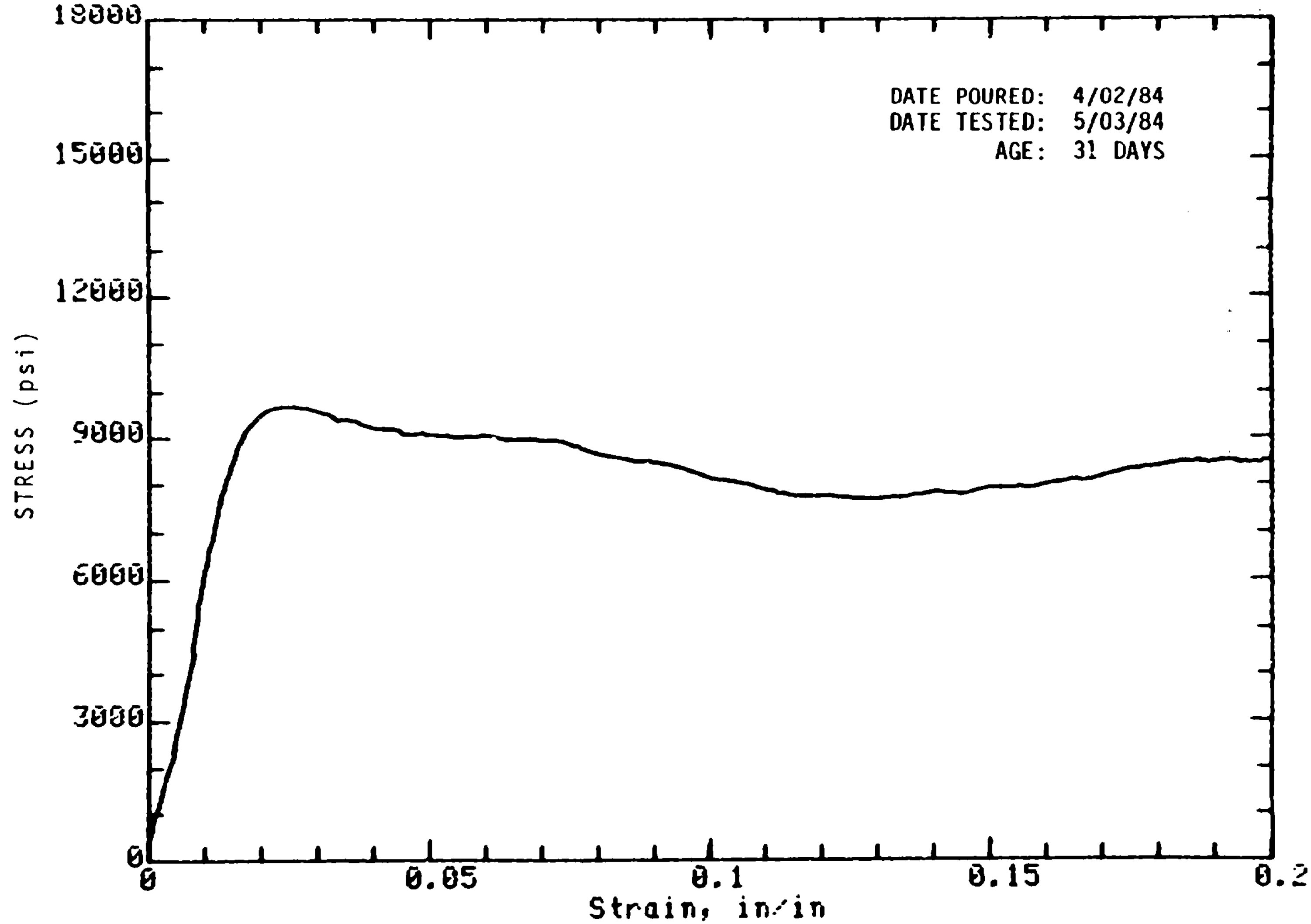

Mark: 10-S2-10 Cored (wall): 2in dia x 4in Cure: Dry
Concrete Sample

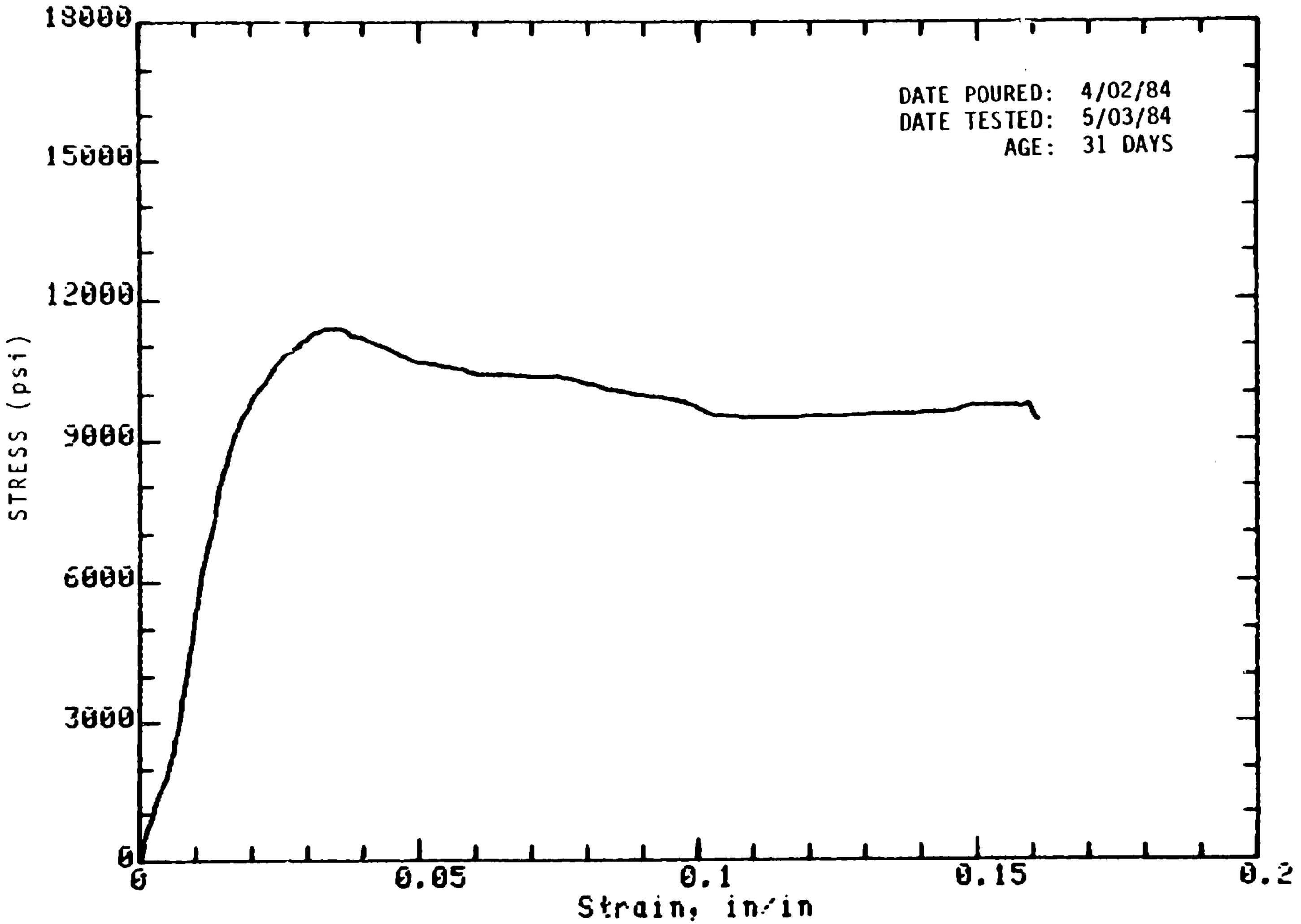

Mark: 10-S2-11 Cored (wall): 2in dia x 4in Cure: Dry
Concrete Sample

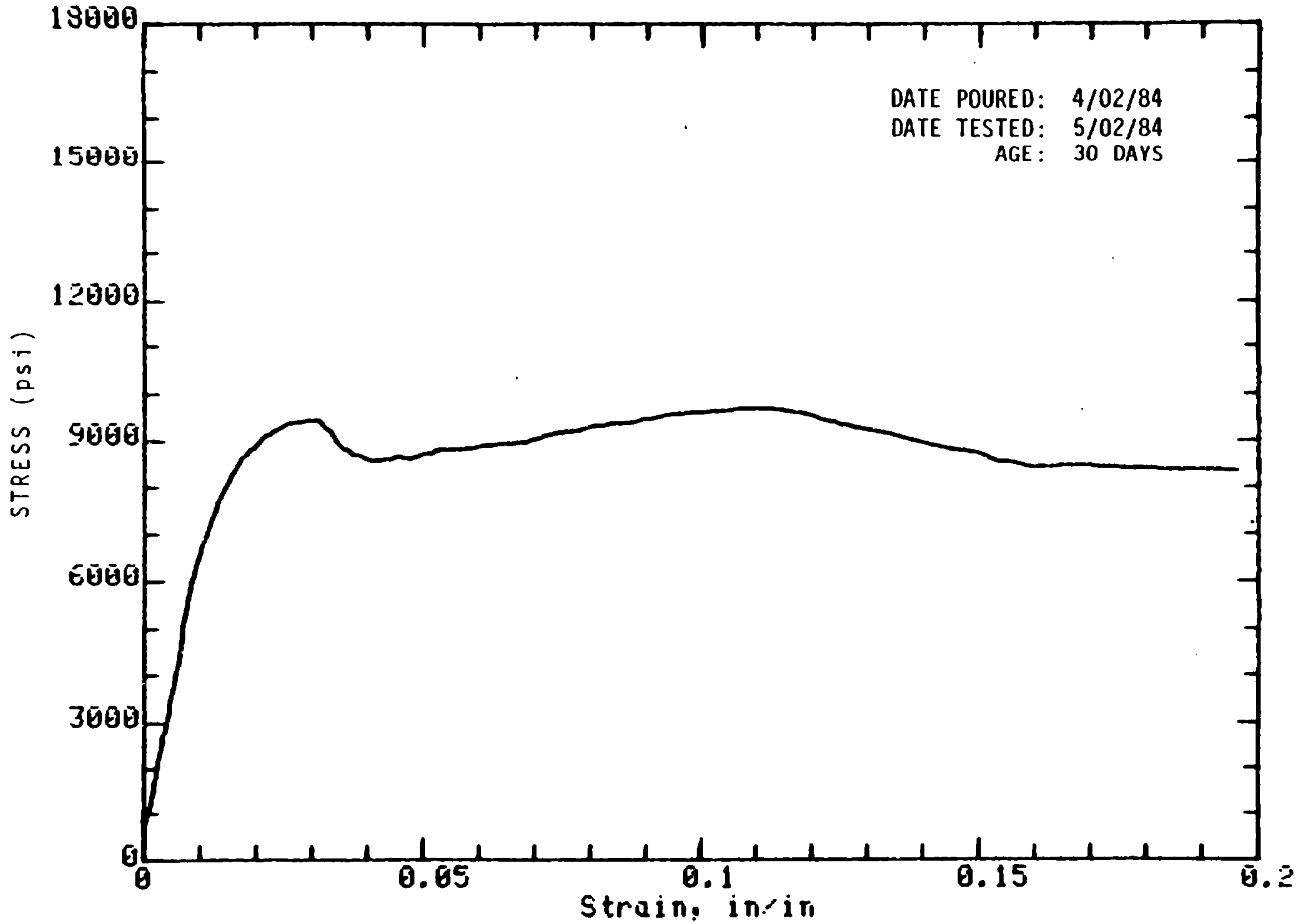

Mark: 10-S2-12 Cored (wall): 2in dia × 4in Cure: Dry
Concrete Sample

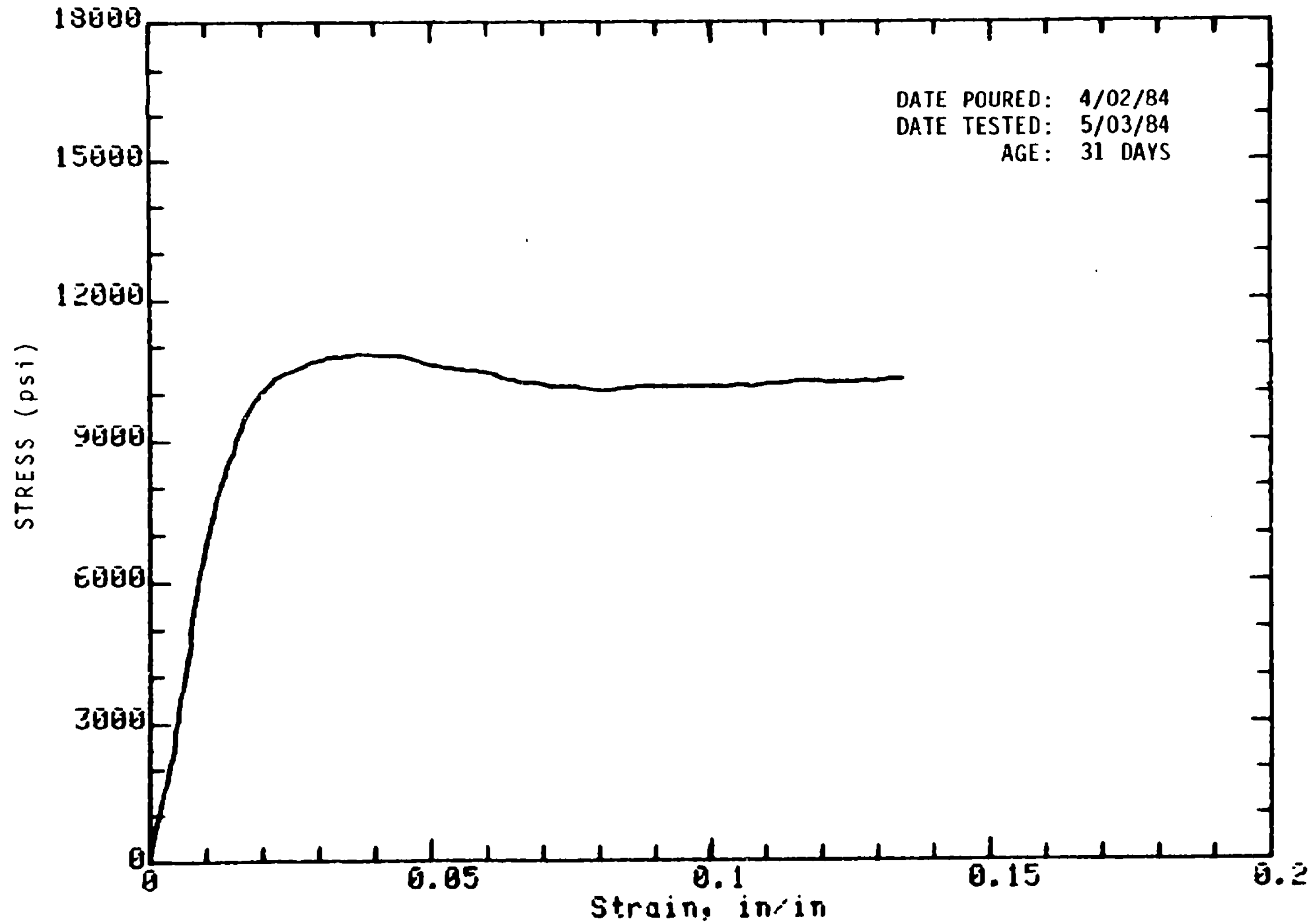

Mark: 10-S2-13 Cored (wall): 2in dia x 4in Cure: Dry
Concrete Sample

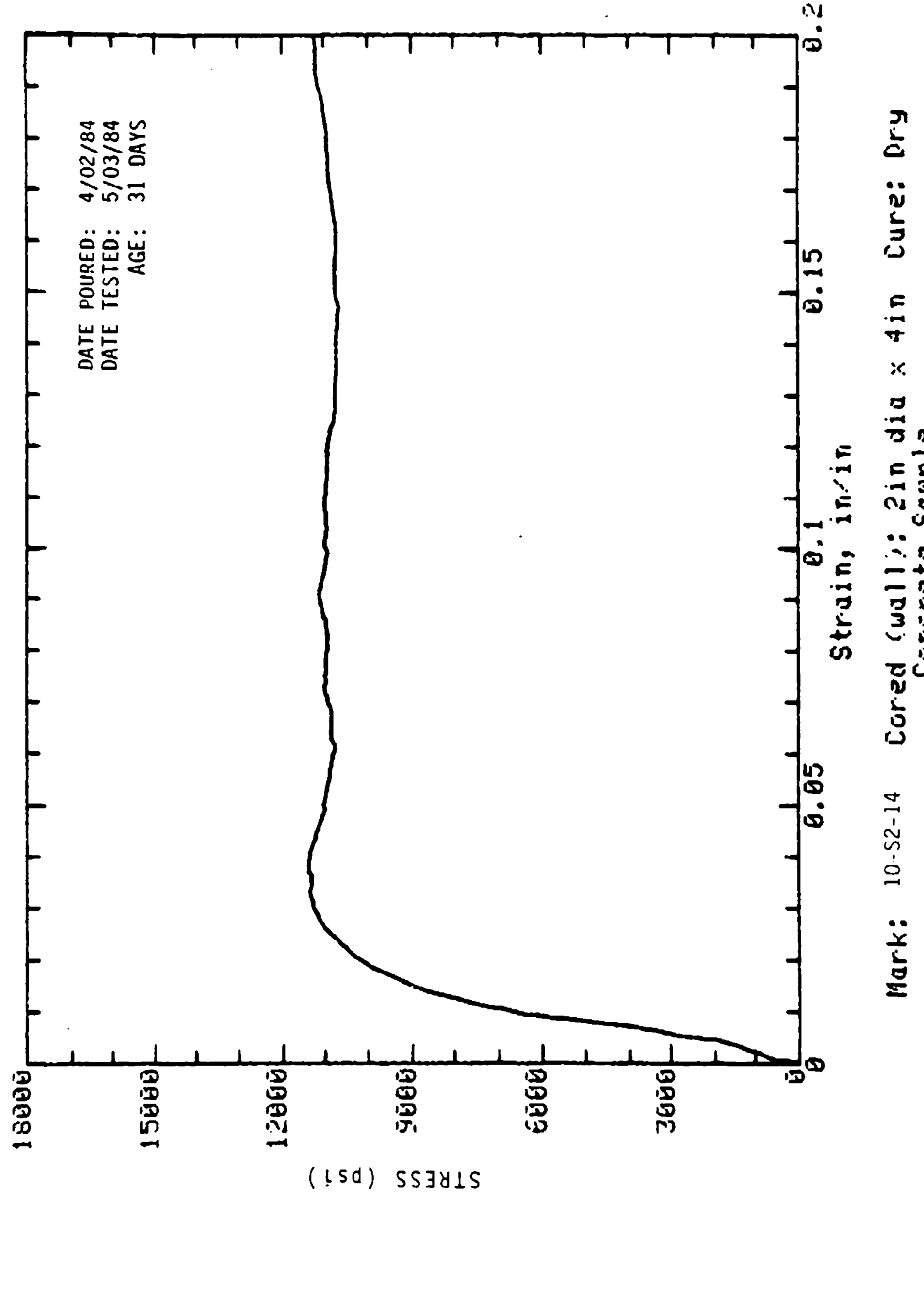
DATE POURED: 4/02/84
DATE TESTED: 5/03/84
AGE: 31 DAYS
STRESS (psi)
0
3000
6000
9000
12000
15000
18000
0
0.05
0.1
0.15
0.2
Strain, in/in
Mark: 10-S2-14 Cored (wall); 2in dia x 4in Cure: Dry
Concrete Sample

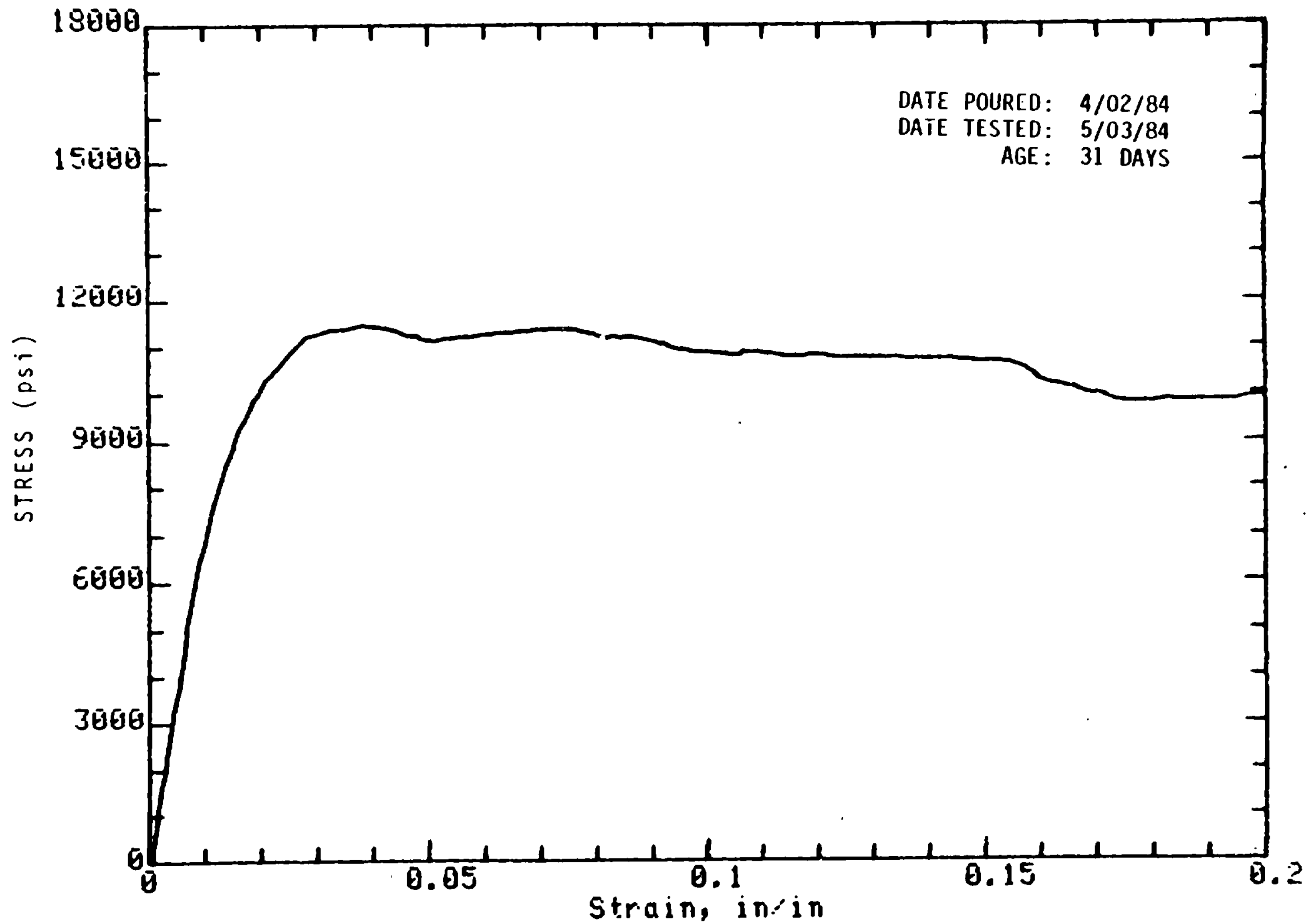

Mark: 10-S2-15 Cored (wall): 2in dia × 4in Cure: Dry
Concrete Sample

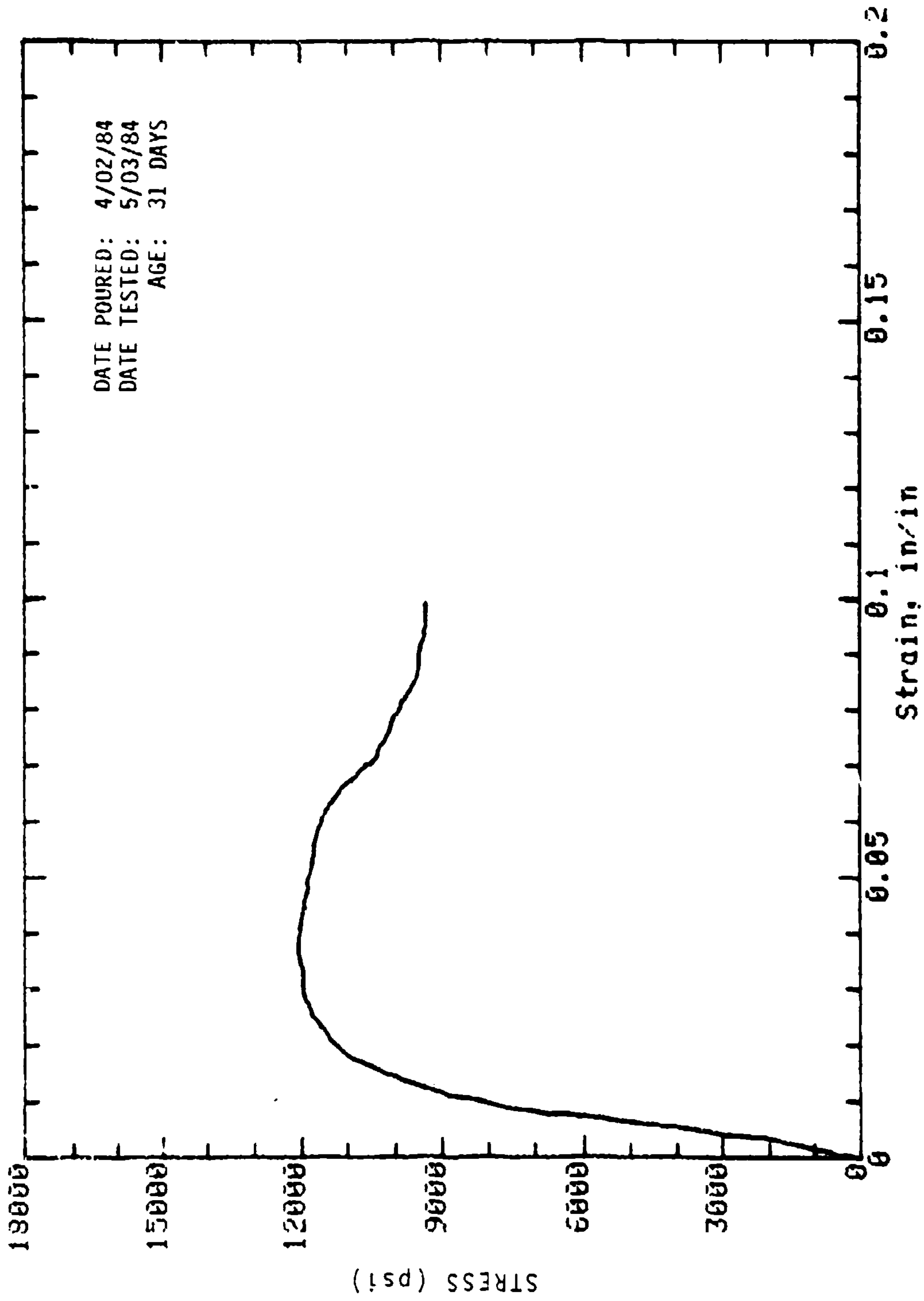

Mark: 10-S2-16 Cored (wall): 2in dia × 4in Cure: Dry
Concrete Sample

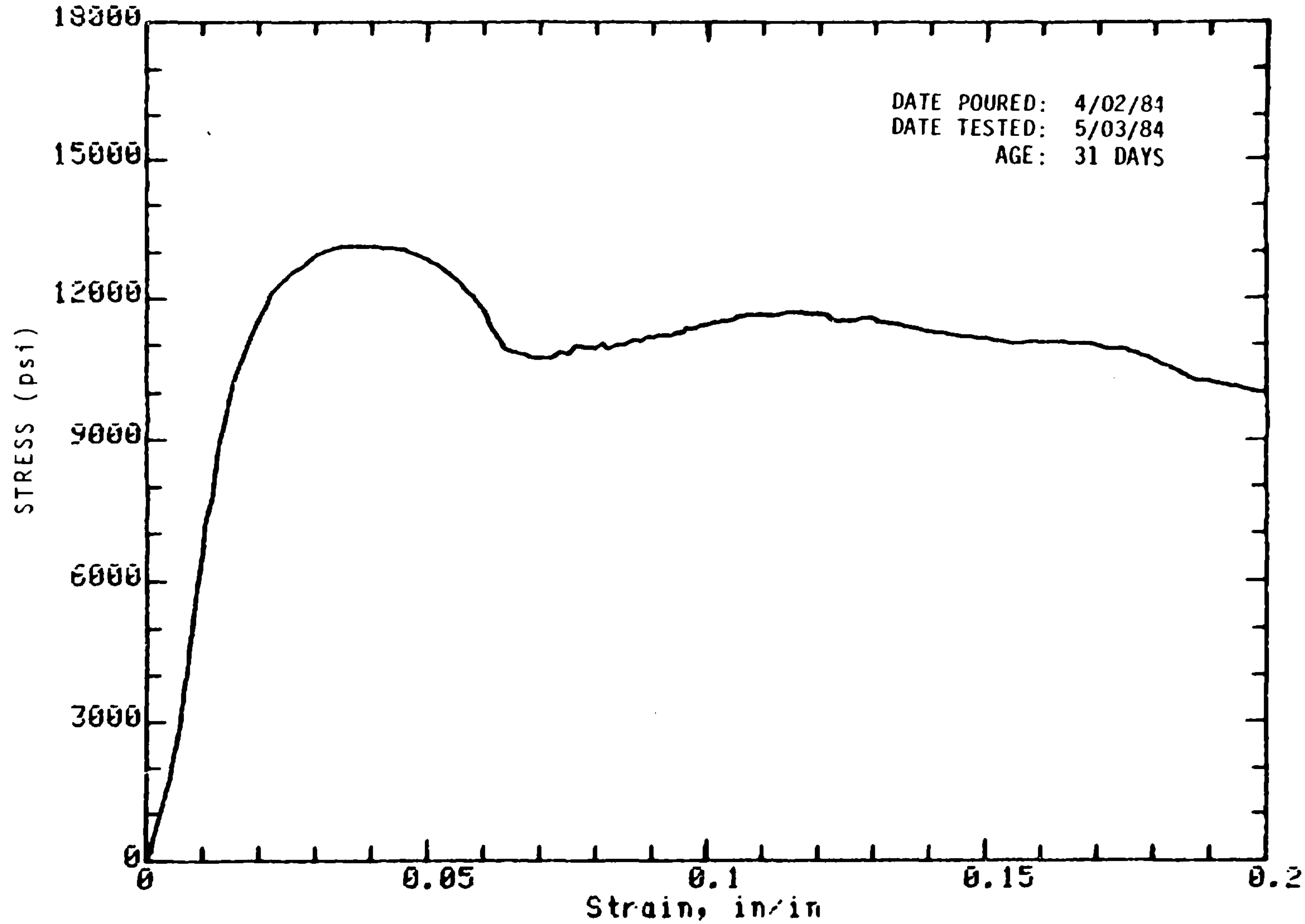

Mark: 10-S2-17 Cored (wall): 2in dia x 4in Cure: Dry
Concrete Sample

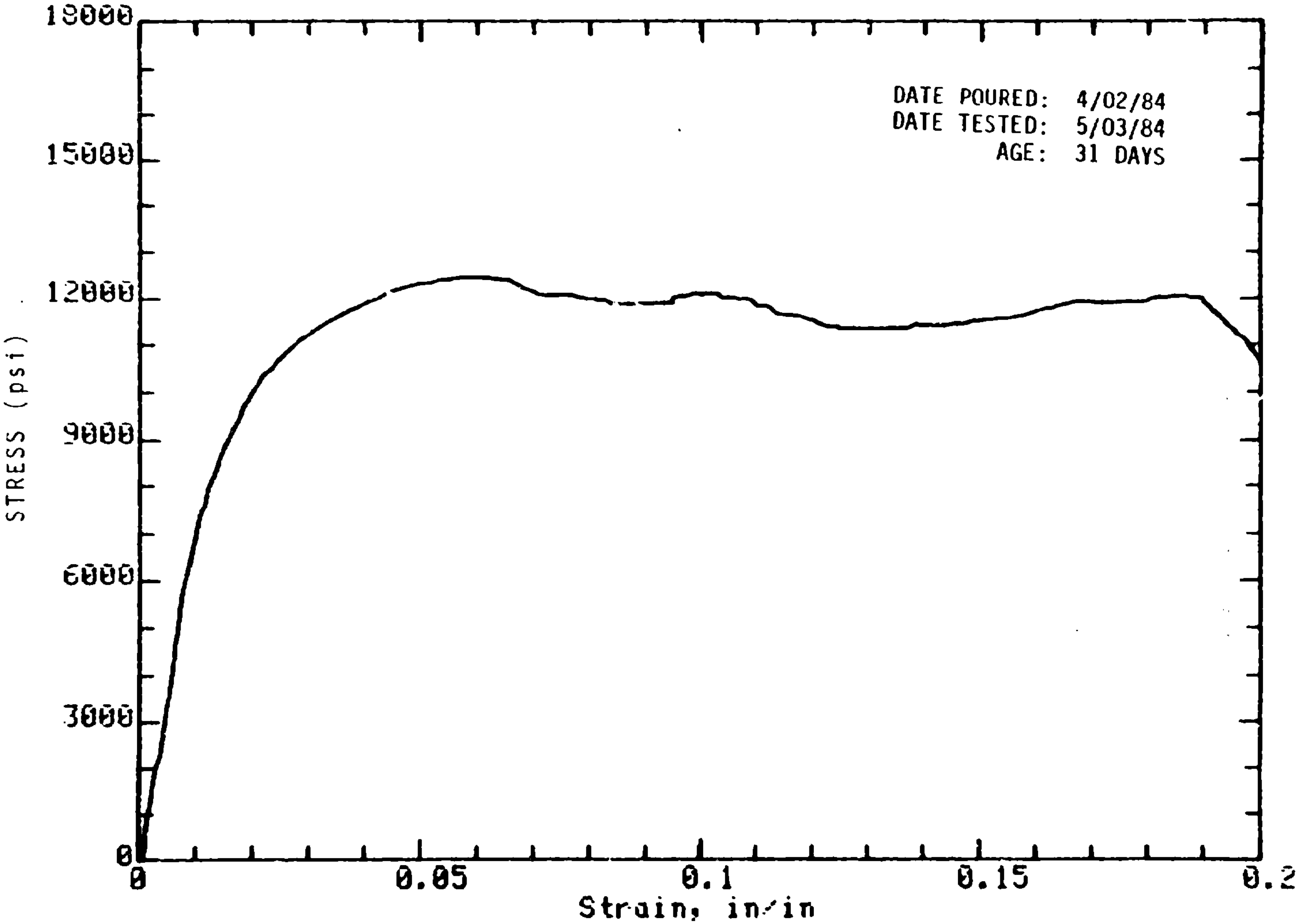

Mark: 10-S2-18 Cored (wall): 2in dia x 4in Cure: Dry
Concrete Sample

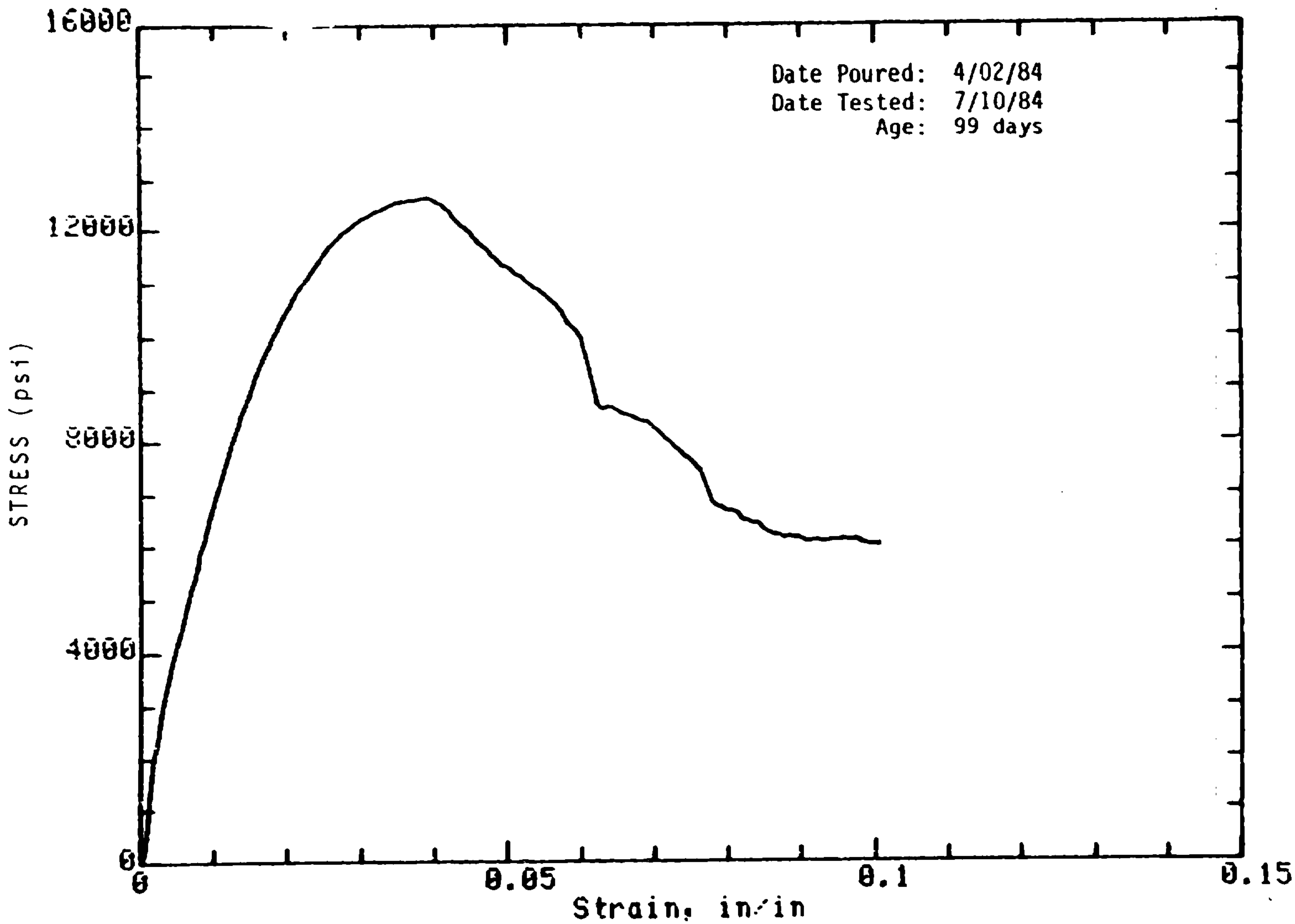

Mark: 10-2 Molded: 4in dia x 8in Cure: Wet
Concrete Sample

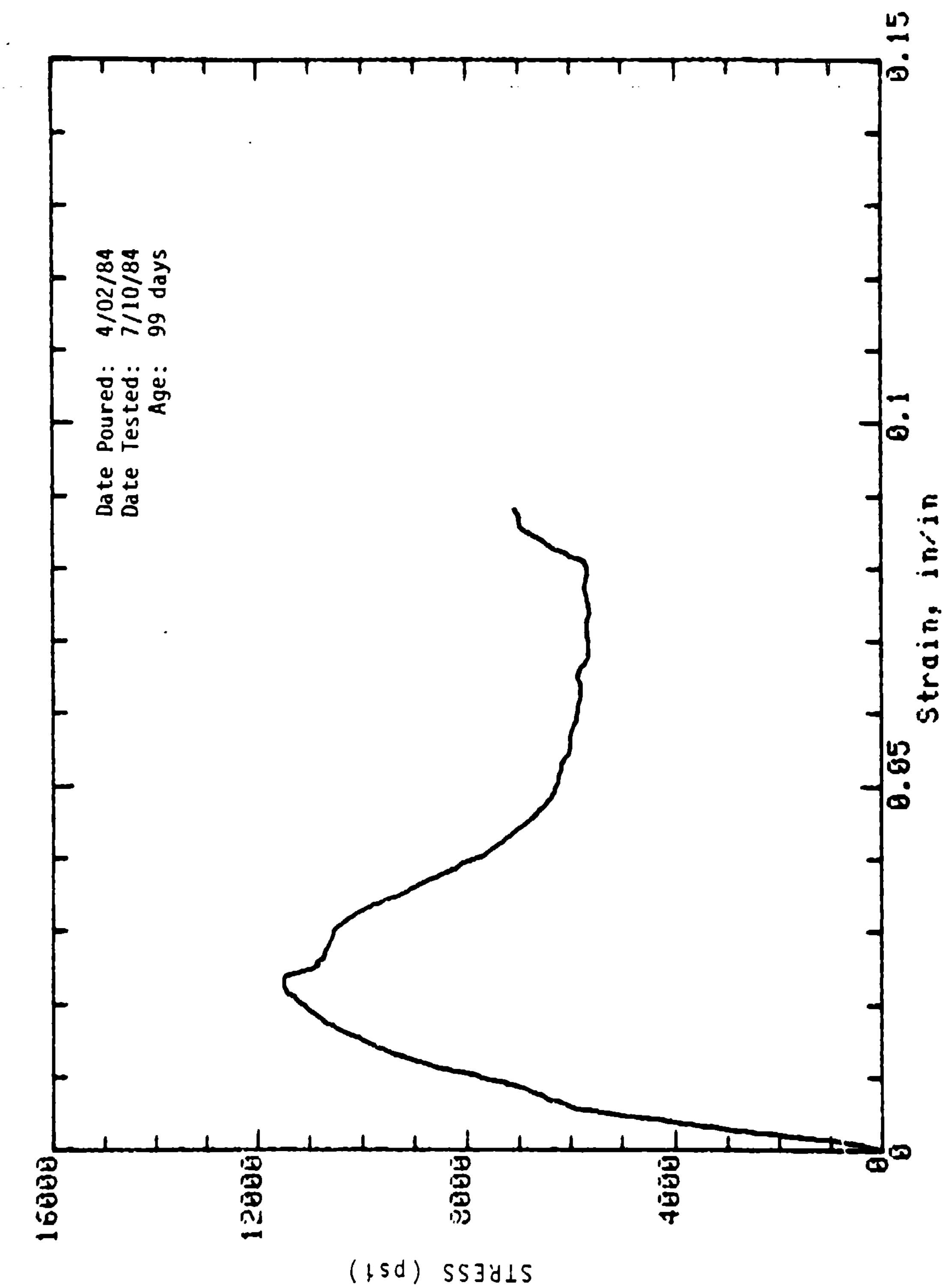

Mark: 10-4 Molded: 4in dia x 8in Cure: Wet
Concrete Sample

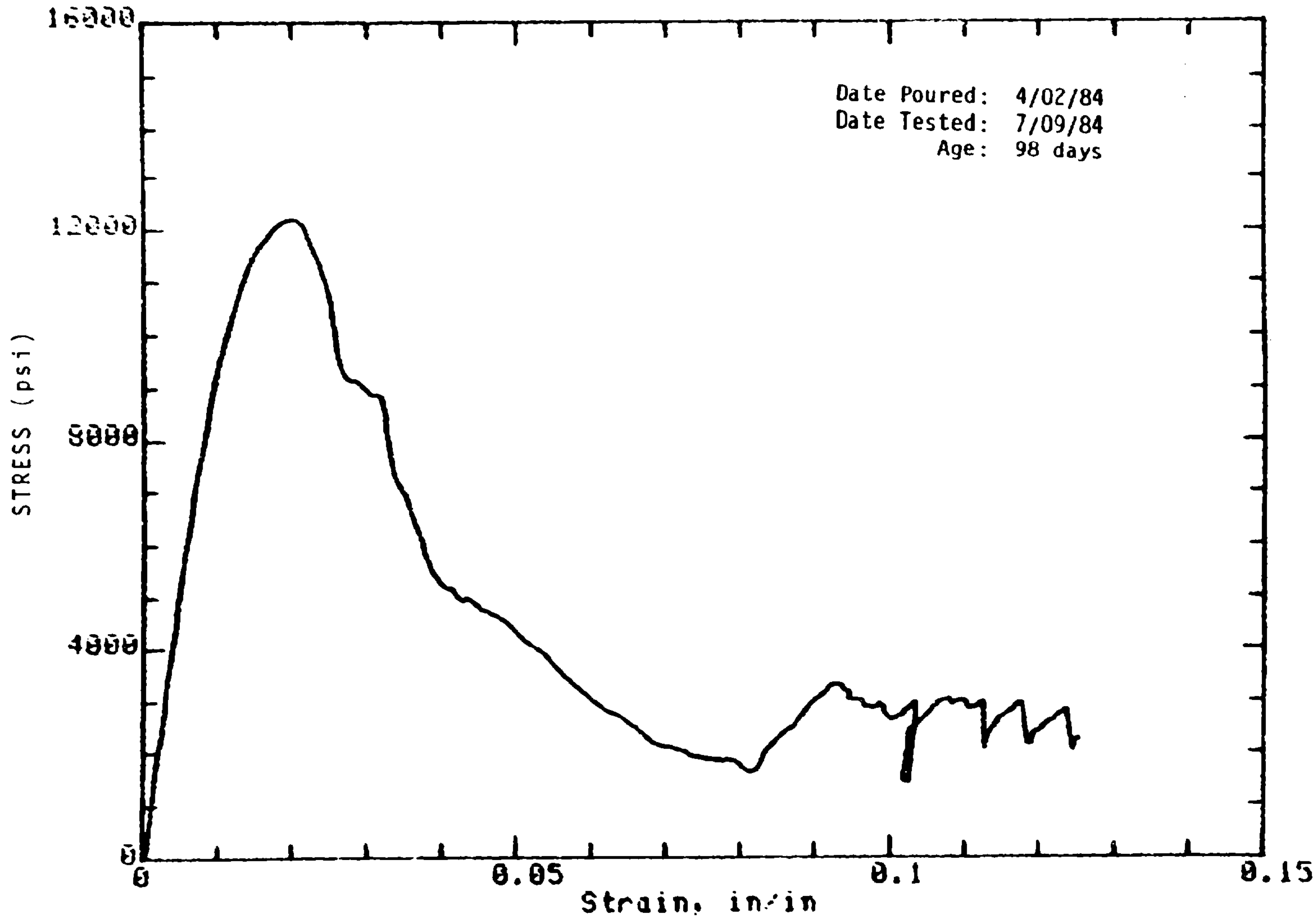

Mark: 10-11 Molded: 4in dia x 8in Cure: Wet
Concrete Sample

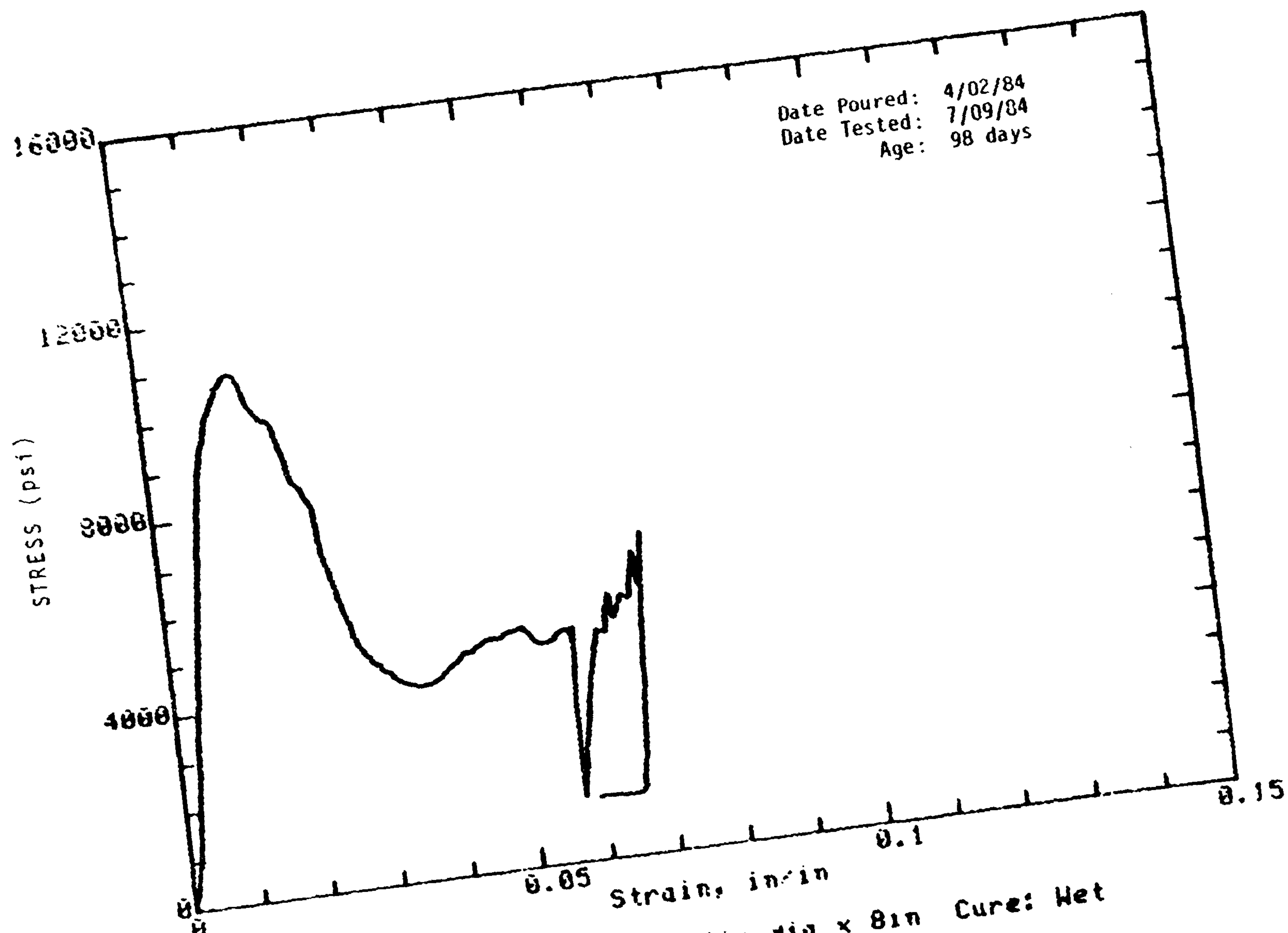

Mark: 10-12 Molded: 4in dia x 8in Cure: Wet
Concrete Sample

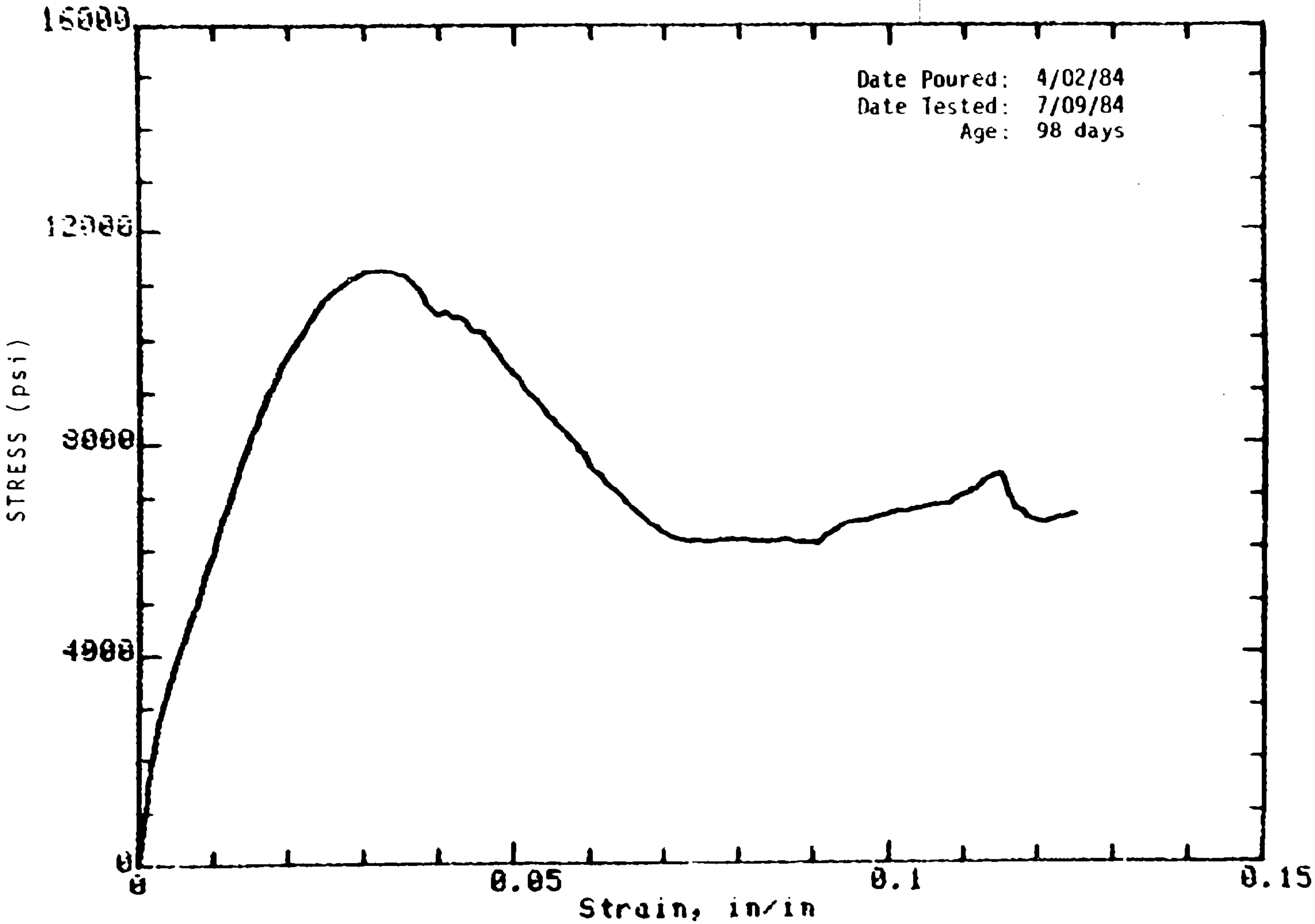

Mark: 10-14 Molded: 4in dia x 8in Cure: Wet
Concrete Sample

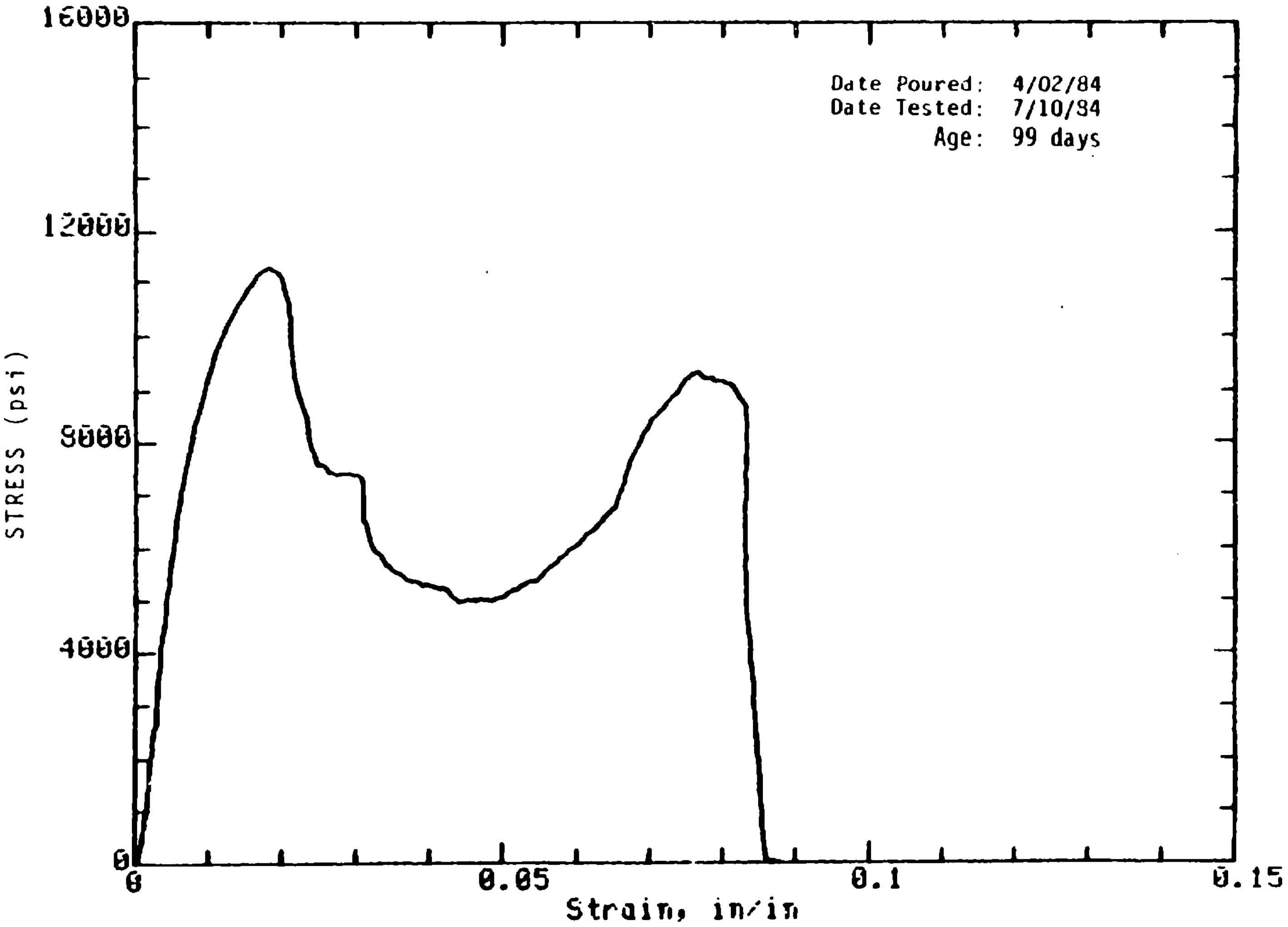

Mark: 10-18 Molded: 4in dia x 8in Cure: Wet
Concrete Sample

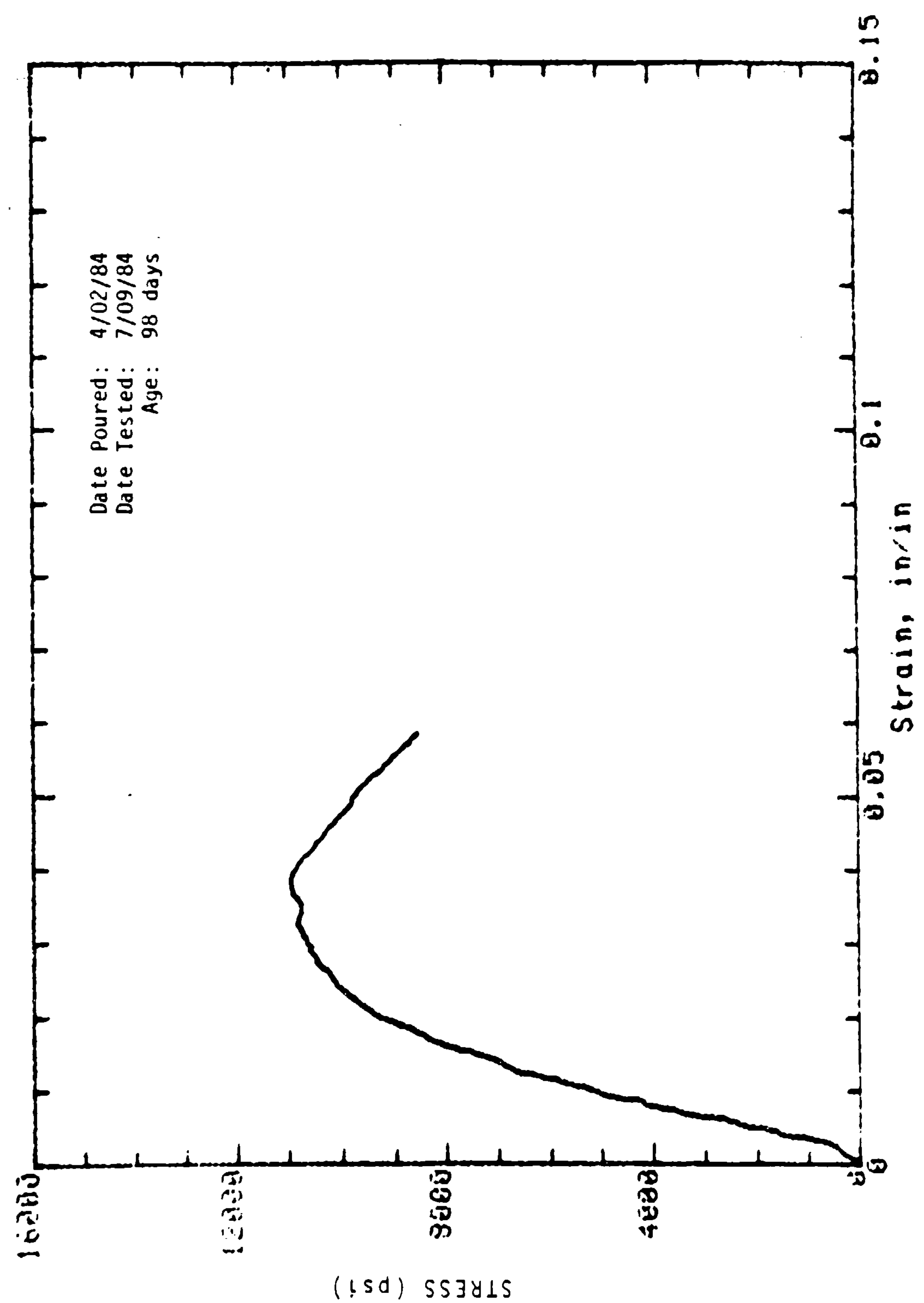

Mark: 10-1 Molded: 4in dia x 8in Cure: Dry
Concrete Sample

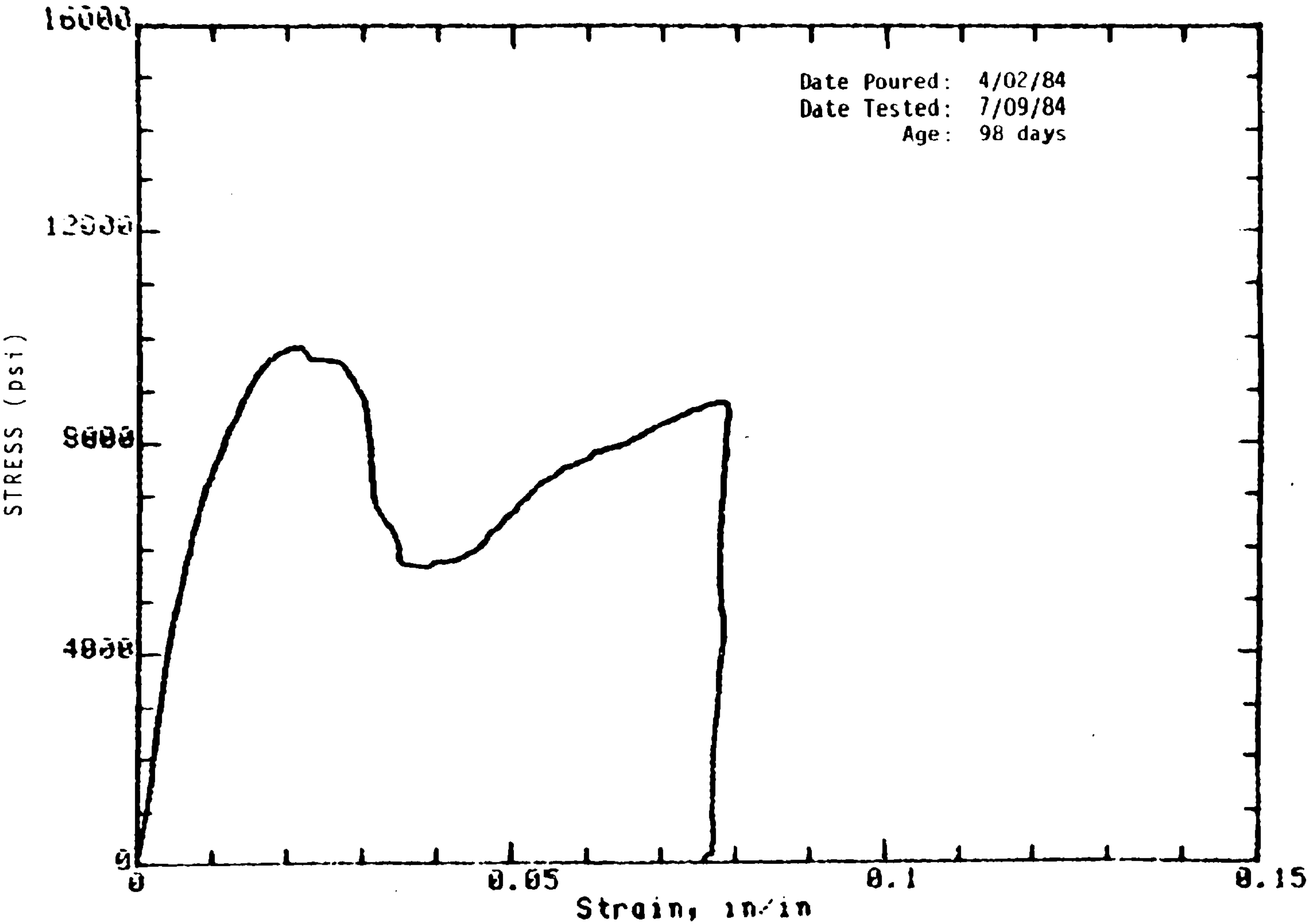

Mark: 10-3 Molded: 4in dia x 8in Cure: Dry
Concrete Sample

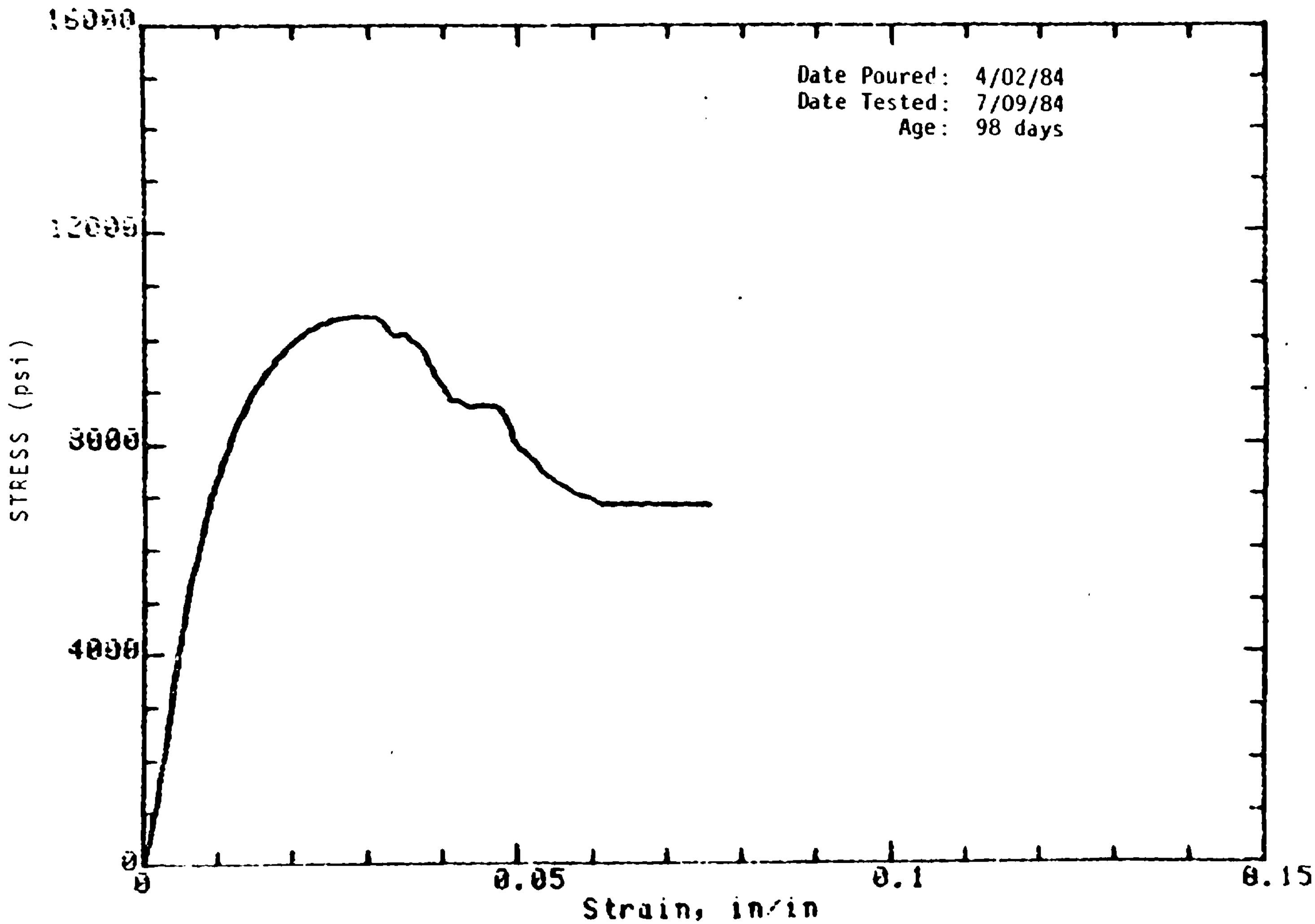

Mark: 10-5 Molded: 4in dia x 8in Cure: Dry
Concrete Sample

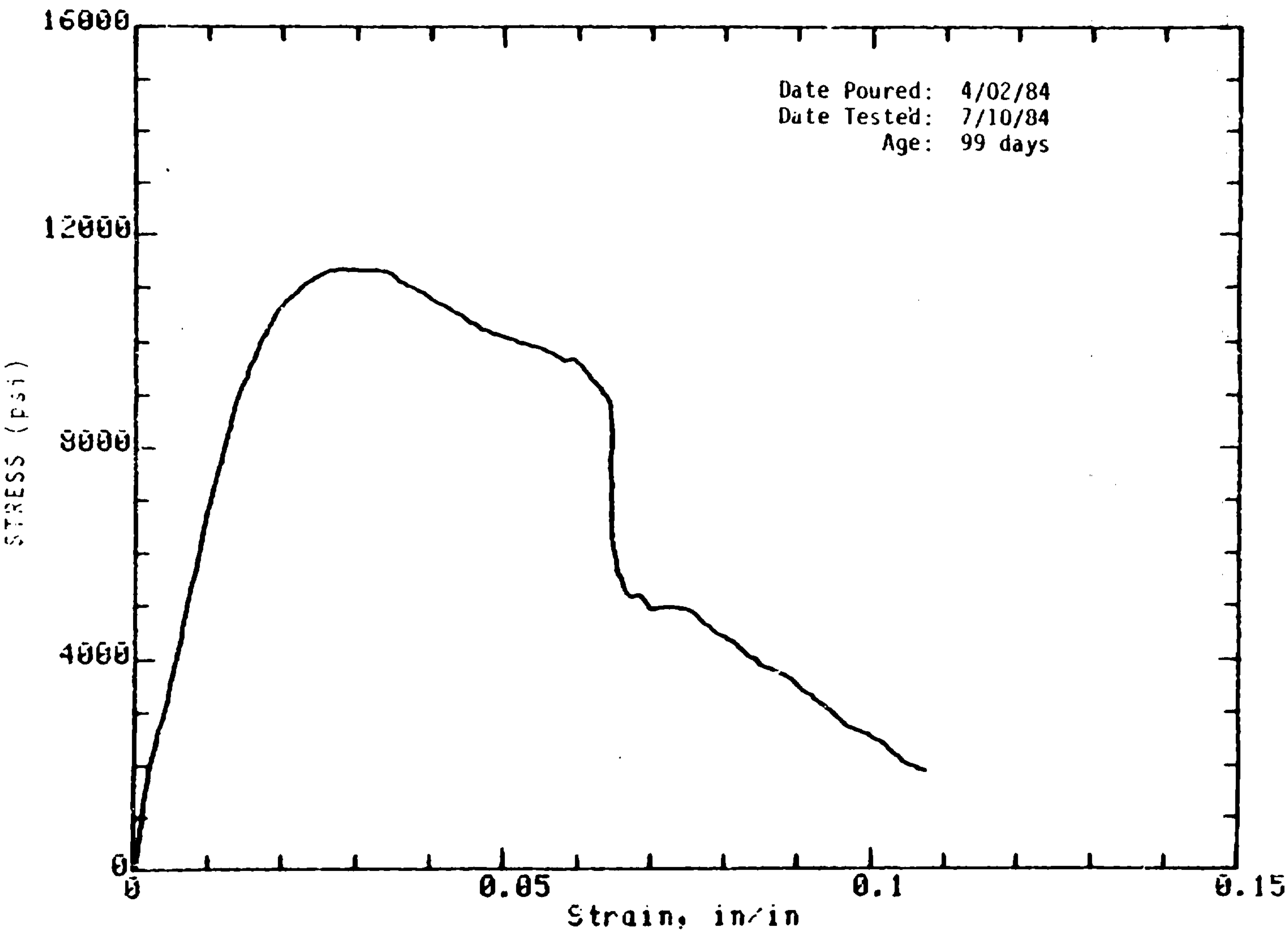

Mark: 10-7 Molded: 4in dia x 8in Cure: Dry
Concrete Sample

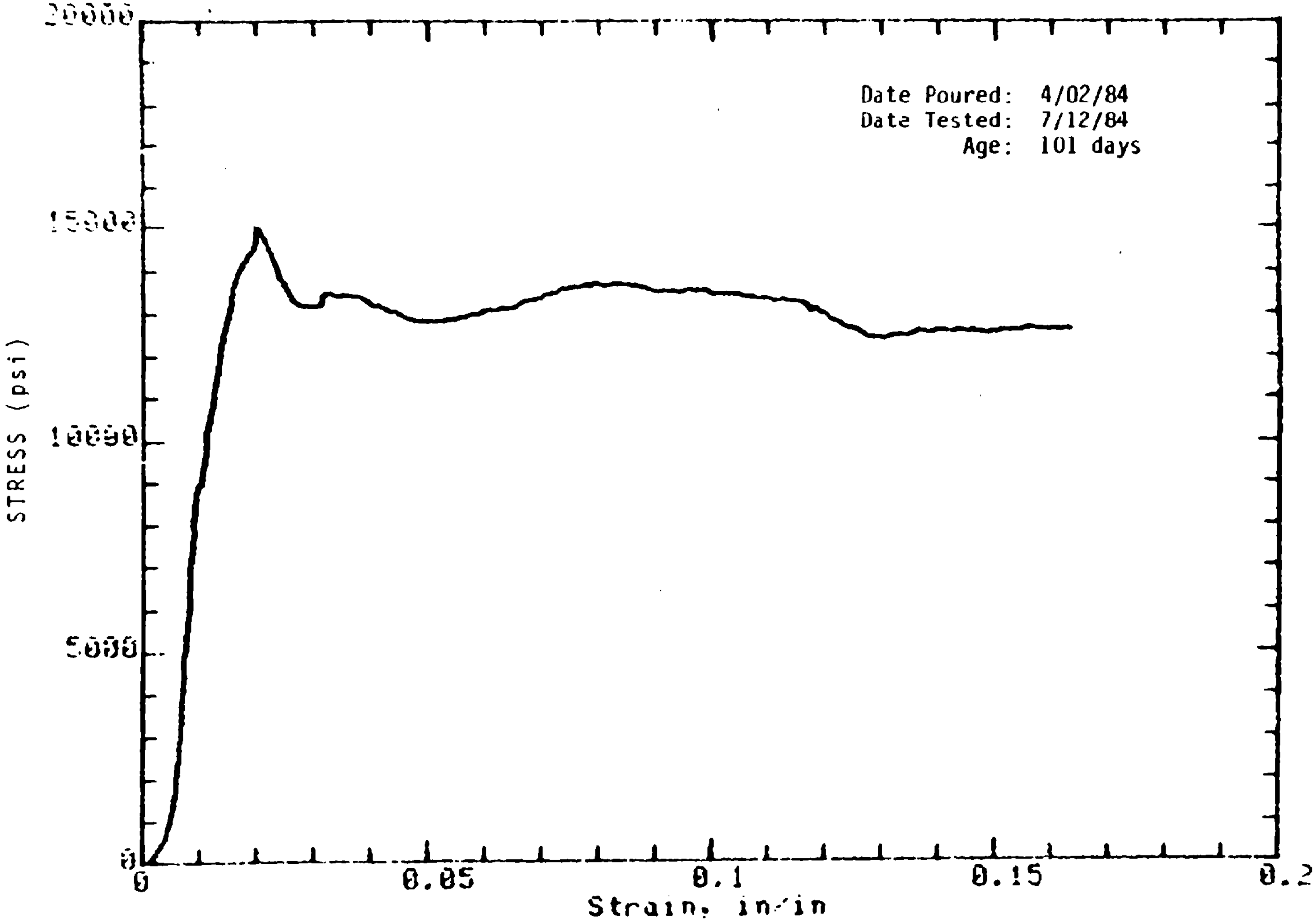

Mark: 1-10-1 Cored (Wall): 2in dia x 4in Cure: Dry
Concrete Sample

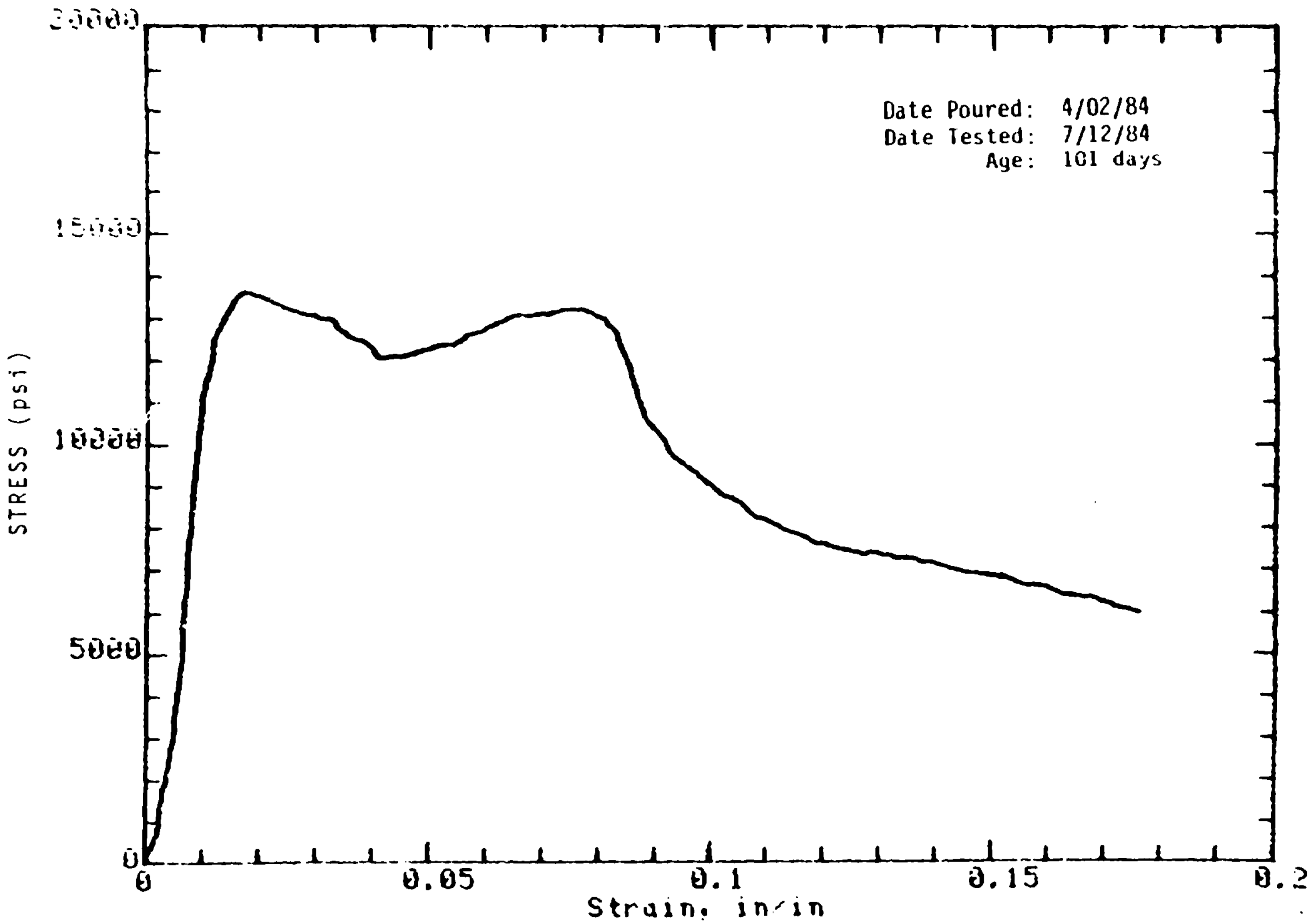

Mark: 1-10-2 Cored (Wall): 2in dia x 4in Cure: Dry
Concrete Sample

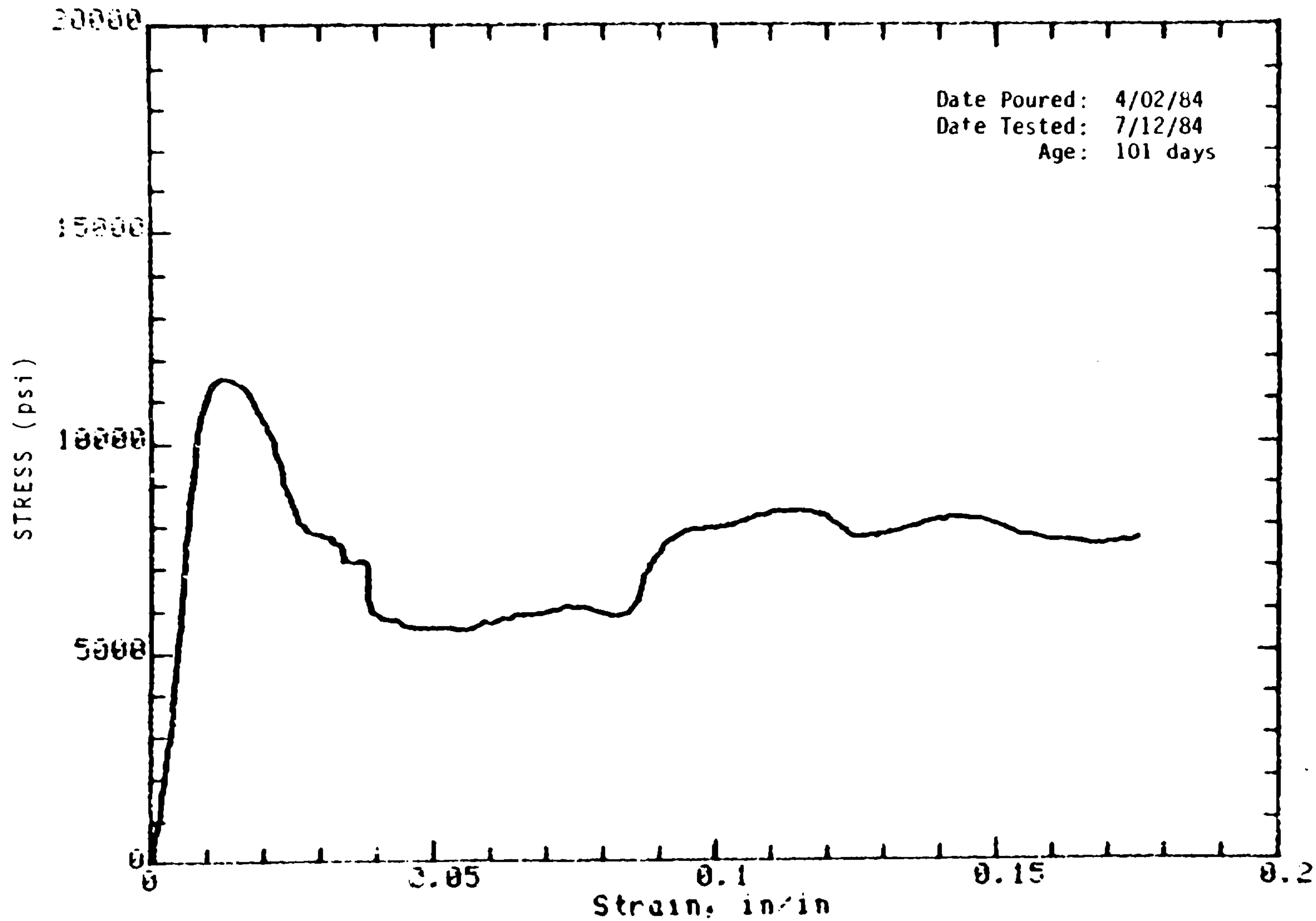

Mark: 1-10-3 Cored (Wall): 2in dia x 4in Cure: Dry
Concrete Sample

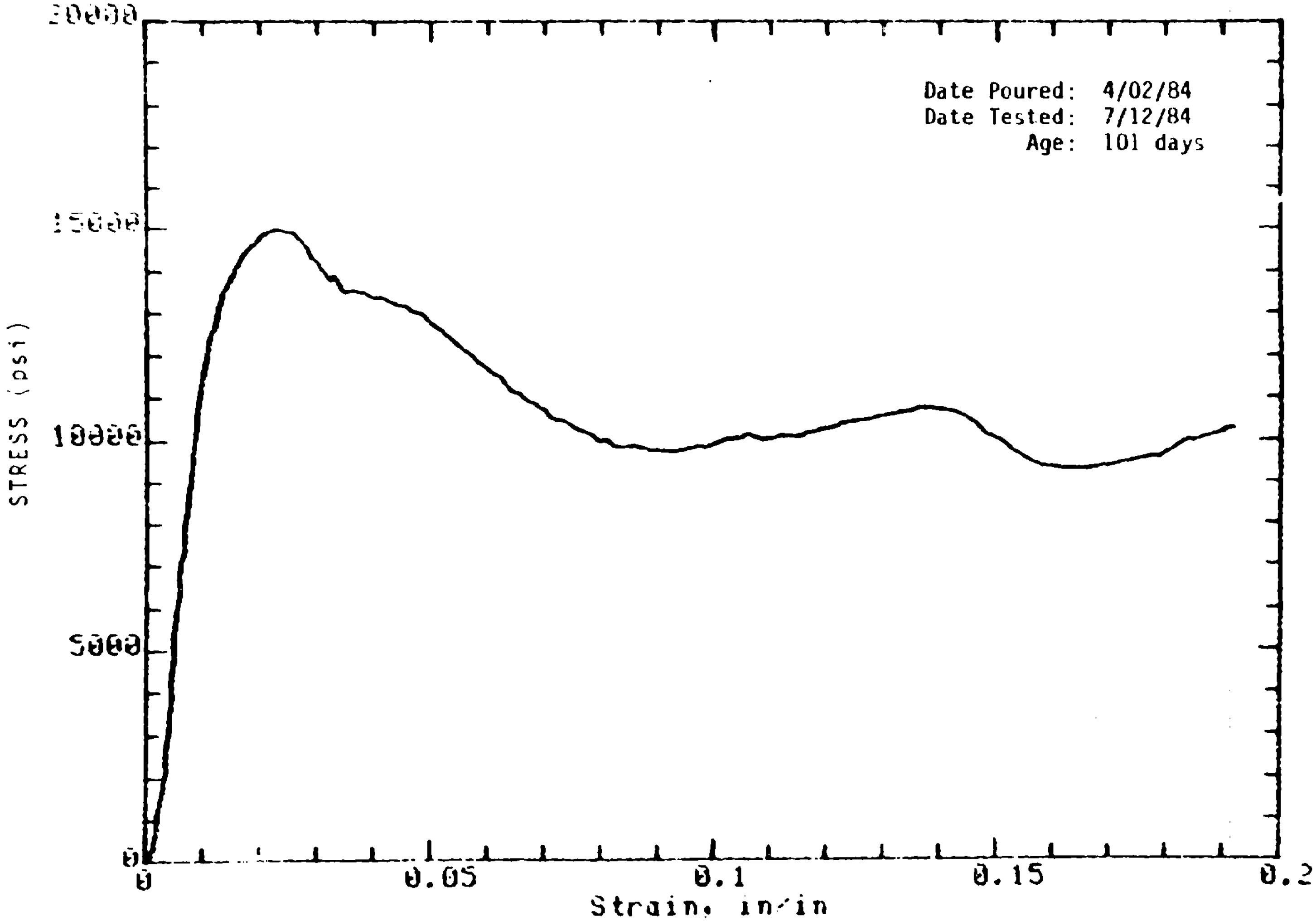

Mark: 1-10-4 Cored (Wall): 2in dia × 4in Cure: Dry
Concrete Sample

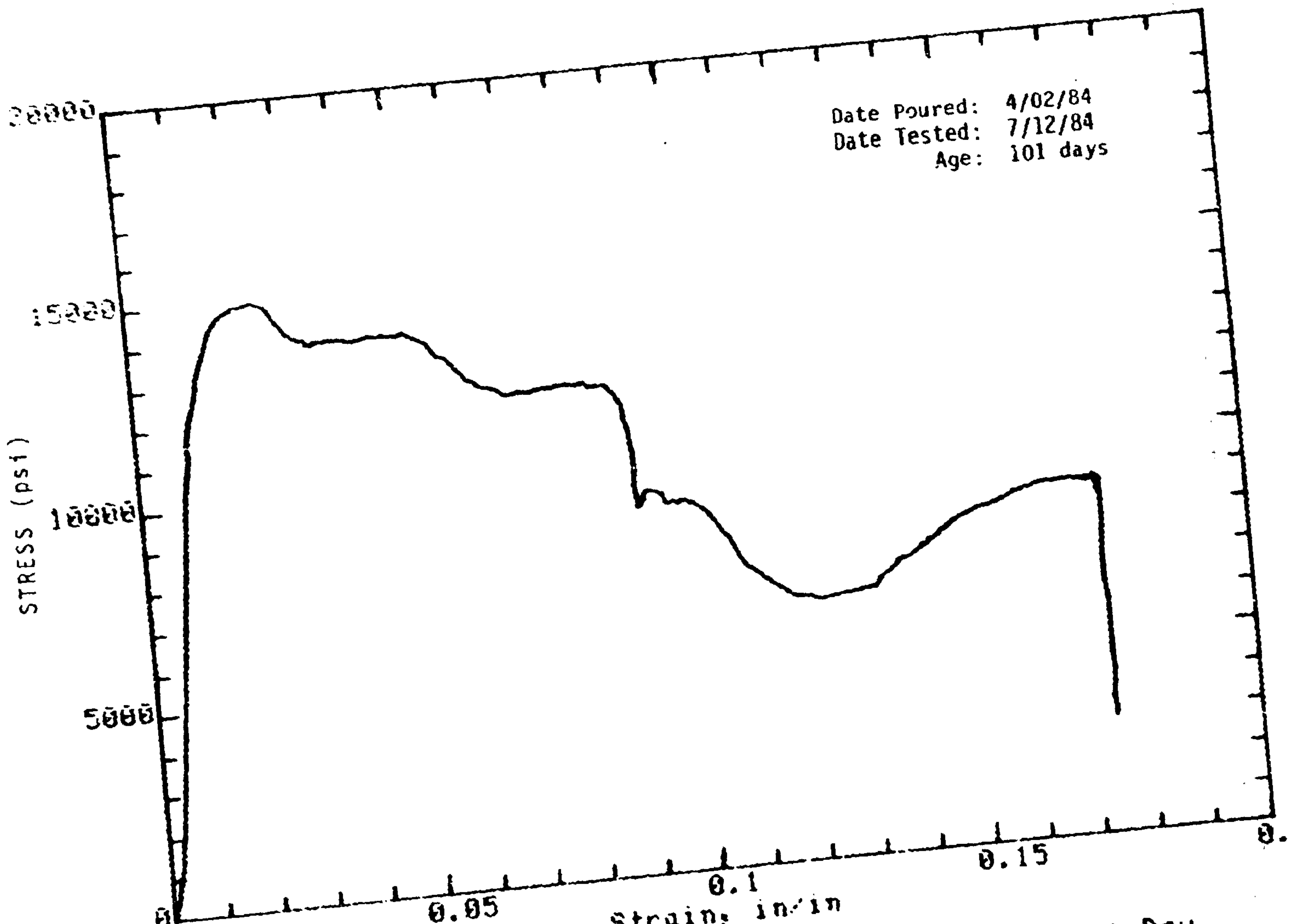

Mark: 1-10-5 Cored (Wall): 2in dia x 4in Cure: Dry
Concrete Sample

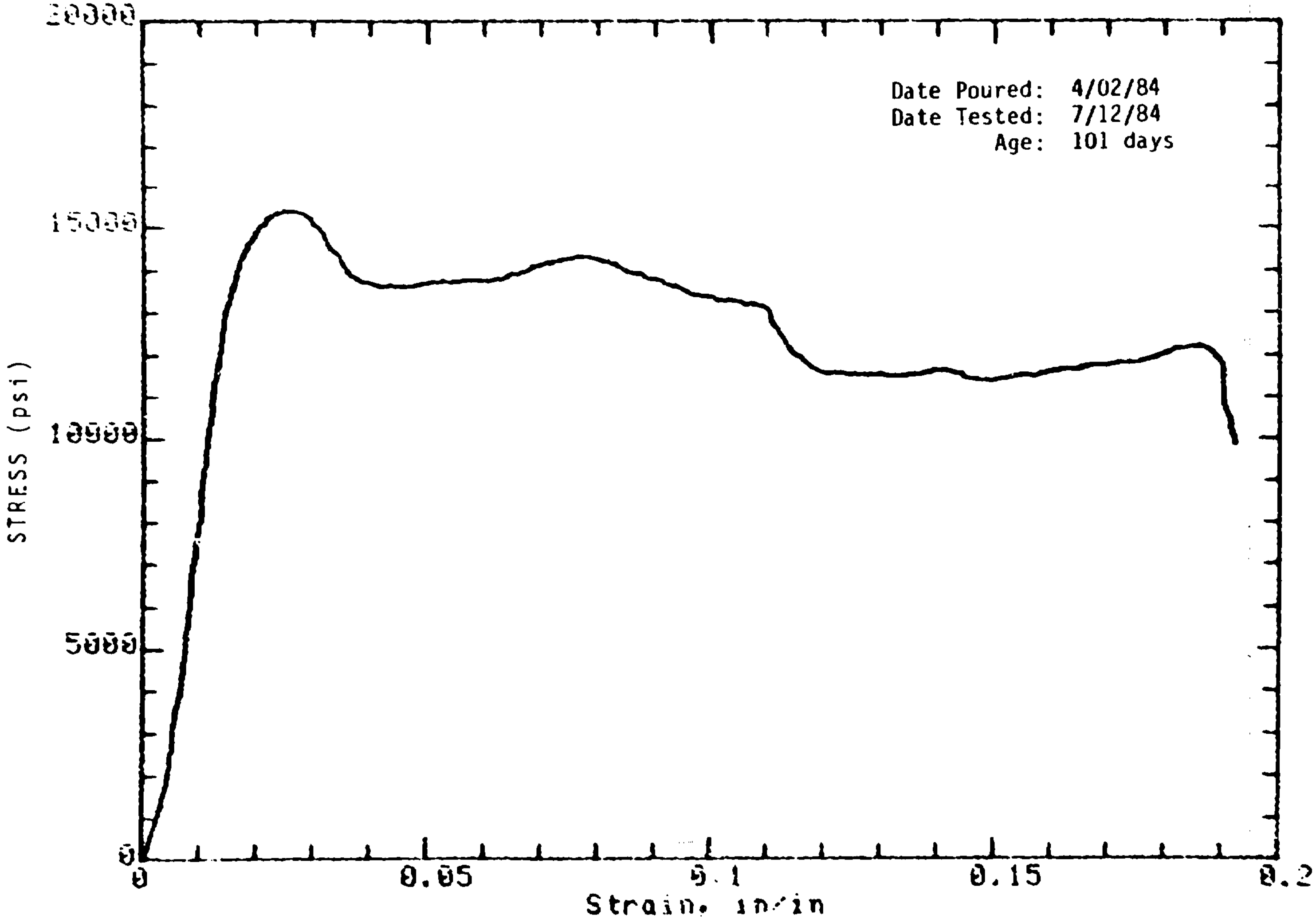

Mark: 1-10-6 Cored (Wall): 2in dia x 4in Cure: Dry
Concrete Sample

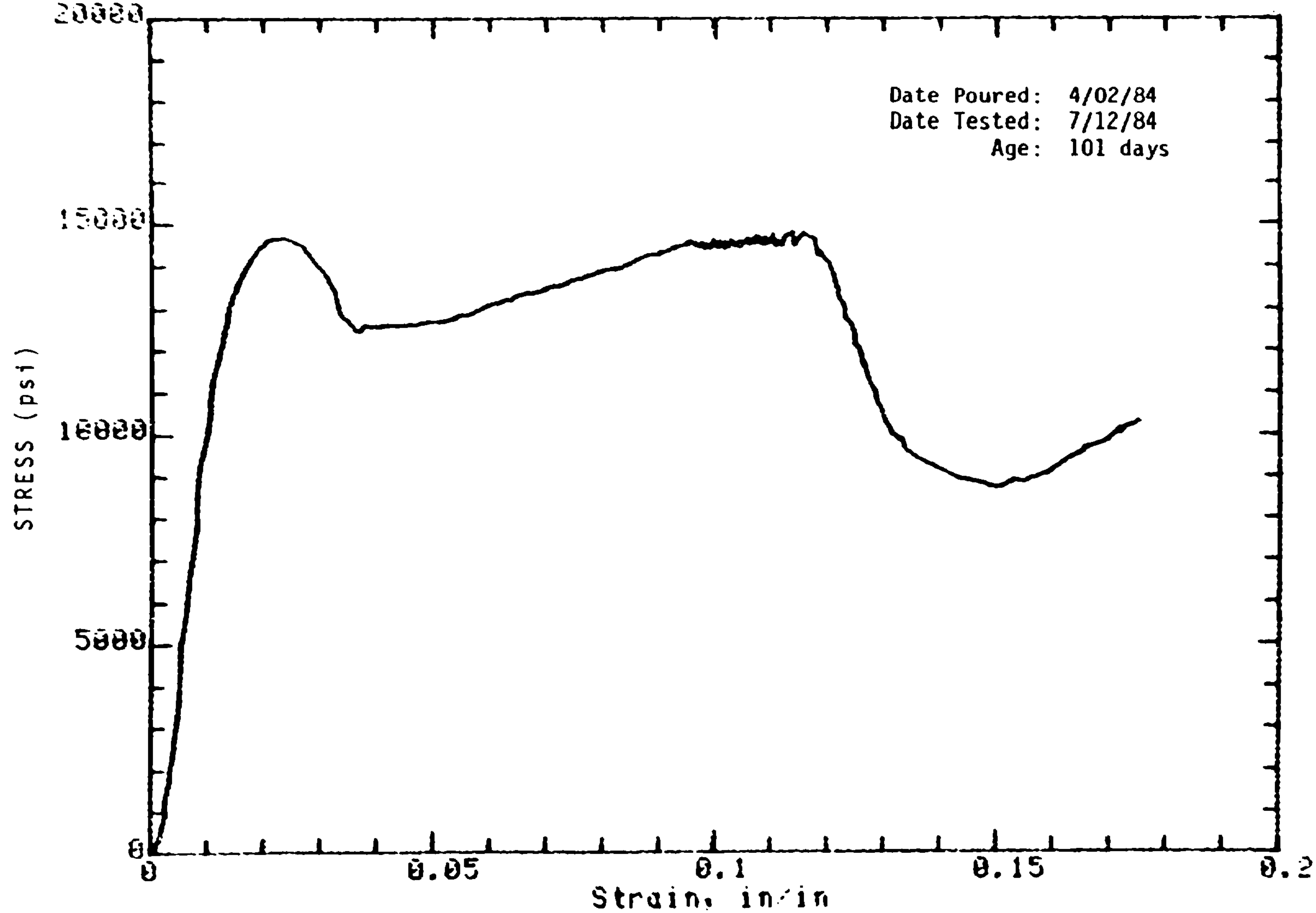

Mark: 1-10-7 Cored (Wall): 2in dia x 4in Cure: Dry
Concrete Sample

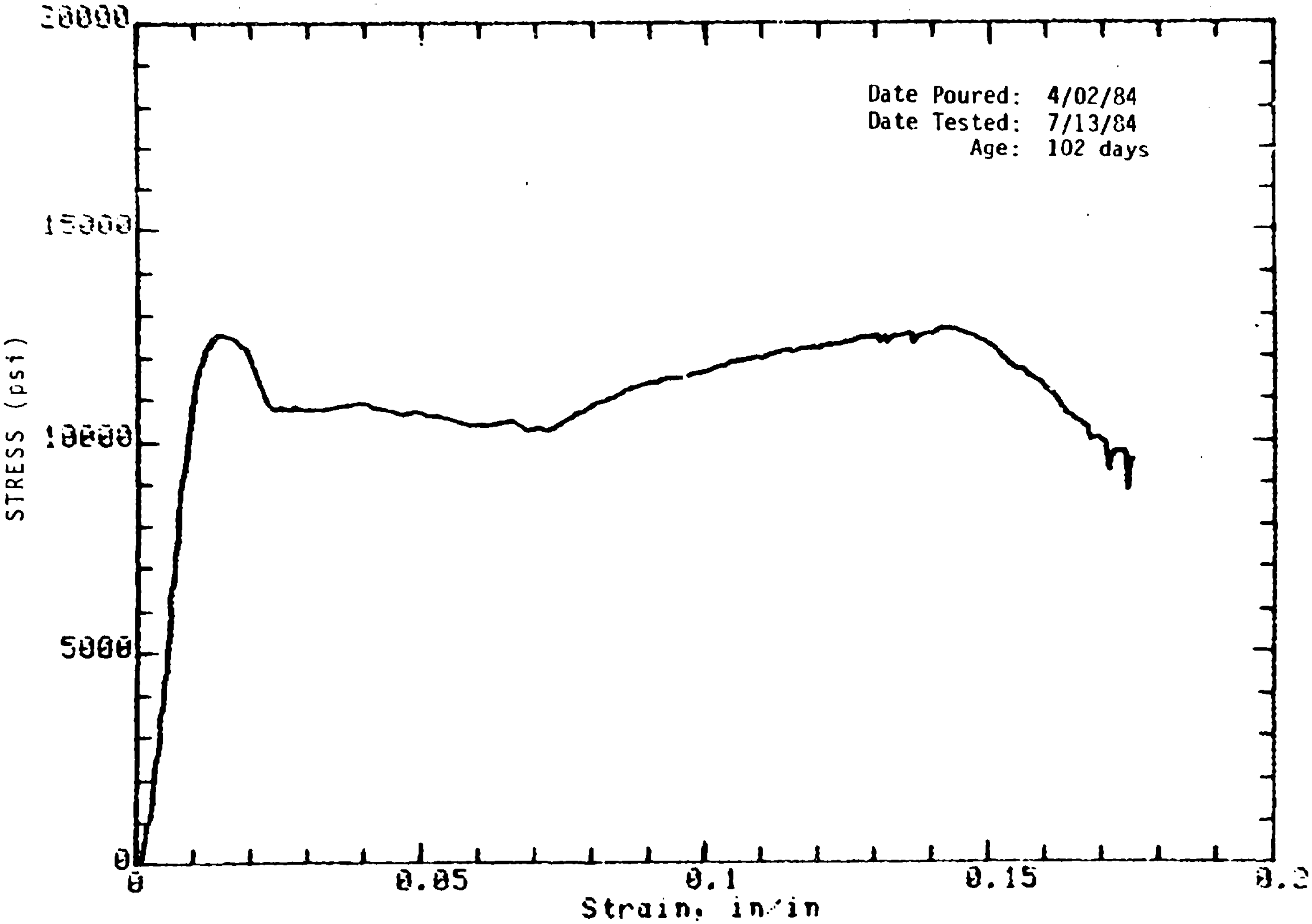

Mark: 1-10-8 Cored (Wall): 2in dia x 4in Cure: Dry
Concrete Sample

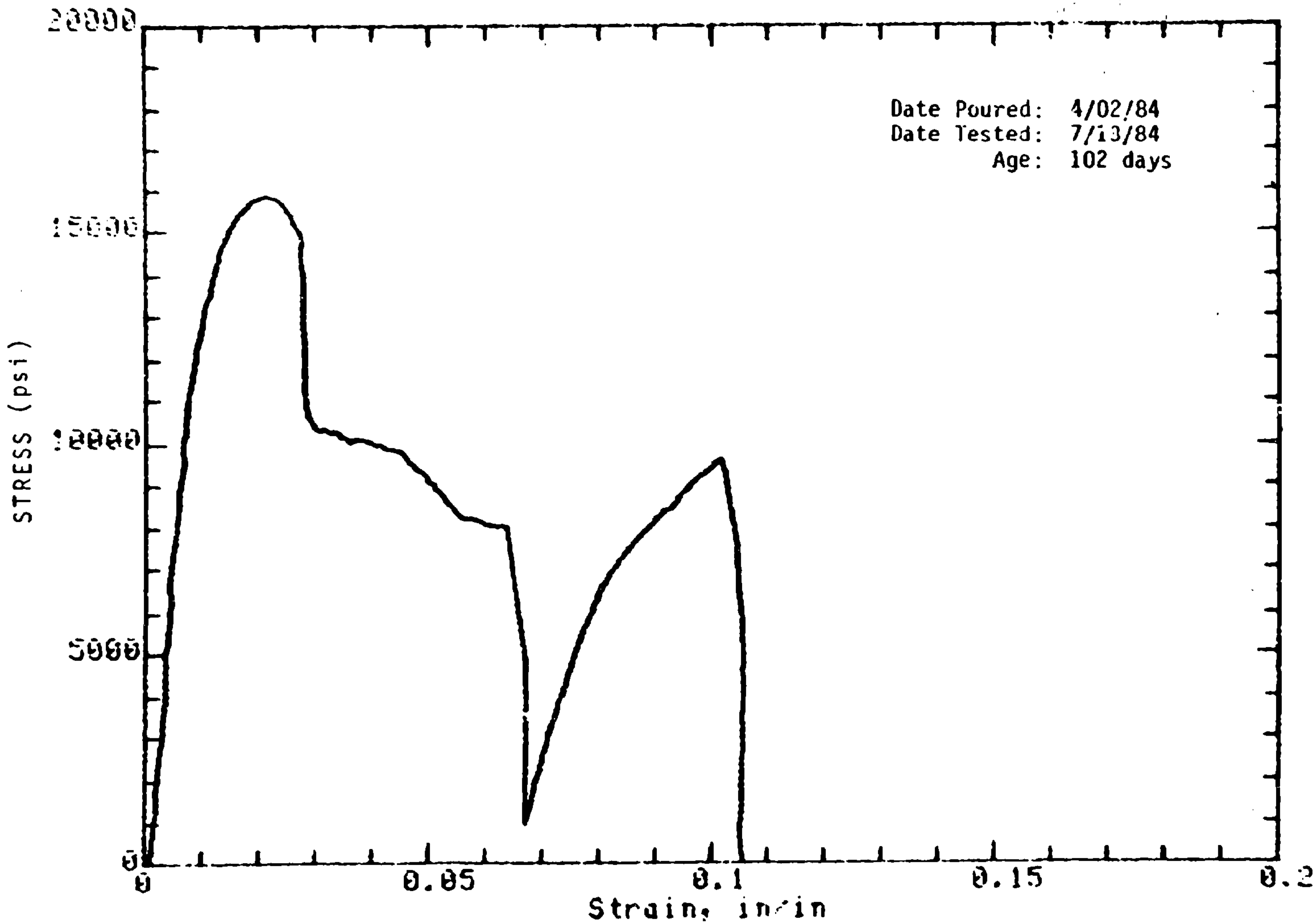

Mark: 1-10-9 Cored (Wall): 2in dia × 4in Cure: Dry
Concrete Sample

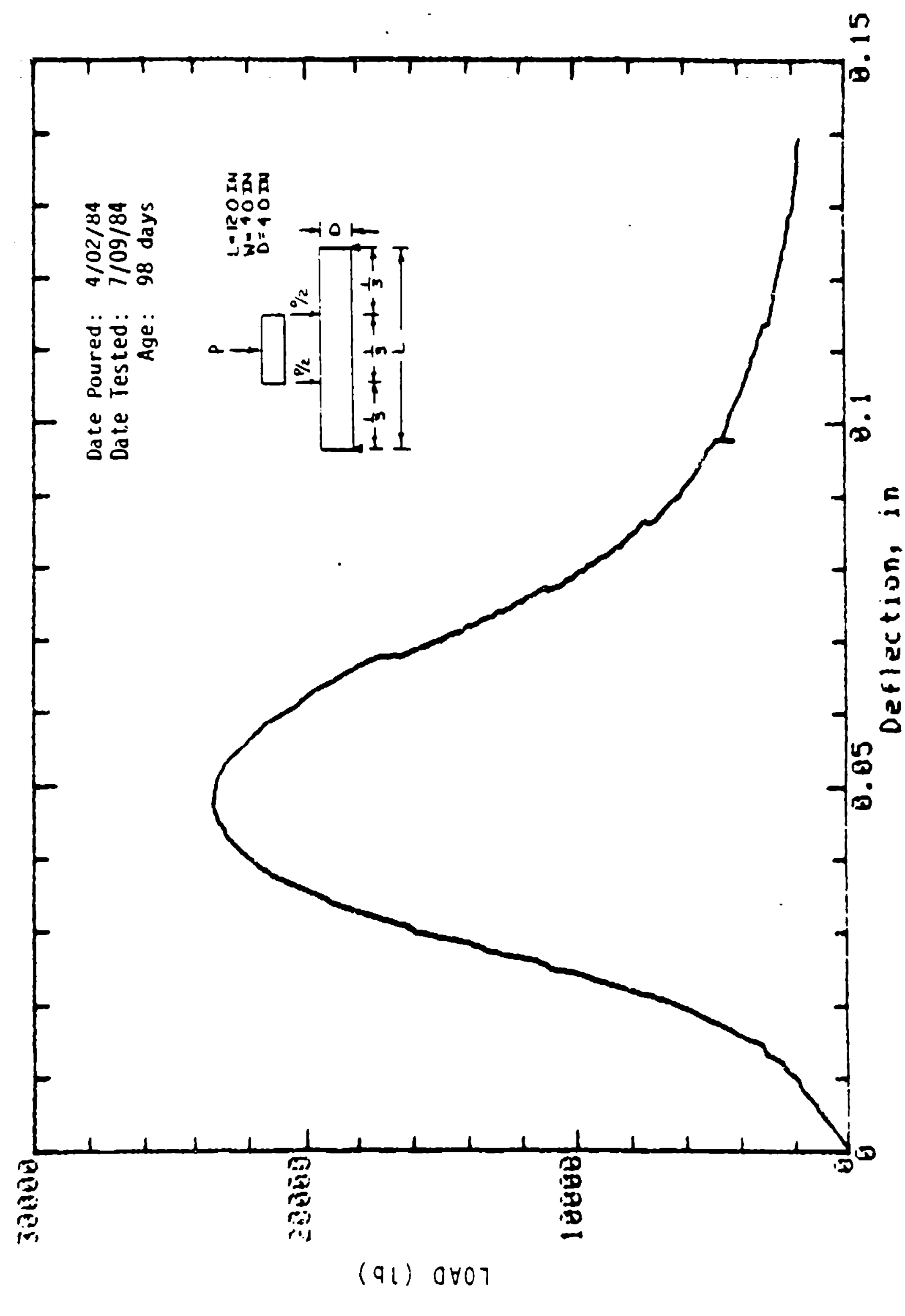

Mark: 10-30 Beam: 4in x 4in Cure: Wet
Concrete Sample

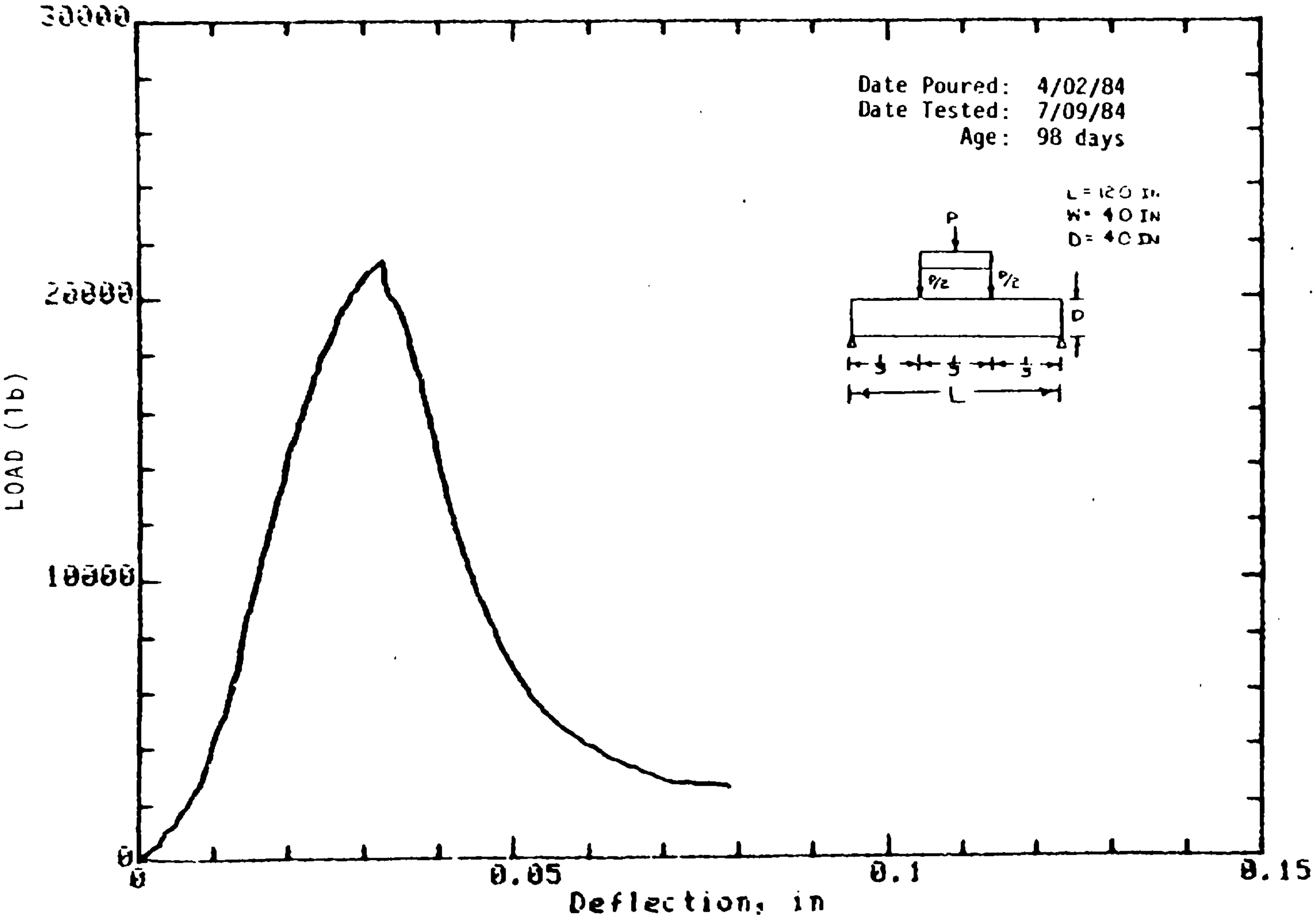

Mark: 10-31 Beam: 4in x 4in Cure: Wet
Concrete Sample

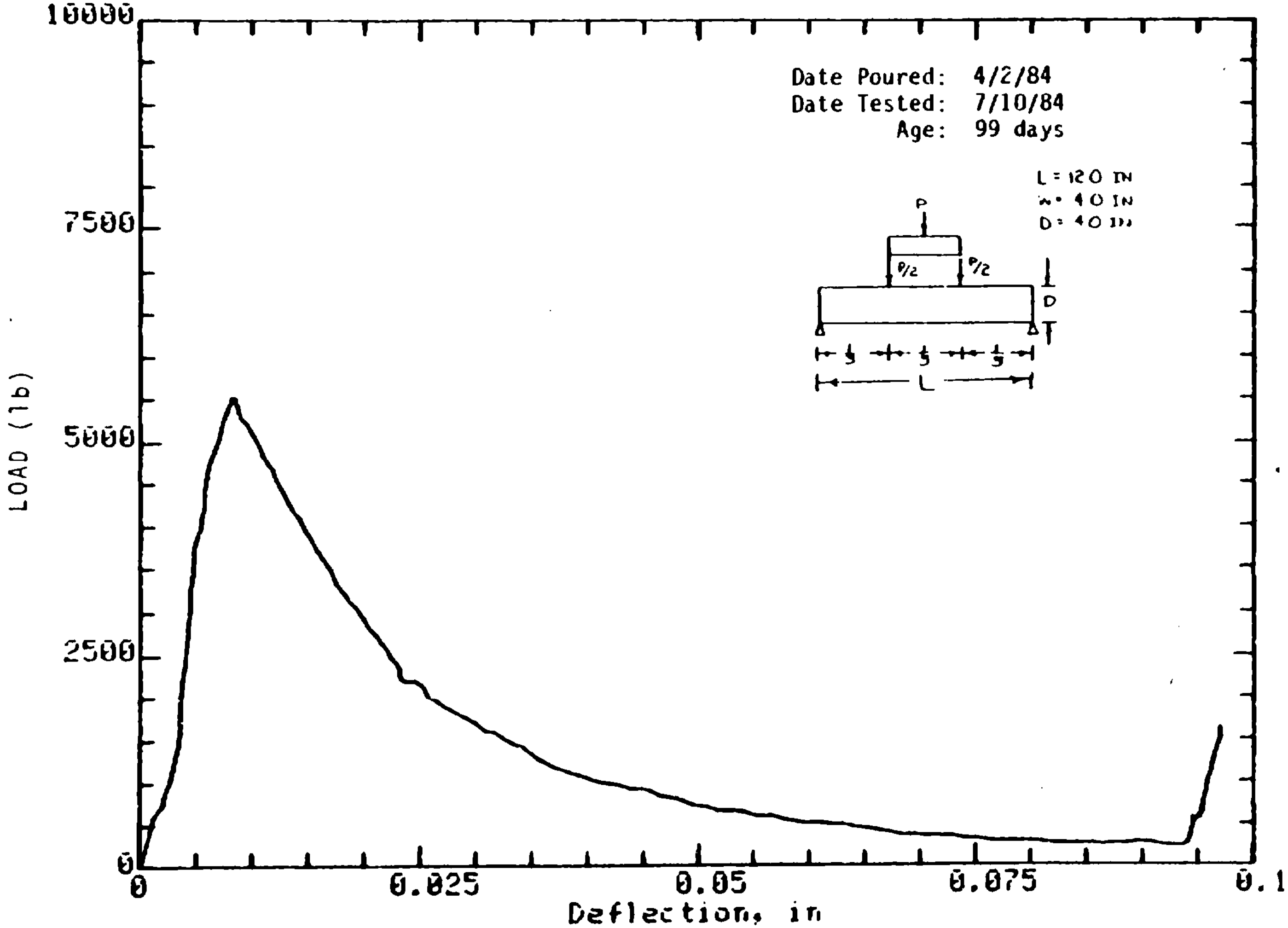

Mark: 10-35 Column: 4in x 4in Cure: Wet
Concrete Sample